frontiers | Research Topics

Territorial spatial evolution process and its ecological resilience

Edited by
Xiao Ouyang, Xue-Chao Wang, Salvador García-Ayllón Veintimilla and Juergen Pilz

Published in
Frontiers in Ecology and Evolution
Frontiers in Environmental Science

ISSN 1664-8714
ISBN 978-2-8325-4454-9
DOI 10.3389/978-2-8325-4454-9

About Frontiers

Frontiers is more than just an open access publisher of scholarly articles: it is a pioneering approach to the world of academia, radically improving the way scholarly research is managed. The grand vision of Frontiers is a world where all people have an equal opportunity to seek, share and generate knowledge. Frontiers provides immediate and permanent online open access to all its publications, but this alone is not enough to realize our grand goals.

Frontiers journal series

The Frontiers journal series is a multi-tier and interdisciplinary set of open-access, online journals, promising a paradigm shift from the current review, selection and dissemination processes in academic publishing. All Frontiers journals are driven by researchers for researchers; therefore, they constitute a service to the scholarly community. At the same time, the *Frontiers journal series* operates on a revolutionary invention, the tiered publishing system, initially addressing specific communities of scholars, and gradually climbing up to broader public understanding, thus serving the interests of the lay society, too.

Dedication to quality

Each Frontiers article is a landmark of the highest quality, thanks to genuinely collaborative interactions between authors and review editors, who include some of the world's best academicians. Research must be certified by peers before entering a stream of knowledge that may eventually reach the public - and shape society; therefore, Frontiers only applies the most rigorous and unbiased reviews. Frontiers revolutionizes research publishing by freely delivering the most outstanding research, evaluated with no bias from both the academic and social point of view. By applying the most advanced information technologies, Frontiers is catapulting scholarly publishing into a new generation.

What are Frontiers Research Topics?

Frontiers Research Topics are very popular trademarks of the *Frontiers journals series*: they are collections of at least ten articles, all centered on a particular subject. With their unique mix of varied contributions from Original Research to Review Articles, Frontiers Research Topics unify the most influential researchers, the latest key findings and historical advances in a hot research area.

Find out more on how to host your own Frontiers Research Topic or contribute to one as an author by contacting the Frontiers editorial office: frontiersin.org/about/contact

Territorial spatial evolution process and its ecological resilience

Topic editors

Xiao Ouyang — Hunan University of Finance and Economics, China
Xue-Chao Wang — Beijing Normal University, China
Salvador García-Ayllón Veintimilla — Polytechnic University of Cartagena, Spain
Juergen Pilz — University of Klagenfurt, Austria

Citation

Ouyang, X., Wang, X.-C., Veintimilla, S. G.-A., Pilz, J., eds. (2024). *Territorial spatial evolution process and its ecological resilience*. Lausanne: Frontiers Media SA.
doi: 10.3389/978-2-8325-4454-9

Table of contents

frontiers | Frontiers in Environmental Science

TYPE Editorial
PUBLISHED 31 January 2024
DOI 10.3389/fenvs.2024.1373672

OPEN ACCESS

EDITED AND REVIEWED BY
Alexander Kokhanovsky,
German Research Centre for Geosciences, Germany

*CORRESPONDENCE
Salvador García-Ayllón,
salvador.ayllon@upct.es

RECEIVED 20 January 2024
ACCEPTED 22 January 2024
PUBLISHED 31 January 2024

CITATION
García-Ayllón S and Pilz J (2024), Editorial: Territorial spatial evolution process and its ecological resilience.
Front. Environ. Sci. 12:1373672.
doi: 10.3389/fenvs.2024.1373672

Editorial: Territorial spatial evolution process and its ecological resilience

Salvador García-Ayllón[1]* and Jürgen Pilz[2]

[1]Department of Mining and Civil Engineering, Technical University of Cartagena, Cartagena, Spain, [2]Institut für Statistik, Universität Klagenfurt, Klagenfurt, Austria

KEYWORDS

territorial spatial evolution, ecological resilience, land use analysis, territorial diffuse anthropization, resilience-related indicators, ecological restoration policy, environmental management, remote sensing analysis

Editorial on the Research Topic
Territorial spatial evolution process and its ecological resilience

The large-scale territorial transformation of our planet is possibly the anthropogenic footprint that most clearly defines the behavioral patterns of human beings today (Bronts et al., 2023). This footprint, which was difficult to analyze a few decades ago due to the absence of real social awareness and evaluation tools, can now be measured precisely. The effects associated with climate change often occur dramatically in scenarios that we can clearly visualize with catastrophic events such as floods, droughts, tornadoes, *etc.* (Lang et al., 2016; Virah-Sawmy et al., 2016; Romera et al., 2017; Mansoor et al., 2022). However, the impact associated with what some authors call diffuse territorial anthropization is much more complex to diagnose because it has more sophisticated cause-effect patterns of functioning.

Thanks to the important methodological advances that exist at a technological level, we are now aware of the true magnitude of the problem we face. This silent enemy that we have called diffuse territorial anthropization can thus be unmasked through a large-scale spatial analysis (Magalhães et al., 2015; Mohamed et al., 2017). The evolution of land space demonstrates the shift of land use types from natural and semi-natural land (e.g., forest land and cropland) to built-up land, altering ecosystem cycling patterns and leading to degradation of ecosystem services in terms of regulation, provisioning and support (Du et al., 2023).

At the same time, production and living space crowding out ecological space brings high potential threats, such as soil erosion (Cao et al., 2024), water imbalances in wetlands and spaces of high ecological value (Garcia-Ayllon and Radke, 2021), alteration of coastal areas (Bianco et al., 2020), forest productivity decline (Yang et al., 2023b)and habitat fragmentation (Li et al., 2022). Accordingly, in response to the problems of imbalanced territorial space development, inefficient resource utilization and ecological environment degradation, how to improve the diversity, stability and sustainability of ecosystems is an urgent issue to promote modernization and green development in the new era of territorial space evolution.

In this field of research, high-resolution remote sensing images have become a very common visual instrument to monitor the characteristics of national land space and ecological environment. However, this is not the only tool in which improvements have

been developed in the field of spatial analysis associated with this subject. There have been numerous technological or methodological advances in recent years in fields such as statistics (García-Santos et al., 2020), economic quantification of impacts (Bianco and García-Ayllón, 2021) or sociological analysis (Ibarra et al., 2023), among others, for the analysis of these phenomena linked to territorial spatial evolution processes and its ecological resilience.

For this reason, this Research Topic wanted to make a review of the state of the art of research that addresses spatial studies by using field survey, remote sensing monitoring, model simulation and other similar technologies. These contributions systematically investigate the evolutionary process of territorial space and ecological resilience to clarify the dynamic trend of ecological resilience under the action of nature and human. The Research Topic also focuses on the establishment of a territorial space simulation model for enhancing ecological resilience the stability and sustainability of the ecosystem and promote the modernization of the harmonious coexistence of human beings and nature.

On this issue, China is probably one of the areas in the world with the greatest intensity and variety of repercussions related to anthropogenic phenomena associated with land transformation. For that reason, this Research Topic has addressed it in a comprehensive way with several studies that focus the hottest topics from the subject. Among them, for example, the effects derived from the significant urbanization growth of large cities stand out. Peng et al. analyze, from a spatiotemporal perspective, the impact of land urbanization on the gross primary productivity of vegetation in the middle reaches of the Yangtze River urban agglomeration, pointing out new evidence from the township scale (Peng et al., 2023).

Wang et al. investigate the mechanism of urbanization on the net primary productivity of vegetation in the Yangtze River Economic Belt, making a comprehensive analysis from global to local effects Wang et al. Shu et al. and Li et al. make similar approaches to analysis from the perspective of the spatiotemporal trends and factors influencing online attention for China's tea industry Shu et al. and the construction of carbon budget balance index and its application in the urban agglomeration around Poyang Lake area Li et al. By last, Meng et al. show an interesting case study on the growing problem of surface urban heat island effect and its spatiotemporal dynamics in cities with case study of the Zhengzhou metropolitan area (Meng et al.).

Other interesting phenomena are addressed from the ecological perspective with the parameterization of the environmental resilience of the territory through the behavior of its high-value natural areas. In this field, Zeng et al. show an interesting example with monitoring and control of water-ecological space in the Dongting Lake region (Zeng et al.). Yang et al. show a different approach for monitoring in their study for digital research on the resilience control of water ecological space under the concept of urban-water coupling (Yang et al.) and Huang et al. design and optimize an ecological security pattern based on landscape ecological risk assessment in the affected area of the Lower Yellow River Huang et al.

Finally, a third pillar of this Research Topic, no less interesting than the previous ones, is the establishment of territorial planning criteria through zoning and the use of ecosystem services. In this field, several authors have carried out enlightening studies: Yin et al. evaluate the factors influencing ecological environment and zoning control for the study case of the Dongting Lake area (Yin et al., 2024) and Ma et al. analyze the spatiotemporal variation and driving factors of habitat quality in the northern foothills of the Qinling Mountains in Xi'an (Ma et al.). On the other hand, other authors address this issue with a different approach: Li et al. adopt a "structure–function" perspective in the analysis of the evolution and zoning of spatial ecosystem functional stability in the southern hilly province of Hunan (Li et al.), Meng et al. research on multilevel evaluations and zones of territorial spatial functions in Yibin Meng et al., Tan et al. study the trade-off/synergy spatiotemporal benefits of ecosystem services and its influencing factors in hilly areas of the southern area of the country (Tan et al., 2024) and Huang et al. analyze the spatiotemporal evolution and influencing factors of ecosystem service in the Changsha-Zhuzhou-Xiangtan urban agglomeration (X. Huang et al., 2024).

In conclusion, it is a quite heterogenous field of research in which there have been great technical advances and important methodological improvements in recent years, but which continues to progress. Even so, further research is needed in this area, as the relationship between the effects of territorial anthropization and their effects is becoming more and more complex, and therefore difficult to analyze. There is and will be no planet B for us or for our generations to come. Therefore, a good spatial analysis of the evolution of the territory will undoubtedly be a determining factor in the future, if we want to make the planet we inhabit ecologically resilient to the footprint we are going to leave on it.

Author contributions

SG-A: Conceptualization, Data curation, Formal Analysis, Funding acquisition, Investigation, Methodology, Project administration, Resources, Software, Supervision, Validation, Visualization, Writing–original draft, Writing–review and editing. JP: Conceptualization, Data curation, Formal Analysis, Funding acquisition, Investigation, Methodology, Project administration, Resources, Software, Supervision, Validation, Visualization, Writing–original draft, Writing–review and editing.

Funding

The author(s) declare that no financial support was received for the research, authorship, and/or publication of this article.

Conflict of interest

The authors declare that the research was conducted in the absence of any commercial or financial relationships that could be construed as a potential conflict of interest.

The author(s) declared that they were an editorial board member of Frontiers, at the time of submission. This had no impact on the peer review process and the final decision.

Publisher's note

References

Bianco, F., Conti, P., García-Ayllon, S., and Pranzini, E. (2020). An integrated approach to analyze sedimentary stock and coastal erosion in vulnerable areas: resilience assessment of san vicenzo's coast (Italy). *Water* 12 (3), 805. doi:10.3390/w12030805

Bianco, F., and García-Ayllón, S. (2021). Coastal resilience potential as an indicator of social and morphological vulnerability to beach management. *Estuar. Coast. Shelf Sci.* 253, 107290. doi:10.1016/j.ecss.2021.107290

Bronts, S., Gerbens-Leenes, P. W., and Guzmán-Luna, P. (2023). The water, land and carbon footprint of conventional and organic dairy systems in The Netherlands and Spain. A case study into the consequences of ecological indicator selection and methodological choices. *Energy Nexus* 11, 100217. doi:10.1016/j.nexus.2023.100217

Cao, Y., Hua, L., Peng, D., Liu, Y., Jiang, L., Tang, Q., et al. (2024). Decoupling the effects of air temperature change on soil erosion in Northeast China. *J. Environ. Manag.* 351, 119626. doi:10.1016/j.jenvman.2023.119626

Du, H., Fan, Y., Luo, L., Liao, J., Li, Z., Liu, X., et al. (2023). Identification of natural and anthropogenic sources and the effects of climatic fluctuations and land use changes on dust emissions variations in the Qinghai-Tibetan Plateau. *Agric. For. Meteorology* 340, 109628. doi:10.1016/j.agrformet.2023.109628

García-Santos, G., Scheiber, M., and Pilz, J. (2020). Spatial interpolation methods to predict airborne pesticide drift deposits on soils using knapsack sprayers. *Chemosphere* 258, 127231. doi:10.1016/j.chemosphere.2020.127231

Garcia-Ayllon, S., and Radke, J. (2021). Diffuse anthropization impacts in vulnerable protected areas: comparative analysis of the spatial correlation between land transformation and ecological deterioration of three wetlands in Spain. *ISPRS Int. J. Geo-Information* 10 (9), 630. doi:10.3390/ijgi10090630

Huang, X., Xie, Y., Lei, F., Cao, L., and Zeng, H. (2024). Analysis on spatio-temporal evolution and influencing factors of ecosystem service in the Changsha-Zhuzhou-Xiangtan urban agglomeration, China. *Front. Environ. Sci.* 11, 1334458. doi:10.3389/fenvs.2023.1334458

Ibarra, J. T., Caviedes, J., Marchant, C., Mathez-Stiefel, S.-L., Navarro-Manquilef, S., and Sarmiento, F. O. (2023). Mountain social-ecological resilience requires transdisciplinarity with Indigenous and local worldviews. *Trends Ecol. Evol.* 38 (11), 1005–1009. doi:10.1016/j.tree.2023.07.004

Lang, W., Radke, J., Chen, T., and Chan, E. (2016). Will affordability policy transcend climate change? A new lens to re-examine equitable access to healthcare in the San Francisco Bay Area. *Cities* 58, 124–136. doi:10.1016/j.cities.2016.05.014

Li, D., Yang, Y., Xia, F., Sun, W., Li, X., and Xie, Y. (2022). Exploring the influences of different processes of habitat fragmentation on ecosystem services. *Landsc. Urban Plan.* 227, 104544. doi:10.1016/j.landurbplan.2022.104544

Magalhães, J. L. L., Lopes, M. A., and Queiroz, H. L. D. (2015). Development of a Flooded Forest Anthropization Index (FFAI) applied to Amazonian areas under pressure from different human activities. *Ecol. Indic.* 48, 440–447. doi:10.1016/j.ecolind.2014.09.002

Mansoor, S., Farooq, I., Kachroo, M. M., Mahmoud, A. E. D., Fawzy, M., Popescu, S. M., et al. (2022). Elevation in wildfire frequencies with respect to the climate change. *J. Environ. Manag.* 301, 113769. doi:10.1016/j.jenvman.2021.113769

Mohamed, A.-S., Leduc, C., Marlin, C., Wagué, O., and Sidi Cheikh, M.-A. (2017). Impacts of climate change and anthropization on groundwater resources in the Nouakchott urban area (coastal Mauritania). *Comptes Rendus Geosci.* 349 (6), 280–289. doi:10.1016/j.crte.2017.09.011

Peng, D., Chen, Y., and Wang, W. (2023). Spatio-temporal analysis of the impact of land urbanization on the gross primary productivity of vegetation in the Middle Reaches of the Yangtze River Urban Agglomeration: new evidence from the township scale. *Front. Ecol. Evol.* 11, 1260641. doi:10.3389/fevo.2023.1260641

Romera, R., Gaertner, M. Á., Sánchez, E., Domínguez, M., González-Alemán, J. J., and Miglietta, M. M. (2017). Climate change projections of medicanes with a large multi-model ensemble of regional climate models. *Glob. Planet. Change* 151, 134–143. doi:10.1016/j.gloplacha.2016.10.008

Tan, F., Lu, Z., and Zeng, F. (2024). Study on the trade-off/synergy spatiotemporal benefits of ecosystem services and its influencing factors in hilly areas of southern China. *Front. Ecol. Evol.* 11, 1342766. doi:10.3389/fevo.2023.1342766

Virah-Sawmy, M., Gillson, L., Gardner, C. J., Anderson, A., Clark, G., and Haberle, S. (2016). A landscape vulnerability framework for identifying integrated conservation and adaptation pathways to climate change: the case of Madagascar's spiny forest. *Landsc. Ecol.* 31 (3), 637–654. doi:10.1007/s10980-015-0269-2

Yang, H., Tao, W., Ma, Q., Xu, H., Chen, L., Dong, H., et al. (2023b). Compound hot extremes exacerbate forest growth decline in dry areas but not in humid areas in the Northern Hemisphere. *Agric. For. Meteorology* 341, 109663. doi:10.1016/j.agrformet.2023.109663

Yin, X., Lslu, Z., and Zhang, B. (2024). Study on the factors influencing ecological environment and zoning control: a study case of the Dongting Lake area. *Front. Ecol. Evol.* 11, 1308310. doi:10.3389/fevo.2023.1308310

frontiers | Frontiers in Ecology and Evolution

TYPE Original Research
PUBLISHED 17 May 2023
DOI 10.3389/fevo.2023.1195833

OPEN ACCESS

EDITED BY
Xiao Ouyang,
Hunan University of Finance and Economics, China

REVIEWED BY
Ying She,
Nanchang Hangkong University, China
Sergio Noce,
Foundation Euro-Mediterranean Center on Climate Change (CMCC), Italy
Cui Shixi,
Liaoning Normal University, China

*CORRESPONDENCE
Yaobin Liu
✉ liuyaobin@ncu.edu.cn

RECEIVED 29 March 2023
ACCEPTED 26 April 2023
PUBLISHED 17 May 2023

CITATION
Li S, Liu Y, Wei G, Sevegnani F and Deng W (2023) Construction of carbon budget balance index and its application in the lake area.
Front. Ecol. Evol. 11:1195833.
doi: 10.3389/fevo.2023.1195833

Construction of carbon budget balance index and its application in the lake area

Shuoshuo Li[1], Yaobin Liu[1]*, Guoen Wei[2], Fábio Sevegnani[3] and Weifeng Deng[1]

[1]School of Economics and Management, Nanchang University, Nanchang, China, [2]School of Resources and Environment, Nanchang University, Nanchang, China, [3]Graduation Program in Production Engineering, Paulista University, São Paulo, Brazil

The imbalance of the carbon cycle in terrestrial ecosystems exacerbates global warming. Identifying the spatial–temporal characteristics and drivers of the carbon budget is important for the effective management of complex ecosystems and the achievement of the United Nations Sustainable Development Goals. Based on the complex ecosystem theory, this article constructs two carbon indicators, carbon carrying capacity–carbon footprint matching degree (Carbon-MD), and carbon carrying capacity–carbon footprint coupling coordination degree (Carbon-CCD). Taking a typical lake region—urban agglomeration around Poyang Lake as an example, the spatial–temporal characteristics and driving factors of the carbon budget from 2000 to 2020 are revealed by GIS technology and geographically–temporally weighted regression model. The results show that there is a significant spatial and temporal variability of carbon budget in Poyang Lake city agglomerations from 2000 to 2020, the Carbon-MD shows a gradually decreasing trend, and the Carbon-CCD shows a gradually increasing characteristic from moderate disorder to basic coordination development. From the spatial pattern, the Carbon-MD of the study area showed an increasing character from the core area to the peripheral area of the lake, and the low-value area of Carbon-MD shows the trend of spreading from point to surface and the Carbon-CCD changes from scattered to group type. In addition, land use type always has a significant effect on the carbon budget, while there is a spatial and temporal heterogeneity in the effects of natural and socioeconomic factors on the carbon budget. The research results show that it is reasonable and scientific to construct carbon budget indicators from the perspective of matching supply and demand and coupling and coordination, which provides a quantitative carbon budget analysis tool for local policymakers.

KEYWORDS

carbon budget, matching degree, coupling coordination degree, spatial–temporal characteristics, driving factors

1. Introduction

Climate warming is a major environmental threat to global sustainable development (Zhenmin and Espinosa, 2019; Wei et al., 2021; Mikulčić et al., 2022), and it has become the consensus of the international community to address global climate change and human activities by promoting a global balance of carbon in terrestrial ecosystems (Fernández-Martínez et al., 2020; Li et al., 2021). Since the release of the IPCC Special Report on Global

Warming of 1.5°C, many countries and regions have specified their timelines and measures to achieve carbon reduction (Climate Change 2021: The Physical Science Basis). Since the twentieth century, accelerated global urbanization has not only increased carbon emissions (Liddle, 2014; Yao et al., 2018; Wang W. Z. et al., 2021; Zhou et al., 2022a; Wei et al., 2023) but also weakened carbon sequestration through changes in land use types (Nathaniel and Adeleye, 2021; Zhou L. et al., 2021), ultimately affecting the state of the carbon budget. Carbon cycle imbalance triggers the greenhouse effect, and rebalancing is an effective means to combat global climate change (Li et al., 2019; Mekonnen et al., 2021). Therefore, it is necessary to study the carbon budget of cities from the perspective of the carbon cycle to seek achievements at the UN sustainable development goals (SDGs) and explore the construction of low-carbon cities.

Carbon emissions from human activities and land use change significantly affect the carbon balance of terrestrial ecosystems (Gatti et al., 2014; Wang H. et al., 2021; Wei et al., 2022). Currently, geographers and biologists have conducted many studies on carbon balance accounting, regional carbon cycle, carbon balance, and carbon offset (De Wit et al., 2015; Guo et al., 2017). The research focuses on the estimation of carbon balance, wetland carbon balance, forest carbon balance, carbon balance of urban functional zones, and factors influencing carbon balance (Nepal et al., 2013; Pingoud et al., 2016; Pukkala, 2017; Dolman and Janssen, 2018; Kondo et al., 2018; Maillard et al., 2018; Chuai et al., 2019; Nag et al., 2019; Yang et al., 2021; Mathias and Trugman, 2022). The research fields mainly focus on biology, ecology, and geography (Berhongaray et al., 2017; Tcherkez et al., 2017; Feng et al., 2019), and focus on the carbon budget of various industries (Dolman and Janssen, 2018), with the scale involving countries, provinces, and cities (Williams et al., 2017; Chen et al., 2019; Zhang et al., 2023).

Under the challenge of increasingly dramatic global warming, revealing the spatial–temporal characteristics and drivers of the carbon budget is crucial for regional carbon management (Li et al., 2021; Wang C. et al., 2021). At present, scholars mostly construct the carbon budget index from the perspective of carbon emission and carbon absorption by subtracting or dividing and then exploring the carbon balance zoning of cities or provinces (Lin et al., 2016; Gao et al., 2022). Some scholars propose that the carbon balance pressure index, by calculating the ratio of energy carbon emissions to vegetation carbon sequestration, can reflect carbon neutrality more objectively and comprehensively and guide the green development of cities (Chen et al., 2021). The improvement of carbon balance has an important influence on the development of rapidly urbanized areas (Chen et al., 2019). It is an important support to promote the high-quality development of the regional economy and the construction of ecological civilization (Chuai et al., 2019). Although the traditional carbon budget index can reflect the regional carbon deficit or carbon surplus, it is difficult to truly reflect the pressure caused by carbon emissions on the ecosystem. This problem can be better solved if the carbon footprint and carbon carrying capacity are studied together. This study aimed to comprehensively analyze the spatial–temporal characteristics of the regional carbon budget through two perspectives of supply and demand matching and coupling and coordination, and further analyze its driving factors and incorporate them into the city carbon management system. This study also contributes to the goals of SDGs12 and SDGs13.

Poyang Lake is the largest freshwater lake in China (Yuan et al., 2019), and the wetland of Poyang Lake is one of the six largest wetlands in the world (Feng et al., 2012). The spatial–temporal distribution of water-ecological resources in the lake area affects the carbon cycle and ecological environment of the terrestrial ecosystem, and then the development of urban agglomeration in the lake area. As a typical urban agglomeration of the lake region, the urban agglomeration around Poyang Lake has a relatively complete ecosystem and is in the key period of rapid urbanization. The "water-dependent" urban agglomeration around Poyang Lake is a powerful carbon source and carbon sink (Dai et al., 2021), and is becoming a key area for regional carbon budget research. At the same time, the city agglomeration around Poyang Lake is also a typical fast-urbanizing area and an important ecological function protection zone (Ye et al., 2013). The rapid expansion of urban agglomerations causes changes in land use landscape patterns. It, in turn, acts on the material cycle and energy flow of urban agglomerations, thereby affecting the process and equilibrium state of the carbon cycle (Ye et al., 2013; Li et al., 2019). To combat global warming, the Chinese government has proposed the goal of "carbon peaking and carbon neutrality." Therefore, taking the specificity and typicality of the urban agglomeration around Poyang Lake into consideration is important to construct a carbon budget index and analyze its spatial–temporal variation characteristics to achieve carbon balance in the lake area.

This study first proposes a comprehensive framework for carbon cycling in urban social–economic–natural complex ecosystems based on the complex ecosystem theory. Second, from the perspective of matching supply and demand, coupling and coordination, two carbon budget balance indicators, carbon carrying capacity–carbon footprint matching degree (Carbon-MD), and carbon carrying capacity–carbon footprint coupling coordination degree (Carbon-CCD), are constructed. Finally, this article takes the urban agglomeration around Poyang Lake as an example to conduct an application study. The third part gives a detailed introduction to the basic situation, data sources, and carbon index calculation model. The fourth part analyzes the spatial–temporal characteristics of carbon indicators of the study area Lake from 2000 to 2020 and further analyzes the driving factors of carbon indicators from land use, natural factors, economic and social factors by using land use transfer matrix, and geographically–temporally weighted regression model. The fifth section focuses on the rationality of the carbon indicator construction process and the scientific validity of the results. The sixth section concludes this study. This study provides a quantitative carbon balance analysis tool for local policymakers and a theoretical and decision basis for policymakers to achieve sustainable carbon management.

2. Carbon cycle framework for urban complex ecosystems

Based on the complex ecosystem theory, the urban social–economic–natural complex ecosystem can be divided into energy subsystem, industry subsystem, and ecological subsystem from the perspective of the carbon cycle (Wang et al., 2011a,b; Yao et al., 2015). The carbon source of the urban complex ecosystem comes from the energy subsystem, industrial subsystem, and ecological subsystem, while its carbon sink is mainly the carbon uptake by vegetation, soil, and water in the ecological subsystem (Houghton et al., 2012; Lai

et al., 2016; Zhou Y. et al., 2021). Carbon flows between the three subsystems in the form of organic carbon or inorganic carbon, and under the action of various physical, chemical, and biological processes in the three subsystems, carbon transformation, and carbon storage occur, and finally enter the natural environment in various forms or formats (Schimel et al., 2015; Battin et al., 2023). Fossil energy sources enter the social–economic–natural complex ecosystem through the energy subsystem, and after electricity and heat production, part of them enter the industrial subsystem as carbon-containing products and energy products together with industrial raw materials, part of them enter the ecological subsystem in the form of solid waste, and finally part of them enter the atmosphere in gaseous form to participate in the carbon cycle of the terrestrial ecosystem (Bassham, 1971; Dusenge et al., 2019). From a long-life cycle perspective, the carbon input, carbon consumption, carbon storage, carbon accumulation, and carbon output of the social–economic–natural complex ecosystem constitute a complete carbon cycle system in the energy subsystem, industrial subsystem, and ecological subsystem. The flow of carbon between the energy subsystem, industrial subsystem, and ecological subsystem constitutes the inner cycle of the carbon cycle of the urban's complex ecosystem. The carbon-containing products and energy products at the carbon export side of the urban complex ecosystem enter the circulation of the consumer market, the carbon-containing waste enters the ecosystem to participate in the natural ecological process again, and the carbon-containing gases enter the atmosphere to participate in the carbon cycle of the terrestrial ecosystem, which constitutes the outer cycle of the carbon cycle of the urban complex ecosystem (Figure 1). Clarifying and characterizing the process of carbon city social–economic–natural complex ecosystems is the basis for carbon budget accounting and spatial–temporal characterization.

3. Materials and methods

3.1. Study area

Poyang Lake is the largest throughput lake in the Yangtze River basin, which plays a great role in regulating the water level of the Yangtze River, connoting water, improving the local climate, and maintaining the ecological balance of surrounding areas (Yuan et al., 2019; Dai et al., 2021). Urban agglomeration around Poyang Lake is a typical basin lake-type urban agglomeration, including five cities and some counties (districts), with a land area of approximately 5.319 million km^2. Its climate is dominated by a subtropical monsoon climate, and the terrain is dominated by lakes and wetlands, and hilly plains. As shown in Figure 2, the spatial–temporal distribution of water resources in the study area is uneven, the towns and rural settlements are mostly distributed near the water area, and human activities have "hydrophilic" characteristics. Its carbon emissions are mainly concentrated in near-water areas where human activities are more frequent, while ecological resources with strong carbon sink capacity, such as forest resources and grassland resources, are mostly concentrated in far-water areas.

Since the twentieth century, the Poyang Lake area has experienced three stages of "deep development (2001–2006)-ecological economic

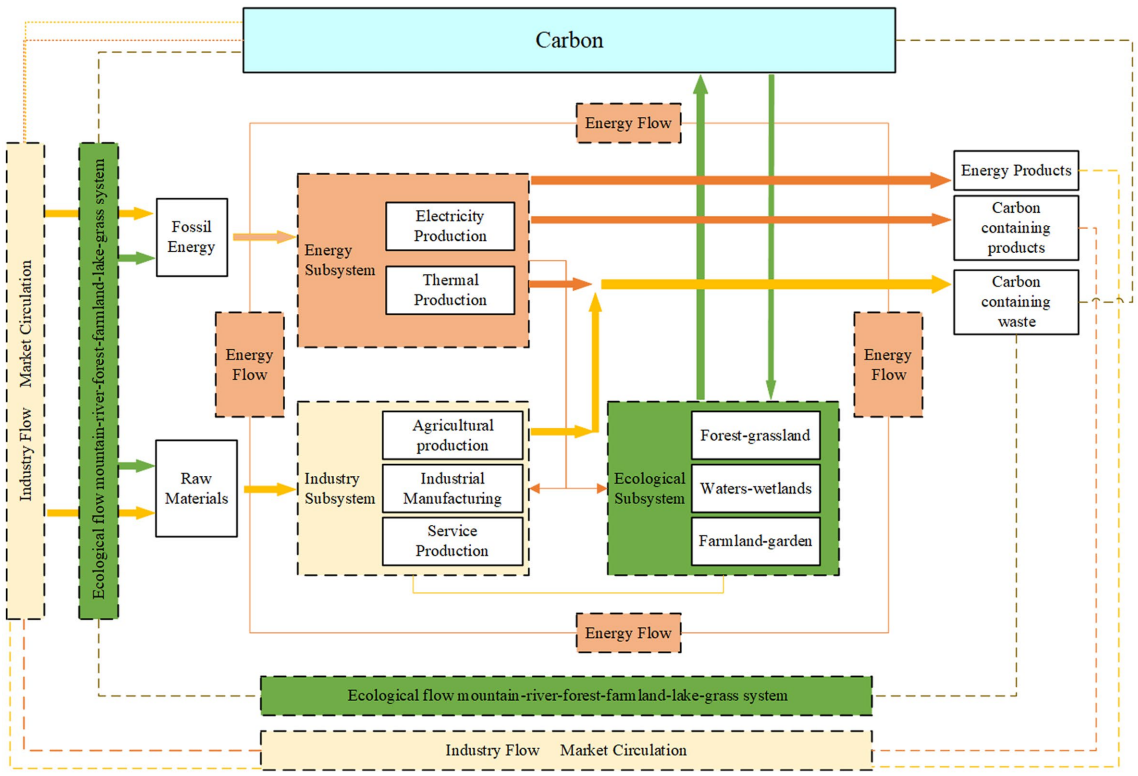

FIGURE 1
Carbon cycle framework for urban social–economic–natural complex ecosystems.

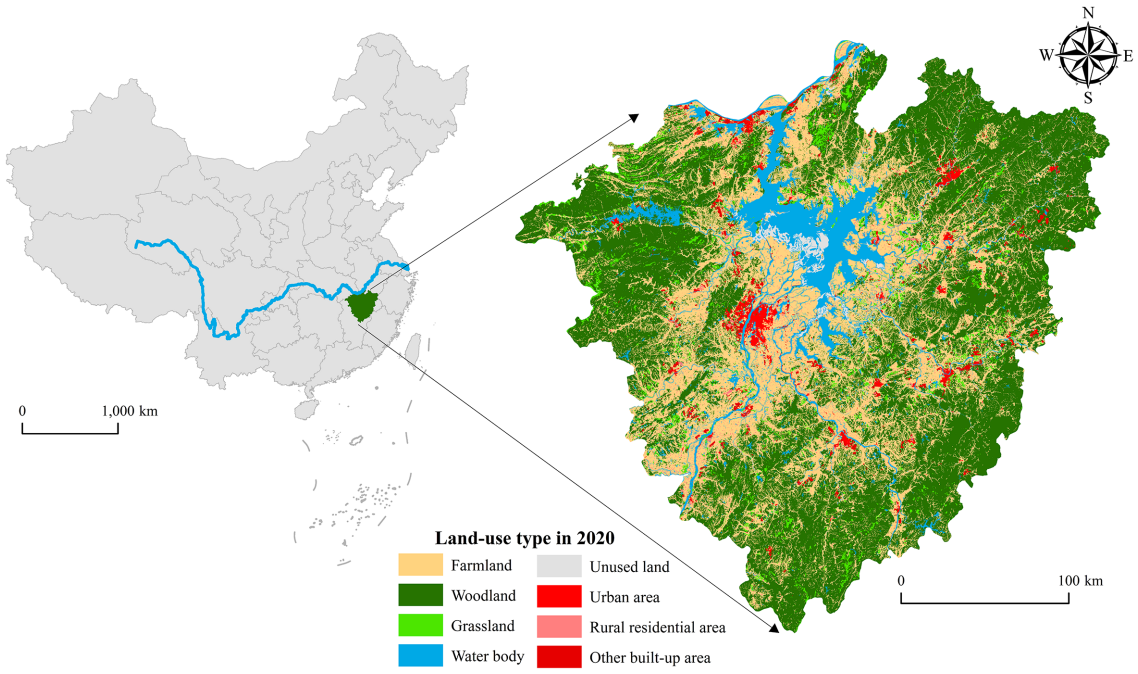

FIGURE 2
Location and land use type of the urban agglomeration around Poyang Lake in China.

zone construction (2007–2014)-ecological urban agglomeration construction (2015-present)." The carbon footprint of the study area has changed greatly since 2000–2020. The study results of this article are important for the carbon balance and ecological protection in the lake area (Figure 2).

3.2. Methods

3.2.1. Carbon emission and carbon sink

The carbon emissions of urban social–economic–natural complex ecosystems originate from the energy subsystem, industrial subsystem, and ecology subsystem (Houghton et al., 2012; Lai et al., 2016; Li et al., 2021). The accounting equation is as follows:

$$C_{ce} = C_{energy} + C_{industry} + C_{ecology} \quad (1)$$

where C_{ce} is the overall carbon emission of the city, C_{energy} is the energy subsystem, $C_{industry}$ is the industry subsystem, and $C_{ecology}$ is the ecology subsystem.

The carbon sinks of urban social–economic–natural complex ecosystems mainly originate from ecological subsystems, specifically water carbon sinks, soil carbon sinks, and vegetation carbon sinks (Guo et al., 2017; Chuai et al., 2019; Li et al., 2021; Gao et al., 2022). On the one hand, scholars have estimated terrestrial vegetation carbon sinks relatively accurately, but the research on soil carbon sinks is relatively weak, and there are large differences in the valuation of soil carbon sinks due to the limitations of knowledge, data, and technology. On the other hand, in different land types, carbon absorbed by agricultural ecosystems is decomposed into the atmosphere during the harvest season, and whether there is a net sink, and the size of the sink is somewhat controversial. Therefore, only the carbon sink functions of forests, water bodies, and grasslands are considered. Considering the forest resource types in the study area and the existing research results (Zhang et al., 2022), the carbon absorption factor of forest land was calculated as 0.644 t C/(hm²·a). Considering regional similarities and in light of existing research results (Wang C. et al., 2021), combining grassland types and climatic zones in the study area, the carbon absorption factor for grasslands was calculated at 0.021 t C/(hm²·a). Poyang Lake is the largest freshwater lake in China, and its wetland ecosystem is one of the most important carbon reservoirs on earth. Considering the difference in carbon sequestration rates between the geographical location of the Lake region and wetland ecosystems in the north and south, the carbon sequestration factor in the water was 0.253 t C/(hm²·a) (Wang C. et al., 2021). The formula is as follows:

$$C_{cs} = \sum_{k=1}^{n} A_K \times \delta_K, \quad (2)$$

where C_{cs} is the total carbon sequestration of water bodies, forests, and grasslands; A_k is the area of the kth land type; δ_k is the carbon emission factor of the kth land type.

3.2.2. Carbon footprint and carbon carrying capacity

Studies on regional carbon footprints mainly focus on carbon emissions generated by human activities, which cannot portray the balanced relationship between carbon emissions and carbon sinks, while combining carbon footprint and carbon carrying capacity can better solve this problem. Carbon footprint can be regarded as the ecological footprint of carbon emissions, which is the area of ecologically productive land that needs to be occupied to absorb

carbon emissions. Carbon carrying capacity can be regarded as the carbon supply capacity of the ecosystem, which is the upper limit of carbon sink capital that can be provided by the ecologically productive land in the region. Net ecosystem production (NEP) reflects the net carbon absorption capacity of terrestrial ecosystems and represents the carbon sequestration capacity of 1 hm^2 (squared hectometers) of vegetation or water body in a year, and the conversion between carbon emissions and carbon footprint can be realized by using NEP. Considering the uniqueness of the lake region, the carbon sink capacity of the water body is included in the carbon footprint and carbon carrying capacity. The calculation formula is as follows:

$$CF = C_{ce} \times \left(\frac{p_f}{NEP_f} + \frac{p_g}{NEP_g} + \frac{p_w}{NEP_w} \right) \quad (3)$$

$$CCC = C_{cs} \times \left(\frac{p_f}{NEP_f} + \frac{p_g}{NEP_g} + \frac{p_w}{NEP_w} \right) \quad (4)$$

where *CF* and CCC are the carbon footprint and carbon carrying capacity, respectively; p_f, p_g, and p_w ratios are the carbon sequestration ratios of forests, grasslands, and water bodies.

3.2.3. Carbon budget balance evaluation index

Based on the Chen et al. (2021), Chuai et al. (2019), and Guo et al. (2017) study, the carbon budget balance evaluation indexes include Carbon-MD and Carbon-CCD. There is a certain threshold value for carbon carrying capacity to bear the carbon footprint, which depends on the local and natural state of the ecosystem and takes subject to the scale and way of carbon footprint. When the regional carbon footprint is within a certain range, the carbon carrying capacity can carry the carbon footprint to the maximum extent through self-regulation and elasticity; but when the carbon footprint exceeds a certain limit, that is, the carbon carrying capacity cannot carry the carbon footprint needs, then carbon spillover will occur.

3.2.3.1 Carbon-MD

Carbon-MD is an important indicator of whether the carbon carrying capacity in the region can carry the demand of carbon footprint, which plays an important role in restraining the intensity of carbon footprint and excessive growth of demand. The Carbon-MD further reflects the surplus status of regional carbon revenue and expenditure and can characterize whether the carbon sink of the ecological production system can offset the carbon source. Its formula is as follows:

$$Carbon - MD = \frac{CCC}{CF}, \begin{cases} < 1 & unable\ to\ carry\ the\ load \\ = 1 & balance \\ > 1 & able\ to\ carry\ the\ load, \end{cases} \quad (5)$$

where Carbon-MD <1 means that the carbon carrying capacity cannot carry carbon footprint [including mildly unbearable grade (0.85, 1.00), barely impossible to carry grade (0.50, 0.85), seriously unbearable grade (0.00, 0.50)], carbon carrying capacity and carbon footprint are in the unbearable state; Carbon-MD =1 means that carbon carrying capacity and carbon footprint are in equilibrium; when Carbon-MD >1, it means that the carbon carrying capacity can carry carbon footprint [including general carrying capacity (1.00, 1.10), good carrying capacity (1.10, 2.00), and high-quality carrying capacity (2.00, +∞)], and the carbon carrying capacity and carbon footprint are in a bearable state.

3.2.3.2 Carbon-CCD

Carbon-CCD characterizes the level of synergistic development between carbon carrying capacity and carbon footprint, reflecting whether the carbon emissions from human activities develop in line with the carbon sinks that ecosystems can provide, which can reveal the potential of regional carbon budget balance. The formula is as follows:

$$C = \frac{2\sqrt{CF \times CCC}}{CF + CCC} \quad (6)$$

$$T = \alpha CF + \beta CCC \quad (7)$$

$$Carbon - CCD(x,y) = \sqrt{C \times T} \quad (8)$$

where C is the coordination index of carbon carrying capacity and carbon footprint; T is the composite development index of carbon carrying capacity and carbon footprint, which reflects the comprehensive level of carbon carrying capacity and carbon footprint, according to the importance degree of carbon sink and carbon emission system, α and β are assigned, α+β=1; Carbon-CCD indicates that under the condition that the composite development benefit (*CF*+*CCC*) of carbon carrying capacity and carbon footprint is certain, to maximize the composite benefits (*CF*×*CCC*), the two carry out the quantitative degree of combined coordination. According to the previous research results and the actual situation, the coupling coordination type of carbon carrying capacity and carbon footprint is subdivided according to the size of the coupling coordination degree Carbon-CCD (Table 1).

3.2.4. Geographically and temporally weighted regression model (GTWR)

GTWR considers the expansion of geographically weighted regressive models by considering the non-stationarity of time, incorporating both temporal and spatial effects (Xu et al., 2023). This enables the model to deal with spatiotemporal heterogeneity at the same time, so it has a clear advantage in exploring spatiotemporal variability of carbon budget influencing factors. The construction formula is as follows:

TABLE 1 Classification of carbon carrying capacity–carbon footprint coupling coordination degree (Carbon-CCD) types.

Carbon-CCD	Coordination level	Carbon-CCD	Coordination level
0<D ≤ 0.2	Severely uncoordinated	0.5<D ≤ 0.6	Moderately coordinated
0.2<D ≤ 0.3	Moderately uncoordinated	0.6<D ≤ 0.8	Good coordinated
0.3<D ≤ 0.4	Mildly uncoordinated	0.8<D ≤ 1	Quality coordinated
0.4<D ≤ 0.5	Mildly coordinated		

$$Y_i = \beta_0(\mu_i, \vartheta_i, t_i) + \sum_k \beta_k(\mu_i, \vartheta_i, t_i) \times X_{ik} + \varepsilon_i \quad (9)$$

where $\beta_0(u_i,v_i,t_i)$ is the regression constant, ε_i is the residual of the model, X_{ik} represents the value of the influencing factor, $\beta_k(u_i,v_i,t_i)$ represents the regression parameter of the variable, that is, the weight factor of the variable in the space–time position (u_i,v_i,t_i).

To measure the beta $\beta_k(u_i,v_i,t_i)$ of each variable k in all space–time location. $\beta_k(u_i,v_i,t_i)$ can be transformed as follows:

$$\hat{\beta}(\mu_i, \vartheta_i, t_i) = \left[X^T W(\mu_i, \vartheta_i, t_i) X\right]^{-1} W^T W(\mu_i, \vartheta_i, t_i) Y \quad (10)$$

where $W(u_i,v_i,t_i)$ is a space–time weighting matrix that takes into consideration space–time effects.

3.3. Data source

Based on 42 counties of the urban agglomeration around Poyang Lake, the data selected in this study include energy consumption data, land use data, and socioeconomic data. Energy consumption and socioeconomic data are obtained from Carbon Emission Accounts and Datasets for emerging economies (CEADs),[1] China Statistical Yearbook (County-level), Jiangxi Statistical Yearbook, and corresponding yearbooks of cities and counties. Land use data were derived from 30 m × 30 m grid data from the Resource and Environmental Science Data Center of the Chinese Academy of Sciences[2] for the years 2000, 2005, 2010, 2015, and 2020.

4. Results

4.1. Spatial–temporal characteristics of carbon footprint and carbon carrying capacity

It selected 50, 100, and 150% of the average carbon footprint and carbon carrying capacity of the urban agglomeration around Poyang Lake from 2000 to 2020 and divided the carbon footprint and carbon carrying capacity into four levels: low, lower, higher, and high. Then, the spatial distribution of carbon footprint and carbon carrying capacity in 2000, 2010, and 2020 was visualized through ArcGIS software (Figure 3).

During the study period, the carbon footprint of the study area shows a dynamic increasing trend from rapid increase to steady increase. Since 2000, the carbon footprint of the study area has increased rapidly from 6,255,395.63 hm^2 to 14,485,241.37 hm^2 in 2010, with an increase in 231.56%. After 2010, its growth rate slowed down but still increased to 27,874,164.9 hm^2 in 2020, with a growth rate of 192.43%. The comparison shows that the construction of the eco-urban agglomeration around Poyang Lake (2015–2030) is beneficial to slow down the growth rate of carbon footprint.

The spatial pattern of the carbon footprint at the county level in the study area shows a "core-periphery" structure with the Nanchang municipal district as the core of high value and gradually decreasing outward. The high-value carbon footprint area in 2000 only included Nanchang City District and Nanchang County, while the rest of the areas had a lower carbon footprint due to the fledgling urbanization, slow economic development, and dispersed population. Compared with 2000, the number of high-value areas and lower-value areas of carbon footprint increased significantly in 2010. In addition to the core area of Nanchang City, the high-value area gradually spreads outward, and Jiujiang City becomes the high-value area of carbon footprint with the advantage of transportation location. By 2020, the number of high-value carbon footprint areas will increase to 14 and the number of low-value areas will shrink to 3. The carbon footprint of prefecture-level municipalities such as Fuzhou City, Jingdezhen City, and Yingtan City will increase significantly due to population concentration and economic development.

During the study period, the carbon carrying capacity of the study area shows a trend of "rising, then falling and finally declining." Since 2000, the carbon-bearing capacity of the study area slowly increased from 15,922,773.77 hm^2 to 15,994,651.77 hm^2 in 2010, with an increase of only 0.45%. Since 2000, the carbon-bearing capacity of the study area slowly increased from 15,922,773.77 hm^2 to 15,994,651.77 hm^2 in 2010, with an increase of only 0.45%. Subsequently, it decreases to 15,591,361.26 hm^2 in 2020, which is 2.52% less than in 2010. After 2010, the urbanization rate of the study area accelerated, and the urban expansion led to the shrinkage of carbon sinks in land areas such as woodland, waterbody, and grassland. The topography of the county with high carbon carrying capacity is mainly mountainous and hilly, with rich forest resources, which provides a large amount of carbon sink. The counties with a low value of carbon carrying capacity are mainly located in the core area around Poyang Lake, the topography of these areas is mainly plain, and the carbon sink capacity is weak.

4.2. Spatial–temporal characteristics analysis of Carbon-MD

The Carbon-MD can quantitatively reflect the carbon budget of the study area. We used ArcGIS10.8 software to divide the county into seven categories of areas: severe unbearable area, barely unbearable area, mild unbearable area, carbon balance area, average bearable area, good bearable area, and high-quality bearable area in 2000, 2005, 2010, 2015, and 2020 (Figure 4).

From 2000 to 2020, the distribution of Carbon-MD in the study area ranges from 0.008 to 47.6597. From the time change, the Carbon-MD of the whole area decreases from 2.5454 in 2000 to 0.5593 in 2020, which decreases by 78.03% in 20 years, from high quality to barely unbearable. This indicates that the carbon budget of urban agglomeration around Poyang Lake gradually turns into a deficit over time, and its carbon carrying capacity does not meet the demand for an internal carbon footprint.

From the spatial pattern, the Carbon-MD in the study area shows the spatial distribution characteristics of increasing from the core area around the lake, where the built-up area is more concentrated, to the peripheral area around the lake with higher elevation. The low value of Carbon-MD is mainly concentrated in the Poyang Lake Plain, especially around municipal districts such as Nanchang and Jiujiang. The high carrying capacity areas are mainly distributed in Wuyi

1 https://www.ceads.net.cn/
2 https://www.resdc.cn/

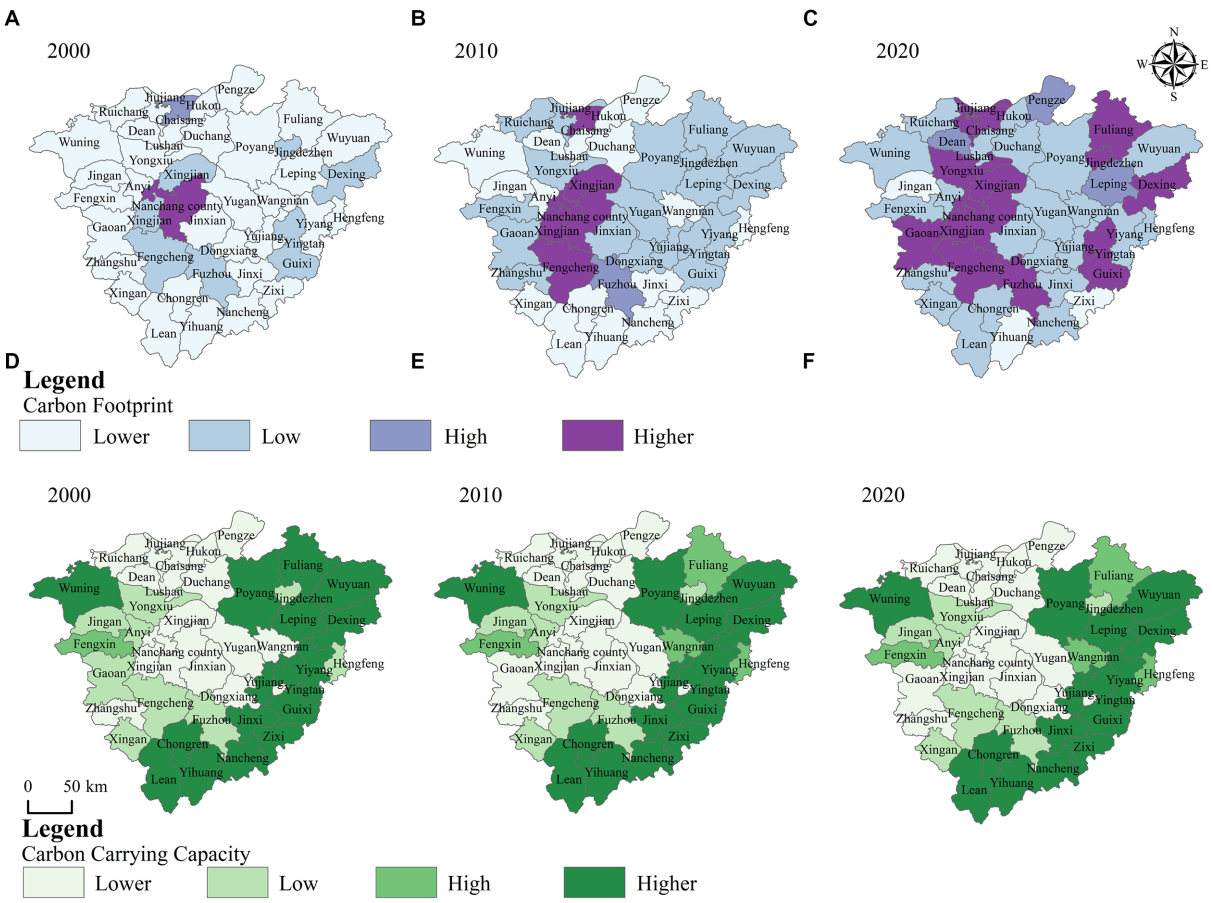

FIGURE 3
Spatial distribution of carbon footprint and carbon carrying capacity.

Mountain in the east of Jiangxi and Luoxiao Mountain area between Jiangxi and Hunan provinces. The spatial distribution characteristics of the Carbon-MD are similar to those of the carbon footprint and opposite to those of the carbon carrying capacity.

From the perspective of spatial evolution, the low-value area of Carbon-MD shows a "point to area" diffusion trend. From 2000 to 2020, the low-value area spreads from Nanchang City and the surrounding counties to the core area around the lake and then to the edge of the lake. In 2000, the Carbon-MD low-value area included only five counties in Nanchang City, Nanchang County, Xinjian County, Jiujiang City, and Chaisang District. By 2010, the low-value area increased to 12 counties, at which time the region-wide carbon revenue and expenditure match was 1.1042, still in a good match stage, indicating that the carbon carrying capacity could still meet the internal carbon footprint at this time. The Carbon-MD low-value area in the study area increases to 20 counties in 2020, concentrated in the core area of the lagoon and the counties in the peripheral area of the lagoon. In addition, due to the vast water area of Poyang County, which is located in the core area of the lagoon, most of its period is in a good bearable and high-quality bearable stage.

In general, the county carbon budget partition has obvious characteristics of the Great Lakes basin, and Poyang County, which is located in the center of the lake, has more water area with a long-term carbon surplus. The core area around the lake is dominated by plains, and the rapid expansion of urbanization in the core area of the "water-dependent" urban agglomeration has led to a carbon deficit. The edge area around Poyang Lake is mainly hilly and mountainous, with rich forest resources and strong carbon sink capacity, while the level of urbanization and industrialization is low due to the topography and terrain, with less carbon emission.

4.3. Spatial–temporal characteristics analysis of Carbon-CCD

There is a coupled interaction between carbon carrying capacity and carbon footprint that promotes and coerces each other. We measured the coupling degree values of county units in the study area in 2000, 2005, 2010, 2015, and 2020, respectively. Then, we spatially visualized the expression by ArcGIS10.8 software to obtain the spatial distribution map of the carbon bearing capacity–carbon footprint coupling degree in the study area (Figure 5).

From 2000 to 2020, the distribution of carbon carrying capacity–carbon footprint coupling degree of each county in the study area ranged from 0.2853 to 1. During the two decades, the overall carbon carrying capacity–carbon footprint coupling degree of the whole study area showed a trend of "rising and then falling." The overall coupling degree of the whole region increased from 0.8999 in 2000 to 0.9987 in 2010 and then decreased to 0.9592 in 2020. It indicates that the whole region of the study area is in a

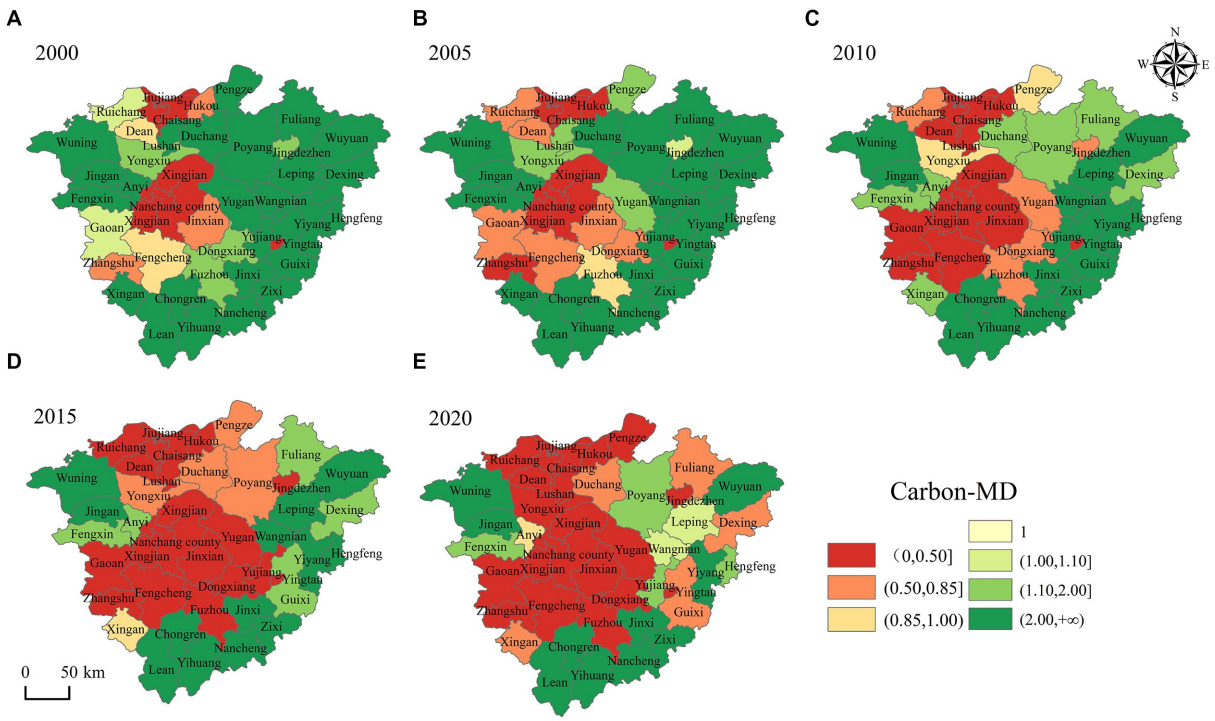

FIGURE 4
Spatial distribution of Carbon-MD.

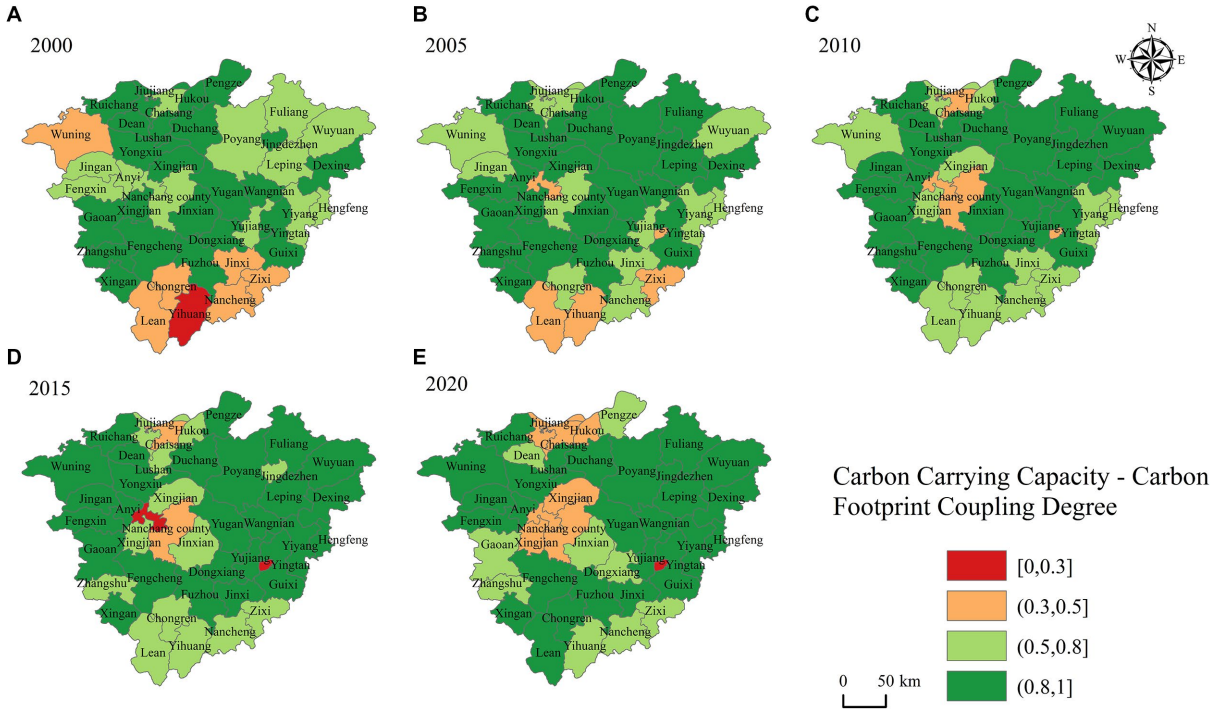

FIGURE 5
Spatial distribution of carbon carrying capacity–carbon footprint coupling degree.

long-term coordinated coupling period, and the carbon carrying capacity and carbon footprint gradually develop in an orderly direction.

From the spatial pattern, the high values of carbon bearing capacity–carbon footprint coupling are concentrated in most of the counties in the peripheral area of the lake ring and the peripheral area

of the lake ring. In 2000 and 2005, the low-value areas were clustered in the southern counties of the study area. After 2010, the low-value areas were concentrated in the municipal districts of Nanchang and Jiujiang and the surrounding areas of both.

From the spatial evolution, the high-value area of carbon carrying capacity–carbon footprint coupling shows an increasing trend year by year, from 21 county units in 2000 to 26 county units in 2020. The coupling degree evolution of some counties shows obvious fluctuation. For example, the Nanchang city municipal area has experienced the process of "friction–antagonism–low coupling–antagonism," and Le'an County, Zixi County has experienced the process from "antagonism" to "antagonism." Le'an County and Zixi County experienced a leap from "antagonism" to "friction" and even "coordinated coupling."

The Carbon-CCD can qualitatively reflect the carbon budget balance of the study area. The distribution range of Carbon-CCD in the study area from 2000 to 2020 is 0.1730 ~ 0.8661. Based on the calculation results, we used ArcGIS10.8 software to classify the county Carbon-CCD in 2000, 2005, 2010, 2015, and 2020 into eight types: severely uncoordinated, mildly uncoordinated, mildly coordinated, moderately uncoordinated, moderately coordinated, well-coordinated, and quality coordinated (Figure 6).

From the spatial pattern, there is a spatial heterogeneity in the distribution of Carbon-CCD of the county unit in the study area, and it shifts from scattered type to group type. The spatial distribution of Carbon-CCD of county units in the study area has a certain correlation, and the high-value area of Carbon-CCD roughly coincides with the high-value area of the coupling degree. The number of low-value areas of Carbon-CCD is much more than the number of low-value areas of coupling degree, but both show the spatial evolution characteristics of gradually spreading outward with Nanchang and Jiujiang municipal districts as the core.

In the time dimension, the Carbon-CCD in the study area showed a gradual increase from moderate disorder to basic coordination, and the average level of coupling coordination increased from 0.3927 to 0.4687. In 2000, the Carbon-CCD ranged from [0.1730, 0.6359], with the lowest value in Hukou County and the highest value in Guixi City. The types of coupling coordination are mainly severely uncoordinated, mildly uncoordinated, mildly coordinated, moderately uncoordinated, moderately coordinated, and good coordination, accounting for 2.38%, 23.81, 30.95, 19.05, 19.05, and 4.76%, respectively. Its overall level is low, and most of them are in mild dissonance. In 2010, the Carbon-CCD was between [0.1440, 0.7524], the lowest value was in Yingtan City, and the highest value was still in Guixi City. The coupling coordination types are the same as those in 2000, but the coordination types of mild and above account for 53.49%, and the overall level has improved, but the increase is not obvious. In 2020, the Carbon-CCD in the study area is between [0.1786, 0.8661], and the lowest and highest value areas are the same as in 2010. The coupling coordination type in Guixi City is improved to the coupling of high-quality coordination, and the coordination type of mild and above accounts for 60.47%. Compared with 2000 and 2010, the proportion of moderate coordination and good coordination increased significantly.

4.4. Natural and anthropogenic factors

Human activities and climate change act together on land cover, which, in turn, leads to significant changes in land use types and

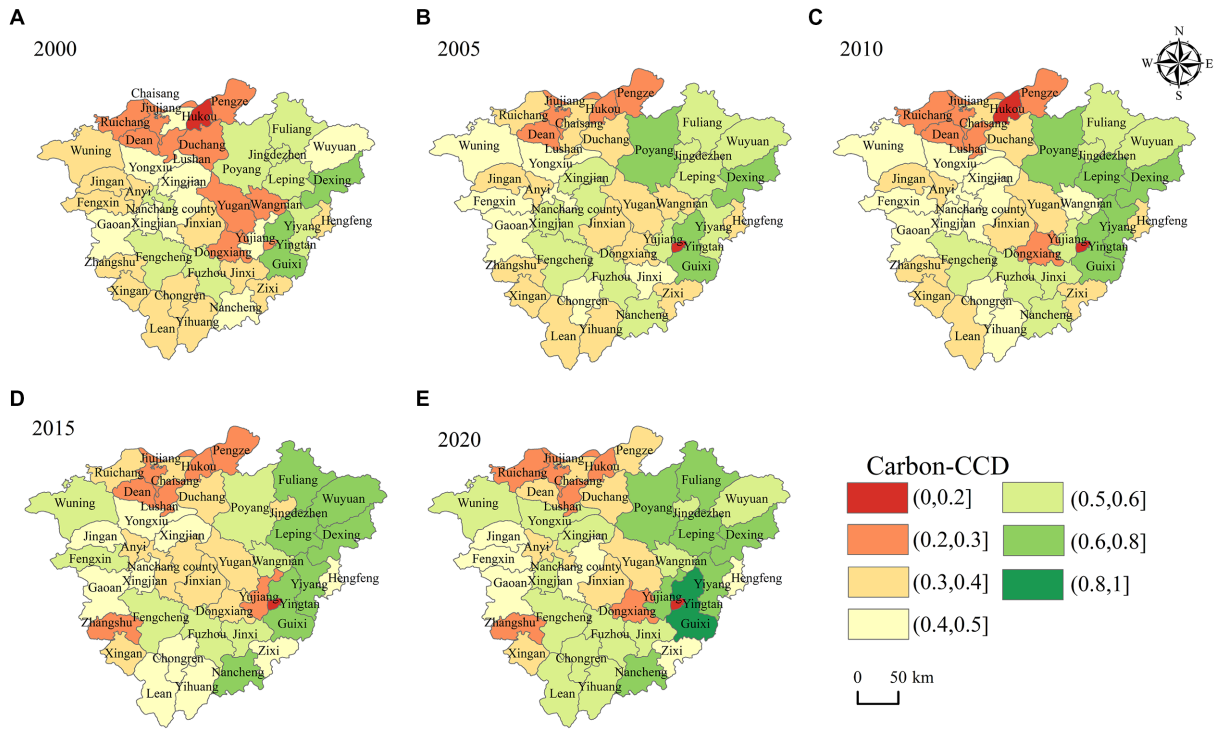

FIGURE 6
Spatial distribution of Carbon-CCD.

affects the carbon emissions and carbon sink of the urban agglomeration ecosystem around Poyang Lake. The mechanisms of land use change on carbon budget include the following two main aspects. There are differences in carbon emissions and carbon sinks between land use types, and land use changes may directly alter the amount of carbon emitted or sequestered. Land use change affects the processes of the carbon cycle in complex social–economic–natural ecosystems, such as energy exchange, carbon metabolism, and geochemical cycling of carbon.

This study made the land use transfer matrix of urban agglomeration around Poyang Lake from 2000 to 2020 through ArcGIS (Table 2). The land type in the study area from 2000 to 2020 has undergone significant changes, which overall show an increase in construction land and water body, and a decrease in farmland, grassland, woodland, and unused land. During the 20 years, the urban agglomeration around Poyang Lake, land use types, except for the same type of conversion, have shifted more unused land to construction land, more grassland to woodland, more construction land to unused land, unused land to a waterbody, and woodland to construction land. By phase, the increase in construction land from 2010 to 2020 is significantly higher than the increase from 2000 to 2010. From 2000 to 2010, the total area of other land types converted to construction land in the study was 35.06 km^2. From 2010 to 2020, it is 919.99 km^2. During this period, the low Carbon-MD of the study area spread rapidly, suggesting that the expansion of construction land is the main cause of its carbon deficit. The land use type shifts between different types from 2000 to 2010 mainly include farmland to a waterbody, grassland to woodland, construction land to farmland, unused land to a waterbody, waterbody to unused land, and woodland to grassland. In addition, the shift of land use types between different types from 2010 to 2020 mainly includes unused land to construction land, grassland to construction land, construction land to unused land, unused land to a waterbody, waterbody to construction land, and woodland to construction land. During this period, the shift between different land use types was dominated by the shift to built-up land.

In addition to land use types, natural factors, and socioeconomic factors are also important factors affecting the carbon budget. Combined with the characteristics of this type of lake city group around Poyang Lake, the lake-ring zoning (LRZ) and normalized difference vegetation index (NDVI) are selected as natural factors. The proportion of built-up area (PBU), regional population density (RPD), and industrial structure (IS) are socioeconomic factors. To avoid interactions between variables, all variables were tested for covariance, and the variance inflation factor values of all variables were found to be less than 10, indicating that there was no significant covariance between variables.

TABLE 2 Land transfer matrix of urban agglomeration around Poyang Lake from 2000 to 2020.

2000–2010	Farmland	Grassland	Construction land	Unused land	Waterbody	Woodland	Total
Farmland	23386.33	38.94	21.21	7.46	262.91	100.30	23817.15
Grassland	8.34	2351.86	0.01	2.24	1.87	17.58	2381.89
Construction land	413.33	18.17	1509.55	1.39	32.80	129.02	2104.25
Unused land	7.48	0.23	0.67	548.96	79.07	0.14	636.55
Waterbody	149.59	16.41	12.79	357.04	5176.17	11.97	5723.97
Woodland	34.32	238.91	0.38	0.03	16.32	34834.95	35124.91
Total	23999.39	2664.51	1544.61	917.12	5569.14	35093.95	69788.73
2010–2020	**Farmland**	**Grassland**	**Construction land**	**Unused land**	**Waterbody**	**Woodland**	**Total**
Farmland	23194.44	0.65	551.78	7.83	61.86	0.59	23817.15
Grassland	0.66	2329.87	45.75	0.09	5.47	0.06	2381.89
Construction land	44.30	0.93	2048.59	0.00	5.27	5.15	2104.25
Unused land	0.07	0.00	1.31	500.11	134.81	0.26	636.55
Waterbody	21.45	2.54	34.95	19.23	5643.28	2.51	5723.97
Woodland	17.29	78.82	286.19	2.03	21.44	34719.14	35124.91
Total	23278.20	2412.82	2968.58	529.29	5872.13	34727.72	69788.73
2000–2020	**Farmland**	**Grassland**	**Construction land**	**Unused land**	**Waterbody**	**Woodland**	**Total**
Farmland	22825.85	9.00	918.33	10.98	201.31	33.92	23999.39
Grassland	38.93	2304.05	66.53	0.22	20.15	234.63	2664.51
Construction land	29.76	0.13	1493.78	0.67	16.11	4.17	1544.61
Unused land	6.54	0.96	2.71	453.61	453.02	0.29	917.12
Waterbody	269.49	4.41	65.81	62.13	5155.36	11.93	5569.14
Woodland	107.63	94.25	421.44	1.68	26.17	34442.78	35093.95
Total	23278.20	2412.82	2968.58	529.29	5872.13	34727.72	69788.73

Red–orange–yellow–light green–dark green, representing the order of area size from one land use type to another (except for the same type of conversion), with red representing the largest area and dark green representing the smallest area.

The GTWR model is an extension of the GWR model considering the non-smoothness of time, which incorporates both temporal and spatial effects into the model, enabling the GTWR model to deal with spatiotemporal heteroskedasticity simultaneously. To test the reliability of the model, we compared the fitting results of the GTWR model with the GWR model, as shown in Table 3. The R2 adjusted value of the GTWR model is significantly higher than that of the GWR model, which indicates that the GTWR model has a better fit than the GWR model.

To compare the spatial–temporal variability of the effects of natural and socioeconomic factors on the Carbon-MD and Carbon-CCD, five periods of data from 2000, 2005, 2010, 2015, and 2020 were selected in this study to calculate the regression coefficients of each influencing factor after standardization. By comparing the magnitude of the absolute values of the regression coefficients of each factor, the dominant factors of each county unit were selected to spatially visualize and express the dominant factors of Carbon-MD and Carbon-CCD in 2000, 2010, and 2020.

As shown in Figure 7, the influence of socioeconomic factors on the Carbon-MD and Carbon-CCD of the study area is stronger in the study period. The area share of built-up area and population density as the highest value is most widely distributed in the county units. In terms of Carbon-MD, the counties with the highest built-up areas are mainly located in the south of the study area and show a trend of "increasing then decreasing" over time, gradually spreading to the northeast. The counties with the highest population density values are mainly located in the northern part of the study area except for Nanchang City and show a trend of "increasing then decreasing" over time and finally distributed in the western and northern parts of the study area. The county units with the highest values of natural factors are mainly distributed in and around the municipal district of Nanchang City, and they show an increasing trend over time. In general, the area dominated by socioeconomic factors gradually decreases, and the area dominated by natural factors increases correspondingly.

From the Carbon-CCD, the number of county units with the built-up area, population density, and NDVI as the dominant factors is relatively balanced. The county units with the percentage of the built-up area as the dominant factor are mainly distributed in the southwestern part of the study area, and gradually expand like the northeastern part, eventually dominated by the peripheral area around the lake. The county units with population density as the dominant factor are mainly located in the northwestern part of the study area and show a decreasing trend. The county units with NDVI as the dominant factor were mainly distributed in the eastern part of the study area and showed a gradually increasing trend. In general, the area of the strong role of socioeconomic factors on the Carbon-CCD is gradually decreasing, and the area of NDVI as the dominant factor is increasing.

5. Discussion

5.1. Rationality of the process and the scientific nature of the results

This study applies the carbon-bearing Carbon-MD and Carbon-CCD for the first time to analyze the spatial–temporal characteristics of the carbon budget in the study area, and it is necessary to explore the rationality of its process and the science of the results. Based on the complex ecosystem theory, this article portrays the complete process of the carbon cycle in the urban complex ecosystem from three perspectives: energy subsystem, industry subsystem, and ecological subsystem, which provides theoretical and framework support for carbon budget accounting in the study area. Existing studies only consider the carbon sink function of forest land and grassland when calculating carbon footprint and carbon carrying capacity (Lenzen et al., 2018). However, inland waterbody and phytoplankton, aquatic plants, heterotrophs, and microorganisms in inland waterbody have great carbon sequestration potential and can share the carbon-neutral pressure of terrestrial ecosystems. Considering the uniqueness of the lake area, this article incorporates the carbon sink of waterbody into the accounting system of carbon footprint and carbon carrying capacity of urban agglomeration around Poyang Lake. Based on the theory of human–land synergy, ecosystem service theory, and landscape ecology theory, the carbon carrying capacity–carbon footprint matching degree and coupling coordination degree indicators are constructed with solid theoretical support. The Carbon-MD and Carbon-CCD are the results of the interaction response between human activities and ecosystems. The harmonization process of the contradictory human–earth relationship is the core theme of geography research (Ouyang et al., 2022). Carbon balance is one of the best means to seek harmonious coexistence between humans and the environment in the context of global climate change (Zhou Y. et al., 2021). Carbon carrying capacity belongs to the regulating services of ecosystem services, and carbon footprint characterizes the degree of pressure of carbon emissions from human activities on natural systems. The carbon balance status of a region is an expression of its landscape pattern. Various methods such as the greenhouse gas inventory method, carbon sequestration inventory method, and

TABLE 3 Statistical results of GTWR and GWR parameters.

	GTWR		GWR					
			2000		2010		2020	
	Carbon-MD	Carbon-CCC	Carbon-MD	Carbon-CCC	Carbon-MD	Carbon-CCC	Carbon-MD	Carbon-CCC
Sigma	1.8408	0.0839	4.6309	0.1095	1.8888	0.1154	17.5376	0.1255
AICc	1074.5100	−346.1520	296.1430	−44.6154	203.3380	−40.2461	0.6462	−33.1832
R^2	0.9205	0.6336	0.8210	0.2057	0.6927	0.2941	116.5740	0.3444
R^2Adjusted	0.9181	0.6228	0.7903	0.0695	0.6400	0.1731	0.7401	0.2320

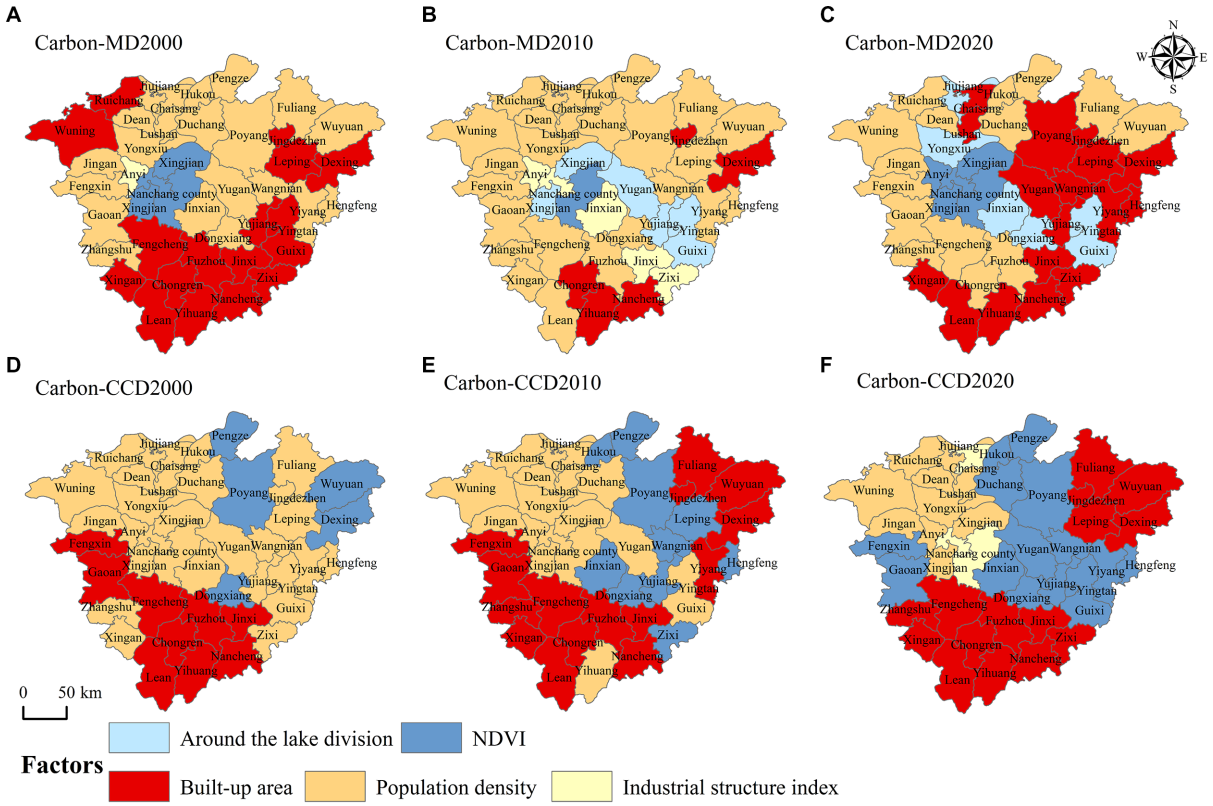

FIGURE 7
Spatial distribution of influencing factors of Carbon-MD and Carbon-CCD.

carbon balance indicator method are used to integrate multisource data such as energy consumption data, land use data, ecological and environmental type data, and socioeconomic data, and the data have objectivity in the process of indicator construction. These provide a guarantee for the scientific base of the results of this article.

Since both carbon indicators are new, this study was compared with other related studies. Guo et al. (2017) used the ratio of carbon sinks to carbon emissions to construct a carbon neutrality factor and found that the unbalanced spatial distribution of carbon emissions and carbon sinks is the main reason for the spatial variation of the carbon neutrality factor. Chen et al. (2021) constructed a carbon balance pressure index using the ratio of carbon emissions to vegetation carbon sequestration to measure the ecological pressure caused by carbon emissions in 77 countries from 2000 to 2015 and found that carbon emissions have become the direct cause of the rising pressure on the global carbon balance. Wang C. et al. (2021) analyzed the spatial pattern of carbon sources, carbon sinks, and carbon balance in the Beijing–Tianjin–Hebei region from the perspective of land use carbon emissions through the difference between carbon sources and carbon sinks. Li et al. (2021) studied the terrestrial carbon sink/source changes in China caused by land use change, and carbon balance partitioning should be conducted for its six regions. Based on previous studies developed by this group, it is scientific to use carbon footprint and carbon carrying capacity to construct carbon budget balance indicators, considering spatial heterogeneity and regional uniqueness, and its comparability on spatial–temporal scales can be applied.

The Carbon-MD F reflects the carrying status of ecosystems to carbon emissions from human activities, and its index value is influenced by the endowment of ecosystems and human activities. Therefore, the differences in ecological resources and human activities determine the spatial and temporal heterogeneity of the Carbon-MD. The Carbon-CCD reflects the coupled coordination relationship between carbon carrying capacity and carbon footprint. The Carbon-CCD reflects the sustainability of the ecosystem's carbon budget balance. Thus, the ecological resource endowment and the degree of carbon emissions from human activities determine the sustainability of the carbon balance. Therefore, the two carbon budget balance indicators of Carbon-MD and Carbon-CCD developed in this study have certain scientific and practicality.

5.2. Factors influencing the spatial–temporal characteristics of carbon indicators

The combination of internal and external factors has led to the heterogeneity of the spatial–temporal distribution of carbon budget balance in the study area. From the internal composition of the index, the carbon footprint has become the direct cause of the decrease of the Carbon-MD in the study area due to the relatively stable change of the carbon carrying capacity. The uneven spatial–temporal distribution of water-ecological resources in the lake area has led to the spatial mismatch of carbon footprint and carbon carrying capacity in the study area. The carbon footprint of the lake-ring edge area and the lake-ring periphery area gradually approaches its carbon carrying capacity, which is the main

reason for the increase of the Carbon-CCD value of these two regional county units. Human activities caused a large shift in land use types, which further affected the carbon budget balance by changing the landscape pattern (Zhou et al., 2020; Ouyang et al., 2021). The research results show that the increase in construction land leads to the main reason for the decrease of Carbon-MD in the study area. Therefore, to achieve the carbon balance goal, urban agglomeration around Poyang Lake should focus on carbon reduction activities first, and adopt sink enhancement means second. In addition to land use types, we quantified the effects of five factors on carbon budget balance from two perspectives of natural factors and socioeconomic factors, focusing on comparing the absolute values of regression coefficients of natural and socioeconomic factors. It was found that the built-up area and population density were the main factors affecting the carbon budget balance of the study area. Compared with natural factors, socioeconomic factors are the main influencing factors of carbon budget balance. This also reflects from the side that the increasing human activities are the main cause of ecosystem disorders (Xing et al., 2021; Li et al., 2022; Zhou et al., 2022b).

5.3. Limitation and future research

This article analyzes the spatial–temporal characteristics of the carbon budget balance of the lake urban agglomeration through two carbon budget balance indicators, Carbon-MD and Carbon-CCD, and has achieved certain results. Since the urban carbon cycle process is extremely complex, it is a challenging task to comprehensively characterize the carbon sources, sinks, and flows in different cities. A framework of the urban carbon cycle was constructed under the guidance of the social–economic–natural complex ecosystem theory, and further measured the carbon sources and sinks of the urban agglomeration around Poyang Lake. However, the carbon source accounting process used in this study does not consider carbon emissions from human and plant, and animal respiration, and carbon emissions from microbial decomposition. Meanwhile, carbon sequestration by soils is a complex process, and our carbon sink accounting process does not include carbon sinks from soils. In terms of influencing factors, we explored the effects of land use type, NDVI, the proportion of built-up area, population density, and industrial structure on the carbon budget of the study area. Considering the special characteristics of the lake area, we analyzed the influence of the distance zoning of the city from the lake center on its carbon budget balance. However, the carbon budget of different regions is subject to different factors and there are interactions among these factors. How to reveal the interactions among multiple factors and their transmission mechanisms on carbon budget balance is one of the directions that need to be urgently researched in future.

6. Conclusion

This study proposes a carbon cycle framework for urban social–economic–natural complex ecosystems from three subsystem perspectives: industrial subsystem, energy subsystem, and ecological subsystem. The framework portrays the carbon cycle process of the city from both vertical and horizontal perspectives, which can provide a scientific reference for low-carbon urban management. Furthermore, this study constructs two carbon balance indicators, Carbon-MD and Carbon-CCD, based on the relationship between carbon carrying capacity and carbon footprint. Unlike previous studies, this study considers both the uniqueness of the lake area for carbon sink accounting and the relationship between people and land and adopts carbon carrying capacity and carbon footprint instead of carbon source and carbon sink. The spatial–temporal variability of the carbon budget balance in the urban agglomeration around Poyang Lake from 2000 to 2020 is significant. The distribution of Carbon-MD in the study area from 2000 to 2020 ranges from 0.008 to 47.6597 and shows a decreasing trend over time. The Carbon-MD in the study area shows the spatial distribution characteristics of increasing from the core area of the lake to the peripheral area of the lake with higher elevation. From 2000 to 2020, the distribution range of Carbon-CCD in the study area is 0.1730 ~ 0.8661, showing a gradual increase from moderate disorder to basic coordination. The distribution of Carbon-CCD is spatially heterogeneous in the study area, and it is shifting from scattered to grouped. Finally, this article analyzes the influencing factors of carbon budget balance in the study area in terms of land use, natural factors, and socioeconomic factors. The two carbon budget balance indicators constructed in this article not only have advantages in describing the spatial and temporal characteristics of regional carbon balance but also are effective tools for regional low-carbon management.

Data availability statement

The original contributions presented in the study are included in the article, further inquiries can be directed to the corresponding author.

Author contributions

SL and YL conceived the study. YL obtained funding for the study. WD and SL performed the statistical analysis. SL produced the figures and tables and wrote the first draft of the manuscript. GW modified and checked this manuscript. All authors contributed to the manuscript and approved the submitted version.

Funding

This study was sponsored by the National Natural Science Foundation of China (NSFC) (Response and simulation of industrial spatial pattern in the urban cluster around Poyang Lake based on the supply and demand of ecosystem services, No. 42271209) and Project of Jiangxi Provincial Humanities and Social Science, grant no. JJ21201.

Acknowledgments

The authors thank the editors and reviewers for their comments on this manuscript.

Conflict of interest

The authors declare that the research was conducted in the absence of any commercial or financial relationships that could be construed as a potential conflict of interest.

Publisher's note

References

Bassham, J. A. (1971). The control of photosynthetic carbon metabolism: photosynthesis of carbon compounds is regulated to allocate intermediates according to metabolic needs. *Science* 172, 526–534. doi: 10.1126/science.172.3983.526

Battin, T. J., Lauerwald, R., Bernhardt, E. S., Bertuzzo, E., Gener, L. G., Hall, R. O., et al. (2023). River ecosystem metabolism and carbon biogeochemistry in a changing world. *Nature* 613, 449–459. doi: 10.1038/s41586-022-05500-8

Berhongaray, G., Verlinden, M. S., Broeckx, L. S., Janssens, I. A., and Ceulemans, R. (2017). Soil carbon and belowground carbon balance of a short-rotation coppice: assessments from three different approaches. *GCB Bioenergy* 9, 299–313. doi: 10.1111/gcbb.12369

Chen, J., Li, Z., Song, M., and Dong, Y. (2021). Decomposing the global carbon balance pressure index: evidence from 77 countries. *Environ. Sci. Pollut. Res.* 28, 7016–7031. doi: 10.1007/s11356-020-11042-1

Chen, C., Wu, Q., and Xin, H. (2019). Carbon balance of marine energy based on carbon emission and low carbon economy: a case study of Shandong Province. *J. Coast. Res.* 98, 167–170. doi: 10.2112/SI98-041.1

Chuai, X., Yuan, Y., Zhang, X., Guo, X., Zhang, X., Xie, F., et al. (2019). Multiangle land use-linked carbon balance examination in Nanjing City, China. *Land Use Policy* 84, 305–315. doi: 10.1016/j.landusepol.2019.03.003

Dai, L., Liu, Y., and Luo, X. (2021). Integrating the MCR and DOI models to construct an ecological security network for the urban agglomeration around Poyang Lake, Chine. *Sci. Total Environ.* 754:141868. doi: 10.1016/j.scitotenv.2020.141868

De Wit, H. A., Austnes, K., Hylen, G., and Dalsgaard, L. (2015). A carbon balance of Norway: terrestrial and aquatic carbon fluxes. *Biogeochemistry* 123, 147–173. doi: 10.1007/s10533-014-0060-5

Dolman, A. J., and Janssen, T. A. J. (2018). The enigma of the Amazonian carbon balance. *Environ. Res. Lett.* 13:061002. doi: 10.1088/1748-9326/aac78e

Dusenge, M. E., Duarte, A. G., and Way, D. A. (2019). Plant carbon metabolism and climate change: elevated CO_2 and temperature impacts on photosynthesis, photorespiration and respiration. *New Phytol.* 221, 32–49. doi: 10.1111/nph.15283

Feng, L., Hu, C., Chen, X., Cai, X., Tian, L., and Gan, W. (2012). Assessment of inundation changes of Poyang Lake using MODIS observations between 2000 and 2010. *Remote Sens. Environ.* 121, 80–92. doi: 10.1016/j.rse.2012.01.014

Feng, L., Raza, M. A., Li, Z., Chen, Y., Khalid, M. H. B., Du, J., et al. (2019). The influence of light intensity and leaf movement on photosynthesis characteristics and carbon balance of soybean. *Front. Plant Sci.* 9:1952. doi: 10.3389/fpls.2018.01952

Fernández-Martínez, M., Sardans, J., Musavi, T., Migliavacca, M., Iturrate-Garcia, M., Scholes, R. J., et al. (2020). The role of climate, foliar stoichiometry and plant diversity on ecosystem carbon balance. *Glob. Chang. Biol.* 26, 7067–7078. doi: 10.1111/gcb.15385

Gao, R., Chuai, X., Ge, J., Wen, J., Zhao, R., and Zuo, T. (2022). An integrated telecoupling analysis for requisition–compensation balance and its influence on carbon storage in China. *Land Use Policy* 116:106057. doi: 10.1016/j.landusepol.2022.106057

Gatti, L. V., Gloor, M., Miller, J. B., Doughty, C. E., Malhi, Y., Domingues, L. G., et al. (2014). Drought sensitivity of Amazonian carbon balance revealed by atmospheric measurements. *Nature* 506, 76–80. doi: 10.1038/nature12957

Guo, R., Zhao, Y., Shi, Y., Li, F., Hu, J., and Yang, H. (2017). Low carbon development and local sustainability from a carbon balance perspective. *Resour. Conserv. Recycl.* 122, 270–279. doi: 10.1016/j.resconrec.2017.02.019

Houghton, R. A., House, J. I., Pongratz, J., Van Der Werf, G. R., Defries, R. S., Hansen, M. C., et al. (2012). Carbon emissions from land use and land-cover change. *Biogeosciences* 9, 5125–5142. doi: 10.5194/bg-9-5125-2012

Kondo, M., Ichii, K., Patra, P. K., Canadell, J. G., Poulter, B., Sitch, S., et al. (2018). Land use change and El Niño-southern oscillation drive decadal carbon balance shifts in Southeast Asia. *Nat. Commun.* 9:1154. doi: 10.1038/s41467-018-03374-x

Lai, L., Huang, X., Yang, H., Chuai, X., Zhang, M., Zhong, T., et al. (2016). Carbon emissions from land-use change and management in China between 1990 and 2010. *Sci. Adv.* 2:e1601063. doi: 10.1126/sciadv.1601063

Lenzen, M., Sun, Y. Y., Faturay, F., Ting, Y. P., Geschke, A., and Malik, A. (2018). The carbon footprint of global tourism. *Nat. Clim. Chang.* 8, 522–528. doi: 10.1038/s41558-018-0141-x

Li, J., Guo, X., Chuai, X., Xie, F., Yang, F., Gao, R., et al. (2021). Reexamine China's terrestrial ecosystem carbon balance under land use-type and climate change. *Land Use Policy* 102:105275. doi: 10.1016/j.landusepol.2020.105275

Li, X., Li, Y., Chen, A., Gao, M., Slette, I. J., and Piao, S. (2019). The impact of the 2009/2010 drought on vegetation growth and terrestrial carbon balance in Southwest China. *Agric. For. Meteorol.* 269-270, 239–248. doi: 10.1016/j.agrformet.2019.01.036

Li, F., Yin, X., and Shao, M. (2022). Natural and anthropogenic factors on China's ecosystem services: comparison and spillover effect perspective. *J. Environ. Manag.* 324:116064. doi: 10.1016/j.jenvman.2022.116064

Liddle, B. (2014). Impact of population, age structure, and urbanization on carbon emissions/energy consumption: evidence from macro-level, cross-country analyses. *Popul. Environ.* 35, 286–304. doi: 10.1007/s11111-013-0198-4

Lin, T., Ge, R., Zhao, Q., Zhang, G., Li, X., Ye, H., et al. (2016). Dynamic changes of a city's carbon balance and its influencing factors: a case study in Xiamen, China. *Carbon Manag.* 7, 149–160. doi: 10.1080/17583004.2016.1180587

Maillard, É., McConkey, B. G., and Angers, D. A. (2018). Each rotation phase can affect soil carbon balance differently over decades. *Can. J. Soil Sci.* 98, 584–588. doi: 10.1139/cjss-2018-0013

Mathias, J. M., and Trugman, A. T. (2022). Climate change impacts plant carbon balance, increasing mean future carbon use efficiency but decreasing total forest extent at dry range edges. *Ecol. Lett.* 25, 498–508. doi: 10.1111/ele.13945

Mekonnen, Z. A., Riley, W. J., Berner, L. T., Bouskill, N. J., Torn, M. S., Iwahana, G., et al. (2021). Arctic tundra shrubification: a review of mechanisms and impacts on ecosystem carbon balance. *Environ. Res. Lett.* 16:053001. doi: 10.1088/1748-9326/abf28b

Mikulčić, H., Baleta, J., Wang, X., Duić, N., and Dewil, R. (2022). Sustainable development in period of climate crisis. *J. Environ. Manag.* 303:114271. doi: 10.1016/j.jenvman.2021.114271

Nag, S. K., Nandy, S. K., Roy, K., Sarkar, U. K., and Das, B. K. (2019). Carbon balance of a sewage-fed aquaculture wetland. *Wetl. Ecol. Manag.* 27, 311–322. doi: 10.1007/s11273-019-09661-8

Nathaniel, S. P., and Adeleye, N. (2021). Environmental preservation amidst carbon emissions, energy consumption, and urbanization in selected African countries: implication for sustainability. *J. Clean. Prod.* 285:125409. doi: 10.1016/j.jclepro.2020.125409

Nepal, P., Ince, P. J., Skog, K. E., and Chang, S. J. (2013). Forest carbon benefits, costs and leakage effects of carbon reserve scenarios in the United States. *J. For. Econ.* 19, 286–306. doi: 10.1016/j.jfe.2013.06.001

Ouyang, X., Tang, L., Wei, X., and Li, Y. (2021). Spatial interaction between urbanization and ecosystem services in Chinese urban agglomerations. *Land Use Policy* 109:105587. doi: 10.1016/j.landusepol.2021.105587

Ouyang, X., Xu, J., Li, J., Wei, X., and Li, Y. (2022). Land space optimization of urban-agriculture-ecological functions in the Changsha-Zhuzhou-Xiangtan urban agglomeration, China. *Land Use Policy* 117:106112. doi: 10.1016/j.landusepol.2022.106112

Pingoud, K., Ekholm, T., Soimakallio, S., and Helin, T. (2016). Carbon balance indicator for forest bioenergy scenarios. *GCB Bioenergy* 8, 171–182. doi: 10.1111/gcbb.12253

Pukkala, T. (2017). Does management improve the carbon balance of forestry? *Forestry* 90, 125–135. doi: 10.1093/forestry/cpw043

Schimel, D., Stephens, B. B., and Fisher, J. B. (2015). Effect of increasing CO2 on the terrestrial carbon cycle. *Proc. Natl. Acad. Sci.* 112, 436–441. doi: 10.1073/pnas.1407302112

Tcherkez, G., Gauthier, P., Buckley, T. N., Busch, F. A., Barbour, M. M., Bruhn, D., et al. (2017). Leaf day respiration: low CO 2 flux but high significance for metabolism and carbon balance. *New Phytol.* 216, 986–1001. doi: 10.1111/nph.14816

Wang, R., Li, F., Hu, D., and Li, B. L. (2011a). Understanding eco-complexity: social-economic-natural complex ecosystem approach. *Ecol. Complex.* 8, 15–29. doi: 10.1016/j.ecocom.2010.11.001

Wang, W. Z., Liu, L. C., Liao, H., and Wei, Y. M. (2021). Impacts of urbanization on carbon emissions: an empirical analysis from OECD countries. *Energy Policy* 151:112171. doi: 10.1016/j.enpol.2021.112171

Wang, H., Lu, S., Lu, B., and Nie, X. (2021). Overt and covert: the relationship between the transfer of land development rights and carbon emissions. *Land Use Policy* 108:105665. doi: 10.1016/j.landusepol.2021.105665

Wang, C., Zhan, J., Zhang, F., Liu, W., and Twumasi-Ankrah, M. J. (2021). Analysis of urban carbon balance based on land use dynamics in the Beijing-Tianjin-Hebei region, China. *J. Clean. Prod.* 281:125138. doi: 10.1016/j.jclepro.2020.125138

Wang, R., Zhou, T., Hu, D., Li, F., and Liu, J. (2011b). Cultivating eco-sustainability: social–economic–natural complex ecosystem case studies in China. *Ecol. Complex.* 8, 273–283. doi: 10.1016/j.ecocom.2011.03.003

Wei, G., Bi, M., Liu, X., Zhang, Z., and He, B. J. (2022). Investigating the impact of multi-dimensional urbanization and FDI on carbon emissions in the belt and road initiative region: direct and spillover effects. *J. Clean. Prod.* 384:135608. doi: 10.1016/j.jclepro.2022.135608

Wei, G., Bi, M., Liu, X., Zhang, Z., and He, B. J. (2023). Investigating the impact of multi-dimensional urbanization and FDI on carbon emissions in the belt and road initiative region: direct and spillover effects. *J. Clean. Prod.* 384:135608. doi: 10.1016/j.jclepro.2022.135608

Wei, G., Zhang, Z., Ouyang, X., Shen, Y., Jiang, S., Liu, B., et al. (2021). Delineating the spatial-temporal variation of air pollution with urbanization in the belt and road initiative area. *Environ. Impact Assess. Rev.* 91:106646. doi: 10.1016/j.eiar.2021.106646

Williams, D. R., Alvarado, F., Green, R. E., Manica, A., Phalan, B., and Balmford, A. (2017). Land-use strategies to balance livestock production, biodiversity conservation and carbon storage in Yucatán, Mexico. *Global Change Biol.* 23, 5260–5272. doi: 10.1111/gcb.13791

Xing, L., Zhu, Y., and Wang, J. (2021). Spatial spillover effects of urbanization on ecosystem services value in Chinese cities. *Ecol. Indic.* 121:107028. doi: 10.1016/j.ecolind.2020.107028

Xu, Y., Dong, Z., and Wu, Y. (2023). The spatiotemporal effects of environmental regulation on green innovation: evidence from Chinese cities. *Sci. Total Environ.* 876:162790. doi: 10.1016/j.scitotenv.2023.162790

Yang, B., Liu, L., and Yin, Y. (2021). Will China's low-carbon policy balance emission reduction and economic development? Evidence from two provinces. *Int. J. Clim. Change Strat. Manag.* 13, 78–94. doi: 10.1108/IJCCSM-08-2020-0093

Yao, X., Kou, D., Shao, S., Li, X., Wang, W., and Zhang, C. (2018). Can urbanization process and carbon emission abatement be harmonious? New evidence from China. *Environ. Impact Assess. Rev.* 71, 70–83. doi: 10.1016/j.eiar.2018.04.005

Yao, L., Liu, J., Wang, R., Yin, K., and Han, B. (2015). A qualitative network model for understanding regional metabolism in the context of social–economic–natural complex ecosystem theory. *Eco. Inform.* 26, 29–34. doi: 10.1016/j.ecoinf.2014.05.014

Ye, X., Zhang, Q., Liu, J., Li, X., and Xu, C. Y. (2013). Distinguishing the relative impacts of climate change and human activities on variation of streamflow in the Poyang Lake catchment, China. *J. Hydrol.* 494, 83–95. doi: 10.1016/j.jhydrol.2013.04.036

Yuan, W., Liu, X., Wang, W., Di, M., and Wang, J. (2019). Microplastic abundance, distribution and composition in water, sediments, and wild fish from Poyang Lake, China. *Ecotoxicol. Environ. Saf.* 170, 180–187. doi: 10.1016/j.ecoenv.2018.11.126

Zhang, D., Zhao, Y., and Wu, J. (2023). Assessment of carbon balance attribution and carbon storage potential in China's terrestrial ecosystem. *Resour. Conserv. Recycl.* 189:106748. doi: 10.1016/j.resconrec.2022.106748

Zhang, C. Y., Zhao, L., Zhang, H., Chen, M. N., Fang, R. Y., Yao, Y., et al. (2022). Spatial-temporal characteristics of carbon emissions from land use change in Yellow River Delta region, China. *Ecol. Indicat.* 136:108623. doi: 10.1016/j.ecolind.2022.108623

Zhenmin, L., and Espinosa, P. (2019). Tackling climate change to accelerate sustainable development. *Nat. Clim. Chang.* 9, 494–496. doi: 10.1038/s41558-019-0519-4

Zhou, Y., Chen, M., Tang, Z., and Mei, Z. (2021). Urbanization, land use change, and carbon emissions: quantitative assessments for city-level carbon emissions in Beijing-Tianjin-Hebei region. *Sustain. Cities Soc.* 66:102701. doi: 10.1016/j.scs.2020.102701

Zhou, L., Dang, X., Mu, H., Wang, B., and Wang, S. (2021). Cities are going uphill: slope gradient analysis of urban expansion and its driving factors in China. *Sci. Total Environ.* 775:145836. doi: 10.1016/j.scitotenv.2021.145836

Zhou, L., Hu, F., Wang, B., Wei, C., Sun, D., and Wang, S. (2022a). Relationship between urban landscape structure and land surface temperature: spatial hierarchy and interaction effects. *Sustain. Cities Soc.* 80:103795. doi: 10.1016/j.scs.2022.103795

Zhou, L., Yuan, B., Hu, F., Wei, C., Dang, X., and Sun, D. (2022b). Understanding the effects of 2D/3D urban morphology on land surface temperature based on local climate zones. *Build. Environ.* 208:108578. doi: 10.1016/j.buildenv.2021.108578

Zhou, L., Zhou, C., Che, L., and Wang, B. (2020). Spatio-temporal evolution and influencing factors of urban green development efficiency in China. *J. Geogr. Sci.* 30, 724–742. doi: 10.1007/s11442-020-1752-5

frontiers | Frontiers in Environmental Science

TYPE Original Research
PUBLISHED 09 June 2023
DOI 10.3389/fenvs.2023.1200513

OPEN ACCESS

EDITED BY
Xiao Ouyang,
Hunan University of Finance and Economics, China

REVIEWED BY
Guoen Wei,
Nanchang University, China
Xue-Chao Wang,
Beijing Normal University, China

*CORRESPONDENCE
Hua Yang,
yh191121626@163.com

RECEIVED 05 April 2023
ACCEPTED 02 May 2023
PUBLISHED 09 June 2023

CITATION
Zeng Z, Yang H, Zhou H, Lai N, Song Q, Ji Q and Ning Q (2023), Monitoring and control of water-ecological space in the Dongting Lake region.
Front. Environ. Sci. 11:1200513.
doi: 10.3389/fenvs.2023.1200513

Monitoring and control of water-ecological space in the Dongting Lake region

Zhiwei Zeng[1,2,3], Hua Yang[4]*, Hui Zhou[4], Nan Lai[4], Qidi Song[4], Qianfu Ji[4] and Qimeng Ning[1,2,3]

[1]College of Architecture and Urban Planning, Hunan City University, Yiyang, China, [2]Key Laboratory of Key Technologies of Digital Urban-Rural Spatial Planning of Hunan Province, Yiyang, China, [3]Key Laboratory of Urban Planning Information Technology of Hunan Provincial Colleges, Yiyang, China, [4]Hunan Provincial Territorial Space Survey and Monitoring Institute, Changsha, China

The territorial spatial planning in the new era strengthens the control of different functional spaces and emphasizes integrated and coordinated development of each functional space. Therefore, it is important to monitor the "structure-function" characteristics of water-ecological space based on the context of territorial spatial planning and develop a management and control framework. Based on land use and social statistics, and with the help of ArcGIS analysis, this paper examined the structure and function of the water-ecological space in the Dongting Lake study for 2010, 2015, and 2020, generating a control framework and proposing key initiatives. The main results are as follows: 1) The overall scale of the water ecological space in the Dongting Lake study is over 7,300 km^2. Water bodies had the largest share, followed by coastal terrestrial areas, while the land-water ecotone was the smallest. There was a small decrease in the water ecological space during the study period. Yueyang had the largest overall scale of water ecological space, while Linli had the smallest. 2) The comprehensive function of water ecological space in the Dongting Lake study was about 0.4000, increasing somewhat during the study period. Among the units, the comprehensive function value was highest in Yuanjiang City, while Jincheng City had the lowest. 3) From the structural elements of water ecological space, scientific planning of functional zoning of water ecological space should be carried out and combined with the delineation of "three zones and three lines." Key initiatives such as multi-scale and multi-level planning and control, use control and access restrictions, determination of water ecological space ownership, pollution control and accountability, and comprehensive water ecological treatment and restoration should be promoted.

KEYWORDS

water-ecological space, structure-function, monitoring and control, Dongting Lake, territorial spatial planning

1 Introduction

Water ecological space pertains to areas that provide for hydrological-ecological processes, maintain the health and stability of water ecosystems, and guarantee water security; as a core constituent of ecological space and the basic support of urban space and agricultural space, it has an important position in the national spatial system (Yang et al., 2017a; Zhu et al., 2017). However, rapid urbanization and industrialization have caused damage to the water ecological environment. Regional water shortage, water pollution,

flooding, and other water-related problems frequently occur, leading to enormous pressures on the water ecological space (Yang et al., 2021). Therefore, under the new territorial spatial planning system, mapping the dynamic evolution of regional water ecological space and enhancing the control and management of regional water ecological space are essential measures to implement territorial spatial use control, optimize territorial spatial layout, and enhance territorial spatial quality, in order to promote high-quality regional development.

Monitoring and control of water-ecological space is to measure and collect data on the real-time status of water spatial structure, hydrology, aquatic biology, water quality, water function and other elements, analyze and evaluate the *status quo* and development trend of water ecosystem on this basis, and propose corresponding regulation and control measures, with the purpose of protecting and restoring water ecological environment. It is the foundation of water ecosystem protection, management and sustainable utilization in the new era (Liu et al., 2022). Domestic and foreign scholars have explored the monitoring and control of water ecological space. Foreign researchers have had an early start, focusing mainly on water quality monitoring (Aina et al., 2015), water ecological habitat (Cecilia et al., 2016), water resource management (Chitresh et al., 2017), and water environment management (Gerald and Galloway, 1997), and attaching importance to the relationship between land use and water ecological space and its impact effect (Ghosh and Maiti, 2021; Baltodano et al., 2022). For example, Benra et al. (2021) used the InVEST model to monitor the service value of the water ecosystem. Alberti et al. (2006) found a clear correlation between the water ecosystem and urban land use structure (Marina et al., 2006). Gerald et al. analyzed the Mississippi River flood in 1993 and proposed a sustainable water space management model that integrates environment, economy and culture. Over time, a systematic paradigm of "classification system-evolution characteristics-control measures" was gradually established in water ecological space research.

Combining international research on water ecological monitoring and control concepts and methods with China's own land ownership, space development, and environmental management systems, domestic scholars have explored traditional water quality detection (Yin et al., 2021) and water resource management (Zuo et al., 2021), expanding into water ecological space classification (Li et al., 2009) and control planning systems (Wu et al., 2021). And with the establishment and improvements in territorial spatial planning, water ecological space classification has gradually become a research hotspot. Local scholars have largely focused on the spatial causes, composition media, and spatial forms of the classification criteria (Deng et al., 2004; Liu C. et al., 2018; Kang et al., 2022). For example, Huang et al. (2012) proposed a zoning method for water ecological space based on regional differences in river basin water ecosystems. Yang et al. (2017b) and Yang et al. (2017c) defined the scope of water ecological space into three types: water ecological protection red line study, water ecological restricted development study, and water security guidance study.

The current concept of water ecological space control and related studies are based on extending the idea of land use control. Research has been conducted in terms of control zones, control systems, and control indicators (Du et al., 2013; Qiu et al., 2017). For instance, Cao et al. (2014) used current ecological elements, important rivers, lakes, reservoirs, wetlands, and green parks and proposed the water ecological control standards for water ecological space. Qiu et al. (2017) explored and analyzed the water ecological space control system based on the supporting requirements of water ecological space. Other studies have analyzed the spatial evolution of the water ecological environment (Su et al., 2021), the water ecological effects of land use and urban activities (Ren et al., 2016), and water ecological civilization (Jiang et al., 2018). In general, domestic and international research on spatial monitoring and control of water-ecology is developing from small to large scales (Yin et al., 2021).

According to system theory, water ecological space can be regarded as a water-centered eco-economic system formed by the interaction of natural and human elements disturbed by human activities; its structure and function are the most fundamental attributes of the system (Liu et al., 2010; Liu W. et al., 2018). Structure reflects the external form of water ecological space, while function harbors its internal role (Bo et al., 2022). Therefore, understanding the dynamic change process and characteristics of the structure and function would be crucial in protecting and optimizing water ecological space and integrating and coordinating national space. The impact of urbanization, population growth, industrial and agricultural production and FDI on changes in the spatial scale of water and ecology has been investigated (Zhou et al., 2022a; Wei et al., 2023), and the relationship between the optimization of water and ecological functions and the coordination of national spatial functions has been discussed (Ouyang et al., 2022). However, there is a paucity of literature on the study of water ecological spaces from an integrated "structure-function" perspective. Most are based on specific management purposes (Zuo et al., 2021), often overlooking the perspective of new territorial spatial planning. Their results are decoupled from the new planning

FIGURE 1
Overview of the study area.

TABLE 1 Indicator system for "structure-function" monitor of the water-ecological space in the Dongting Lake study.

	Secondary classification	Specific indicators		Secondary classification	Specific indicators
Structure	Water space	River channel	Function	Ecology function	Water conservation
		The linear or zonal water surface between the constant water level shorelines of rivers formed by natural or artificial excavation			It can show the ability of water ecological space to retain precipitation, regulate runoff, purify water quality and affect precipitation
		Lakes			Soil-water conservation
		The surface water formed by the natural water level shoreline in the water accumulation study			It reflects the ability of water-ecological spaces to maintain soil and water, regulate sediment and maintain ecological security
		Reservoir pond		Social function	Reservoir pond area
		Artificial interception of the water surface enclosed by the normal water level shoreline and the smaller water surface formed by natural or artificial excavation			It can reflect the water supply capacity of society to a certain extent
	Water-land mosaic zones	Beach			Embankment length
		The study between the flood and flat water levels of river and lake waters			It can reflect the ability of flood control and flood storage to a certain extent
		Swamp		Economic function	Aquatic product yield
		The land where wet plants grow on the surface that is too wet and often waterlogged			The initial product output that can show the output of water ecological space
	Adjacent terrestrial zone	Sparse woodland			Fishery output value
		The study within a certain distance from the water body space, with strong water connotation and soil conservation ability			It can show the economic production capacity of the initial products of water ecological space

TABLE 2 The coefficients of ecosystem service value for various water-ecosystem spaces in the Dongting Lake study (yuan·hm-2*a-1).

Ecological function type	Water space (including rivers, canals, lakes, reservoirs and ponds)	Wetlands (including marsh flats)	Forest land
Water conservation	65,932.31	50,358.29	10,146.56
Soil and water conservation	33.77	5,603.45	12,588.47

system, which is not conducive to the practical operations of territorial spatial zoning, use control, and optimal management. Therefore, based on the new territorial spatial planning context, it is necessary to monitor the regional water ecological environment from the perspective of "structure-function" and explore feasible control strategies for regional territorial spatial planning.

The study area is Dongting Lake, which is the ecological security lifeline of the Yangtze River basin. It is an important storage lake ecological zone in the middle and lower reaches of the Yangtze River, which is a typical fragile zone of interlocking water and land ecology (Chen et al., 2013; Ning et al., 2020). Due to accelerated urbanization, industrial and agricultural activities around Dongting Lake have increased, intensifying land use and damaging the water ecosystem. The region's water areas have shrunk considerably, soil erosion has become common, flooding is frequent, and the water ecological environment has shown a declining trend (Liu and Wang, 2008; Chen Q. et al., 2015). As an important hub of Hunan Province's "one belt, one city" strategy, the protection and construction of Dongting Lake's water ecological space are closely linked to the high-quality development of the province and the Yangtze River Economic Belt. The main scientific question that this study focuses on is how to scientifically and effectively monitor the water and ecological space in the Dongting Lake area in the context of the new territorial spatial planning and the "structure-function" perspective? How to build a reasonable control strategy? This is also the main objective of this study.

2 Study overview, study methods and data sources

2.1 Study overview

The study area is a watershed unit centered on Dongting Lake, transitioning to plains, tablelands, and low hills (Deng

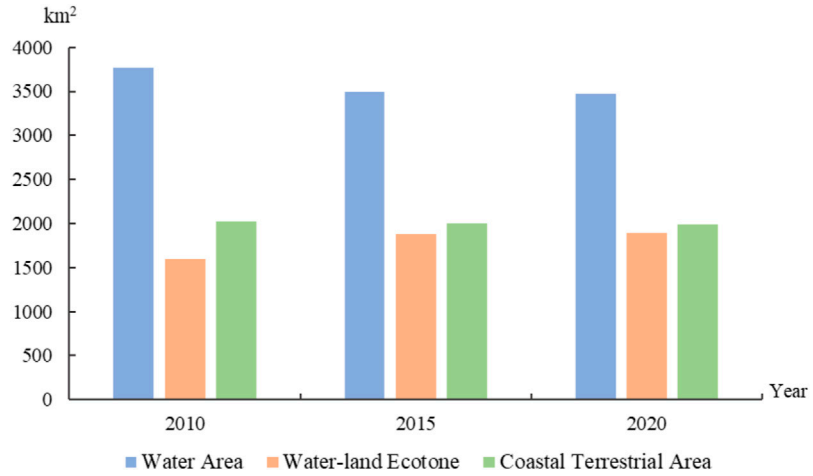

FIGURE 2
Changes in the spatial structure of water ecology in the Dongting Lake region from 2010 to 2020.

TABLE 3 Area of different types of water-ecological space in the Dongting Lake region from 2010 to 2020.

Type of water ecological space	Land type	2010		2015		2020	
Water area	lake	1,901.74	3,772.41	1,622.64	3,499.99	1,604.14	3,470.19
	River channel	684.10		679.96		679.09	
	Reservoir pond	1,186.57		1,197.40		1,186.97	
Water-land mosaic zones	Beach	637.09	1,597.86	917.38	1,877.89	943.38	1,895.81
	Marsh	960.78		960.51		952.430	
Adjacent terrestrial zones	Sparse woodland	2,020.55	2,020.55	2,002.27	2,002.27	1,985.00	1,985.00

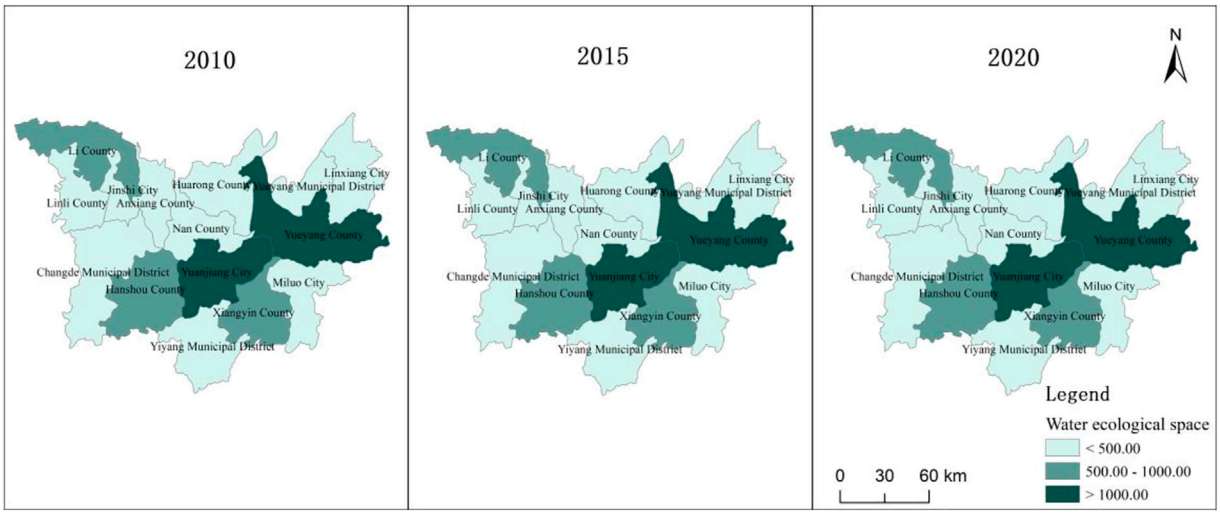

FIGURE 3
Regional Structural Differences in water-ecological Space in the Dongting Lake Region from 2010 to 2020.

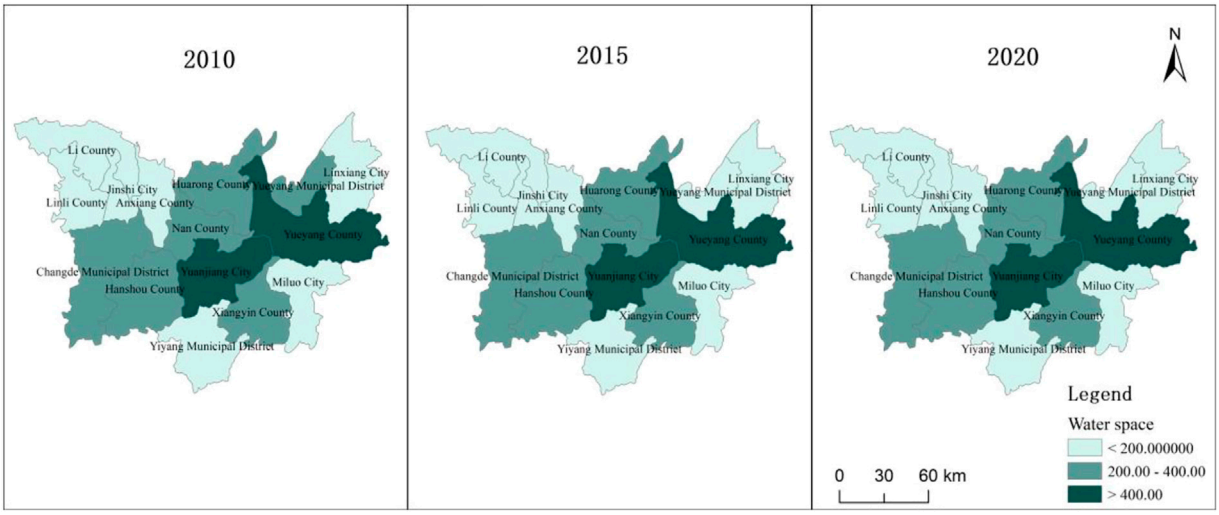

FIGURE 4
Regional structural differences of water bodies in the Dongting Lake region from 2010 to 2020.

et al., 2019). It is located in the northern part of Hunan Province at the confluence of the Xiangjiang, Zijiang, Yuanjiang, and Li rivers and has important hydrological regulating and agricultural production functions in the middle and lower reaches of the Yangtze River (as shown in Figure 1). Most of the study area is at an altitude of 30–50 m, belonging to the subtropical monsoon climate. While the Dongting Lake study site has a dense river network and abundant water, gas, soil, and biological resources, it has significant ecological vulnerability and sensitivity. Given the sharp contradiction between human activities and the water ecological environment (Wang and Tang, 2015), analyzing the monitoring and control system of water ecological space would be of great significance. Nineteen counties (cities, districts) closely related to the Dongting Lake Basin comprised the study site: Yueyang, Changde and Yiyang (Yueyanglou District, Junshan District, Yunxi District, Wuling District, Dingcheng District, Heshan District, Ziyang District) and Yueyang County, Huarong County, Xiangyin County, Miluo City, Linxiang City, Hanshou County, Anxiang County, Lixian County, Linli County, Jinshi City, Nanxian County, Yuanjiang City. The municipal districts of Yueyang, Changde, and Yiyang were each treated as an overall study unit, resulting in a total of 15 study units established for this study.

2.2 Study methods

2.2.1 Construction of the index system

Water ecological space is a vast and intricate system that includes not only bodies of water like lakes, rivers, and reservoirs but also water-land transitional zones like wetlands and mudflats, as well as terrestrial territorial systems close to the shore, which act as its structural components (Yang et al., 2017b). Meanwhile, it is also an important part of the regional landscape structure and a fundamental element of the regional landscape ecosystem (Zhou et al., 2022b). Given the diverse spatial structure, the water ecological space has both natural and human attributes (Tang et al., 2020), providing important values for the health and stability of natural ecosystems (e.g., water containment, soil conservation, and biodiversity maintenance) and fundamental carrying and supporting services to human development, including water supply, flood control and storage, and aquaculture (Zhou et al., 2020a).

Therefore, based on the structural elements and functional attributes of water ecological space, and considering data availability and the regional characteristics of the Dongting Lake water ecological space, three structural monitoring indicators (i.e., water space, water-land ecotone and coastal terrestrial) and three functional monitoring indicators (i.e., ecological function, social function, and economic function) were used in constructing the "structure-function" monitoring system of the aquatic biological space. Among the structural monitoring indicators, rivers/canals, lakes, and reservoirs/ponds were used for water spaces, mudflats and swamps were used for the water-land mosaic zone, and open woodlands were used for the shoreline terrestrial zone. For functional monitoring, water conservation was selected as an ecological indicator, reservoir pond area and bank length were used as social indicators, and fish production and fishery output value were selected as economic indicators. The specific index system is shown in Table 1.

2.2.2 Functional value calculation method

2.2.2.1 Calculation of ecological function value

Soil and water conservation are basic ecosystem service value components of water ecological space (Li et al., 2011). Water conservation and soil-and-water conservation are used in this paper to describe the ecological function of the water ecological space in the Dongting Lake study area. The value of ecosystem services is frequently evaluated using the equivalent factor method in both local and international research. Ecosystem service value refers to the proportional value a specific service contributes to an

ecosystem and is typically converted using the market price of grain output per unit (Chen Y. et al., 2015). Based on the research findings of Costanza et al., Xie et al. (2003) created an equivalent table of ecosystem service value in China. However, due to the large regional differences, the service value of the same ecological type may vary significantly in different regions and may require corrections to the national equivalent factor coefficient. Based on the equivalent factor table developed by Xie Gaodi et al. and referring to the results of Deng et al. (2019), this paper evaluated the service value coefficient for water conservation and for soil and water conservation of different water ecological space types in Dongting Lake (Table 2). The calculation formula for the ecological function value is:

$$W_{ESV} = \sum_{i=1}^{n}(A_i \times VC_{si}) + \sum_{i=1}^{n}(A_i \times VC_{ti}) \Big/ 2 \quad (1)$$

where W_{ESV} is the ecological function value of the water ecological space; A_i is the study of the i th water ecological space type; VC_{si} is the service value coefficient of water conservation of i water ecological space type; VC_{ti} is the service value coefficient of soil conservation of i water ecological space type. The value of n is 3; the calculation results are dimensionless in order to integrate the social and economic function values.

2.2.2.2 Social and economic function value measurement

Social and economic functions support and promote the water ecological space for human economic production and social activities. Using statistical data, the extreme difference standardization method was used on the social and economic indicators. Since the related indicators were all positive, the standardization formula is:

$$X_{ij} = \frac{x_{ij} - \min(x_{ij})}{\max(x_{ij}) - \min(x_{ij})} \quad (2)$$

where $^{X_{ij}}$ is the standardized index value; $^{x_{ij}}$ is the original value of the index; $^{\min(x_{ij})}$ and $^{\max(x_{ij})}$ are the minimum and maximum values in the data set of the index, respectively.

The final values for the social and economic functions were obtained using the weighted average method. The weight setting of each relevant index was determined by the entropy weight method. The calculation formula of the entropy weight method is:

$$e_j = -\frac{1}{\ln(n)} \times \sum_{i=1}^{n} P_{ij} \times \ln(P_{ij}) \quad (3)$$

$$W_j = (1 - e_j) \Big/ \sum_{j=1}^{m}(1 - e_j) \quad (4)$$

where e_j is the information entropy of the corresponding index; W_j is the weight of the corresponding index, such that $P_{ij} = X_{ij} / \sum_{i=1}^{n} X_{ij}$.

2.3 Data sources

The main data used in this study include basic geographic data, land use data and social statistics. Among them, the base map of the basic geographic data was obtained from the National Standard Map Service Platform (http://bzdt.ch.mnr.gov.cn/) with the review number GS (2019) 3333. The land use data was obtained from the Resource and Environment Science and Data Centre, Institute of Geographical Sciences and Resources, Chinese Academy of Sciences (https://www.resdc.cn/), classified with reference to the LUCC classification standard, and spatially analysed in ArcGIS. Social statistics such as length of embankments, fish production and fishery output value were obtained from the Hunan Statistical Yearbook and statistical bulletins of the relevant years.

3 Monitoring of water ecological spatial structure of Dongting Lake

3.1 Overall structure

The water ecological space of the Dongting Lake area is more than 7,300 km^2, accounting for about 28.35% of the total land

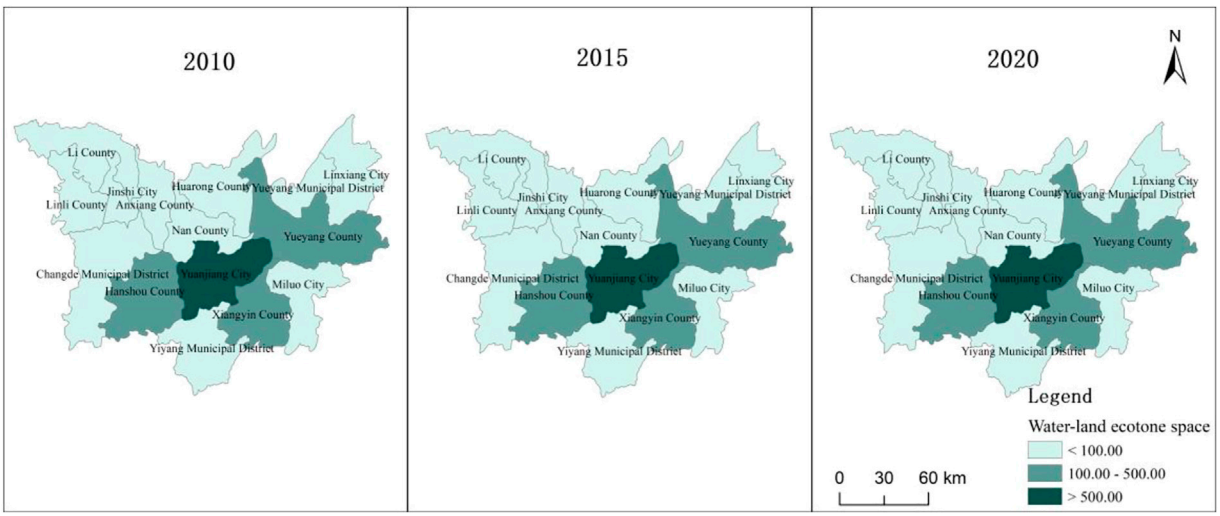

FIGURE 5
Regional structural differences of water-land mosaic zones in the Dongting Lake region from 2010 to 2020.

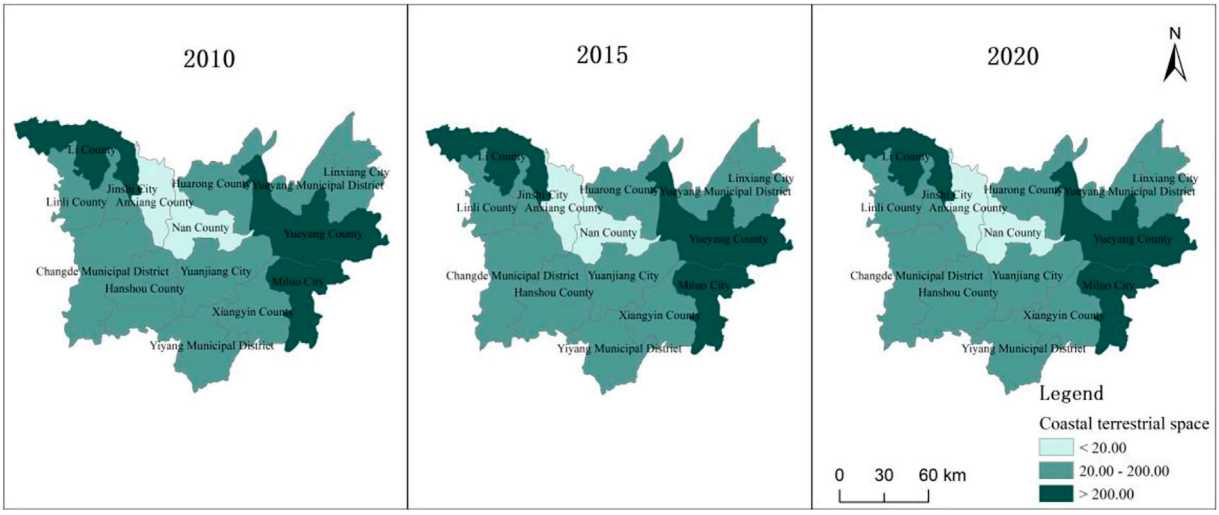

FIGURE 6
Regional structural differences of the adjacent terrestrial zone in the Dongting Lake region from 2010 to 2020.

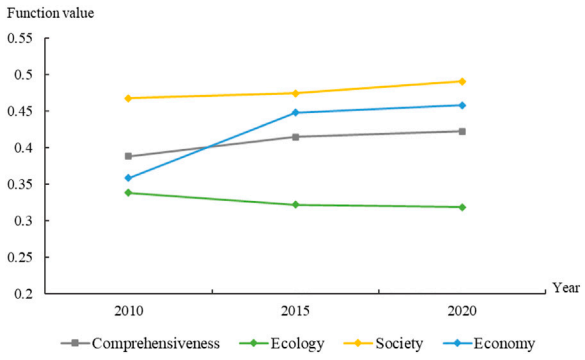

FIGURE 7
Changes in the spatial function of water ecology in the Dongting Lake area.

area. During the study period, the total aquatic ecological space decreased slightly from 7,390.81 km^2 in 2010 to 7,350.99 km^2 in 2020, a decrease of 39.82 km^2. Among the aquatic ecological space types (Figure 2), water area accounted for the largest proportion but decreased significantly during the study period. Water ecological space decreased from 3,772.41 km^2 (51.04%) in 2010 to 3,470.19 km^2 (47.21%) in 2020, a decrease of 302.22 km^2. The largest decrease occurred in 2010–2015, with a total decrease of 272.41 km^2. The land-water ecotone accounted for the smallest proportion but showed a clear upward trend during the study period. Aquatic ecological space increased from 1,597.86 km^2 (21.62%) in 2010 to 1,895.81 km^2 (25.79%), an increase of 297.95 km^2; the growth was largest during 2010–2015, increasing by 280.03 km^2. Coastal terrestrial areas comprised 27.00% of aquatic ecological space, decreasing by only 35.55 km^2 during the study period, from 2,020.55 km^2 in 2010 to 1,985.00 km^2.

In terms of water space, the lake area was the largest, occupying more than 45%. Total lake area decreased from 1,901.74 km^2 (50.41%) in 2010 to 1,604.14 km^2 (46.23%) in 2020, a decrease of 297.60 km^2; the fastest decline occurred during 2010–2015. Reservoir pond was the second largest, increasing from 31.45% to 34.21% during the study period. The spatial area slightly increased by 10.83 km^2 during 2010–2015, then slightly decreased in 2015–2020, but the overall change was not pronounced. The proportion of the river channel was relatively low, accounting for about 680.00 km^2 (19.00%); the change in the area and proportion for river channels was low for the given study period.

In the aquatic-terrestrial ecotone, swamps accounted for more than 50%, with a spatial area of more than 950.00 km^2. During the study period, the proportion of swamps decreased from 60.13% to 50.24%, while its spatial area changed little. The proportion of beach land was relatively small but exhibited a significant upward trend during the study period. The proportion increased from 39.87% to 49.76%, while the area increased from 637.09 to 943.38 km^2. The areas for the different types of water ecological space in Dongting Lake are summarized in Table 3.

3.2 Regional structure

From the perspective of regional units, the water ecological space in the Dongting Lake area has prominent structural differences (Figure 3). As shown in Figure 3, the water ecological spaces in Yueyang County and Yuanjiang City were larger than 1,000 km^2. Water ecological spaces in Yueyang County and Yuanjiang City were 1,332.98 and 1,327.99 km^2 in 2010, 1,323.92 and 1,038.45 km^2 in 2015, and 1,043.94 and 1,043.43 km^2 in 2020. The scale of water ecological space in Xiangyin County, Hanshou County, and Li County was in the second echelon, having an overall scale between 500 and 1,000 km^2. In 2010, the water ecological spaces in Xiangyin

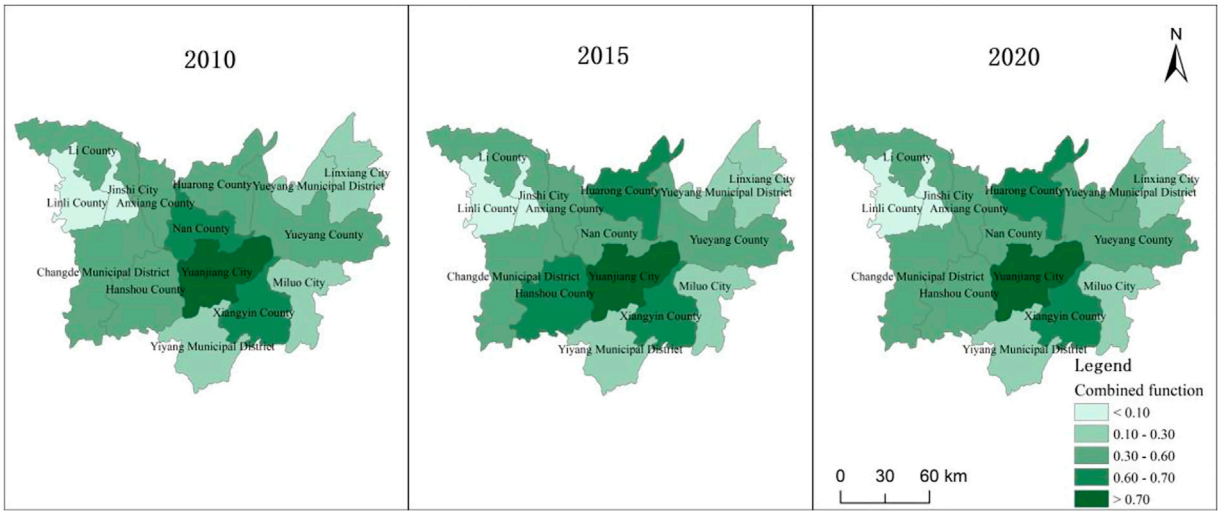

FIGURE 8
Differences in the integrated function value of water-ecological space in the Dongting Lake region from 2010 to 2020.

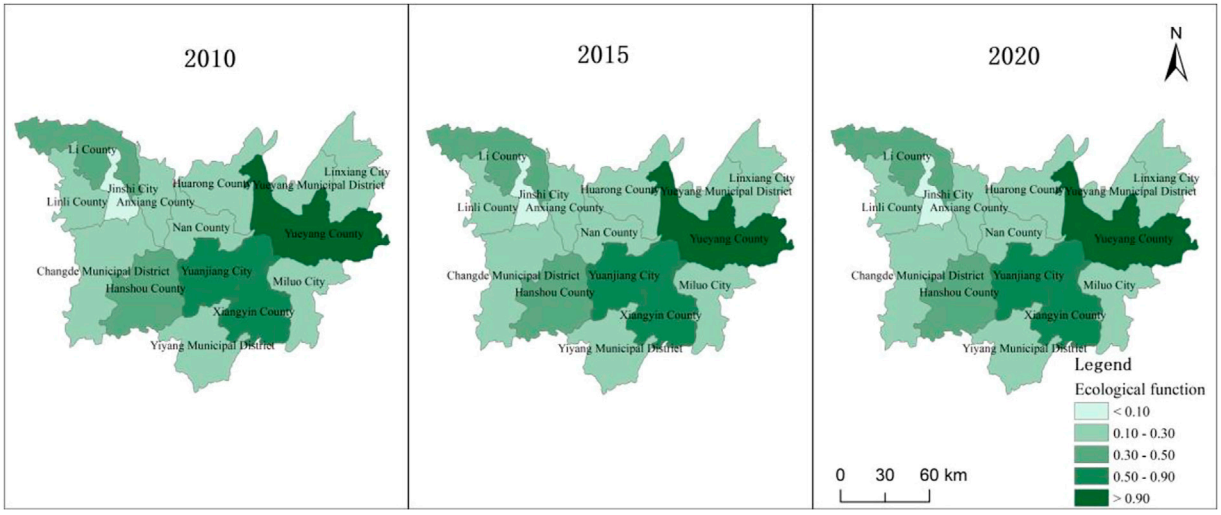

FIGURE 9
Differences in the ecological function value of water-ecological space in the Dongting Lake region from 2010 to 2020.

County, Hanshou County, and Li County were 735.08, 731.52, and 728.04 km^2, 656.17, 659.65, and 659.16 km^2 in 2015, and 522.74, 521.33, and 521.32 km^2 in 2020. In other regional units (e.g., Yueyang City, Changde City, Linxiang City, Miluo City, Huarong County, Linli County, Anxiang County, Jinshi City, and Nanxian County), the water ecological space was below 500 km^2. Linli County had the smallest overall scale, having a water ecological space area of 189.32 km^2 in 2010, 188.09 km^2 in 2015, and 187.57 km^2 in 2020. During the study period, there was no significant structural difference in water ecological space in the Dongting Lake area, and the overall scale in each regional unit slightly fluctuated.

For water space (Figure 4), Yueyang County and Yuanjiang City were larger, with water space areas of more than 400 km^2. Yueyang County's water space area was the largest but decreased significantly for the research period (762.54 km^2 in 2010, 542.76 km^2 in 2015, and 526.40 km^2 in 2020), decreasing by 236.14 km^2 in 10 years. Hanshou County, Xiangyin County, Huarong County, Nanxian County, Changde City, and Yueyang City followed, with water bodies between 200 and 400 km^2; the change in water spaces in these

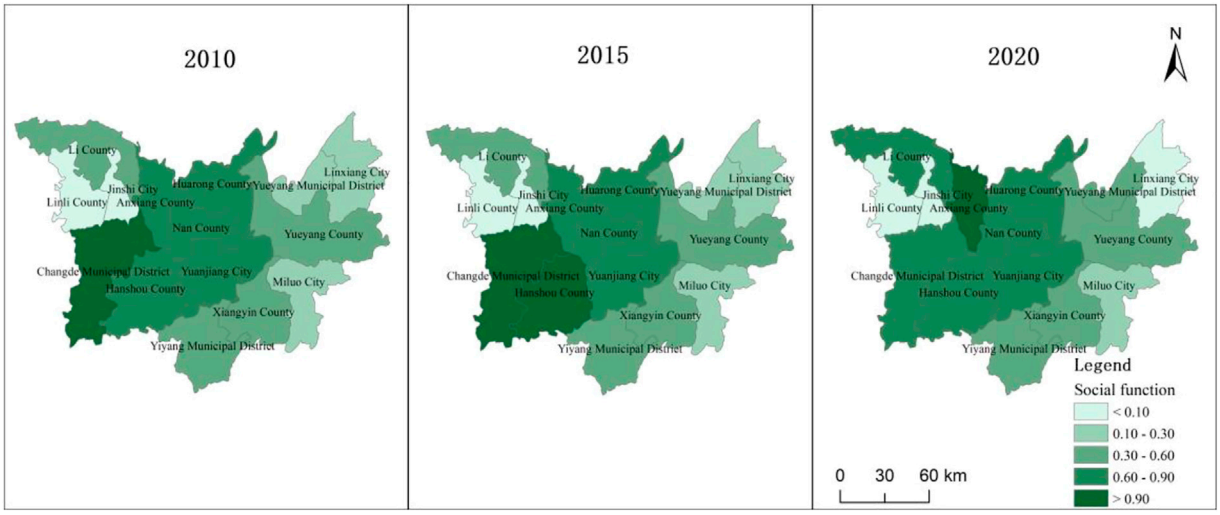

FIGURE 10
Differences in the social function value of water-ecological space in the Dongting Lake region from 2010 to 2020.

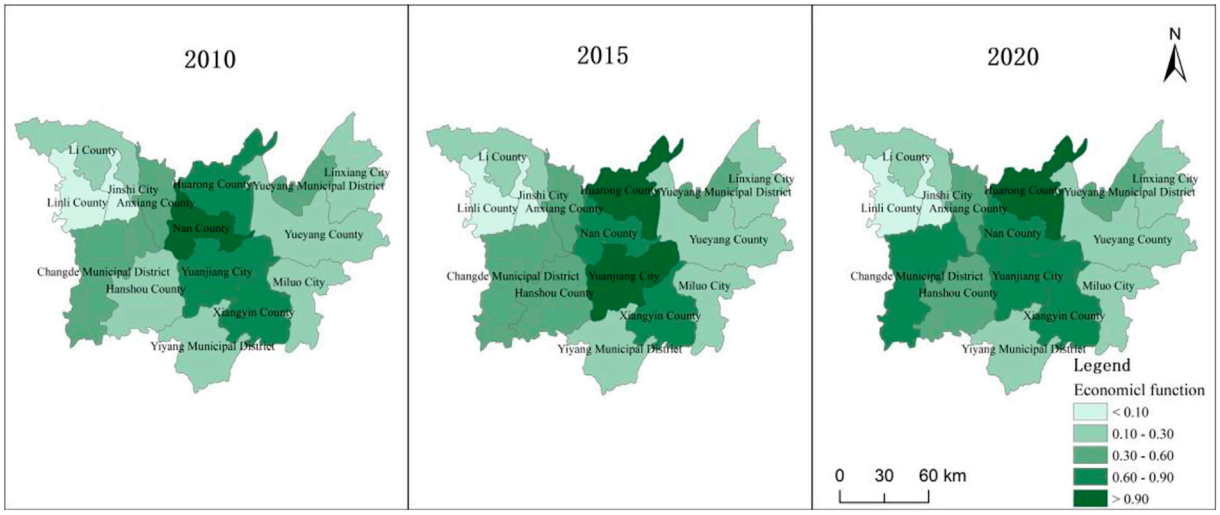

FIGURE 11
Differences in the economic function value of water-ecological space in the Dongting Lake region from 2010 to 2020.

areas was not significant for the study period. In seven regional units (e.g., Linli County, Miluo City, and Jinshi City), the water space scales were relatively small, with areas of less than 200 km^2. Linli County had the smallest water area (about 40 km^2) and exhibited no pronounced spatial change during the study period.

For the water-land mosaic zones (Figure 5), the spatial scale of Yuanjiang City had the largest spatial scale at over 500 km^2, increasing slightly from 568.33 km^2 in 2010 to 569.81 km^2 in 2015 and 575.46 km^2 in 2020. For Yueyang County, the spatial scale of the water-land interface area increased significantly in 2015, reaching 410.87 km^2 and surpassing Xiangyin County; by 2020, it reached 427.10 km^2, increasing 235.78 km^2 in 10 years, mainly due to the increase in beach areas. This is related to the previously mentioned reduction in water spaces, i.e., the conversion of water space into beach land. The spatial scale of the water-land interface area in 11 regional units (e.g., Linli County, Linxiang City, Jincheng City, and Yueyang Municipal District) was relatively small, mostly below 100 km^2; Linli County had the smallest water-land interface area (2.70 km^2). Except for Yueyang County, the changes in the spatial scale of the interlocking land and water areas in the remaining units were not pronounced.

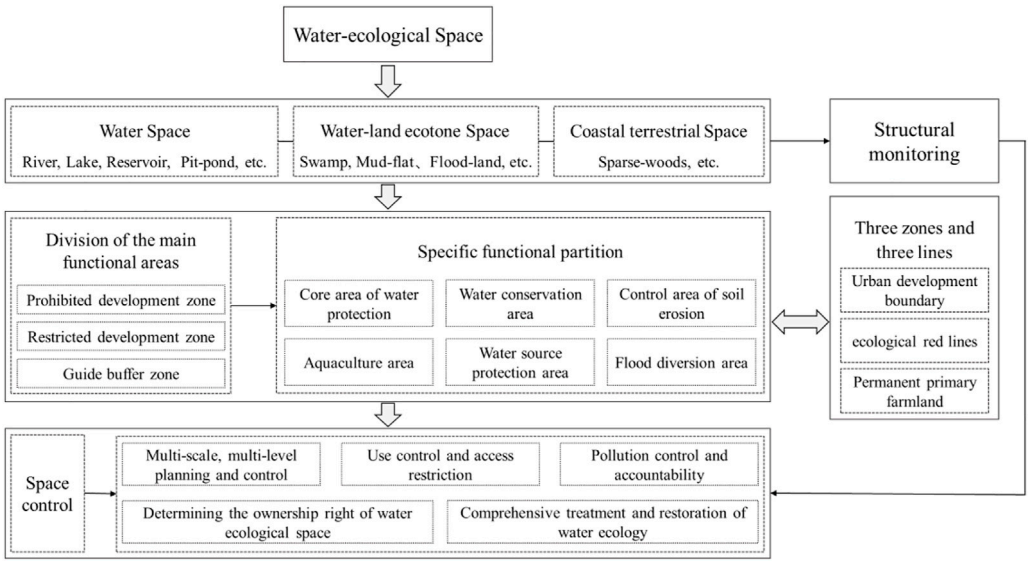

FIGURE 12
Spatial management and control framework for water-ecological space in the Dongting Lake region.

For the adjacent terrestrial zone (Figure 6), Yueyang County had the largest size, with a coastal terrestrial area of 379.11 km^2 in 2010, 374.36 km^2 in 2015, and 370.42 km^2 in 2020. Lixian County came in second with a coastal terrestrial area of 308.59 km^2 in 2010, 306.74 km^2 in 2015, and 306.25 km^2 in 2020. Nanxian County had the smallest coastal terrestrial area, less than 1 km^2, followed by Anxiang County, with about 1.50 km^2 coastal terrestrial area; they had no significant spatial changes in coastal terrestrial extent during the study period.

4 Monitoring of the water ecological space function of Dongting Lake

4.1 Overall function monitoring of water ecological space

As shown in Figure 7, the comprehensive functional value of the water ecological space in the Dongting Lake area improved from 0.3879 in 2010 to 0.4221 in 2020, increasing by 0.0341 and indicating an overall increase in functional service. Growth was most pronounced during 2010–2015, increasing by 0.0264.

Additionally, there were more pronounced differences between units in terms of the integrated function of the water ecological space (Figure 8). Yuanjiang City had the highest integrated function value (0.7185 for 2010, 0.8210 for 2015, and 0.7748 for 2020), experiencing a process of rising and then falling, with a total increase of 0.0563. Huarong County and Xiangyin County had the next highest comprehensive functional values (above 0.6), improving over the given research period. Huarong County increased from 0.6092 in 2010 to 0.6527 in 2020, while Xiangyin County increased from 0.6030 in 2010 to 0.6350 in 2020. The comprehensive function of water ecological space in Jinshi City and Linli County was relatively low, which did not exceed 0.1 and slightly decreased for the study period. Linli County's comprehensive function value decreased from 0.0693 in 2010 to 0.0665 in 2020, while Jinshi City's decreased from 0.0544 to 0.0527. The comprehensive function of water ecological space declined at varying degrees in Linxiang City, Nanxian County, and Hanshou County. In ten units, including Anxiang County, Yueyang Municipal District, and Changde Municipal District, the overall functional value of the water ecological space increased to varying degrees; Anxiang County had the largest increase of 0.1450 among them.

4.2 Ecological function monitoring

From Figure 7, the ecological function of the water ecological space in the study area exhibited a decreasing trend, decreasing from 0.3382 in 2010 to 0.3182 in 2020. This suggests that the ecological service function of the water ecological space in Dongting Lake had been disturbed to a certain extent, leading to a decrease in its natural regulation and support capacity. However, this decline has slowed, decreasing by 0.0167 in 2010–2015 to 0.0032 in 2015–2020, indicating that the construction of ecological civilization has significantly promoted the protection and restoration of water ecological spaces.

The spatial function values of the water ecological space differed significantly between units (Figure 9). In 2010, the unit with the highest ecological function value was Yueyang County (0.9586), followed by Yuanjiang City (0.7448) and Xiangyin County (0.5164), while Jin City had the lowest at 0.0970. The function values in the remaining units were mostly between 0.1 and 0.5, consistent with the distribution of water zones in the Dongting Lake area. The core waters and marshes of Dongting Lake are mainly located in Yueyang County, Yuanjiang City, Xiangyin County, Huarong County, and Yueyang City, so their water conservation value is high. Yueyang County, Xiangyin County, and Li County have wide forest regions,

so their water and soil conservation value is relatively high. In these areas, the ecological function values of water ecological space are comparatively higher than the other units.

The spatial pattern of ecological function values did not change significantly. The largest ecological function value in 2015 and 2020 was still Yueyang County, at 0.9429 and 0.9401, respectively. The next two were still Yuanjiang City and Xiangyin County, with function values of 0.7254 and 0.5049 in 2015 and 0.7277 and 0.50 in 2020, respectively. In most units, the ecological function value of water ecological space decreased at varying degrees; Li County had the largest decrease at 0.0574, while Huarong County had the smallest decrease at 0.0054. Only Anxiang County and Nan County had an increase in the ecological function of water ecological space, but the improvement was relatively weak, both within 0.01.

4.3 Social function monitoring

As shown in Figure 7, the social function value increased from 0.47 in 2010 to 0.49 in 2020. This suggests that the reservoir pit building and shoreline flood management in the Dongting Lake area has improved, boosting the water resource support capacity and strengthening the region's water security.

There were noticeable disparities in the social function values of water ecological space among the different units, with the spatial pattern changing dramatically during the study period (see Figure 10). In 2010, Linli county had the lowest social function value at only 0.0275, followed by Jin city at 0.0498. The remaining units had social function values between 0.1000 and 0.8000. Changde city had the highest social function value at 0.9075, followed by Hanshou county at 0.8997. In 2015, the two still had the highest social function values at 0.9443 and 0.9319, respectively, much higher than in 2010; Linli County and Jincheng City had the lowest at 0.0197 and 0.0455, both lower than in 2010. By 2020, Anxiang County had the highest social function value at 0.9157, followed by Nan County at 0.7826; Linli County (0.0331) and Jinshi City (0.0583) still had the lowest amounts but have greatly improved compared to 2010 and 2015. Ten units, including Anxiang County, Nanxian County, Lixian County, Yueyang Municipal District, and Yiyang Municipal District, had improved social function values; Anxiang County increased by 0.3022, the highest among the five. Changde City, Hanshou County, Linxiang City, Yuanjiang City, and Miluo City had declining values, with Hanshou County having the largest decline, decreasing by 0.2072.

4.4 Economic function monitoring

As observed in Figure 7, the economic function value exhibited an upward trend, rising from 0.3619 in 2010 to 0.4611 in 2020. This indicates that the Dongting Lake area's economic production capacity and efficiency, which depend on water space, have increased and that the economic function of water ecological space has further developed.

For the regional units (see Figure 11), the values of the economic function of water ecological space also varied considerably, exhibiting temporal changes in the spatial pattern. In 2010, Nan County had the highest economic function value at 0.9283, followed by Huarong County at 0.8279 and Xiangyin County at 0.8034. Jin City had the lowest economic function value at 0.0163, followed by Linli County at 0.0427. In the remaining units, the economic function value of water ecological space typically ranged between 0.1000 and 0.8000. In 2015, Yuanjiang City had the largest economic function value of water ecological space at 0.9480 (increasing by 0.2758 from 2010), followed by Huarong County at 0.9431 (increasing by 0.1152 from 2010) and Xiangyin County at 0.8366 (increasing by 0.0333 from 2010). Jinshi City and Linli County came in last with 0.0118 and 0.0484, respectively; Jinshi City decreased by 0.0045 from 2010, while Linli County increased by 0.0057 from 2010. For 2020, Huarong County (0.9827) had the largest economic function value of aquatic ecological space, followed by Yuanjiang City (0.8658) and Xiangyin County (0.8593); the lowest economic function values of water ecological space were still Jinshi City (0.0103) and Linli County (0.0548). During the study period, only Nanxian County and Jinshi City had a decrease in economic function value of water ecological space, declining by 0.1902 and 0.0059. The economic functional value of the other units increased at varying degrees. Changde City's growth rate was the highest, increasing by 0.4581, from 0.3078 in 2010 to 0.7659 in 2020.

5 Water ecological space control strategy of Dongting Lake

5.1 The overall framework of water ecological space control of Dongting Lake

The Dongting Lake area is a regional basin unit with Dongting Lake and several rivers at its core, and its development is centered on water ecological space. The region includes core water spaces, the areas where land and water crisscross, and lands adjacent to water. These form the foundation of the water ecological space and should be considered when managing and controlling the space. Water is a fundamental element that maintains the health and order of natural ecosystems and is vital for human survival. Therefore, the water ecological space has dual attributes, playing a decisive role in environmental sustainability and human development (see Figure 12).

Water ecological space can be divided into different functional zones, such as core water conservation, water source conservation, soil erosion control, water source protection, flood regulation and storage, and aquatic product culture. The key to managing and protecting water ecological space is controlling these different functions. Therefore, this paper developed a water ecological space management and control framework from the perspective of "structure-function", as shown in Figure 12.

The framework construction starts with identifying the structural elements, differentiating the functional spaces, and then delineating the zones (e.g., ecological protection red line, urban development boundary, and permanent basic farmland) to layout the functional regions of water ecological space, and systematic monitoring of this structural system of the water ecological space. We should strictly implement the access list system, improve the water resource confirmation and management system, strengthen source control, control pollution

discharge, and strengthen ecological restoration to improve water quality and promote soil and water conservation.

5.2 Main measures of water ecological space control in Dongting Lake

5.2.1 Multi-scale and multi-level planning control

The Dongting Lake area is crucial in the development of the Yangtze River Economic Belt and an important ecological and economic zone in Hunan Province. It comprises many counties and municipalities, so its management is multi-scale and multi-level. The upper limit of water resources, the bottom line of water environment quality, and the red line of water ecology protection should be used as constraints to scientifically and reasonably develop river and lake management and protection. The Dongting Lake will be integrated with other types of ecological protection red lines and protected areas to form a regional ecological barrier, combined with urban development boundaries and farmland borders, and incorporated into the national spatial planning system at provincial, municipal and county levels. The revisions to the Dongting Lake area plan should be accelerated to determine the strategic focus of spatial control.

5.2.2 Strict use control and access restrictions

The zoning control and hierarchical management should be strengthened from the watershed level, and positive and negative access lists should be developed for each control zone. The water ecological space control methods and systems should be improved, prohibiting water-related activities that do not conform to the positioning of each functional zoning of water ecological space. Existing water ecological space layouts and facilities should be integrated and optimized, promoting green construction that meets ecological requirements. To avoid disorderly development, ecological red lines (e.g., protecting drinking water, water conservation areas, protecting sensitive soil erosion areas) should be classified as prohibited development zones, where large-scale development and construction activities are strictly controlled and ecological core functions are resolutely maintained. Industries and facilities that do not meet the requirements to occupy water ecological spaces should be withdrawn unconditionally.

In restricted development zones, no urban construction activities should be carried out. Existing urban construction areas should be gradually withdrawn under conditions, establishing a scientific and reasonable exit mechanism and promoting technological upgrading and green transformation. Ecological industries should be encouraged in the restricted development zone, building green infrastructure such as ecological corridors and ecological isolation zones. In the buffer guidance area, low-polluting, low-energy consuming, and environment-friendly industrial activities should be supported, encouraging the development of modern waterfront leisure, ecological healthcare, green aquaculture, and other industries. The production activities of high pollution and high energy consumption should be carefully monitored and managed, controlling the scale of urban construction and building a compound layout integrated with water ecology.

5.2.3 Accelerate the determination of water ecological space ownership

The watershed is a systematic, holistic, and tightly connected area with strong interactions and constraints between upstream and downstream, trunk and tributaries, and left and right banks. Since it also involves different regions and sectors, spatial ownership and synergistic regional management should be clarified to promote high-quality development of the water ecological spaces. Water ecological space rights should be properly identified based on the waters, shorelines, staggered areas, and the scope of each delineated control area. The ownership and use rights of waters and shorelines (e.g., rivers, lake beaches, reservoir pits, ponds, wetland marshes) should be established to improve the utilization and management of water resources use. Market allocation and a market-oriented system of water ecological space property rights should be established, giving full play to the ecological, resource, social, and economic values of water spaces and guiding relevant interests to solve problems through market means. In addition, efforts should be made to build a regional collaborative governance mechanism, strengthen intra- and inter-regional synergy, and create a collaborative governance community with regional linkage, government organization, enterprise promotion and public participation. Differentiated ecological compensation standards should be developed for different regions, improving the docking mechanism of upstream, downstream, trunk, and tributaries and building a networked ecological compensation system.

5.2.4 Strengthen pollution control and accountability

The water resources and water quality management system should be improved, and the total water resources index should be decomposed to the relevant county-level administrative regions according to the actual situation of each unit. The total amount of restricted discharge of each municipal, county, and administrative unit should be decomposed step by step, and pollution restriction plans should be formulated in stages and regions. A suitable water quality assessment network should be established, strengthening the monitoring of water quantity, quality, and ecological value of important ecological function areas. A regional water ecological space quality monitoring and management index system should be established, and water ecological space control target assessment should be implemented based on the index system. Furthermore, the regional sewage reward and punishment system should be improved, cracking down on illegal and illicit sewage discharge and increasing administrative penalties.

5.2.5 Increase the comprehensive management and restoration of water ecology

Adhering to the concept of integrated management of "mountains, rivers, forests, fields, lakes, grass and sand," the comprehensive management and restoration of water ecological space in the Dongting Lake area should be promoted. Polluted water bodies should be treated, and the water quality of the watershed should be improved. The treatment and restoration of mudflats and swamps should be increased to improve the ecological functions of wetlands and bring into play their great water purification, storage, and transfer values. The return of farming to the lake and forest should be scientifically and orderly promoted,

developing a modern, green, and comprehensive agricultural industry system that reduces encroachment on water bodies and water-land intersection areas and avoids further shrinkage of Dongting Lake waters. At the same time, afforestation measures in the upstream areas should be strengthened to enhance water and soil ecosystem services and increase regional water security. In addition, a diversified water ecology governance and restoration system should be actively explored. The government can adopt purchasing services to attract social capital to participate in water ecology restoration and protection and adopt restoration and protection funds to support areas with weak payment capacity and improve water ecology governance and protection.

6 Conclusion and discussion

6.1 Conclusion

From the "function-structure" standpoint, this paper investigated the monitoring and control of water-ecological space in the Dongting Lake area. The structure and function of the water ecological space were assessed in 2010, 2015, and 2020 using land-use and related statistical data and ArcGIS analysis, and the framework system and key initiatives for spatial control were explored. The main conclusions obtained are as follows:

(1) The scale of water ecological space in the Dongting Lake area is more than 7,300 km^2. The water area accounts for the largest proportion, accounting for about 50%, while the land-water ecotone accounts for the smallest proportion, accounting for about 24%. During the study period, the total area of aquatic ecological space decreased slightly; the decrease in water space was most pronounced, its proportion decreasing from 51.04% to 47.21%, while the area of land-water ecotone increased from 21.62% to 25.79%. In addition, there were considerable variations in the scale of water ecological space among the different administrative units. Yueyang County and Yuanjiang City had water ecological spaces larger than 1,000 km^2, while Linli County and Jinshi City had below 200 km^2.

(2) The comprehensive function of water ecological space in Dongting Lake increased from 0.3879 in 2010 to 0.4221 in 2010, indicating improved overall functional service. In particular, the social and economic function values increased considerably, while the ecological function value somewhat decreased. Yuanjiang City had the highest comprehensive function with a value of over 0.7000, while Jinshi City and Linli County had the lowest value of less than 0.1000. For ecological functions, the highest value was Yueyang County, while the lowest was Jinshi City. For social functions, the highest was Changde City and Anxiang County and the lowest was Linli County. For economic functions, the highest values were Nanxian Yuanjiang and Huarong while the lowest was Jinshi.

(3) The concept of harmony between man and nature should guide the management and control of the water ecological space in the Dongting Lake area. Starting with the structural components of the water ecological space, the various functional areas should be logically separated, the functional zoning of the water ecological space should be scientifically planned and laid out, and the delineation of ecological protection red lines, urban development boundaries, and permanent basic farmland should be combined. Based on this, multi-scale and multi-level planning oversight should be improved, access and use restrictions should be strictly regulated, the ownership of water ecological space should be properly defined, water quality monitoring and treatment should be integrated, pollution control and accountability should be improved, and comprehensive management and restoration of water ecology should be increased.

6.2 Discussion

According to the research idea of "land use foundation-structural function system-pattern evolution monitoring-control system construction," this paper explored the theory and method of water ecological space monitoring and control in the context of land space optimization. This study provides an in-depth analysis of water ecological space control, expanding the literature on water ecological space and offering a comprehensive perspective of micro-monitoring and single-function measurement. It is also a development in the study of national spatial planning for the modern era, advancing the reasonable delineation and adjustment of the "three zones and three lines" and crucial to the control of spatial use of national land and the preservation and high-quality development of water ecological spaces. In the age of ecological civilization, resolving conflicts between people and land and people and water is crucial in economic and social advancement (Zhou et al., 2020b). To mitigate the adverse effects of human activity on water ecosystems and promote water sustainability, it is crucial to explore and understand the various functions of water ecological spaces and the relationship between function and structure.

However, it should be noted that the classification system of water ecological space structure and function in this paper is still not sufficiently detailed due to limitations in data availability. For example, the subdivision structure and function did not include climate regulation, biodiversity maintenance, flood storage capacity, and other water ecological functions (e.g., waterfront leisure area, paddy field, and water buffer zone), limiting the current analysis depth. Subsequent studies should collect more data through multiple channels and means to establish a more comprehensive and detailed "structure-function" classification system. Additionally, due to space constraints, this paper did not address micro-water ecological quality monitoring and restoration issues, including water quality monitoring, aquatic organism quantity and diversity monitoring, water purification, and water resources supply management. This may limit future research on the quality supervision of water ecological space. In future research, the theory and technique for monitoring the pattern and quality of the landscape should integrate macro,

meso, and micro scales to thoroughly assess the dynamic evolution of the water ecological space and carry out thorough scientific management and control.

Data availability statement

The original contributions presented in the study are included in the article/Supplementary Material, further inquiries can be directed to the corresponding author.

Author contributions

ZZ: Conceptualization, methodology, software, formal analysis, writing—original draft and review and editing, project administration. HY: Methodology and formal analysis. HZ: Methodology, formal analysis, writing—review and editing. NL: Writing—review and editing, supervision, and funding acquisition. QS: Writing—review and editing, supervision. QJ: Writing—review and editing, supervision. QN: Writing—review and editing, supervision. All authors contributed to the article and approved the submitted version.

Funding

This research was funded by the "Research project of Hunan Geological Institute" (HNGSTP202206), "Scientific Research Foundation of Hunan Provincial Education Department of China" (No. 21A0506) and "National Science Foundation of Hunan Province of China" (No. 2022JJ50271).

Conflict of interest

The authors declare that the research was conducted in the absence of any commercial or financial relationships that could be construed as a potential conflict of interest.

Publisher's note

References

Aina, G., Bárbara, O., and Araceli, P. (2015). Environmental risk assessment of water quality in harbor areas: A new methodology applied to European ports. *J. Environ. Manag.* 155, 77–78. doi:10.1016/j.jenvman.2015.01.042

Alberti, M., Booth, D., Hill, K., Coburn, B., Avolio, C., Coe, S., et al. (2006). The impact of urban patterns on aquatic ecosystems: An empirical analysis in Puget lowland sub basins. *Landsc. Urban Plan.* 80 (4), 345–361. doi:10.1016/j.landurbplan.2006.08.001

Baltodano, A., Agramont, A., Reusen, I., and van Griensven, A. (2022). Land cover change and water quality: How remote sensing can help understand driver-impact relations in the lake titicaca basin. *Water* 14 (7), 1021. doi:10.3390/w14071021

Benra, F., De Frutos, A., Gaglio, M., Álvarez-Garretón, C., Felipe-Lucia, M., and Bonn, A. (2021). Mapping water ecosystem services: Evaluating InVEST model predictions in data scarce regions. *Environ. Model. Softw.* 138, e104982. doi:10.1016/j.envsoft.2021.104982

Bo, L. M., Wei, W., Yin, L., Zhao, L., and Xia, J. N. (2022). Changes in the spatial pattern of water ecology in the Yangtze River Economic Belt and its influencing factors from 2000 to 2020. *China Environ. Sci.* 2022. doi:10.19674/j.cnki.issn1000-6923.20220915.010

Cao, J., Wang, L., Chen, T. T., and Wei, Z. C. (2014). From ideal to reality: The construction of basic ecological space in cities: An example of the basic ecological space plan of feidong county, hefei city. *Planner* 30 (6), 51–57. doi:10.3969/j.issn.1006-0022.2014.06.008

Cecília, G. L., Paulo, S. P., Toby, A. G., Leitão, R. P., Hughes, R. M., Kaufmann, P. R., et al. (2016). Multi-scale assessment of human-induced changes to Amazonian instream habitats. *Landsc. Ecol.* 31 (8), 1725–1745. doi:10.1007/s10980-016-0358-x

Chen, D. L., Peng, B. F., and Xiong, J. X. (2013). The coupling characteristics of ecological and economic systems in the Dongting Lake area. *Geoscience* 33 (11), 1338–1346. doi:10.13249/j.cnki.sgs.2013.11.007

Chen, Q., Chen, Y. H., Wang, M. J., Jiang, W. G., Hou, P., and Li, Y. (2015a). Remote sensing comprehensive evaluation and change analysis of Dongting Lake ecosystem quality from 2001 to 2010. *J. Ecol.* 35 (13), 4347–4356. doi:10.5846/stxb201403250557

Chen, Y., Zhang, J. J., Du, G. M., Fu, M. C., and Liu, L. L. (2015b). Spatial and temporal evolution of ecosystem service values in the northern Sanjiang Plain. *J. Ecol.* 35 (18), 6157–6164. doi:10.5846/stxb201401020014

Chitresh, S., Binaya, K. M., and Pankaj, K. (2017). Integrated urban water management scenario modeling for sustainable water governance in Kathmandu Valley, Nepal. *Sustain. Sci.* 12 (6), 1037–1053. doi:10.1007/s11625-017-0471-z

Deng, C. X., Zhong, X. L., Xie, B. G., Wan, Y. L., and Song, X. W. (2019). Spatial and temporal variation in the service value of land ecosystems in the Dongting Lake area. *Geogr. Res.* 38 (04), 844–855. doi:10.11821/dlyj020170999

Deng, W., Yan, D. H., He, Y., and Zhang, G. X. (2004). Research on water ecological space in watersheds. *Adv. Water Sci.* 3, 341–345. doi:10.14042/j.cnki.32.1309.2004.03.014

Du, Z., Zhang, G., and Shen, L. F. (2013). Research on ecological space control in Chengdu. *Urban Plan.* 37 (8), 84–88.

Gerald, E., and Galloway, M. (1997). river basin management in the 21st century: Blending development with economic, ecologic, and cultural sustainability. *Water Int.* 22 (2), 82–89. doi:10.1080/02508069708686675

Ghosh, A., and Maiti, R. (2021). Development of new Ecological Susceptibility Index (ESI) for monitoring ecological risk of river corridor using FAHP and AHP and its application on the Mayurakshi river of Eastern India. *Ecol. Inf.* 63, 101318. doi:10.1016/j.ecoinf.2021.101318

Huang, X. X., Jiang, Y., Xiong, X., He, K. J., and Zhang, Y. (2012). Research on water ecological function zoning. *Water Resour. Conserv.* 3, 22–27. doi:10.3969/j.issn.1004-6933.2012.03.004

Jiang, C., Liu, H. Y., Chen, Z., Rao, C., and Li, Z. D. (2018). GIS-based land use change and water quality response in the Hongfeng Lake watershed. *J. Agric. Environ. Sci.* 37 (6), 1232–1239. doi:10.11654/jaes.2017-1598

Kang, L. T., Hu, X. J., Luo, Z. W., Wei, B. J., and Zhou, D. M. (2022). Spatial identification of county water ecology and its distribution characteristics. *J. Soil Water Conservation* 36 (01), 170–181. doi:10.13870/j.cnki.stbcxb.2022.01.023

Li, J. C., Wang, W. L., and Hu, G. Y. (2011). Impacts of land use and cover changes on ecosystem service value in Zoige Plateau. *Acta Ecol. Sin.* 31 (12), 3451–3459.

Li, Y. M., Zeng, W. X., and Zhou, Q. X. (2009). Research progress of water ecological function zoning. *J. Appl. Ecol.* 20 (12), 3101–3108. doi:10.13287/j.1001-9332.2009.042

Liu, C., Xu, Y. Q., Liu, Y. X., Sun, P. L., Huang, A., and Zhou, J. (2018a). A system theory-based multifunctional land use classification and evaluation index system. *J. Peking Univ. Nat. Sci. Ed.* 54 (1), 181–188. doi:10.13209/j.0479-8023.2017.132

Liu, M., and Wang, K. L. (2008). Landscape pattern change and its driving forces in middle and upper reaches of Dongting Lake watershed. *J. Appl. Ecol.* 19 (6), 1317–1324. doi:10.13287/j.1001-9332.2008.0231

Liu, P., Duan, J. N., Wang, W., and Zeng, M. (2010). Study on functional classification and evaluation system of land use system. *J. Hunan Agric. Univ. Nat. Sci. Ed.* 36 (1), 113–118.

Liu, W., Yang, Q., Zhang, M. R., Zhao, W., and Zhai, Y. (2018b). Research on building a watershed-based spatial control system for water ecology. *China Water Resour.* 5, 27–31.

Liu, Z., Zhang, N., Peng, D. H., Zhang, Y. Z., Zhang, D., and Qin, X. C. (2022). DNAJA4 promotes the replication of the Chinese giant salamander iridovirus. *Environ. Monit. China* 38 (01), 58–71. doi:10.3390/genes14010058

Ning, Q. M., Ouyang, H. Y., Tang, F. H., and Zeng, Z. W. (2020). Spatial and temporal evolution of landscape patterns in the Dongting Lake area under the influence of land use change. *Econ. Geogr.* 40 (09), 196–203. doi:10.15957/j.cnki.jjdl.2020.09.021

Ouyang, X., Xu, J., Li, J. Y., Wei, X., and Li, Y. H. (2022). Land space optimization of urban-agriculture-ecological functions in the Changsha-Zhuzhou-Xiangtan Urban Agglomeration, China. *Land Use Policy* 117, 1061112. doi:10.1016/j.landusepol.2022.106112

Qiu, B., Liu, W., Zhang, J. Y., Zhang, M. R., and Zhao, W. (2017). Exploration of water ecological spatial control system construction. *China Water Resour.* 16, 16–20.

Ren, J. L., Li, H., Wu, X. M., and Li, X. S. (2016). Evaluation of water ecological civilization in provincial capital cities of Yangtze River Economic Belt based on principal component analysis. *Yangtze River Basin Resour. Environ.* 25 (10), 1537–1544. doi:10.11870/cjlyzyyhj201610008

Su, C. W., Deng, Z. B., Li, L. P., Wen, J. X., and Cao, Y. F. (2021). Spatial pattern evolution and convergence of water eco-civilization development index in China. *J. Nat. Resour.* 36 (05), 1282–1301. doi:10.31497/zrzyxb.20210515

Tang, Y., WangWang, C. G. W. Q., Huang, H. J., and Yuan, Y. (2020). Multifunctional classification of aquatic habitats for remote sensing data. *Adv. Geoscience* 39 (3), 454–460. doi:10.18306/dlkxjz.2020.03.010

Wang, Q., and Tang, F. H. (2015). Spatial and temporal differentiation of the coupled and coordinated development of ecological-economic-social systems in the Dongting Lake area. *Econ. Geogr.* 35 (12), 161–167. doi:10.15957/j.cnki.jjdl.2015.12.023

Wei, G. E., Bi, M., Liu, X., Zhang, Z. K., and He, B. J. (2023). Investigating the impact of multi-dimensional urbanization and FDI on carbon emissions in the belt and road initiative region: Direct and spillover effects. *J. Clean. Prod.* 384, 135608. doi:10.1016/j.jclepro.2022.135608

Wu, D., Zhang, L., Yu, L., Ding, N., and Tang, Z. (2021). Research on ecological management of water affairs under the high quality development of land space: The case of guangming district, shenzhen. *J. Urban Plan.* 4, 66–73. doi:10.16361/j.upf.202104010

Xie, G. D., Lu, C. X., Leng, Y. F., Zheng, D., and Li, S. C. (2003). Valuation of ecological assets on the Qinghai-Tibet Plateau[J]. *J. Nat. Resour.* 18 (2), 189–196.

Yang, F., Li, Z., Luo, W. L., Wu, G., Lippuner, K., and Hunziker, E. B. (2021). Anticytokine Activity Enhances Osteogenesis of Bioactive Implants. *Econ. Geogr.* 41 (08), 177–186. doi:10.1089/ten.TEA.2020.0067

Yang, Q., Wang, X. H., Zhang, J. Y., Zhao, W., Jia, R., Zhu, D., et al. (2017a). GoTLR7 but not GoTLR21 mediated antiviral immune responses against low pathogenic H9N2 AIV and Newcastle disease virus infection. *China Water Resour.* 3, 6–15. doi:10.1016/j.imlet.2016.11.001

Yang, Q., Zhang, M. R., Zhao, W., Zhang, J. Y., and Wang, X. H. (2017b). Water ecological spatial function and control classification. *China Water Resour.* 12, 3–5. doi:10.13201/j.issn.1001-1781.2017.01.002

Yang, Q., Zhao, W., Zhang, J. Y., and Wang, X. H. (2017c). Construction of water ecological space control index system. *China Water Resour.* 9, 1–5.

Yin, K., Liu, H. J., Wang, G., and Jin, X. W. (2021). Overview of habitat monitoring methods under spatial control of watershed water ecology. *Environ. Sci.* 42 (03), 1581–1590. doi:10.13227/j.hjkx.202007287

Zhou, L., Dang, X. W., Mu, H. W., Wang, B., and Wang, S. H. (2020b). Cities are going uphill: Slope gradient analysis of urban expansion and its driving factors in China. *Sci. Total Environ.* 775, 145836–145910. doi:10.1016/j.scitotenv.2021.145836

Zhou, L., Hu, F. N., Wang, B., Wei, C. Z., Sun, D. Q., and Wang, S. H. (2022b). Relationship between urban landscape structure and land surface temperature: spatial hierarchy and interaction effects. *Sustain. Cities Soc.* 80, 103795–103812. doi:10.1016/j.scs.2022.103795

Zhou, L., Yuan, B., Hu, F. N., Wei, C. Z., Dang, X. W., and Sun, D. Q. (2022a). Understanding the effects of 2D/3D urban morphology on land surface temperature based on local climate zones. *Build. Environ.* 208, 108578–108610. doi:10.1016/j.buildenv.2021.108578

Zhou, L., Zhou, C. H., Che, L., and Wang, B. (2020a). Spatio-temporal evolution and influencing factors of urban green development efficiency in China. *J. Geogr. Sci.* 30 (5), 724–742. doi:10.1007/s11442-020-1752-5

Zhu, D. S., Zhang, J. Y., Wang, X. H., and Yang, Q. (2017). Ideas for promoting spatial control of water ecology in China. *China Water Resour.* 16, 1–5.

Zuo, Q. T., Zhang, Z. Z., and Ma, J. X. (2021). Classification scheme of water resources and its disciplinary system. *Resour. Sci.* 43 (11), 2215–2223. doi:10.18402/resci.2021.11.06

frontiers | Frontiers in Environmental Science

TYPE Original Research
PUBLISHED 13 June 2023
DOI 10.3389/fenvs.2023.1206705

OPEN ACCESS

EDITED BY
Salvador García-Ayllón Veintimilla,
Technical University of cartagena, Spain

REVIEWED BY
Zheng Shiyong,
Guilin University of Electronic Technology, China
Amar Razzaq,
Huanggang Normal University, China

*CORRESPONDENCE
Jingyi Xiao,
xiaojingyi@qhnu.edu.cn
Zhucheng Su,
20070173@zafu.edu.cn

RECEIVED 16 April 2023
ACCEPTED 31 May 2023
PUBLISHED 13 June 2023

CITATION
Shu R, Xiao J and Su Z (2023), Spatiotemporal trends and factors influencing online attention for China's tea industry.
Front. Environ. Sci. 11:1206705.
doi: 10.3389/fenvs.2023.1206705

Spatiotemporal trends and factors influencing online attention for China's tea industry

Rentian Shu[1,2], Jingyi Xiao[1,2]* and Zhucheng Su[3]*

[1]School of Geographical Sciences, Qinghai Normal University, Xining, China, [2]Key Laboratory of Natural Geography and Environmental Processes of Qinghai Province, Xining, China, [3]College of Tea Science and Tea Culture, Zhejiang Agriculture and Forestry University, Hangzhou, China

In the context of the "Internet plus" era, the study of tea industry online attention is a new perspective in research on the tea industry and an opportunity for the sustainable and high-quality development of this industry. Based on the Baidu index, this paper obtains web attention data from 2012 to 2021, analyzes the spatial and temporal evolution characteristics of online attention using the seasonal concentration index and geographic concentration index, and quantitatively discusses the influencing factors using correlation analysis and GeoDetector. The results show the following: The interannual change in China's tea industry online attention shows "rapid growth, high level of stability, slow decline," the monthly distribution has an intense concentration, mainly in March-April and October, and the interday distribution of attention peaks on weekdays. The spatial distribution shows an intense geographical concentration, with an overall trend of "light concentration first, then light dispersion." The migration trajectory of the center of attention is tilted toward the southwest. Economic development status, residents' income, the natural environment of tea growing, the leisure time of followers, and the price level of tea are the essential factors affecting the of the tea industry online attention. In contrast, the other factors we have chosen have a weaker impact on online attention compared to the few factors just mentioned.

KEYWORDS

internet plus, tea industry, online attention, influencing factors, GeoDetector, baidu index, spatiotemporal trends

1 Introduction

1.1 Background and literature review

China is the birthplace of tea (Meegahakumbura et al., 2017), and tea culture has a long history. Tea is an essential traditional economic crop in China. Over the past 40 years, China's modern tea industry has been developing rapidly, with tea plantation area, tea production, and domestic tea consumption ranking first globally. However, with "Internet plus" and globalization vision, the traditional model of the tea industry is facing unprecedented challenges. With the rapid development of network applications, "Internet plus" is becoming a catalyst for dramatic changes in various fields and industries. The development of the "Internet plus tea industry" model is a crucial way to promote regional development, improve the living standards of residents, and support rural revitalization and industrial integration and is a typical example of the transformation of the

development of traditional industries and a new opportunity for the high-quality development of the tea industry.

Online attention (OA) refers to the users' degree of concern and demand for information through online searches for relevant information (He et al., 2017), which reflects the degree of concern and request of users according to the search volume, and its data sample size is large and time-sensitive (Sun et al., 2017). Chinese users mainly use the search engines Baidu, Bing, and Google, of which Baidu accounts for approximately 72.4%, so the Baidu index, as one of the big data indicators for studying online attention, can broadly reflect the temporal and spatial characteristics of Chinese users in regard to the tea industry online attention (Abbreviated as TIOA). Producers release information to the public through online platforms. Consumers, in turn, follow, understand and access information through Internet channels to inform their decisions. Online attention on the one hand becomes an important channel for followers to obtain information and assist in decision-making. On the one hand, researchers and some industry personnel can use big data technology to analyze and mine the historical data and dynamic evolution, summarize industrial development laws, patterns and predict development trends. The study of the spatial and temporal characteristics of network attention and its influencing factors has certain guiding significance for production information management and online marketing.

Research on online attention was first started by Western scholars (Katz and Aspden, 1997; Kwan et al., 2006), mainly exploring topics such as search behavior and consumer decision-making based on Google Trends. It is found that Internet search data reflect users' attention to a certain phenomenon or thing to a certain extent, and to a certain extent there is a correlation with real social behavior (Ginsberg et al., 2008). In recent years, global scholars have focused their research on online attention in tourism (Yang et al., 2015; Zhang et al., 2022), media (Holt et al., 2013), disease surveillance (Hu et al., 2022), hazard monitoring (Guo et al., 2022), finance and trade (Jue et al., 2017; Cheraghali et al., 2022). This research is mainly concerned with the spatiotemporal characteristics (Zhang et al., 2016), marketing strategies (Cai et al., 2016), and empirical coupling studies (Ju et al., 2017) of online attention.

Research on "Internet plus" in the tea industry has focused on the following areas. Hu's research review provides an outlook on Internet + tea through concept definition, overview framework, and application prospects (Hu, 2015). In terms of empirical research, Shen conducted a sample of respondents through in-depth interviews in the field. It was concluded that the media and the Internet provide opportunities for the development of small and medium scale, pointing out the contribution made to the economy of the tea industry and rural revitalization (Shen and Chou, 2022). Paul developed a conceptual model of a BCT-driven tea supply chain by integrating BCT into the tea supply chain and investigated its positive impact on the tea supply chain based on the structural equation of partial least squares regression (Paul et al., 2021). Dou et al. (2021) used data from yearbooks, statistical handbooks, *etc.* An evaluation index system affecting the price of pu-erh tea was established and an empirical study was conducted using TOPSIS method. It was pointed out that economic development factors and Internet development level factors have a great influence on the price, so it proposed that the need to use Internet thinking is an important work for the tea industry in the future (Dou et al., 2021). Liu et al., studied an IoT-aware machine learning (ML) approach for early prediction of disease probability in agricultural environment, which plays an active role in the application of precision agriculture (Liu K. et al., 2022). Xu adopted a mixed-method approach and conducted a questionnaire survey of key practitioners, the public sector, and domestic and international tourists during fieldwork in the West Lake Longjing tea region, with the aim of analyzing the problems and proposing countermeasures for the development of tea tourism in China in the era of the experience economy (Xu, 2022). KHAN used a structured questionnaire and constructed a structural equation model. The extent of customers' decision to purchase tea was studied in terms of social influence, shared vision, psychological evaluation and mutual trust, concluding that internet always has a crucial role in individuals' decision to purchase, use and change their perception. (Khan et al., 2021). For concern people, information was usually obtained through TV, radio, books, and conversations, but nowadays, the Internet can be used to obtain a large amount of information easily and quickly. For researchers and practitioners, data are usually obtained through field research, in-depth interviews, volunteer experiments, statistical yearbooks, *etc.*, which is more difficult to obtain information and the amount of data is limited. Compared with traditional information dissemination methods, Internet+ and big data have convenient and efficient features, which make up for these problems very well.

Internet data is rich in value, which helps to discover the development rules of the industry and provide information for industry decision-making. Baidu index is used to conduct statistics and analysis of internet search attention of the tea industry, with a view to providing reference for tea industry producers to better understand and grasp market demand. It has certain significance for the tea industry to formulate regionalized, seasonal and precise marketing strategies and deploy transportation resources, revealing the precursor effect and spatio-temporal characteristics of online attention, and providing scientific reference for the layout of the tea industry. The application of Internet + helps the transformation and optimization of the tea industry, a traditional industry, to upgrade.

From the research method, the current research is mostly qualitative research, and the results of quantitative research are relatively few. From the data sources, it is mostly questionnaire interviews, statistical data and yearbook data, and the data types are mostly cross-sectional data. In terms of research content, the fields involved are relatively broad, and there are fewer studies combining Internet + tea with geography. Therefore, compared with previous studies, this paper is innovative in terms of research design.

In the context of "Internet + tea industry", there are more achievements in other fields, but there are fewer studies on the tea industry online networks, and the tea industry "Internet+" has not been studied quantitatively using big data. Studies of the tea online attention perspective based on internet big data are even rarer. Thus, As for the innovation point of this paper, a cross-disciplinary study of the spatial and spatiotemporal distribution characteristics and influencing factors of China's tea industry online attention is conducted based on a multidisciplinary perspective and geographic spatiotemporal thinking and using internet big data.

In addition, in the research of influencing factors, compared with the same type of research, qualitative analysis, GWR model and correlation analysis are mostly used, and we introduce GeoDetector to detect factors and interact with influencing factors, which are less used in the same type of research. The aim of this paper is to provide data support for the marketing decisions of the tea industry, which is helpful for accurately understanding demand so that targeted products and services can be offered and is greatly significant for the high-quality and sustainable development of the tea industry.

1.2 Study area overview

The research object of this paper is the tea industry online attention in 31 provincial administrative regions in China, excluding Hong Kong, Macao and Taiwan. In this paper, China is divided into tea production and marketing areas according to the production status of the tea industry (Xiao et al., 2018). The production and marketing area, that is, the tea production area, is mainly distributed in the latitude range of 18°N~37°N and the longitude range of 95°E~122°E. It is primarily classified into four tea regions, namely, the North Yangtze, South Yangtze, South China and Southwest tea regions. Warm weather, suitable ground that is acid and not alkali, and shade, not Sun, are best for growing tea, so the tea industry and the distribution of tea-producing areas and the geographical environment of tea growth are closely linked. The tea production distribution map of China was drawn based on tea production data from 2012 to 2021 (Figure 1). The spatial distribution of the tea industry reflects the tea production of each province. Provinces with high production include Hubei, Zhejiang, Yunnan, Fujian, Anhui, Jiangsu, Sichuan and Henan. These provinces are the main tea-producing areas in China and have more complete supportive industrial chains, with higher production and marketing value and a more intensive tea industry. Other provinces such as Shaanxi and Shandong also have a small amount of tea industry distribution. The above areas are the production and marketing areas of China's tea industry, and other areas are the sales areas of China's tea industry. In general, the distribution of China's tea industry has a "dense south and sparse north" pattern.

2 Theoretical framework

The theory of limited attention is derived from psychology and was first applied to research in the field of investment. It focuses on the relationship between asset prices and investor behavior. Scholars have concluded in their research that people can only pay attention to one thing within a time period, and it is difficult to pay attention to more than one thing at the same time (Cherry, 1953). People cannot obtain and understand information in a timely manner due to limited time and energy and can only analyze and judge the information that attracts their attention. For followers and potential followers, there is a large amount of information about the tea industry on the Internet, and usually only a limited amount of attention will be directed to attractive content at a certain time. This also leads to differences in the degree of attention received by different regions at different times, which provides the basis for this paper to analyze the spatial and temporal differences in the online attention of the tea industry in China and the influencing factors.

Spatio-temporal thinking is one of the characteristics of geographic research. Temporal thinking is reflected as ephemeral research, cotemporal research and anticipatory research; spatial thinking is reflected as spatial distribution, spatial structure and spatial relationship (Yao-feng et al., 2011). The organic combination of spatial thinking and temporal thinking reflects the unity of ephemerality and co-occurrence. In this paper, the use of Spatio-temporal thinking helps to enhance the depth and scientificity of research on issues such as spatial evolution and temporal research.

As a new subdiscipline of geography, cyberspace geography is an extension of real space to virtual space, which transforms the traditional human-land relationship into a new human-land-net relationship (Gao et al., 2019). Big data technology has "6 V" characteristics: volume, variety, velocity, veracity, value, and valence. Based on the principle of big data visualization to visualize abstract data in visual graphics, geospatial thinking is used to present the information and Spatio-temporal dynamic laws implied in the data.

Hypotheses H1. and H2 were proposed based on limited attention theory and Spatio-temporal thinking theory, and the hypotheses were verified using geospatial statistical methods, correlation analysis and geographic detectors.

H1. Chinese tea industry network attention has significant divergent characteristics in Spatio-temporal distribution.

H2. Natural factors, economic factors and social factors have a significant influence on the spatial pattern of attention.

To study the distribution characteristics of network attention, first, hypothesis H1H2 is proposed based on theories such as limited attention theory, Spatio-temporal thinking and network spatial geography theory. Second, the Spatio-temporal pattern of Chinese tea industry network attention is analyzed with the theoretical framework of the scale-pattern-process-mechanism; geospatial statistical methods, correlation analysis and geographic detectors are used to study the influencing factors to verify the hypothesis of H1H2 (Figure 2).

3 Materials and methods

3.1 Data source

Since the study area of this paper is China, we used the Baidu index, which is owned by Baidu, the world's largest Chinese search engine, with the aim of improving the accuracy of the study. For this paper, we use "cha (tea)" and "cha ye (tea leaf)" as keywords in the Baidu index platform to obtain daily, monthly and yearly data on the internet attention of 31 provincial-level administrative regions (Hong Kong, Macao and Taiwan are not included in the study because the values for these areas are too low). The Baidu index data for this term started in February 2011. For the sake of data integrity, 2012 is taken as the starting year of data, and 2021 is taken as the cutoff year of data. The climate data and socioeconomic statistics from 2012 to 2021are

obtained from the statistical yearbooks, statistical bulletins and government work reports of each province (autonomous region).

3.2 Research methods

3.2.1 Interannual variation index

The interannual variation index is an index that describes the interannual variation in web attention based on the average value of web attention over many years, where *Yv* is the interannual variation index, N_i is the value of web attention in year i, and n represents the number of study years. The closer to 100% the value of *Yv* tends to be, the less the interyear variation of online attention is, and the more stable the online attention is, and *vice versa*. A *Yv* value greater than 100% indicates that the web concern of the place is higher than the overall average. A *Yv* value less than 100% indicates that it is lower than the overall average (Bao and Chen, 2017; Wang et al., 2022; Yan, 2023).

$$Y_v = \frac{N_i}{\frac{\sum_{i=0}^{n} N_i}{n}} \times 100\% \tag{1}$$

3.2.2 Seasonal concentration index

This index is used to reflect the concentration of the research subjects in monthly time (Zhang et al., 2016). In this index, xi is the proportion of the attention of each month in the whole year, and *R* is the seasonal concentration index. The more *R* tends to zero, the more uniform the monthly online attention distribution and the smaller the seasonal concentration; the more significant the *R* value is, the more dispersed the attention distribution and the greater the seasonal concentration (Ma and Long, 2017; Tang and Bao, 2018; Guan et al., 2022).

$$R = \sqrt{\frac{\sum_{i=1}^{12} (x_i - 8.33)^2}{12}} \tag{2}$$

3.2.3 Geographical concentration index

This index is an indicator of the degree of geographical concentration of an economic activity (Xiao et al., 2018), reflecting the concentration or dispersion of the regional distribution of the tea industry online attention. In the formula, p_j indicates the tea industry online attention in region *j*; *p* indicates the total amount of tea industry online attention, and *G* is the geographical concentration index, *n* represents the number of regions. The closer *G* is to 100, the more concentrated the online attention is in a particular region, and *vice versa*, the more dispersed it is (Frandsen, 2005; Wren, 2012).

$$G = 100 \times \sqrt{\sum_{j=1}^{n} \left(p_j / p\right)^2} \tag{3}$$

3.2.4 Intra-weekly distribution skewness index

This index is used to measure the concentrated distribution characteristics of the tea industry online attention on the micro time scale within weeks. The calculation formula is:

$$W = 100 \times \frac{2}{7}\left(\sum_{i=1}^{7} i f_i - \frac{(7+1)}{2}\right) \tag{4}$$

In the formula, if_i is the ratio of online attention on day *i* to online attention in the week. If $W < 0$, the online attention is distributed in the early part of the week; if $W > 0$, the attention is mostly concentrated in the late part of the week; and if $W = 0$, the attention is symmetrically distributed throughout the week (Liu et al., 2010; Qiu and Zheng, 2017; Rosselló and Sansó, 2017).

3.2.5 GeoDetector

GeoDetector (GD) is a model that is used to detect spatial heterogeneity, explain the explanatory strength of the differential driving forces behind its influencing factors, and reveal factor interactions (Wang et al., 2016). In this paper, we use the factor detection and interaction detection functions to clarify the explanatory strength of each influencing factor on the attention of the tea industry online and to detect the interaction between each influencing factor indicator.

$$q = 1 - \frac{\sum_{h=1}^{L} N_h \sigma_h^2}{N\sigma^2} \tag{5}$$

The *q* in the formula is the impact factor impact strength detection value, N_h is the number of cells contained in the probe element and the whole area, and *N* is the variance between the element layer *h* and the Y value of the whole area, *L* is the stratification (Strata) of variable Y or factor X, representing the classification or partition. *q* has a value range between 0 and 1 if the stratification is generated by the independent variable *X*; the larger the *q* value is, the more substantial the explanatory power of the independent variable *X* on the attribute *Y*, and *vice versa* (Liao et al., 2021; Liu Z. et al., 2022).

4 Results

According to the theoretical analysis framework of "scale - pattern - process - mechanism", the research results mainly illustrate three academic issues: firstly, to explore the temporal characteristics of the Chinese tea industry online attention; secondly, to explore the evolution of the spatial distribution pattern of the Chinese tea industry online attention; thirdly, to establish the index system of the influencing factors of the tea industry online attention, and to study the influencing factors based on qualitative and quantitative analysis and geographic detectors.

4.1 Temporal distribution trends of TIOA

There are various scales for analyzing the temporal characteristics of online attention, and this study aims to analyze the temporal characteristics of online attention in detail and specifically through three time scales: annual, monthly, and intra-weekly, and to provide reference for production operators to develop seasonal and seasonal production and marketing strategies through temporal characteristics.

TABLE 1 Seasonal intensity index and intraweekly distribution skewness index of China's tea industry online attention from 2012 to 2021.

Year	2012	2013	2014	2015	2016	2017	2018	2019	2020	2021
R	8.247	8.247	8.238	8.231	8.226	8.227	8.233	8.232	8.247	8.252
W	−2.472	−7.725	−2.088	−1.705	−0.644	−1.144	−1.221	−1.391	−2.362	−1.291

4.1.1 Inter-annual characteristics

The interannual variation index was used to quantify the interannual variation in tea industry online attention (Figure 3). The resulting Yv values all ranged from 50% to 120%. When Y_v is closer to 100%, it indicates that the interannual variation in online attention is more stable. A Y_v value greater than 100% indicates a good development trend. Y_v rose from 2012 to 2017 and peaked in 2017. From 2017 to 2019, the online attention remained relatively stable at a high level, and after 2019, the online attention gradually declined. Among these years, the one with the most significant increase in online attention is 2013–2014, with a rise of 32.12%, and the largest decline is 2019–2020, with a decrease of 12.98%; the rate of decline for 2020–2021 is 2.89%, slowing down the rate of decline. Y_v values after 2014 are more significant than 100%, and the overall development trend of the tea industry online degree is good. The 2017 tea industry online attention peaked, which may be related to the professional qualification certificate of tea artisan "return", China's first discovery of the tea tree genome, the death of tea industry titan Zhang Tianfu and other public opinion events related to the tea industry. The inter-year characteristics show us the trend of concern in different years.

4.1.2 Monthly characteristics

Online attention is a reflection of consumer demand and search behavior on the internet. Visualize the monthly distribution of online attention in China's tea industry from 2012–2021, roughly showing a bimodal pattern (Figure 4). The peak periods are March to May and October every year. The rest of the months have a more even distribution of tea industry online attention, which is the trough period of attention. Overall, the tea industry online attention has more obvious seasonal characteristics, with the highest attention in spring, followed by autumn, and the lowest online attention in winter. It is initially speculated that the monthly change in tea industry online attention may be related to the climate, which will be verified later.

Mathematical model analysis was used to enhance the accuracy of the study, based on the visual presentation of monthly characteristics, the seasonal intensity index *R* is used to analyze the degree of temporal concentration of the Chinese tea industry online attention. A larger value of *R* indicates more significant monthly differences, and *vice versa*, it tends to be evenly distributed. As shown in Table 1, the R values of Chinese tea industry online attention are all concentrated between 8.2 and 8.3, and the seasonal concentration index is relatively stable. Among them, the *R*-value of 2021 is the largest, indicating that the monthly variation in tea industry online attention is the largest in 2021, and the R-value of 2017 is the smallest, which means that the monthly variation in 2017 is the smallest. This indicates that the distribution characteristics of tea industry online attention have a strong monthly concentration. Through the monthly distribution characteristics analysis, we can see a "bimodal", indicating that the tea industry online attention in a year there are 2 periods of higher attention.

4.1.3 Interday characteristics

The intraweekly distribution of tea industry online attention was further analyzed using the intraweekly distribution skewness index W. The results are shown in Table 1. The results show that W < 0 from 2012 to 2021, and the value of W does not vary significantly, indicating that the intraweekly distribution of tea industry online attention is skewed toward the front part of the week and that the degree of skewness does not vary significantly. Among them, the smallest W value in 2013 indicates that the degree of intraweek bias is the largest, and the largest W value in 2016 tends to 0, indicating that the intraweek distribution bias in that year is the weakest and tends to the average intraweek distribution.

The data superimposed on daily attention from 2012 to 2021 are superimposed, and the average value is needed to obtain the distribution of online attention within each year. Its distribution is consistent and generally manifests as the characteristics of high working days and low weekends. The highest value is Monday, and the minimum attention value is Saturday (Figure 5). Therefore, it is speculated that the distribution characteristics of the tea industry online may be related to work needs. The intra-week distribution study aims to explore whether weekends have an impact on the attention of the tea network.

4.2 Spatial distribution characteristics of TIOA

This section aims to explore, through visualization, whether there are spatially concentrated characteristics of online attention, how differences are presented, what kind of differences are presented, and how the center of gravity of spatial distribution is shifted in direction.

4.2.1 Spatial aggregation characteristics

To analyze the spatial distribution clustering characteristics of China's TIOA, a quantitative analysis with the geographical concentration index was conducted.

First, the geographical concentration index was used to measure the spatial concentration degree of tea industry online attention. Assuming that tea industry online attention is uniformly distributed across 31 provincial administrative regions, the geographical concentration index $\bar{G}$ was calculated as 17.96. As shown in Table 2, the geographical concentration index of attention from 2012 to 2021 is greater than $\bar{G}$, indicating that the degree of concentration of attention distribution is greater than the concentration when it is uniformly distributed. From 2012 to

TABLE 2 2012–2021 China's TIOA geographic concentration index.

Year	2012	2013	2014	2015	2016	2017	2018	2019	2020	2021
G	19.927	19.757	19.838	19.943	20.050	19.931	19.877	19.841	19.680	19.540

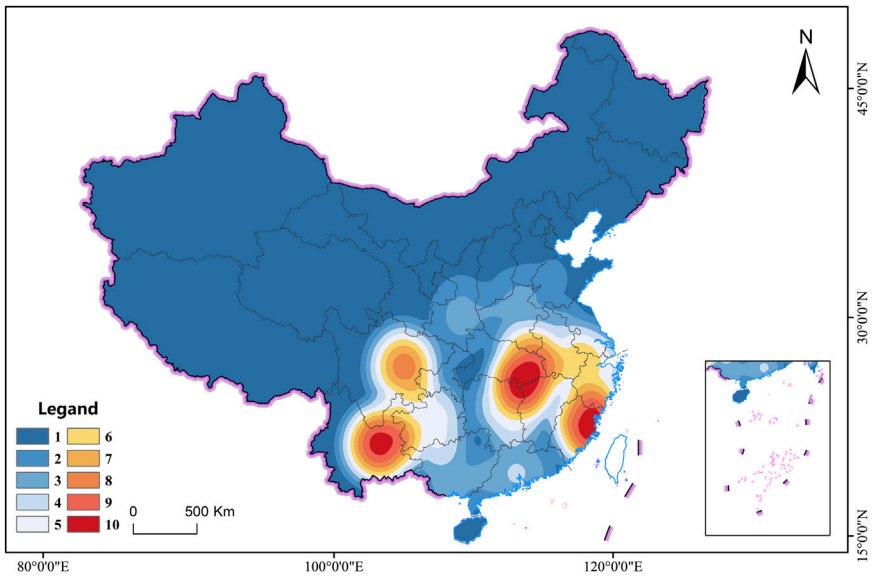

FIGURE 1
Tea-producing areas and production distribution in China.

2021, the degree of attention *G* first showed an overall increase and then decreased. In 2016, the geographical concentration index was the highest, indicating that the degree of attention was most concentrated at this time. Overall, the spatial distribution of online attention shows a trend of mild concentration and then slight dispersion, and there is no drastic change in the attention of each year, indicating that the spatial distribution is relatively stable. It is preliminarily speculated that the changes in the geographical concentration index after 2016 may be related to factors such as the popularity of regional internet and the rise of the concept of "health preservation" in recent years, making tea popular in more regions, so the attention tends to be scattered. The study of "Spatial aggregation characteristics" based on the geographical concentration index aims to initially determine whether the Chinese tea industry network attention is spatially clustered.

4.2.2 Spatial divergence characteristics

Using ArcGIS 10.8, the spatial distribution characteristics of China's tea industry online attention were visualized and analyzed. The values of tea industry online attention in each province in 2012, 2015, 2018 and 2021 were selected for stratified coloring, and the results are shown in Figure 6.

The overall spatial distribution of the TIOA shows the characteristics of "China's east more west less, coastal high inland low". The north and south have high value area distributions, and the difference between the north and south is not significant. From a spatial point of view, the TIOA is the highest in Guangdong Province, and Jiangsu, Zhejiang, and Shandong also have a high degree of concern. The provinces with the lowest attention are Tibet, Qinghai and Ningxia. In addition, the online attention of Sichuan is higher than that of surrounding provinces, forming an island of high values; the online attention of Shanxi, Chongqing, Guangxi and Jiangxi is also significantly lower than that of neighboring provinces, forming a low value area. From a regional point of view, the value of online attention in each year by regional summation from high to low, in order, are as follows: East China, followed by North China, Southwest China, South China, Central China, Northwest China and Northeast China, with the overall spatial distribution of tea industry online attention around those that are more stable. It is preliminarily speculated that East China may have the highest ranking because of the degree of economic development in the region. The regional economic status and material conditions largely determine the level and volume of regional consumption, determine the development scale of the industry, and thus affect online attention. The lower TIOA in Northwest China is presumed to be related to the local dietary habits and preferences as well as the smaller population and lack of enough people to pay attention and search.

Referring to the research method of scholars (Tang and Xu, 2021). The rank order of online attention in each province and region was divided into cold spot and hot spot areas (Figure 7). The 1st-15th place of attention ranking is the hot spot area, and the 16th-31st place is the cold spot area. Meanwhile, the ranking changes are divided into growing, stable and declining. The average rank order and rank order change rate of online attention of each province and region from 2012 to 2021 were visualized, and the rank order and

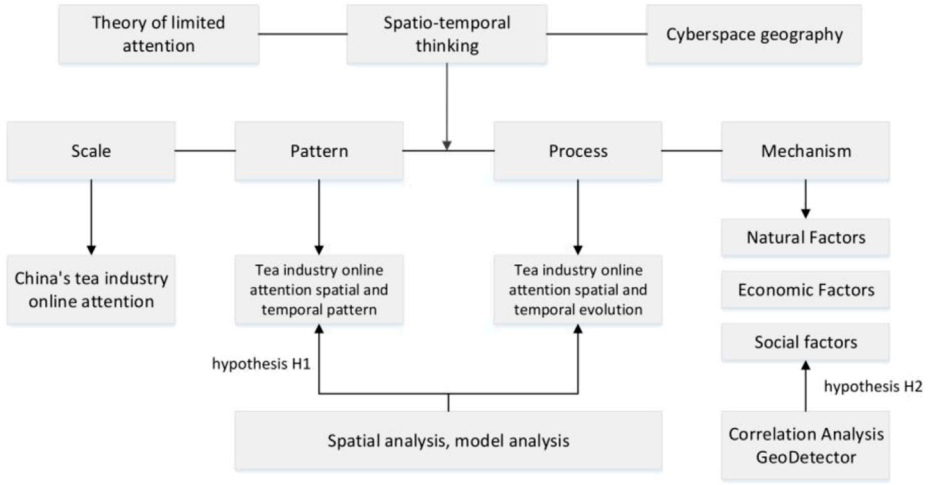

FIGURE 2
Theoretical framework.

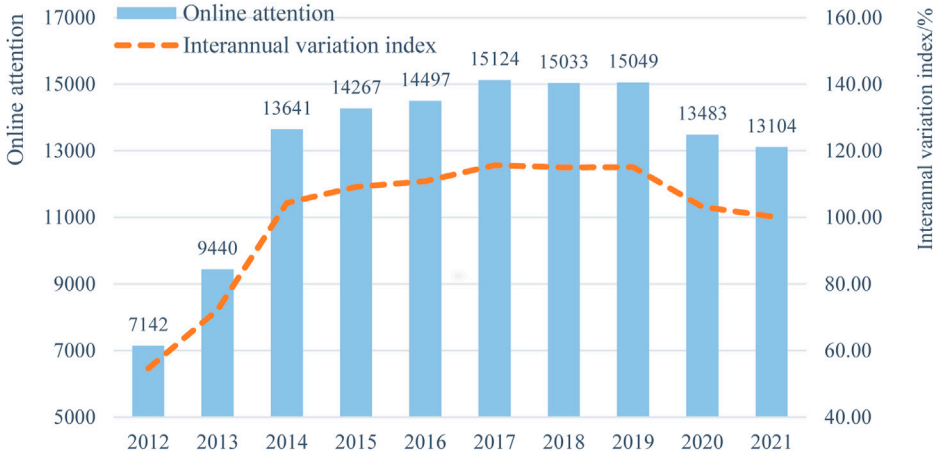

FIGURE 3
Interannual change index of China's TIOA from 2012 to 2021.

change rate were divided into six types. In terms of bit order characteristics, the top ten provinces in terms of online attention are Guangdong, Zhejiang, Jiangsu, Shandong, Beijing, Henan, Fujian, Sichuan, Hebei and Shanghai, in that order. In terms of the rate of change, provinces and regions with faster growth in rank order include Jiangsu, Yunnan, Anhui and Chongqing; provinces and regions with faster decline in rank order include Beijing, Fujian and Tianjin. Provinces and regions such as Guangdong, Zhejiang, Fujian and Hunan have a stable ranking while maintaining a high level of online attention. Provinces and regions such as Tibet, Qinghai, Hainan and Ningxia have lower and more stable attention. In addition, among the top 10 provinces of China's TIOA, 7 provinces are the production areas of China's tea industry and have better development of this industry and related industries. The spatial pattern of China's tea industry reality has a certain coupling with the spatial pattern of online attention. Based on the Spatial Interpolation Chart and rank order change diagram of China's tea industry online attention, the aim is to clarify which provinces have high attention and which provinces have low attention, and to analyze the overall trend of change in the attention of these provinces.

4.2.3 Spatial orientation characteristics

The standard deviation ellipse tool (SDE) and the center of gravity model tool in ArcGIS 10.8 were used to visualize and analyze the center of gravity of the distribution of TIOA, and the results are shown in Figure 8. The standard deviation ellipse distribution of China's TIOA from 2012 to 2021 is relatively stable, and its long axis, short axis, flatness and distribution direction have not changed significantly, which indicates that the geographical space of the tea industry online attention distribution is also relatively stable. The mean center tool was used to determine that the center of gravity of the Chinese tea industry online attention is located in Henan Province. From 2012 to 2013, the center of gravity of attention

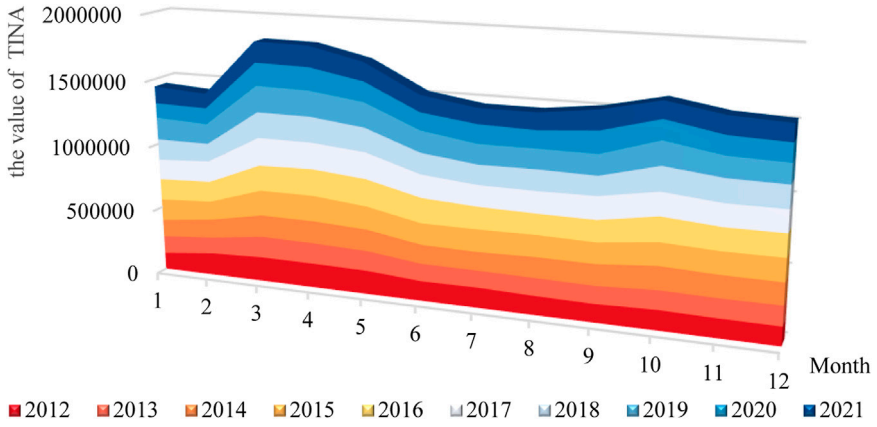

FIGURE 4
Monthly distribution characteristics of China's TIOA from 2012 to 2021.

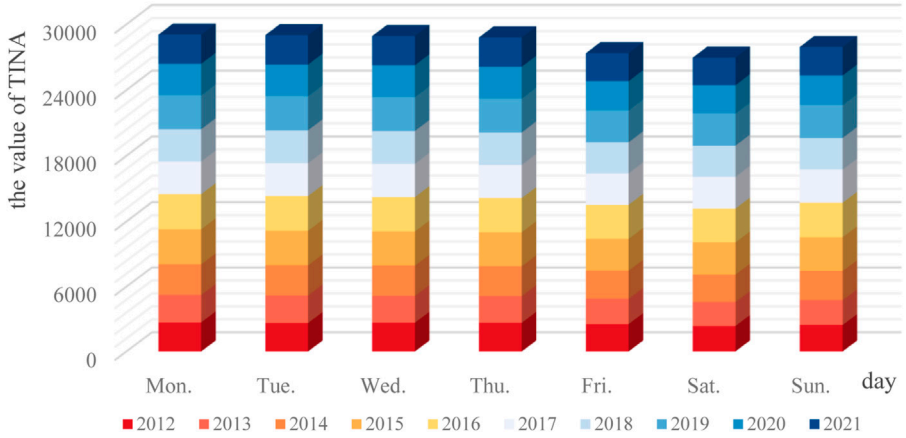

FIGURE 5
Intra-week distribution characteristics of China's TIOA from 2012 to 2021.

was located in the Yicheng District of Henan Province, in 2020, it was located in Tongbai County, and for the rest of the years, it was located in Biyang County. The migration trajectory of the center of attention shows a shift from the northeast to the southwest, Combining the direction of change of the long axis of the SDE, i.e., the Chinese tea industry online attention tends to the southwest of China. In the study of the ranking characteristics above, among the 11 provinces that have risen in the ranking of China's tea industry, the southwest region accounts for 4 places. Since 2012, tea production and sales, planting area and other indicators in Yunnan, Guizhou and Sichuan have grown rapidly. The reality of the rapid development of the tea industry in Southwest China in recent years is consistent with the fact that the center of gravity of China's tea industry online attention is shifting to the southwest. Spatial orientation characteristics aims to explore which part of China's regions are developing faster in terms of online attention from a more macro perspective, and to explore whether there is a coupling between the online attention situation and reality.

4.3 Influencing factors of TIOA

Scholars believe that any factor that can influence the needs and access to information of followers is a factor that affects online attention (Dann, 1977; Tang and Xu, 2021). Based on the research of scholars (Zhang et al., 2016; Li et al., 2019; Mei et al., 2020; Hu et al., 2022), combined with the spatial and temporal characteristics of TIOA, this paper uses a combination of quantitative and qualitative approaches to explore the influencing factors that may affect tea industry online attention in natural, economic and social dimensions and uses a geographic detector to validate the influencing factors and measure the degree of influence of different factors.

4.3.1 Selection and analysis of influencing factors

This section aims to make a preliminary exploration of the influencing factors by correlation analysis of the influencing factors. in order to prepare for the geographic probe in the latter part.

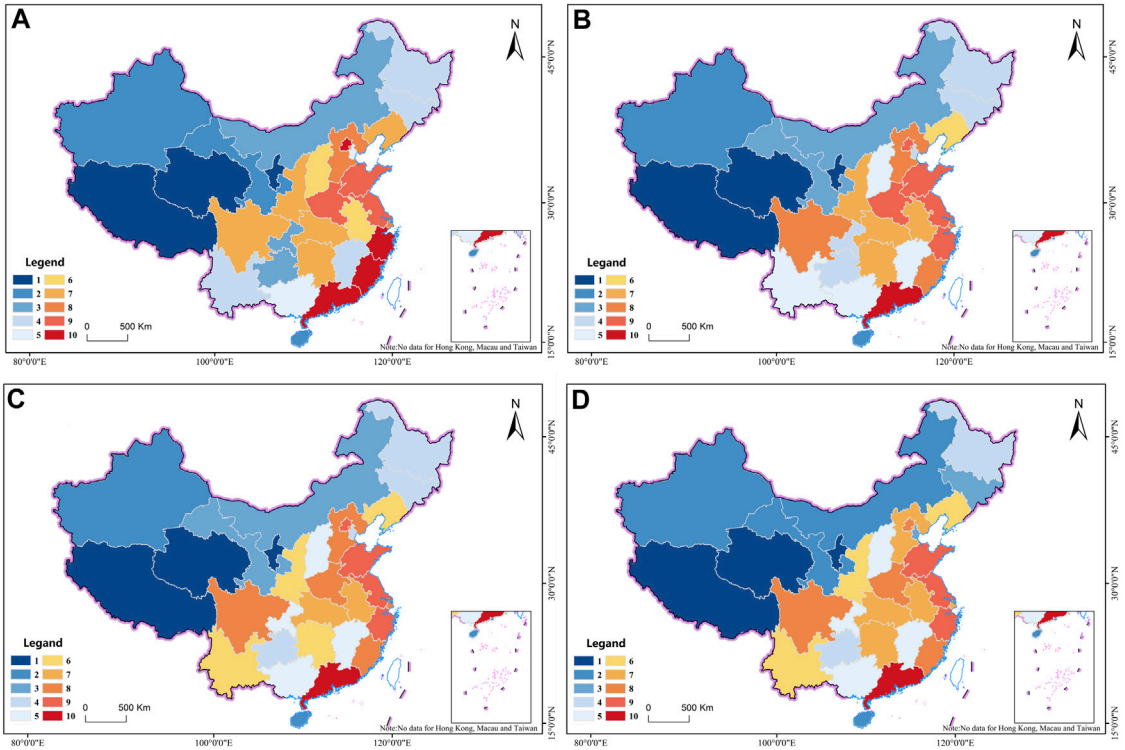

FIGURE 6
(A) is 2012's spatial interpolation chart of China's TIOA, **(B)** is 2015's spatial interpolation chart of China's TIOA, **(C)** is 2018's spatial interpolation chart of China's TIOA, **(D)** is 2021's spatial interpolation chart of China's TIOA.

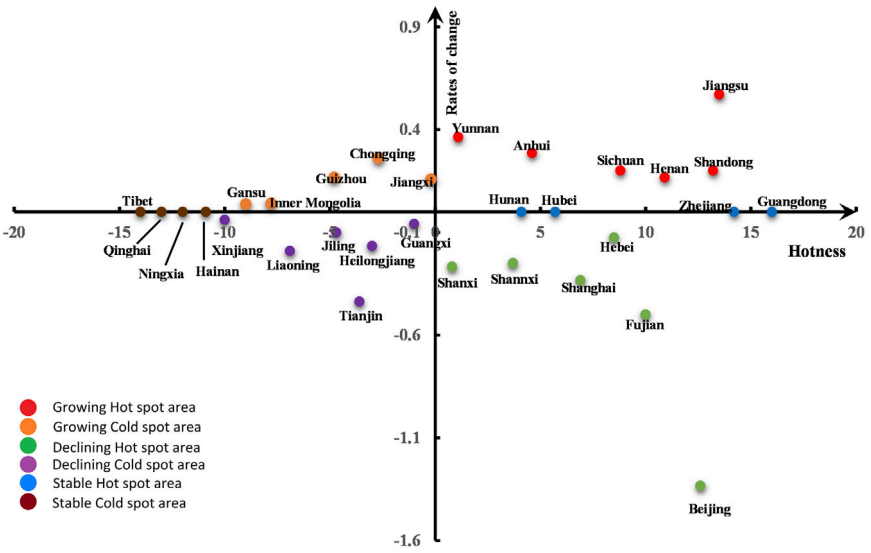

FIGURE 7
Average rank order and change rate of TIOA by provinces and regions from 2012 to 2021.

4.3.1.1 Natural factors

Natural factors are the fundamental factors that affect attention. Tea is the material basis of the tea industry. If we only study the influencing factors of the tea industry from economic and social perspectives, we will split the natural attributes of the tea industry. The spatial distribution of tea

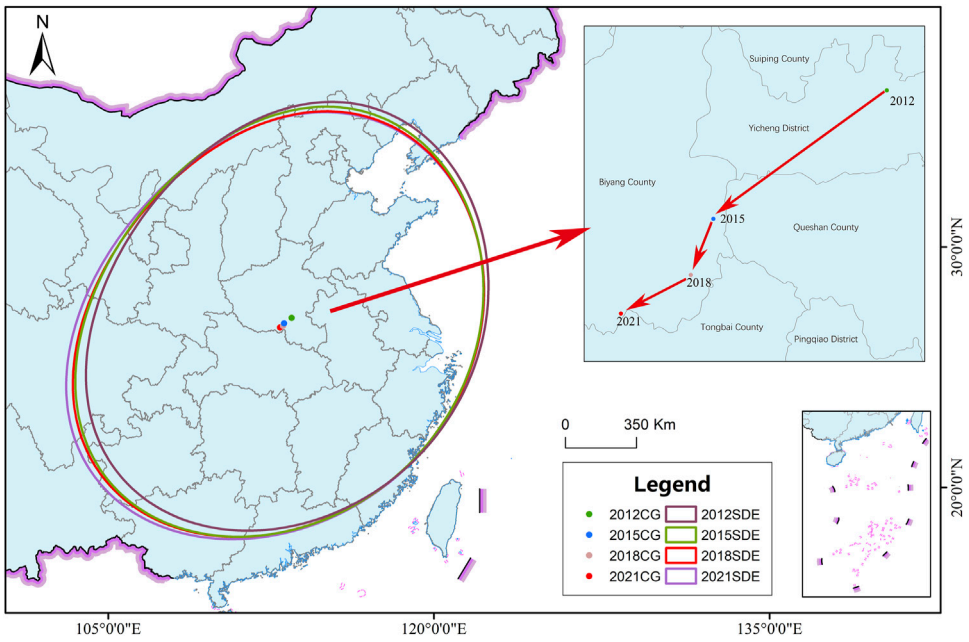

FIGURE 8
The SDE of TIOA distribution and the migration trajectory of center of gravity from 2012 to 2021.

industry online attention is closely related to the distribution of tea-producing areas and the geographical environment of tea growth. The environmental factors that affect the distribution of tea mainly include moisture, accumulated temperature, light, soil pH, drought and flood disasters. A good climate and natural environment are conducive to the growth of tea, while unsuitable natural environmental conditions make it difficult for the tea industry to develop, which in turn affects attention to the tea industry on the internet. Considering the availability of national-scale data, precipitation, temperature, sunshine and humidity were selected as indicators of natural factors affecting the attention of the TIOA (Lu et al., 2018; Shimei et al., 2018; Guo et al., 2022), and Pearson correlation analysis was conducted with the online attention of the tea industry. The results are shown in Table 3.

The tea season is the best period for natural conditions and tea growth and is therefore an important factor influencing the attention of the TIOA. According to the monthly distribution characteristics of the tea industry, two peaks of attention are formed in March to April and October every year. March to April coincides with the tea season dates of spring tea every year, while October corresponds with the autumn tea season every year. Every year, when a large number of new teas are listed in the tea season, it is not only the peak of consumers' attention to the tea industry but also the peak time for each tea production operator to obtain information, which drives up the TIOA under the joint action of production and consumer demand. The correlation analysis initially showed that natural factors are one of the factors influencing online attention.

4.3.1.2 Economic and social factors

Economic and social factors are the direct factors affecting the attention of the TIOA. Referring to the relevant literature, GDP, income, industrial base, and output were selected as the indicators to measure economic factors (Liu and Liao, 2021; Liu et al., 2023). For consumers, the economic level determines the income consumption level and purchasing power of residents. The more developed the economy is, the stronger the potential willingness to buy, and the higher the demand for information, which in turn affects online attention. Tea is a nonessential good, and tea consumption can also reflect its income consumption level to a certain extent. Second, for producers, the economic level determines the level of tea industry funds, technical base and related supporting facilities. The industrial base determines the integrity of the upstream and downstream industrial chain of the tea industry, which in turn affects the level of development of the tea industry and ultimately affects the yield and healthy development of the tea industry. Combined with the actual situation in China, the level of economic development and marketization of the eastern coastal region is higher than that of the central and western regions during the same period, which is also one of the reasons for the divergence between east and west in the presentation of tea industry network attention (Sang et al., 2023).

In terms of social factors, the factors that affect the TIOA mainly include the online penetration rate, brand density, tea price index, education level and age of the followers (Lin, 2021; Wenjing and Gang, 2021; Zhao et al., 2022; Chen et al., 2023). Since population bases and internet user bases vary among different places, it is not accurate enough to adopt the number of internet users as the influencing factor, as the online attention penetration rate can directly affect the number of users who can search for information about the tea industry through the internet.

Brand density can reflect the level of development of the tea industry and the level of awareness of property rights protection in a certain place, and this paper uses the number of "China's top ten famous teas" and geographical indication products as the basis for

TABLE 3 Correlation analysis of influencing factors of TIOA.

	Factor	Index	Pearson correlation coefficient (two-tailed)
Natural Factors	Precipitation	Annual precipitation	0.503**
	Temperature	Average annual temperature	0.417*
	Sunlight	Annual sunlight hours	−0.389*
	Humidity	Relative humidity	0.372*
Economic factors	GDP	GDP	0.918***
	Income	Disposable income *per capita*	0.510**
	Industrial Base	Percentage of primary industry	−0.448*
	Capacity	Tea production	0.345*
Social factors	Internet	Internet penetration rate	0.584***
	Brands	Geographical Indication Tea Brands	0.403*
	Price	Tea price indices	0.508***
	Education level	Percentage of higher education	0.382*
Other factors	Leisure time	Social Virtual Index	0.901***

TABLE 4 Intra-week TIOA and social virtual indicators table.

	Mon.	Tue.	Wed.	Thu.	Fri.	Sat.	Sun.
NA	29,062.59	29,015.66	28,930.12	28,810.44	27,368.25	26,961.29	27,932.74
H_i	1	0.95	0.9	0.85	0.7	0.25	0.5

measuring brand density. Third, price is a reflection of demand, which can have an impact on the production arrangement of producers and the consumption intention of residents, which in turn can convey the degree of attention to information about the tea industry. In addition, demographic characteristics are also important factors that influence the online attention of the tea industry. For example, the age and education level of the followers are important factors that affect the degree of users' usage of the online and the way they use it. Pearson correlation analysis was conducted between the above influencing factors and tea industry online attention, and the results are shown in Table 3. Most of the factors showed moderate correlation, and the *p* values of all factors passed the significance test.

The correlation analysis initially showed that Economic and social factors are one of the factors influencing online attention.

4.3.1.3 Other factors

The intraweekly distribution skewness characteristics above show that weekdays and nonworking days have an impact on tea online attention. Since leisure time is difficult to quantify, on the basis of reference to scholars' assignments (Lijun et al., 2011; Zhang et al., 2016; Wang and Meng, 2023), a social virtual index (Hi) was used to assign a value between 0 and 1 to the degree of leisure in the intraweekly distribution from 2012 to 2021. 1 is busy, and 0 is leisure. Correlation analysis was performed between Hi and the mean value of online attention from 2012 to 2021, and the Pearson correlation coefficient was 0.901 and $p < 0.001$, which passed the consistency test (Table 4).

The second factor is the impact of festival activities or special events on the tea industry online attention. Relevant studies by scholars show that public opinion events and events also have a significant impact on online attention (Luo et al., 2011). For example, in March 2018, on the day when the "first bamboo tea" of Mengdingshan tea was launched, the attention of the tea industry online increased significantly. Major events not only drive the development of related industries but also play a positive role in stimulating demand, and some factors are not easily quantifiable. Examples include the personal preferences, living habits, consumption habits, and regional cultural background of the followers. The formation of living habits is a product of the natural climate, economy, culture and other factors formed under long-term effects. For example, the difference between the northern and southern tea drinking habits, the difference between coastal and inland areas, the demand for tea and the demand for tea types, clear drinking and blending and other drinking methods are also different, and these individual preferences also have an impact on attention. The correlation analysis tentatively showed that other factors were one of the factors influencing network attention, but we did not include other factors in the GeoDetector because they were not easily quantifiable.

TABLE 5 TIOA influence factor detection results.

	Factor	Index	*q*
Natural Factors	X_1	Annual precipitation	0.45
	X_2	Average annual temperature	0.353
	X_3	Annual sunlight hours	0.435
	X_4	Relative humidity	0.223
Economic Factors	Y_1	GDP	0.884
	Y_2	Disposable income *per capita*	0.51
	Y_3	Percentage of primary industry	0.31
	Y_4	Tea production	0.436
Social factors	Z_1	Internet penetration rate	0.373
	Z_2	Geographical Indication Tea Brands	0.306
	Z_3	Tea price indices	0.447
	Z_4	Percentage of higher education	0.289

4.3.2 Validation of impact factors based on geodector

The methods that scholars have used to research influencing factors mainly include correlation analysis, multiple linear regression (Xiao et al., 2017), and GWR models (He et al., 2018) among others. GeoDetector is an effective tool for studying and analyzing driving factors. Since GeoDetector can only detect the intensity of the impact factor and cannot discern the direction of the impact, correlation analysis needs to be performed first, and then GeoDetector can be used to verify the impact factor.

4.3.2.1 Factor detection

As shown in Table 5, all factors passed the Pearson correlation analysis as well as the *p*-value significance test. The data mean value was processed, and the influence factor data were clustered and discretized based on the Jenks natural break method to generate type data. Finally, each influence factor was imported into the geographic detector for influence q-value measurement to analyze the strength of the explanatory power between the influence factors and attention values of Chinese tea industry online attention. A total of 3 major categories and 12 index systems were established.

Referring to the classification method of scholars on the q-value of influencing factors (Ruan et al., 2019), the influencing factors were classified into three categories: core influencing factors ($q \geq 0.5$), important influencing factors ($0.4 \leq q < 0.5$) and general influencing factors ($q < 0.4$). Among them, Y1 (GDP) and Y2 (*per capita* disposable income) are core influencing factors, X3 (annual sunshine hours), Y4 (tea yield), and Z3 (tea price index) are important influencing factors, other detection factors have relatively low q values, and the relative humidity (X4) and the education level of followers (Z4) have a weak degree of influence on the attention of the TIOA. The factor detection aims to know which factors have a strong influence on the attention and which factors have a weak influence on it.

4.3.2.2 Interaction detection

Interaction detection is mainly used to analyze whether there are interactions among the factors that influence tea industry attention. The interactions are classified into the following five categories according to the relevant definitions. If $q(X1\cap x2)<\text{Min}\ (q(X1), q(X2))$, the interaction shows nonlinear weakening; if $\text{Min}\ (q(X1), q(X2))< q(X1\cap X2)<\text{Max}\ (q(X1), q(X2))$, it shows one-factor nonlinear weakening; when $q(X1\cap X2)>\text{Max}\ (q(X1), q(X2))$, both show bifactor enhancement; when $q(X1\cap X2) = q(X1)+q(X2)$, it exhibits independence; and finally, when $q(X1\cap X2))> q(X1)+ q(X2)$, it exhibits nonlinear enhancement. Interaction detection aims to analyze whether the joint effect between factors presents a positive or negative effect on attention.

As shown in Table 6, the interaction types of each main influencing factor were two types of two-factor enhanced and nonlinear enhanced. Among them, there were 51 groups of the two-factor enhanced type and 27 groups of each nonlinear enhanced type. The interaction detection results show that there is an interaction between any two influencing factors, and the results all show that the interaction enhances the strength of the explanation of the TIOA. That is, the two-factor interaction is stronger than the single-factor effect strength. This indicates that the spatial and temporal characteristics of tea industry online attention are influenced not only by the natural environment, society and economy but also by the joint effect of the interaction of each factor that finally forms the spatial and temporal distribution pattern of TIOA.

5 Discussion

At present, some progress has been made in the research on online attention, but there are few research results with a certain industry or a certain product as the research object, and it does not involve the tea industry for the time being, so further research is needed. In addition, due to the dual natural and social attributes of the tea industry, this paper differs from those of scholars in terms of influencing factors regarding online attention, so the selection of indicators has been innovated. Unlike most scholars who only analyze 1 year or individual years, we focus on Chinese tea industry online attention from 2012 to 2021 as the data source, which has a longer time span and helps to better reveal the spatial and temporal divergence pattern of tea industry online attention. This paper takes internet big data as the data source, which enriches the perspective of tea industry research from geographic spatiotemporal thinking and provides a useful reference for the high-quality development of the tea industry under the perspective of "Internet+".

Since natural factors are the innate and limiting factors affecting the attention of the tea industry network, natural conditions such as climate, precipitation are difficult to change, therefore the optimization measures in this study are mainly from economic and social factors. As agriculture, disorderly development must be avoided and attention needs to be paid to the ecological harmony between human and nature. In the context of the "Internet +" era, the following suggestions are proposed based on the optimization of China's TIOA and the sustainable and high-quality development of the tea industry:

TABLE 6 TIOA influence factor interaction detection results.

	X1	X2	X3	X4	Y1	Y2	Y3	Y4	Z1	Z2	Z3	Z4
X1	0.450											
X2	0.643	0.353										
X3	0.775	0.676	0.435									
X4	0.641	0.502	**0.840**	0.223								
Y1	0.966	0.987	0.979	0.987	0.884							
Y2	0.975	**0.954**	0.968	**0.919**	0.950	0.510						
Y3	0.790	**0.866**	**0.874**	**0.918**	0.938	0.788	0.310					
Y4	0.797	0.691	0.746	0.679	0.923	0.834	0.762	0.436				
Z1	**0.899**	**0.861**	**0.897**	**0.752**	0.950	0.827	**0.905**	0.809	0.373			
Z2	0.670	0.664	0.690	**0.582**	0.943	**0.868**	**0.837**	0.641	**0.754**	0.305		
Z3	**0.978**	**0.935**	**0.931**	**0.915**	0.940	0.555	0.755	0.828	0.807	**0.830**	0.447	
Z4	**0.912**	**0.862**	**0.893**	**0.797**	0.931	0.810	**0.673**	**0.790**	0.611	**0.751**	0.722	0.288

Bold text indicates nonlinear enhanced type.

Economic factors are important elements that influence the attention of the tea industry network. We propose suggested measures based on Y1-Y4, GDP, disposable income, share of primary production, and tea production from the perspective of product, culture, and industry. (1) First, for the product side, the technological content of tea production should be improved, the product system should be further developed, and product quality should be optimized to create the core competitiveness of the tea industry. (2) Second, for the cultural aspect, the tea industry is a traditional industry with thousands of years of heritage and should involve the active inheritance and promotion of traditional tea culture and the enhancement of the cultural connotation of products in this industry. (3) For industrial integration, the new "Internet + tea" and "tea + tourism" business models should be actively promoted. Relying on internet technology, through the Internet + agricultural e-commerce model, there is a direct connection between consumers and tea industry business entities, extending the tea industry chain, broadening the distribution channels, and promoting the transformation of traditional agricultural industries to modern agriculture. Combined with tea resources and seasonal characteristics, local conditions are used to create a tea tourism area and develop tea tourism, study, experience and other forms to achieve the interactive development of the tea industry and tourism. (4) For the spatial and temporal characteristics of online attention and Price Index (Z3), a differentiated and accurate marketing strategy should first be developed. Spatially, for the lower attention to the northwest and northern regions, the tea industry market should be actively explored, new channels should be developed, potential markets should be targeted, *etc.* At the same time, the eastern and central advantageous markets should be consolidated, and products and services should be improved; in terms of time, the tea industry online attention has strong seasonal characteristics. Therefore, off-season marketing, differentiated marketing, anti-seasonal promotion and other measures can be carried out; in terms of population characteristics, as preferences for tea vary across different regions and age groups, product differentiation and precision strategies should be implemented to provide diversified and multiple price options. At the same time, for the trend of tea drinking younger, traditional marketing methods should also be adjusted. (5) For the spatial and temporal characteristics and geographical indication tea brand (Z2), followed by the strengthening of publicity efforts. In the context of the Internet +, a combination of online and offline marketing should be utilized. For online publicity, the internet and new media platforms should be actively employed for publicity and promotion to enrich the channels of information understanding. Offline publicity can be organized through the tea industry fair, "National Tea Day" and other high-quality activities to promote the local tea industry and representative industry brands to enhance the visibility of the industry. At the meantime, it should actively declare geographical indication products and do a good job of brand protection. It also improves customer satisfaction by increasing brand reputation and loyalty, and in the long term (Gong et al., 2021). (6) Internet penetration (Z1) is an important indicator that affects online attention, based on this, the internet can be used to build a comprehensive information service platform for the tea industry. In the context of Internet +, the internet has become an important platform for information elements. First, the construction of web infrastructure should be improved, and internet platforms should be well built and maintained. The second step is to build a wisdom platform for the tea industry based on internet big data. Big data, cloud computing, the Internet of Things and other technologies can be used to support tea industry production and processing, sales promotion of agricultural products, consumer shopping and other preproduction and postproduction digital information sharing and linkage to provide producers and consumers with intelligent services. At the same time, agricultural big data application services should be put to good use. This includes using agricultural environment big data, production and marketing big data, *etc.*, to provide scientific and

efficient technical support for decision-making and high-quality development in the tea industry. (7) At the government level, the relevant departments should do a top design, while giving production operators to develop "Internet + tea industry" funding and policy support (Cui and Xu, 2022). In addition, the proportion of higher education (Z4) is also an important factor affecting the online attention, and "Internet +" should be used to train highly qualified personnel in modern agriculture and improve the literacy level of practitioners through continuing education. At the same time to strengthen cross-regional collaboration in the tea industry, the integration of the advantages of local resources, to achieve resource sharing, complementary advantages, mutual benefit and win-win.

This paper has some shortcomings. Due to the use of different keywords and different search engines, the presented results are not the same. In addition, the Baidu index does not comprehensively reflect the demographic attributes of users, so future research can integrate online and offline data in terms of data sources to improve the completeness and reliability of the data. In addition, the factors influencing online attention are complex and multifaceted, and this paper is not sufficiently comprehensive in selecting the index system. In terms of research scale, further small-scale, microlevel, and refined research on tea industry online attention, as well as comparative research at different regional levels, can be carried out in the future to enrich the depth and breadth of research.

6 Conclusion

(1) In terms of temporal characteristics, the interannual characteristics of China's tea industry online attention from 2012 to 2021 show a trend of rapid growth, a high and stable period, and then a slow decline. In 2017, tea industry online attention reached its highest peak. In terms of monthly characteristics, the seasonal intensity index of attention is 8.2, with a strong monthly concentration. March to April and October in each year are the two peaks of TIOA, which coincides with the tea seasons of spring tea and autumn tea. In terms of intraweekly distribution, the intraweekly distribution skewness index is negative, indicating that the online attention is mainly concentrated in the first part of the week, i.e., weekdays, and the TIOA is significantly lower on Fridays and weekends.

(2) In terms of spatial characteristics, the geographic concentration index *G* of online attention from 2012 to 2021 is approximately 19, and the overall value is stable, showing a trend of mild concentration first and then mild dispersion. The interprovincial differences in online attention are relatively obvious. The migration trajectory of the center of attention shows a shift from the northeast to the southwest, and the online attention of China's tea industry has a tendency to tilt toward the southwest.

(3) In terms of influencing factors, the core factors of TIOA are economic development and residents' income. The natural environmental conditions of tea growth, leisure time of followers and tea price level are important factors affecting attention but are less influential. Each factor presents nonlinear enhancement and dual-factor enhancement, and the dual-factor interaction is stronger than the single-factor effect. Under the joint action of each factor, the spatiotemporal distribution pattern of TIOA is finally formed.

Data availability statement

The raw data supporting the conclusion of this article will be made available by the authors, without undue reservation.

Author contributions

Conceptualization, RS. Formal analysis, RS. Methodology, RS. and JX. Investigation, RS. and ZS. Writing—original draft preparation, RS. Writing—review and editing, JX and ZS. Visualization, RS. Supervision, JX. Funding acquisition, JX and ZS. All authors contributed to the article and approved the submitted version.

Funding

This research was supported by the Key Project of Zhejiang Province Philosophy and Social Science Planning (grant No.17NDJC040Z), the Social Science Planning Project of Qinghai Province (grant No. 19027), the Social Science Planning Project of Qinghai Province (grant No. 2022ZCY033).

Conflict of interest

The authors declare that the research was conducted in the absence of any commercial or financial relationships that could be construed as a potential conflict of interest.

Publisher's note

References

Bao, F. H., and Chen, Y. (2017). Research on the spatial-temporal distribution characteristics of China's outbound tourism in the past 10 years. *World Reg. Stud.* 26, 127–139. doi:10.3969/j.issn.1004-9479.2017.02.014

Cai, W. M., Peng, J., and Qin, J. J. (2016). A study on national network attention heat matrix and promotion strategy in shaoshan. *Tour. Sci.* 30, 61–72. doi:10.16323/j.cnki.lykx.2016.04.005

Chen, J., Sun, H., Wu, Y. C., Chou, T. Y., and Cheng, Y. C. (2023). Network attention and carbon dioxide emission performance of agricultural enterprises: Empirical evidence from China's baidu search index. *Front. Environ. Sci.* 11, 198–205. doi:10.1016/j.lungcan.2023.02.015

Cheraghali, H., Igeh, S. A., Lin, K. H., Molnar, P., and Wijerathne, I. (2022). Online attention and mutual fund performance: Evidence from Norway. *Finance Res. Lett.* 49, 103139. doi:10.1016/j.frl.2022.103139

Cherry, E. C. (1953). Some experiments on the recognition of speech, with one and with two ears. *J. Acoust. Soc. Am.* 25, 975–979. doi:10.1121/1.1907229

Cui, X., Xu, B., and Razzaq, A. (2022). Can application of artificial intelligence in enterprises promote the corporate governance? *Front. Environ. Sci.* 980. doi:10.3389/fenvs.2022.944467

Dann, G. M. (1977). Anomie, ego-enhancement and tourism. *Ann. Tour. Res.* 4, 184–194. doi:10.1016/0160-7383(77)90037-8

Dou, Z. W., Ji, M. X., Shao, Y. N., and Wang, M. (2021). Research on the price impact mechanism of Pu'er tea under Internet + environment. *Acta Agric. Scand. Sect. B-Soil Plant Sci.* 71, 17–27. doi:10.1080/09064710.2020.1840619

Frandsen, T. F. (2005). Geographical concentration - the case of economics journals. *Scientometrics* 63, 69–83. doi:10.1007/s11192-005-0204-4

Gao, C., Guo, Q., Jiang, D., Wang, Z., Fang, C., and Hao, M. (2019). Theoretical basis and technical methods of cyberspace geography. *J. Geogr. Sci.* 29, 1949–1964. doi:10.1007/s11442-019-1698-7

Ginsberg, J., Mohebbi, M. H., Patel, R. S., Brammer, L., Smolinski, M. S., and Brilliant, L. (2008). Detecting influenza epidemics using search engine query data. *Nature* 457, 1012–1014. doi:10.1038/nature07634

Gong, X., Razzaq, A., and Wang, W. (2021). "More haste, less speed: How update frequency of mobile apps influences consumer interest," in *Journal of theoretical and applied electronic commerce research*.

Guan, H., Li, W., Zhao, J., and Fan, Y. (2022). Implications of tourism seasonal intensity for the development of ice and snow tourism in the south. *Tour. Manag. Technol. Econ.* 5, 6–10.

Guo, X. J., Yao, H. L., Chen, X. P., and Li, Y. (2022). A study on the online attention of emergency events of torrential rain in shanxi and henan. *Water* 14, 2183. doi:10.3390/w14142183

He, X. Q., Liu, Y., and Wu, F. M. (2017). Analysis on temporal and spatial characteristics of network attention of hot spring tourism based on baidu index. *Areal Res. Dev.* 36, 103–108. doi:10.3969/j.issn.1003-2363.2017.01.019

He, C., Halik, W., and Zhu, Y. (2018). Spatial-temporal differences of xinjiang tourism attention and its influencing factors. *J. Nat. Sci. Hunan Normal Univ.* 41, 16–24. doi:10.7612/j.issn.2096-5281.2018.03.003

Holt, K., Shehata, A., Stromback, J., and Ljungberg, E. (2013). Age and the effects of news media attention and social media use on political interest and participation: Do social media function as leveller? *Eur. J. Commun.* 28, 19–34. doi:10.1177/0267323112465369

Hu, F., Qiu, L. P., Xia, W., Liu, C. F., Xi, X., Zhao, S., et al. (2022). Spatiotemporal evolution of online attention to vaccines since 2011: An empirical study in China. *Front. Public Health* 10, 949482. doi:10.3389/fpubh.2022.949482

Hu, G. (2015). "internet plus"tea industry. *J. Comput. Sci. Eng.* 21.

Ju, S. L., Tao, Z. M., and Hang, Y. L. (2017). Coupling coordination degree between rural scenic tourist network attention and gravity in nanjing city. *Econ. Geogr.* 37, 220–228. doi:10.15957/j.cnki.jjdl.2017.11.027

Jue, W., Lanyi, H. U., and Chen, Q. I. (2017). Prediction of bulk commodities based on internet concerns. *Syst. Engineer. Theory Pract.* 37, 1163–1171.

Katz, J., and Aspden, P. (1997). Motivations for and barriers to internet usage: Results of a national public opinion survey. *Internet Res. Electron. Netw. Appl. Policy* 7, 170–188. doi:10.1108/10662249710171814

Khan, T. H., Yuzhen, D., Ali, S., and Ariyesti, F. R. (2021). Tea culture and industry: Customer tea buying decision-making power shaped by social capital in the presence of mutual trust. *J. Public Aff.* 21, e2127. doi:10.1002/pa.2127

Kwan, I., Fong, J., and Wong, H. K. (2006). An e-customer behavior model with online analytical mining for internet marketing planning. *Decis. Support Syst.* 41, 189–204. doi:10.1016/j.dss.2004.11.012

Li, H., Li, D., Dong, X., and Xu, N. (2019). Spatial patterns of 5a-level tourist attractions and their network attention degrees in China. *J. Arid. Land Resour. Environ.* 33, 178–184. doi:10.13448/j.cnki.jalre.2019.305

Liao, J. J., Yu, C. Y., Feng, Z., Zhao, H. F., Wu, K. N., and Ma, X. (2021). Spatial differentiation characteristics and driving factors of agricultural eco-efficiency in Chinese provinces from the perspective of ecosystem services. *J. Clean. Prod.* 288, 125466. doi:10.1016/j.jclepro.2020.125466

Lijun, M., Gennian, S., and Yunma, H. (2011). A correlative analysis on the relationship between domestic tourists and network attention. *Econ. Geogr.* 31, 680–685. doi:10.15957/j.cnki.jjdl.2011.04.026

Lin, M. (2021). Influencing factors of social service satisfaction of the elderly under the background of internet attention. *Complexity* 2021, 1–10. doi:10.1155/2021/9985280

Liu, Y. W., and Liao, W. (2021). Spatial characteristics of the tourism flows in China: A study based on the baidu index. *Isprs Int. J. Geo-Inf.* 10, 378. doi:10.3390/ijgi10060378

Liu, Z., Li, H., Shi, C., Wang, X., and Zhang, H. (2010). The response of short term tourist flows to spatial structure of regional tourism: A case study of tourist flows of yunnan in golden weeks. *Acta Geogr. Sin.* 65, 1624–1632.

Liu, Y., Chen, Y., and Han, F. (2023). Exploring temporal and spatial structure of tourism market through a big data approach: Whether geographic distance still matters? *J. Hosp. Tour. Manag.* 55, 292–299. doi:10.1016/j.jhtm.2023.03.017

Liu, K., Xue, Y. T., Lan, Y., and Fu, Y. X. (2022). Agricultural water utilization efficiency in China: Evaluation, spatial differences, and related factors. *Water* 14, 684. doi:10.3390/w14050684

Liu, Z., Bashir, R. N., Iqbal, S., Shahid, M. M. A., Tausif, M., and Umer, Q. (2022). Internet of things (iot) and machine learning model of plant disease prediction–blister blight for tea plant. *Ieee Access* 10, 44934–44944. doi:10.1109/access.2022.3169147

Lu, L., Yi-ran, W., Yan, Y. U., Shu-yu, Y. I., Shi-mei, P., and Chen, Z. (2018). Optimal data partitioning, multispecies coalescent and Bayesian concordance analyses resolve early divergences of the grape family (Vitaceae). *J. Southwest China Normal Univ. Nat. Sci. Ed.* 43, 57–77. doi:10.1111/cla.12191

Luo, Q., Pang, J., and Jin, W. (2011). An empirical study on the economic impact of the events with input-output model: A case study of canton fair, China. *Acta Geogr. Sin.* 4, 57–73. doi:10.11821/xb201104006

Ma, L. J., and Long, Y. (2017). Spatiotemporal characteristics of residents tourism demand for typical scenic spots in hunan province based on network attention. *Econ. Geogr.* 37, 201–208. doi:10.15957/j.cnki.jjdl.2017.02.027

Meegahakumbura, M. K., Wambulwa, M. C., Li, M. M., Thapa, K. K., Sun, Y. S., Möller, M., et al. (2017). Domestication origin and breeding history of the tea plant (camellia sinensis) in China and India based on nuclear microsatellites and cpDNA sequence data. *Front. Plant Sci.* 8, 2270. doi:10.3389/fpls.2017.02270

Mei, D., Xiu, C., and Feng, X. (2020). Analysis on the evolution characteristics and driving factors of urban information network structure in China. World reg. *Stud* 29, 717–727. doi:10.3969/j.issn.1004-9479.2020.04.2019284

Paul, T., Mondal, S., Islam, N., and Rakshit, S. (2021). The impact of blockchain technology on the tea supply chain and its sustainable performance. *Technol. Forecast. Soc. Change* 173, 121163. doi:10.1016/j.techfore.2021.121163

Qiu, Q., and Zheng, T. (2017). Study on the spatial-temporal distribution of tourist flow in the scenic spots: Taking golden weeks as examples. *J. Tour. Hosp.* 6. doi:10.4172/2167-0269.1000330

Rosselló, J., and Sansó, A. (2017). Yearly, monthly and weekly seasonality of tourism demand: A decomposition analysis. *Tour. Manag.* 60, 379–389. doi:10.1016/j.tourman.2016.12.019

Ruan, W., Zhang, S., Li, Y., and Zheng, X. (2019). Spatiotemporal differentiation and influencing factors of Chinese's tourism demand to Thailand. *Tour. Trib.* 34, 76–89. doi:10.19765/j.cnki.1002-5006.2019.05.010

Sang, X., Luo, X., Razzaq, A., Huang, Y., and Erfanian, S. (2023). Can agricultural mechanization services narrow the income gap in rural China? *Heliyon* 9, e13367. doi:10.1016/j.heliyon.2023.e13367

Shen, J., and Chou, R. (2022). Rural revitalization of xiamei: The development experiences of integrating tea tourism with ancient village preservation. *J. Rural Stud.* 90, 42–52. doi:10.1016/j.jrurstud.2022.01.006

Shimei, P., Yi, S., Wang, Y., Sun, S., and Jiang, H. (2018). Climate change and its impacts on tourism in yantai. *J. Agric.* 8, 60.

Sun, Y., Zhang, H., Liu, P. X., and Zhang, J. (2017). Forecast of tourism flow volume of tourist attraction based on degree of tourist attention of travel network: A case study of baidu index of different clients. *Hum. Geogr.* 32, 152–160.

Tang, H. J., and Bao, J. G. (2018). Spatio-temporal characteristics and influencing factors of tourists from main inbound tourist source for mainland China. *Econ. Geogr.* 38, 222–230.

Tang, H., and Xu, C. X. (2021). Spatio-temporal evolution and influencing factors of Chinese red tourism classic scenic spots network attention. *J. Nat. Resour.* 36, 1792–1810. doi:10.31497/zrzyxb.20210712

Wang, G., and Meng, Y. (2023). The clustering characteristics and driving mechanisms of tourist preference for 5a scenic spots from the dynamic spatio-temporal perspective: A case of jiangsu in eastern coastal area of China. *Sustainability* 15, 1626. doi:10.3390/su15021626

Wang, J., Zhang, T., and Fu, B. (2016). A measure of spatial stratified heterogeneity. *Ecol. Indic.* 67, 250–256. doi:10.1016/j.ecolind.2016.02.052

Wang, S., Fang, Z., and Wu, D. (2022). Internet of things-enabled tourism economic data analysis and supply chain modeling. *Technol. Econ. Dev. Econ.*, 1–18. doi:10.3846/tede.2022.17120

Wenjing, Z., and Gang, Z. (2021). "Temporal and spatial attention network model based evolution model for bulk commodity price fluctuation risk," in 2021 IEEE International Conference on Big Data (Big Data) (IEEE).

Wren, C. (2012). Geographic concentration and the temporal scope of agglomeration economies: An index decomposition. *Regional Sci. Urban Econ.* 42, 681–690. doi:10.1016/j.regsciurbeco.2012.03.004

Xiao, W. U., Shaozhi, C., and Rong, Z. (2017). Analysis of impact factors on forest park passenger flow based on baidu index. *For. Resour. Wanagement*, 27–30. doi:10.13466/j.cnki.lyzygl.2017.01.006

Xiao, Z., Huang, X., Zang, Z., and Yang, H. (2018). Spatio-temporal variation and the driving forces of tea production in China over the last 30 years. *J. Geogr. Sci.* 28, 275–290. doi:10.1007/s11442-018-1472-2

Xu, J. (2022). *Tea tourism development in China entering experience economy era under the strategic background of rural revitalization: A case study of West Lake longjing tea area and damushan tea garden area in zhejiang province*. Universitat de les Illes Balears.

Yan, H. (2023). Study on the evolution of the temporal and spatial structure of inbound tourist market in shaanxi province. *Acad. J. Manag. Soc. Sci.* 2, 36–42. doi:10.54097/ajmss.v2i2.7530

Yang, X., Bing, P., Evans, J. A., and Lv, B. (2015). Forecasting Chinese tourist volume with search engine data. *Tour. Manag.* 46, 386–397. doi:10.1016/j.tourman.2014.07.019

Yao-feng, M. A., Jun, G., and Chuang-xin, L. I. (2011). On tourism research and application of time-space-thinking principle and its enlightenment. *Tour. Tribune/Lvyou Xuekan* 26.

Zhang, X. M., Cheng, S. W., Liu, X. L., Wang, Q., and Zhao-Hong, L. I. (2016). Spatial-temporal characteristics and influencing factors of network attention to ancient city destination: A case of pingyao. *Econ. Geogr.* 36, 196–202.

Zhang, Y., Jin, X., Wang, Y. W., Liu, R. T., and Jing, Y. (2022). Characterizing spatial-temporal variation of cultural tourism internet attention in Western triangle economic zone, China. *Land* 11, 2221. doi:10.3390/land11122221

Zhao, Y. L., Li, J. K., Liu, K., and Wang, J. E. (2022). Analyzing the spatio-temporal characteristics and influencing factors of "AI + education" network attention in China. *Math. Problems Eng.* 2022, 1–17. doi:10.1155/2022/5101967

frontiers | Frontiers in Ecology and Evolution

TYPE Original Research
PUBLISHED 12 July 2023
DOI 10.3389/fevo.2023.1231487

OPEN ACCESS

EDITED BY
Juergen Pilz,
University of Klagenfurt, Austria

REVIEWED BY
Shengnan Jiang,
Changzhou University, China
Haimeng Liu,
Chinese Academy of Sciences (CAS), China

*CORRESPONDENCE
Yuemin Fan
fanyuemin@gdufe.edu.cn

RECEIVED 30 May 2023
ACCEPTED 22 June 2023
PUBLISHED 12 July 2023

CITATION
Wang S, Wei G, Gao M and Fan Y (2023) Investigating the mechanism of urbanization on the net primary productivity of vegetation in the Yangtze River Economic Belt: a comprehensive analysis from global and local effects. *Front. Ecol. Evol.* 11:1231487. doi: 10.3389/fevo.2023.1231487

Investigating the mechanism of urbanization on the net primary productivity of vegetation in the Yangtze River Economic Belt: a comprehensive analysis from global and local effects

Sicheng Wang[1,2], Guoen Wei[3], Mingming Gao[1] and Yuemin Fan[4]*

[1]College of Architecture and Urban Planning, Guizhou University, Guiyang, China, [2]College of Urban and Environmental Sciences, Peking University, Beijing, China, [3]College of Resources and Environment, Nanchang University, Nanchang, China, [4]New Development Institute, Guangdong University of Finance & Economics, Guangzhou, China

The stressful effects of urbanization on vegetation net primary productivity (NPP) and vegetation–carbon cycle functions within the Yangtze River Economic Belt (YEB) under the sustainable development goals (SDG) and the concept of coordinated regional development, have garnered growing attention. Existing studies have been insufficient in comprehensively examining both the global effects and local variations resulting from urbanization in the region. Additionally, insufficient attention has been given to the heterogeneity of the ecological negative effects of urbanization in the three major urban agglomerations within the YEB. Based on multivariate remote sensing image and socioeconomic statistics data, this study integrates population, economic and land dimensions to construct comprehensive urbanization indexes and quantify the spatio-temporal evolution patterns of NPP and urbanization in the YEB. The focus is on detecting the global response of NPP to urbanization using the Spatial Durbin model and discussing the local heterogeneity of the effect in the Yangtze River Delta urban agglomeration (YRD), the middle reaches of Yangtze River urban agglomeration (MRYRU), and the Chengdu-Chongqing urban agglomeration (CCU) based on a geographically weighted regression model. The results show that the average NPP of the YEB increased from 592g*c/m^2 to 670g*c/m^2 at a rate of 0.621% from 2000 to 2020, with the most significant growth in the CCU, and the overall pattern of change is "increased in the north and decreased in the south". The negative spatial autocorrelation between urbanization and NPP is becoming increasingly significant, and the negatively correlated clusters is the dominant type of local autocorrelation, among which the number of "High-Low" type cities is the largest and growing, mainly located in the northern regions of Anhui and Jiangsu. The significant negative effect of urbanization on the productive capacity of vegetation cover systems was verified, and a negative spillover effect that far exceeded the local negative effect was also confirmed. The effect of urbanization on NPP has significant local variability and gradually shifts to the effect pattern of positive effect in the east and negative effect in the

west, while the pattern of urbanization-driven effects in the three urban agglomerations also continues to change. This study increases the concern about the negative ecological effects of urbanization, and more importantly, provides a basis for the joint action of ecological restoration and management in the Yangtze River Economic Belt and the implementation of differentiated governance policies around urban agglomerations.

KEYWORDS

net primary productivity of vegetation, urbanization, driving effect, ecological restoration, Yangtze River Economic Belt (YEB)

1 Introduction

Net primary productivity (NPP) of vegetation is the residual of the total organic matter produced by photosynthesis in a green plant community per unit area and per unit time, after deducting the organic matter required for its own respiration (Zhong et al., 2023). NPP is a key element in measuring the health and resilience of terrestrial ecosystems. It has also been shown to be an important indicator for regulating the "structure-function" of ecosystems, their carbon sequestration capacity, sustainability of material cycles and even the evolution of ecosystem dynamics (Yang et al., 2021). NPP's response to long-term global climate change has been confirmed by numerous investigations. Climate change factors such as precipitation, temperature, and humidity affect NPP levels through direct or indirect pathways and have complex implications for ecosystem suitability management in human settlements (Wei et al., 2021). As human activities have increased, the increasing conflicts between human and natural systems due to the migration of residents, urban land expansion, and predatory exploitation of natural resources have attracted worldwide attention (Liu et al., 2019; Wang et al., 2022; Wei et al., 2023; Wei G.E. et al., 2023). In particular, the global urban land area grew from 239,000 km^2 to 519,800 km^2 in the first two decades of the 21st century, an increase of 117.49% (Liu et al., 2019). Accelerated urbanization has changed the structure of urban land use and the size of built-up areas, and consequently affected soil fertility, space for vegetation growth and the risk of growth pollution (Muhammad et al., 2023). These process pathways put a heavy burden on urban landscape ecological patterns and global vegetation cover systems, and have become important constraints on sustainable urban development goals such as sustainable urban construction (Goal11, SDG), maintenance of ecosystem carbon cycles (Goal13, SDG), and ecosystem conservation (Goal15, SDG) (Chen et al., 2023). Therefore, it is important to reveal the response pattern of NPP to urbanization and provide macro-management strategies to mitigate the stressful effects of urbanization. This is important for deepening the knowledge and understanding of global environmental change, promoting urban ecosystem restoration and resilience enhancement, and even sustainability of urban planning and land use management (Tang et al., 2023; Wei et al., 2022).

To mitigate the negative effects of human activities on NPP represented by urbanization, national organizations and local governments have put a lot of practice based on consensus frameworks such as the 2030 Agenda for Sustainable Development, the Paris Agreement, and the International Geosphere-Biosphere Programme (IGBP) (Saiu et al., 2022). For example, the U.S. Strategic Plan for the Conservation of Ecosystems and Biodiversity, China's Plan for the Advancement of Ecological Civilization, and Europe's Biodiversity Strategy 2020 all consider harmonious, orderly, and healthy urban development as an important area for restoring the carbon storage and species conservation capacity of vegetated ecosystems (Guido et al., 2017). Scholars have mainly developed case studies on the mechanisms of urbanization on NPP in terms of the impact of urban land expansion, population urbanization and economic urbanization processes on NPP and the simulation of future trends of this impact. For example, Liu et al. (2020) investigated global built-up land expansion encroaching on terrestrial vegetation NPP at a rate of 22.4 Tg-C per year in the early decade of the 21st century and offsetting 30% of climate change-driven NPP growth. Li et al. (2022) revealed that there are direct and indirect effects of urbanization on NPP, and the direct effects have significant spatial non-stationarity characteristics, providing evidence for the development of differentiated urban ecological governance strategies. These studies have focused more on the negative ecological effects of urbanization unidimensionally on NPP, while rarely examining the integrated effects of urbanization as a systemic project on NPP in multiple domains such as residential migration, economic growth, and land use change. This has led to a significant reduction in quantitative support for relevant urbanization management strategies (Wu et al., 2014). In addition, the transboundary spillover effects of urbanization on NPP have not been generally appreciated, which clearly lacks support for carrying out joint conservation and restoration strategies for regional vegetated ecosystems (Zhong et al., 2021).

The Yangtze River Economic Belt (YEB) is a major national strategic development region spanning three geographic regions in China: the east, the middle and the west, and an inland urban economic belt with global influence. It contains the Yangtze River Delta urban agglomeration (YRD), the middle reaches of Yangtze River urban agglomeration (MRYRU), and the Chengdu-Chongqing urban agglomeration (CCU), which are strategic national urban

agglomerations in China and bring together internationally important cities such as Shanghai, Wuhan, Chengdu and Chongqing (Liu et al., 2023). According to data from China's National Bureau of Statistics, the YEB has a key position in China's macroeconomic growth and human capital market with a total GDP and population of 47.15 trillion yuan and 606 million people in 2020, accounting for 46.4% and 42.92% of China's total, respectively (Yang et al., 2022). The rapid clustering of economic and demographic elements promotes rapid urbanization and changes the form, compactness and structure of urban land, which in turn affects regional landscape patterns and ecological networks. This generates ecological problems such as habitat degradation, species loss, carbon sequestration and water retention capacity decay (Yan et al., 2021). Although in 2016, the Chinese government issued the initiative of "Grasping great protection and not engaging in great development" for the YEB, and released the Ecological Protection Plan for the YEB focusing on key ecological elements such as vegetation cover systems. It aims to enhance the conservation of ecosystem diversity, resilience, and sustainability in the region (Bai et al., 2023). However, monitoring the response rule of vegetation ecosystem production capacity to urbanization is still an urgent issue to understand the ecological carbon cycle process and ecological sustainable development path in the YEB.

Existing studies have focused more on changes in vegetation ecosystem response to human urban construction activities in a single province or urban agglomeration in the YEB, providing an effective reference for ecosystem restoration and management in the region. For example, Li et al. (2022) analyzed the local direct and spatial spillover effects of urbanization on NPP using the CCU as a case study; Wang et al. (2021) measured changes in vegetation carbon stocks in the Yangtze River basin based on NPP data and revealed the synergistic effects of urbanization-dominated human activities and climate factors on different segments of the Yangtze River basin. However, as an important strategic region crossing different economic and topographic divisions and population density boundaries in China (the "Heihe-Tengchong" line), significant regional differences in industrial structure, urban form, and population migration patterns dominated by urban agglomerations have developed within the YEB (Li et al., 2022). More often, existing studies need to focus more on the intrinsic variability of urbanization impacts on NPP in the YEB in the context of such significant cross-regional differences in natural (topography, climate, etc.) and human factors (population size, city size, etc.) (Chen et al., 2023; Xia and Zhai, 2022). Otherwise, this will create a realistic gap that makes it difficult to provide site-specific and systematic urbanization optimization strategies and urban vegetation ecological conservation solutions for the YEB from a theoretical perspective.

In summary, existing studies have made prominent contributions to the understanding of the spatial dependence pattern of NPP, the response of NPP under the influence of climate change and human activities represented by urbanization, but the exploration of the mechanism of the impact of urbanization on NPP in the YEB is still far from being addressed: (1) Rarely considered urbanization as a multi-dimensional whole encompassing residential migration, economic growth and land use change, and considered the driving impact of integrated urbanization on NPP; (2) The comprehensive assessment of the local direct effects and cross-border spillover effects of urbanization on NPP in the YEB needs to be strengthened; (3) The response mechanism of NPP to urbanization in the YEB is clearly site-specific, influenced by the disparities in topography, urbanization stage and economic base, while previous studies have paid insufficient attention to the local heterogeneity of the influence mechanism within it dominated by urban agglomerations. To fill these knowledge gaps, our study uses the YEB as a case study to analyze the spatio-temporal evolution patterns of NPP based on MODIS-17A3HF NPP image products. The comprehensive urbanization index is also constructed based on population urbanization, land urbanization and economic urbanization. The focus is on investigating the global and local effects of comprehensive urbanization on the impact of NPP in the Yangtze River Economic Zone using spatial econometric regression models and geographically weighted regression models. The focus is on the use of spatial regression models to investigate the global effects of integrated urbanization on NPP impacts in the YEB, and the local effects and spatial heterogeneity of the impacts of the three major urban agglomerations are further diagnosed under Geographically Weighted Regression (GWR) models.

2 Study area, methods and data sources

2.1 Study area

The YEB is a major national strategic development area in China with the Yangtze River basin as the main trunk, which contains three national strategic urban agglomerations: YRD, MRYRU and CCU (Figure 1). YEB involves 130 prefecture-level cities in 11 provinces and municipalities, including Shanghai, Jiangsu, Zhejiang, Anhui, Jiangxi, Hubei, Hunan, Chongqing, Sichuan, Yunnan, and Guizhou (Chen et al., 2023). This study takes the YEB as the case study, with 130 cities within it as the research sample. The Yangtze River basin, with its warm climate, abundant rainfall, numerous tributary lakes and rich species resources, is a concentrated distribution area for rare and endangered wildlife in China. The per capita GDP of Yangtze River Economic Zone increased from 7506.25 yuan to 71,102.70 yuan from 2000 to 2020, an increase of 8.472 times, and the population density increased from 454.65 person/km^2 to 490.6 person/km^2, an increase of 7.907%. Despite the Chinese government's initiative of "Grasping the big protection, not big development", the conservation and restoration of forest and ecological space in the YEB has achieved significant achievements. However, the rapid growth of economic scale and population size, as well as the significant disparities between provinces and cities in socio-economic and natural contexts have led to the continued contradiction between human urban activities and ecological environmental protection in the region. Therefore, it is important to study the impact mechanism of urbanization on NPP in the YEB for the construction of ecological resilience and sustainable development in the region.

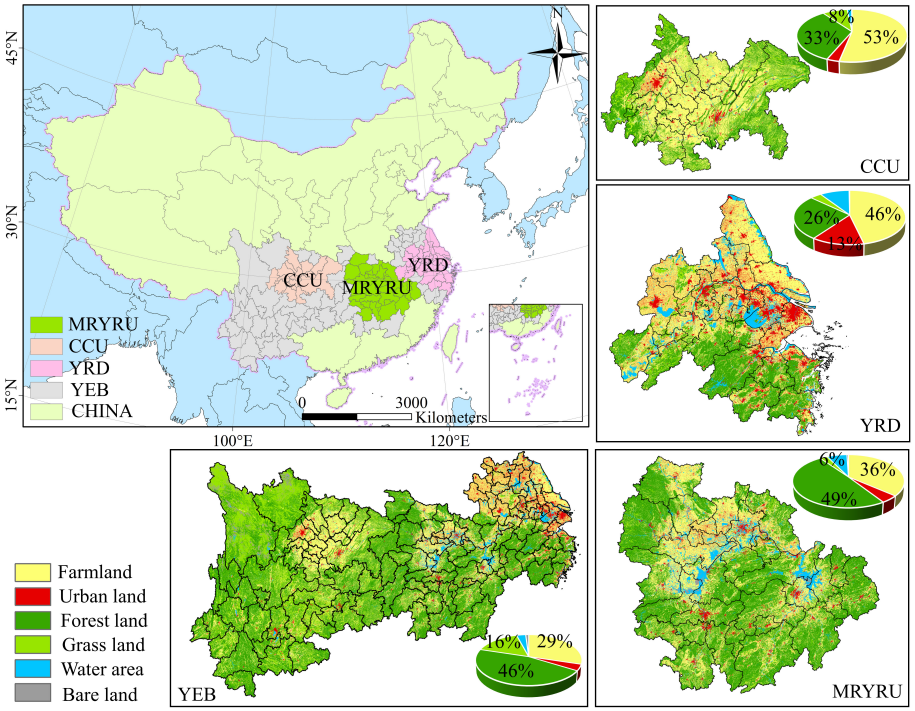

FIGURE 1
Study area.

2.2 Methods

2.2.1 Comprehensive urbanization level accounting

Urbanization is a systemic project involving multi-domain contents such as urban population growth, land expansion and economic revitalization (Figure 2). The comprehensive urbanization level referred to in this study includes three dimensions of population, land and economic urbanization. Referring to the studies of Peng et al. (2020), Wei G. et al. (2023) and Ouyang et al. (2021), the above indicators were measured in terms of urban resident population share, urban land area share and GDP density. Based on Chen et al. (2022), the data of urbanization sub-dimension indicators were standardized based on the extreme value method, and the standardized results were summed and averaged to obtain the comprehensive urbanization level of each city in the YEB. The formula is as follows:

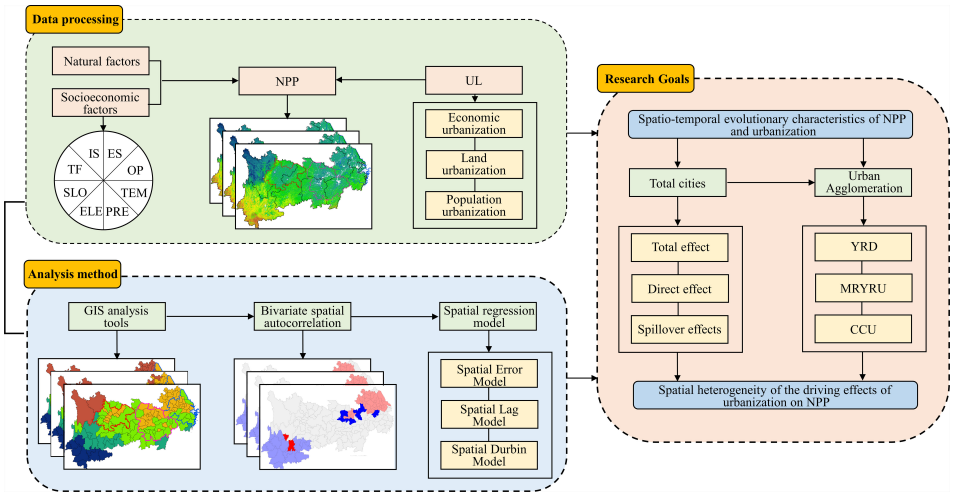

FIGURE 2
Study route.

$$x_{ij}{}' - \frac{x_{ij} - \min\{x_{ij,} \cdots x_{ij}\}}{\max\{x_{ij,} \cdots x_{ij}\} - \min\{x_{ij,} \cdots x_{ij}\}} \quad (1)$$

$$UL_i = \frac{x_{iPU} + x_{iLU} + x_{iEU}}{3} \quad (2)$$

Where: x_{ij}' is the standardized value of the j indicator of city i; x_{iPU}, x_{iLU} and x_{iEU} are the indexes of city i after standardization, respectively; UL_i is the comprehensive urbanization level of city i.

2.2.2 Bivariate spatial autocorrelation

The bivariate spatial autocorrelation model is used to analyze the spatial correlation between integrated urbanization and NPP. Among them, the local bivariate spatial autocorrelation is calculated as:

$$I = \frac{UL_i - \overline{UL}}{\sigma_{UL}} \cdot \sum_{j=l}^{n} \left(W_{ij} \frac{NPP_j - \overline{NPP}}{\sigma_{NPP}} \right) \quad (3)$$

Where: W_{ij} is the spatial weight matrix; UL_i and NPP_j are the UL and NPP of cells i and j, respectively; σUL and σNPP are the variances of UL and NPP_l, respectively (Dong et al., 2023).

2.2.3 Spatial regression model

The study investigates the global driving effect of urbanization on NPP in the YEB with a spatial regression model. Compared to the Spatial error model (SEM) and Spatial lag model (SLM), the Spatial Durbin model (SDM) integrates the quantitative advantages of both for exogenous and endogenous interaction effects of variables and can decompose the driving effects into direct and spillover effects based on partial differential equations (P.D.E.) (Guo et al., 2023). The calculation formula of SDM is as follows:

$$NPP_{it} = \rho WNPP_{it} + \beta(UL_{it} \sim PRE_{it}) + \theta W(UL_{it} \sim PRE_{it}) + \epsilon_{it} \quad (4)$$

Where: NPP_{it} is the explanatory variable NPP for region i in period t; UL_{it}~PRE_{it} is the explanatory variable for region i in period t, containing the key explanatory variables integrated urbanization and other control variables (including natural and socioeconomic control variables); ϵ is a normally distributed random disturbance term; ρ, β and θ are parameters to be estimated; W is the spatial weight matrix; WY is the spatial lagged dependent variable; and WX is the spatial error independent variable. The Lagrange multiplier (LM) was used to assess the necessity of incorporating spatial effects into the regression model; the Likelihood Ratio estimation (LR) was used to evaluate whether the SDM can be reduced to SLM or SEM.

2.2.4 Geographically weighted regression model

This study measures the local variation effect of urbanization on NPP in the YEB based on the GWR model for discussing the differential performance of the driving effect among the three major urban agglomerations (Tian et al., 2023). The model is calculated as follows:

$$NPP_{it} = \beta_0(u_i, v_i) + \sum_{j=l}^{k} \beta(u_i, v_i)(UL_i \sim PRE_i) + \epsilon_i \quad (5)$$

Where: (u_i, v_i) is the geographic location coordinates of region i; β_i is the corresponding geospatial location function of region i; UL_i~PRE_i are the explanatory variables for region i, containing the key explanatory variable UL and other control variables.

2.3 Data sources

2.3.1 Urbanization level

The three urbanization dimensions of population urbanization, land urbanization and economic urbanization are measured by the percentage of urban resident population, the percentage of urban land area and GDP density, respectively. Among them, the data of urban resident population ratio are mainly from the statistics of population number in China Urban Statistical Yearbook, China Statistical Yearbook; the data of urban land area and GDP density are from the remote sensing dataset of land use (30m) and spatialized dataset of GDP density (1km) provided by the Environment and Resources Data Center of Chinese Academy of Sciences (http://www.resdc.cn).

2.3.2 Net primary productivity of vegetation

The NPP data were taken from the MOD17A3 Global Net Primary Productivity product (https://modis.gsfc.nasa.gov/) from NTSG (Numerical Terradynamic Simulation Group), USA, with a spatial resolution of 500m. This dataset has now been used in a large number of research areas such as global NPP spatial distribution and carbon cycle.

2.3.3 Control variables

In addition to urbanization, regional physical context and socioeconomic development are also considered to have important effects on NPP in existing research and theoretical systems. Referring to studies such as Yue et al. (2022) and Sun et al. (2016), we also selected socioeconomic indicators such as industrial structure share, energy consumption, actual utilization of foreign investment, and pressure on transportation infrastructure, as well as natural indicators such as slope, elevation, average annual precipitation, and average annual temperature as control variables to improve the fit of the regression model (Table 1). Among them, the data of natural control variables were mainly obtained from the relevant data products provided by the Geographic Data Cloud Platform of CAS (http://www.gscloud.cn/sources/index) and the Earth System Science Data Center (http://www.geodata.cn/). We extracted the dataset of 130 prefecture-level cities in the Yangtze River Economic Belt based on the image cropping and zoning statistics tools of ArcGIS platform. The socio-economic control variables were mainly obtained from the China City Statistical Yearbook, the China Energy Statistical Yearbook, and the statistics of relevant index data from the provincial and municipal statistical yearbooks. We extracted the dataset of 130 prefecture-level cities in the Yangtze River Economic Belt based on the image cropping and zoning statistics tools of ArcGIS platform. The socio-economic control variables data were mainly obtained from the China City Statistical Yearbook, the China Energy Statistical Yearbook, and the statistics of relevant index data from the provincial and municipal statistical yearbooks.

TABLE 1 Indicator data sources.

Data type	Variables	Unit	Data name	Data sources	Abbreviation
Socioeconomic	Population urbanization	%	Urban resident population as a share of total population	Urban statistical yearbook of China	PU
	Land urbanization	%	Land use data in 2000, 2010, 2020	Data Centre for Resources and Environmental Sciences of the Chinese Academy of Sciences (http://www.resdc.cn)	LU
	Economic urbanization	yuan/km2	GDP density grid data set in 2000, 2010, 2020	Data Centre for Resources and Environmental Sciences of the Chinese Academy of Sciences (http://www.resdc.cn)	EU
	Industrial structure	%	Value added of tertiary industry as a percentage of GDP (%)	Urban statistical yearbook of China	IS
	Energy consumption	Billion kwh	Electricity consumption	Energy Statistics Yearbook of China	ES
	Openness	USD million	Actual use of foreign capital	Urban statistical yearbook of China	OP
	Transportation infrastructure pressure	Million people	Road passenger volume	Urban statistical yearbook of China	TIP
Natural	Slope	°	Slope	Geospatial Digital Cloud Platform of Chinese Academy of Sciences (http://www.gscloud.cn/sources/index)	SLO
	Elevation	m	DEM digital elevation data	Geospatial Digital Cloud Platform of Chinese Academy of Sciences (http://www.gscloud.cn/sources/index)	ELE
	Average annual precipitation	mm	China's monthly precipitation data in 2000, 2010, 2020	National earth system science data science (http://www.geodata.cn/)	PRE
	Average annual temperature	°C	China's monthly precipitation data in 2000, 2010, 2020	National earth system science data science (http://www.geodata.cn/)	TEM
	Net primary productivity	g*c/m2	NPP data from MODIS-MOD17A3	MODIS-17A3HF data products are available on the NASA website (https://modis.gsfc.nasa.gov/)	NPP

3 Result

3.1 Spatio-temporal evolution patterns of NPP and urbanization in the YEB

Combining GIS zoning statistics tools and spatial interpolation techniques to measure the dynamic trend of NPP in the YEB, as shown in Figures 3, 4. The investigation shows that the average NPP in the YEB increased from 592 g*c/m^2 to 670 g*c/m^2 at a rate of 0.621% from 2000 to 2020 (Figure 3A). Among them, the NPP growth of CCU is the most significant, with an increase of 39.387% from 2000 to 2020, followed by MYRYU and YRD, with increases of 14.867% and 6.495%, respectively. In terms of spatio-temporal dynamics, the NPP level in the YEB shows a clustering pattern of "high in the south and low in the north, high in the west and low in the east" (Figure 4), both in terms of remote sensing images and distribution based on administrative districts. The three major low-value clusters (NPP<450 g*c/m^2) in the eastern, central and western

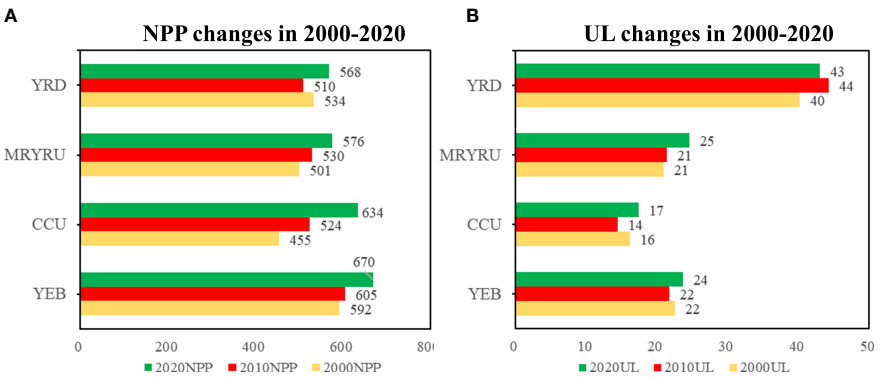

FIGURE 3
Dynamics of NPP (g*c/m2) **(A)** and urbanization (%) (Bs) **(B)**, 2000–2020.

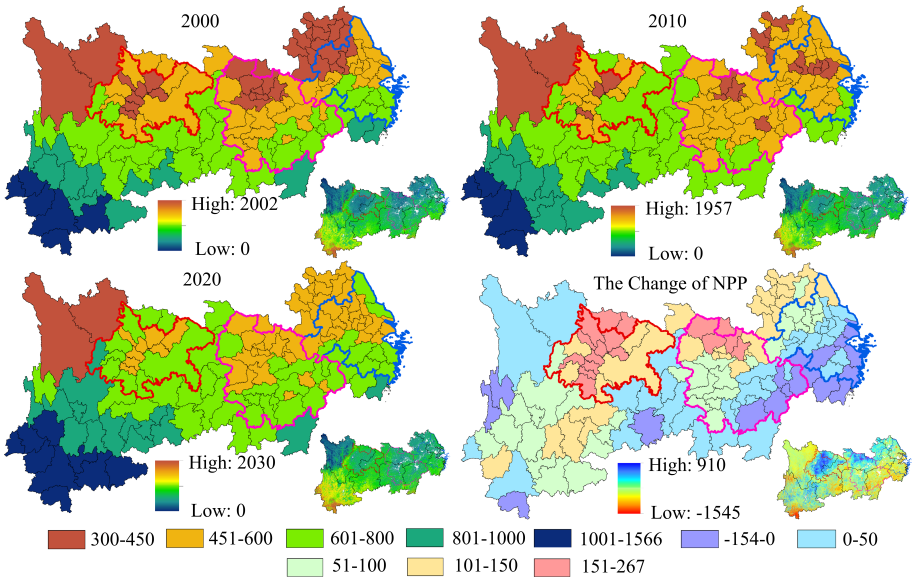

FIGURE 4
Spatio-temporal changes of NPP in YEB, 2000–2020.

parts of the study area in 2000 gradually developed toward dispersion in 2020, and the high-value clusters, mainly in Yunnan Province, spread further in 2020. In terms of the change trend, the average NPP of the YEB shows a general pattern of change of "increased in the north and decreased in the south". The NPP degraded cities with 13.178% of all cities are mainly located in the southeastern and southern part of the YEB. The most prominent NPP degradation is Xishuangbanna and Lishui, with decreases of 9.787% and 4.575%, respectively. The cities with high values of NPP growth are mostly distributed in the CCU and northern areas of the MYRYU, especially Suining and Ziyang with increases of 84.486% and 78.810%, respectively.

The overall average UL index of the YEB grew from 22.485% to 23.652% with an average annual growth rate of 0.253% from 2000 to 2020 (Figure 5). Among them, the UL index of the MYRYU has the most significant growth, with an increase of 17.455% from 2000 to 2020, followed by CCU and YRD, while the UL index of YRD is usually the highest, with a UL index of 42.982% in 2020. In terms of spatio-temporal dynamic distribution, the level of urbanization in the YEB gradually changes from "high in the east and low in the west" to a distribution pattern with urban agglomerations as the regional core. In 2000, it was presented as the eastern UL high-value group with Shanghai as the core. By 2010 and 2020, the UL indexes of Wuhan, Changsha, Chongqing and other central cities in the central and western regions grew rapidly, gradually forming a pattern of UL high-value distribution led by the core cities of urban agglomerations. In terms of the change trend, 37.984% of the cities in the YEB have a decreasing trend in UL index, mainly in the northwestern cities represented by Aba and the northeastern cities represented by Bozhou. However, this does not imply a degradation of the urbanization process, as the UL index is performed based on a standardized formula (Eq. 2), the variation of the UL index mainly shows the degree of difference in urbanization levels and the change in the rank order among cities in the YEB. The cities with significant UL index growth are mainly located in the eastern part of the MYRYU and the southern part of the YRD. In particular, the UL indexes of Jiujiang, Suzhou and Changsha increased by 17.747%, 14.900% and 15.444%, respectively.

3.2 Spatial correlation analysis of urbanization and NPP in YEB

Figure 6 shows the change trend of bivariate global autocorrelation and local autocorrelation of UL index with NPP in YEB from 2000 to 2020. The global Moran's I for UL and NPP in 2000, 2010 and 2020 are −0.350, −0.380 and −0.419 (p-value = 0.001), respectively, which indicate an overall increasingly significant negative spatial autocorrelation between urbanization and NPP in the YEB. In terms of bivariate local autocorrelations, UL and NPP negatively correlated cluster cities (containing both High-Low and Low-High cluster types) are dominant, and the share increases from 24.806% to 33.333% during the study period. This validates the increasingly significant negative spatial autocorrelation between urbanization and NPP in the YEB, and confirms the urgent need to adjust urbanization pathways in the region to reduce the negative impacts on vegetation ecosystems and carbon cycle functions. "High-Low" is the dominant cluster type in the bivariate spatial correlation, and the number of cities increased from 13.178% to 20.930%, followed by "Low-High" clusters, whose overall share also increased from 11.628% to 12.403%. In terms of spatio-temporal evolution, the distribution pattern of bivariate local spatial autocorrelation cluster types is relatively stable during the study period. Specifically, the "High-Low" negative correlation clusters are mainly located in Bozhou, Huai'an and other cities in Anhui and northern Jiangsu. The prominent scale of population,

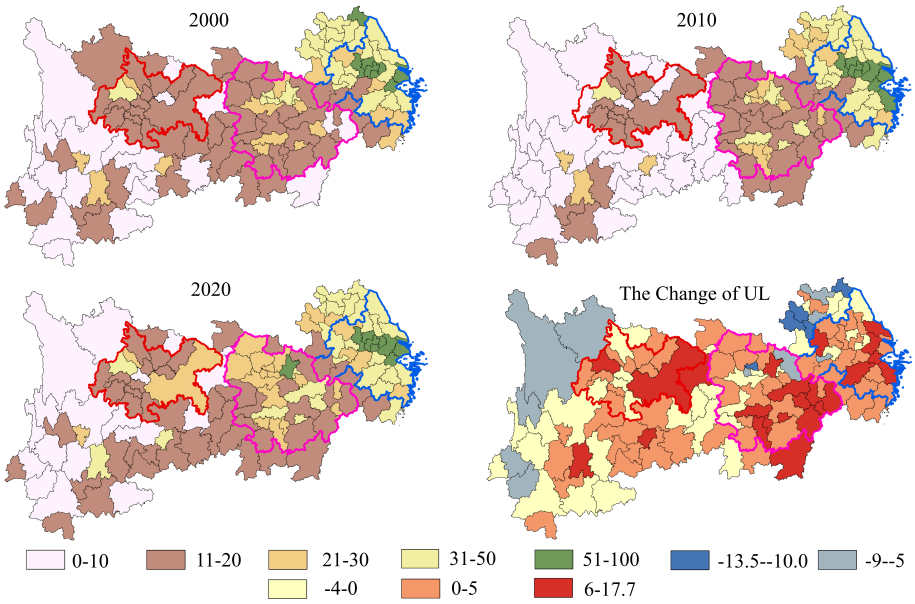

FIGURE 5
Spatio-temporal changes in urbanization levels in the YEB, 2000–2020.

arable land, and construction land in these cities (Figure 1) generates significant encroachment on vegetated ecosystems, resulting in relatively high levels of urbanization and relatively low NPP in the region.

The "Low-High" negative correlation clusters cities are generally located in the southwestern region, such as Xishuangbanna, Lincang and Pu'er. These cities are located near the "Hu Huanyong population density line" in China, where the human footprint is relatively sparse and the terrain is complex, with many forested and mountainous areas off the beaten path. The excellent natural ecological background and the low intensity of urban development have contributed to the low level of urbanization but high quality plant ecosystems in the area. The "High-High" positive correlation clusters are mainly located in Kunming, reflecting the high quality ecological environment and the strong "siphon effect" of population, industry and resources in the region. The "Low-Low" positive correlation agglomeration is mainly laid out in Huanggang, Jingzhou and Jingmen and other cities in the middle reaches of the Yangtze River. Combined with the performance of multidimensional urbanization, these cities have low levels of land and economic

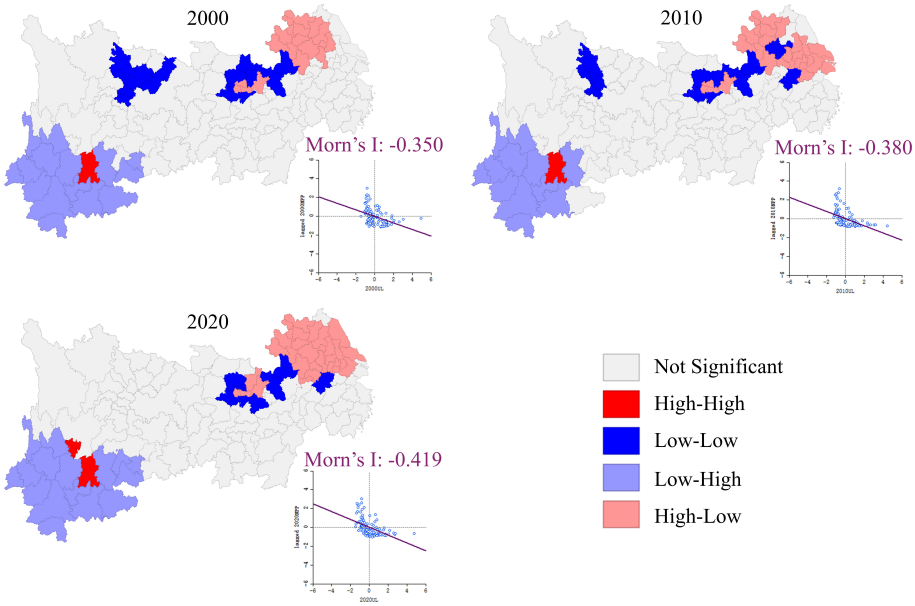

FIGURE 6
Bivariate spatial global autocorrelation scatter plot and local autocorrelation LISA plot of urbanization and NPP in YEB, 2000–2020.

urbanization, have significant gaps in urban development intensity compared to Wuhan, and are subject to significant resource siphoning. At the same time, due to the location in Jianghan Plain, organic matter produced by photosynthesis of grassland vegetation is more disadvantaged than that of mountainous woodlands in humid climate, resulting in relatively disadvantaged urbanization level and vegetation ecosystem productivity in this region.

3.3 Analysis of the driving impact of urbanization on NPP in the YEB

3.3.1 Driving impact of urbanization on NPP in a global perspective

All variables after logarithmization and normalization passed the multi-collinearity and Moran tests, while LM-SLM, LM-SEM tests and LR-SLM and LR-SEM significantly rejected the original hypothesis at 1% confidence level (Table 2). Based on this, we used SDM model to detect the driving impact of urbanization on NPP, and the regression results are shown in Table 2. It was found that the driving effect of UL on NPP was significantly negative in different periods, verifying the significant negative feeder effect of urbanization on the productive capacity of vegetation cover systems in the YEB. In terms of coefficient changes, the driving influence of UL showed an inverted "U" shape, with statistically significant regression coefficients of −0.165, −0.223 and −0.166 in 2000, 2010 and 2020, respectively. The effect of control variables also received further attention. For example, the driving influence of the value added of the tertiary sector as a share of GDP on NPP is significantly positive in different periods. This indicates that the tertiary sector not only has low consumption and emission characteristics, but also the businesses involved in computer and digital information technology contribute to the restoration and management of urban vegetation ecosystem. Slope and elevation had a significantly positive effect on NPP during some periods, indicating that slope and elevation also played a significant role in contributing to the conservation of vegetated ecosystems.

TABLE 2 Regression results based on SDM model.

	SDM_2000	SDM_2010	SDM_2020
UL	−0.165* (−1.957)	−0.223** (−2.235)	−0.166* (−1.948)
lnELE	0.047 (1.584)	0.089** (2.913)	0.048 (1.586)
lnSLO	0.081* (1.684)	0.010 (0.190)	0.080* (1.655)
lnTEM	−0.108 (−1.030)	−0.041 (−0.381)	−0.110 (−1.039)
lnPRE	0.049 (0.553)	−0.008 (−0.086)	0.050 (0.568)
lnIS	0.102** (2.000)	0.152*** (3.666)	0.104** (2.022)
lnES	0.011 (0.735)	0.008 (0.822)	0.011 (0.739)
lnOP	0.001 (0.179)	0.001 (0.251)	0.001 (0.155)
lnTIP	−0.003 (−0.356)	−0.024** (−2.209)	−0.003 (−0.351)
*W*UL*	−0.071 (−0.420)	0.203 (1.148)	−0.070 (−0.420)
*W*lnELE*	−0.022 (−0.639)	−0.008 (−0.214)	−0.020 (−0.577)
*W*lnSLO*	−0.141** (−2.246)	−0.116 (−1.597)	−0.143** (−2.256)
*W*lnTEM*	0.337** (2.080)	0.189 (1.074)	0.350** (2.143)
*W*lnPRE*	−0.035 (−0.328)	−0.021 (−0.187)	−0.037 (−0.342)
*W*lnIS*	−0.086 (−1.035)	0.321*** (3.664)	−0.077 (−0.917)
*W*lnES*	0.037 (1.300)	−0.028 (−1.296)	0.038 (1.313)
*W*lnOP*	−0.010 (−1.127)	0.024 (1.341)	−0.010 (−1.153)
*W*lnTIP*	0.021 (1.250)	−0.057*** (−2.784)	0.020 (1.232)
Direct effect (UL)	−0.274** (−1.997)	−0.212* (−1.853)	−0.277* (−1.941)
Spillover effect (UL)	−1.463*** (−4.034)	0.127 (0.149)	−1.319*** (−3.930)
R-squared	0.662	0.869	0.675
Log-likelihood	184.044	174.645	183.694
sigma^2	0.003	0.004	0.003
LM-SLM	5624.942***	4214.041***	4587.462***
LM-SEM	53.273***	45.427***	53.321***
Moran's I	0.519***	0.440***	0.420***

*, **, and *** indicate significance at the confidence level of 10%, 5%, and 1%, respectively.

However, according to LeSage and Pace (2009), the SDM coefficients do not reflect either the direct, spillover, or total effects of the independent variables. This is because analyzing the spatial spillover effects between regions through simple point regressions would produce erroneous estimates, and a decomposition with reference to P.D.E is needed to better understand the effect of urbanization on NPP. It is found that urbanization in both local and neighboring regions has a significant negative effect on NPP in the Yangtze River Economic Zone in some periods. For example, every 1% increase in the UL index in 2020 will directly lead to a 0.277% decrease in local NPP and indirectly lead to a 1.319% decrease of NPP in neighboring regions. Among them, the direct negative effect of urbanization is statistically significant in all periods, and this direct effect generally fluctuates in growth, with direct effect elasticity coefficients of −0.274 and −0.277 in 2000 and 2020, respectively. Although the elasticity coefficient is not significant in 2010, the spillover effect of urbanization on the impact of NPP achieves an overall convergence from 2000 to 2020. The elasticity coefficients of spillover effects for UL are −1.463 and −1.319 in 2000 and 2020, respectively, with an absolute decrease of 9.843% in the regression coefficient. This indicates that the negative effect of urbanization on NPP in neighboring areas has converged. In addition, the comparison of the direct effect with the spillover effect raises concern, as the survey shows that the spillover effect of urbanization on NPP is much more than the direct effect in a statistical sense. For example, the elasticity coefficient of the direct effect of urbanization in 2000 is −0.274, while the spillover effect is −1.463.

3.3.2 Driving impact of urbanization on NPP in a local perspective

To further analyze the local effects of urbanization on the NPP in the YEB, especially to reveal the local heterogeneous characteristics of the impact in the three major urban agglomerations, we constructed a GWR analysis model based on ArcGIS platform (Figure 7). The investigation showed that the Adjusted R2 was 0.945, 0.909 and 0.971, Sigma was 57.816, 78.262 and 46.461, and AICc was 1430.183, 1508.319 and 1374.427 for the three periods in GWR estimation, respectively. The spatially heterogeneous characteristics of the impact of urbanization on NPP in the YEB are significant, validating the need to monitor the driving effects from a local perspective. Specifically, urbanization in the west maintains a significant negative shock, while the overall pattern of the driving effect of UL on NPP gradually shifts to a regional heterogeneity of positive in the east and negative in the west. The reason may be that western cities such as Lincang and Baoshan are located on the Yunnan-Guizhou Plateau where forest vegetation is abundant, and the base of urban development intensity is low, but the risk sensitivity of the forest cover system is higher, and they are more affected by the disturbance of human activities in the crude urban construction activities. In contrast, with the continuous development of urban ecological resilience construction concepts and low-carbon green development technologies in the eastern region, the impact of urbanization on vegetation ecosystems and their productivity has gradually diminished. It even promotes the growth of urban NPP to some extent based on urban ecological planning policies such as park cities and green corridors.

In terms of the divergent performance of the urban agglomerations, the effect of UL on NPP is negative for all of the YRD in 2000. While most of the cities in the MYRYU show negative effects, the effects in western mountainous cities such as Jingmen, Xiangyang and Yichang are positive. The driving influence of UL in the western cities of CCU is significantly negative, while Chongqing and Dazhou show positive effects. In 2010, the negative effect of UL in the YRD urban agglomeration further increases and shows a gradient pattern of decreasing from east to west. The pattern of regression coefficients is more stable in the MYRYU, but the negative effect of UL on NPP increases overall, and the UL turns negative in the whole area of CCU. In 2020, the impact of UL on NPP for cities in the whole YRD turns from negative to positive, the positive effect cities in the

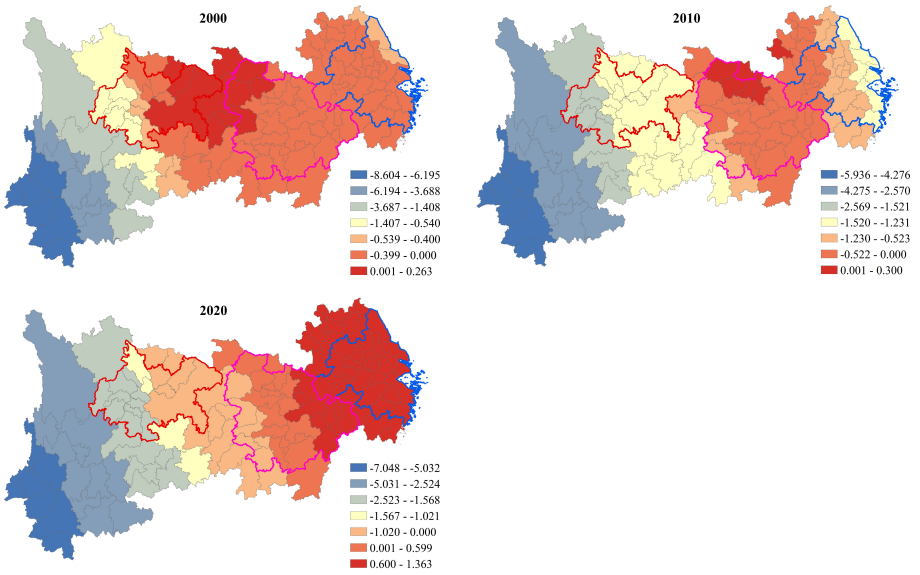

FIGURE 7
Distribution of regression coefficients based on GWR model.

MYRYU shift to eastern cities such as Shangrao, Huanggang and Jiujiang, and the impact of UL on NPP for cities in CCU are still all negative, but the overall negative impact has converged.

4 Discussion

4.1 Direct and spillover effects of the impact of urbanization on NPP

The direct effect of urbanization on NPP has been confirmed in previous studies, which emphasize the substantial conversion of ecological spaces such as grasslands and woodlands to production-living spaces during urbanization, resulting in the derogation of vegetation cover systems and leading to a decrease in regional NPP levels (Yang et al., 2021). Our study considers urbanization as a unified system, integrating urbanization elements such as population urbanization, economic urbanization, and land urbanization, providing an comprehensive perspective for investigating the impact of urbanization on NPP (Chen et al., 2020). The findings emphasize that the negative effect of urbanization on NPP is not only in the local area, but more widely a spillover effect that goes far beyond the local effect. The former may be related to the inherent resource-consuming activities of cities (Sharma et al., 2022; Zhong et al., 2021; Chen et al., 2023). Urban population migration and industrial boom increase the demand for natural resources and production-living space, while land urbanization implies the conversion of a large amount of ecological space to artificial impervious surfaces. These urbanization processes have, to some extent, directly or indirectly enhanced the encroachment on native vegetation cover systems and challenged the carbon cycling capacity of vegetation. The latter may have some connection with the regional integration construction of the Yangtze River Economic Belt. As a national strategic development region in China, the Yangtze River Economic Belt forms an integrated cooperation space with Shanghai as the leader and urban agglomerations along the route as the core. The region has gradually built synergistic channels in technological innovation, data integration, and industrial chain construction (Tian and Pang, 2022). With the support of regional integration, ecological product consumption actions can influence neighboring urban markets through the integrated "land, water, and air" channel, thus indirectly causing cross-regional ecological consumption of vegetation (Wang et al., 2022).

4.2 Heterogeneity in the impact of urbanization on NPP in three major urban agglomerations

The spatial heterogeneity of the impact of UL on NPP in urban agglomerations in the YEB is verified in this study, which complements previous studies based on individual urban agglomerations or the YEB as a whole. For example, Qiao and Huang (2022) assessed the ecosystem health of the YRD and evaluated the impact of land urbanization on ecosystem health. Chen et al. (2022) based on NDVI index explored the ecosystem health level of the MYRYU, and pointed out a U-shaped relationship between urbanization and ecosystem health. Our investigation finds that the NPP of the CCU is most strongly influenced by UL, especially the negative influence of western cities is significantly stronger than that of eastern cities such as Chongqing. The reason for this phenomenon may be that the western part of the CCU is surrounded by mountains and hills, with a high quality forest ecological substrate and carbon sequestration capacity, and urban development activities have modified the local forest ecosystem to a more obvious extent. In contrast, most of the eastern cities such as Chongqing are located in the plains and have relatively more homogeneous NPP of grassland ecosystems, which, together with more modern urban planning and green economy construction, contribute to the ecological resilience of these cities to resist urbanization (Li et al., 2023; Luo et al., 2023). The distribution pattern of UL effects in the MYRYU remains relatively stable, but it is noteworthy that the UL of cities in the eastern part of the urban agglomeration is positive in 2020. This may have some synergistic relevance to urban ecological planning in the region (Chen et al., 2022; Liu et al., 2023; Ma et al., 2023). At the end of 2009, China released the "Poyang Lake Ecological Economic Zone Plan", which tries to build the Poyang Lake area into an advanced and efficient ecological industrial cluster and gradually build a new urban agglomeration with ecological livability. This promotes the ecological restoration of vegetation and the sustainable construction of urbanization in the area. The driving effect of UL on NPP in the YRD turns from negative to positive, which may be related to the implementation of ecological co-protection planning in the region. By proliferating green production processes, circular economy technologies and energy saving and emission reduction standards of the core cities of Shanghai, Nanjing, Hangzhou and Hefei, the overall ecological restoration governance and urban sustainability of the YRD urban agglomeration can be promoted (Luo et al., 2021; He et al., 2023).

4.3 Policy implications

Our study confirms that widespread significant negative ecological effects of urbanization exist in the YEB, where vegetation carbon cycle function and ecological stability were challenged, and ecological resilience building strategies based on optimal urbanization management perspectives should receive attention. In terms of land urbanization, constraints on the rough expansion of production-living space should be strengthened, and more attention should be paid to the vegetation protection and land development approval in new urban areas. The renewal of urban parks, corridors, green space construction and intensive and optimal use of land in old urban areas should also be mentioned more often. In terms of population urbanization, a concept that focuses on green and low-carbon living and consumption should be mentioned more often, with attention to people-centered vegetation and ecological restoration efforts. In terms of economic urbanization, we will strengthen the breakthrough of circular economy and green production process, and accelerate the transformation of low carbon and green industry for alleviating the plundering of vegetation and ecological resources by urban economic development. Moreover, our study confirms that the negative ecological effect of urbanization has a significant spillover

effect, which actually provides fundamental evidence for the joint regional ecological management of the YEB. More improved communication channels on information technology, greening industrial chains and pollutant emission standards should be established between cities. Meanwhile, the sharing of information related to ecological monitoring, pollution emission and climate change should be enhanced to optimize the urbanization paths and patterns of the YEB from an overall perspective. From the direction of urban agglomeration optimization, the CCU needs to strengthen the ecological restoration of vegetation in western cities and formulate gradual construction of human settlements and resource extraction activities. The MYRYU should pay more attention to the ecological conservation work in the western Hunan region, and strengthen the protection of mountainous forests and grassland management. The YRD should further improve urban ecological planning policies and enhance urban livability, focusing on the transmission of urban ecological resilience construction ideas and the diffusion effect of green production technologies. In this way, to promote the YEB to form a green development path guided by urban agglomerations.

5 Conclusion

Previous studies have rarely considered the global and local effects of urbanization on NPP in the YEB, and the direct and spillover effects of urbanization have rarely been systematically investigated. This study analyzed the spatio-temporal dynamic patterns of NPP and urbanization levels in the YEB based on remote sensing images and socioeconomic statistics, and investigated the global and local impacts of urbanization on NPP based on the SDM and GWR model. The highlight of our study is to focus on the direct and spillover effects of urbanization on NPP, in particular, we also explore the regional heterogeneity of the impact of urbanization on NPP at the scale of urban agglomerations based on local effects analysis. To our knowledge, this is rare in previous studies on the linkage between urbanization and ecological environment in the Yangtze River Economic Belt, especially since the natural and socio-economic differences among the three major urban agglomerations prompt this impact differentiation analysis to be more instructive. Some meaningful conclusions are drawn as a result: (1) From 2000 to 2020, the average NPP of Yangtze River Economic Zone increased from 592g*c/m^2 to 670g*c/m^2 at a rate of 0.621% (Figure 3A), and showed a distribution pattern of "high in the south and low in the north, high in the west and low in the east" and the change pattern of "increasing in the north and decreasing in the south". (2) The average UL index of the YEB in general grew from 22.485% to 23.652% with an average annual growth rate of 0.253% from 2000 to 2020, and gradually changed to a clustering pattern with urban agglomerations as the regional core. (3) There is an increasingly significant negative spatial autocorrelation between urbanization and NPP in general, with "High-Low" being the dominant cluster type in the bivariate spatial correlation between UL and NPP, followed by "Low-High" clusters. (4) The negative direct effect of urbanization on NPP in the Yangtze River Economic Zone shows a fluctuating growth trend, while a negative spillover effect, which far exceeds the direct effect and declines slowly, is widespread. In addition, the local non-stationarity of the impact of urbanization on NPP is verified, and the three major urban agglomerations show a differentiated pattern and development direction of the driving effect. More importantly, based on the "population–land–nature" complex ecosystem theory, our study explores the optimal strategies for vegetation ecological security maintenance and sustainable urban development in the YEB. Mainly from various aspects, including multi-dimensional urbanization management, joint spatial governance and ecological conservation paths of urban agglomerations.

This study provides new evidence to reveal the driving mechanism of vegetation net primary productivity by urbanization construction in the YEB. The study of local changes in the mechanisms of the impact of urbanization on vegetation ecosystems can provide important conditions for the development of vegetation ecosystem management strategies in the YEB. The discussion of direct and spillover effects has the potential to provide the necessary support for joint urban governance and ecological synergistic optimization pathways. There are still some shortcomings. First, the study is based on cross-sectional data, which makes it difficult to observe long-term continuous changes in the impact of urbanization on NPP. In the future, a panel database will be established to focus on the long time series variation of the driving effects based on the SPDM model. Second, the study focused on the driving effect of the combined urbanization indicators on NPP, but the decomposition effects of population urbanization, economic urbanization, and land urbanization on NPP could not be investigated. The heterogeneity of the effects of urbanization sub-dimensional indicators on NPP will be further analyzed in the future.

Data availability statement

Publicly available datasets were analyzed in this study. This data can be found here: http://www.geodata.cn/.

Author contributions

SW and GW conceived the study. SW obtained funding for the study. SW, MG and YF performed the statistical analysis. SW produced the figures and tables and wrote the first draft of the manuscript. GW and YF modified and checked this manuscript. All authors contributed to the article and approved the submitted version.

Funding

This research was supported by Guizhou Provincial Science and Technology Projects (Qian Ke He Ji Chu-ZK[2022] General 234).

Conflict of interest

The authors declare that the research was conducted in the absence of any commercial or financial relationships that could be construed as a potential conflict of interest.

Publisher's note

References

Bai, J., Guo, K., Liu, M., and Jiang, T. (2023). Spatial variability, evolution, and agglomeration of eco-environmental risks in the Yangtze river economic belt, China. *Ecol. Indic.* 152, 110375. doi: 10.1016/j.ecolind.2023.110375

Chen, W., Gu, T., and Zeng, J. (2022). Urbanisation and ecosystem health in the middle reaches of the Yangtze river urban agglomerations, China: a U-curve relationship. *J. Environ. Manage.* 318. doi: 10.1016/j.jenvman.2022.115565

Chen, M., Jia, W., Du, C., Shi, M., Henebry, G., and Wang, K. (2023). Carbon saving potential of urban parks due to heat mitigation in Yangtze river economic belt. *J. Cleaner Production* 385, 135713. doi: 10.1016/j.jclepro.2022.135713

Chen, Y. X., Liu, C., Li, H. F., and Xue, X. Z. (2023). How do countries along the maritime silk road perform in sustainable use of natural resources? progress of natural resources-related SDGs. *Ecol. Indic.* 149, 110194. doi: 10.1016/j.ecolind.2023.110194

Chen, J., Wang, L. J., and Li, Y. Y. (2020). Research on the impact of multi-dimensional urbanization on china's carbon emissions under the background of COP21. *J. Environ. Manage.* 273, 111123. doi: 10.1016/j.jenvman.2020.111123

Dong, Y., Peng, F., Li, H., and Men, Y. (2023). Spatial autocorrelation and spatial heterogeneity of underground parking space development in Chinese megacities based on multisource open data. *Appl. Geogr.* 153, 102897. doi: 10.1016/j.apgeog.2023.102897

Guido, S., Christian, K., Katerina, T., David, D., and Jeffrey, D. S. (2017). National baselines for the sustainable development goals assessed in the SDG index and dashboards. *Nat. Geosci.* 10 (8), 547–555. doi: 10.1038/ngeo2985

Guo, Q., Dong, Y., Feng, B., and Zhang, H. (2023). Can green finance development promote total-factor energy efficiency? empirical evidence from China based on a spatial durbin model. *Energy Policy* 177, 113523. doi: 10.1016/j.enpol.2023.113523

He, T., Dai, X., Li, W., Zhou, J., Zhang, J., Li, C., et al. (2023). Response of net primary productivity of vegetation to drought: a case study of qinba mountainous area, China, (2001–2018). *Ecol. Indic.* 149, 110148. doi: 10.1016/j.ecolind.2023.110148

Lesage, J. P., and Pace, R. K. (2009). *Introduction to spatial econometrics* (Boca Raton, FL: CRC Press).

Li, J., Bi, M., and Wei, G. (2022). Investigating the impacts of urbanization on vegetation net primary productivity: a case study of Chengdu–Chongqing urban agglomeration from the perspective of townships. *Land* 11 (11), 2077. doi: 10.3390/land11112077

Li, W., Kang, J., and Wang, Y. (2023). Spatiotemporal changes and driving forces of ecological security in the chengdu-chongqing urban agglomeration, China: quantification using health-services-risk framework. *J. Cleaner Production* 389, 136135. doi: 10.1016/j.jclepro.2023.136135

Li, W., Zhang, Y., Yang, C., Gong, W., Wang, C., and Zhang, R. (2022). Does producer services agglomeration improve urban green development performance of the Yangtze river economic belt in China? *Ecol. Indic.* 145, 109581. doi: 10.1016/J.ECOLIND.2022.109581

Liu, X., Huang, Y., Xu, X., Li, X., Ciais, P., Lin, P., et al. (2020). High-spatiotemporal-resolution mapping of global urban change from 1985 to 2015. *Nat. Sustainability* 3 (7), 564-570. doi: 10.1038/s41893-020-0521-x

Liu, X., Pei, F., Wen, Y., Li, X., Wang, S., Wu, C., et al. (2019). Global urban expansion offsets climate-driven increases in terrestrial net primary productivity. *Nat. Commun.* 10 (1), 1–8. doi: 10.1038/s41467-019-13462-1

Liu, L., Yang, Y., Liu, S., Gong, X., Zhao, Y., Jin, R., et al. (2023). A comparative study of green growth efficiency in Yangtze river economic belt and yellow river basin between 2010 and 2020. *Ecol. Indic.* 150, 110214. doi: 10.1016/j.ecolind.2023.110214

Luo, D., Liang, L., Wang, Z., Chen, L., and Zhang, F. (2021). Exploration of coupling effects in the economy–Society–Environment system in urban areas: case study of the Yangtze river delta urban agglomeration. *Ecol. Indic.* 128, 107858.

Luo, T., Zeng, J., Chen, W., Wang, Y., Gu, T., and Huang, C. (2023). Ecosystem services balance and its influencing factors detection in China: a case study in chengdu-chongqing urban agglomerations. *Ecol. Indic.* 151, 110330. doi: 10.1016/j.ecolind.2023.110330

Ma, F., Wang, J., He, Y., Luo, Y., Zhang, R., Tian, D., et al. (2023). Nitrogen enrichment differentially regulates the response of ecosystem stability to extreme dry versus wet events. *Sci. total Environ.* 887, 164152. doi: 10.1016/J.SCITOTENV.2023.164152

Muhammad, Y. R., Maruf, H. M., and Chen, Y. (2023). Role of economic growth, urbanization and energy consumption on climate change in Bangladesh. *Energy Strategy Rev.* 2023, 47. doi: 10.1016/J.ESR.2023.101088

Ouyang, X., Tang, L., Wei, X., and Li, Y. (2021). Spatial interaction between urbanization and ecosystem services in Chinese urban agglomerations. *Land Use Policy* 2021, 109. doi: 10.1016/j.landusepol.2021.105587

Peng, J., Wang, X. Y., Liu, Y. X., Zhao, Y., Xu, Z., Zhao, M., et al. (2020). Urbanization impact on the supply-demand budget of ecosystem services: decoupling analysis. *Ecosystem Serv.* 44, 101139. doi: 10.1016/j.ecoser.2020.101139

Qiao, W., and Huang, X. (2022). The impact of land urbanization on ecosystem health in the Yangtze river delta urban agglomerations, China. *Cities* 130, 103981. doi: 10.1016/j.cities.2022.103981

Saiu, V., Blečić, I., and Meloni, I. (2022). Making sustainability development goals (SDGs) operational at suburban level: potentials and limitations of neighbourhood sustainability assessment tools. *Environ. Impact Assess. Rev.* 96, 106845. doi: 10.1016/j.eiar.2022.106845

Sharma, S., Joshi, P. K., and Fürst, C. (2022). Unravelling net primary productivity dynamics under urbanization and climate change in the western Himalaya. *Ecological Indicators* 144, 109508.

Sun, B., Zhao, H., and Wang, X. (2016). Effects of drought on net primary productivity: roles of temperature, drought intensity, and duration. *Chin. Geographical Sci.* 26 (2), 270–282. doi: 10.1007/s11769-016-0804-3

Tang, J., Zhou, L., Dang, X. W., Hu, F. N., Yuan, B., Yuan, Z. F., et al. (2023). Impacts and predictions of urban expansion on habitat quality in the densely populated areas: a case study of the yellow river basin, China. *Ecol. Indic.* 151, 110320. doi: 10.1016/j.ecolind.2023.110320

Tian, Y., and Pang, J. (2022). The role of internet development on green total-factor productivity–an empirical analysis based on 109 cities in Yangtze river economic belt. *J. Cleaner Production* 378, 134415. doi: 10.1016/j.jclepro.2022.134415

Tian, A., Xu, T., Gao, J., Liu, C., and Han, L. (2023). Multi-scale spatiotemporal wetland loss and its critical influencing factors in China determined using innovative grid-based GWR. *Ecol. Indic.* 149, 110320. doi: 10.1016/j.ecolind.2023.110144

Wang, J., Delang, C. O., Hou, G., Gao, L., and Lu, X. (2021). Net primary production increases in the Yangtze river basin within the latest two decades. *Global Ecol. Conserv.* 26, e01497. doi: 10.1016/j.gecco.2021.e01497

Wang, S. C., Lu, F., and Wei, G. E. (2022). Direct and spillover effects of urban land expansion on habitat quality in chengdu-chongqing urban agglomeration. *Sustainability* 14 (22), 14931. doi: 10.3390/su142214931

Wang, Y., Yu, X., Zhao, B., Xiong, X., Li, Y., and Zhang, M. (2022). Evaluation of ecological carrying capacity in Yangtze river economic belt and analysis of its spatial pattern evolution. *Ecol. Indic.* 144, 109535. doi: 10.1016/j.ecolind.2022.109535

Wei, G., Bi, M., Liu, X., Zhang, Z., and He, B. (2023). Investigating the impact of multi-dimensional urbanization and FDI on carbon emissions in the belt and road initiative region: direct and spillover effects. *J. Cleaner Production* 384, 135608. doi: 10.1016/j.jclepro.2022.135608

Wei, G. E., He, B. J., Sun, P. J., Liu, Y. B., Li, R. Z., Luo, K., et al. (2023). Evolutionary trends of urban expansion and its sustainable development: evidence from 80 representative cities in the belt and road initiative region. *Cities* 138, 104353. doi: 10.1016/j.cities.2023.104353

Wei, X. D., Yang, J., Luo, P. P., Lin, L. G., Lin, K. L., and Guan, J. M. (2022). Assessment of the variation and influencing factors of vegetation NPP and carbon sink capacity under different natural conditions. *Ecol. Indic.* 138. doi: 10.1016/j.ecolind.2022.108834

Wei, G., Zhang, Z., Ouyang, X., Shen, Y., Jiang, S., Liu, B., et al. (2021). Delineating the spatial-temporal variation of air pollution with urbanization in the Belt and Road Initiative area. *Environmental Impact Assessment Review* 91, 106646.

Wu, S., Zhou, S., Chen, D., Wei, Z., Dai, L., and Li, X. (2014). Determining the contributions of urbanisation and climate change to NPP variations over the last decade in the Yangtze river delta, China. *Sci. Total Environ.* 472, 397–406. doi: 10.1016/j.scitotenv.2013.10.128

Xia, C., and Zhai, G. (2022). The spatiotemporal evolution pattern of urban resilience in the Yangtze river delta urban agglomeration based on TOPSIS-PSO-ELM. *Sustain. Cities Soc.* 87, 104223. doi: 10.1016/J.SCS.2022.104223

Yan, Y., Wu, C., and Wen, Y. (2021). Determining the impacts of climate change and urban expansion on net primary productivity using the spatio-temporal fusion of remote sensing data. *Ecol. Indic.* 127, 107737. doi: 10.1016/j.ecolind.2021.107737

Yang, H., Zhong, X., Deng, S., and Xu, H. (2021). Assessment of the impact of LUCC on NPP and its influencing factors in the Yangtze river basin, China. *Catena* 206, 105542. doi: 10.1016/j.catena.2021.105542

Yang, T., Zhou, K., and Ding, T. (2022). Air pollution impacts on public health: evidence from 110 cities in Yangtze river economic belt of China. *Sci. total Environ.* 851 (P1), 158125. doi: 10.1016/J.SCITOTENV.2022.158125

Yue, D., Zhou, Y., Guo, J., Chao, Z., and Guo, X. (2022). Relationship between net primary productivity and soil water content in the Shule River Basin. *Catena* 208, 105770.

Zhong, S., Liu, P. K., Jiao, C., Lian, C., Xu, C., and Zhou, C. (2021). Assessing the comprehensive impacts of different urbanization process on vegetation net primary productivity in Wuhan, China, from 1990 to 2020. *Sustainable Cities and Society* 75, 103295.

Zhong, J., Jiao, L. M., Droin, A., Liu, J. F., Lian, X. H., and Taubenböck, H. (2023). Greener cities cost more green: examining the impacts of different urban expansion patterns on NPP. *Building Environ.* 228, 109876. doi: 10.1016/j.buildenv.2022.109876

frontiers | Frontiers in Ecology and Evolution

TYPE Original Research
PUBLISHED 21 August 2023
DOI 10.3389/fevo.2023.1260641

OPEN ACCESS

EDITED BY
Xiao Ouyang,
Hunan University of Finance and Economics, China

REVIEWED BY
Lang Yi,
Hunan University of Finance and Economics, China
Wenfang Pu,
Huazhong Agricultural University, China

*CORRESPONDENCE
Duming Peng
15111018295@163.com

RECEIVED 18 July 2023
ACCEPTED 31 July 2023
PUBLISHED 21 August 2023

CITATION
Peng D, Chen Y and Wang W (2023) Spatio-temporal analysis of the impact of land urbanization on the gross primary productivity of vegetation in the Middle Reaches of the Yangtze River Urban Agglomeration: new evidence from the township scale.
Front. Ecol. Evol. 11:1260641.
doi: 10.3389/fevo.2023.1260641

Spatio-temporal analysis of the impact of land urbanization on the gross primary productivity of vegetation in the Middle Reaches of the Yangtze River Urban Agglomeration: new evidence from the township scale

Duming Peng[1]*, Yakai Chen[1] and Wulin Wang[2]

[1]Hunan Provincial Institute of Land and Resources Planning, Changsha, China, [2]College of Tourism, Hunan Normal University, Changsha, China

The urgent need to maintain ecosystem provisioning services and achieve urban sustainable development goals has led to a long-standing focus on the driving effects of land urbanization (LU) in the Middle Reaches of the Yangtze River Urban Agglomeration (MRYRU) on vegetation cover system productivity. Previous studies have lacked consideration for the long-term correlation between land urbanization (LU) and the Gross Primary Productivity (GPP) of vegetation, as well as the spatial non-stationarity of LU's impact in the region. This study is based on land cover remote sensing data and GPP imagery data to monitor the long-term evolution trends of LU and GPP in MRYRU from the perspectives of townships and grids. It further investigates the spatial correlation and clustering characteristics between the two using bivariate spatial autocorrelation method. Additionally, a Geographically and Temporally Weighted Regression (GTWR) model was employed to analyze the spatial effects of LU on GPP. The results indicate that the GPP of MRYRU grows to 1572.88gCm^{-2}a^{-1} with an average annual growth rate of 0.848% from 2000 to 2020. High-value areas are distributed in the central and eastern mountainous of the urban agglomeration, while low-value areas gradually formed an "n"-shaped clustered distribution pattern. The negative spatial autocorrelation between LU and GPP shows a general upward trend, and Low-High is the dominant agglomeration type, concentrated in Hengyang and some mountainous cities in Jiangxi Province. The overall negative impact of land urbanization on GPP in MRYRU is maintained in the spatially nonstationary pattern of driving coefficients, with negative impact areas mostly concentrated in the city's main city zone and positive impact areas concentrated in the urban agglomeration's mountainous townships. This study provides support for MRYRU to adopt more resilient land optimization management strategies and vegetation ecological restoration plans.

KEYWORDS

land urbanization, vegetation gross primary productivity, GWTR, driving influence, Middle Reaches of the Yangtze River Urban Agglomeration (MRYRU)

1 Introduction

Gross Primary Productivity (GPP) is the amount of organic matter produced from carbon dioxide fixation by photosynthesis in green plants per unit area per unit time. It determines the initial organic matter and energy that enters terrestrial ecosystems and directly or indirectly determines the ecosystem's provision of product services such as food, fiber, and fuel needed for human survival (Kim et al., 2017; Jia et al., 2022; Wang et al., 2022). GPP is also commonly used as a key element in measuring terrestrial ecosystem health and land-atmosphere CO_2 exchange. GPP has an irreplaceable contribution to the regulation of the global bio-carbon balance, the maintenance of global climate stability and the sustainability of the material cycle, and is the ecological basis for the survival and development of human society (Guido et al., 2017; Dyvavani et al., 2023; Yang et al., 2023). Regional GPP variations due to global changes in environmental and biological factors have been recognized in previous studies, such as temperature, humidity and solar radiation, and changes in vegetation phenology (Zhong et al., 2021; Zhao et al., 2022; Guo et al., 2023; Tan et al., 2023). However, with the rise of the human footprint and urban construction activities, it has changed urban land use functions, scale, and product services of vegetation ecosystems, and as a result, posed risks to soil fertility, vegetation growing space, and bio-carbon cycling processes (Hu et al., 2022; Wei et al., 2023b). For example, a study by Liu et al. (2019) confirms that global urban land expansion encroached on terrestrial vegetation net primary productivity (NPP) at a rate of 22.4 Tg·C per year in the first decade of the 21st century and offset 30% of climate change-driven NPP growth. In particular, the encroachment of urban production-living space on ecological space during land urbanization has placed a heavy burden on the ecological pattern of urban landscapes and the global vegetation cover system and its productivity, as well as posing a challenge to the maintenance of the carbon cycle in urban ecosystems and the construction of sustainable cities (Tan et al., 2023; Xu et al., 2023). How to measure the change in the intensity of intrusion of land urbanization process on vegetation ecosystems and the response pattern of GPP to urban land transformation is of great significance for urban ecological environment governance and sustainable land management.

During the past 20 years of the 21st century, the global urban land area grew from 239,900 km^2 to 519,800 km^2, expanding by 117.49%, especially in Asia, where the urban land area grew by 133,700 km^2 (Liu et al., 2019; Wei et al., 2023b). Governments have developed a series of binding strategies based on macro-consensus strategies such as the Global Assessment Report on Biodiversity and Ecosystem Services and the International Geosphere-Biosphere Program (IGBP) (Guido et al., 2017; Xie et al., 2022). Aiming to mitigate the encroachment of urban sprawl on the productive capacity of vegetated ecosystems in order to better serve the urban sustainable development goals of sustainable urbanization (Goal11, SDG), maintenance of the ecosystem carbon cycle (Goal13, SDG) and ecosystem conservation (Goal15, SDG). For example, China has recently issued policies such as the Opinions on Comprehensively Implementing the Forest Chief System and the Natural Forest Protection and Restoration System Program to mitigate the negative ecological impacts of urban construction activities, to increase natural ecosystem and environmental protection, and to promote the protection and ecological restoration of pristine forests (Zhao et al., 2022). Similar policies have been implemented in the United States in terms of financial disbursement, where a national ecological compensation program, the Land Fallow Conservation Program (CRP), has been implemented to achieve the objectives of returning ecologically fragile agricultural lands to forests, restoring vegetation cover, improving forest land quality, and enhancing the carbon storage capacity of forests. Scholars have mainly developed case studies on the long-term trends of land urbanization and vegetation cover systems and the prospects for sustainability, the driving effects and correlations of urbanization on vegetation production capacity under climate change, and the externalities and indirect effects of the impacts of land urban expansion (Chen et al., 2019; Gui et al., 2021; Wang et al., 2021). For example, Zhou et al. (2023) constructed an "urbanization-vegetation cover coordination index" to analyze the coordinated relationship between urbanization and vegetation cover systems and their productivity in China, and found that the expansion of urban land use has caused a significant decline in the greenness of urban areas in China, with the degradation of new urban areas being the most significant. Zhuang et al. (2022) investigated the joint mechanism of "climate-urbanization-soil" driving spatio-temporal changes in NPP, and found that soil salinization has a stronger impact on the productive capacity of vegetation cover systems than urbanization. Zafar et al. (2023) predicted the future trends in the productive capacity of urban and rural vegetation in a typical Pakistani city and analyzed the long-term impact of urbanization on urban and rural vegetation and environmental vulnerability. Mu et al. (2023) estimated the trend of NPP in the Central Plains Urban Agglomeration over the past 40 years, and found that NPP showed a continuous downward trend under rapid urbanization, and that the indirect impact of urbanization on the high-speed developing cities was higher than that of the medium- and low-speed cities. These studies provide support for building sustainable and resilient urban agglomerations and green and sustainable urban planning policies. However, whether land urbanization contributes to or coerces total vegetation productivity? As well as the potential correlation and the estimation of the spatial effects of land urbanization on GPP are still insufficiently integrated. This is clearly detrimental to the development of site-specific regional vegetation ecosystem restoration strategies and green urban planning policies.

The Middle Reaches of the Yangtze River Urban Agglomeration (MRYRU) is another strategic urban cluster in China after the Beijing-Tianjin-Hebei Urban Agglomeration, the Yangtze River Delta Urban Agglomeration, the Guangdong-Hong Kong-Macao Greater Bay Area, and the Chengdu-Chongqing Urban Agglomeration, and the region brings together Wuhan, Changsha, and Nanchang, which are important supportive cities in China (Yang et al., 2022; Zeng et al., 2023). According to data released by China's Bureau of Statistics, the total GDP and population of the city cluster in the middle reaches of the Yangtze River in 2020 will be 9.3 trillion and 120 million people, accounting for 9.175% and

9.207% of China's total, respectively. Rapid clustering of population, knowledge, information and technology factors has contributed to the rapid development of the socio-economic level of MRYRU, but also generated mutant expansion of urban land to meet the demand for the construction of transportation, housing, factories and power generation sites in the urban agglomeration (Su et al., 2013). A large number of ecosystem protection and restoration projects have been constructed in the region since the implementation of the "Development Plan for the Urban Agglomeration in the Middle Reaches of the Yangtze River" to achieve a green and low-carbon transition and ecological civilization. However, the long-term evolution of land urbanization and GPP and the impact of land urbanization on the vegetation ecology of MRYRU in the context of the human-land conflict of "development and conservation" still need to be further explored (Zhu and He, 2021; Ma et al., 2022). This is an urgent issue for understanding the eco-carbon cycle process and ecologically sustainable development pathways of MRYRU. MRYRU contains three key regions, that is, Wuhan City Circle, Changsha-Zhuzhou-Xiangtan Urban Agglomeration and Poyang Lake Urban Agglomeration, and the existing studies focus more on the evolutionary trends of land urbanization and vegetation ecosystems in these subregions. The quantification of the overall evolutionary pattern and spatial correlation characteristics of land urbanization and GPP in MRYRU is still insufficient (Luo et al., 2020). In particular, there is a lack of impact analysis experiments based on township or grid perspectives, and few studies have focused on the regional heterogeneity of impacts exerted by land urbanization (Chen and Chi, 2022). This is not conducive to providing targeted green urban planning strategies, vegetation ecological resilience development and ecological conservation programs for the MRYRU.

Overall, the existing studies provide a rich practical basis for revealing the effects of land urbanization on vegetation GPP from a doctrinal perspective, but further discussion is needed on the spatial effects of land urbanization on the vegetation cover systems in MRYRU: (1) Insufficient attention has been paid to the spatial correlation between land urbanization and vegetation GPP; (2) the study scale usually focuses on the individual analysis of subdivided urban agglomerations, and seldom concerns the comprehensive impacts of land urbanization in the urban agglomeration areas in the MRYRU from the townships perspective; (3) the estimation of the spatial effects of land urbanization on vegetation GPP needs to be improved, in order to accommodate the spatial heterogeneity of the driving impacts brought about by regional differences in topography, meteorology, urbanization processes and socio-economic levels. Based on multivariate remote sensing image data, this study utilizes GIS spatial analysis techniques, land use transfer matrix and bivariate spatial autocorrelation to monitor the long-term trends and spatially correlated clustering features of land urbanization process and GPP in the MRYRU, both from the grid and the township perspectives. Further integrating anthropogenic and natural control variables such as climate, topography, spatial distance and socio-economic factors, a Geographically and Temporally Weighted Regression (GTWR) model was used to investigate the spatially differentiated impacts of land urbanization on GPP under the township perspective. The purpose is to provide a decision-making reference and scientific guidance for MRYRU to adopt more resilient land optimization management strategies and vegetation ecological restoration programs.

2 Study area, methods and data sources

2.1 Study area

MRYRU is a Chinese strategic urban agglomeration with Wuhan City Circle, Changsha-Zhuzhou-Xiangtan Urban Agglomeration and the Urban Agglomeration around Poyang Lake as the main components, and is also an important part of the Yangtze River Economic Belt, which involves the three provincial-level central cities of Wuhan, Changsha, and Nanchang as well as 28 prefectural-level municipalities, and contains 4,037 townships units in total. Our study takes 4037 townships as the study sample to explore the spatio-temporal evolution and spatial correlation between land urbanization and GPP, and to reveal the spatio-temporal impact effect of land urbanization on the GPP in the MRYRU region. MRYRU is an important part of the Yangtze River Basin, which belongs to the subtropical monsoon climate region and the evergreen broad-leaved forest belt. With its warm climate, abundant rainfall, well-developed water system, lush vegetation and rich species resources, the region is a concentrated area for a large number of rare and endangered wild animals and plants in China. However, owing to the high population density and long history of urbanization, the coercion on the vegetation cover system by population movement, land use expansion and economic factor agglomeration under the land urbanization process still need to be mitigated. In particular, under the regional differences in the "natural-social-economic" complex ecosystems of urban agglomerations, the complexity of vegetation ecosystem restoration and resilience building projects and the coordination of "urban construction-ecological protection" need more attention. Therefore, studying the impact of land urbanization on GPP in MRYRU has great practical and doctrinal value for building ecological resilience and sustainable development in the region (Figure 1).

2.2 Methods

2.2.1 Accounting for land urbanization levels

Land urbanization is generally regarded as the proportion of built-up land area to all land area in a city, reflecting the process of urbanization in which urban built-up land is increasing and rural land is contracting. It is a core indicator for evaluating the level of urbanization, along with population urbanization and economic urbanization. Drawing on the studies of Peng et al. (2020) and Wei et al. (2023a), the spatio-temporal dynamic evolution of the land urbanization level in the MRYRU is measured using the proportion of urban land size to the overall land size. The calculation formula is as follows:

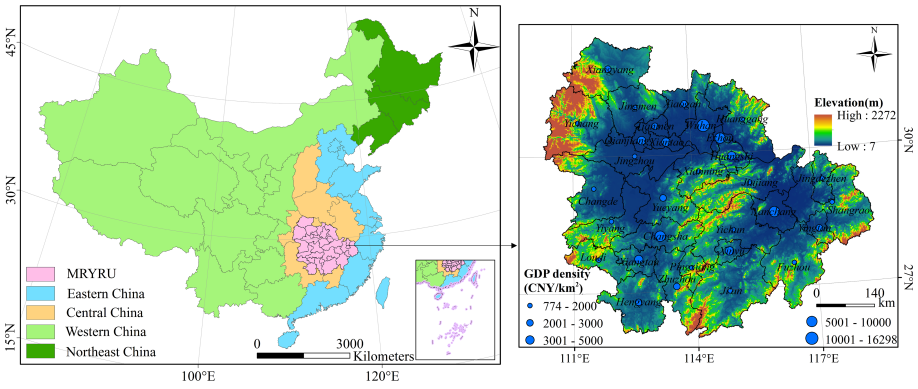

FIGURE 1
Study area.

$$LU_i = \frac{U_{urban}}{U_{total}} \times 100\,\% \tag{1}$$

where LU_i is the land urbanization level of unit i; U_{urban} is the urban land area; and U_{total} is the total urban area.

2.2.2 Land-use transfer matrix

Land urbanization is intuitively reflected in the variation and scale change of urban land use types. We use the land use transfer matrix to quantify the area conversion process of each land use type in the urban agglomeration in the MRYRU from 2000 to 2020 for showing the encroachment of urban land on other types of land use and the dynamic change of scale (Yang and Liu, 2022; Tan et al., 2023). The land use transfer matrix is calculated in the ArcGIS platform with the following formula:

$$S_{ij} = \begin{bmatrix} S_{11} S_{12} & \cdots & S_{1n} \\ \vdots & \ddots & \vdots \\ S_{n1} S_{n2} & \cdots & S_{nn} \end{bmatrix} \tag{2}$$

Where S is the area of a certain land use type in the city; n is the number of land use types; and S_{ij} is the area of conversion from land use type i to land use type j in a certain period of time.

2.2.3 Bivariate spatial autocorrelation

Bivariate spatial autocorrelation models are used to analyze the spatial correlation between land urbanization and GPP. The method can test the global and local correlation features that exist between the two systems in geospatial terms. Among them, the local bivariate spatial autocorrelation is calculated as:

$$\mathrm{I} = \frac{\mathrm{LU_i} - \overline{\mathrm{LU}}}{\sigma_{\mathrm{LU}}} \sum_{\mathrm{j=1}}^{\mathrm{n}} (\mathrm{W_{ij}} \frac{\mathrm{GPP_j} - \overline{\mathrm{GPP}}}{\sigma_{\mathrm{GPP}}}) \tag{3}$$

where W_{ij} is the spatial weight matrix; LU_i and GPP_j are the land urbanization level and total vegetation productivity of units i and j, respectively; σ_{LU} and σ_{GPP} are the variances of LU and GPP_l, respectively (Dong et al., 2023).

2.2.4 Geographically and temporally weighted regression

The GWR model focuses on the effect of spatial heterogeneity in local areas on the overall regression fit, and can be used to test for individual spatial variation in regression coefficients (Tian et al., 2022). The GTWR model takes into account the expansion of geographically weighted regression models due to the non-stationarity of time, and incorporates both temporal and spatial effects into the model, which allows the model to deal with spatial-temporal heteroskedasticity at the same time. In this study, the local variation effect of the impact of land urbanization on the GPP of MRYRU was measured based on the GTWR model for discussing the spatio-temporal characteristics of the impacts generated by land urbanization (Tian et al., 2023). The model calculation formula is as follows:

$$Y_i = \beta_0(u_i, v_i, t_i) + \sum_k \beta_k(u_i, v_i, t_i) \times X_{ik} + \epsilon_i \tag{4}$$

Where $\beta_0(u_i,v_i,t_i)$ is the regression constant; ϵ_i is the residuals of the model; the X_{ik} table is the observed values of the drivers, including the key explanatory variable LU and the other control variables; and $\beta_k(u_i,v_i,t_i)$ is the regression coefficients of the variables, i.e., the weighting coefficients of the variables at the spatio-temporal location (u_i,v_i,t_i).

To measure $\beta_k(u_i,v_i,t_i)$ for each variable k in all spatio-temporal positions i, $\beta_k(u_i,v_i,t_i)$ can be transformed as follows:

$$\hat{\beta}(u_i, v_i, t_i) = [X^t W(u_i, v_i, t_i) X]^{-1} W^T W(u_i, v_i, t_i) Y \tag{5}$$

Where $W(u_i,v_i,t_i)$ is the spatio-temporal weight matrix taking into account spatio-temporal effects.

2.3 Data sources

2.3.1 Land cover remote sensing data

The land urbanization level measurement was based on land cover remote sensing data, which was obtained from the Environment and Resources Data Center of the Chinese Academy

of Sciences (http://www.resdc.cn) with a spatial resolution of 30m (CNLUCC). The dataset is a national-scale multi-period land-use thematic database of China constructed through manual visual interpretation, using Landsat TM/ETM and Landsat 8 remote sensing images as the main information source. The dataset involves 25 land-use types, which can be grouped into six primary classifications: cropland, forest land, grassland, watershed, urban land and bare land, and has been widely used in many research fields, such as land urbanization, expansion of urban land, carbon storage and ecological spatial dynamics evolution (Table 1).

2.3.2 Gross primary productivity

Gross primary productivity (GPP) of vegetation is an important basis for food production and the ecological-carbon cycle in terrestrial ecosystems. Internationally recognized methods for estimating GPP include continuous observation at flux stations, estimation by terrestrial ecological process models, and other methods. In this study, we used the GPP dataset provided by Fan et al. (2023) in China Scientific Data Platform. This dataset is based on the long-term networked observation data and open datasets of ChinaFLUX, combining biological, climatic and soil factors, and using the random forest regression tree model to simulate GPP per unit of leaf area to construct the GPP dataset of China from 2000 to 2020, with a spatial resolution of 30 arcsec (Dataset doi: 10.57760/sciencedb.o00119.00077).

2.3.3 Natural and socio-economic control variables

In addition to land urbanization, the natural geographic context and socio-economic conditions are also considered to have important effects on terrestrial vegetation ecosystems. Referring to the study of Li et al. (2022), we selected natural indicators such as temperature, wind speed, humidity, and distance to rivers, and anthropogenic indicators such as GDP density, population density, distance to county administrative centers, and distance to railroads and highways as control variables to be introduced into the regression model in order to improve the degree of model fit. The data for the natural control variables are mainly derived from relevant data products provided by the Geographic Data Cloud Platform (http://www.gscloud.cn/sources/index) and the Earth System Science Data Center (http://www.geodata.cn/) of the Chinese Academy of Sciences. The GDP density among the anthropogenic control variables is mainly derived from the grid dataset of China's regional GDP density with a spatial resolution of 1km constructed by the Resource and Environmental Science Data Center of the Chinese Academy of Sciences (https://www.resdc.cn/). Population densities are expressed as Landscan Global Population Statistics Analysis data, developed by the U.S. Department of Energy's Oak Ridge National Laboratory (ORNL), with a spatial resolution of nearly 1km x 1km (https://www.satpalda.com/product/landscan/).

3 Result

3.1 Evolution of the spatio-temporal dynamics of the GPP

From the grid perspective, the overall average GPP of MYRYU increased from 1328.40 $gCm^{-2}a^{-1}$ to 1572.88 $gCm^{-2}a^{-1}$ at an average annual growth rate of 0.848% from 2000 to 2020, which is an increase of 18.404% (Figures 2A–C). This indicates that ecosystem vegetation cover and productivity in MYRYU showed a rapid increasing trend in the first two decades of the 21st century. From the township perspective, the overall GPP also showed an increasing trend from 2000 to 2020, with the mean value of GPP increasing from 1166.649 $gCm^{-2}a^{-1}$ to 1368.795 $gCm^{-2}a^{-1}$, an increase of 17.733% (Figures 2E–G). The spatial distribution pattern of GPP is relatively stable, with high values distributed in the Luoxiao Mountains in the central part of the urban agglomeration, the Mofu Mountains and the Wuyi Mountains in the east. These areas have sparse human footprints, lush vegetation, and vegetation ecosystems that maintain good carbon sequestration and production services. Low-value areas are concentrated in the Wuhan, Changsha and Nanchang metropolitan areas and the surrounding densely populated urban areas, and gradually forming an "n" shaped cluster distribution

TABLE 1 Variable settings and attributes.

Data type	Variables	Unit	Abbreviations
Explained variable	Gross Primary Productivity	$gCm^{-2}a^{-1}$	GPP
Explanatory variables	Land urbanization	%	LU
Control variables	GDP density	$10000CNY/km^2$	GDP
	Population density	$person/km^2$	PD
	Distance to the county administrative center	m	Dis-county
	Distance to highway	m	Dis-highway
	Distance to railroad	m	Dis-railroad
	Temperature	°	TEM
	Wind	m/s	WIND
	Distance to river	m	Dis-river

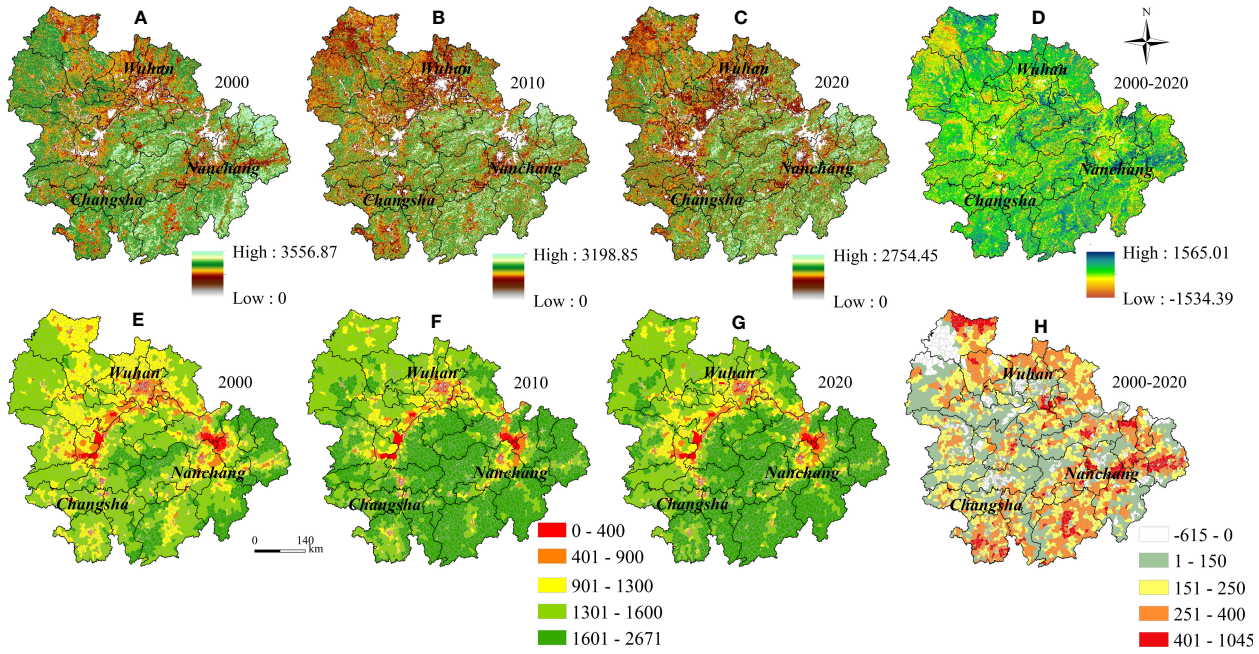

FIGURE 2
2000-2020 GPP distribution **(A–C)** and trends **(D)** of MRYRU at grid scale; GPP distribution **(E–G)** and trends **(H)** at township scales.

pattern. However, the overall upward trend in GPP does not mean that the level of vegetation coverage levels and productivity are increasing across MYRYU. In terms of changing trends, despite significant GPP growth in the southern and eastern regions of the urban agglomeration from 2000 to 2020, the GPP in parts of the main city zone of the cities of Wuhan, Changsha, Nanchang, Xiangyang and Yichang showed a significant downward trend. This may be due to the gradual degradation of the natural habitat and vegetation cover of the ecosystem as a result of the crowding out of a large amount of ecological space by productive-living space in the main city zone during the study period (Figures 2D, H).

3.2 Evolution of the spatio-temporal dynamics of land urbanization

The land use types of MYRYU are dominated by two categories, farmland and forest land, which are distributed in the plain areas (Jianghan Plain, Dongting Lake Plain and Poyang Lake Plain) and the mountainous areas (Luoxiao Mountains, Shufu Mountains and Wuyi Mountains, etc.) of the urban agglomeration, respectively. The average share of them was 37.091% and 49.588% in 2000 and 2020, respectively, but decreased by 4,798.480km^2 and 2,063.764km^2 during the study period (Figures 3A–C). The urban land in MYRYU increased from 9,098.238km^2 to 15,394.108km^2 at an average annual growth rate of 2.664% from 2000 to 2020 (Figure 3E). According to the land use transfer matrix information, the growth of urban land in MYRYU from 2000 to 2020 is mainly realized by encroachment on farmland and forest land. Especially in 2000-2010, the scale of conversion of farmland and forest land to urban land was 2882.403km^2 and 1048.1643km^2, respectively, and in 2010-2020, the scale of conversion was 1487.278km^2 and 293.614km^2, respectively (Figure 3E). These new urban land uses occurred mainly in the areas surrounding the Wuhan, Changsha and Nanchang metropolitan areas (Figure 3D). The LU level of MRYRU increased from 2.657% in 2000 to 4.496% in 2020. And the high value area were clustered in point-shaped distribution centered on the main city zone of the provincial capital city in 2000, and by 2020 are gradually shifting to a face-shaped cluster centered on the metropolitan area of the provincial capital cities, such as Wuhan metropolitan (Wuhan-Xiaogan-Xiantao-Jingzhou) and the Changsha metropolitan (Changsha-Zhuzhou-Xiangtan). Geographically, the distribution of high values has formed a "ring-shaped" due to the socio-economic disparity of the region and the mountain range barrier (Figure 4).

3.3 Spatio-temporal correlation between land urbanization and GPP

The bivariate global spatial autocorrelation indices of LU and GPP for MYRYU are -0.499, -0.510 and -0.504 in 2000, 2010 and 2020, respectively (Figure 5). This showed that the negative correlation between land urbanization and vegetation GPP in MYRYU is on a general upward trend in geospatial terms, and an urgent need to regulate the correlation among them. Negative correlation clusters (including High-Low and Low-High) are the main type of local spatial autocorrelation of the LU and GPP bivariate at the township scale, with the share increasing from 27.467% in 2000 to 29.607% in 2020. In particular, Low-High clusters accounted for more than 18% of all townships in each of the study periods. This suggests that land urbanization is an important geographic factor associated with the productivity of vegetated ecosystems, and that there is an urgent need for MYRYU to regulate land expansion strategies to reduce the negative impacts on the stability of vegetated

10.3389/fevo.2023.1260641

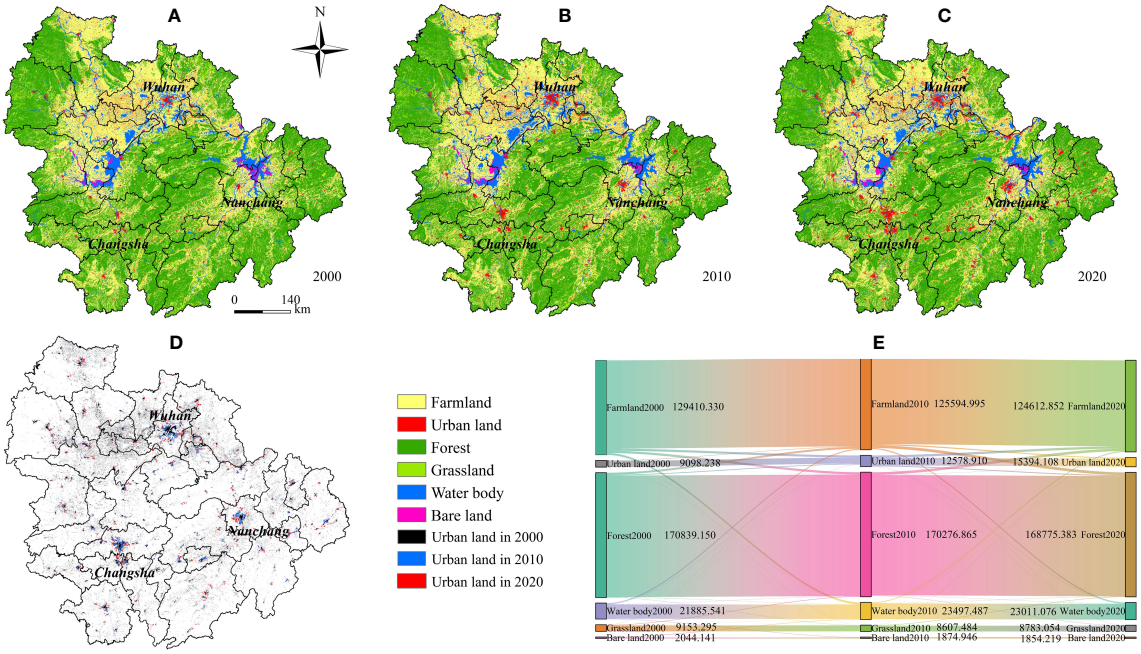

FIGURE 3
Trends in land-use transformation **(A–C)**, urban expansion process **(D)** and the land-use transfer matrix **(E)** in MRYRU, 2000–2020.

ecosystems and carbon stock functions. In terms of spatial distribution, High-Low cluster townships are stably distributed around the main city zone of Wuhan, Nanchang, and Changsha-Zhuzhou-Xiangtan, while Low-High cluster townships are mainly distributed in Hengyang and some mountainous cities in the Urban Agglomeration around Poyang Lake (Yichun, Ji'an, Fuzhou, Yingtan and Shangrao). Low-Low cluster townships are distributed in the mountainous areas at the junction of Hunan, Hubei and Jiangxi provinces, and High-High type townships are in a fragmented layout.

3.4 Spatio-temporal impacts of land urbanization on GPP based on the GTWR model

The control variables were selected to input into the GTWR model (spatial distribution of control variables shown in Figure 6), and the Adjusted R2 of the model was 0.619, 0.632, and 0.756 for 2000, 2010, and 2020, respectively (Figure 7). Our study confirms that the regression coefficients of land urbanization in MYRYU have significant spatial non-stationary properties in 2000, 2010 and 2020, validating the importance of investigating the impact of LU on GPP from a spatially localized perspective. Overall, the LUs of more than 2/3 of the MYRYU townships exert a negative depressing effect on the GPP in the study period, especially in the 2020 when 77.241% of the townships are in a negative impact. Geospatially, the spatial effect of LU on GPP shows obvious steadily characteristics, and the negatively affected areas are concentrated in the main city zone of the cities, especially in Changsha-Zhuzhou-Xiangtan area, Wuhan, JingZhou and Nanchang. The reason for this phenomenon may lie in the long history of disturbance of the vegetation cover system in the main city zone by urban construction activities, with a large amount of vegetated ecological space being crowded out by houses, factories and transportation routes. However, with the implementation of the concepts of urban ecological resilience and sustainable development, the three major urban agglomerations with the centers in Wuhan, Changsha and Nanchang, respectively, have proposed urban land optimization management plans and the concepts of forest city and

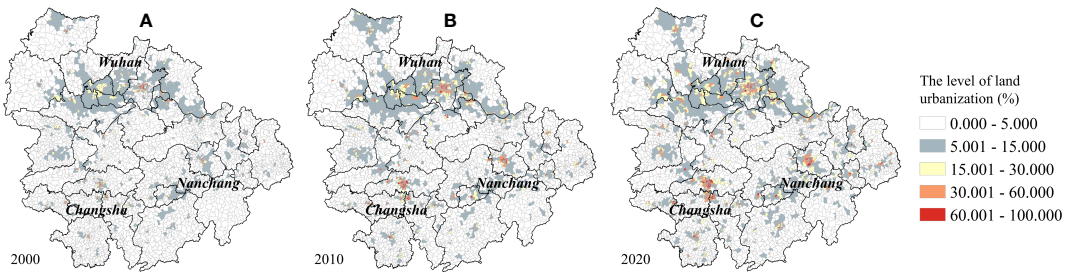

FIGURE 4
Trends in spatio-temporal distribution of land urbanization levels in MRYRU, 2000 **(A)**, 2010 **(B)** and 2020 **(C)**.

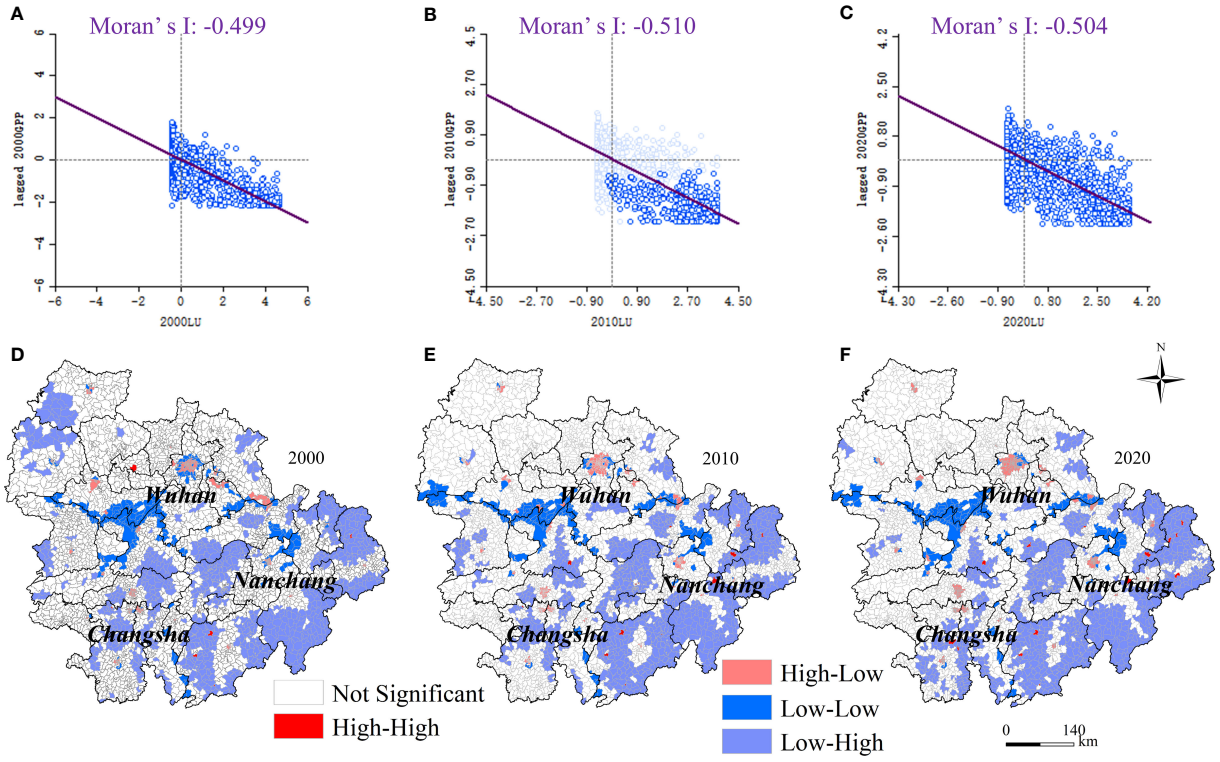

FIGURE 5
Evolution of global **(A–C)** and local bivariate spatial correlation pattern **(D–F)** between land urbanization and GPP in MRYRU, 2000-2020.

park city. This will provide more possibilities for regulating the relationship between the demand for urban landuse and the total primary productivity of the ecosystem. The townships where LU has a positive impact on GPP account for about 22% of the whole number of townships in MYRYU, and are mainly located in Xiangyang, Yichang, and the southern counties of Zhuzhou (Youxian, Chaling, and Yanling counties). A possible reason is that these areas are covered with high-quality vegetation cover, and the terrain is mainly mountainous and hillyhave. For example, Xiangyang and Yichang are located in the mountains of western Hubei, and the southern counties of Zhuzhou are located in the hills of central Hunan, which are more resilient to land urbanization and human remodeling activities, and have a certain degree of resistance to ecological risks and disruptive capacity. Furthermore, a series of ecological restoration measures taken by the national and local governments in the Yangtze River Basin Ecological Conservation Area optimized the environmental conditions for the vegetation growth and the ecological suitability of urban expansion activities, and may have contributed to the increase in vegetation cover and productivity.

4 Discussion

4.1 Driving mechanisms and spatial heterogeneity effect of LU on GPP

Natural variations in temperature, precipitation, and photosynthesis of vegetation can shape the long-term steady-state evolution of vegetation cover and productivity, while anthropogenic programs such as land urbanization, farmland expansion, and predatory exploitation of forest resources can shift this stable evolution process, resulting in abrupt changes in the vegetation GPP (Qin and Sha, 2023). However, green urban planning, environmental regulation and eco-engineering are considered to be an optimization measure that can achieve the gradual harmonization of "development and conservation" objectives at the land urbanization level. The pathway is to control the pattern of land urbanization at the front end of ecological restoration, to modulate the input technology, capital and knowledge of ecological restoration at the middle end, and to strengthen comprehensive ecological management at the end (Guan et al., 2019; Zafar et al., 2023; Zhang et al., 2023). Our study confirms the joint growth trend of LU and GPP at the township level in the MYRYU region, however, the encroachment of vegetation by urbanization is still occurring, especially in the major urban areas where the significant decline in GPP and the rapid growth of LU are forming an opposite. Although the high quality ecological substrate of MYRYU itself is trying hard to whitewash the overall increase in vegetation GPP in the area, investigations based on the GWTR model confirm that the negative impacts of the LU are in control of the bigger picture in the long term, and that the rapid growth of the main city zone in particular is exacerbating this productivity deprivation. This has been mentioned in previous studies that the effects of deep modification of human settlements on the productivity of vegetation cover systems are significant and sustained over time (Zhong et al., 2021; Muntasir et al., 2022; Mu et al., 2023). The study

10.3389/fevo.2023.1260641

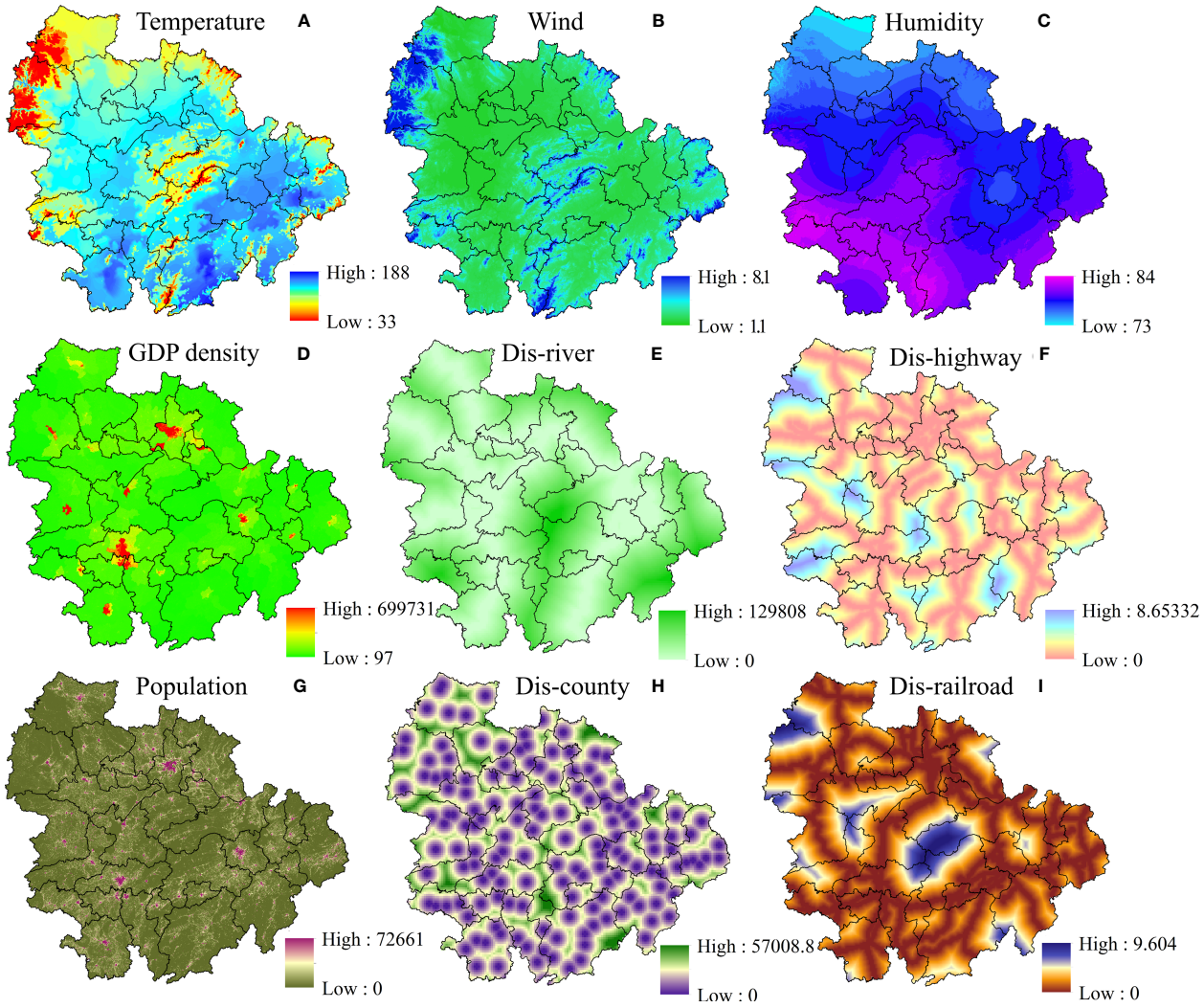

FIGURE 6
Spatial distribution of control variables: temperature **(A)**; wind **(B)**; humidity **(C)**; GDP density **(D)**; distance to river **(E)**; distance to highway **(F)**; population density **(G)**; distance to county **(H)**; distance to railroad **(I)**.

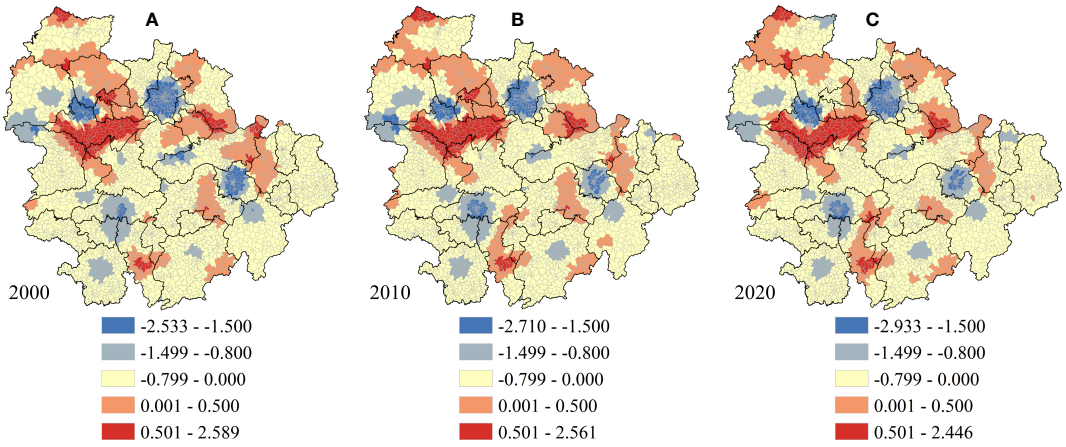

FIGURE 7
Distribution of regression coefficients for land urbanization under the GTWR model in 2000 **(A)**, 2010 **(B)** and 2020 **(C)**.

also further observed some success in the conservation of mountain vegetation. In contrast to the declining trend of GPP in the main city zone and the metropolitan area of the provincial capital city, the mountainous cities around MYRYU have a significant trend of GPP growth and land urbanization has a positive impact on GPP in some mountainous areas. This is similar to the findings of several studies (Asif and Almagul, 2022; Hu et al., 2023; Liu et al., 2023). We suggest that this is related to the implementation of tightened and sustainable environmental regulations, urban planning and ecological engineering policies in the Yangtze River Basin in China in recent years. For example, the Action Plan for the Protection and Restoration of the Yangtze River, the 13th Five-Year Plan for Environmental Protection in Hubei Province, and Hunan Provincial Government's "No. 1 Key Project". These policies focus on building ecological corridors along the river, strengthening the conservation and ecological restoration of forests, wetlands and other ecosystems, and helping to enhance the service functions and productivity of various types of ecosystems. These policies pay attention to the construction of ecological corridors along the rivers, strengthening the conservation and ecological restoration of forests, wetlands and other ecosystems in mountainous areas, and helping to enhance the service functions and productivity of various ecosystems.

4.2 Policy implications and shortcomings

The long-term spatial correlation between land urbanization and GPP was confirmed in this study, and a macro-optimization strategy of the vegetation cover system and its productivity based on the land urbanization perspective should be given first priority. First of all, the development strategy of the Yangtze River Basin of "grasping great protection, not engaging in great development" should be further practiced. The development of a resource-saving and ecologically optimized industrial structure and production and living style should be promoted, as these factors largely determine the process of land urbanization and the demand for urban land. Secondly, strict curbing of disorderly development activities and nature modification activities in urban agglomerations should be emphasized. A range of ecological protection measures should be mentioned, such as the construction of urban green corridors, park cities and forest cities. More over, the spatial non-smoothness of the impact of land urbanization on GPP is confirmed, and it is time for differentiated urbanization management strategies and ecological restoration policies based on the mountainous areas around urban agglomerations and the main city zone to be further mentioned. In the case of main city zone, vegetation system productivity enhancement projects with more resilient and ecologically resilient should be implemented. These areas should take into account the ecological value, landscape integrity, and connectivity of the city in urban planning practices, improve the urban ecological environment management system, and emphasize the economic, residential, and ecological functions of main city zone. In the case of mountainous cities with high ecological quality and a relative lack of urbanization activities, further monitoring of risks and challenges is needed, despite the relatively minor impacts of land urbanization and the positive increase in regional GPP. These areas should continue to implement projects such as returning farmland to forest and planting artificial forests and grasses, strengthening ecological protection and management of vegetation in mountainous areas, and constructing green barriers for soil and water conservation, water protection and other vegetation ecological security. Adequate and sustainable financial investment is also important. The establishment of ecological compensation mechanisms, such as resource development compensation and watershed compensation, should be explored, and comprehensive forest and grassland ecological improvement and monitoring management systems should be strengthened. The key is to address the coordinated relationship between regional socio-economic development and ecological protection, increase the rate of intensive urban land use and the rate of integrated resource development, and support more effective and flexible policies for environmental restoration of vegetation growth.

This study has several shortcomings. First, the mediating mechanisms through which land urbanization affects GPP are insufficiently quantified. In the future, mediating variables such as ecosystem organization, structure, and provisioning service functions can be included, and the theoretical thinking of economics and geography can be combined to further explore the profound mechanism of the impact of LU on GPP. Second, GWTR well illustrates the long-term comprehensive impact of LU on GPP. However, in the future, we can focus on the comparative differences in the impacts of land urbanization patterns on vegetation cover systems and their productivity, and the paths that can be taken for land ecological management between MYRYU and other urban agglomerations in the Yangtze River Economic Belt, as well as in China and globally, from a broader perspective. This is important to further enrich the global value and macro-reference of the study. Third, population and economic urbanization as important areas of urbanization were not considered in this study. In the future, population, land and economic urbanization can be integrated to monitor the mechanisms of urbanization impacts on vegetation ecological resources, structure and function.

5 Conclusion

Previous studies have paid little attention to the associative relationship between land urbanization and vegetation GPP in MYRYU, and the spatially localized effects of land urbanization on GPP have been less comprehensively investigated. This study explores the spatio-temporal evolution of land urbanization and GPP in MYRYU from a township perspective based on multivariate remote sensing datasets. The spatial correlation properties of the two were further investigated, as well as the spatial effects of LU to produce driving impacts were analyzed based on the GTWR model. This study has drawn widespread attention to ecological engineering in mountainous areas and green urban planning in the main city zone of the city, and more importantly the findings provide evidence for a subject area and regionally differentiated

management strategies for ecological restoration of vegetation in MRYRU. This leads to some interesting conclusions: (1) The average GPP of MYRYU grows overall to 1572.88 $gCm^{-2}a^{-1}$ from 2000 to 2020. High-value areas are distributed in the central and eastern mountainous areas, while low-value areas gradually form an "n"-shaped cluster distribution pattern, and the GPP of some areas in the main city zone has decreased significantly. (2) The negative spatial autocorrelation between LU and GPP shows a general upward trend, and Low-High is the dominant cluster type for the bivariate spatial correlation, followed by High-Low. (3) The impact of land urbanization on GPP has obvious spatial non-stationary distribution characteristics, and is dominated by negative impact. More importantly, based on the theory of "population-land-nature" complex ecosystem, our study explores the coordinated and optimized strategies and sustainable development paths of land urbanization and vegetation ecosystem productivity in MYRYU from the perspectives of land policy, green urban planning, and ecological engineering.

Data availability statement

The original contributions presented in the study are included in the article/supplementary files. Further inquiries can be directed to the corresponding author.

Author contributions

DP: Conceptualization, Data curation, Formal Analysis, Investigation, Methodology, Software, Writing – original draft. YC: Methodology, Project administration, Resources, Writing – review & editing. WW: Data curation, Funding acquisition, Investigation, Methodology, Project administration, Resources, Validation, Writing – review & editing. All authors contributed to the article and approved the submitted version.

Conflict of interest

The authors declare that the research was conducted in the absence of any commercial or financial relationships that could be construed as a potential conflict of interest.

Publisher's note

References

Asif, R., and Almagul, T. (2022). Dynamic impacts of economic growth, energy use, urbanization, agricultural productivity, and forested area on carbon emissions: New insights from Kazakhstan. *World Dev. Sustain.* 1.

Chen, W., and Chi, G. (2022). Urbanization and ecosystem services: The multi-scale spatial spillover effects and spatial variations. *Land Use Policy* 114, 105964. doi: 10.1016/j.landusepol.2021.105964

Chen, W., Zhu, D., Huang, C., Ciais, P., Yao, Y., Friedlingstein, P., et al. (2019). Negative extreme events in gross primary productivity and their drivers in China during the past three decades. *Agric. For. Meteorol.* 275, 47–58.

Dong, Y., Peng, F., Li, H., and Men, Y. (2023). Spatial autocorrelation and spatial heterogeneity of underground parking space development in chinese megacities based on multisource open data. *Appl. Geogr.* 153, 102897. doi: 10.1016/j.apgeog.2023.102897

Dyvavani K, K., Taibanganba, W., Hitendra, P., Ritika, S., and Subrata, N. (2023). Improved gross primary productivity estimation using semi-empirical (PRELES) model for moist Indian sal forest. *Ecol. Model.* 475, 110175.

Fan, R. X., Zhu, X., Chen, Z., Yu, G., Zhang, W., Han, L., et al. (2023). A dataset of annual gross primary productivity over Chinese terrestrial ecosystems during 2000-2020. *Sci. Data Bank* V3, 1–20. doi: 10.57760/sciencedb.o00119.0007

Guan, X., Shen, H., Li, X., Gan, X., and Zhang, L. (2019). A long-term and comprehensive assessment of the urbanization-induced impacts on vegetation net primary productivity. *Sci. Total Environ.* 669, 342–352. doi: 10.1016/j.scitotenv.2019.02.361

Gui, X., Wang, L., Su, X., Yi, X., Chen, X., Yao, R., et al. (2021). Environmental factors modulate the diffuse fertilization effect on gross primary productivity across Chinese ecosystems. *Sci. total Environ.* 793, 148443. doi: 10.1016/J.SCITOTENV.2021.148443

Guido, S., Christian, K., Katerina, T., David, D., and Jeffrey, D. S. (2017). National baselines for the Sustainable Development Goals assessed in the SDG Index and Dashboards. *Nat. Geosci.* 10 (8), 547–555. doi: 10.1038/ngeo2985

Guo, H., Zhou, X., Dong, Y., Wang, Y., and Li, S. (2023). On the use of machine learning methods to improve the estimation of gross primary productivity of maize field with drip irrigation. *Ecol. Model.* 476, 110250. doi: 10.1016/j.ecolmodel.2022.110250

Hu, Z., Piao, S., Knapp, A. K., Wang, X., Peng, S., Yuan, W., et al. (2022). Decoupling of greenness and gross primary productivity as aridity decreases. *Remote Sens. Environ.* 279, 113120. doi: 10.1016/j.rse.2022.113120

Hu, Q., Shen, W., and Zhang, Z. (2023). How does urbanization affect the evolution of territorial space composite function? *Appl. Geogr.* 155, 102976. doi: 10.1016/J.APGEOG.2023.102976

Jia, J., Gao, Y., Qin, B., Dungait, J., Liu, Y., Lu, Y., et al. (2022). Evolving geographical gross primary productivity patterns in global lake systems and controlling mechanisms of associated phytoplankton communities since the 1950s. *Earth-Science Rev.* 234, 104221. doi: 10.1016/j.earscirev.2022.104221

Kim, J., Kug, J., Jeong, S., Deborah, N.H., Anna, M., Christopher, R. S., et al. (2017). Reduced North American terrestrial primary productivity linked to anomalous Arctic warming. *Nat. Geosci.* 10 (8), 572–576. doi: 10.1038/ngeo2986

Li, W., Zhang, Y., Yang, C., Gong, W., Wang, C., and Zhang, R. (2022). Does producer services agglomeration improve urban green development performance of the yangtze river economic belt in China? *Ecol. Indic.* 145, 109581. doi: 10.1016/j.ecolind.2022.109581

Liu, R., Dong, X., Wang, X., Zhang, P., Liu, M., and Zhang, Y. (2023). Relationship and driving factors between urbanization and natural ecosystem health in China. *Ecol. Indic.* 147, 109972. doi: 10.1016/j.ecolind.2023.109972

Liu, X., Pei, F., Wen, Y., Li, X., Wang, S., Wu, C., et al. (2019). Global urban expansion offsets climate-driven increases in terrestrial net primary productivity. *Nat. Commun.* 10 (1), 18866. doi: 10.1038/s41467-019-13462-1

Luo, Q., Zhou, J., Li, Z., and Yu, B. (2020). Spatial differences of ecosystem services and their driving factors: A comparation analysis among three urban agglomerations in China's Yangtze River Economic Belt. *Sci. Total Environ.* 725, 138452. doi: 10.1016/j.scitotenv.2020.138452

Ma, L., Xiang, L., Wang, C., Chen, N., and Wang, W. (2022). Spatiotemporal evolution of urban carbon balance and its response to new-type urbanization: A case of the middle reaches of the Yangtze River Urban Agglomerations, China. *J. Clean. Prod.* 380, 135122. doi: 10.1016/j.jclepro.2022.135122

Mu, W., Zhu, X., Ma, W., Han, Y., Huang, H., and Huang, X. (2023). Impact assessment of urbanization on vegetation net primary productivity: A case study of the core development area in central plains urban agglomeration, China. *Environ. Res.* 229, 115995. doi: 10.1016/j.envres.2023.115995

Muntasir, M., Nicholas, A., Shabbir, M. A., Khan, U., and Mahmud, S. (2022). The impacts of renewable energy, financial inclusivity, globalization, economic growth, and urbanization on carbon productivity: Evidence from the net moderation and mediation

effects of energy efficiency gains. *Renewable Energy* 196, 824–838. doi: 10.1016/J.RENENE.2022.07.012

Peng, J., Wang, X. Y., Liu, Y. X., Zhao, Y., Xu, Z., Zhao, M., et al. (2020). Urbanization impact on the supply-demand budget of ecosystem services: Decoupling analysis. *Ecosystem Serv.* 44, 101139.

Qin, Z., and Sha, Z. (2023). Modeling the impact of urbanization and climate changes on terrestrial vegetation productivity in China by a neighborhood substitution analysis. *Ecol. Model.* 482, 110405. doi: 10.1016/j.ecolmodel.2023.110405

Su, M., Fath, D., Yang, Z., Chen, B., and Liu, G. (2013). Ecosystem health pattern analysis of urban clusters based on emergy synthesis: Results and implication for management. *Energy Policy* 59, 600–613. doi: 10.1016/j.enpol.2013.04.015

Tan, X., Jia, Y., Yang, D., Niu, C., and Hao, C. (2023). Turning points in the impact of earlier green-up on evapotranspiration and gross primary productivity in a semi-arid grassland watershed. *J. Hydrol.* 616, 128755. doi: 10.1016/j.jhydrol.2022.128755

Tian, J., Cai, D., Han, K., and Zhou, K. (2022). Understanding peasant household's land transfer decision-making: A perspective of financial literacy. *Land Use Policy* 119, 106189. doi: 10.1016/J.LANDUSEPOL.2022.106189

Tian, A., Xu, T., Gao, J., Liu, C., and Han, L. (2023). Multi-scale spatiotemporal wetland loss and its critical influencing factors in china determined using innovative grid-based GWR. *Ecol. Indic.* 149, 110144. doi: 10.1016/j.ecolind.2023.110144

Wang, J., Delang, C., Hou, G., Gao, L., and Lu, X. (2021). Net primary production increases in the Yangtze River Basin within the latest two decades. *Global Ecol. Conserv.* 26, e01497. doi: 10.1016/j.gecco.2021.e01497

Wang, Y., Yu, X., Zhao, B., Xiong, X., Li, Y., and Zhang, M. (2022). Evaluation of ecological carrying capacity in Yangtze River Economic Belt and analysis of its spatial pattern evolution. *Ecol. Indic.* 144, 109535. doi: 10.1016/j.ecolind.2022.109535

Wei, G., Bi, M., Liu, X., Zhang, Z., and He, B. (2023a). Investigating the impact of multi-dimensional urbanization and FDI on carbon emissions in the belt and road initiative region: Direct and spillover effects. *J. Clean. Prod.* 384, 135608. doi: 10.1016/j.jclepro.2022.135608

Wei, G., He, B., Sun, P., Liu, Y., Li, R., Ouyang, X., et al. (2023b). Evolutionary trends of urban expansion and its sustainable development: Evidence from 80 representative cities in the belt and road initiative region. *Cities* 138, 104353. doi: 10.1016/j.cities.2023.104353

Xie, X., Tian, J., Wu, C., Li, A., Jin, H., Bian, J., et al. (2022). Long-term topographic effect on remotely sensed vegetation index-based gross primary productivity (GPP) estimation at the watershed scale. *Int. J. Appl. Earth Observ. Geoinform.* 108, 102755. doi: 10.1016/j.jag.2022.102755

Xu, H., Zhang, Z., Wu, X., and Wan, J. (2023). Light use efficiency models incorporating diffuse radiation impacts for simulating terrestrial ecosystem gross primary productivity: A global comparison. *Agric. For. Meteorol.* 332, 109376. doi: 10.1016/J.AGRFORMET.2023.109376

Yang, Z., Huang, Y., Duan, Z., and Tang, J. (2023). Capturing the spatiotemporal variations in the gross primary productivity in coastal wetlands by integrating eddy covariance, Landsat, and MODIS satellite data: A case study in the Yangtze Estuary, China. *Ecol. Indic.* 149, 110154. doi: 10.1016/j.ecolind.2023.110154

Yang, X., and Liu, X. (2022). Carbon conduction effect and temporal-spatial difference caused by land type transfer in Chang-Zhu-Tan urban agglomeration from 1995 to 2018. *Acta Ecol. Sin.* 42 (4), 338–347. doi: 10.1016/j.chnaes.2022.02.004

Yang, B., Zhang, Z., and Wu, H. (2022). Detection and attribution of changes in agricultural eco-efficiency within rapid urbanized areas: A case study in the Urban agglomeration in the middle Reaches of Yangtze River, China. *Ecol. Indic.* 144, 109533. doi: 10.1016/j.ecolind.2022.109533

Zafar, Z., Mehmood, M. S., Zhai, S., Zubair, M., Sajjad, M., and Qin, Y. (2023). Fostering deep learning approaches to evaluate the impact of urbanization on vegetation and future prospects. *Ecol. Indic.* 146, 109788. doi: 10.1016/j.ecolind.2022.109788

Zeng, X., Ma, Y., Ren, J., and He, B. (2023). Assessing the network characteristics and structural effects of eco-efficiency: A case study in the urban agglomerations in the middle reaches of Yangtze River, China. *Ecol. Indic.* 150, 110169. doi: 10.1016/j.ecolind.2023.110169

Zhang, T., Zhou, J., Yu, P., Li, J., Kang, Y., and Zhang, B. (2023). Response of ecosystem gross primary productivity to drought in northern China based on multi-source remote sensing data. *J. Hydrol.* 616, 128808. doi: 10.1016/j.jhydrol.2022.128808

Zhao, Y., Peng, J., Ding, Z., Qiu, S., Liu, X., Wu, J., et al. (2022). Divergent dynamics between grassland greenness and gross primary productivity across China. *Ecol. Indic.* 142, 109100. doi: 10.1016/j.ecolind.2022.109100

Zhong, J., Liu, J., Jiao, L., Lian, X., Xu, Z., and Zhou, Z. (2021). Assessing the comprehensive impacts of different urbanization processes on vegetation net primary productivity in Wuhan, China, from 1990 to 2020. *Sustain. Cities Soc.* 75, 103295. doi: 10.1016/J.SCS.2021.103295

Zhou, T., Liu, H., Gou, P., and Xu, N. (2023). Conflict or Coordination? measuring the relationships between urbanization and vegetation cover in China. *Ecol. Indic.* 147, 109993. doi: 10.1016/j.ecolind.2023.109993

Zhu, Z., and He, Q. (2021). Spatio-temporal evaluation of the urban agglomeration expansion in the middle reaches of the Yangtze River and its impact on ecological lands. *Sci. Total Environ.* 790, 148150. doi: 10.1016/J.SCITOTENV.2021.148150

Zhuang, Q., Shao, Z., Li, D., Huang, X., Cai, B., Altan, O., et al. (2022). Unequal weakening of urbanization and soil salinization on vegetation production capacity. *Geoderma* 411, 115712. doi: 10.1016/j.geoderma.2022.115712

frontiers | Frontiers in Environmental Science

TYPE Original Research
PUBLISHED 25 August 2023
DOI 10.3389/fenvs.2023.1247046

OPEN ACCESS

EDITED BY
Xiao Ouyang,
Hunan University of Finance and Economics, China

REVIEWED BY
Wei Liao,
Hunan University of Finance and Economics, China
Shaohua Zhao,
Ministry of Ecology and Environment Center for Satellite Application on Ecology and Environment, China

*CORRESPONDENCE
Guanghui Tian,
tianguanghui@xcu.edu.cn

RECEIVED 25 June 2023
ACCEPTED 14 August 2023
PUBLISHED 25 August 2023

CITATION
Meng F, Yan S, Tian G and Wang Y (2023), Surface urban heat island effect and its spatiotemporal dynamics in metropolitan area: a case study in the Zhengzhou metropolitan area, China.
Front. Environ. Sci. 11:1247046.
doi: 10.3389/fenvs.2023.1247046

Surface urban heat island effect and its spatiotemporal dynamics in metropolitan area: a case study in the Zhengzhou metropolitan area, China

Fei Meng[1], Shuling Yan[1], Guanghui Tian[2]* and Yudong Wang[3]

[1]School of Foreign Languages and Tourism, Henan Institute of Economics and Trade, Zhengzhou, China, [2]College of Urban and Environmental Sciences, Xuchang University, Xuchang, China, [3]Key Research Institute of Yellow River Civilization and Sustainable Development and Collaborative Innovation Center on Yellow River Civilization, Henan University, Kaifeng, China

The deterioration of the urban surface thermal environment has seriously affected regional environments and human health, becoming a critical ecological problem faced by cities worldwide. This study focused on surface urban heat island effect in metropolitan area and selected the emerging metropolitan area of Zhengzhou, China, as a case study. Based on the MODIS land surface temperature data obtained from the Google Earth Engine the surface urban heat island intensity (SUHII) was calculated and its temporal and spatial dynamics were analyzed from 2003 to 2022. The main findings indicated that Zhengzhou, the core city of the metropolitan area, had the strongest urban heat island effect with day surface urban heat island intensity of 1.10°C and night SUHII of 1.39°C). Generally, the average annual SUHII was higher during the day than at night, and the maximum value was detected in summer (2.43°C). SUHII showed an increasing trend at night, especially in summer during the study period. It decreased obviously in urban centers during the day, while it increased obviously in the outer urban areas at night. The results of this study contributed to the understanding of the spatiotemporal dynamics of the urban heat island effect in the Zhengzhou metropolitan area.

KEYWORDS

urban heat island effect, surface heat island intensity, trend analysis, spatial disparities, GEE

1 Introduction

The urban heat island effect is defined as the phenomenon by which temperatures in urban areas are higher than those in surrounding rural areas. This effect can have an impact on the microclimate, atmospheric environment, and the wellbeing and health of urban residents (Manoli et al., 2019; Yang D. et al., 2022; Vinayak et al., 2022; Ma and Dong, 2023). Within the context of global climate change, urban heat islands exacerbate the risk of heat-related deaths (Wang J. et al., 2021; Tong et al., 2021). With the acceleration of urbanization, the urban heat island effect has become an important environmental issue. The phenomenon is caused by the gradual replacement of natural land surfaces (vegetation and water bodies) with impermeable surfaces and by the increase in heat emissions derived from urban human activities. As China's massive urbanization continues to progress, the expansion of urban

land use and population growth will continue to have a significant impact on the urban heat island effect (Chen et al., 2018; Vinayak et al., 2022). Studying urban heat islands can provide a theoretical basis for urban planning and sustainable development, which is urgently needed and have significant practical implications for improving the living environment of urban residents.

Extensive research has already been conducted on the urban heat island effect. In terms of measurement methods, it is common to calculate the air temperature or land surface temperature differences between urban and suburban areas based on data obtained on-site or using remote sensing technology (Khan and Chatterjee, 2016; Levermore et al., 2018; Zhang X. et al., 2022). In recent years, the urban heat island effect has been increasingly and primarily quantified by calculating the surface urban heat island intensity (SUHII) using land surface temperature data derived from remote sensing (Deilami et al., 2018; Kumar and Mishra, 2019; Yao et al., 2019). The temporal and spatial characteristics of SUHII and its influencing factors are the main focus of current research. Typically, Meng et al. (2018) conducted a temporal analysis of the urban heat island effect in Beijing and found a higher average daytime SUHII, which was associated with higher density of impervious surfaces (Meng et al., 2018). Wang et al. (2021) investigated urban heat island and the influences of air pollutants in cities in the Yangtze River Delta during 2015–2019 and also documented that annual average daytime SUHII was higher than nighttime SUHII, and O_3 concentration presented a significant positive correlation with daytime SUHII (Wang Y. et al., 2021). Zhang et al. (2022) documented a decrease in SUHII in the Yangtze River Delta, Beijing-Tianjin-Hebei region, and the middle reaches of the Yangtze River from 2003 to 2019, as well as an increase in SUHII in the Chengdu-Chongqing and Pearl River Delta urban agglomerations, with significant impacts of land cover changes on the urban heat island effect in the Beijing-Tianjin-Hebei, Yangtze River Delta, and Chengdu-Chongqing urban agglomerations (Zhang H. et al., 2022). Additionally, Siddiqui et al. (2021) investigated the temporal variations of SUHII in three cities in India from 2001 to 2019, revealing a significant increasing trend in annual average SUHII in Kolkata and Pune, with particularly high warming rates during summer, especially at night. (Siddiqui et al., 2021). Generally, previous studies have mainly shown that the urban heat island effect is obvious in summer and at night. Aspects of the underlying surface, including land use/cover, urban morphology, landscape pattern, as well as anthropogenic heat and atmospheric pollution, are considered to be major factors influencing the urban heat island effect (Wang et al., 2018; Li et al., 2020; Wang J. et al., 2021; Yang F. et al., 2022; Sun et al., 2022). Regional climate conditions also have an important impact on the urban heat island effect. For example, Wu et al. (2019) explored the heat islands of 44 cities in South America based on the Köppen-Geiger climate zones and found that the average SUHII in all climate zones (except for arid zones) was higher during the day than at night (Wu et al., 2019).

In China, research is concerned with this issue in multiple cities or at the national scale (Peng et al., 2012; Debbage and Shepherd, 2015; Zhao et al., 2016; Yang et al., 2019; Liu Y. et al., 2020; Ke et al., 2021; Marando et al., 2022), especially where major megacities are located, such as the Yangtze River Delta region and the Beijing-Tianjin-Hebei region (Zhao et al., 2016; Liu X. et al., 2020; Zhang X. et al., 2022). These studies have greatly contributed to understanding this harmful phenomenon and the mechanisms that influence it. While, urban heat island effects may have different temporal and spatial characteristics in different regions and at different stages of urban expansion. Particularly, with the development of urban agglomerations, the urban heat island effect may extend beyond individual cities and spread throughout the entire urban agglomeration. While there have been numerous studies on the urban heat island effect in single cities or megacities, research specifically focusing on urban agglomerations remains relatively limited. Previous studies have mainly examined the temporal variations of the overall urban heat island effect in single cities and the differences among different cities (Meng et al., 2018; Yang et al., 2019). Some scholars have also investigated the spatial differences of the urban heat island effect within urban areas, such as the differences among different urban functional zones (Zhao et al., 2016; Ke et al., 2021). However, less attention has been given the temporal trends of the urban heat island effect within urban areas and its spatial differences. Therefore, further investigation is warranted to explore these aspects.

Therefore, to bridge this knowledge gap, long-term MODIS land surface temperature data obtained from the Google Earth Engine (GEE) cloud platform and related auxiliary data were here used to measure the SUHII of each city in the Zhengzhou metropolitan area from 2003 to 2022. Then, the annual variation and seasonal differences in SUHII during the day and at night were analyzed. Finally, the temporal trends of this parameter and its spatial differences within the cities in the area were further explored. The aim was to describe the spatiotemporal dynamics of the urban heat island effect and provide support for the formulation of policies to mitigate this harmful phenomenon in the Zhengzhou metropolitan area.

2 Materials and methods

2.1 Study area

The Zhengzhou metropolitan area is located in the central and lower reaches of the Yellow River in China, a favorable geographical location at the center of China (Figure 1). Its total area is about 15.90 thousand square kilometers. It consists of five cities, i.e., Zhengzhou, Kaifeng, Xuchang, Xinxiang, and Jiaozuo, among which Zhengzhou is one of the nine national central cities of China. The Zhengzhou metropolitan area is characterized by a mainly flat terrain and mild climate. It is a key development area in Henan Province, and its economic hinterland is vast and has a great potential for future expansion. In 2021, the permanent population in the Zhengzhou metropolitan area was 31.60 million people, accounting for 32% of the total population in Henan Province; the regional gross domestic product was 2.43 trillion RMB, accounting for 41% of that of Henan Province (Henan Province Bureau of Statistics, 2022). It is one of the most developed and fastest-growing regions in central and western China. However, the rapid expansion of cities has damaged the urban ecological environment, leading to changes in the thermal environment and to the consequent urban heat island effect in this region.

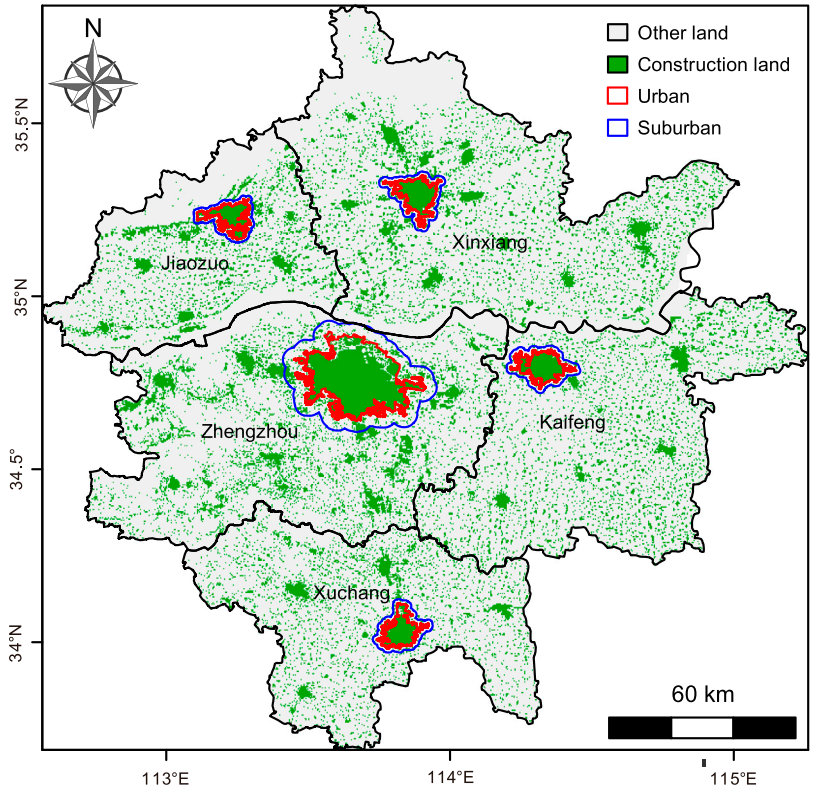

FIGURE 1
Map of the Zhengzhou metropolitan area and its urban and suburban areas.

2.2 Data sources and preprocessing

2.2.1 Surface temperature data

In previous studies, surface temperature has been used as a common indicator to quantify the urban heat island effect (Schwarz et al., 2011; Halder et al., 2021; Sekertekin and Zadbagher, 2021). In this study, the MODIS surface temperature product dataset, MYD11A2 V6.1, was obtained from the NASA's Land Processes Distributed Active Archive Center (LP DAAC, https://lpdaac.usgs.gov) through the GEE platform. This dataset has a spatial resolution of 1 km and provides daytime and nighttime surface temperatures over an average period of 8 days. The images in the form of average values were synthesized to obtain the 20-year, annual, and seasonal land surface temperatures for the Zhengzhou metropolitan area on the GEE. Seasons were defined based on the traditional Chinese classification: spring (from March to May), summer (from June to August), autumn (from September to November), and winter (from December to February of the following year). The MYD11A2 dataset is available from 4 July 2002, therefore data from 1 March 2003, to 28 February 2023, were used in the present investigation.

2.2.2 Land use data

Land use data were obtained from the China National Land Use/Cover Change dataset at the Resource and Environment Science and Data Center (https://www.resdc.cn/). This dataset is a national-scale thematic database of variations in land use/cover in China that was compiled through manual visual interpretation of Landsat-derived remote sensing images. The dataset, which has been updated to 2020, adopts a two-level classification system, with Level 1 consisting of six categories: cultivated land, forest land, grassland, water area, construction land, and unused land; the spatial resolution is 30 m.

2.3 Methods

2.3.1 Subdivision of urban and suburban areas

A core issue in the remote sensing-based monitoring of urban heat islands is how to subdivide urban and suburban areas. In this study, an area buffer method was developed to determine the boundary between urban and suburban areas based on relevant previous investigations (Clinton and Gong, 2013; Zhou et al., 2014; Tan and Li, 2015; Liu X. et al., 2020). This method consisted of four steps. Firstly, land use data were processed using a binary system; construction land was defined as 1 and other land cover types were defined as 0. Secondly, the largest urban patches were identified and selected, and a 3 × 3 convolution filter was applied to extract urban boundaries. Thirdly, the "holes" formed by non-urban land cover within the urban boundary were filled to obtain a complete urban boundary. The resolution was very high: some patches north and east of Zhengzhou are separated from urban Zhengzhou by the Jialu River, Lian-Huo highway, and their green belt. In reality, these patches are also part of Zhengzhou's urban area (they are main areas of Huiji District and Zhengdong New District). Thus, mask processing was applied to gap areas north and east of

Zhengzhou. Finally, equal-area buffers were established outside the urban boundary to determine the suburban area (Liao et al., 2021). The derived urban and suburban boundaries are shown in Figure 1. The method ensures that urban built-up areas are concentrated contiguous areas, and the urban area is similar to the outer area, which is conducive to the comparison of surface temperature in the two regions.

2.3.2 Surface urban heat island intensity

SUHII is commonly measured by calculating the differences in surface temperature between urban area or sites and suburban area or sites. Based on the above-mentioned preprocessing of daytime and nighttime surface temperature data at the interannual and seasonal scales, we calculated the difference in the average surface temperature of all pixels between the urban and suburban areas of each city and considered it as the surface heat island intensity of each city. The following equation was applied:

$$SUHII = \frac{\sum_{u=1}^{n} T_u}{n} - \frac{\sum_{s=1}^{m} T_s}{m}$$

where *SUHII* is the surface urban heat island intensity, n and m represent the total number of pixels in urban and suburban areas, respectively. T_u is the surface temperature in pixel u in urban areas, and T_s is the surface temperature in pixel s in suburban areas.

2.3.3 Sen's slope

Sen's slope, also known as Theil-Sen median, is a robust nonparametric statistical method used to calculate trends. As it has a high computational efficiency and is insensitive to measurement errors and outliers, this method is commonly used in trend analyses of long time series data. It is described by the following equation:

$$\beta = mean\left(\frac{x_j - x_i}{j - i}\right), \quad (j > i)$$

where, x_i and x_j are the time series of observed values (surface temperature in the current study). A β value higher than 0 indicates an upward trend in the time series, while a β value lower than 0 indicates a downward trend.

The Sen's slope method is usually applied in combination with the Mann–Kendall test.

2.3.4 Mann-Kendall test

The Mann-Kendall test is a nonparametric statistical method. Its null hypothesis assumes the absence of a trend, while the alternative hypothesis assumes the existence of some trend. Through this test, the difference between each data point and all subsequent data points in a given time series was calculated, and the trend of the time series was then determined based on the sign of the differences obtained. Finally, by applying the rank-sum test it was established whether the trend was significant or not. A significant test result indicated the presence of a trend in the time series; otherwise, it was concluded that there was no trend.

The test was described as follows:

The standardized test statistic Z for time series $X_i, i = 1, 2, \cdots, i, \cdots, j, \cdots, n$, is defined as:

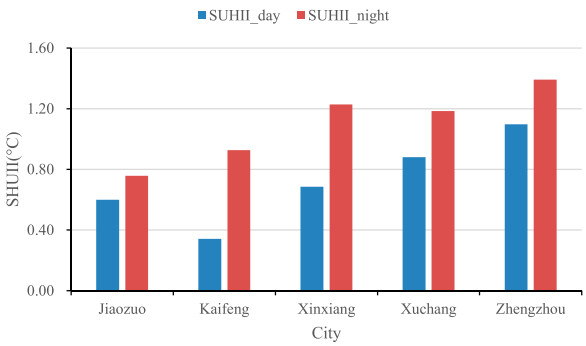

FIGURE 2
Average daytime and nighttime surface heat island intensity in each city of the Zhengzhou metropolitan area.

$$Z = \begin{cases} \frac{S}{\sqrt{VAR(S)}} & (S > 0) \\ 0 & (S = 0) \\ \frac{S+1}{\sqrt{VAR(S)}} & (S < 0) \end{cases}$$

$$S = \sum_{i=1}^{n-1} \sum_{j=i+1}^{n} sign(x_j - x_i)$$

$$sign(\theta) = \begin{cases} 1 & (\theta > 0) \\ 0 & (\theta = 0) \\ -1 & (\theta < 0) \end{cases}$$

where, x_i and x_j are the time series, and n is the time series length. If $n \geq 8$, the expectation and variance of S is:

$$E(S) = 0$$

$$VAR(S) = \frac{n(n-1)(2n+5)}{18}$$

If $|Z| > Z_{1-\frac{\alpha}{2}}$ (α is the given significance level), the time series exhibits a significant variation trend. When α is 0.05, $Z = 1.96$. If $|Z| > 1.96$, the variation trend is significant at the confidence level of 95%.

3 Results

3.1 Daytime and nighttime SUHIIs in each city of the Zhengzhou metropolitan area

3.1.1 Average daytime and nighttime SUHIIs in each city

Based on the daytime and nighttime land surface temperature data from 2003 to 2022, the multi-year average land surface temperatures of urban and suburban areas and the annual average SUHIIs of each city during the day and at night were calculated and are shown in Figure 2. Among the cities in the Zhengzhou metropolitan area, Zhengzhou showed the strongest SUHII during the day (1.10°C) and at night (1.39°C). The annual average SUHIIs during the day in the other cities were all less than 1°C. However, at night, Xinxiang and Xuchang exhibited SUHII higher than 1°C, reaching 1.23°C and 1.18°C, respectively. The lowest annual average SUHII

TABLE 1 Surface heat island intensity in each city of the Zhengzhou metropolitan area across seasons.

City	Day				Night			
	Spring	Summer	Autumn	Winter	Spring	Summer	Autumn	Winter
Jiaozuo	1.04	1.53	0.34	−0.54	0.94	0.95	0.77	0.71
Kaifeng	0.67	1.89	0.26	−0.70	1.12	0.90	1.10	1.14
Xinxiang	2.05	1.78	0.06	−0.72	1.46	1.27	1.27	1.38
Xuchang	2.11	1.68	0.35	−0.26	1.57	1.19	1.28	1.33
Zhengzhou	1.36	2.43	0.78	−0.28	1.47	1.35	1.40	1.67
Mean	1.44	1.86	0.36	−0.50	1.31	1.13	1.16	1.25

during the day was 0.34°C, detected in Kaifeng, while the lowest value at night was 0.76°C, detected in Jiaozuo. Overall, the multi-year average land surface temperatures of urban and suburban areas in the Zhengzhou metropolitan area during the day were 26.38°C and 25.66°C, respectively, while at night they were 10.34°C, and 9.24°C, respectively. The SUHII in the Zhengzhou metropolitan area was higher at night (1.10°C) than during the day (0.72°C).

3.1.2 Daytime and nighttime SUHIIs in different seasons in each city

Subsequently, the average daytime and nighttime SUHIIs in each city in different seasons were calculated, and the results are shown in Table 1. The highest daytime SUHII was detected in Xuchang in spring (2.11°C), followed by that in Xinxiang (2.05°C), while that in Kaifeng was the lowest (0.67°C). In summer, the highest SUHII was detected in Zhengzhou, where it reached 2.43°C, while the values in other cities were all below 2.00°C. In autumn, the SUHII in Zhengzhou was still the highest, reaching 0.78°C, while that in Xinxiang was the lowest, at only 0.06°C. In winter, the SUHIIs in all cities were negative due to the cold island effect. The strongest and weakest effects were detected in Xinxiang (−0.72°C) and Zhengzhou (−0.28°C), respectively.

At night, the highest SUHII was recorded in Xuchang in spring (1.57°C), followed by the values in Zhengzhou (1.47°C) and Xinxiang (1.46°C). The lowest SUHII in spring was detected in Kaifeng (0.94°C). In summer, Zhengzhou exhibited the highest SUHII (1.35°C), followed by Xinxiang (1.27°C) and Xuchang (1.19°C), while the lowest value was detected in Kaifeng (0.90°C). In autumn, the highest SUHII was still recorded in Zhengzhou (1.40°C), followed by Xuchang (1.28°C) and Xinxiang (1.27°C). In winter, Zhengzhou again recorded the highest SUHII (1.67°C), followed by Xinxiang (1.38°C) and Xuchang (1.33°C), while the lowest intensity was recorded in Jiaozuo (0.71°C).

Among the four seasons, spring and summer recorded higher SUHIIs in each city during the day. Among the examined cities, similarly to the results reported in Figure 1, Zhengzhou, Xuchang, and Xinxiang exhibited relatively high SUHIIs, while the values in Kaifeng and Jiaozuo were low.

3.2 Temporal variation of daytime and nighttime SUHIIs

3.2.1 Interannual variation of daytime and nighttime SUHIIs

The annual average daytime and nighttime SUHIIs in each city from 2003 to 2022 were plotted to determine temporal variations, and the results are shown in Figure 3. During the day, the SUHII in Kaifeng and Jiaozuo showed a fluctuating downward trend from 2003 to 2018, while that in Zhengzhou, Xuchang, and Xinxiang showed an increasing trend from 2003 to 2008 and a fluctuating downward trend from 2008 to 2018 (Figure 3A). After 2018, the overall trend in all cities except for Jiaozuo showed a significant increase. The daytime SUHII in Zhengzhou was positive in all years examined, while in the other cities it was positive in most years and negative in some years. Specifically, in Kaifeng, SUHII was negative in 2016, 2019, and 2022, with values of −0.04°C, −0.14°C, and −0.10°C, respectively. In Jiaozuo and Xinxiang, this parameter was negative in 2018, with values of −0.02°C and −0.38°C, respectively. In Xuchang, it was negative in 2013, with a value of −0.18°C.

In all cities except for Jiaozuo, SUHII showed a fluctuating upward trend at night. In 2003, the nighttime SUHIIs in Kaifeng, Xinxiang, Xuchang, and Zhengzhou were 0.67°C, 0.87°C, 1.04°C, and 0.92°C, respectively. By 2022, these values had increased to 1.12°C, 0.98°C, 1.33°C, and 1.69°C, respectively.

The daytime and nighttime SUHIIs in the study area in summer and winter from 2003 to 2022 were plotted to analyze temporal variations in different seasons. The temporal changes in SUHII during summer days reported in Figure 4 indicate no significant increasing or decreasing trends in the cities examined. Among these, Zhengzhou exhibited a relatively large fluctuation in SUHII values during summer days. However, during summer nights, the intensities generally increased in all cities, and the increase was significant especially between 2003 and 2010 (Figure 4B). During winter days, SUHII showed a decreasing trend in all cities before 2009 and displayed interannual non-significant fluctuations after 2009, which basically indicated the presence of the cold island effect (Figure 4C). During winter nights, SUHII did not very significantly in Jiaozuo, but in the other cities it generally showed an increasing trend (Figure 4D).

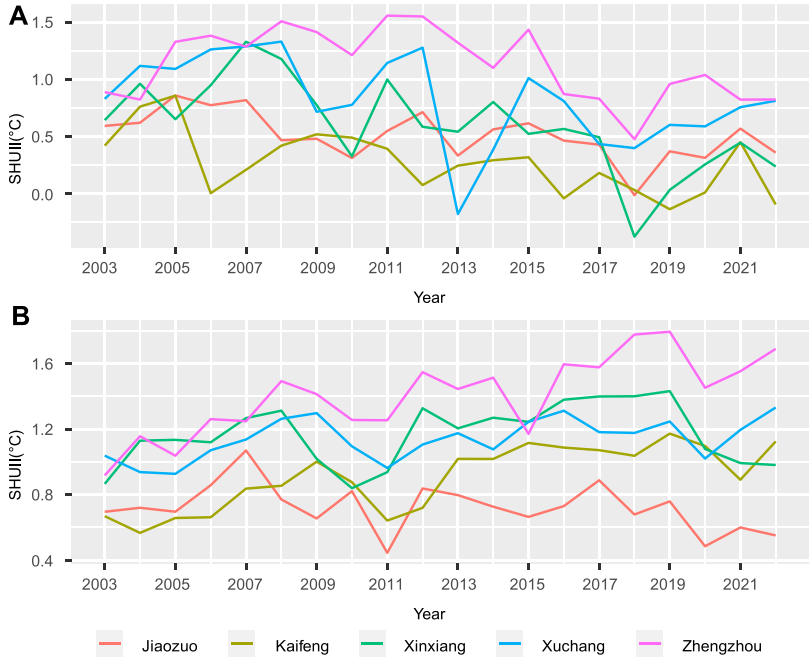

FIGURE 3
Temporal variation of surface heat island intensity in each city of the Zhengzhou metropolitan area between 2003 and 2022: **(A)** day, **(B)** night.

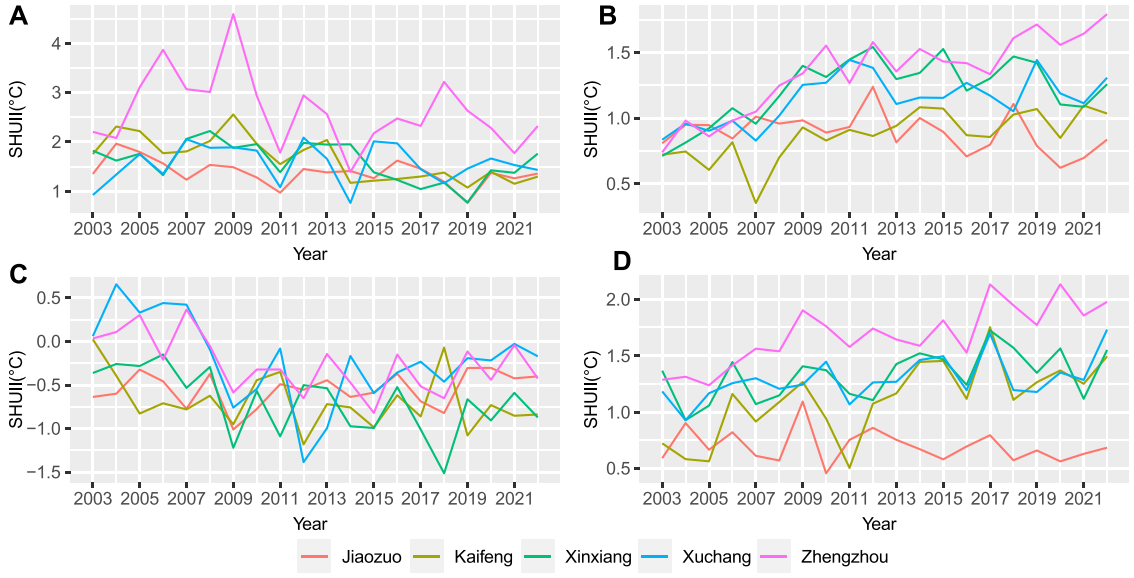

FIGURE 4
Temporal variation of SUHII in each city of the Zhengzhou metropolitan area during summer and winter from 2003 to 2022: **(A)** summer daytime, **(B)** summer nighttime, **(C)** winter daytime, **(D)** winter nighttime.

3.3 Variations and spatial differences in daytime and nighttime SUHIIs within cities

SUHII was expected to vary at different locations within each city. The pixel-scale SUHII was here calculated based on the daytime and nighttime surface temperatures of urban and suburban areas in each city from 2003 to 2022. Then, based on the values obtained for each year, the Sen's slope was calculated at the pixel scale and the Mann–Kendall trend test was conducted. Using a confidence level of 95% (α = 0.05, Z = 1.96), the SUHII trends of all cities were categorized into four types: significant increase, non-significant increase, significant decrease, and non-significant decrease.

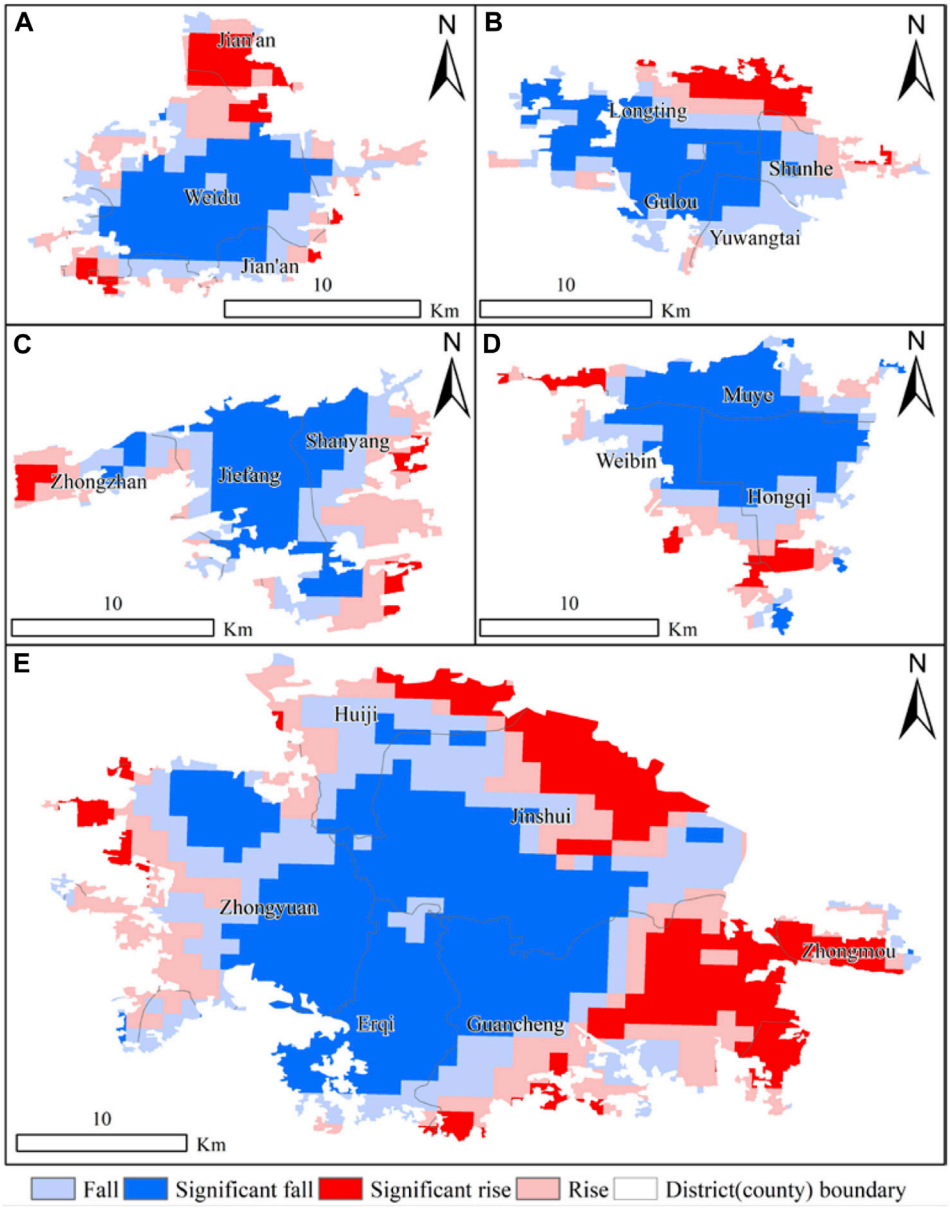

FIGURE 5
Spatial distribution of daytime SUHII trends in different cities within the Zhengzhou metropolitan area: **(A)** Xuchang, **(B)** Kaifeng, **(C)** Jiaozuo, **(D)** Xinxiang, **(E)** Zhengzhou.

Figure 5 shows the spatial distribution of daytime SUHII trends in the five cities examined. This parameter significantly decreased during the day in the old city areas and increased primarily in the peripheral urban areas, namely, in the northern parts of Xuchang (Figure 5A) and Kaifeng (Figure 5B), the eastern and western parts of Jiaozuo (Figure 5C), the western and southern parts of Xinxiang (Figure 5D), and the northeastern and southeastern parts of Zhengzhou (Figure 5E). The proportion of areas showing a significant decrease in SUHII during the daytime was relatively large in each city (Table 2). Specifically, the proportion in the urban area of Xinxiang was the largest, at 55.11%, while that in the urban area of Zhengzhou was the smallest, but still up to 39.67%. The areas in each city showing a significant increase in SUHII during the daytime were relatively small. The largest proportion (18.02%) was detected in the urban area of Zhengzhou, followed by Xuchang (12.04%) and Kaifeng (10.44%). In both the urban areas of Xinxiang and Jiaozuo, the proportion was lower than 7.00%.

Figure 6 shows the spatial distribution of nighttime SUHII trends for the five cities examined. A significant decrease in nighttime SUHII was detected southwest of Xuchang (Figure 6A), while a significant increase was observed northeast of this city. In other areas, the upward or downward trends were not significant. In Kaifeng, most areas northwest of Longting District showed a significant increase in SUHII at night, while other areas mainly exhibited non-significant upward or downward trends (Figure 6B). In the southern part of Jiaozuo, the nighttime SUHII

TABLE 2 Proportion of areas (%) showing increasing (Rise) or decreasing (Fall) trends in SUHII during the day and at night in different cities within the Zhengzhou metropolitan area.

City	Day				Night			
	Fall	Fall*	Rise*	Rise	Fall	Fall*	Rise*	Rise
Jiaozuo	26.24	43.05	5.08	25.62	36.27	35.86	13.93	13.93
Kaifeng	31.10	43.96	10.44	14.50	27.61	6.18	41.15	25.07
Xinxiang	25.24	55.11	6.92	12.73	29.63	4.65	14.70	51.02
Xuchang	25.39	40.25	12.04	22.32	31.98	10.11	28.38	29.54
Zhengzhou	23.58	39.67	18.02	18.73	16.43	4.66	51.51	27.41

Note: *represents significant values.

increased significantly, while in some central, northeastern, and northwestern areas of the city, this parameter showed a significant decrease (Figure 6C). Significant increases in nighttime SUHII were observed in some eastern, southeastern, and northern areas of Xinxiang (Figure 6D), while some small areas northwest and southwest of this city showed significant decreases in this parameter. In most other areas, the upward or downward trends were not significant. Significant increases in nighttime SUHII were observed in most southeastern, northwestern, and southwestern areas of Zhengzhou (Figure 6E), while individual areas northeast and southwest of this city showed a significant decrease in this parameter. The values in the old city area and its surroundings exhibited a downward and upward trend, respectively, but these were not significant.

Based on the data reported in Table 2, large areas of Kaifeng (51.51%) and Zhengzhou (41.14%) exhibited a significant increase in nighttime SUHII, while this trend was observed in relatively small areas in Jiaozuo (13.93%) and Xinxiang (14.70%). The largest area showing a significant decrease in nighttime SUHII was detected in Jiaozuo, reaching 35.86%, followed by Xuchang at 10.11%. In all the other cities, the proportions were smaller than 6.50%.

Several studies have been conducted to investigate urban heat island in the study area. However, previous research has primarily focused on Zhengzhou. Notably, Min et al. (2018) and Yang et al. (2022) examined the temporal and spatial variations of urban heat island using radiation brightness temperature data for the periods of 1996–2014 and 2006–2020, respectively (Min et al., 2018; Yang Y. et al., 2022). These studies analyzed the spatial patterns of urban heat island and documented the area of urban heat island generally increased during over the study periods. Additionally, Min et al. (2018) reported an overall rise in average land surface temperature during 1996–2014. Furthermore, Zhou et al. (2022) investigated the temporal and spatial variations of land surface temperature across the entire city of Zhengzhou, encompassing both urban and rural areas (Zhou et al., 2022). The study utilized the MODIS land surface temperature data from 2005 to 2020 and found that the average land surface temperature exhibited an upward trend, with the urban heat island predominantly concentrated in the main city. It is important to note that these aforementioned studies differ significantly from the present study, as they used land surface temperature as a metric to characterize urban heat island and focused on analyzing the spatial distribution and temporal changes of land surface temperature. Nevertheless, there were some similar findings indicating a general increasing trend in surface temperature within Zhengzhou (see Fig. A1 and Fig. A2).

4 Discussion

In this study, the SUHII in the cities of the Zhengzhou metropolitan area was calculated and its temporal variation, seasonal differences, and spatial differences during the day and at night were analyzed. The core city of the metropolitan area, Zhengzhou, exhibited the strongest SUHII and, in all cities examined, this parameter was higher during the day than at night. Significant seasonal differences in SUHII were detected in each city, with generally stronger daytime intensities in summer and cold island effects in winter. From 2003 to 2022, the annual average SUHII at night and the average SUHII in summer and winter nights showed overall increasing trends in all cities except for Jiaozuo. Values varied significantly in different areas within each city during the day, with significant downward trends detected in the central areas (referred to as “old city”) and significant upward trends in some peripheral areas. Significant regional differences in the increase or decrease of nighttime SUHII in each city were also observed.

The urban heat island effect is a widespread phenomenon, especially in large cities (Yang et al., 2019), and the present study confirmed that the city of Zhengzhou had the strongest SUHII in the metropolitan area. In comparison, the values detected in Kaifeng and Jiaozuo were relatively low, and this difference is closely related to the geographical environment of these two cities. Kaifeng, known as the “water city” of northern China, has many water bodies in its urban area, which result in a weak heat island effect. Due to the exposure of Jiaozuo to the Taihang Mountain in the north and its winds, the nighttime surface temperature in this city was lower than 1°C, and SUHII was also consequently low. As reported in previous studies of the seasonal patterns of SUHII in Chinese cities (Zhou et al., 2014; Wang et al., 2015), the present study found that the daytime heat island effect in the Zhengzhou metropolitan area was the strongest in summer, followed by that in spring, autumn, and winter, while the nighttime heat island effect was stronger in spring and winter and weaker in summer and autumn. The Zhengzhou metropolitan area is located in the temperate monsoon climate zone of the northern hemisphere and is characterized by long sunshine hours and a high solar elevation angle in summer. The continuous heat storage by artificial surfaces in urban areas causes

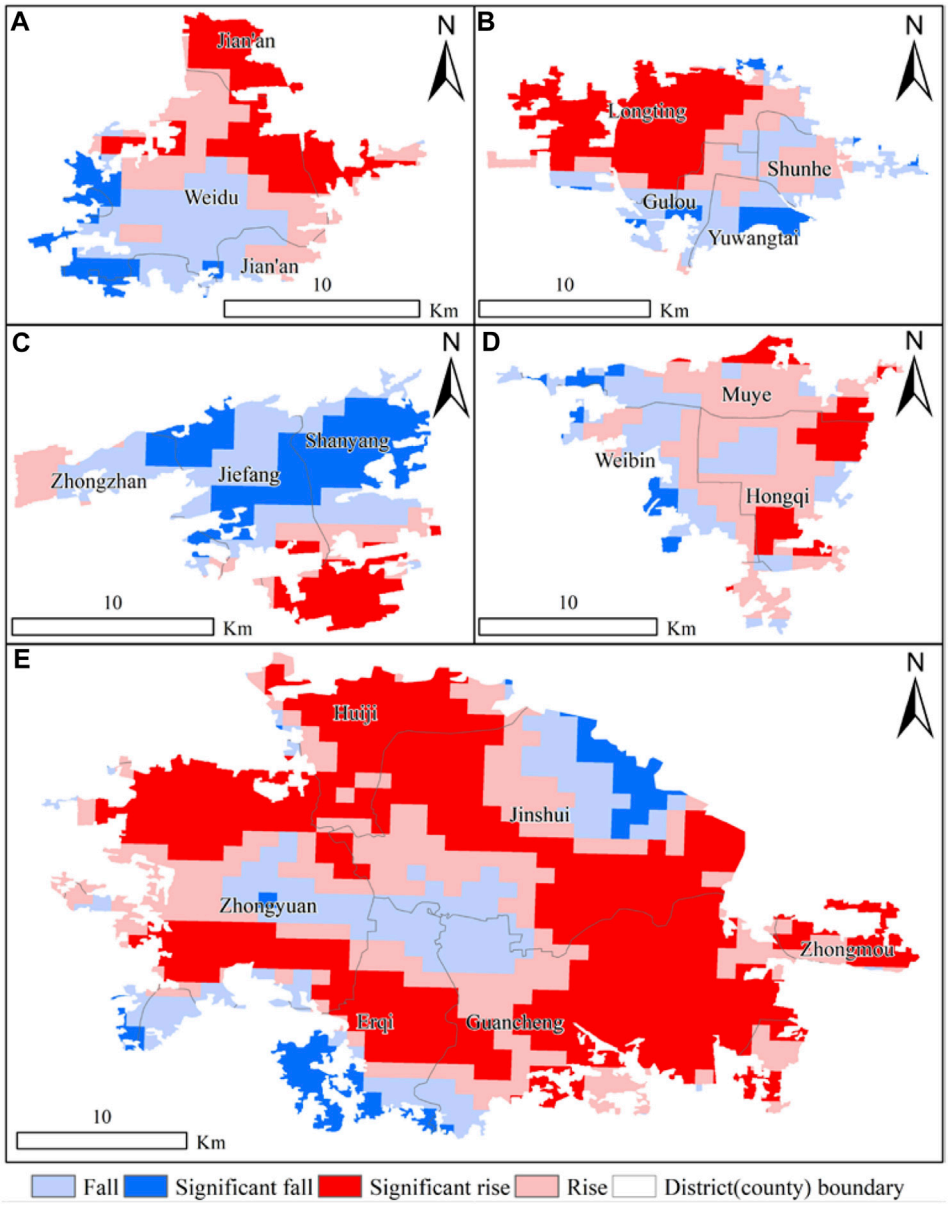

FIGURE 6
Spatial distribution of nighttime SUHII trends in different cities within the Zhengzhou metropolitan area: **(A)** Xuchang, **(B)** Kaifeng, **(C)** Jiaozuo, **(D)** Xinxiang, **(E)** Zhengzhou.

higher daytime surface temperatures that result in stronger daytime SUHIIs in summer. In contrast, in suburban areas, where there are more agricultural activities or forest vegetation, the evapotranspiration effect of plants reduces surface temperatures (Yao et al., 2019; Meng et al., 2023). In this study, the lowest SUHIIs were detected in winter, indicating the presence of the cold island effect, which is associated with weak solar radiation and differences in the thermal properties of urban and suburban areas. This effect has been shown to vary in different regions. At night, suburban vegetation activity and reduced surface reflectivity as well as human-induced heat emissions cause higher surface temperatures in urban areas than in suburban areas in all seasons (Yang et al., 2019).

In terms of the interannual variation of daytime and nighttime SUHIIs, we found no significant trends during the day in any of the cities examined, except for Jiaozuo. However, the SUHII at night showed an increasing trend in all cities except for Jiaozuo. In terms of seasonal variation, no clear trend in daytime SUHII was detected either in winter or summer. However, the nighttime SUHII in summer showed a clear increasing trend in all cities, while that in winter showed a clear increasing trend for all cities except for Jiaozuo. Similar findings have also been reported in other studies (Zhou et al., 2016; Meng et al., 2018). The present study also revealed the spatial differences in SUHII within urban areas. During the day, this parameter exhibited a significant decreasing trend in the "old city" areas and a non-

significant decreasing trend in the surrounding areas. On the other hand, some areas on the outskirts of the cities examined showed a significant increasing trend. This indicated that the urban heat islands effect shifts from central cities to the suburbs, and we believe that this phenomenon is related to the processes of urbanization and spatial expansion of cities. The earliest increases in surface temperature and SUHII were recorded in the central areas of cities, which were developed first. With the expansion of cities, the surface temperature in the peripheral areas increased rapidly, leading to an increase in surface temperature in the suburbs. At the same time, the surface temperature in the old cities increased relatively slowly due to the higher initial surface temperature. Consequently, the difference in the increase of surface temperature between the central and peripheral areas (see Figure A1) resulted in a weaker increase in SUHII in the central area, and even in a decreasing trend. At night, obvious differences among cities were detected in the areas where SUHII significantly increased or decreased. This was due to the main direction of urban expansion and to the population and industrial concentrations in each city. Over the past 20 years, Xuchang has mainly expanded to the northeast, Kaifeng has expanded on a large scale in Longting District, and Jiaozuo and Xuchang have expanded toward their southeastern/eastern areas. In contrast, in Zhengzhou, the areas of urban and population expansion have been the eastern Zhengdong New District, southeastern Economic Development Zone, northwestern High-Tech Zone, and Huiji District, and they have been rapidly developed moving from the city center toward the periphery.

The above findings can contribute to the understanding of the spatiotemporal dynamics of the urban heat island effect in the study area. Especially, the spatial differences in SUHII within urban areas, which previous studies have focused less on, were also revealed. The specific mechanisms that determine the urban heat island effect in each city and its influencing factors are different and complex and need to be further investigated. However, urbanization and urban expansion undoubtedly resulted in spatial differences in the increase of surface temperature (Figure A2) and SUHII within each city. In addition, the large area of the water body (in Kaifeng) effectively mitigates the urban heat island effect from the comparison of heat island effects in the five cities. Thus, these findings have important practical policy implications for the ongoing urban renewal projects and urbanization development planning in China. It is recommended to add more green vegetation around buildings, city roads, and large squares, and to include new water urban bodies, and increase the existing urban water bodies according to the area of urban function zones. The plan for ventilation corridors and green belts between urban function zones should be given full attention in future urbanization and urban agglomeration development.

There were two main aspects of limitation that needed clarification in this study. The first was the coarse resolution of the surface temperature data. A resolution of 1 km is sufficient to reveal spatial differences in surface temperatures at a regional or national scale, but it fails to capture the spatial variability in temperature within urban areas effectively. Fortunately, significant progress has been made in producing finer resolution surface temperature data products, such as 100 m and 30 m, based on the Landsat data (Wang et al., 2020; Cheng et al., 2021). Therefore, finer-resolution surface temperature product data should be applied in future studies. The second limitation stems from the division of urban areas and suburban areas. Urban areas are dynamic and rapidly expand into rural regions. In urban agglomerations, some cities are even adjacent to each other through critical infrastructure and functional zones, blurring the boundaries between urban and suburban areas. Consequently, some urban areas may be excluded in this study. More scientific and effective quantization methods for defining urban and suburban areas should be explored, particularly in urban agglomerations.

5 Conclusion

In this study, the SUHIIs of cities in the Zhengzhou metropolitan area were calculated based on the difference in surface temperature between urban and suburban areas. Then, the differences in this parameter during the day and at night, as well as its seasonal variation, temporal trends, and spatial differences among different cities were analyzed. Overall, it was shown that Zhengzhou, the core city of the metropolitan area, had the strongest urban heat island effect. The nighttime SUHII of each city examined exhibited a clear increasing trend; however, the daytime SUHIIs outside the urban areas showed a significant decreasing trend, while the nighttime values in the main regions of urban expansion in each city showed a clear increasing trend. The results obtained provided a knowledge base to understand the spatiotemporal variation of the urban heat island effect in the Zhengzhou metropolitan area.

Data availability statement

The original contributions presented in the study are included in the article/Supplementary Material, further inquiries can be directed to the corresponding author.

Author contributions

GT conceived and designed the study. FM initiated the study and undertook statistical analysis and manuscript writing. FM undertook data curation and revised the manuscript. YW designed the methodology. SY provided useful suggestions. All authors contributed to the article and approved the submitted version.

Funding

This study was sponsored by the Key Scientific and Technological Project of Henan Province, China (Grant No. 222400410101).

Conflict of interest

The authors declare that the research was conducted in the absence of any commercial or financial relationships that could be construed as a potential conflict of interest.

Publisher's note

References

Chen, M., Liu, W., Lu, D., Chen, H., and Ye, C. Progress of China's new-type urbanization construction since 2014: A preliminary assessment. *Cities* 2018, 78, 180–193. doi:10.1016/j.cities.2018.02.012

Cheng, Jie., Meng, X., Dong, S., and Liang, S. Generating the 30-m land surface temperature product over continental China and USA from landsat 5/7/8 data. *Sci. Remote Sens.* 2021, 4: 100032. doi:10.1016/j.srs.2021.100032

Clinton, N., and Gong, P. MODIS detected surface urban heat islands and sinks: Global locations and controls. *Remote Sens. Environ.* 2013, 134, 294–304. doi:10.1016/j.rse.2013.03.008

Debbage, N., and Shepherd, J. M. The urban heat island effect and city contiguity. *Comput. Environ. Urban Syst.* 2015, 54, 181–194. doi:10.1016/j.compenvurbsys.2015.08.002

Deilami, K., Kamruzzaman, M., and Liu, Y. Urban heat island effect: A systematic review of spatio-temporal factors, data, methods, and mitigation measures. *Int. J. Appl. Earth Obs. Geoinf.* 2018, 67, 30–42. doi:10.1016/j.jag.2017.12.009

Halder, B., Bandyopadhyay, J., and Banik, P. Evaluation of the climate change impact on urban heat island based on land surface temperature and geospatial indicators. *Int. J. Environ. Res.* 2021, 15, 819–835. doi:10.1007/s41742-021-00356-8

Henan Province Bureau of Statistics,. 2022 *Henan statistical yearbook*. Beijing, China: China Statistics Press.

Ke, X., Men, H., Zhou, T., Li, Z., and Zhu, F. Variance of the impact of urban green space on the urban heat island effect among different urban functional zones: A case study in wuhan. *Urban For. Urban Green.* 2021, 62, 127159, doi:10.1016/j.ufug.2021.127159

Khan, A., and Chatterjee, S. Numerical simulation of urban heat island intensity under urban–suburban surface and reference site in Kolkata, India. *Earth Syst. Environ.* 2016, 2, 71, doi:10.1007/s40808-016-0119-5

Kumar, R., and Mishra, V. Decline in surface urban heat island intensity in India during heatwaves. *Environ. Res. Commun.* 2019, 1, 031001, doi:10.1088/2515-7620/ab121d

Levermore, G., Parkinson, J., Lee, K., Laycock, P., and Lindley, S. The increasing trend of the urban heat island intensity. *Urban Clim.* 2018, 24, 360–368. doi:10.1016/j.uclim.2017.02.004

Li, Y., Schubert, S., Kropp, J. P., and Rybski, D. On the influence of density and morphology on the urban heat island intensity. *Nat. Commun.* 2020, 11, 2647, doi:10.1038/s41467-020-16461-9

Liao, W., Cai, Z., Feng, Ye., Gan, D., and Li, X. A simple and easy method to quantify the cool island intensity of urban greenspace. *Urban For. Urban Green.* 2021,62: 127173, doi:10.1016/j.ufug.2021.127173

Liu, X., Zhou, Y., Yue, W., Li, X., Liu, Y., and Lu, D. Spatiotemporal patterns of summer urban heat island in Beijing, China using an improved land surface temperature. *J. Clean. Prod.* 2020b, 257, 120529, doi:10.1016/j.jclepro.2020.120529

Liu, Y., Li, Q., Yang, L., Mu, K., Zhang, M., and Liu, J. Urban heat island effects of various urban morphologies under regional climate conditions. *Sci. Total Environ.* 2020a, 743, 140589, doi:10.1016/j.scitotenv.2020.140589

Ma, J., Dong, G., Yao, B., Giannousis, P., Thoolen, M., Ye, Q., et al. Periodicity and variability in daily activity satisfaction: Toward a space-time modeling of subjective well-being. *Ann. Am. Assoc. Geogr.* 2023, 1, 1–19. doi:10.1080/00498254.2023.2245459

Manoli, G., Fatichi, S., Schläpfer, M., Yu, K., Crowther, T. W., Meili, N., et al. Magnitude of urban heat islands largely explained by climate and population. *Nature* 2019, 573, 55–60. doi:10.1038/s41586-019-1512-9

Marando, F., Heris, M. P., Zulian, G., Udías, A., Mentaschi, L., Chrysoulakis, N., et al. Urban heat island mitigation by green infrastructure in European functional urban areas. *Sustain. Cities Soc.* 2022, 77, 103564, doi:10.1016/j.scs.2021.103564

Meng, Q., Zhang, L., Sun, Z., Meng, F., Wang, L., and Sun, Y. Characterizing spatial and temporal trends of surface urban heat island effect in an urban main built-up area: A 12-year case study in Beijing, China. *Remote Sens. Environ.* 2018, 204, 826–837. doi:10.1016/j.rse.2017.09.019

Meng, X., Pi, H., Gao, X., He, P., and Lei, J. A high-accuracy vegetation restoration potential mapping model integrating similar habitat and machine learning. *L. Degrad. Dev.* 2023, 34, 1208–1224. doi:10.1002/ldr.4527

Min, M., Zhao, H., and Miao, C. Spatio-temporal evolution analysis of the urban heat island: A case study of Zhengzhou city, China. *Sustainability* 2018, 10, 1992; doi:10.3390/su10061992

Peng, S., Piao, S., Ciais, P., Friedlingstein, P., Ottle, C., Bréon, F.-M., et al. Surface urban heat island across 419 global big cities. *Environ. Sci. Technol.* 2012, 46, 696–703. doi:10.1021/es2030438

Schwarz, N., Lautenbach, S., and Seppelt, R. Exploring indicators for quantifying surface urban heat islands of European cities with MODIS land surface temperatures. *Remote Sens. Environ.* 2011, 115, 3175–3186. doi:10.1016/j.rse.2011.07.003

Sekertekin, A., and Zadbagher, E. Simulation of future land surface temperature distribution and evaluating surface urban heat island based on impervious surface area. *Ecol. Indic.* 2021, 122, 107230, doi:10.1016/j.ecolind.2020.107230

Siddiqui, A., Kushwaha, G., Nikam, B., Srivastav, S. K., Shelar, A., and Kumar, P. Analysing the day/night seasonal and annual changes and trends in land surface temperature and surface urban heat island intensity (SUHII) for Indian cities. *Sustain. Cities Soc.* 2021, 75:103374, doi:10.1016/j.scs.2021.103374

Sun, Z., Li, Z., and Zhong, J. Analysis of the impact of landscape patterns on urban heat islands: A case study of Chengdu, China. *Int. J. Environ. Res. Public Health* 2022, 19, 13297, doi:10.3390/ijerph192013297

Tan, M., and Li, X. Quantifying the effects of settlement size on urban heat islands in fairly uniform geographic areas. *Habitat Int.* 2015, 49, 100–106. doi:10.1016/j.habitatint.2015.05.013

Tong, S., Prior, J., McGregor, G., Shi, X., and Kinney, P. Urban heat: An increasing threat to global health. *BMJ* 2021, 375, n2467, doi:10.1136/bmj.n2467

Vinayak, B., Lee, H. S., Gedam, S., and Latha, R. Impacts of future urbanization on urban microclimate and thermal comfort over the Mumbai metropolitan region, India. *Sustain. Cities Soc.* 2022, 79, 103703, doi:10.1016/j.scs.2022.103703

Wang, J., Chen, Y., Liao, W., He, G., Tett, S. F. B., Yan, Z., et al. Anthropogenic emissions and urbanization increase risk of compound hot extremes in cities. *Nat. Clim. Chang.* 2021a, 11, 1084–1089. doi:10.1038/s41558-021-01196-2

Wang, J., Huang, B., Fu, D., and Atkinson, P. M. Spatiotemporal variation in surface urban heat island intensity and associated determinants across major Chinese cities. *Remote Sens.* 2015, 7, 3670–3689. doi:10.3390/rs70403670

Wang, M., Zhang, Z., Hu, T., Wang, G., He, G., Zhang, Z., et al. An efficient framework for producing landsat-based land surface temperature data using Google Earth engine. *IEEE J. Sel. Top. Appl. Earth Observations Remote Sens.* 2020, 13: 4689–4701. doi:10.1109/JSTARS.2020.3014586

Wang, X., Tian, G., Yang, D., Zhang, W., Lu, D., and Liu, Z. Responses of PM2.5 pollution to urbanization in China. *Energy Policy* 2018, 123, 602–610. doi:10.1016/j.enpol.2018.09.001

Wang, Y., Guo, Z., and Han, J. The relationship between urban heat island and air pollutants and them with influencing factors in the Yangtze River Delta, China. *Ecol. Indic.* 2021b,129: 107976, doi:10.1016/j.ecolind.2021.107976

Wu, X., Wang, G., Yao, R., Wang, L., Yu, D., and Gui, X. Investigating surface urban heat islands in South America based on MODIS data from 2003–2016. *Remote Sens.* 2019, 11, 1212, doi:10.3390/rs11101212

Yang, D., Meng, F., Liu, Y., Dong, G., and Lu, D. Scale effects and regional disparities of land use in influencing pm 2.5 concentrations: A case study in the Zhengzhou metropolitan area, China. *Land* 2022a, 11, 1538, doi:10.3390/land11091538

Yang, F., Li, S., Gao, Y., Li, M., and Wu, P. Inconsistent carbon budget estimation using dynamic/static carbon density under land use and land cover change: A case study in henan Province, China. *Land* 2022b, 11, 2232, doi:10.3390/land11122232

Yang, Q., Huang, X., and Tang, Q. The footprint of urban heat island effect in 302 Chinese cities: Temporal trends and associated factors. *Sci. Total Environ.* 2019, 655, 652–662. doi:10.1016/j.scitotenv.2018.11.171

Yang, Y., Song, F., Ma, J., Wei, Z., Song, L., and Cao, W. Spatial and temporal variation of heat islands in the main urban area of Zhengzhou under the two-way influence of urbanization and urban forestry. *PLoS ONE* 2022c, 17(8): e0272626. doi:10.1371/journal.pone.0272626

Yao, R., Wang, L., Huang, X., Gong, W., and Xia, X. Greening in rural areas increases the surface urban heat island intensity. *Geophys. Res. Lett.* 2019, 46, 2204–2212. doi:10.1029/2018GL081816

Zhang, H., Yin, Y., An, H., Lei, J., Li, M., Song, J., et al. Surface urban heat island and its relationship with land cover change in five urban agglomerations in China based on GEE. *Environ. Sci. Pollut. Res.* 2022b, 29: 82271–82285. doi:10.1007/s11356-022-21452-y

Zhang, X., Chen, L., Jiang, W., and Jin, X. Urban heat island of Yangtze River Delta urban agglomeration in China: Multi-time scale characteristics and influencing factors. *Urban Clim.* 2022a, 43, 101180, doi:10.1016/j.uclim.2022.101180

Zhao, M., Cai, H., Qiao, Z., and Xu, X. Influence of urban expansion on the urban heat island effect in shanghai. *Int. J. Geogr. Inf. Sci.* 2016, 30, 2421–2441. doi:10.1080/13658816.2016.1178389

Zhou, D., Zhang, L., Hao, L., Sun, G., Liu, Y., and Zhu, C. Spatiotemporal trends of urban heat island effect along the urban development intensity gradient in China. *Sci. Total Environ.* 2016, 544, 617–626. doi:10.1016/j.scitotenv.2015.11.168

Zhou, D., Zhao, S., Liu, S., Zhang, L., and Zhu, C. Surface urban heat island in China's 32 major cities: Spatial patterns and drivers. *Remote Sens. Environ.* 2014, 152, 51–61. doi:10.1016/j.rse.2014.05.017

Zhou, S., Liu, D., Zhu, M., Tang, W., Chi, Q., Ye, S., et al. Temporal and spatial variation of land surface temperature and its driving factors in Zhengzhou city in China from 2005 to 2020. *Remote Sens.*2022, 14, 4281. doi:10.3390/rs14174281

Appendix

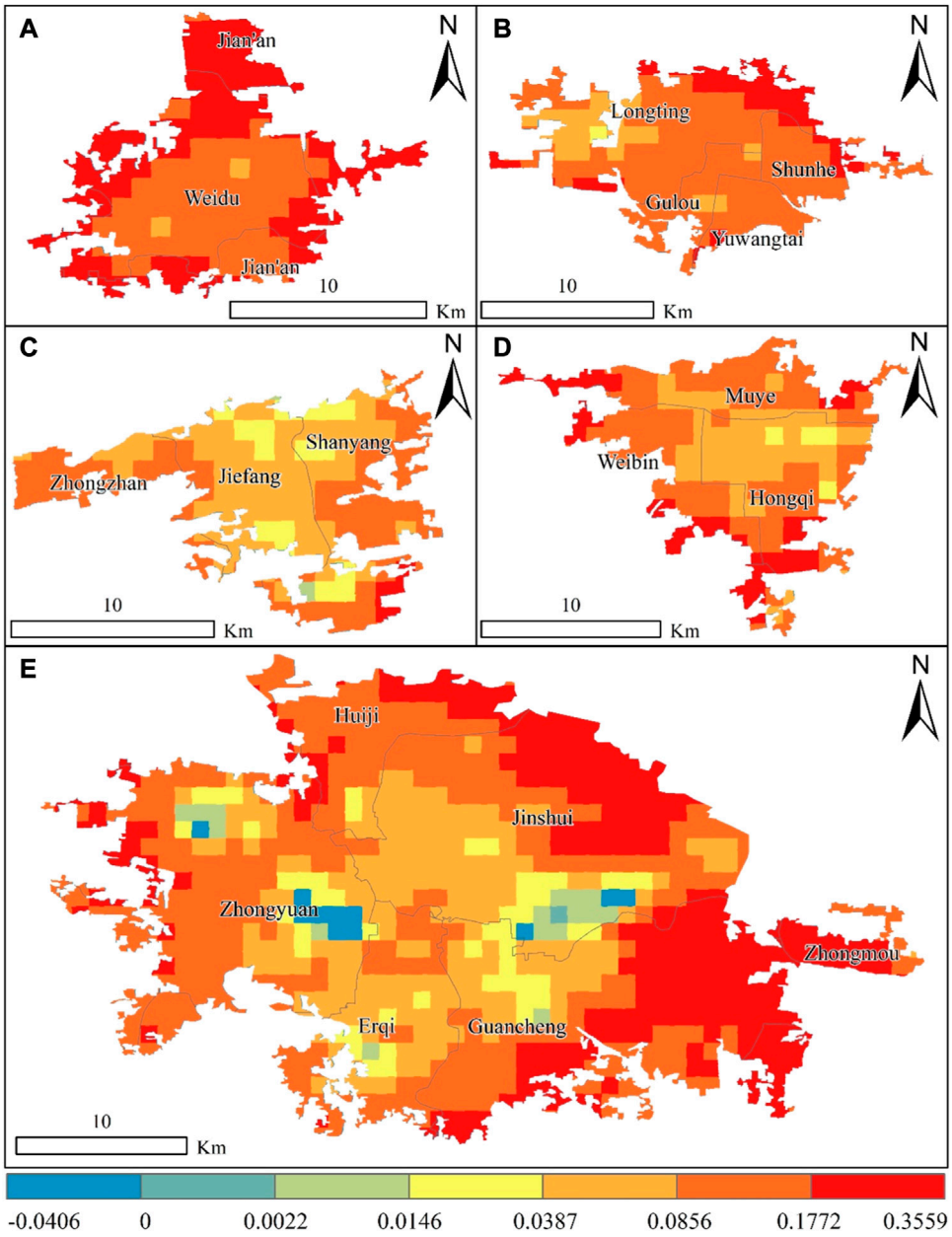

FIGURE A1
Spatial distribution of daytime surface temperature trends in different cities within the Zhengzhou metropolitan area.

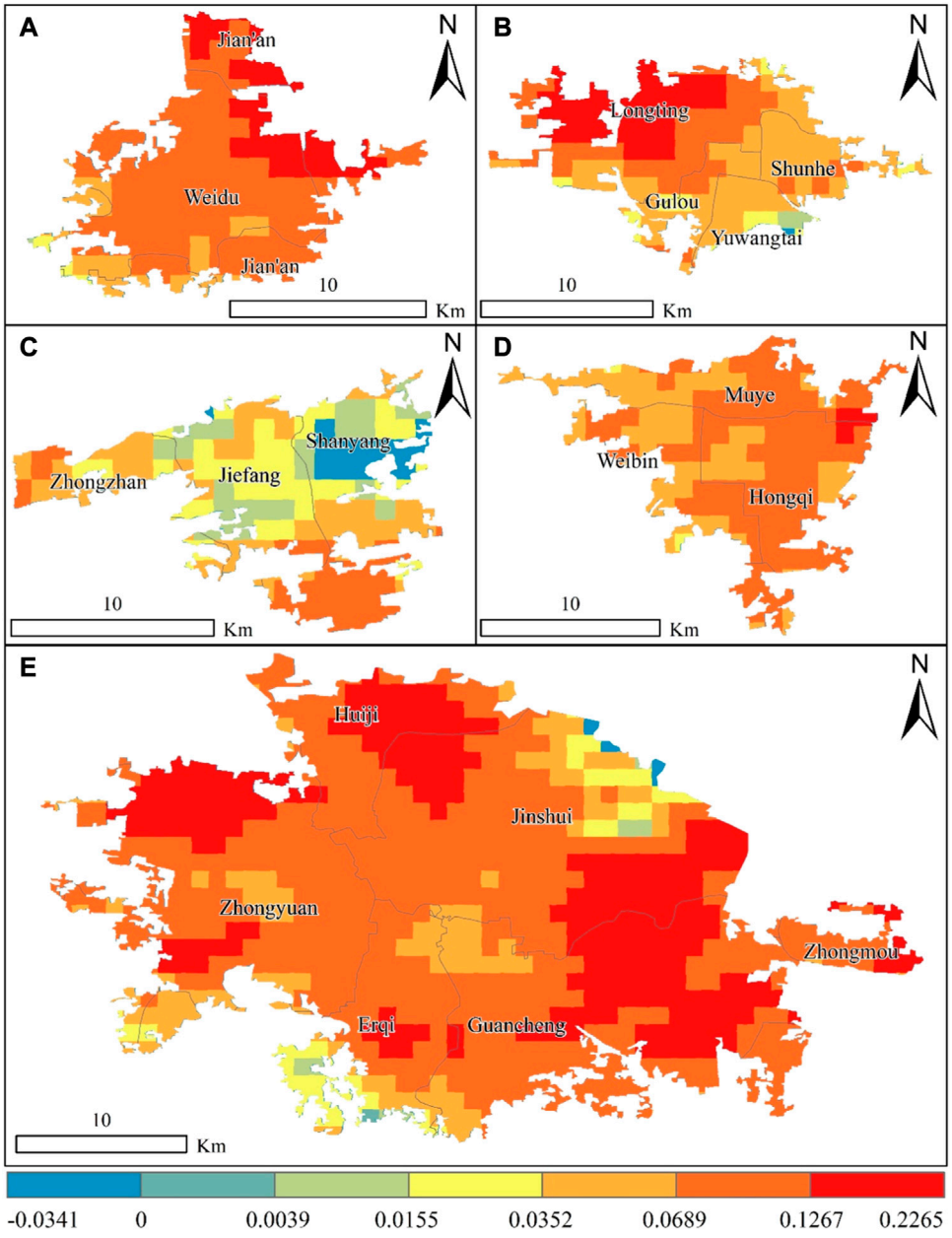

FIGURE A2
Spatial distribution of nighttime surface temperature trends in different cities within the Zhengzhou metropolitan area.

frontiers | Frontiers in Environmental Science

TYPE Original Research
PUBLISHED 26 October 2023
DOI 10.3389/fenvs.2023.1270921

OPEN ACCESS

EDITED BY
Xue-Chao Wang,
Beijing Normal University, China

REVIEWED BY
Xiao Ouyang,
Hunan University of Finance and Economics, China
Kun Wang,
Guangxi University Nanning, China in collaboration with reviewer XO
Guoen Wei,
Nanchang University, China

*CORRESPONDENCE
Qimeng Ning,
ningqimeng@hncu.edu.cn

RECEIVED 01 August 2023
ACCEPTED 09 October 2023
PUBLISHED 26 October 2023

CITATION
Yang H, Ning Q, Zhou H, Lai N, Song Q, Ji Q and Zeng Z (2023), Digital research on the resilience control of water ecological space under the concept of urban-water coupling.
Front. Environ. Sci. 11:1270921.
doi: 10.3389/fenvs.2023.1270921

Digital research on the resilience control of water ecological space under the concept of urban-water coupling

Hua Yang[1], Qimeng Ning[2]*, Hui Zhou[1], Nan Lai[1], Qidi Song[1], Qianfu Ji[1] and Zhiwei Zeng[2]

[1]Hunan Provincial Territorial Space Survey and Monitoring Institute, Changsha, China, [2]College of Architecture and Urban Planning, Hunan City University, Yiyang, China

Introduction: The construction of digital governance of national land space depends greatly on the development of a digital model for robust control of water and ecological space. However, how changes to the urban-water coupling relationships affect the resilience control of water ecological space is rarely reported.

Methods: The evolution characteristics of urban and water space in the study area from 2000 to 2020 and the correlation between them are analyzed based on the grid analysis using InVEST and Moran'I methods. Based on the theory of human-environment interaction territorial system to provide a theoretical framework to explain the urban and water space. We used digital to construct an resilience control framework in the Dongting Lake area based on the correlation between the urban and water space.

Results: The results show that: 1) From 2000 to 2020, the geographical evolution of towns and cities in the research area displayed obvious spatial variation in intensity, indicating a process of expansion and change. The regional and temporal fluctuations of the water conservation function are significant. The mountainous areas in the east, south, and northwest are where the high values of the water conservation function are primarily found. These regions have more vegetation, which increases the water conservation function. 2) According to the results of local binary spatial autocorrelation analysis, it can be seen that from 2000 to 2020, the high-high agglomeration of town space and water-related is mainly distributed in Linxiang City, Yueyang County, Miluo City, Li County, and Yiyang City, and the low-low agglomeration is mainly distributed in Dongting Lake, Datong Lake, and along the Yangtze River. 3) Based on how urban spatial evolution affects water ecological space, we construct a theoretical framework of urban-water coupling and establish a digital model of water ecological space resilience control in the Dongting Lake area from four perspectives: threshold, visualization, dynamics, and intelligence.

KEYWORDS

urban-water coupling, water ecological space, resilience control, digitalization, Dongting lake area

1 Introduction

Digital governance of land space is an important component of the modernization of the national governance system and governance capacity (Corodescu-Roșca et al., 2023). In May 2019, "Several Opinions of the State Council of the Central Committee of the Communist Party of China on Establishing a Land Space Planning System and Supervising its Implementation" were issued, and land space governance entered a new stage of development. The Proposal of the CPC Central Committee on Formulating the 14th Five-Year Plan for National Economic and Social Development and the 2035 Visionary Goals proposes to realize the digitization, networking and intelligence of the whole process of national land spatial governance and build a new pattern of national land spatial development and protection. Therefore, relying on digital technology to promote the digital transformation of land space governance has become an inevitable choice for the refinement of land space governance under the new situation. Rapid urbanization has caused the destruction of water ecological space, and the government now needs to learn more about its structure and function in order to build a digital model of toughness control that will allow it to assess, monitor, and control changes to water ecological space in an efficient manner (Zeng et al., 2023). This is important for the digital governance of national land space in the Dongting Lake area.

High-urbanization areas in China are generally characterized by more artificial intervention in ecosystems and stronger ecological vulnerability (Zhang et al., 2023). For a long time, the construction of various water conservancy engineering facilities such as river hardening, cut-off and straightening, sluice gates, reservoirs and artificial drainage ditches has changed the connectivity and infiltration capacity of surface water systems, resulting in the reduction of water ecosystem functions (Jaiswal and Pandey, 2021; Wang et al., 2023). Driven by urban expansion, the construction of lake-fenced and reclaimed land has caused a significant reduction in the area of rivers, lakes and wetlands and seriously damaged the circulation system of rivers and wetlands, weakening the ecosystem service role of water ecosystems in storing rain and floods, purifying water bodies, regulating microclimate, controlling soil erosion and beautifying the environment (Paiva et al., 2020; Yao et al., 2021). In the practice of urban spatial planning, how to organize the spatial form, functional layout, road system, open space, infrastructure and other elements of the city to achieve coordination and adaptation with the characteristics of the urban water ecological environment has also been a common concern of planning scholars and local governments in recent years (Huang et al., 2023). Meanwhile, the research on the interaction between urban and water environments shows a development trend from empirical analysis to quantitative and data-based research, and scholars at home and abroad analyze the interaction between urban development and water environments more systematically and completely by combining various computer simulation models such as urban growth models, hydrological models, and ecological models. For example, Maeve McBride and Derek Booth (2005) analyzed the scale sensitivity of the effect of urban construction on water systems and the effect of urban land form through regression models of the physical environmental characteristics of water systems in urban areas and urban construction in watersheds (McBride and Booth, 2005). Bach et al. (2013) simulated the interaction between plot-scale, water-sensitive infrastructure construction (Bhaskar et al., 2016). And Bhaskar et al., 2016 applied the SLEUTH model, which simulates urban spatial growth, and the ParFlow model, which simulates the water circulation system, to study the characteristics of surface vegetation and the water circulation system in Baltimore, United States, as urban spatial growth occurs, and found that urban expansion will lead to a decrease in surface water and that the sensitivity of the water environment varies among different locations. The sensitivity of the water environment varies, and the surface water in some sensitive areas will be more significantly affected by the spatial growth of the town (Bhaskar et al., 2016). Xu Kang et al. (2013) applied a cellular automaton (CA) model and a regional hydrological model (SCS) to simulate the proportion and risk of urban flooding under different urban growth rates, and then guided the delineation of urban growth boundaries (XU et al., 2013). Zhang et al. (2021) used the distributed metacellular automata model (CA) and BP neural network model to construct an urban land use change and water quality response simulation model to simulate regional urban land use change, predict the response relationship of upstream and downstream water quality to urban area pollution discharge, and quantitatively analyze the characteristic law between urban spatial expansion and water environment quality change (Zhang et al., 2021).

There are close interactions and interactions between urban spatial development and water environmental protection, both in terms of constraints and coercion, as well as reciprocal promotion and enhancement (Meng, 2021) (Table 1). Further research is needed on the kind of relationship between urban and water and how to improve the resilience of water ecological space in the process of urban spatial evolution. As an example, this thesis uses the Dongting Lake area to apply the theory of "urban-water coupling concept" and the technical framework of spatio-temporal interaction to identify the urban-water contradiction in the Dongting Lake area, construct a theoretical framework of urban-water coupling, and build a digital model of water-ecological spatial resilience control in the Dongting Lake area from four aspects: threshold, visualization, dynamization, and intelligence. It is investigated how to put the concept of ecological civilization into practice in the field of spatial planning in order to advance the theoretical and methodological framework for the digitalization of territorial spatial governance.

2 Study area, methods and data sources

2.1 Study area

Dongting Lake Eco-Economic Zone is located at 28°30′N-29°40′N, 113°10′E-114°40′E, in the north of Hunan Province and the south of Hubei Province, and is the second largest freshwater lake in China, as well as an important storage lake and ecological security function area in the Yangtze River Basin. The overall plain is dominant, but there are still many types of landforms, which can be roughly divided into four types: lake water bodies and continental beaches, plains and hills around the lake, hills and low mountains around the lake area, and river valley plains and hills (Zeng et al., 2023). It is a typical subtropical monsoonal climate, with simultaneous rain and heat, long sunshine hours, abundant precipitation, and a dense network of rivers in the lake area, through which the Xiang, Zizhi, Yuan and Li rivers flow. The region has good coastline resources, thriving interior river ports like Yueyang Port and

TABLE 1 The core control index system of water ecological space.

Urban space evolution	Population urbanization rate	GDP
	Natural population growth rate	GDP *per capita*
	Density of population	GDP annual rate of growth
	Proportion of impermeable ground surface	Industrialization level index
	Million yuan GDP wastewater emissions	Water consumption per million yuan of GDP
Water ecological space	Landscape fragmentation index (water wetland)	Household water consumption
	Water wetland area	Daily water consumption *per capita*
	Change rate of water wetland area	Domestic wastewater discharge per unit area of living area
	Water conservation	Urban domestic sewage discharge rate
	Natural shoreline retention rate	Sewage centralized treatment rate

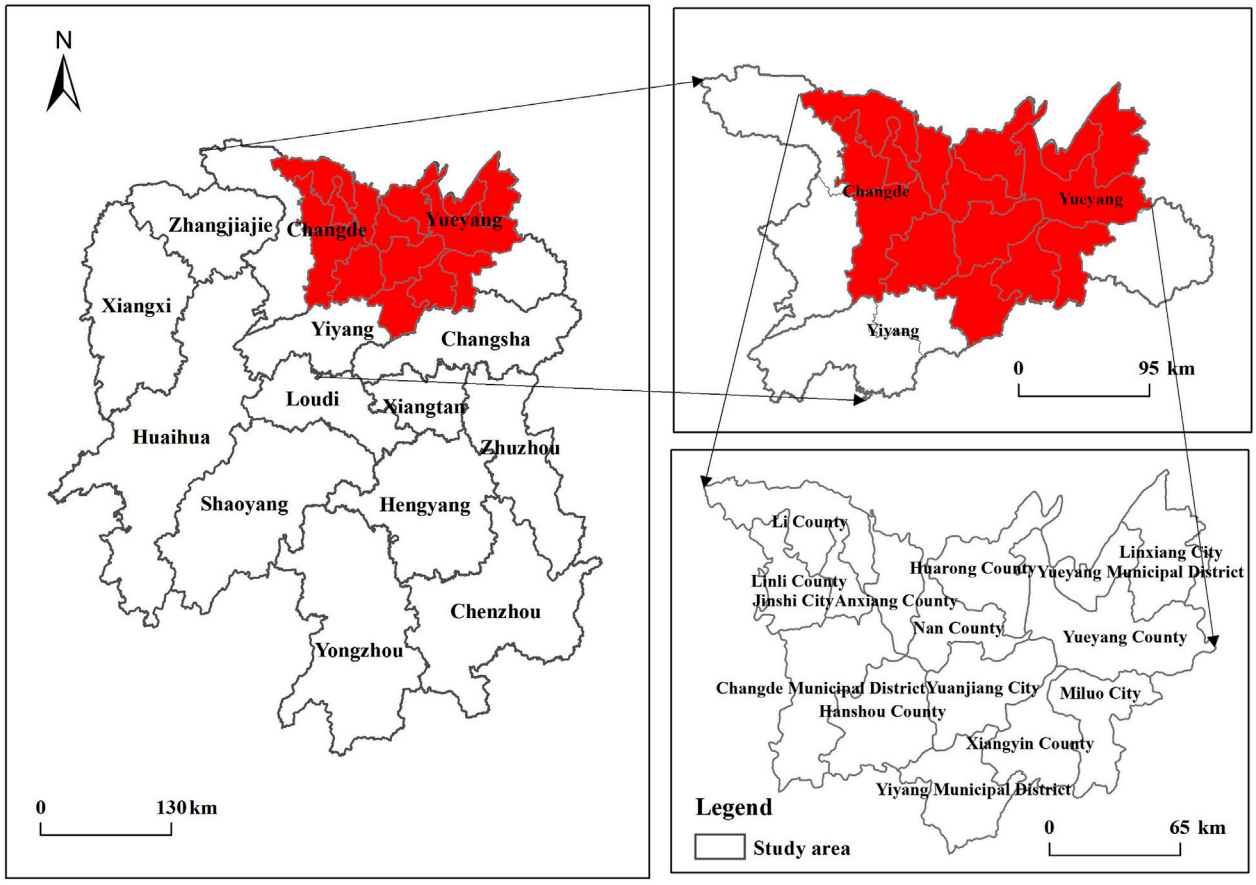

FIGURE 1
Study area.

Jingzhou Port, and is well-served by a variety of transportation modes including high-speed rail, highway, railroad, water transport, and air transport. The area has a thriving agricultural products processing business and is a key producer of agricultural goods such as grain, cotton, oil, and freshwater fish in China (Xiong et al., 2022). Here, some counties (cities and districts) in three prefecture-level cities of Yueyang, Yiyang, and Changde in the Dongting Lake Ecological and Economic Zone were selected as the study area, including Yueyang city, Linxiang city, Yueyang county, Huarong county, Miluo city, Xiangyin county, Yiyang city, Yuanjiang city, Nan county (including Datong lake area), Changde city, Hanshou county, Anxiang county, Li county, Jin city, and Linli county, a total of 19 counties (cities and districts) (the study area in the following refers to this range), as shown in Figure 1, with a total area of about 25,800 km2, accounting

for about 12.18% of Hunan Province, a resident population of about 10,075,800 as of the end of 2020, accounting for 16.11% of the province, and a gross product of about 710.44 billion yuan, accounting for about 17% of the province.

2.2 Methods

2.2.1 Spatial expansion intensity of urban land

The spatial expansion intensity of urban land (*USEI*) indicates the percentage of the spatial size of a cell town to its cell area in different periods, and is used to analyze the size of spatial expansion intensity of towns in different periods (Wang et al., 2022), in %. Its formula is:

$$USEI = \left(U_{urban} / U_{fishnet}\right) \times 100\% \quad (1)$$

Where: U_{fishnet}、 U_{urban} represent respectively the area of each cell and the sum of the urban space area.

2.2.2 Water production service

The water production service is generally defined as the difference between precipitation and evapotranspiration and is one of the measures of the water availability of an ecosystem. Based on the Budyko coupled water-energy balance theory (Jin et al., 2022), the InVEST model's water production service module (water yield) determines the average annual water yield by subtracting the average annual precipitation from the actual annual evapotranspiration. The calculating formula is as follows:

$$Y_{ij} = \left(1 - \frac{AET_{ij}}{\mathrm{P}_i}\right) \cdot P_i \quad (2)$$

Where: Y_{ij} is the annual water yield (mm) of grid unit; AET_{ij} represents the annual actual evapotranspiration (mm) of grid unit ; P_i indicates the annual precipitation (mm) of grid unit i.

2.3 Data sources

The Urban land, Annual actual evapotranspiration and Annual precipitation datasets were obtained from the Resource and Environmental Science and Data Center of the Chinese Academy of Sciences, accessible through the specific website (https://www.resdc.cn/).

3 Results analysis

3.1 Spatial-temporal evolutionary characteristics of urban land intensity and water-related function

Along with the beginning and speeding up of urbanization, the amount of agricultural land being converted into non-agricultural construction land has accelerated and expanded, and the intensity of land disturbance by human activities has steadily increased. This is partially reflected in the spatial evolution of towns. From Figures 2A–C, it can be seen that the intensity of urban spatial evolution in the study area from 2000 to 2020 shows obvious spatial divergence characteristics and exhibits a process of growth and change. In general, the low intensity is mainly distributed in Dongting Lake, coastal rivers and lakes and mountainous hilly areas, while the high intensity is concentrated in areas with higher urbanization levels such as urban counties and cities. The higher intensity is located in the combined urban-rural areas around towns, the medium intensity is mainly distributed in the fringe areas of combined urban-rural areas, and the lower intensity is mainly concentrated around ecologically sound areas such as rivers and hills. From 2000 to 2010, the area of high intensity has shrunk, mainly showing the obvious reduction of high intensity areas in Yiyang city, Miluo city, Huarong county and Nan county; the distribution range of higher intensity has slightly expanded, mainly transformed by the high intensity area in 2000; while the area of low intensity, lower intensity and medium intensity is more stable. This reflects the slow urbanization process, slow population concentration and small scale of economic activities in the ecological economic zone of Dongting Lake during this period, resulting in a small change in the overall land use intensity. From 2010 to 2020, there is a significant increase in land use intensity in the study area, mainly in the high-intensity areas of Huarong County, Nan County, Yuanjiang City, Yiyang City, Changde City, Miluo City and Yueyang County At the same time, the low-intensity area in the northern waters of Dongting Lake, Linxiang City and the eastern side of Yueyang County decreased significantly, while the lower-intensity area increased significantly. In the eastern, southern and western shore areas of Dongting Lake, the higher-intensity and medium-intensity areas also expanded to a certain extent compared with 2010. This is related to the accelerated urbanization in recent years, the increasing concentration of population, the accelerated expansion of construction land, the sharp changes in the original land use structure, and the increased economic pressure on land. Thus, the change process of land use intensity from 2000 to 2018 indicates the importance of continuing to implement the concept of ecological civilization and the development plan of an ecological economic zone in the future study area, vigorously developing the ecological economy, accelerating industrial transformation and upgrading, and strengthening ecological environmental protection.

In terms of the water-related function (Figures 2D–F), the spatial and temporal variation of the water-related function from 2000 to 2020 is large. The highest value of the water-related function is found mostly in the eastern, southern, and northwestern mountainous areas, where the vegetation cover is dense and thus the water-related function is high. From 2000 to 2010, the distribution area of high water-related function increased slightly, mainly in Changde city, Linli county, Yiyang city and Miluo city; from 2010 to 2020, the area of high water-related function decreased significantly in Linli county, southern Changde city, Yueyang county, Linxiang city and Miluo city. In 2010–2020, the area of high water-related function in Linli County, the southern part of Changde City, Yueyang County, Linxiang City and Miluo City decreased significantly. At the same time, the area of higher water content function in the study area is always shrinking, as the ecological and economic zone of Dongting Lake is in the stage of accelerated urbanization and the scope of human activities is expanding, and the regional water content function is obviously

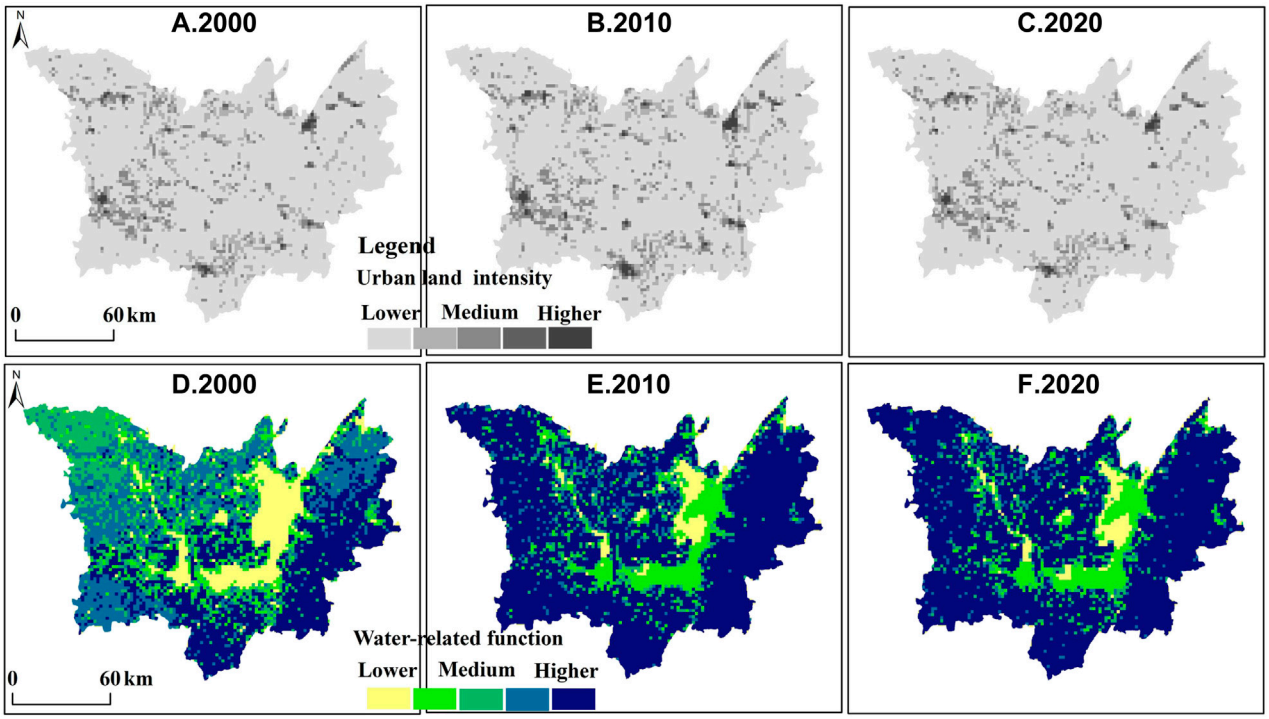

FIGURE 2
Spatial distribution of urban and water ecology in study area 2000–2020.

reduced due to the influence of anthropogenic activities such as forest land reclamation and sloping land development, etc. From 2000 to 2020, the area of medium water content function is characterized by a continuous increase, which is manifested in the plains on the west bank of Dongting Lake and the hills and mountains in the east and south. From 2000 to 2020, the area of medium water-related function is characterized by a continuous increase, as shown by the plain on the west bank of Dongting Lake and the hilly mountains in the east and south. The lower values of the water-related function are mainly distributed along the Dongting Lake watershed, Datong Lake, along the Yangtze River, the western part of Xiangyin County, Changde City, and Jincheng City, and their distribution is relatively stable from 2000 to 2020, with little spatial change.

3.2 Spatial-temporal interaction analysis between urban and water ecology

The greater the intensity of urban spatial evolution, the deeper the impact of human activities on water ecology, which will eventually contribute to the decline and reduction of water ecological functions. The analysis of the spatial evolutionary intensity of towns and cities and the spatio-temporal relationship between water ecological functions is of great relevance to the realization of sustainable development. From the results of the local binary spatial autocorrelation analysis (Figure 3), it can be seen that in the local spatial autocorrelation distribution of the spatial evolutionary intensity of towns and cities and water ecological functions, the high-high concentration is mainly distributed in Linxiang City, Yueyang County, Miluo City, Li County and Yiyang City, and from 2000 to 2010, its distribution area shows a shrinking feature, while there is a small expansion in Changde City and Yiyang City; From 2010 to 2020, its distribution area increases, and the expansion is more obvious in Yueyang County, Miluo City, Xiangyin County, Yiyang City, Li County and Linli County. Low-low agglomeration is mainly concentrated in Dongting Lake, Datong Lake and along the Yangtze River; From 2000 to 2010, its distribution area in Datong Lake and North Dongting Lake showed a small increase, and its spatial pattern did not change much from 2010 to 2020. The low-high concentration is mainly located in Li County, Linxiang City, Yueyang County, Miluo City, Linli County, Yiyang City and the southern part of Changde City, and its area has an increasing trend; From 2000 to 2010, the area of low-high concentration in Linli County, the southern part of Changde City, the southern part of Yiyang City and the southeast of Linxiang City increased significantly; From 2010 to 2020, its distribution in Linli County, Changde City, Linxiang City and Yueyang County. From 2010 to 2020, the distribution area in Linli County, Changde City, Linxiang City and Yueyang County decreased significantly, while the distribution area in Yiyang City increased. The area of high-low agglomeration is smaller and more concentrated on the south bank of Dongting Lake, the south bank of the Yangtze River and the Changde urban area. From 2000 to 2010, its area in Xiangyin County showed a large increase, but the area of high-low agglomeration remained basically the same from 2010 to 2020.

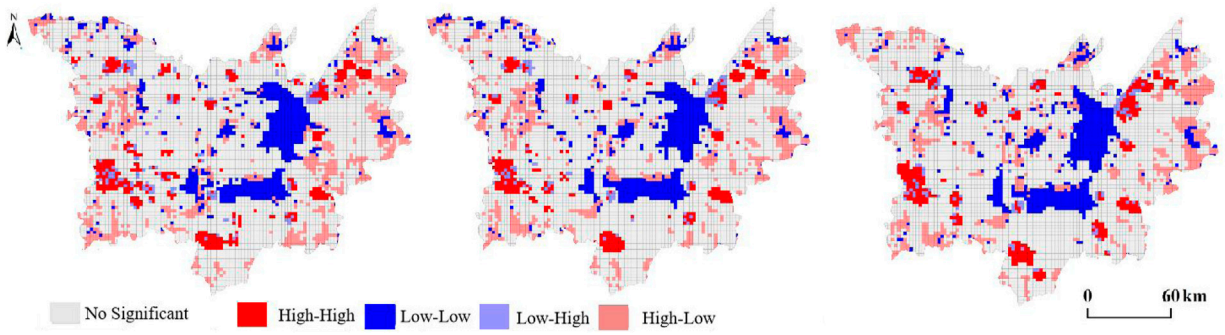

FIGURE 3
Spatio-temporal interaction between towns and water ecology.

4 Digital intelligence control mode of water ecological space under urban water coupling

The urban space in the Dongting Lake area shows the characteristics of spreading expansion, polycentric structure evolution and jumping land expansion. The analysis of water ecological functions reveals that while pressure on the supply of water ecological functions is relieved with the implementation of projects like the return of farmland to the lake in the Dongting Lake area, the problem of water ecological space risk remains severe and water ecological space, such as waters and wetlands, is reduced in a significant amount of urban space (Namavar et al., 2023).

4.1 Theoretical framework of urban water coupling

Established studies have employed a range of quantitative variables to assess the regional population, industrial scale, industrial structure, etc. with regard to the pressure that urban socio-economic development has on the aquatic environment. Among them, for the measurement of population pressure, some studies have used indicators such as population urbanization rate (Lu et al., 2019), natural population growth rate, and population density (Duan et al., 2021) to directly quantify the population scale, arguing that the carrying pressure on the water environment is also higher in regions with a higher population scale; or they have used household water consumption, *per capita* daily domestic water consumption, domestic wastewater discharge per unit area of living area, urban domestic wastewater discharge rate (Bi et al., 2023) and other indicators to measure the pressure on the water environment caused by domestic water use and sewage discharge. Similarly, for industrial scale and industrial structure, evaluation indexes such as GDP, *per capita* GDP, annual growth rate of GDP, industrialization level index, water consumption per 10,000 yuan GDP, and wastewater discharge per 10,000 yuan GDP (Ferrer et al., 2012) can be used. According to the principle of representativeness, this study adopts a pressure measurement index that integrates the level of population and economic development, the water resources load index to measure the change in pressure exerted on the water environment by socioeconomic development.

The pressure that urban development has put on the aquatic environment is mostly manifested in the alteration of the original hydrogeomorphological characteristics and the rise in pollutants in surface runoff. As mentioned above, the process of urban construction has the problem of filling small water bodies and rivers and changing the connected structure of water systems, which causes a change in the water flow state and habitat of aquatic animals and plants (Wei et al., 2023a; Wei et al., 2023b). Drawing on the landscape pattern index method of landscape ecology (Yu et al., 2019), this study used the landscape fragmentation index of watershed wetlands to measure the magnitude of changes in hydrogeomorphic characteristics caused by urban construction. For the problem of surface runoff pollution caused by urban construction, which mainly originates from the runoff pollution of impervious surface surfaces in cities and towns, the percentage of impervious surface surfaces is used as an evaluation index, which can be calculated by extracting remote sensing images, and the data are available and connected with the manageable indexes of territorial spatial planning.

4.2 Water ecology spatial digital intelligence control model

Digital intelligence control of territorial space has been emphasized in China's planning community, but the main control contents are mostly qualitative planning effectiveness and macro-socio-economic indicators, while there is a lack of specific policy evaluation, external evaluation and dynamic monitoring of the implementation process. Therefore, the development trend of the digital intelligence control model must achieve threshold identification, dynamic visualization and intelligence, and improve all aspects of digital intelligence control of land space (Wei et al., 2023a). Thresholds: The indicator thresholds are essentially the boundaries of the numerical interval of the constraints in the water ecology spatial digital intelligence control, which is the key information for the implementation of supervision (Ouyang et al., 2019). The key to measuring indicator thresholds is to

identify the key indicators related to human activities, sort out how system components interact, and take into account exogenous factors like large-scale climate change and regional main functions, along with the goals of territorial spatial planning and indicator sets, to establish the many-to-many relationship between human activities and the resource environment. Based on this, the relationship between key indicators and each resource and environmental component is quantified employing system model simulation, and the indicator thresholds are then determined by identifying abrupt change points. The current assessment methods for water resource carrying capacity mainly include the empirical formula method, the multi-objective decision method, the system analysis method, the artificial intelligence algorithm, etc. To determine the threshold value of urban space scale, we need to estimate the total amount of regional water resources and the upper limit of water resource carrying capacity. Then, using the aforementioned method, we can forecast future urban production and living water demand. Based on *per capita* water consumption, we can then determine the size of the urban population that can be supported by regional water resources, or we can directly forecast it using the aforementioned method. Finally, we can multiply the size of the urban population by the *per capita* urban construction land area of the planning target. Additionally, the buildable land area of the entire region must be taken into account. The appropriate scale of urban construction land is determined by taking the smaller value of the buildable land area and the maximum scale of urban construction land carried by water resources.

Dynamic: By establishing a long-term monitoring system for national spatial planning, it can realize dynamic mastery of the implementation and operation of the plan and provide powerful support for the development and utilization of national spatial resources and planning management (Ouyang et al., 2022). The scope of long-term monitoring should include monitoring of land use changes, monitoring of planning implementation and approval, monitoring of planning target indicators, etc. The monitoring department should compare the most recent data of each indicator obtained by the system with the historical data and target values, respectively. Through the former, it can learn the benefits and drawbacks of the corresponding planning policies brought on by implementation and change trends, and through the latter, it can clarify the status of planning implementation as well as the next focus and direction of action. Extending the application of artificial intelligence (AI) and regional block chain technology in the field of territorial spatial planning, integrating the complex supervisory views of all social parties, and conducting scientific calculations on the revision of territorial spatial planning to as closely match the needs of all parties as possible.

Visualization: Identifying the key information from a large number of complex data sets to create an interactive image, implementing the two- and three-dimensional integrated graph-number linkage visualization so that the supervision results can be presented to regulators, technical parties, and the general public in a clear and efficient manner, and comprehensively integrating changes to multi-period remote sensing image changes (Eilola et al., 2023). Automatic extraction, video image interpretation, real-time processing of UAV aerial data flow, and other technical means are all realized, as are quick monitoring and verification and quick modeling of three-dimensional situations. Investigate the integration of 3D GIS, BIM, and IOT technology, develop a spatial planning management and application system based on an urban information model (CIM), and provide visual technical support for intelligent scenario simulation.

Intelligent: Form a feedback process of implementation evaluation-planning adjustment for two-way improvement. Therefore, during the decision-making process, the administrative bodies should conduct evaluations and gather feedback data in a timely manner (Ghavami et al., 2022). They should also build a real-time interactive and co-consultative urban spatial governance platform using the metaverse and digital twin city, and they should use a variety of tools like model algorithms to analyze and correct the implementation of policies and regulations, technical standards, and operating guidelines of the territorial spatial planning and enhance the entire system for spatial planning. We will improve the scientific and intelligent level of all aspects of spatial planning and focus on the system construction and platform development of systems for intelligent review of planning results, intelligent approval of construction projects, auxiliary site selection for major projects, intelligent supervision of the whole planning process, and dynamic evaluation of planning implementation.

5 Conclusion and discussion

5.1 Conclusion

1) From 2000 to 2020, the spatial evolutionary intensity of towns in the study area shows obvious spatial differentiation characteristics and exhibits a process of growth and change. The high intensity is concentrated in areas with high urbanization levels, such as urban counties and cities; the higher intensity is located in the urban-rural combination areas around the towns; the medium intensity is mainly distributed in the fringe areas of the urban-rural combination; and the lower intensity is mainly concentrated around ecologically sound areas, such as rivers and hills. The spatial and temporal variation of the water-related function is large. The high value of the water-related function is mainly distributed in the eastern, southern and northwestern mountainous areas, where the vegetation cover is higher and thus the water-related function is higher.
2) According to the results of the local binary spatial autocorrelation analysis, the high-high urban space and water-related agglomerations are primarily distributed in Linxiang City, Yueyang County, Miluo City, Li County, and Yiyang City from 2000 to 2020, while the low-low agglomerations are primarily distributed in Dongting Lake, Datong Lake, and along the Yangtze River.
3) The theoretical framework of urban-water coupling is sorted out, the core index system of digital intelligence control is constructed, and the digital model of water-ecological spatial toughness control in the Dongting Lake area is built from four aspects: threshold, visualization, dynamization, and intelligence.

5.2 Discussion

How to understand the dynamic interaction between urban space and the water environment system from the perspective of spatial planning is one of the core issues of this paper. On the basis of sustainable development theory, ecological adaptability theory, coupling relationship theory and other theories on the harmonious coexistence of humans and nature (Huang et al., 2022), this paper identifies the interaction between urban spatial evolution and water ecological space through a spatial autocorrelation model, constructs a framework for coupling urban spatial evolution and water ecological space, and sorts out and summarizes the core index system for the control of urban spatial and water ecological space. In the current territorial spatial planning, the ecological protection red line mainly refers to the boundary line of spatial management to protect important ecological function areas and sensitive areas (Liu et al., 2023), but for water ecosystems, water quality, water quantity and water ecological space are all three key factors to maintaining the health of water ecosystems, so some scholars propose to construct the water ecological red line framework from the three dimensions of structure-function-quality (Zeng et al., 2023). This paper agrees with and perpetuates this idea of water ecology protection and takes Dongting Lake as an example to discuss the spatial control model of water ecology in the region. Specifically, it is suggested to set the core control indexes related to water ecological space related to urban space and the water environment and to clarify the bottom line of water ecological protection. This paper proposes to use different non-linear methods to get the thresholds of different indexes, and at the same time, it integrates technologies such as the metaverse and digital twin cities to explore the control strategy of water ecological space in a spatial planning system through thresholds, visualization, dynamics and intelligence. For the territorial spatial system, it is not only necessary to couple the relationship between the urban and the water environment, but also to comprehensively coordinate the relationship between other ecological and environmental protection needs, basic farmland protection needs, etc., (Qu et al., 2023). And the water ecological space. Therefore, the spatial planning strategy proposed in this study can be used as a special study on water environment in the process of spatial planning of the whole area, and the complete delineation of "three zones and three lines" should also integrate other ecological environment elements and basic farmland protection related research results. Water ecological space monitoring is a complex project. This paper attempts to construct a digital technology of resilience from the perspective of urban-water relationship, which is an innovation. However, a comprehensive framework should be further constructed for monitoring in the future.

Data availability statement

The original contributions presented in the study are included in the article/Supplementary material, further inquiries can be directed to the corresponding author.

Author contributions

HY: Conceptualization, Data curation, Writing–original draft. QN: Formal Analysis, Methodology, Writing–review and editing. HZ: Data curation, Formal Analysis, Writing–review and editing. NL: Software, Validation, Writing–review and editing. QS: Data curation, Investigation, Writing–review and editing. QJ: Methodology, Writing–review and editing. ZZ: Conceptualization, Validation, Writing–review and editing.

Funding

This research was funded by the "Research project of Hunan Geological Institute" (HNGSTP202206) and "National Science Foundation of Hunan Province of China" (2022JJ50271).

Conflict of interest

The authors declare that the research was conducted in the absence of any commercial or financial relationships that could be construed as a potential conflict of interest.

Publisher's note

All claims expressed in this article are solely those of the authors and do not necessarily represent those of their affiliated organizations, or those of the publisher, the editors and the reviewers. Any product that may be evaluated in this article, or claim that may be made by its manufacturer, is not guaranteed or endorsed by the publisher.

References

BachDeletic, P. M. A., Urich, C., Sitzenfrei, R., Kleidorfer, M., Rauch, W., and McCarthy, D. T. (2013). Modelling interactions between lot-scale decentralised water infrastructure and urban form - a case study on infiltration systems. *Water Resour. Manage* 27, 4845–4863. doi:10.1007/s11269-013-0442-9

Bhaskar, A. S., Jantz, C., Welty, C., Drzyzga, S. A., and Miller, A. J. (2016). Coupling of the water cycle with patterns of urban growth in the Baltimore Metropolitan Region, United States. *J. Am. Water Resour. Assoc.* 52, 1509–1523. doi:10.1111/1752-1688.12479

Bi, Y., Zheng, L., Wang, Y., Li, J., Yang, H., and Zhang, B. (2023). Coupling relationship between urbanization and water-related ecosystem services in China's Yangtze River economic Belt and its socio-ecological driving forces: a county-level perspective. *Ecol. Indic.* 146, 109871. doi:10.1016/j.ecolind.2023.109871

Corodescu-Rosca, E., Hamdouch, A., and Iatu, C. (2023). Innovation in urban governance and economic resilience. The case of two Romanian regional metropolises: timişoara and Cluj Napoca. *CITIES* 132, 104090. doi:10.1016/j.cities.2022.104090

Duan, T., Feng, J., Zhou, Y., Chang, X., and Li, Y. (2021). Systematic evaluation of management measure effects on the water environment based on the DPSIR-Tapio decoupling model: a case study in the Chaohu Lake watershed, China. *Sci. Total Environ.* 801, 149528. doi:10.1016/j.scitotenv.2021.149528

Eilola, S., Jaalama, K., Kangassalo, P., Nummi, P., Staffans, A., and Fagerholm, N. (2023). 3D visualisations for communicative urban and landscape planning: what systematic mapping of academic literature can tell us of their potential? *Landsc. Urban Plan.* 234, 104716. doi:10.1016/j.landurbplan.2023.104716

Ferrer, J., Pérez-Martín, M. A., Jiménez, S., Estrela, T., and Andreu, J. (2012). GIS-based models for water quantity and quality assessment in the Júcar River Basin, Spain, including climate change effects. *Sci. Total Environ.* 440, 42–59. doi:10.1016/j.scitotenv.2012.08.032

Ghavami, S. M., Taleai, M., and Arentze, T. (2022). An intelligent web-based spatial group decision support system to investigate the role of the opponents' modeling in urban land use planning. *Land Use Policy* 120, 106256. doi:10.1016/j.landusepol.2022.106256

Huang, M., Li, Y., Xia, C., Zeng, C., and Zhang, B. (2022). Coupling responses of landscape pattern to human activity and their drivers in the hinterland of Three Gorges Reservoir Area. *Glob. Ecol. Conservation* 33, e01992. doi:10.1016/j.gecco.2021.e01992

Huang, X., Liu, J., Peng, S., and Huang, B. (2023). The impact of multi-scenario land use change on the water conservation in central Yunnan urban agglomeration, China. *Ecol. Indic.* 147, 109922. doi:10.1016/j.ecolind.2023.109922

Jin, T., Yan, L., Wang, S., and Gong, J. (2022). Spatiotemporal variation in ecological risk on water yield service via land-use and climate change simulations: a case study of the ziwuling mountainous region, China. *Front. Environ. Sci.* 10, 908057. doi:10.3389/fenvs.2022.908057

Jaiswal, D., and Pandey, J. (2021). Human-driven changes in sediment-water interactions may increase the degradation of ecosystem functioning in the Ganga River. *J. Hydrology* 598, 126261. doi:10.1016/j.jhydrol.2021.126261

Liu, Y., Wang, L., Lu, Y., Zou, Q., Yang, L., He, Y., et al. (2023). Identification and optimization methods for delineating ecological red lines in Sichuan Province of southwest China. *Ecol. Indic.* 146, 109786. doi:10.1016/j.ecolind.2022.109786

Lu, W., Xu, C., Wu, J., and Cheng, S. (2019). Ecological effect assessment based on the DPSIR model of a polluted urban river during restoration: a case study of the Nanfei River, China. *Ecol. Indic.* 96, 146–152. doi:10.1016/j.ecolind.2018.08.054

McBride, M., and Booth, D. B. (2005). Urban impacts on physical stream condition: effects of spatial scale, connectivity, and longitudinal trends. *J. Am. Water Resour. Assoc.* 41, 565–580. doi:10.1111/j.1752-1688.2005.tb03755.x

Meng, C. L. (2021). Water balance scheme development for urban modelling. *Urban Clim.* 37, 100843. doi:10.1016/j.uclim.2021.100843

Namavar, M., Moghaddam, M. R. A., and Shafiei, M. (2023). Developing an indicator-based assessment framework for assessing the sustainability of urban water management. *Sustain. Prod. Consum.* 40, 1–12. doi:10.1016/j.spc.2023.06.006

Ouyang, X., Xu, J., Li, J., Wei, X., and Li, Y. (2022). Land space optimization of urban-agriculture-ecological functions in the Changsha-Zhuzhou-Xiangtan Urban Agglomeration, China. *Land Use Policy* 117, 106112. doi:10.1016/j.landusepol.2022.106112

Ouyang, X., Shao, Q., Zhu, X., He, Q., Xiang, C., and Wei, G. (2019). Environmental regulation, economic growth and air pollution: panel threshold analysis for OECD countries. *Sci. Total Environ.* 657, 234–241. doi:10.1016/j.scitotenv.2018.12.056

Paiva, A. C. D. E., Nascimento, N., Rodriguez, D. A., Tomasella, J., Carriello, F., and Rezende, F. S. (2020). Urban expansion and its impact on water security: the case of the Paraíba do Sul River Basin, São Paulo, Brazil. *Sci. Total Environ.* 720, 137509. doi:10.1016/j.scitotenv.2020.137509

Qu, Y., Dong, X., Su, D., Jiang, G., and Ma, W. (2023). How to balance protection and development? A comprehensive analysis framework for territorial space utilization scale, function and pattern. *J. Environ. Manag.* 339, 117809. doi:10.1016/j.jenvman.2023.117809

Wang, H., Huang, L., Zhang, H., Fu, Y., Guo, W., Jiao, X., et al. (2023). Development of a decision framework for river health and water yield ecosystem service in watershed. *J. Hydrology* 623, 129773. doi:10.1016/j.jhydrol.2023.129773

Wang, K., Ouyang, X., He, Q. Y., and Zhu, X. (2022). Impact of urban land expansion efficiency on ecosystem services: a case study of the three major urban agglomerations along the Yangtze River economic belt. *Land* 11, 1591. doi:10.3390/land11091591

Wei, G., He, B., Sun, P., Liu, Y., Li, R., Ouyang, X., et al. (2023a). Evolutionary trends of urban expansion and its sustainable development: evidence from 80 representative cities in the belt and road initiative region. *Cities* 138, 104353. doi:10.1016/j.cities.2023.104353

Wei, G., Bi, M., Liu, X., Zhang, Z., and He, B. (2023b). Investigating the impact of multi-dimensional urbanization and FDI on carbon emissions in the belt and road initiative region: direct and spillover effects. *J. Clean. Prod.*, 384. doi:10.1016/j.jclepro.2022.13560

Xiong, J., Wang, X., Zhao, D., and Zhao, Y. (2022). Spatiotemporal pattern and driving forces of ecological carrying capacity during urbanization process in the Dongting Lake area, China. *Ecol. Indic.* 144, 109486. doi:10.1016/j.ecolind.2022.109486

Xu, K., Wu, S. H., Chen, D. X., Dai, L., and Zhou, S. L. (2013). The urban growth boundary determination based on hydrology effect: taking xinminzhou as an example. *Sci. Geogr. Sin.* 33 (08), 979–985. doi:10.13249/j.cnki.sgs.2013.08.979

Yao, Y., Ma, L., Che, X., and Dou, H. (2021). Simulation study of urban expansion under ecological constraint—taking Yuzhong County, China as an example. *Urban For. Urban Green.* 57, 126933. doi:10.1016/j.ufug.2020.126933

Yu, H., Liu, X., Kong, B., Li, R., and Wang, G. (2019). Landscape ecology development supported by geospatial technologies: a review. *Ecol. Inf.* 51, 185–192. doi:10.1016/j.ecoinf.2019.03.006

Zeng, Z., Yang, H., Zhou, H., Lai, N., Song, Q., Ji, Q., et al. (2023). Monitoring and control of water-ecological space in the Dongting Lake region. *Front. Environ. Sci.* 11, 1200513. doi:10.3389/fenvs.2023.1200513

Zhang, X., Wang, J., Yue, C., Ma, S., Hou, L., and Wang, L. (2023). Impact of wetland change on ecosystem services in different urbanization stages: a case study in the Hang-Jia-Hu region, China. *Ecol. Indic.* 153, 110382. doi:10.1016/j.ecolind.2023.110382

Zhang, Y., Chang, X., Liu, Y., Lu, Y., Wang, Y., and Liu, Y. (2021). Urban expansion simulation under constraint of multiple ecosystem services (MESs) based on cellular automata (CA)-Markov model: scenario analysis and policy implications. *Land Use Policy* 108, 105667. doi:10.1016/j.landusepol.2021.105667

frontiers | Frontiers in Ecology and Evolution

TYPE Original Research
PUBLISHED 01 November 2023
DOI 10.3389/fevo.2023.1271352

OPEN ACCESS

EDITED BY
Xiao Ouyang,
Hunan University of Finance and Economics, China

REVIEWED BY
Kunlun Qi,
China University of Geosciences Wuhan, China
Liang Zhou,
Lanzhou Jiaotong University, China
Yue Liu,
Guangzhou Institute of Geography, China

*CORRESPONDENCE
Yongpeng Song
10130085@vip.henu.edu.cn
Pengyan Zhang
pengyanzh@126.com

RECEIVED 02 August 2023
ACCEPTED 18 October 2023
PUBLISHED 01 November 2023

CITATION
Huang Y, Zhang J, Zhang P, Chen Z, Zhang X, Lu R, Li M, Xing G and Song Y (2023) Construction and optimization of ecological security pattern based on landscape ecological risk assessment in the affected area of the Lower Yellow River. *Front. Ecol. Evol.* 11:1271352. doi: 10.3389/fevo.2023.1271352

Construction and optimization of ecological security pattern based on landscape ecological risk assessment in the affected area of the Lower Yellow River

Yicheng Huang[1], Jinbing Zhang[1], Pengyan Zhang[1,2,3]*, Zhuo Chen[4], Xinyue Zhang[1], Rong Lu[1], Mengfan Li[1], Guangrui Xing[1] and Yongpeng Song[1]*

[1]College of Geography and Environmental Science, Henan University, Kaifeng, China, [2]School of Urban Economics and Public Administration, Capital University of Economics and Business, Beijing, China, [3]Xinyang Vocational and Technical College, Xinyang, China, [4]School of Medicine, Case Western Reserve University, Cleveland, OH, United States

In the context of urban expansion and climate change, the world is under pressure from multiple ecological risks. Key ecological protection areas play a pivotal role in preserving ecological stability and promoting development. Due to its unique geographical conditions, the Yellow River basin has been facing huge ecological risk pressure. In the affected area of the Lower Yellow River (AALYR) as an agricultural hub, ecological protection has gradually become a key factor restricting the development of cities and agriculture. Taking AALYR as an example, the landscape ecological risk assessment (LERA) system is established based on three aspects "natural environment—human society—landscape pattern". We construct a comprehensive cumulative resistance surface based on the risk assessment results as the basis for the future study. Ecological corridors are identified by minimum cumulative resistance (MCR) models to establish and optimize Ecological security pattern (ESP) in the AALYR. We found that the landscape ecological risks (LER) in the study area show a uniform spatial distribution, with a slightly higher distribution in the northeast than the southwest. The ecological risk levels are generally high in AALYR, indicating a more severe risk problem in this area. A total of 56 ecological sources were identified, with a total area of 21176 km^2. The ecological sensitivity of AALYR was high, and 99 ecological corridors and 59 ecological nodes were extracted. Ecological corridors and nodes were consistently and densely distributed throughout the study area. The network analysis method improves the stability of the network structure after optimization. Based on the key components of the ESP, with the combination of geographical characteristics and local policy planning guidance, we constructed the "One Belt and One Axis, Two Cores

and Two Corridors, Four zones" ESP. The study results may offer guidance and suggestions for the construction of ESP and ecological environment protection system in the world's major river basins, and may also provide information for ecological planning of other similar river basins in the world.

KEYWORDS

landscape ecological risk assessment, ecological security patterns, spatial principal component analysis, minimum cumulative resistance model, the affected area of the Lower Yellow River

1 Introduction

Technological advances and population growth have changed the global environment and led to a range of ecological problems such as global warming (Schiermeier et al., 2019; Rong et al., 2022), deteriorating air quality (Castells-Quintana et al., 2021) and declining biodiversity (Mupepele et al., 2021). Ecological problems in many watershed areas have the potential to worsen ecological security risks (Luo et al., 2018). Ecological risk assessment has also become a hot topic of discussion and research for domestic and international scholars. Landscape ecological risk assessment (LERA) as an important subfield of ecological risk at the regional scale is widely used for risk area identification. LER refers to the possible negative effects of the interaction between landscape pattern and ecological process (Gong et al., 2020). Recently, researchers have carried out a lot of fruitful exploration of LERA by choosing relevant indicators, methods and models for different regions and different assessment purposes (Kayumba et al., 2021). However, there have been few studies on the multi-faceted quantitative assessment of ecological risks in basin landscapes from both "natural-social" dimensions (Zhu et al., 2022). Therefore, the combination of the landscape pattern index and the "natural-social" multi-source elements of the basin into the basin LERA system could offer a basis for building safety patterns (Chen et al., 2022). As an ecological space consisting of key locations, positions, and spatial connections in the landscape (Yang et al., 2022c), the Ecological Security Pattern (ESP) should prioritize resource elements that link human well-being and construct relevant ecological sources, nodes and corridors, etc. to optimize regional ESP in a targeted manner and make practical suggestions. By constructing a reasonable land ESP, the ecological security problems brought about by river basin development planning can be effectively guaranteed (Gao et al., 2021).

Concepts similar to ESP include urban growth boundaries (Dawkins and Nelson, 2002), ecological networks (Chen et al., 2023), green infrastructure (Zhang et al., 2022b), ecological control lines (Chen et al., 2021). In 1960s. Warntz and Woldenberg (1967) point, line and surface model for constructing flow surfaces provides a good picture of the "ecological flow" process in the landscape. McHarg (1969) used a "lasagna" superimposed model to reveal vertical links between vegetation, animals, soils and human activities in the landscape. Odum and Barrett (1971) proposed a regional ecosystem development strategy based on systems theory. In 1990s, Forman (1995) proposed a "patch-corridor-matrix" model of landscape ecology based on theories of landscape and regional ecology, laying the foundation for the study of landscape patterns. Subsequent research has focused mainly on ecological reserve zoning and regional landscape planning from the perspective of biodiversity. For example, Budaeva et al. (2021) planned the nature park reserve using a multi-criteria decision analysis method, which provided a reference for the nature conservation and tourism development of the park through sensitive zoning results. Otuoze et al. (2021) used cellular automata theory to construct a dynamic model to simulate and quantitatively predict urban growth, strengthened scientific urban planning and control of green space patterns. Zhelonkina et al. (2021) promoted regional conservation planning by identifying key spatial components of ecological conservation and evolutionary processes from the perspective of biodiversity conservation. Saleh and Abeer (2021) and Saleem et al. (2022) used correlation to assess land suitability and provided a theoretical basis for regional urban and rural land planning and forestry planning.

Following the proposal of the concept of landscape ESP for biological conservation by Yu (1999), Chinese scholars have conducted in-depth exploration and research on regional LER and the ESP based on theories and methods such as "source and sink" and landscape patterns. Existing research areas in LERA are mainly focused on ecologically fragile areas. Examples include large urban areas (Zhang et al., 2021), river basins (Wei et al., 2022), industrial, mining areas (Xu et al., 2021) and Wetland Nature Reserve (Yang et al., 2022a). Early LERA mainly continued the "source-sink" theory of regional ecological risk assessment (Zhu et al., 2020), calculating the ecological risk of a target unit by predicting the spatial dispersion effect of risk sources in a given landscape pattern (Li et al., 2023b). In the aspect of ESP, the study paradigm of "identifying sources—establishing resistance surfaces—extracting corridors—discerning the ESP" has been developed in the development practice (Zhang et al., 2022a). More research results have been achieved at national (Li et al., 2022b), provincial and municipal scales (Li et al., 2022c), as well as in urban clusters (Ran et al., 2022), basins (Wei et al., 2022a) and counties (Fan et al., 2021). The main research methods are graph theory (Urban and Keitt, 2001), circuit theory (Wang et al., 2022a) and the minimum cumulative resistance (MCR) model (Chen et al., 2020). The MCR model is the most commonly used and the study gradually attempted to establish a "bridge" between LERA and the

construction of the ESP (Li et al., 2023a). Previous studies have identified sources and constructed general ideas for ESP by analyzing morphological spatial patterns and the importance of ecological services (Lin et al., 2021). There are relatively few studies on the construction of ESP from the perspective of LERA (Chen et al., 2022). Therefore, this study uses the "source—sink" theory to assess the LER areas in basin areas, construct ESP and propose locally appropriate protection strategies.

The affected area of the Lower Yellow River (AALYR) is currently relatively ecologically fragile, with low flows in the lower basin and shrinking estuarine wetlands starting to occur in some places. Five of the 14 concentrated contiguous destitute areas across the country involve the Yellow River basin (Wohlfart et al., 2016). The AALYR as the basin continues to develop socially and economically, the basin will be further exposed to ecological pressures and risks caused by economic growth and land use expansion (Zhang et al., 2020; Tang et al., 2023). Due to the interference and destruction of human activities in recent years, the spatial differentiation characteristics of landscape pattern in the AALYR are significant (Lou et al., 2022). Serious problems such as severe alkalinization, desertification, drought, waterlogging and poor drainage have occurred in the basin, resulting in serious damage to the ecological risk and the ESP of the basin. Ecological security issues pose a serious challenge to maintaining the LER issues in the AALYR. As one of the key areas for the ecological civilization construction in the Yellow River basin, the construction and optimization of ESP is of strong practical significance for the management of the AALYR. Therefore, the aim of this study is to assess the ecological risk of the AALYR using a LERA method. Overall, the study takes the AALYR as an example. Firstly, The SPCA is used to analyze the spatial distribution of LER in the AALYR. Then, the method of ecological sensitivity assessment is combined to extract high-value areas, which are considered as ecological sources. Finally, the ecological corridors are extracted using the MCR model to build an ESP (Figure 1). Research results can provide important information and reference for the development, utilization and conservation planning of the Yellow River basin.

2 Materials and methods

2.1 Study area

Lower Yellow River is 785.6 km in length. According to existing studies on the division of the AALYR (Cen et al., 2019), and taking into account the Yellow River basin irrigation area, the integrity of regional urban development, and administrative divisions, 20 prefecture-level cities in Henan and Shandong provinces with a total area of 148,100 km^2 are considered as the affected areas of the lower Yellow River (Figure 2). It is a flat plain area that contains seven major landscape types: cultivated land, forest, shrub, wetland, water, bare land and construction land. The cultivated land accounts for 68.67% of the total area; followed by built-up land,

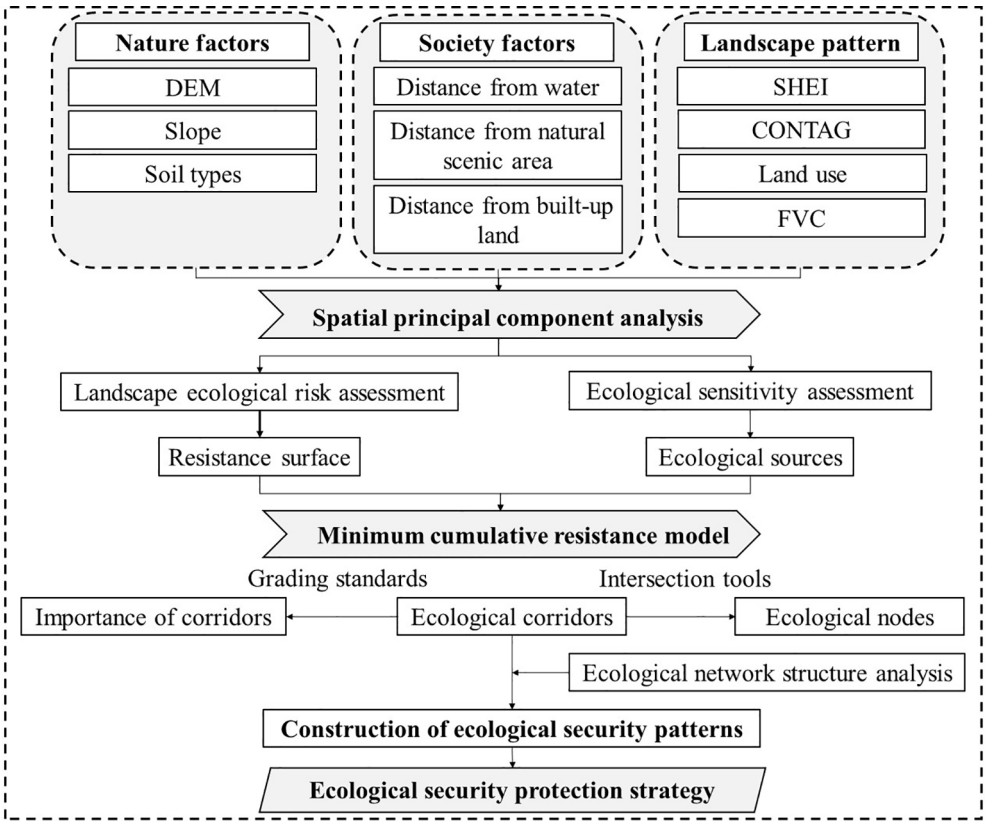

FIGURE 1
Research framework. (DEM, Digital Elevation Model; SHEI, Shannon's evenness index; CONTAG, Contagion; FVC, Fraction Vegetation Coverage).

which accounts for 18.94% of total area; Forestland and grassland account for only 7.12% of the total area. Considering the development of the lower Yellow River area in recent years and the availability of data, this study selected 2018 data to analyze. Since Laiwu, Shandong Province was approved by the State Council to be abolished as a district in 2019, it is still considered to be a prefecture-level city in our study. The terrain of the affected area of the AALYR is dominated by plains, mountains and hills. At the end of 2018, the total GDP of the study area reached 6.63 trillion RMB, accounting for>40 percent of the total GDP of the basin. In 2019, ecological protection and high-quality development of the Yellow River basin were upgraded as a major national strategy, providing unprecedented opportunities for regional development. Therefore, it is urgent to study the status of ecological risk in the lower reaches of the Yellow River area and to analyze the influencing factors in order to provide relevant policy suggestions for the study of regional ecological protection research in small and medium-sized basins and similar areas.

2.2 Data sources

The study data include land use, digital elevation model (DEM), soil types and other geographic data in 2018.

(1) Land use from the Resource and Environmental Science Data Center (http://www.resdc.cn). Land use is divided into cultivated land, forestland, grassland, built-up land, water, and unused land. The spatial resolution is 30 m.

(2) DEM from Geospatial Data Cloud (http://www.gscloud.cn). The spatial resolution is 30m.

(3) Vegetation cover from United States Land Processes Distributed Data Archive center's (https://e4ftl01.cr.usgs.gov/MOLT/MOD13Q1.006/) MOD13A3 dataset product. Data products have a time resolution of 16 days and a spatial resolution of 250 m.

(4) Soil types data from the Chinese soil dataset (http://www.fao.org/home/en/) of the World Soil Database. The spatial resolution is 1 km.

(5) Other basic geographic data from the Global Geographic Information Resources Directory Service System (https://www.webmap.cn). The scale of natural scenic spots, built-up land and water are 1: 250000. The spatial resolution is 30 m.

2.3 Methods

This study mainly aiming at the current situation of ecological environment in the study area, and selects indicators from the natural environment, human society, and landscape pattern as the evaluation elements of the LER of the study area, and constructs a three-dimensional comprehensive LREA system, which is based on the "nature-human society-landscape pattern". Construct a three-dimensional comprehensive LERA system of "nature—human society—landscape pattern". The results of LREA were used as evaluation factors for landscape pattern resistance, and the ecological source was identified by combining with ecological sensitivity assessment, and ESP optimization was carried out by using the MCR model and network structure analysis method.

2.3.1 Selection of ecological risk assessment indexes

According to the natural environment and economic development of the AALYR, and considering the scientific soundness and data availability, we selected 10 influencing factors from three perspectives: nature, human disturbance, and landscape

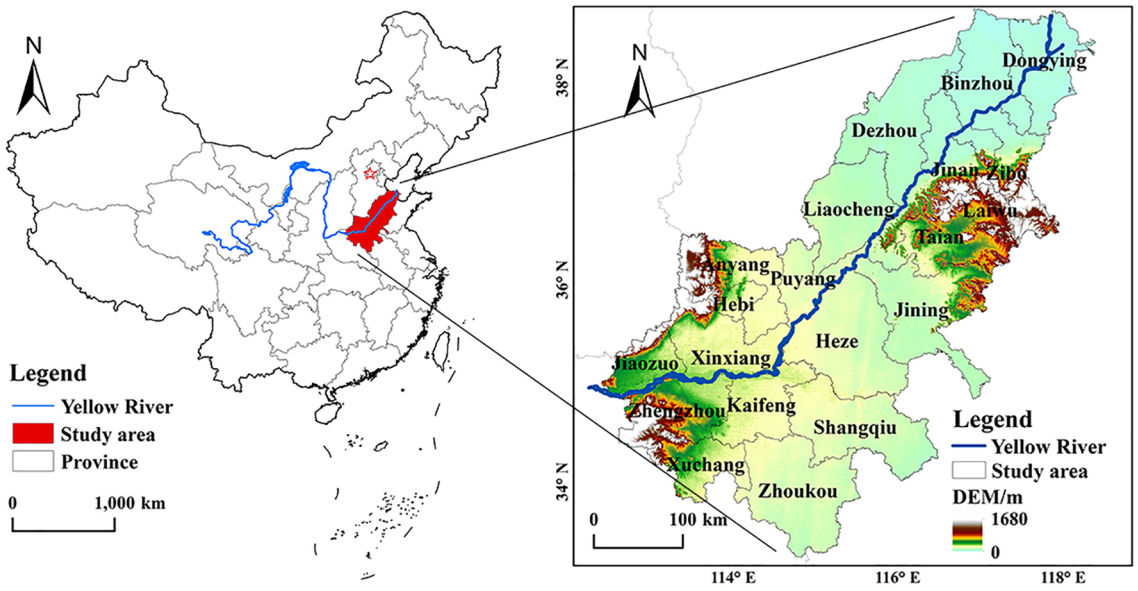

FIGURE 2
Location of the study area.

pattern, to assess the LER of the study area. These include: DEM, Slope, Soil types, Distance from water, Distance from built-up land, Distance from natural scenic, Shannon's evenness index (SHEI), Contagion (CONTAG), Land use, Fraction vegetation coverage (FVC). Indicators of natural factors: the DEM, the higher the risk of landscape ecology; the higher the slope, the higher the risk of the existence of landscape ecology; soil type can reflect the growing condition of crops, which has a good improvement effect. Due to human interference and highway construction, the original ecological conditions have been altered and the original landscape pattern has been disturbed. The closer the distance from the built-up land, the higher the LER; The greater distance from the water and distance from the natural scenic higher ecological risk to the landscape; Landscape factor indicators: The higher the Shannon evenness index, the higher the ecological stability of the area; The lower contagion index corresponds to the vulnerability of the disturbance to external activities in the landscape pattern; Vegetation cover indicates the degree of greening of an area, with larger values indicating a better ecological environment. Land use is classified according to the first-level reclassification. The selection of assessment indicators is based on relevant literature (Chi et al., 2022) and the environmental conditions of the AALYR. The ecological security classification standards for each factor in the study area are formulated using the natural breakpoint method, which divides the factors into 5 levels (Table 1). Figure 3 classifies the indicators by using the reclassification tool.

2.3.2 Spatial principal component analysis

Spatial principal component analysis (SPCA) is widely used in ecological risk assessment (Wei et al., 2020). The key risk factors are identified by extracting the principal components of the original assessment factors to remove the correlation and redundancy of the influencing factors, so that the calculation results of the principal component factors are uniformly presented on each corresponding raster in space, with good spatial visualization effect (Wang et al., 2021). The principal component factors are weighted and superimposed using the raster calculation tool in ArcGIS 10.6 software. Equation is as follows:

$$E = \sum_{i=1}^{m}\sum_{j=1}^{n} a_{ij}F_j \tag{1}$$

Where E is the comprehensive assessment results of LER. a_{ij} is the j principal component corresponding to the i raster. F_j indicates the eigenvalue contribution rate of the j principal component.

2.3.3 Construction and optimization of ESP

The MCR model is often used to simulate the minimum cost path of the cost of species crossing different landscape substrates from the source (Yi et al., 2022). Early on, the concept of MCR model was proposed by Dutch scholars (Knaapen et al., 1992), and then it was improved by Chinese scholar Yu (1999) and has been widely studied in the field of regional ESP. Its advantages include convenient data processing, comprehensive process analysis and visual results. In addition, the MCR model not only analyzes the superposition of vertical factors, but also uses the geographic information system to analyze the horizontal flow trend of land landscape units, making it one of the important models for connectivity and suitability analysis of large-scale space. Equation is as follows:

$$MCR = f_{\min}\sum_{i=1}^{m}\sum_{j=1}^{n} D_{ij}W_j \tag{2}$$

TABLE 1 Landscape ecological risk indicators and assessment grading criteria for the AALYR.

Index type	Assessment index	Unit	Grading standard				
			Level 1	Level 2	Level 3	Level 4	Level 5
Natural	DEM	m	0-97	97-244	244-442	442-752	752-1680
	Slop	degree	0-3	3-8	8-15	15-25	>25
	Soil types	–	lime concretion black soil, brown soil, Alluvial soils	Cinnamon soil, Yellow-cinnamon, Skeletol soils, Red clay soils	Cultivated loessial soils, Aeolian soils, Solonetzs	Fluvo-aquic, soils, Bog soils, Solonchaks, Paddy soils	Meadow soils, Litho soils
Society	Distance from water	m	0-1000	1000-2000	2000-3000	3000-4000	>4000
	Distance from natural scenic area	m	0-1000	1000-3000	3000-5000	5000-7000	>10000
	Distance from built-up land	m	>13500	10000-13500	7000-10000	3500-7000	0-3500
Landscape pattern	SHEI	–	0.8-1	0.6-0.8	0.4-0.6	0.2-0.4	0-0.2
	CONTAG	%	>67	54-67	41-54	18-41	0-18
	Land use	–	forestland, water	grassland	cultivated land	unused land	built-up land
	FVC	–	>0.85	0.69-0.85	0.49-0.69	0.20-0.49	0-0.20

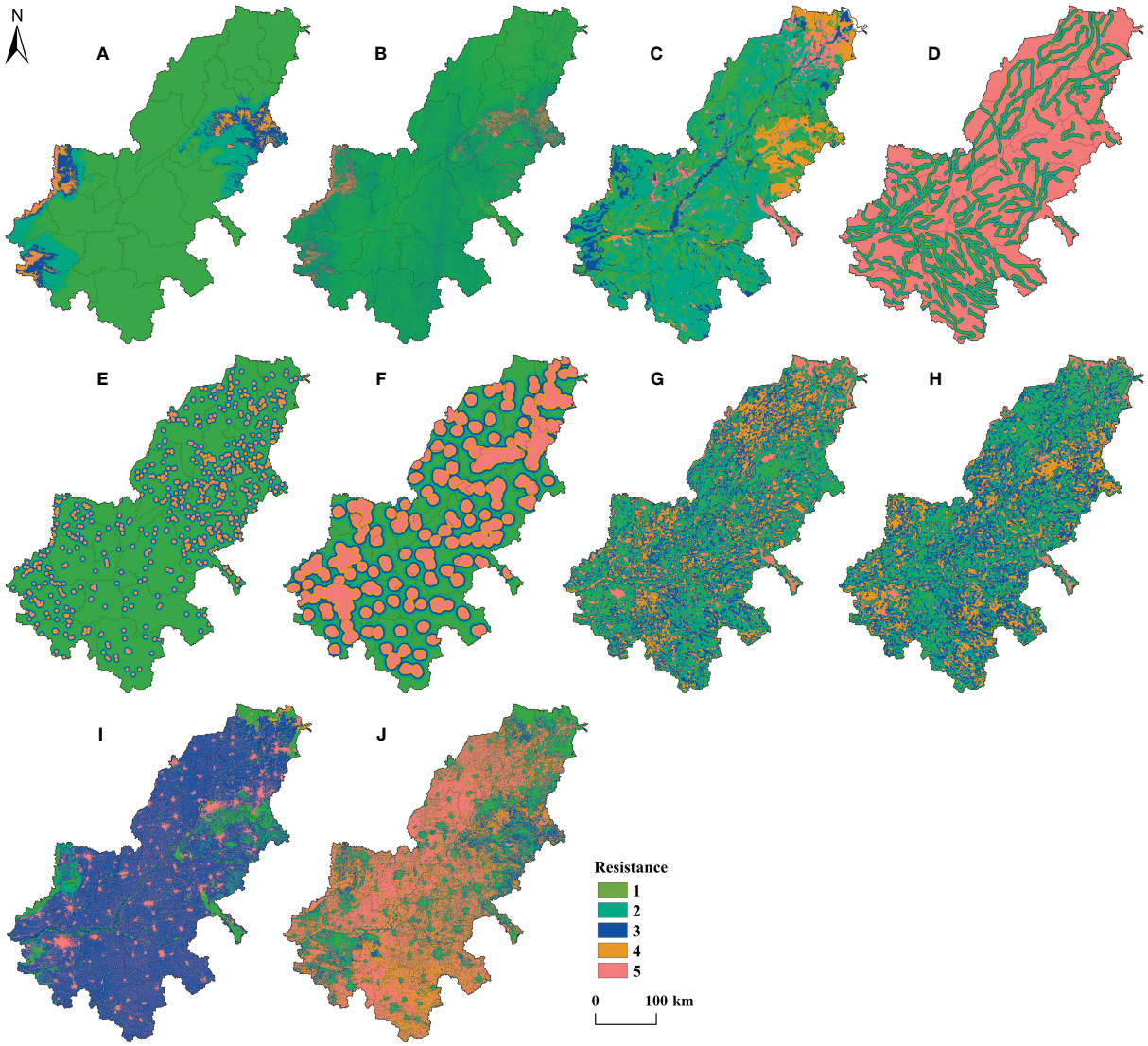

FIGURE 3
Spatial visualization of ecological risk levels of assessment index in the AALYR. **(A)** DEM, **(B)** Slope, **(C)** Soil types, **(D)** Distance from water, **(E)** Distance from natural scenic area, **(F)** Distance from built-up land, **(G)** SHEI, **(H)** CONTAG, **(I)** Land use, **(J)** FVC).

Where *MCR* is the cumulative value of the minimum resistance between the ecological source *j* and any grid *i*. D_{ij} is the path distance of species form source *j* to another possible destination *i* of a source or region. W_i is the resistance value of the *i* grid on the landscape resistance surface to the ecological flow.

(1) Identification of ecological sources. Source areas, as habitat patches, are crucial for improving the optimization of landscape patterns. They serve as source points for species migration and maintenance, with good stability and expansion potential (Ding et al., 2022). In this study, we employ the ecological sensitivity assessment method to identify ecological sources. Ecological sensitivity refers to the ability of ecological factors to adapt to external pressure or human disturbance when the environmental quality does not decrease (Wang et al., 2017b). Specifically, this method first constructs the index system and assigns a weight to each index, then superposes and analyzes each ecological factor, and finally obtains the ecological sensitivity distribution of a region in space. Considering the ecological characteristics of the lower Yellow River and the applicability of the data, a total of 5 ecological factors were selected (DEM, slope, FVC, water, and land use). Combined with analytic hierarchy process (CR=0.0356<0.1, pass the test) to determine the weight of each factor (0.10, 0.15, 0.29, 0.22, and 0.24). The areas with higher ecological sensitivity are relatively rich in ecological resources, and most of the current situation is dominated by woodlands and hills with higher slopes, which have high ecosystem service values (Du et al., 2020; Cui et al., 2022). Finally, taking into account the description of ecological sensitivity classification in the National Ecological Function Zoning issued by the Ministry of Environmental Protection of China in 2015 (No.61 of 2015) and related studies

(Jin et al., 2021). on this basis, we extracted a large area of patches in highly sensitive areas as ecological sources.

(2) Determination of resistance surfaces. The resistance surface is calculated using the results of the basin LERA and the screened sources as the basis for the generation of the resistance surface of the landscape pattern, and the size of the integrated resistance surface is classified into 1-5 grades using the natural breaks method. Table 2 shows the graded criteria.

(3) Extraction of ecological corridors. The shortest consumption paths for the exchange of materials and energy between different ecological source areas are referred to as corridors (Li et al., 2022d). The length of the corridor is divided into 3 levels, the first level corridor is greater than 50 km, the second level corridor is between 30 km and 50 km, and the third corridor is less than 30 km.

(4) Identification of ecological nodes. Nodes are areas on the ecological corridor where ecological functions are weakest and need to be identified and protected as a priority (Yu et al., 2021). The extraction of ecological nodes was performed by utilizing the intersection tool of hydrological analysis.

(5) Assessment of ecological network structure. The assessment indicators mainly include: closure index (α), connectivity rate (β) and linkage index (γ). These indicators show the relationship between the number of corridors and nodes, and also the complexity of the network structure, with larger values indicating a more complex network structure and a better ecological environment. Closure index is used to indicate the extent to which network loops occur (Equation 3), the range of change is between 0-1, and the larger the number, the more species transport paths and the better the circulation of the network. Connectivity indicates the degree of connectivity of the intersection points in the ecological network (Equation 4), the range of change is between 0-1, connectivity rate represents the average connectivity probability between the nodes of the ecological network (Equation 5), β<1 shows that the network structure is dendritic, β=1 explain that the network is the structure of a one-route circuit, and β>1 indicates a complicated network shape. Equation is as follows:

$$\alpha = \frac{L - V + 1}{2V - 5} \tag{3}$$

TABLE 2 Grading standard for cumulative resistance of landscape pattern in the AALYR.

Resistance grade	Cumulative resistance value
1	0-44023
2	44023-76759
3	76759-116267
4	116267-163677
5	163677-287846

$$\gamma = \frac{L}{3(V - 2)} \tag{4}$$

$$\beta = \frac{L}{V} \tag{5}$$

Where L is used to mean the number of corridors, V is used to mean the number of nodes.

3 Result

3.1 LERA

3.1.1 Assessment of ecological resistance of landscape pattern

In this study, 10 influencing factors were selected, including DEM, Slope, Soil types, Distance from water, Distance from natural scenic, Distance from built-up land, SHEI, CONTAG, Land use, and FVC. Table 3 shows the characteristic roots and cumulative contribution rates. We extracted factors with characteristic roots and cumulative contribution rate above 85% to improve the reasonableness of the ecological resistance pattern of the AALYR. Table 4 shows the values of the loadings of the assessment factors that correspond to every principal component. From a natural factors point of view, the results indicate that DEM, slope, and soil types have lower loadings on the third principal component compared to the other index factors. Specifically, the loading value of soil types is 0.590, indicating a higher loading on the sixth principal component. This suggests that natural indicators have a weaker effect on LER, and that soil types have a more significant impact on the integrated risk. Among the indicators of human interference, the Distance from water factor had the highest factor load in the second principal component with a value of 0.937, indicating the strongest influence on the comprehensive LER. The Distance from natural scenic area index had a higher factor load of 0.739 in the first principal component, indicating a significant impact on the comprehensive risk. As for the aspects Landscape pattern, the SHEI has the highest loading of 0.596 in the third principal component factor; the FVC has a higher loading of 0.559 in the fourth principal component factor and the CONTAG has a loading of 0.731 in the tenth principal component factor. This shows that CONTAG, FVC and SHEI contribute significantly to the integrated ecological risk of the landscape.

3.1.2 Spatial analysis of LER

Figure 4A shows the spatial distribution characteristics shown by the results of the LERA in the AALYR region: (1) Highest ecological risk area. The risk index was 3.30-4.95, and the area was 26106.36 km^2. It is centered in the southwest area of the AALYR and some areas with built-up land and settlement distribution in the northeast region. This pattern is mainly caused by the municipality being the administrative center unit and the large interference from human activities, resulting in a serious LER. (2) Higher ecological risk area. The risk index was 2.85-3.30 and the area was 44466.70 km^2. Such regions are mainly located at the edge of high-risk areas and are affected by parts of industrial land and urban built-up land. (3) Middle ecological risk area.

TABLE 3 Principal component related indicators.

Principal component	Characteristic value	Contribution rate/%	Cumulative contribution rate/%
1	0.06342	22.5784	22.5784
2	0.05265	18.7439	41.3223
3	0.03726	13.2639	54.5862
4	0.03307	11.7740	66.3602
5	0.02816	10.0270	76.3872
6	0.02219	7.8994	84.2866
7	0.01835	6.5314	90.8180
8	0.01436	5.1129	95.9310
9	0.00636	2.2629	98.1939
10	0.00507	1.8061	100%

The risk index is 2.39-2.85 and the area is 43751.21 km^2. This risk area is uniformly distributed throughout the study area and occupies the largest area. (4) Lower ecological risk area. The risk index was 1.07-2.39, and the area was 20926.18 km^2. These risk areas are mostly located at the edge of the medium ecological risk area. (5) Lowest ecological risk area. The risk index is 0-1.07, and the area is 12849.55 km^2, which is the smallest proportion of the study area. This area is mainly located in regions with high vegetation cover and along river corridors, where ecosystem services have a high value and human interference is relatively low. These conditions are conducive to the gathering of natural species and the maintenance of ecological balance in this type of habitat.

3.2 Construction of the ESP

3.2.1 Identify ecological sources

Figure 4B shows the integrated ecological sensitivity assessment obtained by AALYR after weighting and superimposing single-factor ecological sensitivity indicators. The Natural Break was used for grading treatment, and five grades were obtained: non-sensitive, light sensitive, medium sensitivity, highly sensitive and extremely sensitive. From Figure 4B, highly sensitive areas are distributed in Dezhou, Liaocheng, Puyang, and Zhengzhou, mainly because the area is close to the Yellow River. The landscape substrate is mainly forestland and grassland, the landscape types are rich, and the ecological environment is high and sensitive. Areas with low ecological risk sensitivity are located in populated areas, urban built-up land and settlements are densely distributed, and the ecological sensitivity is relatively low due to the destruction of human activities. In order to ensure the relevance and integrity of source areas within the AALYR, as well as the appropriate patch size, a careful screening process was carried out to identify ecological sources. After comparing different patch area sizes, patches with high sensitivity areas larger than 200 km^2 were selected as ecological sources. A total of 56 sources were identified, covering an area of 21176 km^2, which represents 14.30% of the total study area. Figure 5A shows that most of the sources are concentrated in the northeastern and southwestern parts of the

TABLE 4 Principal component loading matrix.

Evaluation factor	1	2	3	4	5	6	7	8	9	10	Weight
DEM	0.025	0.161	-0.218	-0.101	0.303	-0.125	-0.189	0.346	-0.800	0.115	0.018
Slope	-0.004	0.096	-0.231	0.008	0.330	-0.167	-0.242	0.650	0.563	-0.050	0.100
Soil types	0.022	0.124	0.061	-0.653	0.053	0.590	0.376	0.246	0.034	-0.018	0.079
Distance from water	0.032	0.937	0.244	0.219	-0.102	0.027	0.013	-0.024	0.038	-0.005	0.187
Distance from natural scenic area	0.739	-0.160	0.370	0.282	0.296	0.318	-0.137	0.058	-0.023	0.016	0.226
Distance from built-up land	0.324	0.095	-0.059	-0.204	0.410	-0.547	0.556	-0.240	0.079	0.011	0.065
SHEI	-0.256	-0.072	0.596	-0.213	0.148	-0.185	-0.154	0.031	0.073	0.665	0.133
CONTAG	0.235	0.076	-0.546	0.131	-0.166	0.189	0.083	-0.083	0.112	0.731	0.023
Land use	0.189	-0.132	0.200	0.141	-0.572	-0.271	0.397	0.559	-0.111	0.054	0.051
FVC	-0.437	-0.091	0.036	0.559	0.391	0.252	0.498	0.124	-0.058	0.067	0.118

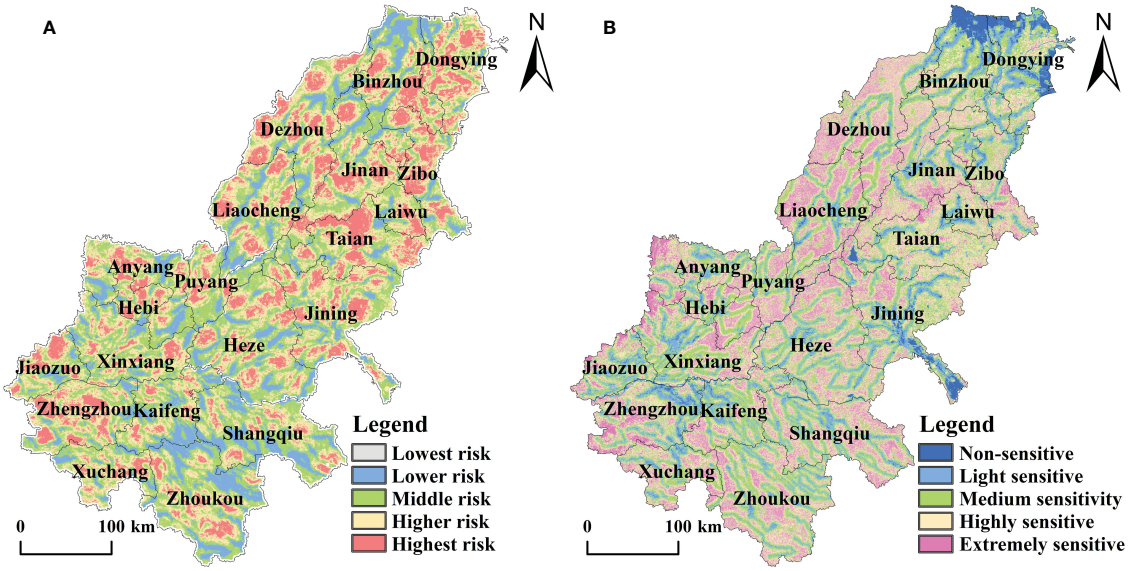

FIGURE 4
(A) Classification of landscape ecological risks in the AALYR; **(B)** Spatial distribution of ecological sensitivity in the AALYR.

AALYR, where the high vegetation cover and rich biodiversity are conducive to the dispersal and conservation of species.

3.2.2 Integrated ecological resistance surface

Based on the ecological source and integrated resistance surface as the reference surface, the MCR surface of the AALYR is calculated by using the cost distance tool. Figure 5B shows the spatial distribution characteristics of the resistance surface: (1) The lowest resistance area is the largest in range, with a total area of 38847.90 km^2, mostly distributed in the northeast and southwest regions and in areas with high vegetation cover. (2) Lower resistance area of 7159.58 km^2, 3.13% of the total study area, mostly distributed in Zhengzhou, Xuchang, Kaifeng, Xinxiang, Zhoukou, Shangqiu, Jinan, Taizhou, Liaocheng, Binzhou, and Dongying. (3) Middle resistance area is 32800.07 km^2, 22.15% of the total study area, mainly located in the peripheral edge region of lower resistance. (4) Higher resistance area is mostly located in the study area in various types of areas such as cultivated land, grassland and unused land, 14.31%, and the area was 21186.08 km^2. (5) Highest resistance area makes up the smallest percentage,

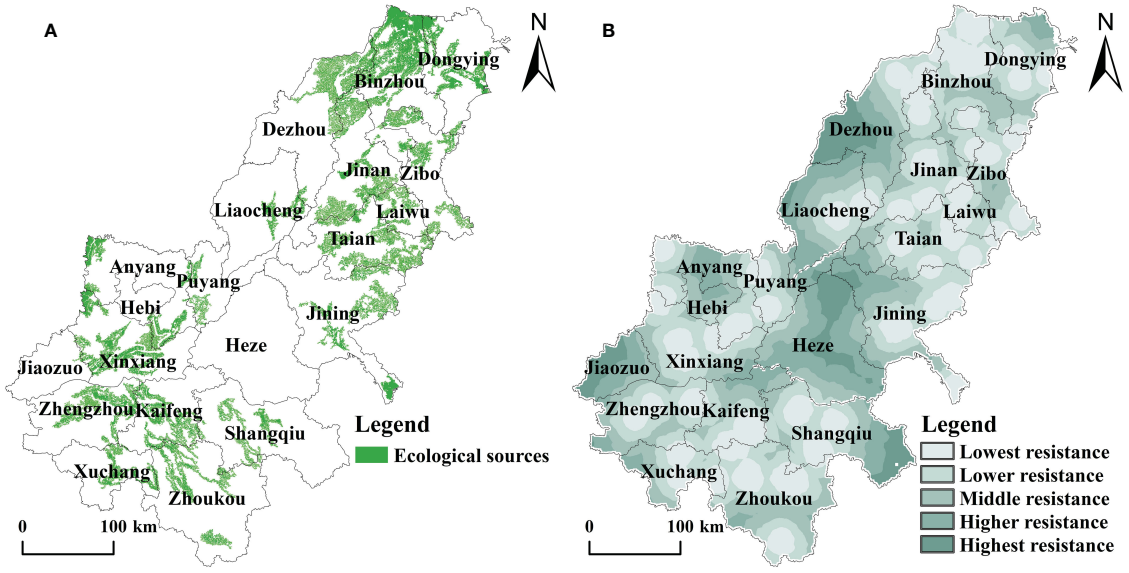

FIGURE 5
(A) Spatial distribution of ecological source area of the AALYR; **(B)** Spatial distribution of resistance in landscape patterns in the AALYR.

accounting for 6.19%. The area is 9,164.50 km^2, mostly concentrated in the central areas of Dezhou and Heze in the AALYR. The main reason is that the region has historically seen several major Yellow River migrations, influenced by factors such as floodway, flow velocity and wind, resulting in a spatial distribution characterized by higher and undulating terrain and poorer connectivity between source sites in high resistance areas and larger patches, creating greater resistance to the flow between species. The lowest resistance values occur in the middle of the Henan and Shandong regions of the basin, so it is necessary to build corresponding ecological corridors to make the resistance surface of the AALYR connected to the ecological source and to obtain the exchange between energy.

3.2.3 Extraction of ecological corridors

Corridor extraction is based on the technical principle of using the geometric centroid of the source site as the source input and clustering the remaining n-1 (where n means the number of ecological source geometric centroids) to create target output clusters. Figure 6A shows that Cost path tool was used to extract the shortest costly paths for clusters of source centroids and target points to obtain ecological corridors between ecological source sites. 99 corridors were built in the study area, with a total length of 3670 km, 51.65% of the total length. The results show: (1) There are 27 first-level ecological corridors whose total length is 1933.004 km, and most of the first-level ecological corridors are concentrated in the area of dense source patches, mainly in Dongying, Binzhou, Jinan, Liaocheng, Jining, Shangqiu, and Zhengzhou, and have a high degree of connectivity. The primary ecological corridor mainly connects the entire the AALYR with its length, thus facilitating movement of species and exchange of energy within the study area. This forms an important hub for maintaining ecological balance in the relevant areas. (2) There are 32 second-level ecological corridors, which are short and scattered, but they are distributed in the AALYR, effectively linking the scattered ecological sources in the study area with smaller regions, improving biodiversity and increasing the value of ecological services. The total length is 1268.14 km, 33.88%. Second-level ecological corridors are mainly distributed with the cities of Laiwu, Taian, Xinxiang, and Zhoukou. (3) There are 41 three-level ecological corridors, with a total length of 541.65 km, only 14.47% of the length of all corridors. Due to the lack of a relatively perfect ecological corridor network system, the ecological connection is weak and cannot adapt to the circulation between "ecological flows".

3.2.4 Identify ecosystem nodes

Figure 6A shows the ecological nodes. The identification of nodes is obtained by extracting the valley lines of the cumulative resistance surface and intersecting the corridors. We identified 59 ecological nodes, including 30 primary and 29 secondaries nodes. The primary ecological nodes intersect the first-level corridors mainly with the least costly paths and play a strategic position in the construction of ESP. The secondary ecological nodes intersect with the second-level and three-level corridors with the maximum cumulative resistance path, forming a radiation driving effect on the surrounding fragile ecological pattern. Ecological nodes are key points of weak ecological functions and should be given key ecological protection and construction.

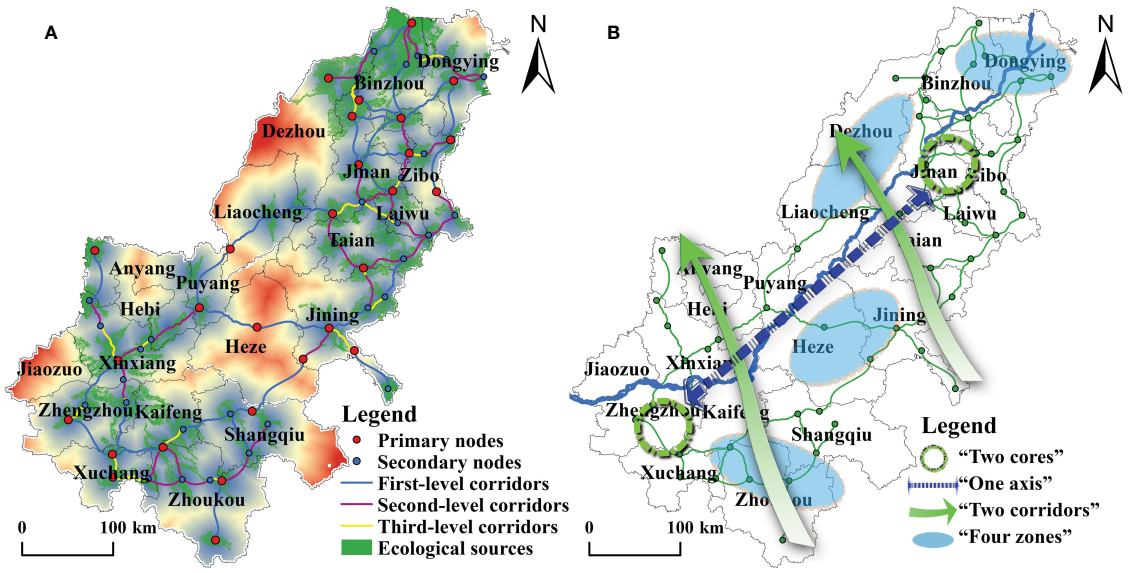

FIGURE 6
(A) Length of ecological corridors and number of ecological nodes in the AALYR; **(B)** The optimized framework to better balance ecological conservation and economic development in the AALYR.

3.2.5 Optimization of ecological network structure

Table 5 shows the calculation results of ecological network indexes before and after optimization. Optimized connectivity was significantly improved, which promoted the stability of ESP in the study area. γ before and after optimization are 0.5789, 0.5819, indicating that the ecological network nodes before optimization are sparse and poorly connected to each other, and the connection of the ecological network nodes after optimization is improved. α before and after optimization are 0.3628, 0.3675. It reflected that there were fewer ways of species migration and diffusion in the AALYR before optimization, and the circulation was poor, which increased the material, energy and information exchange capacity between landscape patches after optimization, and promoted the interoperability between ecological patches. β before and after optimization are 1.6780, 1.5885, indicating that the ecological network is no longer a tree or a single loop network, but a more complex network structure. The stability of the network structure is enhanced by proposing optimized paths for adding some ecological sources, corridors and nodes in the study area.

3.2.6 Optimization framework of the ESP

Identifying and preventing LER is an important prerequisite for improving regional ecological security. From this perspective, this paper proposes to construct a trans-administrative boundary basin ESP, which is of great significance for solving large-scale regional ecological security problems. Combine various landscape elements to optimize ESP. The distribution of corridors, the construction of sources and the selection of nodes are important parts of the construction of ESP. The analysis showed that the AALYR is most affected by human interference, as well as the relatively complex and heterogeneous land use types within the ecological source region. Corridors selection aspect, unlike other research methods, this paper only connects the edges of the source's region, ignoring the connectivity within the source region. In addition, the role of primary nodes is to focus more on the protection and adjustment of current environmental conditions and to provide optimal conditions for species movement, while secondary nodes are mainly used to improve the balance between human destruction and ecological protection and to enhance the basic requirements for species movement between source regions. Based on this, the ESP strategy for the AALYR was established by combining the spatial distribution of ecology, agriculture and cities in Shandong and Henan provinces, as well as the ecological networks constructed. Specifically, with the Yellow River basin as the guiding main line, Zhengzhou and Jinan as the main cores have established an optimization framework based on "One Belt and One Axis, Two Cores and Two corridors, Four zones" (Figure 6B).

4 Discussion

4.1 Comparison and connection with similar studies

Based on the results of ecological security assessment, the present situation of ESP and ecological risks in the AALYR were further clarified. We conclude that the LER in the study area continues to intensify, and the northeast is higher than the southwest, and the LER in the basin area is increased by the influence of man-made destruction, which is consistent with the research results of other similar basins (Ai et al., 2022). At present, China's ecological protection policy is based on the ecological protection red line (Gao et al., 2020), evaluating important ecological sources according to the importance of ecosystem services and ecological sensitivity, and dividing areas far from the scope of human activities according to their importance (Wang et al., 2017a). Source areas are identified by analyzing methods of ecological sensitivity assessment and taking into account the impact of environmental and human activities when selecting sources. This paper mainly draws on the research ideas of other similar basins (Li et al., 2020), compared with the method of directly selecting a nature reserve or a fixed patch of forestland as an ecological source, this study overcomes the limitations of single-factor assessments, enabling a more comprehensive evaluation of ecosystem benefits and providing valuable insights. This is similar to the ESP of the Minjiang River Basin (Wang et al., 2022b). A total of 56 ecological source areas were extracted, and 99 ecological corridors and 59 ecological nodes were identified. The distribution characteristics of the corridors were mostly concentrated in areas with low resistance accumulation and dense source patches, which provided convenience for the exchange of matter and energy, which was consistent with the research results of other similar basins (Li et al., 2022a). Moreover, there is growing evidence that fertile agricultural and forestland areas are often taken up by construction activities, resulting in urban sprawl and ecological land loss (Yang et al., 2022b; Zhou et al., 2023). At present, the methods and standards for constructing resistance surfaces are not unified (Su et al., 2016), and some scholars construct resistance value

TABLE 5 Landscape optimization assessment.

	The number of corridors (*L*)	The number of nodes (*V*)	Linkage index (γ)	Closure index (α)	Connectivity rate (β)
Before optimization	99	59	0.5789	0.3628	1.6780
After optimization	103	61	0.5819	0.3675	1.6885

coefficient by biodiversity conservation (Fu et al., 2019). Therefore, the construction of the resistance surface should fully consider regional differences to improve the reliability of simulation results. In addition, biologists (Salviano et al., 2021) have shown that an ecological corridor of 60-100 m was the best width for species migration and had a better ecological conservation effect. Narrow corridors do not meet the basic needs of migrating species, while wide corridors increase the need for additional land and elevate conflict with landowners (Dong et al., 2020). Therefore, we set the width as 100 m for the extracted first-level ecological corridors and 60 m for the other ecological corridors. In summary, our constructed ESP is scientifically sound and can provide more accurate information for maintaining ecological security when compared to existing research and ecological policies.

4.2 Reasonableness of the LERA

With further urban development and use, landscape fragmentation is not only limited to change the shape of the landscape, but further affect the internal environment, eventually leading to changes in landscape structure and function. Research has shown that changes in landscape patterns and internal relationships are dynamic processes that cannot simply be analyzed in terms of landscape fragmentation and connectivity. Rather, it is important to consider these patterns in relation to specific temporal and spatial changes (Yang et al., 2023; Zou et al., 2022). Therefore, in the management and planning of urban space in the AALYR, corresponding measures are required according to the different development stages of urbanization, not only to coordinate the contradiction of land use, but also to optimize the internal structure, especially to improvement of cultivated land quality. For the more developed Jinan and Zhengzhou, the need for socio-economic development needs to be seriously considered. At the same time, it is important to protect areas where natural habitats are concentrated, especially habitat margins and corridors, in order to achieve a positive balance between natural and economic interests (Liu et al., 2022). This approach can promote regional planning and support the healthy development of the city.

4.3 Limitations and future research directions

This research not only ensures the integrity of the ecosystem, but also provides direct insights for policy makers and planners. However, a number of important issues related to the ESP need to be further explored. Firstly, in establishing the resistance surface factors, although an attempt was made to adequately reflect the natural and socio-economic elements, the socio-economic factors were still generalized due to the lack of regionally corrected ecosystem service values, and the values quoted only reflect the relative differences between the factors rather than reflecting the absolute values (Geng et al., 2022). The selection of ecological sources only relied on what can be ecological sources, and there is no in-depth research on the issue of the scale of ecological sources and how large an area can meet the function of ecological land. Meanwhile, the construction of ecological corridors will inevitably change the land use structure, and the resulting changes in the environment are also a research direction that should be concerned in the future. Our study only analyzed the current ESP based on land use data, and researchers can predict future pattern trends in the context of the corresponding development status.

This study takes the AALYR as the research object. On the one hand, it is because the study area is rich in natural conditions and biodiversity resources; on the other hand, the rapid urbanization and frequent anthropogenic damage have led to environmental degradation, which seriously threatens the regional ecological security. The results of this study expand the understanding of the ecological characteristics of the area and provide suggestions for urban planning and environmental protection in the AALYR and other areas facing similar challenges.

5 Conclusions

Planning urban ecological space is effective in weakening threats to ecological security from urban sprawl at the landscape scale. In this study, we analyzed the ESP of the basin with the by the aid of LERA and MCR model. Figure 6B shows our proposed optimal ecological optimization framework of “One Belt and One Axis, Two Cores and Two Corridors, Four zones”. We followed the sequence of “determining the sources, building the resistance surface, selecting corridors and nodes, constructing and optimizing the ESP”, which is a more scientific approach. This allowed us to propose specific countermeasures for optimizing the ecological service pattern. It is recommended that a part of the plantation forestland be added, the protective zone on both sides of the river be expanded and an ecological reserve be built to enhance the ecological protection of the AALYR. In order to optimize the ecological environment in the AALYR, local government departments should focus on the construction of ESP and reasonably plan and allocate control measures such as ecological land and built-up land. In addition, in the context of promoting ecological conservation and ecological restoration in the Yellow River basin, it is necessary consider the effectiveness of differentiated policy development at different scales.

Data availability statement

The original contributions presented in the study are included in the article/supplementary material. Further inquiries can be directed to the corresponding authors.

Author contributions

YH: Conceptualization, Methodology, Writing – original draft. JZ: Writing – review & editing, Data curation, Investigation. PZ: Funding acquisition, Methodology, Project administration, Writing – review & editing. ZC: Writing – review & editing. XZ: Data curation, Writing – review & editing. RL: Data curation, Writing – review & editing. ML: Data curation, Writing – review & editing. GX: Data curation, Writing – review & editing. YS: Funding acquisition, Project administration, Writing – review & editing.

Funding

The author(s) declare financial support was received for the research, authorship, and/or publication of this article. This research was funded by the National Natural Science Foundation of China, grant number 41601175, 41801362, the Program for Innovative Research Talent in University of Henan Province, grant number 20HASTIT017, 2020 Philosophy and Social Science Planning Project of Henan Province, grant number 2020BJJ020, and 2022 Program for youth talent of Zhongyuan, The Belt and Road Special Foundation of the State Key Laboratory of Hydrology-Water Resources and Hydraulic Engineering, grant number 2021490111, Funding for the construction of the key Laboratory for Agricultural non-point Source pollution Control on the Huang-Huai-Hai Plain in 2023, grant number 2023HNNPSCL-HNDX001. We also thank the Geographical Science Data Center of The Greater Bay Area for providing the relevant data in this study.

Conflict of interest

The authors declare that the research was conducted in the absence of any commercial or financial relationships that could be construed as a potential conflict of interest.

Publisher's note

References

Ai, J. W., Yu, K. Y., Zeng, Z., Yang, L. Q., Liu, Y. F., and Liu, J. (2022). Assessing the dynamic landscape ecological risk and its driving forces in an island city based on optimal spatial scales: Haitan Island, China. *Ecol. Indic.* 137, 108771. doi: 10.1016/j.ecolind.2022.108771

Budaeva, D. G., Sharaldaeva, V. D., and Maksanova, L. (2021). "Some peculiarities of functional zoning in specially protected natural territories: case study of the Tunkinsky National Park, Russia," in *IOP Conference Series: Earth and Environmental Science*, Vol. 885. 012051. doi: 10.1088/1755-1315/885/1/012051

Castells-Quintana, D., Dienesch, E., and Krause, M. (2021). Air pollution in an urban world: a global view on density, cities and emissions. *Ecol. Econ.* 189, 107153. doi: 10.1016/j.ecolecon.2021.107153

Chen, C. L., Shi, L., Lu, Y., Yang, S., and Liu, S. F. (2020). The optimization of urban ecological network planning based on the minimum cumulative resistance model and granularity reverse method: a case study of Haikou, China. *IEEE Access.* 8, 43592–43605. doi: 10.1109/ACCESS.2020.2976548

Chen, J., Wang, S. S., and Zou, Y. T. (2022). Construction of an ecological security pattern based on ecosystem sensitivity and the importance of ecological services: a case study of the Guanzhong Plain urban agglomeration, China. *Ecol. Indic.* 136, 108688. doi: 10.1016/j.ecolind.2022.108688

Chi, J. Y., Xu, G. L., Yang, Q. Q., Liu, Y. T., and Sun, J. X. (2022). Evolutionary characteristics of ecosystem services and ecological risks at highly developed economic region: A case study on Yangtze River Delta, China. *Environ. Sci. Pollut. Res.* doi: 10.1007/s11356-022-22313-4

Chen, X. Q., Guan, Q. H., Li, F. L., Liu, D., Han, C. H., and Zhang, W. J. (2021). Study on the ecological control line in the major leakage area of Baotu spring in Shandong province, eastern China. *Ecol. Indic.* 133, 108467. doi: 10.1016/j.ecolind.2021.108467

Chen, X. Q., Kang, B. Y., Li, M. Y., Du, Z. B., Zhang, L., and Li, H. Y. (2023). Identification of priority areas for territorial ecological conservation and restoration based on ecological networks: a case study of Tianjin City, China. *Ecol. Indic.* 146, 109809. doi: 10.1016/j.ecolind.2022.109809

Cui, X. F., Deng, W., Yang, J. X., Huang, W., and de Vries Walter, T. (2022). Construction and optimization of ecological security patterns based on social equity perspective: A case study in Wuhan, China. *Ecol. Indic.* 136, 108714. doi: 10.1016/j.ecolind.2022.108714

Cen, Y. F., Zhang, P. Y., Yan, Y. H., Jing, W. L., Zhang, Y., Li, Y. Y., et al. (2019). Spatial and temporal agglomeration characteristics and coupling relationship of urban built-up land and economic hinterland—a case study of the Lower Yellow River, China. *Sustainability.* 11, 5218. doi: 10.3390/su11195218

Dawkins, C. J., and Nelson, A. C. (2002). Urban Containment Policies and Housing Prices: an international comparison with implications for future research. *Land Use Policy.* 19, 1–12. doi: 10.1016/S0264-8377(01)00038-2

Ding, M. M., Liu, W., Xiao, L., Zhong, F. X., Lu, N., Zhang, J., et al. (2022). Construction and optimization strategy of ecological security pattern in a rapidly urbanizing region: a case study in central-south China. *Ecol. Indic.* 136, 108604. doi: 10.1016/j.ecolind.2022.108604

Dong, J. Q., Peng, J., Liu, Y. X., Qiu, S. J., and Han, Y. N. (2020). Integrating spatial continuous wavelet transform and kernel density estimation to identify ecological corridors in megacities. *Landsc Urban Plan.* 199, 103815. doi: 10.1016/j.landurbplan.2020.103815

Du, T. F., Qi, W., Zhu, X. C., Wang, X., Zhang, Y., and Zhang, L. (2020). Precise identification and control method of natural resources space based on ecological security pat tern in mountainous hilly area. *J. Ecol. Nat. Resour.* 35 (5), 1190–1200. doi: 10.31497/zrzyxb.20200514

Fan, F. F., Wen, X. J., Feng, Z. M., Gao, Y., and Li, W. J. (2021). Optimizing urban ecological space based on the scenario of ecological security patterns: The case of central Wuhan, China. *Appl. Geogr.* 138, 102619. doi: 10.1016/j.apgeog.2021.102619

Forman, R. T. T. (1995). Some general principles of landscape and regional ecology. *Landsc Ecol.* 10, 133–142. doi: 10.1007/BF00133027

Fu, C. H., Xu, Y., Bundy, A., Gruss, A., Coll, M., Heymans, J. J., et al. (2019). Making ecological indicators management ready: Assessing the specificity, sensitivity, and threshold response of ecological indicators. *Ecol. Indic.* 105, 16–28. doi: 10.1016/j.ecolind.2019.05.055

Gao, J. X., Wang, Y., Zou, C. X., Xu, D. L., Lin, N. F., Wang, L. X., et al. (2020). China's ecological conservation redline: A solution for future nature conservation. *Ambio* 49 (9), 1519–1529. doi: 10.1007/s13280-019-01307-6

Gao, J. B., Du, F. J., Zuo, L. Y., and Jiang, Y. (2021). Integrating ecosystem services and rocky desertification into identification of karst ecological security pattern. *Landsc Ecol.* 36, 2113–2133. doi: 10.1007/s10980-020-01100-x

Geng, W. L., Li, Y. Y., Zhang, P. Y., Yang, D., Jing, W. L., and Rong, T. Q. (2022). Analyzing spatio-temporal changes and trade-offs/synergies among ecosystem services in the Yellow River Basin, China. *Ecol. Indic.* 138, 108825. doi: 10.1016/j.ecolind.2022.108825

Gong, J., Cao, E. J., Xie, Y. C., Xu, C. X., Li, H. Y., and Yan, L. L. (2020). Integrating ecosystem services and landscape ecological risk into adaptive management: Insights from a western mountain-basin area, China. *J. Environ. Manage* 281, 111817. doi: 10.1016/j.jenvman.2020.111817

Jin, X., Wei, L., Wang, Y. I., and Lu, Y. (2021). Construction of ecological security pattern based on the importance of ecosystem service functions and ecological sensitivity assessment: a case study in Fengxian County of Jiangsu Province, China. *Environ. Dev. Sustain.* 23 (1), 563–590. doi: 10.1007/s10668-020-00596-2

Kayumba, P. M., Chen, Y. N., Mingje, R., Mindje, M., Li, X. Y., Maniraho, A. P., et al. (2021). Geospatial land surface-based thermal scenarios for wetland ecological risk assessment and its landscape dynamics simulation in Bayanbulak Wetland, Northwestern China. *Landsc Ecol.* 36, 1699–1723. doi: 10.1007/s10980-021-01240-8

Knaapen, J. P., Seheffer, M., and Harms, B. (1992). Eetimating habitat isolation in landscape planning. *Landsc Urban Plan.* 23, 1–16. doi: 10.1016/0169-2046(92)90060-D

Li, S. K., He, W. X., Wang, L., Zhang, Z., Chen, X. Q., Lei, T. C., et al. (2023a). Optimization of landscape pattern in China Luojiang Xiaoxi basin based on landscape ecological risk assessment. *Ecol. Indic.* 146, 109887. doi: 10.1016/j.ecolind.2023.109887

Li, L., Huang, X. J., Wu, D. F., Wang, Z. L., and Yang, H. (2022a). Optimization of ecological security patterns considering both natural and social disturbances in China's largest urban agglomeration. *Ecol. Eng.* 180, 106647. doi: 10.1016/j.ecoleng.2022.106647

Li, Z. T., Li, M., and Xia, B. C. (2020). Spatio-temporal dynamics of ecological security pattern of the Pearl River Delta urban agglomeration based on LUCC simulation. *Ecol. Indic.* 114, 106319. doi: 10.1016/j.ecolind.2020.106319

Li, H. F., Su, F. L., Guo, C. J., Dong, L. L., Song, F., Wei, C., et al. (2023b). Landscape ecological risk assessment and driving mechanism of coastal estuarine tidal flats—a case study of the liaohe estuary wetlands. *Front. Environ. Sci.* 10. doi: 10.3389/fenvs.2022.1070009

Li, C., Wu, Y. M., Gao, B. P., Zheng, K. J., Wu, Y., and Wang, M. J. (2022b). Construction of ecological security pattern of national ecological barriers for ecosystem health maintenance. *Ecol. Indic.* 146, 109801. doi: 10.1016/j.ecolind.2022.109801

Li, H., Zhang, T., Cao, X. S., and Zhang, Q. Q. (2022c). Establishing and optimizing the ecological security pattern in Shaanxi province (China) for ecological restoration of land space. *Forests.* 13, 766. doi: 10.3390/f13050766

Li, Y. M., Zhao, J. Z., Yuan, J., Ji, P. K., Deng, X. L., and Yang, Y. M. (2022d). Constructing the ecological security pattern of Nujiang Prefecture Based on the framework of "Importance–Sensitivity–Connectivity". *Int. J. Env. Res. Pub He.* 19, 10869. doi: 10.3390/ijerph191710869

Lin, Q. X., Eladawy, A., Sha, J. M., Li, X. M., Wang, J. L., Kurbanov, E., et al. (2021). Remotely sensed ecological protection redline and security pattern construction: a comparative analysis of Pingtan (China) and Durban (South Africa). *Remote Sens.* 13, 2865. doi: 10.3390/rs13152865

Liu, H. M., Xing, L., Wang, C. X., and Zhang, H. Y. (2022). Sustainability assessment of coupled human and natural systems from the perspective of the supply and demand of ecosystem services. *Front. Earth Sci.* 10. doi: 10.3389/feart.2022.1025787

Lou, Y. Y., Yang, D., Zhang, P. Y., Zhang, Y., Song, M. L., Huang, Y. C., et al. (2022). Multi-Scenario simulation of land use changes with ecosystem service value in the Yellow River Basin. *Land.* 11, 992. doi: 10.3390/land11070992

Luo, F. H., Liu, Y. X., Peng, J., and Wu, J. S. (2018). Assessing urban landscape ecological risk through an adaptive cycle framework. *Landsc Urban Plan.* 180, 125–134. doi: 10.1016/j.landurbplan.2018.08.014

McHarg, I. L. (1969). *Design with nature* (New York: american museum of Natural History).

Mupepele, A. C., Bruelheide, H., Bruhl, C., Dauber, J., Fenske, M., Freibauer, A., et al. (2021). Biodiversity in European agricultural landscapes: transformative societal changes needed. *Trends Ecol. Evol.* 36, 1067–1070. doi: 10.1016/j.tree.2021.08.014

Odum, E. P., and Barrett, G. W. (1971). *Fundamentals of ecology* (Philadelphia: Saunders).

Otuoze, S. H., Hunt, D. V. L., and Jefferson, I. F. (2021). Monitoring spatial-temporal transition dynamics of transport infrastructure space in urban growth phenomena: a case study of Lagos—Nigeria. *Front. Future Transp.* 2. doi: 10.3389/ffutr.2021.673110

Ran, Y. J., Lei, D. M., Li, J., Gao, L. P., Mo, J. X., and Liu, X. (2022). Identification of crucial areas of territorial ecological restoration based on ecological security pattern: a case study of the central Yunnan urban agglomeration, China. *Ecol. Indic.* 143, 109318. doi: 10.1016/j.ecolind.2022.109318

Rong, T. Q., Zhang, P. Y., Zhu, H. R., Jiang, L., Li, Y. Y., and Liu, Z. Y. (2022). Spatial correlation evolution and prediction scenario of land use carbon emissions in China. *Ecol. Inform.* 71, 101802. doi: 10.1016/j.ecoinf.2022.101802

Saleem, J., Ahmad, S. S., and Shabbir, R. (2022). Evaluating land suitability analysis for urban services planning in coal clusters of punjab using AHP, WOM, and TOPSIS method. *Arab. J. Geosci.* 15, 324. doi: 10.1007/s12517-022-09510-8

Saleh, D., and Abeer, A. E. K. (2021). Problematic soil risk assessment approach for sustainable spatial suitability of urban land use in new cities by using GIS and remote sensing: a case study of new East Port Said city. *Int. J. Sus. Dev. Plann* 16, 615–628. doi: 10.18280/IJSDP.160402

Salviano, I. R., Gardon, F. R., and dos Santos, R. F. (2021). Ecological corridors and landscape planning: a model to select priority areas for connectivity maintenance. *Landscape Ecol.* 36 (11), 3311–3328. doi: 10.1007/s10980-021-01305-8

Schiermeier, Q., Atkinson, K., Mega, E. R., Padma, T. V., Stoye, E., Tollefson, J., et al. (2019). Scientists worldwide join strikes for climate change. *Nature.* 573, 472–473. doi: 10.1038/d41586-019-02791-2

Su, Y. X., Chen, X. Z., Liao, J. S., Zhang, H. O., Wang, C. J., Ye, Y. Y., et al. (2016). Modeling the optimal ecological security pattern for guiding the urban constructed land expansions. *Urban For Urban Green.* 19, 35–46. doi: 10.1016/j.ufug.2016.06.013

Tang, J. J., Zhou, L., Dang, X. W., Hu, F. N., Yuan, B., Yuan, Z. F., et al. (2023). Impacts and predictions of urban expansion on habitat quality in the densely populated areas: A case study of the Yellow River Basin, China. *Ecol. Indic.* 151, 110320. doi: 10.1016/j.ecolind.2023.110320

Urban, D., and Keitt, T. (2001). Landscape connectivity: a graph-theoretic perspective. *J. Ecol.* 82, 1205–1218. doi: 10.2307/2679983

Wang, Y., Zou, C. X., Xu, D. L., Wang, L. X., Jin, Y., and Wu, D. (2017a). Identifying ecologically valuable and sensitive areas: a case study analysis from China. *J. Nat. Conserv* 40, 49–63. doi: 10.1007/s13280-019-01307-6

Wang, Y., Gao, J. X., Zou, C. C., Xu, D. L., Wang, L. X., Jin, Y., et al. (2017b). Identifying ecologically valuable and sensitive areas—A case study analysis from China. *J. Nat. Conserv.* 40, 1617–1381. doi: 10.1016/j.jnc.2017.08.005

Wang, Y. J., Qu, Z., Zhong, Q. C., Zhang, Q. P., Zhang, L., Zhang, R., et al. (2022a). Delimitation of ecological corridors in a highly urbanizing region based on circuit theory and MSPA. *Ecol. Indic.* 142, 109258. doi: 10.1016/j.ecolind.2022.109258

Wang, Z. Y., Shi, P. J., Zhang, X. B., Tong, H. L., Zhang, W. P., and Liu, Y. (2021). Research on landscape pattern construction and ecological restoration of Jiuquan city based on ecological security evaluation. *Sustainability.* 13, 5732. doi: 10.3390/su13105732

Wang, X. K., Xie, X. Q., Wang, Z. F., Lin, H., Liu, Y., Xie, H. L., et al. (2022b). Construction and optimization of an ecological security pattern based on the MCR model: a case study of the Minjiang River Basin in Eastern China. *Int. J. Environ. Health* 19, 8370. doi: 10.3390/ijerph19148370

Warntz, W., and Woldenberg, M. (1967). *Geography and the properties of surface, concepts and applications-spatial order* (Harvard Papers in Theoretical Geography: Harvard university cambridge mass lab for computer graphics).

Wei, Q. Q., Halike, A., Yao, K. X., Chen, L. M., and Balati, M. (2022a). Construction and optimization of ecological security pattern in Ebinur Lake Basin based on MSPA-MCR models. *Ecol. Indic.* 138, 108857. doi: 10.1016/j.ecolind.2022.108857

Wei, W., Shi, S. H., Zhang, X. Y., Zhou, L., Xie, B. B., Zhou, J. J., et al. (2020). Regional-scale assessment of environmental vulnerability in an arid inland basin. *Ecol. Indic.* 109, 105792. doi: 10.1016/j.ecolind.2019.105792

Wei, L., Zhou, L., Sun, D. Q., Yuan, B., and Hu, F. N. (2022b). Evaluating the impact of urban expansion on the habitat quality and constructing ecological security patterns: a case study of Jiziwan in the Yellow River Basin, China. *Ecol. Indic.* 145, 109544. doi: 10.1016/J.ECOLIND.2022.109544

Wohlfart, C., Kuenzer, C., Chen, C., and Liu, G. H. (2016). Social–ecological challenges in the Yellow River basin (China): a review. *Environ. Earth Sci.* 75, 1866–6280. doi: 10.1007/s12665-016-5864-2

Xu, W. X., Wang, J. M., Zhang, M., and Li, S. L. (2021). Construction of landscape ecological network based on landscape ecological risk assessment in a large-scale opencast coal mine area. *J. Clean. Prod.* 286, 125523. doi: 10.1016/j.jclepro.2020.125523

Yang, C., Deng, W., Yuan, Q. Z., and Zhang, S. Y. (2022a). Changes in landscape pattern and an ecological risk assessment of the Changshagongma wetland nature reserve. *Front. Ecol. Evol.* 10. doi: 10.3389/fevo.2022.843714

Yang, D., Lou, Y. Y., Zhang, P. Y., and Jiang, L. (2022b). Spillover effects of built-up land expansion under ecological security constraint at multiple spatial scales. *Front. Ecol. Evol.* 10. doi: 10.3389/fevo.2022.907691

Yang, K., Wang, S. F., Cao, Y. G., Li, S. P., Zhou, W. X., Liu, S. H., et al. (2022c). Ecological restoration of a loess open-cast mining area in China: perspective from an ecological security pattern. *Forests.* 13, 269. doi: 10.3390/f13020269

Yang, D., Zhang, P. Y., Liu, Z. Y., Huang, Y. C., Chen, Z., Chang, Y. H., et al. (2023). How does urbanization process affect ecological landscape pattern? an empirical analysis based on scale effects. *Ecol. Indic.* 154, 110921. doi: 10.1016/j.ecolind.2023.110921

Yi, S. Q., Zhou, Y., and Li, Q. (2022). A new perspective for urban development boundary delineation based on the MCR model and CA-Markov model. *Land.* 11, 401. doi: 10.3390/land11030401

Yu, K. J. (1999). Landscape ecological security patterns in biological conservation. *Acta Eco. Sin.* 1, 10–17. doi: 10.1016/S0169-2046(96)00331-3

Yu, H. C., Huang, J., Ji, C. N., and Li, Z. A. (2021). Construction of a landscape ecological network for a large-scale energy and chemical industrial base: a case study of Ningdong, China. *Land.* 10, 344. doi: 10.3390/land10040344

Zhang, Y. Z., Jiang, Z. Y., Li, Y. Y., Yang, Z. G., Wang, X. H., and Li, X. B. (2021). Construction and optimization of an urban ecological security pattern based on habitat quality assessment and the minimum cumulative resistance model in Shenzhen city, China. *Forests.* 12, 847. doi: 10.3390/f12070847

Zhang, X. Y., Liu, G., and Zheng, Z. (2022a). Construction of an ecological security pattern based on functional wetland theory: A case study in a landscape city. *Front. Environ. Sci.* 10. doi: 10.3389/fenvs.2022.955230

Zhang, P. Y., Yang, D., Qin, M. Z., and Jing, W. L. (2020). Spatial heterogeneity analysis and driving forces exploring of built-up land development intensity in Chinese prefecture-level cities and implications for future Urban Land intensive use. *Land Use Policy.* 99, 104958. doi: 10.1016/j.landusepol.2020.104958

Zhang, J. B., Zhu, H. R., Zhang, P. Y., Song, Y. P., Zhang, Y., Li, Y. Y., et al. (2022b). Construction of GI network based on MSPA and PLUS model in the main urban area of Zhengzhou: a case study. *Front. Environ. Sci.* 10. doi: 10.3389/fenvs.2022.878656

Zhelonkina, E. E., Pafnutova, I. D., and Emelyanova, T. A. (2021). Conditions for territorial biodiversity conservation affected by technogenesis in the North. *IOP Conf. Environ. Earth Sci.* 867, 12075. doi: 10.1088/1755-1315/867/1/012075

Zhou, T. Y., Liu, H. M., Gou, P., and Xu, N. (2023). Conflict or Coordination? measuring the relationships between urbanization and vegetation cover in China. *Ecol. Indic.* 147, 109993. doi: 10.1016/j.ecolind.2023.109993

Zhu, K. W., Chen, Y. C., Zhang, S., Yang, Z. M., Huang, L., Lei, B., et al. (2020). Identification and prevention of agricultural non-point source pollution risk based on the minimum cumulative resistance model. *Glob. Ecol. Conserv.* 23, e01149. doi: 10.1016/j.gecco.2020.e01149

Zhu, Z. Y., Mei, Z. K., Xu, X. Y., Feng, Y. Z., and Ren, G. X. (2022). Landscape ecological risk assessment based on land use change in the Yellow River Basin of Shaanxi, China. *Int. J. Env. Res. Pub He.* 19, 9547. doi: 10.3390/ijerph19159547

Zou, L. L., Wang, J. Y., and Bai, M. D. (2022). Assessing spatial–temporal heterogeneity of China's landscape fragmentation in 1980–2020. *Ecol. Indic.* 136, 108654. doi: 10.1016/j.ecolind.2022.108654

frontiers | Frontiers in Environmental Science

TYPE Original Research
PUBLISHED 21 November 2023
DOI 10.3389/fenvs.2023.1285020

OPEN ACCESS

EDITED BY
Salvador García-Ayllón Veintimilla,
Polytechnic University of Cartagena,
Spain

REVIEWED BY
Chenxi Li,
Xi'an University of Architecture and Technology, China
Shunbo Yao,
Northwest A and F University, China

*CORRESPONDENCE
Shaoyao Zhang,
zhangsyxs@sicnu.edu.cn

RECEIVED 29 August 2023
ACCEPTED 09 November 2023
PUBLISHED 21 November 2023

CITATION
Meng B, Zhang S, Deng W and Peng L (2023), Research on multilevel evaluations and zones of territorial spatial functions in Yibin, China.
Front. Environ. Sci. 11:1285020.
doi: 10.3389/fenvs.2023.1285020

Research on multilevel evaluations and zones of territorial spatial functions in Yibin, China

Bao Meng[1], Shaoyao Zhang[2]*, Wei Deng[2] and Li Peng[2]

[1]Faculty of Economics and Business Administration, Yibin University, Yibin, China, [2]The Faculty Geography Resource Sciences, Sichuan Normal University, Chengdu, China

Objectively evaluating and defining territorial spatial functions are important prerequisites for optimizing the use of territorial space. However, the results of the evaluation of functions at different levels may differ significantly. How to integrate the evaluation results and guide the spatial utilization at different levels more effectively is worth exploring. This study takes as the research area Yibin City, China, a node city along the Yangtze River in the upper reaches of the Yangtze River. In the study, 185 towns in that city were taken as the primary evaluation units for an indicator system of territorial spatial function constructed on the basis of multivariate data. Research methods such as the entropy method and cluster analysis were adopted to do multilevel evaluations and zoning of territorial spatial functions in Yibin City. The results suggest the following: 1) The distribution of agricultural production, rural living, and ecological regulation functions among the second-level production-living-ecological (PLE) functions of townships were relatively balanced in Yibin City. The production function of industry and mining, urban life function, and ecological product supply function showed spatial directivity. 2) The evaluation results of the first-level PLE functions of townships showed that the areas with substantial PLE functions accounted for approximately 20%, whereas the areas with insignificant functions accounted for approximately 80%, which reflected the "80/20 rule" of spatial functions. 3) In accordance with the cluster analysis of the multilevel evaluation results, the township functions in Yibin were divided into 5 functional areas: urban life-industrial production advantage areas (12%), urban life-rural life advantage areas (8%), rural life-agricultural production-ecological function product supply advantage areas (29%), rural life-agricultural production-ecological service function advantage areas (20%), and ecological service function-agricultural production function advantage areas (31%). 4) In the future, Yibin City should focus on 20% of the significant functional areas and attach importance to the relativity of spatial functions to form a high-quality territorial spatial protection and development pattern. Based on the objectives and requirements of the new territorial spatial planning in China, this study reconstructed the municipal territorial spatial functional areas through a multilevel functional evaluation, which has theoretical and practical significance for forming a new pattern of territorial spatial development and use with joint production, living, and ecological functions.

KEYWORDS

80/20 rule, function evaluation, production-living-ecological function, territorial spatial function, township scale

1 Introduction

Since China's Reform and Opening Up, with the rapid development of industrialization and urbanization, the use pattern of territorial space has been reshaped constantly, and the spatial functions based on spatial patterns have become disordered (Kim and Arnhold, 2018). It is difficult to guarantee a "production-living-ecological" (PLE) functional form and demands, which will greatly restrict regional sustainable development (Cheng et al., 2022; Qiu et al., 2023). Especially in the key river basins (e.g., Yangtze River and Yellow River) of China, the optimization of territorial spatial functions is associated with national ecological security and has been highly valued by the Chinese government in recent years (Xi et al., 2020; Niu et al., 2022). The proposal to promote "well-coordinated environmental conservation and avoid excessive development" in the Yangtze River basin has brought new challenges to the territorial spatial development and functional trade-offs of the basin, especially in the upper reaches of the Yangtze River (Fan et al., 2015; Zhao et al., 2022a). Research on current functional identification and zone optimization might lead to improved policy insights for the best development of watershed territorial space.

According to regional function-structure theory, differences in spatial function are determined by spatial heterogeneity. There are differences in the components or quantity compositions of spatial elements in each region, the effect of natural evolution, and human activities, which result in various spatial patterns (Xie et al., 2021a; Zhao et al., 2022b). The failure of those patterns to adapt to sustainable human development is regarded as spatial dysfunction, which can be balanced by artificial planning constraints (Fu et al., 2021; Zhang, 2022). The evolution of territorial space also follows the general laws of geography: the initial pattern and process determine the pattern and the corresponding functions, while the pattern in turn affects the evolution of the process (Fu, 2002; Brooks and Lee, 2019). After a territorial spatial pattern and its corresponding functions are formed, the pattern will be stable for some time, but the evolution of its driving mechanism and process can be influenced by human planning. That planning will affect the spatial state and quality of the pattern and functions and provide decision-making support for spatial optimization and use (as shown in Figure 1) (Wei et al., 2021; Wang et al., 2022).The spatial scope of various resource allocation and development demands results in no unified model for dividing territorial spatial functions. However, there is a consensus to scientifically define a region's most appropriate regional function in a specific development stage through evaluation. The function should be conducive to the increase of the sustainability of spatial use and the positive effect (Li et al., 2021a). It should also enable top-down spatial control and formulating a spatial intervention policy (Ma et al., 2022). As a direct basis for the division of territorial spatial functions, evaluating spatial suitability and primary zones is vital. In particular, selecting evaluation units and evaluation perspectives and methods is a focus of research and practice.

The main methods for identifying territorial spatial functions are evaluating resources and environmental carrying capacity and determining the suitability of territorial spatial development (referred to as a "double evaluation") (Wang et al., 2019). Those methods have already been used by the Chinese government, and they provide scientific support for planning China's "urban-agricultural-ecological" spaces (Hsu et al., 2021). Different from the urban, agricultural, and ecological functions, the current spatial production-living-ecological (PLE) function originated from the agricultural multifunctional classification system of the European Union. Later, with the rise of research on land multifunctionality, the PLE function concept was introduced in land use classification and spatial policies (Callo-Concha and Denich, 2014; Xue et al., 2022). For example, the Chinese government's PLE space division and development aspirations are expressed as promoting intensive and efficient production spaces, livable and moderate living spaces, and beautiful ecological spaces (Yang et al., 2020).That emphasis at the national strategic level has attracted academic attention, and the comprehensive index of the PLE function has become the basis for spatial function, identification, and comprehensive spatial governance (Xie et al., 2021b; Hou et al., 2022). The current

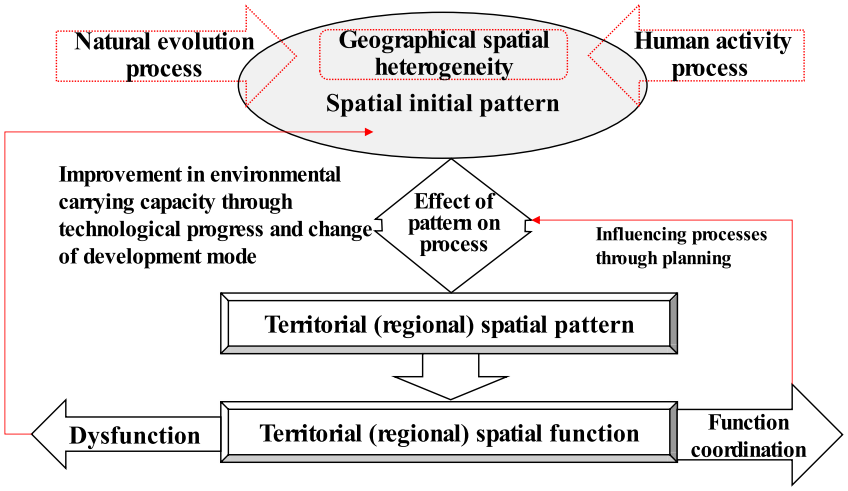

FIGURE 1
Pattern and process of territorial space function.

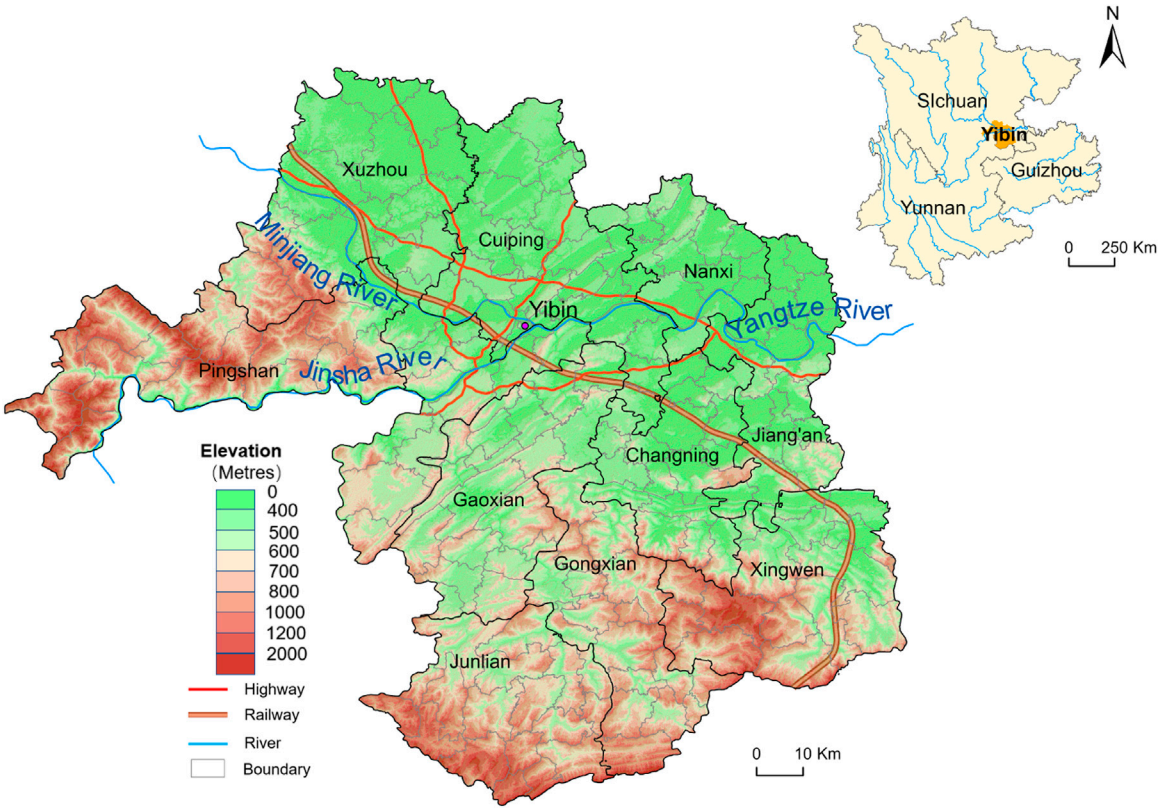

FIGURE 2
Location of Yibin city.

research on evaluating the PLE territorial spatial function is essential to understanding the spatial quantitative structure, function level, and function divisions of territorial space. That includes selecting stable and reasonable spatial evaluation units and establishing an evaluation system and model (Zhang and Xu, 2021; Xiao et al., 2022; Zhang et al., 2022). As for the scale, regional and watershed-level evaluations are based primarily on grid units (30 m × 30 m, 100 m × 100 m, 1,000 m × 1,000 m) or standard evaluation units (nomenclature of territorial units for statistics) (Fu et al., 2022; Liao et al., 2022).Generally, the evaluation results offer little guidance for arranging industrial land use types in a city or for spatial control zoning. Therefore, great importance has been attached to evaluating a county's territorial spatial function (Li et al., 2021b; Fu and Zhang, 2021). To construct a scientific evaluation model as a breakthrough focus, the evaluations involve using powerful computing hardware, mathematical methods, and 3S technology (geographic information system technology, global positioning system technology, remote sensing technology) (Ling et al., 2022). Data from multiple sources, such as remote sensing images, geographical conditions, and internet points of interest (POI) have also been comprehensively adopted (Han et al., 2019; Li et al., 2022a). For example, the development of a land suitability evaluation model, the Intelligent Geographical Information System (LEIGIS) (Kalogirou, 2002), and a suitability evaluation of a particular type of crop planting area for agriculture (Ostovari et al., 2019). Current research often focuses on a function (life, production, or ecology) as an entry point. Few studies of multifunctional fusion zones based on a dominant function have been done, and evaluating single functions is done at the level of data sources. In practice, that fails to obtain sufficient richnesses of the functional connotation and practical guidance because the evaluation unit cannot match the primary administrative unit (the township). The township is the smallest socio-economic management unit in China, which takes into account the socio-economic unity, the integrity of the natural ecosystem and the scientificity of spatial management. How to scientifically conduct multilevel territorial spatial function evaluation and comprehensive zoning at township scale is a scientific issue worth exploring. For the complexity and evolution of spatial functions, a multilevel evaluation of spatial functions that aligns with the control subject is better adapted to the characteristics of the functional area and more conducive to integrating multiple functions under the dominant function. It is also more conducive to a detailed analysis of evaluation results and to obtaining practical guidance for optimizing territorial spatial development.

Yibin City, in the upper reaches of China's Yangtze River Economic Belt, was this study's research area. Considering the administrative subject of spatial control and the scope of the research area, this study adopted 185 townships in Yibin City as the primary evaluation units. In accordance with the spatial and statistical data, the basic concept of PLE space was applied to evaluate the research area's spatial functions. The evaluation was divided into three levels: a second-level PLE function, a first-level PLE function, and a comprehensive PLE function. The second-level

PLE function of a township evaluated the dominant spatial functions of different townships: urban living, rural living, industrial and mining production, agricultural production, ecological regulation, and ecological product supply. Based on the second-level PLE functions of a township, its first-level PLE functions (production, living, and ecological functions) were obtained. Then, based on the evaluation results of spatial functions at various levels and the dominant spatial function, the comprehensive PLE functions area is divided. This study aims to explore the evaluation and comprehensive zoning methods of multi-level spatial functions to define the territorial spatial functions more scientifically, and to understand the territorial spatial functions of townships (the lowest and most direct level of spatial control subjects in the current Chinese system) more objectively in the spatial utilization and management.

2 Study area

Yibin, a city in China's Sichuan Province, is located in the upper reaches of the Yangtze River, where the Jinsha and Minjiang rivers converge to form the Yangtze River (Figure 2). With an area of 13,283 km^2, it covers 3 districts, 7 counties, and 185 townships. By the end of 2018, the registered population of Yibin was 5.523 million, and the permanent population was 4.556 million. The annual GDP of the region was 234.931 billion yuan, and the ratio of the three industrial structures was 12.2:49.7:38.1. Yibin is in the transition zone from the Sichuan Basin to the Yunnan-Guizhou Plateau. That zone is characterized by a transition from low and mild hills to steep hills and low mountains with an altitude of 500–2,000 m and marked differences in territorial spaces. The Jinsha and Minjiang rivers intersect in the central urban area, then become the Yangtze River's mainstream, traversing central and eastern Yibin from west to east. The spatial functional zone is important because of the influence of the geomorphic pattern, which further affects the use complexity.

Yibin has entered an accelerated stage of urbanization and industrialization driven by the development of western China and the strong development of its urban economy, the changes in its transport methods (multi-transportation such as water transport and high-speed railway), and its interregional location (central city of southern Sichuan Province).From the perspective of the watershed ecosystem, Yibin City plays a major part in the ecological barrier in the upper reaches of the Yangtze River. Because of the ecological environment protection in the Yangtze River Basin, the territorial spatial function of Yibin City is mainly ecological, which is of great significance for maintaining the ecological security pattern in the upper reaches of the Yangtze River (Li et al., 2022b). As a modern economic location, Yibin is developing into a growth point that extends westward along the Yangtze River Industrial Belt. It is a subcentral city in Sichuan Province and a central city in the southern region of Sichuan Province, whose urban development functions are also important. From the perspective of development status, territorial spatial development is not only extensive; it is also constrained by national and provincial policies such as the grain for green project, transformation development, environmental protection requirements, and ecological environment restoration in the Yangtze River basin. The rapid expansion of urban and industrial land has encroached on cultivated and ecological lands, which changed the original territorial spatial structure and functions and had a marked effect on the sustainable development of the territorial space (Zhou et al., 2017). Therefore, scientifically evaluating and defining territorial spatial functions and guiding the formation of a new pattern of territorial spatial development and use are conducive to offering guidance to the high-quality development of Yibin's territorial space. They also lay a scientific foundation for constructing and developing the upper reaches of the Yangtze River economic belt.

3 Data and methods

3.1 Data sources

This study's datasets include spatial, statistical, survey, generated, and report data (Table 1).

3.2 Research methods

3.2.1 Construction and description of evaluation indicators

Based on the PLE classification of territorial space, this study's evaluation divided the production function into agricultural production and industrial and mining production. The living function was divided into rural and urban life, and the ecological function was divided into ecological regulation and product provision, forming a criterion layer. Because the evaluation was based on the township as the primary research unit, the form and content of statistical data items at the township level and statistical yearbooks at the district and county levels were not uniform, and there were differences between the main statistical items, so an attempt was made to adopt the indicator data with unified statistics for each township. Referring to the relevant literature (Yang et al., 2020; Xie et al., 2021b; Wang et al., 2023), taking the actual situation of territorial spatial development and the pertinence, stability, scientificalness, and accessibility of indicators into consideration in Yibin City, the final evaluation index system comprised 3 target layers, 6 criterion layers, and 28 indicator items, as shown in Table 2.

3.2.1.1 Indicators of the production function

Soil thickness, nutrient level, soil erosion intensity, and cultivated land slope are the key indicators that characterize the geographical conditions of cultivated land and can be used as natural factor conditions for agricultural production functions. The current cultivated land area was the result of the influence of cultivation conditions and cultivation willingness and reflected the foundation of agricultural production functions. Therefore, it was included in the indicator system.

In the industrial and mining production functions, the regional gross domestic product, value added by secondary industries, and the number of industrial enterprises can effectively represent the current regional industrial development. (The secondary industries' added value was chosen as a factor because the industries contribute

TABLE 1 Research data description.

Data type	Content	Source
Statistical	Gross domestic product in renminbi (RMB 10,000), the added value of the second industry (RMB 10,000), number of industrial enterprises, *per capita* disposable income of rural residents (RMB), permanent population of urban build-up areas, and total retail sales of consumer goods (RMB 10,000)	Statistical Yearbook and Bulletin of Each District and County in Yibin City in 2018 (provided by District and County Statistical Bureau)
Spatial	Cultivated land slope, cultivated land area, distance from the main urban area, altitude, topographic relief, geo-hazards, water area, and drainage density	The Resource and Environment Science and Data Center of the Chinese Academy of Sciences (https://www.resdc.cn/)
Survey	Soil thickness, soil nutrient levels (organic matter, available phosphorus, available potassium), soil erosion intensity, bamboo forest area (km^2), garden area (km^2), tea garden area (km^2), and foundation-bearing capacity (level)	Functional departments: Yibin City Agricultural and Rural Bureau and Yibin Natural Resources and Planning Bureau
Generated	POI types and density of each township	POI classification coding table of the Gaode map API (extracted with Python)
Report	The rural poor population, mineral resource development, and industrial park situation	Report of precision poverty alleviation work in Yibin and the 13th Five-Year Industrial Development Plan of Yibin City

TABLE 2 Function evaluation index system and weight allocation of the current situation of the PLE space in Yibin City.

Criterion layer	Indicator layer/unit	Weight	Criterion layer	Indicator layer/unit	Weight
Urban living function	Permanent population in urban built-up areas	0.093	Rural living function	Per capita disposable income of rural residents	0.156
	Total retail sales of social consumer goods	0.240			
	Urban construction land area	0.283		Rural poor population	0.128
	Geo-hazards	0.025		Altitude	0.237
	Foundation-bearing capacity	0.063		Road network density	0.255
	POI type	0.010		POI type	0.029
	POI density	0.286		POI density	0.195
Industrial and mining production functions	Regional gross domestic product (10,000 yuan)	0.126	Agricultural production function	Cultivated land slope	0.106
	Value added of the secondary industry (10,000 yuan)	0.177		Soil thickness	0.046
	Number of industrial enterprises	0.081		Organic matter	0.134
	Industrial park situation	0.334		Available phosphorus	0.256
	Development of mineral resources	0.254		Available potassium	0.103
	Regional gross domestic product (10,000 yuan)	0.018		Soil erosion intensity	0.108
	Value added of the secondary industry (10,000 yuan)	0.010		Cultivated land area	0.248
Ecological regulation function	NDVI	0.512	Ecological product supply function	Bamboo forest area	0.240
	Water area	0.146		Garden area	0.344
	Drainage density	0.342		Tea Garden Area	0.416

much to the regional gross domestic product in Yibin City.)The parks included industrial parks, agricultural industrial parks, and comprehensive industrial parks (e.g., logistics and specialty commerce), which were assigned values based on their quantity and scale. The assigned values for the planned parks were halved.

The reason for adding the terrain undulation is that Yibin City is a low-mountain and hilly area with few flat land resources, whereas the areas with minor terrain undulations and abundant flat land resources can provide alternative land for industrial and mining layouts.

3.2.1.2 Indicators of living function

The rural residents' *per capita* disposable income and the impoverished population in rural areas were important current

indicators of rural living functions. Although at the time of the study Yibin City had no absolute poverty, it aimed to help people out of poverty. Therefore, the number of poor people at the beginning of targeted poverty alleviation reflected the overall rural human settlements and living conditions to some extent. Altitude and traffic accessibility, which directly affect the environment and conditions of rural entrepreneurship, had an important effect on the return of rural youth laborers and was adopted to be an important indicator for evaluating the rural living function.

As for the urban living functions, the permanent population of the built-up area and the total retail sales of social consumer goods effectively represented the current urban living situation. Geo-hazards and foundation-bearing capacity were included in the index system, which focused on the deep dependence of high-density living facilities on urban environments.

3.2.1.3 Indicators of ecological function

The ecological product supply function was evaluated based on the advantageous tea and bamboo industries in Yibin City (the capital of bamboo in China and the famous hometown of tea in early China). Bamboo forest, garden, and tea garden areas were taken as evaluation criteria.

3.2.2 Comparative advantage index

The first step was to build the original matrix of indicator based on the indicator system. The second step was normalizing the original matrix to obtain a new one. During that process, attention was paid to the distinction between positive and negative indicators. The third step was calculating the entropy and weight of the functional area indicators by the entropy weight method. The specific weights of each indicator are shown in Table 2. To better understand the patterns and statuses of the PLE functions of townships at the municipal level, the normalized revealed comparative advantage index ($NRCA$) was applied to calculate the comparative advantage index of the PLE function of each township:

$$NRCA_{ij} = X_{ij}/X - X_j X_i/XX \tag{1}$$

where X_{ij} refers to the ith functional value of the jth township, X refers to the sum of all functional values of the township, X_j refers to the sum of the jth function of the township, and X_i refers to the sum of all functions of the ith township. When $NRCA$ >0, it indicates that a function (living, production, or ecological) of the township has a comparative advantage in the city; otherwise, the function has no comparative advantage.

3.2.3 Ward system clustering method

The ward system clustering method used the sum of squared deviations to calculate the distance. The sum of square Euclidean distances from each element in a class to the class center of gravity (i.e., the class mean) is called the sum of squared deviations in a class. Assuming that G_K and G_L are clustering as a new class G_M, the sum of squared deviations within the classes of G_K, G_M and G_L are shown in Eqs (2), (3), and (4) respectively:

$$W_K = \sum_{x_i \in G_K} (x_i - \bar{x}_K)'(x_i - \bar{x}_K) \tag{2}$$

$$W_L = \sum_{x_i \in G_L} (x_i - \bar{x}_L)'(x_i - \bar{x}_L) \tag{3}$$

$$W_M = \sum_{x_i \in G_M} (x_i - \bar{x}_M)'(x_i - \bar{x}_M) \tag{4}$$

Assuming that when G_K and G_L are merged into a new class G_M, $W_M > W_K + W_L$, the sum of squared deviations within the class increases. If G_K is close to G_L, the sum of squared deviations should be smaller. Therefore, the squared distance of G_K and G_L was calculated by Eq 5:

$$D^2_{KL} = W_M - (W_K + W_L) \tag{5}$$

It can be seen that the ward-clustering analysis applied the analysis of variance to classification, making the sum of squares of deviation in the same category small, which suggested the high similarity between samples. If the sum of squares of deviations between different classes were large, the similarity between samples would be low. By studying the first-level territorial spatial classification of PLE values as the clustering analysis factors, the comprehensive spatial clustering analysis results of PLE space at the township level in Yibin City were obtained through ward system clustering.

4 Results and analysis

Based on the total scores of different functional properties of each township calculated by the methods mentioned above, they were divided into 4 levels with natural breaks: high-value area, higher-value area, lower-value area, and low-value area. The visualization display and analysis follow.

4.1 Classification and evaluation of second-level functions of PLE space

The evaluation results of urban and rural living functions at the township level in Yibin are shown in Figure 3. Six townships were in high-value areas of urban living functions, 16 townships were in higher-value areas, 124 townships were in lower-value areas, and 39 townships were in low-value areas. The proportions of high, higher, lower, and low-value areas in the study area were 3%, 8%, 71%, and 18% respectively. The proportions of townships with high, higher, lower, and low value living functions in rural areas were 41, 84, 49, and 11 respectively, accounting for 15%, 46%, 30%, and 9% of the study area respectively. From the perspective of the living functions in the city, most areas were mainly rural living functions; the areas with high and higher urban living functions accounted for only 11%.

From the perspective of distribution, the townships with a high value for urban living functions in Yibin were distributed mainly in the central urban areas along the Yangtze River, including the current streets in Cuiping District, Baixi Town in Xuzhou District, Nanxi Street in Nanxi District, and Jiang'an Town in Jiang'an County. In addition, it included Xunchang Town and Changning Town. The towns with higher value were mainly the central towns of the district and county, whereas townships with a low urban living function were distributed mainly in the southern part of middle- and low-mountain counties such as Xingwen County, Changning County, Gong County, and Junlian. The

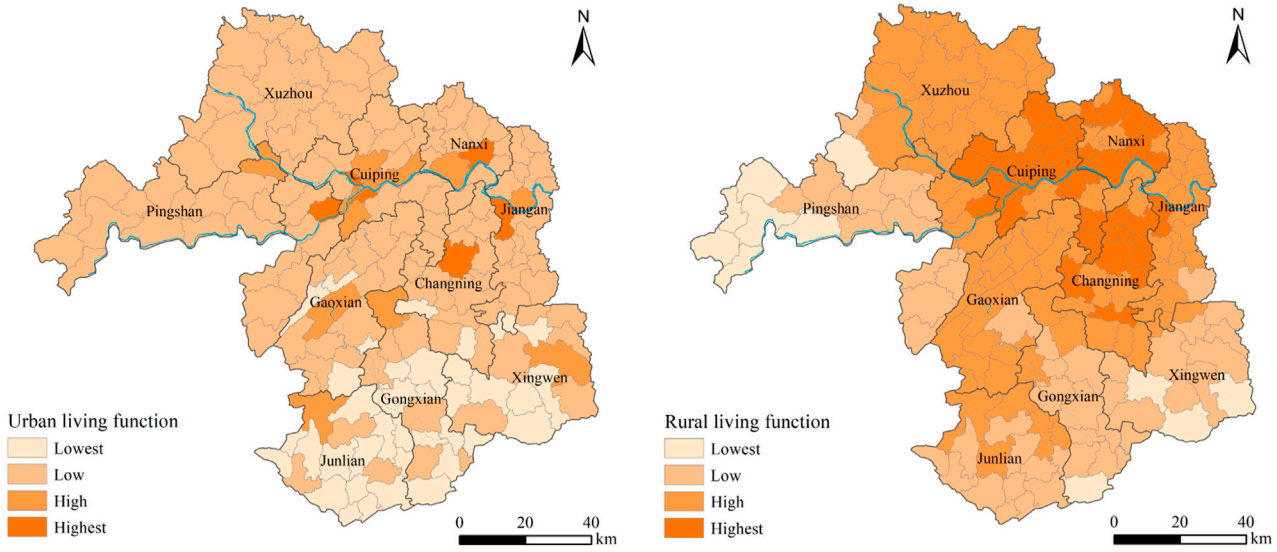

FIGURE 3
Urban living and rural living function zones of townships in Yibin.

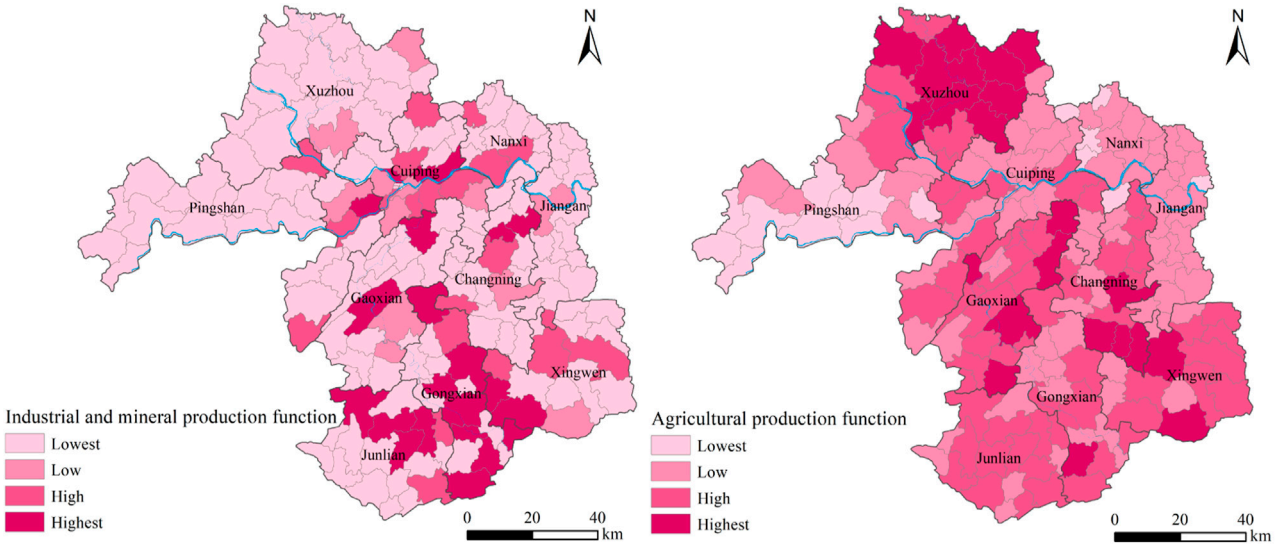

FIGURE 4
Industrial and mineral production function and agricultural production function zones.

areas with high value for rural living functions in Yibin included Cuiping District, Nanxi District, and most northern townships in Changning County. The areas with higher value were mainly the townships in Xuzhou District, Jiangan County, and Gao County, and the areas with low value included the townships in the western part of Pingshan County and three Miao townships in the southern part of Xingwen County. The areas with high value for urban and rural living functions reflected the characteristics of concentrated distribution along the Yangtze River. Because of many flat dams along the river, intensive production factors, and earlier development history driven by the advantages of water transportation, it became the first choice for the layout of living areas. In mountainous and hilly areas with little flat land, the shoreline areas along the river that were unaffected by floods greatly attracted urban and rural residents.

The evaluation results of the production function of each township's industrial and mining industry are shown in Figure 4. The numbers of townships with high-value, higher-value, lower-value, and low-value industrial and mining production functions were 22, 19, 14, and 130 respectively, accounting for 13%, 11%, 9%, and 67% of the study area respectively. The distribution of high-value areas with Yibin industrial and mining production functions

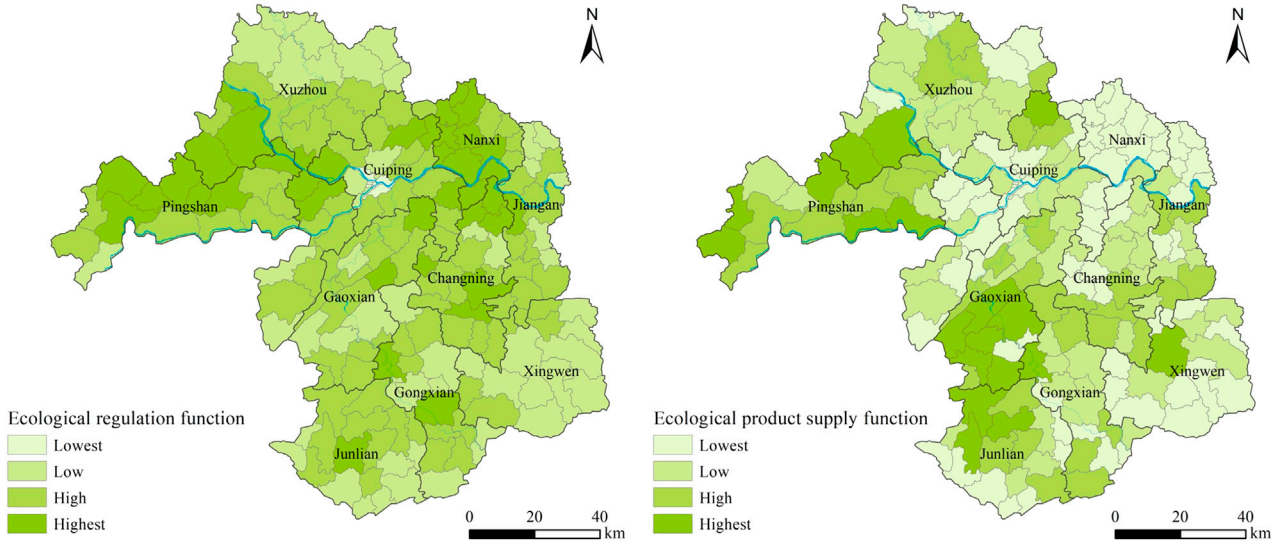

FIGURE 5
Ecological regulation function and evaluation zones of ecological product supply function townships in Yibin.

had two basic characteristics: First, they were distributed in the central towns where the district and county governments were. There were convenient transportation and infrastructures in those towns, which were located near government departments, making it easy to lay out the industrial parks or industrial development concentration areas. Second, they were distributed in some townships with resource advantages. For example, Guhe Town in Changning County, Didong Town and Luodu Miao Township in Gong County, and Mu'ai Town in Junlian played an important part in shale gas development. However, such a phenomenon is not consistent. For example, although Qingping Yi Township in Pingshan County had mineral resources like basalt, it was in the safety zone of Xiangjiaba hydropower station, where mining was prohibited. Therefore, it was a low-value township with industrial and mining production functions.

The number of townships with high, higher, lower, and low agricultural production functions was 21, 64, 81, and 19 respectively, accounting for 19%, 36%, 36%, and 9% of the study area respectively. It can be seen that the towns with a high value of agricultural production function in Yibin were distributed mainly in Xuzhou District. Some townships were located mainly in the northern part of Xuzhou District, e.g., Liujia Town and Guluo Town. The higher-value areas were distributed in Shengtian Town in Gao County, Zhuhai Town in Changning County, and Bowangshan Town in Xingwen County. From a geomorphologic perspective, those areas were composed mainly of low and gentle hills, not along the river or in the middle and low mountains. The agricultural production functions were dominant because they were under little pressure from urban and ecological spaces. Townships unsuitable for agricultural production were distributed mainly in the central and western parts of Pingshan County. The evaluation results of the built-up area in Cuiping District were also suitable; they were affected mainly by the natural basement conditions. From a practical perspective, most of those areas were urban built-up areas, and although there were good functional conditions for developing agriculture, they were forced to give in to the industrial and urban areas.

As shown in Figure 5, the numbers of townships with high, higher, lower, and low ecological regulation functions were 38, 89, 51, and 7 respectively, accounting for 23%, 47%, 29%, and 1% of the study area respectively. High-functional and higher-value areas accounted for 60%, and lower and low-value areas accounted for 40%. The numbers of townships with high-value, higher-value, lower-value, and low-value ecological product supply functions were 19, 36, 53, and 77 respectively, accounting for 16%, 24%, 29%, and 31% respectively. The proportion of functional high and higher-value areas was 40%, and the proportion of lower and low-value areas was 60%, which was opposite to the proportion of ecological regulation functions. That suggested that 60% of the city area in Yibin currently had good ecological regulation functions. Considering the overlap of the two, approximately 40%–50% of that 60% of townships had favorable ecological regulations and ecological product supply; for example, the resources of camphor trees and bamboo forests had dual ecological functions.

From the distribution perspective, the ecological regulation function was evenly distributed in the city. Except for the old central urban area where the three rivers join, the high-value areas of ecological regulation functions were mainly middle- and low-mountain areas such as Pingshan, Gao, and Junlian counties. The low and gentle hills in the northern part of Nanxi District were also high-value areas of the ecological regulation function. The townships with the highest ecological supply capacities were mainly the villages along the Jinsha River in Pingshan County, the northern towns, the southern towns such as Qingfu Town in Gao County, and several townships in Junlian and Xingwen County. The features common to those towns were the wide distribution of bamboo forests and tea gardens, the low level of industrialization and urbanization, and the outstanding ecological background. The distribution of areas with low ecological supply functions was

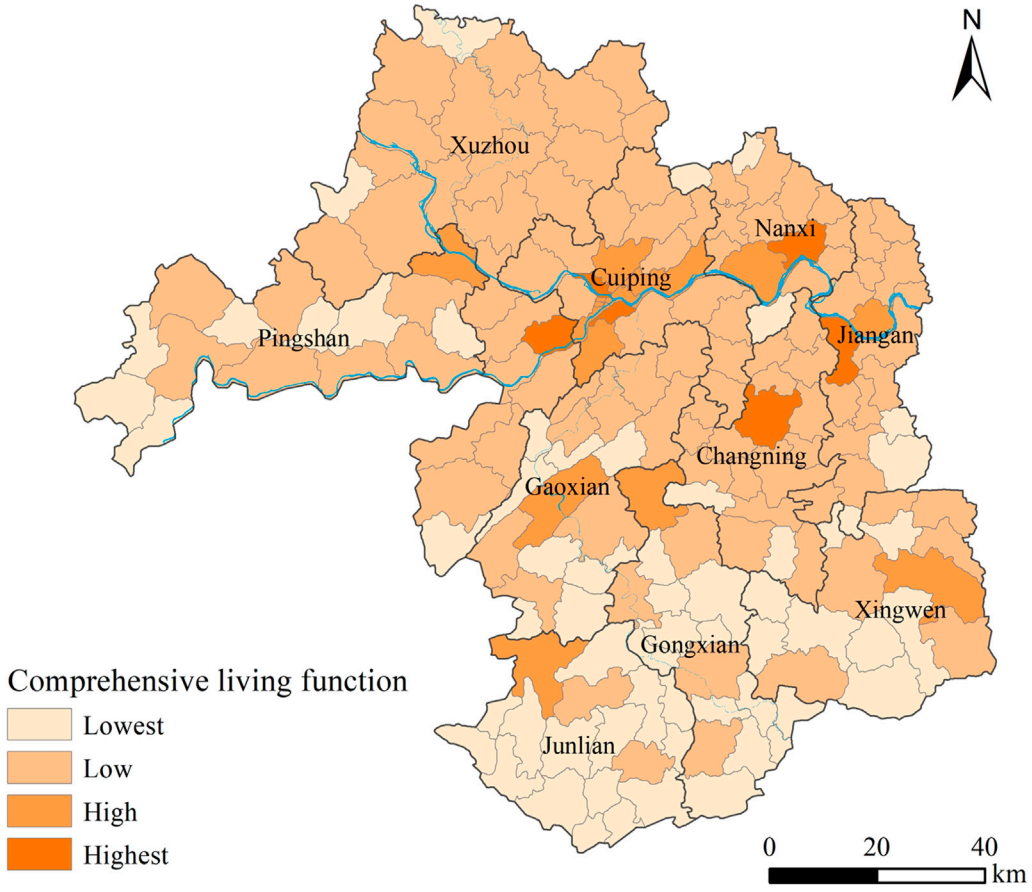

FIGURE 6
First level of living function zones of townships in Yibin.

mainly in the regions along the Yangtze River of Xuzhou District, the Nanxi District, and to the north of Jiang'an County.

4.2 First-level function evaluation of PLE space

The territorial spatial function of a township has a complex nature. Although a township's second-level territorial spatial function has the characteristic of spatial heterogeneity, their functions are diversified and coexisting in some extent. To better express a township's comprehensive functions at the territorial PLE space level, 6 second-level functional indicators of a territorial PLE space were used to evaluate its first-level PLE function.

The numbers of townships with high value, higher value, lower value, and low values of first-level living functions (Figure 6) were 9, 14, 100, and 62 respectively. The proportion of townships with higher and high values was 13%, and the proportion with lower and low values was 87%. The area proportions of high, higher, lower, and low-value areas in the city area were 5%, 11%, 58%, and 26% respectively. The areas of higher and high-value townships accounted for 16%, and the areas of lower and low-value townships accounted for 74%. The high-value areas were almost consistent with the current central urban area and the central town where the district and county governments were. The low-value areas with first-level living functions included mainly the townships in Pingshan County and most towns in the southern part of the city. Some of the townships in mosaic shapes, such as Yachi Township, Majia Township, Furong Town, Dongdi Town, and other low-living function areas, might have been related to the selection of indicators and the calculation of specific indices. From the evaluation perspective, the high-value function areas were not absolute, especially the townships that were administrative units whose boundaries were unstable and easily affected by external factors; for example, the trunk roads (highway or industrial park construction). They neither weakened nor enhanced the functional differences between adjacent administrative districts.

The numbers of townships with high, higher, lower, and low first-level production functions (Figure 7) were 16, 24, 26, and 119 respectively. Townships with higher and high values accounted for 22%, and townships with lower and low values accounted for 78%, which was almost the same as the numbers and proportions of townships with industrial and mining production functions. The area proportions of high, higher, lower, and low-value areas in the city area were 9%, 14%, 16%, and 61% respectively. The areas of higher and high-value townships

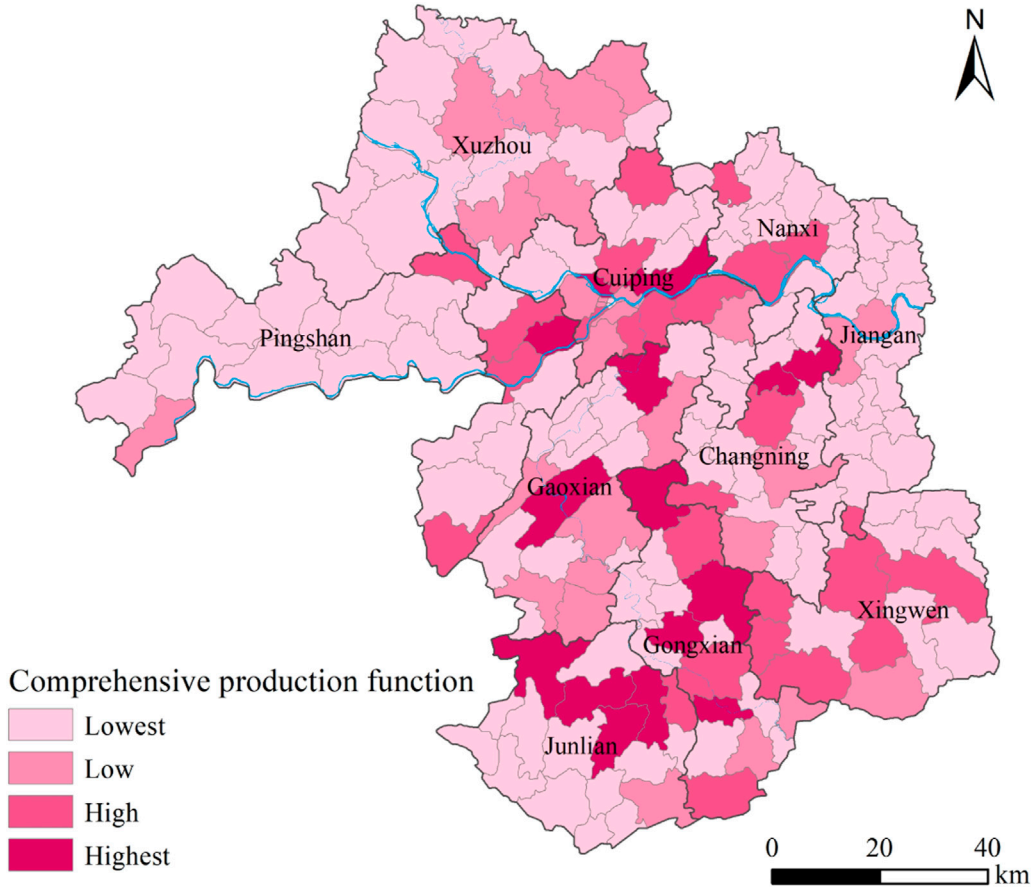

FIGURE 7
First-level production function zones of townships in Yibin.

accounted for 23%, and the areas of lower and low-value townships accounted for 77%. Their distribution was highly similar to the overall pattern of industrial and mining production functions (Figure 4). That was because the general level of the current agricultural development was not high, but in a low-level equilibrium state in Yibin City. However, because industry greatly relied on transportation, location, and natural resource endowment, there were marked regional differences in industrial and mining production functions. Therefore, the spatial difference distribution of first-level production functions was similar to that of industrial and mining production functions.

The numbers of townships with high, higher, lower, and low first-level ecological functions (Figure 8) were 11, 31, 49, and 94 respectively. The proportion of townships with higher and high values was 23%, and the proportion with lower and low values was 77%. The area proportions of the city's high-, higher-, lower-, and low-value areas were 8%, 20%, 27%, and 45% respectively. The areas of higher and high-value townships accounted for 28%, and the areas of lower- and low-value townships accounted for 72%. The first-level ecological function patterns of the townships in Figure 8 were similar to the ecological product supply function of the townships in Figure 5, which suggests that the ecological service function was relatively balanced in the cities like Yibin with a good ecological foundation. In the future, the ecological supply should be given priority in future ecological civilization construction: it should not only meet the essential ecological services and generate pure ecological benefits but also provide ecological products and bring corresponding economic benefits. Because of the comprehensive value of the ecological effect, the ecological function of territorial space becomes an important direction and approach to optimize the use of territorial space.

4.3 Zone and development guidance for a comprehensive PLE function

Based on the evaluation of the PLE function of basic spatial units in townships, the ward system clustering method was adopted to obtain the zone result of a comprehensive PLE function of the territorial space in Yibin City (Figure 9). That space was divided into 5 comprehensive PLE function areas: urban life-industrial production advantage, urban life-rural life advantage, rural life-agricultural production-ecological function product supply advantage, rural life-agricultural production-ecological service function advantage, and ecological service function-agricultural production function advantage.

Twenty-three townships were in the urban life-industrial production advantage area, accounting for 12.04% of the total

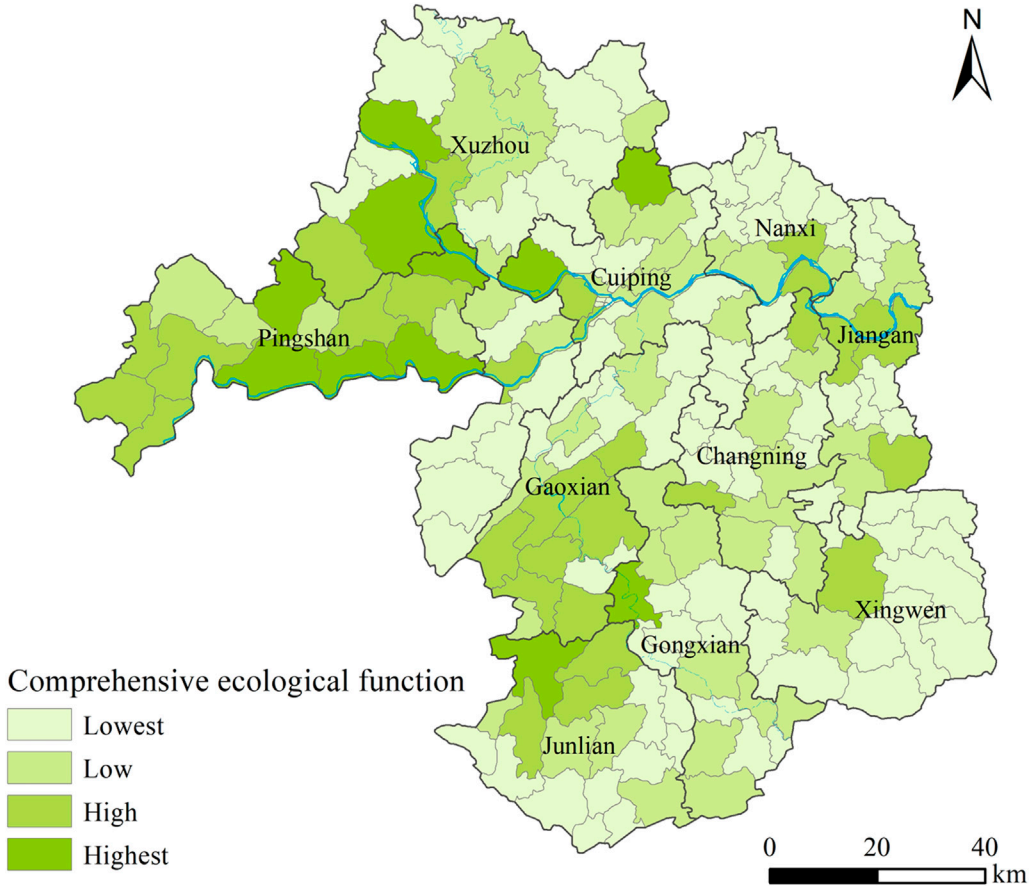

FIGURE 8
First-level ecological function zones of townships in Yibin.

townships and 9.25% of the area. That functional area combined urban life and industrial production functions, focusing on centralized urban construction and developing green industries with low environmental friendliness. The area included mainly streets and townships where the central cities along the river were located. Note that Pu'an, Gaodian, and Xijie towns and Liangjiang Township were classified into this category but not as a direct result of clustering. Instead, they were appropriately revised based on the current planning of urban expansion and industrial concentration areas in Yibin City. The current planning had included them in the central urban expansion area or key industrial parks.

An urban life-rural life advantage area focuses mainly on urban living space and also serves as a rural living space. An urban and rural life advantage zone is an area that focuses mainly on urban and rural living spaces. Its distribution is characterized by being geographically close to the central city (e.g., Nanguang and Lizhuang towns) or being far away from the central city. However, other areas belonged in this category, including a total of 14 townships in the city with prominent central characteristics, long development histories, and vast rural hinterlands (e.g., Junlian and Gusong towns), or towns where important tourist attractions were located (for example, Zhuhai and Shihai towns). They accounted for 8% of the total townships and 8.81% of the area.

A rural life-agricultural production-ecological function product supply advantage area is a township comprising mainly rural life, agriculture, or other business forms around the extension of a modern agricultural industry chain as the leading industry and values the development of ecological agriculture. Although those townships are dominated by rural life and agricultural production, they attach great importance to developing beautiful new villages and the economic benefits of ecological construction driven by a rural revitalization strategy. Such strategies include improving the quality of the ecological product supply of bamboo food, high-quality early tea, and ecotourism. Fifty-three townships were in this area, accounting for 29% of the total townships and 31.14% of the area.

A rural life-agricultural production-ecological service functional advantage area is similar to a rural life-agricultural production-ecological function product supply advantage area, but the former attaches greater importance to ecological service benefits than the latter. That type of area covered 37 townships, accounting for 20% of the total number and 22.55% of the area.

An ecological service function-agricultural production function advantage area puts the achievement of ecological service functions as the top priority and has a scale of agricultural production functions. From a distribution perspective, that area was located in the city's southern, western, and northern parts because they were

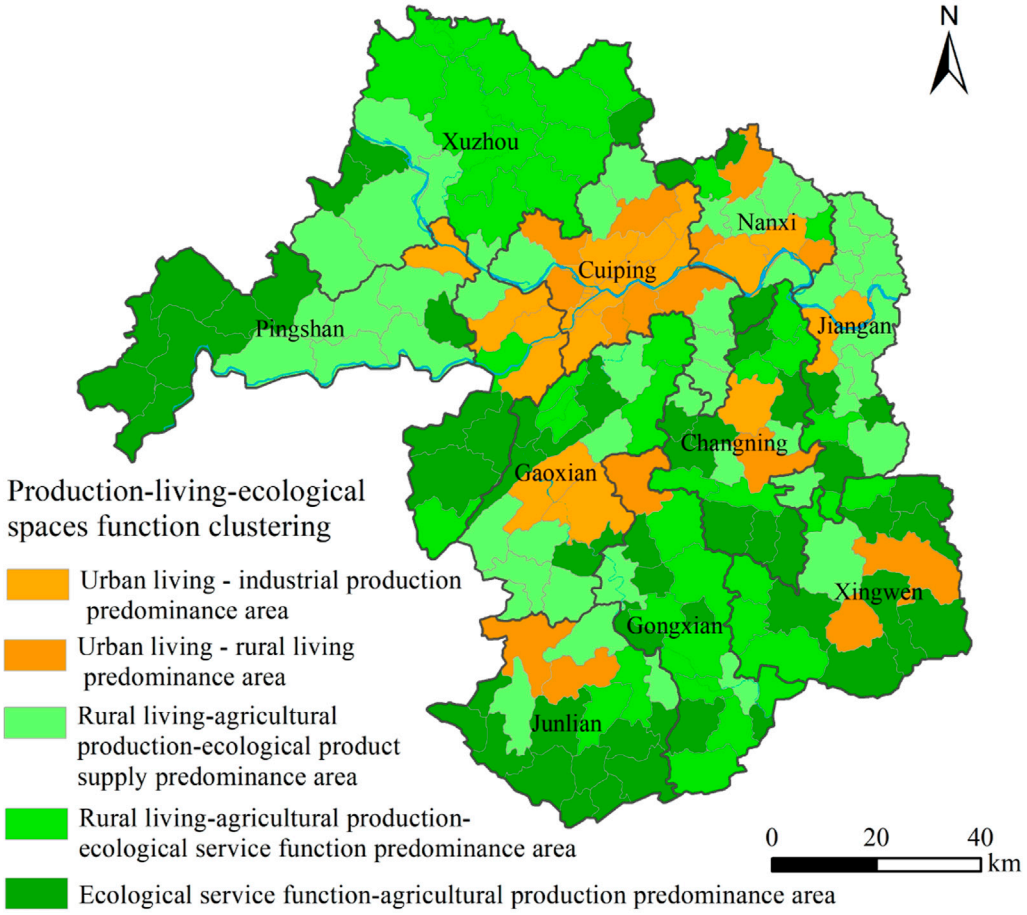

FIGURE 9
Comprehensive PLE space function clustering results of townships in Yibin.

mainly mountainous and hilly. Such areas covered 58 townships, accounting for 31% of the total number and 25.46% of the area.

5 Discussion

5.1 The 80/20 rule of space: occasional or objective?

Taking 2018 as the evaluation base year and townships as the primary evaluation unit, this study evaluated the territorial spatial function of Yibin City at 3 levels This study put forward a multi-level territorial spatial function evaluation and comprehensive zoning method, which had important guiding significance for coordinating the territorial spatial function of Yibin City and scientifically carrying out the protection, development and utilization of territorial space. The evaluation results showed an important phenomenon: from the perspective of the comprehensive PLE functions, the towns with higher values and high values and the towns with lower values and low values showed a 2:8 distribution pattern (Table 3).

In other words, the territorial space with important functions in the PLE function accounted for approximately 20% and insignificant functions approximately 80%. Because the 80/20 rule is usually used in social and economic fields, further research is required to determine whether that phenomenon existed in the objective regional space or was an occasional or universal phenomenon. However, the present research partially characterized that phenomenon. For example, an evaluation of the environmental function in Guangxi showed that the high and higher development and construction areas in Guangxi accounted for 15% of the total area of the autonomous region (Bu et al., 2018). Another emulation measured the suitability of the PLE function in the Bailong River Basin, Gansu Province, and showed that the area of highly suitable and appropriate production functions in the basin accounted for 28.78% of the available space (Liu et al., 2019). This may prove the rationality of the territorial spatial function zoning results in this study to some extent. But how to understand and deal with the contradiction of spatial functions at different levels? The 80/20 rule of territorial spatial function demonstrates that, for a particular type of function, whether it is developing, protecting, or optimizing, more than 20% of the functional areas should be focused on, the input-output ratio of space should be improved, space use efficiency should be increased, space governance should be improved, and regional social and economic development should be served. For example, the current Chinese government's guarantee of

TABLE 3 Area proportion of various functional areas in the evaluation results of the PLE function.

	Urban life (%)	Rural life (%)	Industrial and mining production (%)	Agricultural production (%)	Ecological regulation (%)	Ecological product supply (%)	Comprehensive		
							Living function (%)	Production function (%)	Ecological function (%)
Proportion of functional areas (high and higher-value areas)	11	61	24	55	60	40	16	23	28
Proportion of insignificant functional areas (low and lower-value areas)	89	39	76	45	40	60	84	77	72

functional areas for grain planting should make good use of 20% of the plains areas rather than take mountainous and hilly areas as the key areas for grain planting.

5.2 Relativity of spatial functions

The comprehensive zoning results of PLE function are the result of comprehensive clustering based on the first-level PLE functions, reflecting the commonality of spatial functions and development directions among regions and playing a macro-guiding role for regional development. Therefore, the comprehensive partition results have important reference significance for the gradual optimization of the current function. Note that this study's evaluation of the PLE function was based on social economic indicators and few natural background indicators, with administrative regions (townships) as the primary evaluation unit. The township boundaries were unstable, and major adjustments of townships at the county level in Sichuan have increased in recent years. However, the evaluation results can be used only as a reference for gradually optimizing the current functional areas. Also, the current functional status is often the result of the joint action of spatial base conditions, the historical inertia of development, and the selection of practical development requirements, which have a strong current situational and developmental selectivity. As the lowest and most direct level of spatial control subjects in the current Chinese system, townships will further explore the functional orientation more in line with their own development on the basis of the comprehensive PLE function zoning results according to their development reality.

According to the evaluation results, Shaping Street belonged to the urban life-industrial production advantage area. As for the current situation, it was the core area for urban spatial expansion in Yibin City. However, before 2009, Shaping Street belonged to a typical agricultural area along the river. The agriculture was mainly rice planting, characteristic breeding (for example, chickens and ducks), and characteristic fruit (for example, kiwi, honey pomelo, and citrus) planting. With the vigorous development of the port economy in Yibin City, that area has been transformed from the original agricultural space to urban and industrial production spaces. Also, the living space has been changed from decentralized rural dominance to compact urban dominance. The area of the production space has expanded and increased gradually, and the ecological space has been compressed and divided into an isolated-island distribution (Figure 10). In accordance with the planning, that area will become the core area of the Sanjiang New District, the first provincial-level new district in Sichuan Province. Therefore, the built-up area will be further expanded, and the breakthrough of function definitions will continue to iterate: rural life-agricultural production-ecological functional product supply advantage area → urban life-industrial production advantage area → High-quality urban living space and strategic emerging industry demonstration area. Although the spatial function is relative, for the special ecological sensitive area of the upper reaches of the Yangtze River, the cities along the river should strictly abide by the ecological bottom line in the process of expansion. Some riverside shorelines and wetlands should ensure the absoluteness of their functions to curb the degradation trend of their ecological functions.

5.3 Conservation and development

Coordinating the relationship between territorial spatial conservation and development and optimizing its pattern are important parts in achieving the construction of ecological civilization. The limited spatial resources and the multi-suitability of spatial functions will lead to conflicts between spatial functions, directly affecting the sustainable regional development (Zou et al., 2019). However, how to coordinate and optimize the various territorial spatial functions, alleviate functional conflicts, and realize the high-quality development of the territorial space is an issue that must be paid attention to in the regional territorial spatial protection and development.

Ecological security is the most important reflection of national strategy in the upper reaches of the Yangtze River economic belt. Therefore, at the national level, it is first necessary to satisfy ecological functions such as ecological barrier construction, soil and water conservation, water conservation, aquatic organism protection, water security in the basin, and coastal spatial protection. Of course, that economic belt is also expected to achieve regional economic and social development while fulfilling

FIGURE 10
High-resolution image of Shaping Street from 1990 to 2018.

ecological functions and considering food security and overall basin development (Qian, 2021; Liu et al., 2023). However, local governments such as in Yibin City should focus on how to increase regional development, how to achieve leapfrog development by actively connecting with major national and provincial strategies, and how to increase new industrial economic growth points by doing an industrial transfer, which will help to improve quality and compete for position. Different perspectives on national and regional development lead to different trends in spatial use: conservation demands at the national level require maintaining ecological functions, which might lead to the compression of current production and living spaces in the region. The development demands at the local level drive the continuous expansion of urban and industrial areas, causing an increase in nonagricultural production space, a transformation of traditional agricultural spatial development models and landscapes, and the pursuit of a diversified output of ecological spaces. Therefore, investigating and tackling the relation between development and protection play a key role in the spatial function of that region. For example, great importance should be attached to a more scientific understanding and positioning of ecological functions, the combination of elastic and rigid management, and the integrated development and protection of watersheds. In the future, the maintenance of the spatial function in the upper reaches of the Yangtze River should not only guarantee the reasonable spatial scope, but also pay more attention to the evaluation of the spatial function efficiency, so as to alleviate the direct functional conflicts and coordinate the relationship between protection and development.

6 Conclusion

This By taking 185 townships in Yibin City as evaluation units, this study adopted multivariate data to evaluate the PLE function of Yibin City in 2018 from 3 levels. The results show that:

(1) For the second-level PLE space of the townships in Yibin City, the high-value areas for urban and rural living functions reflected the characteristics of a concentrated distribution along the Yangtze River. The characteristics of the concentrated distribution of high-value industrial and mining production areas were the distribution around the central townships where the district and county government were located and the concentrated distribution of some townships with mineral resource advantages. High-value areas for agricultural production functions were distributed mainly in shallow-hill and flat areas with better light, heat, and water resources in the northern part of the city. The ecological regulation functional areas were evenly distributed throughout the city. The high-value areas of the ecological product supply function were distributed mainly in areas with dense ecological resources such as tea, camphor trees, and bamboo forests.

(2) The distribution of high-value areas for the first-level PLE spatial function of the townships in Yibin City was as follows: high-value areas with first-level living functions were basically consistent with the current central urban areas and central towns where the governments of each district and county were located. The overall pattern of the first-level production function was very similar to that of the industrial and mining production function. The major functional areas were distributed mainly in some central townships with resource advantages. The distribution of first-level ecological functions was similar to the pattern of ecological product supply in various townships, and the major functional areas covered a larger area of bamboo forests and tea gardens in Yibin City.

(3) As for the characteristics of the 80/20 rule of the proportion of significant and insignificant areas in the comprehensive PLE function in the townships, the significant areas accounted for approximately 20%, whereas the insignificant areas accounted for approximately 80%. By applying a cluster analysis to the evaluation results, the functions of townships in Yibin City were divided into 5 types of comprehensive PLE function areas: urban life-industrial production advantage (12%), urban life-rural life advantage (8%), rural life-agricultural production-ecological function product supply advantage (29%), rural life-agricultural production-ecological service function advantage (20%), and ecological service function-agricultural production function advantage (31%). The 5 types of functional areas showed important spatial differences.

In addition to multiple data sources and multilevel function evaluations, importance should be attached to how to use the functional effects of a particular type of functional advantage area and reduce the pressure of multifunctional and functional integration in disadvantaged areas. Moreover, the evaluation of territorial spatial functions is a dynamic process, and conventional function evaluation mechanisms should be explored in the future.

Data availability statement

Publicly available datasets were analyzed in this study. This data can be found here: https://www.resdc.cn/.

Author contributions

BM: Conceptualization, Formal Analysis, Investigation, Methodology, Software, Writing–original draft. SZ: Methodology, Software, Visualization, Writing–review and editing. WD: Conceptualization, Funding acquisition, Supervision, Validation, Writing–review and editing. LP: Conceptualization, Data curation, Project administration, Supervision, Validation, Writing–review and editing.

Funding

The author(s) declare financial support was received for the research, authorship, and/or publication of this article. This research was funded by the high-level talent "QiHang" program of Yibin University (No. 2021QH037), the National Natural Science Foundation of China (Nos: 41930651 and 42101244) and the program of Sichuan Center for Rural Development Research of Sichuan Agricultural University (No. CR2113).

Conflict of interest

The authors declare that the research was conducted in the absence of any commercial or financial relationships that could be construed as a potential conflict of interest.

Publisher's note

All claims expressed in this article are solely those of the authors and do not necessarily represent those of their affiliated organizations, or those of the publisher, the editors and the reviewers. Any product that may be evaluated in this article, or claim that may be made by its manufacturer, is not guaranteed or endorsed by the publisher.

References

Brooks, B. G. J., and Lee, D. C. (2019). Feasibility of pattern type classification for landscape patterns using the ag-curve. *Landsc. Ecol.* 34, 2149–2157. doi:10.1007/s10980-019-00869-w

Bu, X. Q., Luo, R. T., Zhao, H. J., Ma, W. C., and Zeng, G. Q. (2018). A study on the comprehensive assessment of environmental function and its spatial differentiation in Guangxi. *J. Fudan Univ. Nat. Sci.* 57, 68–78.

Callo-Concha, D., and Denich, M. (2014). A participatory framework to assess multifunctional land-use systems with multicriteria and multivariate analyses: a case study on agrobiodiversity of agroforestry systems in Tomé Açú, Brazil. *Change Adapt. Socio-Ecological Syst.* 1, 40–50. doi:10.2478/cass-2014-0005

Cheng, Z. L., Zhang, Y. J., Wang, L. Z., Wei, L. Y., and Wu, X. Y. (2022). An analysis of land-use conflict potential based on the perspective of production–living–ecological function. *Sustainability* 14, 5936. doi:10.3390/su14105936

Fan, J., Wang, Y. F., Chen, D., Zhou, C. H., Ma, J. H., Yafei, W., et al. (2015). Analysis on the spatial development structure of the yangtze River Economic belt. *Prog. Geogr.* 34, 1336–1344. doi:10.18306/dlkxjz.2015.11.001

Fu, B. J. (2002). Ecological and environmental effects of land-use changes in the Loess Plateau of China. *J. Chin. Sci. Bull.* 67, 3769–3779. doi:10.1360/tb-2022-0543

Fu, J. C., and Zhang, S. L. (2021). Functional assessment and coordination characteristics of production, living, ecological function—a case study of Henan province, China. *Int. J. Environ. Res. Public Health* 18, 8051. doi:10.3390/ijerph18158051

Fu, J. Y., Bu, Z. Q., Jiang, D., Lin, G., and Li, X. (2022). Sustainable land use diagnosis based on the perspective of production-living-ecological spaces in China. *Land Use Pol.* 122, 106386–6386. doi:10.1016/j.landusepol.2022.106386

Fu, X. X., Wang, X. F., Zhou, J. T., and Ma, J. H. (2021). Optimizing the production-living-ecological space for reducing the ecosystem services deficit. *Land* 10, 1001. doi:10.3390/land10101001

Han, Q., Sun, Z. Y., Sun, C. M., Li, D., and Liu, Y. P. (2019). Establishment and application of one map of current situation of territorial spatial planning according to the foundations of natural resources: taking Qingdao city as an example. *J. Nat. Resour.* 34, 2150–2162. doi:10.31497/zrzyxb.20191011

Hou, Y. Z., Zhang, Z. L., Wang, Y. R., Sun, H. H., and Xu, C. (2022). Function evaluation and coordination analysis of production–living–ecological space based on the perspective of type-intensity-connection: a case study of suzhou, China. *Land* 11, 1954. doi:10.3390/land11111954

Hsu, W. L., Shen, X. J., Xu, H. Y., Zhang, C. M., Liu, H. L., and Shiau, Y. C. (2021). Integrated evaluations of resource and environment carrying capacity of the Huaihe river ecological and economic belt in China. *Land* 10, 1168. doi:10.3390/land10111168

Kalogirou, S. (2002). Expert systems and GIS: an application of land suitability evaluation. *Environ. Urban Syst.* 26, 89–112. doi:10.1016/S0198-9715(01)00031-X

Kim, I., and Arnhold, S. (2018). Mapping environmental land use conflict potentials and ecosystem services in agricultural watersheds. *Sci. Total Environ.* 630, 827–838. doi:10.1016/j.scitotenv.2018.02.176

Li, S. N., Lv, X., Yin, R., Fang, B., and Jin, T. (2021b). Spatial equilibrium state and its time evolution of the multi-functionalization of regional landuse in the eastern China. *Pol. J. Environ. Stud.* 30, 2827–2841. doi:10.15244/pjoes/128538

Li, S. N., Zhao, X. Q., Pu, J. W., Miao, P. P., Wang, Q., and Tan, K. (2021a). Optimize and control territorial spatial functional areas to improve the ecological stability and total environment in karst areas of Southwest China. *Land Use Pol.* 100, 104940–4940. doi:10.1016/j.landusepol.2020.104940

Li, W. J., Fu, J., Jiang, D., Lin, G., and Cao, C. (2022a). Land use optimization in Ningbo City with a coupled GA and PLUS model. *J. Clean. Prod.* 375, 134004. doi:10.1016/j.jclepro.2022.134004

Li, W. J., Wu, J. P., Du, H. B., Wan, Y., Yang, S. F., Xiao, Y., et al. (2022b). Impact assessment of waterway development on the socioeconomic conditions and ecosystem in the upper Yangtze River. *River Res. Appl.* 38, 988–999. doi:10.1002/rra.3955

Liao, G. T., He, P., Gao, X. S., Lin, Z. Y., Huang, C. Y., Zhou, W., et al. (2022). Land use optimization of rural production–living–ecological space at different scales based on the BP–ANN and clues models. *Ecol. Indic.* 137, 108710. doi:10.1016/j.ecolind.2022.108710

Ling, Z. Y., Jiang, W. G., Liao, C. M., Li, Y. S., Ling, Y. R., Peng, K. F., et al. (2022). Evaluation of production–living–ecological functions in support of SDG target 11.a: case study of the Guangxi beibu gulf urban agglomeration, China. *Diversity* 14, 469. doi:10.3390/d14060469

Liu, D. Q., Zhang, J. X., Gong, J., and Cao, E. J. (2019). Ecological function zoning in Bailongjiang Watershed of Gansu based on production living-ecological function clusters. *Chin. J. Ecol.* 38, 1258–1266.

Liu, X. Q., Wang, X., Chen, K. L., and Li, D. (2023). Simulation and prediction of multi-scenario evolution of ecological space based on flus model: a case study of the yangtze river economic belt, China. *J. Geogr. Sci.* 33, 373–391. doi:10.1007/s11442-023-2087-9

Ma, Y., Xue, F., and Yang, Z. (2022). Coupling study on territory space suitability evaluation and construction land expansion simulation: a case study of Jiangxi province, China. *Environ. Dev. Sustain.* 25 (8), 8279–8298. doi:10.1007/s10668-022-02399-z

Niu, G. Y., Wang, G. L., Lu, Q. C., and Xiong, C. H. (2022). Function evaluation and optimal strategies of three types of space in cross-provincial areas from the perspective of high-quality development: a case study of Yangtze River delta, China. *Pol. J. Environ. Stud.* 3, 2763–2777. doi:10.15244/pjoes/144910

Ostovari, Y., Honarbakhsh, A., Sangoony, H., Zolfaghari, F., Maleki, K., and Ingram, B. (2019). GIS and multi-criteria decision-making analysis assessment of land suitability for rapeseed farming in calcareous soils of semi-arid regions. *Ecol. Indic.* 103, 479–487. doi:10.1016/j.ecolind.2019.04.051

Qian, C. (2021). Study on the coordination degree of regional economy-ecological environment coupling in the Yangtze River Economic Zone. *Fresenius Environ. Bull.* 30, 12063–12071.

Qiu, Y., Zhou, A. G., Li, M. H., Guo, Y. X., Cui, H., and Ma, C. M. (2023). Territorial spatial usage regulation based on resources endowment and sustainable development: a case of Wuhan, China. *J. Clean. Prod.* 385, 135771. doi:10.1016/j.jclepro.2022.135771

Wang, J., Liu, B., and Zhou, T. (2023). The category identification and transformation mechanism of rural regional function based on SOFM model: a case study of Central Plains Urban Agglomeration, China. *Ecol. Indic.* 147, 109926. doi:10.1016/j.ecolind.2023.109926

Wang, S. L., Qu, Y. B., Zhao, W. Y., Guan, M., and Ping, Z. L. (2022). Evolution and optimization of territorial-space structure based on regional function orientation. *Land* 11, 505. doi:10.3390/land11040505

Wang, Y. F., Fan, J., and Zhou, K. (2019). Territorial function optimization regionalization based on the integration of "Double Evaluation. *Geogr. Res.* 38, 2415–2429. doi:10.11821/dlyj020190327

Wei, L. Y., Zhang, Y. J., Wang, L. Z., Mi, X. Y., Wu, X. Y., and Cheng, Z. L. (2021). Spatiotemporal evolution patterns of "production-living-ecological" spaces and the coordination level and optimization of the functions in Jilin Province. *Sustainability* 13, 13192. doi:10.3390/su132313192

Xi, F. R., Wang, R. P., Shi, J. S., Zhang, J. D., Yu, Y., Wang, N., et al. (2020). Spatio-temporal pattern and conflict identification of production-living-ecological space in the Yellow River Basin. *Land* 11 (5), 744. doi:10.3390/land11050744

Xiao, P. N., Xu, J., and Zhao, C. (2022). Conflict identification and zoning optimization of "Production-Living-Ecological" space. *Int. J. Environ. Res. Public Health* 19, 7990. doi:10.3390/ijerph19137990

Xie, X. T., Li, X. S., Fan, H. P., and He, W. K. (2021a). Correction to: spatial analysis of production-living-ecological functions and zoning method under symbiosis theory of Henan, China. *Environ. Sci. Pollut. Res.* 28, 69111–69110. doi:10.1007/s11356-021-15714-4

Xie, X. T., Li, X. S., Fan, H. P., and He, W. K. (2021b). Spatial analysis of production-living-ecological functions and zoning method under symbiosis theory of Henan, China. *Environ. Sci. Pollut. Res.* 28, 69093–69110. doi:10.1007/s11356-021-15165-x

Xue, M. Q., Wang, H. W., Wei, Y. M., Ma, C., and Yin, Y. C. (2022). Spatial characteristics of land use multifunctionality and their trade-off/synergy in Urumqi, China: implication for land space zoning management. *Sustainability* 14 (15), 9285. doi:10.3390/su14159285

Yang, Y. Y., Bao, W. K., and Liu, Y. S. (2020). Coupling coordination analysis of rural production-living-ecological space in the Beijing-Tianjin-Hebei region. *Ecol. Indic.* 117, 106512. doi:10.1016/j.ecolind.2020.106512

Zhang, R. T. (2022). Spatial differentiation and tradeoff-synergy of rural multifunction at the county scale in anhui province in the China's traditional agricultural areas. *Int. J. Environ. Res. Public Health* 19, 13604. doi:10.3390/ijerph192013604

Zhang, X. S., and Xu, Z. J. (2021). Functional coupling degree and human activity intensity of production–living–ecological space in underdeveloped regions in China: case study of Guizhou province. *Land* 10, 56. doi:10.3390/land10010056

Zhang, Y. H., Wang, Z., Hu, S. G., Song, Z. Y., Cui, X. G., and Afriyie, D. (2022). Spatial and temporal evolution and prediction of the coordination level of "production-living-ecological" function coupling in the Yellow River Basin, China. *Int. J. Environ. Res. Public Health* 19, 14530. doi:10.3390/ijerph192114530

Zhao, T. Y., Cheng, Y. N., Fan, Y. Y., and Fan, X. N. (2022b). Functional tradeoffs and feature recognition of rural production–living–ecological spaces. *Land* 11, 1103. doi:10.3390/land11071103

Zhao, T. Y., Zhao, Y. L., and Yang, X. P. (2022a). Evolution characteristics and driving mechanism of the territorial space pattern in the yangtze River Economic belt, China. *Land* 11, 1447. doi:10.3390/land11091447

Zhou, H., Wang, P., and Jiang, H. B. (2017). Suitability evaluation of land spatial development of the yangtze River Economic belt in sichuan province. *Geospatial Inf.* 15, 26–30. doi:10.3969/j.issn.1672-4623.2017.07.008

Zou, L., Liu, Y., Wang, J., Yang, Y., and Wang, Y. (2019). Land use conflict identification and sustainable development scenario simulation on China's southeast coast. *J. Clean. Prod.* 238, 117899. doi:10.1016/j.jclepro.2019.117899

frontiers | Frontiers in Ecology and Evolution

TYPE Original Research
PUBLISHED 13 December 2023
DOI 10.3389/fevo.2023.1284281

OPEN ACCESS

EDITED BY
Xue-Chao Wang,
Beijing Normal University, China

REVIEWED BY
Zhe Feng,
China University of Geosciences, China
Caige Sun,
South China Normal University, China

*CORRESPONDENCE
Ling Ma
nwu201920833@stumail.nwu.edu.cn

RECEIVED 28 August 2023
ACCEPTED 24 November 2023
PUBLISHED 13 December 2023

CITATION
Ma L, Wang C, Wang L, Jin S and Kou X (2023) Study of spatiotemporal variation and driving factors of habitat quality in the northern foothills of the Qinling Mountains: a case study of Xi'an, China.
Front. Ecol. Evol. 11:1284281.
doi: 10.3389/fevo.2023.1284281

Study of spatiotemporal variation and driving factors of habitat quality in the northern foothills of the Qinling Mountains: a case study of Xi'an, China

Ling Ma[1,2]*, Chuanming Wang[1,2], Liyang Wang[1], Shumeng Jin[1] and Xiaomei Kou[1]

[1]Northwest Engineering Corporation Limited, Xi'an, China, [2]Shaanxi Union Research Center of University and Enterprise for River and Lake Ecosystems Protection and Restoration, Xi'an, China

As earth surface human activities become more frequent, global ecosystem service functions and especially biodiversity maintenance functions are challenged. This study aimed to analyze spatiotemporal changes in Xi'an section of the northern foothills of the Qinling Mountains from 1990 to 2020. Temporal and spatial changes in habitat quality in the study area were visualized using InVEST model and land use data, and factors affecting habitat quality were analyzed using Geodetector. The results showed that during the study period, the cultivated land, grassland, and water decreased by 16.40%, 74.37%, and 35.39%, respectively, while the area of forest land and construction land increased, among which the construction land increased by 117.70%, the largest increase, and the forest land increased by 8.47%. The main changes in land use are the conversion of cultivated land into forest land and construction land, and the conversion of grassland into forest land and cultivated land. During the period 1990–2020, the average habitat quality index in the study area changed from 0.8617 to 0.8585, showing a slow decreasing trend. The spatial distribution of habitat quality showed a trend of "high in the south, moderate in the north, and low in the northwest". The high habitat quality was mainly concentrated in the southern forest land, the middle habitat quality was mainly distributed in the northern cultivated land, and the low habitat quality was mainly distributed in the northwest construction land. The land use type has a great influence on habitat quality, and the interaction between any two factors is stronger than that of a single factor. The temporal and spatial variation of habitat quality is influenced by both natural and human factors. This study provides a theoretical basis for ecological protection and nature reserve planning in the Qinling Mountains region.

KEYWORDS

habitat quality, InVEST model, land use change, spatiotemporal change, Geodetector

Introduction

Habitat quality (HQ) can represent the supply capacity of ecosystem services and biodiversity in a region and is an important basis for ensuring ecological security and reflecting the pros and cons of the human living environment (Silvis, 2012; Zhang et al., 2020). In recent years, with the rapid growth of population and the continuous development of the social economy, the excessive occupation of land resources and the rapid change of land use mode has caused a series of environmental problems, resulting in serious damage to ecosystem service functions and endangering human welfare (Newbold et al., 2015; Sallustio et al., 2017; Li et al., 2020a; Li et al., 2020b). Therefore, it is of great practical significance for realizing sustainable development of resources and maintaining ecosystem security to analyze and study the habitat quality in the region and evaluate the changing trend of the ecosystem service function.

The methods of habitat quality assessment are mainly divided into the quantitative index method and model method. The quantitative index method is to obtain the relevant parameters of habitat quality through field investigation and construct an evaluation index system for comprehensive evaluation (Wynne and Côté, 2007; Yang et al., 2021a). Due to the large amount of human and material resources invested in the evaluation process and the lack of universality, it is not suitable for large-scale regional and long-term time series research (Chen et al., 2019; Muñoz-Barcia et al., 2019). The model rule uses mathematical models to quantitatively assess habitat quality, which has the advantages of convenience, speed, and low cost (Moreina et al., 2018). ARtificial Intelligence for Ecosystem Services (ARIES), Social Values for Ecosystem Services (SoIVES), and Integrated Valuation of Ecosystem Services and Trade-offs (InVEST) are widely used in related research (Bagstad et al., 2011; Mushet et al., 2014; Sherrouse et al., 2014; Huang et al., 2020). Among these models, the InVEST model jointly developed by Stanford University, the World Wide Fund for Nature, and The Nature Conservancy is the most well-developed, with advantages such as easy access to data and strong visibility of results (Huang et al., 2020).

Qianqian et al. (2022) analyzed the habitat quality and degree of degradation in the Ebinur Lake Basin of Xinjiang from 1990 to 2020, and predicted the spatiotemporal changes in habitat quality in the Ebinur Lake Basin under inertial development and ecological protection scenarios. Cao et al. (2017) studied the impact of the urbanization process on ecosystem service function in Zhoushan Island and revealed the response relationship between urban expansion encroachment on other land use types and temporal and spatial changes in habitat quality. Pan et al. (2022) explored the temporal and spatial changes in habitat quality in the source region of the Yellow River and analyzed the effects of vegetation cover change and human activities on habitat quality combined with NDVI and land use data. Wang and Cheng (2022) conducted a study on the spatial aggregation characteristics of habitat quality under different topographies using DEM, and analyzed the distribution patterns of habitat quality in different altitude areas. At present, a large number of studies mainly explore the characteristics of habitat quality changes based on different land use, climate types, geomorphic features, and altitude (Arunyawat and Shrestha, 2016; Wu et al., 2021; Zhang et al., 2022a). However, there are relatively few studies on the spatiotemporal evolution of habitat quality in complex areas in geographical transition regions.

As an important natural geographical transition area in China, the Qinling Mountains plays a key role in water conservation and biodiversity maintenance, has important ecological service value, and is an indispensable natural ecological barrier in China (Li et al., 2013; Zhang et al., 2017; Zhang et al., 2019). However, the climate, terrain, and biological species of Qinling Mountain are complex and varied, and its ecological environment has obvious spatial differences under the dual influence of climate change and human activities (Shu-Yan, 2002), which has become the main focus of most studies at present (Ma et al., 2019; Zhao et al., 2021; Zhang et al., 2022b). Ting et al. (2014) evaluated the ecological benefits of soil and water conservation in the Qinling Mountains region using the InVEST model. Ning et al. (2020) analyzed the spatiotemporal changes in the water conservation function of the Qinling Mountains. These studies mostly focus on the evaluation of ecosystem service functions in the Qinling Mountains, lacking research on the spatiotemporal changes of habitat quality over a long time series. Xi'an, at the northern foothills of the Qinling Mountains, has always had a large population and high intensity of human activities, which have a profound impact on the natural environment. Especially in recent years, with the continuous advancement of urbanization and the rapid increase of urban construction land, the natural ecosystem and ecological functions in the region have been affected (Zhou and Li, 2017; Li et al., 2019). Therefore, based on NDVI, land use, night light, and other data, this paper uses InVEST model to analyze the temporal and spatial changes of habitat quality in the Xi'an section of the northern foothills of the Qinling Mountains from 1990 to 2020 and discusses the impact of urban expansion on habitat, to provide the scientific basis for ecological civilization construction in the Qinling Mountains.

Materials and methods

Study area

Referring to the narrow definition of the Qinling Mountains as defined in the "Overall Plan for Ecological Environment Protection in Qinling Mountains, Shaanxi Province" (http://www.shaanxi.gov.cn/zfxxgk/zfgb/2020/d17q/202009/t20200921_1728563.html), the northern and southern slopes of Qinling Mountain and the eastern and western borders of Shaanxi Province are defined as Qinling boundary. Combined with the administrative division of Xi'an City, the Xi'an section at the northern foothills of the Qinling Mountains was selected as the study area (Figure 1). The geographical range was 107° 24′–109°49′E, 33°45′–34°22′N, the climate type is the warm temperate semi-humid climate, and the vegetation is mainly warm temperate deciduous broad-leaved forest.

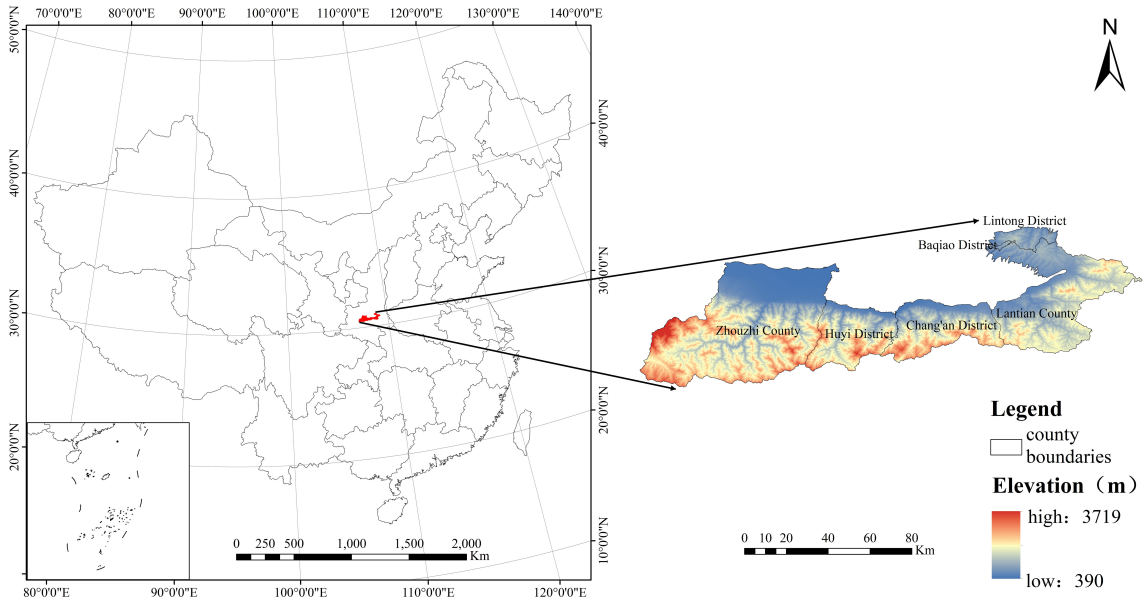

FIGURE 1
The map of study area.

Data source

The land use raster datasets with 30 m resolution ratio of the Qinling mountains in 1990, 2000, 2010 and 2020, the Normalized Differential Vegetation Index (NDVI), night light, temperature, and precipitation data resolution ratio were acquired from the Resource and Environment Science and Data Center (http://www.resdc.cn). Among them, land use data is obtained from the visual interpretation of landSat 8 remote sensing images, The annual dataset of night light is processed based on DMSP/OLS and NPP-VIIRS satellite night light remote sensing image data, precipitation and air temperature grid data is generated based on the spatial interpolation of Anuspl interpolation software, and NDVI data is obtained by the maximum synthesis method of remote sensing images. DEM data is downloaded from Geospatial data (http://www.gscloud.cn/). The population density data with 1 km resolution ratio are derived from the worldpop database (www.worldpop.org.uk). Traffic data are from the National Geographic Information Center of China (https://www.ngcc.cn). All raster data unified the resolution to 30 m using resampling and clipped by the study area for Geodetector analysis.

Methods

Assessment of habitat quality

Referring to the principle of InVEST model, the calculation formula of habitat quality is as follows:

$$D_{xj} = \sum_{r=1}^{R}\sum_{y=1}^{Y_r} r_y \left(\frac{w_r}{\sum_{r=1}^{R} w_r}\right) r_j i_{rxy} \beta_x S_{jr} \quad (1)$$

$$i_{rxy} = 1 - \left(\frac{d_{xy}}{d_{r\ \max}}\right)(liner) \quad (2)$$

$$i_{rxy} = 1 - \left(\frac{-2.99 d_{xy}}{d_{r\ \max}}\right)(exponential) \quad (3)$$

Where: D_{xj} is the degree of habitat degradation in the grid cell x with habitat type j, and R is the number of potential threats. Y_r is the grid number of r on the grid plot; r_y is the strength of the grid cell y; ω_r represents the weight of the threat source; the distance between the habitat and the threat source is represented by i_{rxy}. β_x represents the antiinterference level of the grid cell x; S_{jr} indicates the relative sensitivity of habitat type j to the threat source r; d_{xy} represents the distance between grid cells x and y; and $d_{r\ max}$ represents the maximum impact distance of the threat source.

$$Q_{xj} = H_j \left[1 - \left(\frac{D_{xj}^{\ z}}{D_{xj}^{\ z} + K^z}\right)\right] \quad (4)$$

Where: Q_{xj} is the habitat quality of pixel x in land-use/cover type j, D_{xj} is the threat level of pixel x in land-use/cover type j, H_j is the habitat suitability of land-use/cover type j, and K is half the saturation constant (which is half of the maximum value of D_{xj}). z is a default parameter in the model and is set as 2.5 (Chen et al., 2021).

InVEST's habitat quality model is based on land use data, habitat threat source data, habitat threat source weights, sensitivity of different land classes to threat sources, and habitat suitability of local classes. Many studies have selected different threats factors and related parameters, this study referred to the InVEST model manual (Sharp et al., 2020) and other relevant studies (Fan et al., 2021; Cui et al., 2022; Qianqian et al., 2022), based on the spatial scale of this study and expert consultation, the relevant parameters are determined as follows (Tables 1, 2):

TABLE 1 Threat factors and maximum effect distances, weights of threat factors, and decay types identified in the study area.

Threats factor	Max distance of influence (km)	Weights	Decay type
Cultivated land	4	0.4	linear
Construction land	8	1	exponential
Highway	3	0.6	linear
Main road	2	0.5	linear
Railway	5	0.9	linear

Where: The max distance of influence is defined as the maximum range of the threats factors on the quality of surrounding habitats, the weight represents the relative destructiveness of threats factors to all habitats, which the value range is [0,1]. Decay type is used to describe the attenuation of environmental threats by threats factors as distance increases, divided into linear attenuation and exponential attenuation (Sharp et al., 2020).

Where: The sensitivity parameters included habitat suitability parameters for each land use type and sensitivity parameters of each land use type to stressors, all ranging from 0 to 1.

Geodetector

Geodetector is a model used to detect the spatial heterogeneity of geographical elements and identify the interaction between multiple factors. Through the analysis based on the spatial stratification characteristics of variables rather than linear relationships, the explanatory power and mutual relationship of different factors on habitat quality can be truly and accurately reflected (Ma et al., 2022; Chen et al., 2023). Detectors are divided into four types: factor detector, ecological detector, interaction detector, and risk detector, which are widely used in the ecological research field (Jing et al., 2017; Sun et al., 2021; Qu et al., 2022). In this study, an interaction detector was used to analyze the interaction between different factors. The calculation formula is as follows:

$$q = 1 - \frac{\sum_{i=1}^{m} n_i \sigma_i^2}{n\sigma^2} = 1 - \frac{SSW}{SST}$$
$$SSW = \sum_{i=1}^{m} n_i \sigma_i^2, \quad (5)$$
$$SST = n\sigma^2$$

where i (i = 1, 2,…, l) is the stratification of dependent variable y or independent variable %, i.e., classification or partition; n_i and n are the unit numbers of layer i and the whole region, respectively; σ_i^2 and σ^2 are the variances of layer i and region Y, respectively; SSW and SST are the sum of variances within the layer and the total variances of the whole region, respectively; and the value range of q is [0, 1], where the larger the value, the stronger the explanatory power of independent variable % to dependent variable y.

The interaction detector is to determine the interaction between various factors and assess whether multiple factors work together to increase or reduce the driving force of HQ, or whether there is an interaction between these factors (Table 3). The habitat quality of the ecosystem is the result of the interaction of multiple factors. In terms of natural factors, considering the influence of topography and climate, the distribution of vegetation is closely related to topography, and the distribution of vegetation in different land forms is quite different, which affects the habitat quality. Therefore, elevation are selected as influence factors in terms of topographic factors. Land use type influences the spatial distribution of habitat quality, so land use data was chosen as the influence factor. Climate factors on land cover affect habitat quality, so precipitation and temperature are selected as influence factors; vegetation can reflect habitat quality to some extent, and vegetation growth through the vegetation normalization index (NDVI). In terms of socioeconomic factors, population density and the night light index are important indicators of the intensity of human activity, which can also have an impact on habitat quality. The habitat quality is used as the dependent variable, and the natural break point method is used as the independent variable. Habitat quality was treated as dependent variable and each driver as independent variable and discretized by natural break point method. The ArcGIS software was used to create fishing nets, and the sampling interval was set at 1 km after multiple debugging. The spatial analyst-extraction analyst-sampling tool was used to input the independent variable and dependent variable layer. The sampling point was the fishing net point in the study area, and the values of the independent variables and dependent variables were extracted and input into the geographic detector model.

Results

Land-use change in the northern foothills of the Qinling Mountains

Land use changed dramatically during 1990–2020 as in Table 4. The cultivated land and grassland showed a continuous decreasing trend,

TABLE 2 Habitat suitability and sensitivity of land use types to each threat factor.

Land-use	Habitat suitability	Cultivated land	Construction land	Highway	Main road	Railway
Cultivated land	0.6	0.0	0.9	0.7	0.4	0.6
Woodland	1	0.5	0.8	0.7	0.5	0.8
Grassland	0.9	0.2	0.5	0.5	0.4	0.5
Water area	0.8	0.4	0.7	0.6	0.4	0.5
Construction land	0.0	0.0	0.0	0.0	0.0	0.0

TABLE 3 Types of interactions between two Covariates to HQ.

Judgments based	Interaction
$q(x1\cap x2)<\min(q(x1),q(x2))$	Non-linear weaken
$\min(q(x1),q(x2))<q(x1\cap x2)<\max(q(x1),q(x2))$	Single-factor nonlinearity weaken
$q(x1\cap x2)>\max(q(x1),q(x2))$	Two-factor enhancement
$q(x1\cap x2)=q(x1)+q(x2)$	Independent
$q(x1\cap x2)>q(x1)+q(x2)$	Nonlinear enhancement

decreasing by 16% and 74% respectively. Forest land and construction land showed a trend of continuous growth, increasing by 8% and 118% respectively. Water area shrank significantly during 1990 to 2000, however, it has increased between 2000 to 2020. As shown in the graph below, the major types of land use in the study are forest land and cultivated land. In the study cultivated land is mainly distributed in the north of the study area which account for about 24% of the total area; where forest land is primarily distributed in the southern part of the study area and it account for about 70% of the total area; The remainder grassland and water area is distributed dismissively. Lastly, the construction land is mainly distributed in the northwest of the study area.

This research is based on the four stages land use data (Figure 2), combined with the land use transfer matrix. From 1990 to 2020, land use transformation in the study area mainly involves cultivated land, forest land, grassland, and construction land (Table 5). The cultivated land was mainly changed into forest land of 240.22 m^2, indicating that the project of returning farmland to forest was implemented in the local area during the study period. In addition, 90.35 km^2 of cultivated land has been transformed into construction land, indicating that the urbanization of urban suburbs is relatively significant. The forestland mainly flows into cultivated land, which accounts for about 77% of the forestland outflow area. 190.05 km^2 and 38.64 km^2 of grassland were mainly converted into forest land and cultivated land. The water area is mainly converted into cultivated land and construction land, both of which are 4.87 km^2. Construction land was mainly converted into cultivated land, with an area of 8.23 km^2, accounting for 79% of the transferred area.

Temporal and spatial variation of habitat quality

Natural break-point method is often used for grading the results of habitat quality, most studies generally classify the habitat quality level into 3 or 5 levels (Fan et al., 2021; Yang et al., 2021b; Cui et al., 2022; He et al., 2023). Using the natural breakpoint method, based on the calculation results of the habitat quality and the range of the study area, the habitat quality retention at 1 decimal point from 1990 to 2020 was divided into three levels: low (0–0.4), medium (0.4–0.8), and high (0.8–1.0). Habitat area and percentage at each level in the four periods are summarized below (Table 6). From the perspective of time scale, the mean value of habitat quality in the study area decreased slightly during 1990–2020, but the range of change was small. The mean values were 0.8617, 0.8629, 0.8604, and 0.8585. Overall, the area proportion of high-quality habitat increased, the area of medium-quality habitat gradually decreased, and the area of low-quality habitat increased slowly.

From a spatial perspective (Figure 3), regions with high habitat quality were mainly distributed in the southern mountains of the study area, where regions with low habitat quality were mainly distributed in the northwestern part of the study area, and regions with medium habitat quality were mainly distributed in the northern part of the study area. The habitat quality of construction land is low. The land type of the region with high habitat quality is mainly forest land, the land type of the region with medium habitat quality is mainly cultivated land, and the land type of the region with low habitat quality is mainly construction land.

To further understand the spatiotemporal variation characteristics of habitat quality in the study area, the arcgis10.8 software was used to make the spatiotemporal variation map of habitat quality levels in the study area from 1990 to 2020 (Figure 4). During 1990–2020, habitat quality levels in most areas of the study area remained stable (Table 7). About 93% of the total area of the habitat quality grade remained unchanged, about 5% of the total area of the habitat quality grade increased, and about 2% of the total area of the habitat quality grade decreased. medium to high area accounts for about 3% of the total area, showing an east-west zonal distribution in space, mainly distributed in the area of human production and living and the border zone of high-altitude mountains. Low to medium areas are mainly distributed in the northeast of the study area, and High to medium areas account for about 2% of the total area, mainly distributed in the eastern part of the study area and scattered in the southern mountain settlements. The area of Medium to low is mainly distributed in the northern part of the study area where the altitude is lower and the population is denser.

Factors influencing spatial variations in HQ

Single factor analysis

The results of the geographic detector analysis (Table 8) show that there are differences in the driving forces (q values) of various

TABLE 4 Variations in the areas of different land types in study area (km^2) from 1990 to 2020.

LULC	1990	2000	2010	2020	Change (km^2)	Change (%)
Cultivated land	1577.63	1533.27	1459.43	1318.83	−258.8	−16.40
Woodland	4519.47	4647.54	4755.28	4902.09	382.62	8.47
Grassland	276.70	183.23	115.21	70.92	−205.78	−74.37
Water area	12.84	3.76	6.22	8.27	−4.57	−35.59
Construction land	73.52	92.37	124.03	160.05	86.53	117.70

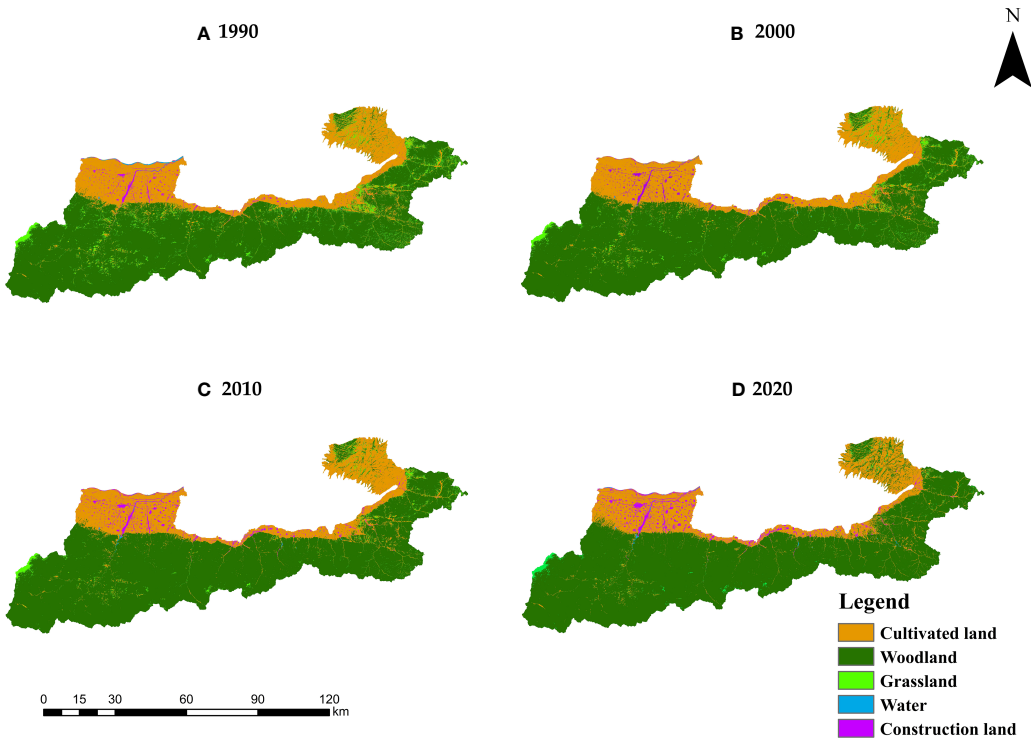

FIGURE 2
Land use type in 1990 **(A)**, 2000 **(B)**, 2010 **(C)**, 2020 **(D)**.

factors affecting the change of HQ. The order of q value is land use type (X3) > NDVI (X5) > altitude (X4) > temperature (X6) > precipitation (X7) > population density (X2) > night light index (X1). Thus, land use type was identified as the key factor affecting HQ change (q = 0.788), followed by NDVI (q = 0.467). Temperature, rainfall, population density, elevation, and night light index are weak in explaining the spatial variation of habitat quality, but these factors need to be considered. In general, natural factors (land use type, NDVI) had a significant impact on the spatial distribution pattern of habitat quality, and its q value was greater than that of terrain (altitude), meteorological (precipitation, temperature), and social economy (night light index, population density).

TABLE 5 Land-use change transfer matrix of the study area (km^2) from 1990 to 2020.

Land-use type	Cultivated land	Woodland	Grassland	Water area	Construction land
Cultivated land	1229.41	240.22	14.94	2.72	90.35
Woodland	37.68	4471.34	9.66	0.31	0.48
Grassland	38.64	190.05	46.17	0.58	1.27
Water area	4.87	0.25	0.08	2.78	4.87
Construction land	8.23	0.23	0.08	1.89	63.09

TABLE 6 Areas and proportions of HQ levels in study area from 1990 to 2020.

HQ grade	1990		2000		2010		2020	
	km^2	%	km^2	%	km^2	%	km^2	%
Low	113.04	2	126.33	3	163.23	3	217.05	3
Medium	1810.24	28	1762.80	27	1684.46	26	1565.16	24
High	4542.57	70	4576.72	70	4618.16	71	4683.65	73
Mean	0.8617		0.8629		0.8604		0.8585	

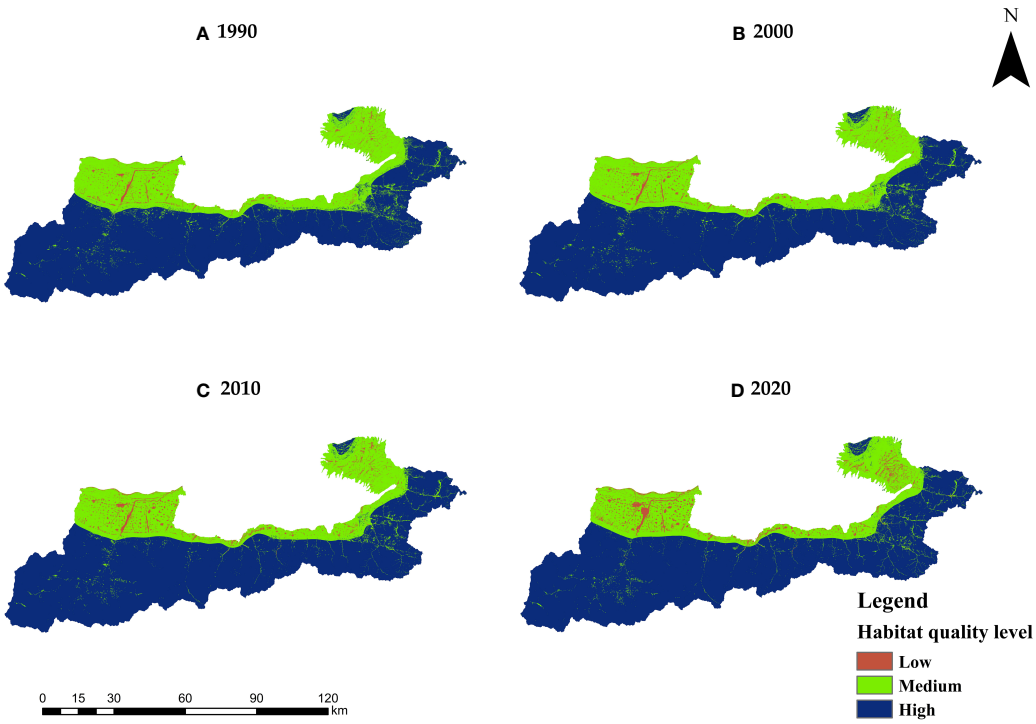

FIGURE 3
Habitat quality in 1990 **(A)**, 2000 **(B)**, 2010 **(C)**, 2020 **(D)**.

Analysis of interactions between bi-factors

The driving force of two-factor interaction on HQ was analyzed using the interaction detector of the geographical detector. The results (Table 9) show that the *q* value of two-factor interaction is greater than that of a single factor. The interaction was characterized by two-factor enhancement. The most significant interaction effect on spatial variation of habitat quality is land use ∩ temperature (0.865), followed by land use ∩ altitude (0.860). When one dominant single factor (land use type) is combined with another factor, the interaction of dominant factors is most significant, indicating that different land use types determine the distribution pattern of ecosystem types. The interaction of NDVI with precipitation, temperature, and elevation showed a considerable driving force, indicating that natural factors such as temperature, precipitation, and slope had a certain impact on the change of land use type and habitat quality. While the single-factor drivers of nighttime lighting and population density are low, interactions with other factors outweigh the single-factor drivers.

TABLE 7 Habitat quality level transfer matrix from 1990 to 2020.

1990	2020		
	Low	Medium	High
Low	77.16	35.22	0.46
Medium	138.85	1457.70	210.01
High	0.99	70.6554	4469.2263

Discussion

In this study, the InVEST habitat quality model and interactive detector were applied to analyze the temporal and spatial changes and influencing factors of habitat quality in the Xi'an section of the northern foothills of the Qinling Mountains from 1990 to 2020, which has great practical significance in the protection of ecological diversity and the construction of ecological civilization in the Qinling Mountains.

The relationship of land use change and habitat quality

Land use change is the direct reflection of the interaction between humans and the natural environment, it is also an important reason for changes in habitat quality (Li S. et al., 2020a). Research shows that the land use of the northern foot of the Qinling Mountains has changed enormously in the past 30 years; cultivated land, forest land, and construction land are the main types of land use in the region.And the area of cultivated land and grassland continued to decrease between 1990 and 2020, while the area of construction land continued to increase, the development of social economy and the rapid expansion of cities have been the main reasons for the rapid changes in land use in China in recent decades (Ma et al., 2022; Qu et al., 2022).

There is a certain response relationship between the spatiotemporal changes in habitat quality and land use changes. From 1990 to 2020,

TABLE 8 *q* Values of factors influencing spatial variations in HQ.

Driving factor	X1	X2	X3	X4	X5	X6	X7
Driving force (*q*)	0.300	0.326	0.788	0.448	0.467	0.431	0.371
p Value	0	0	0	0	0	0	0

the mean value of habitat quality in the northern foot of the Qinling Mountains decreased slightly, showing an overall trend of first increasing and then decreasing. The areas with improved habitat quality are mainly concentrated in the north and central regions, these areas are supported by a series of ecological protection policies such as returning farmland to forests, naturally protected forest (Liu et al., 2018). Therefore, the land use in this region has mostly shifted from arable land to forest land. The areas with declining habitat quality are mainly concentrated in the densely populated areas of Xi'an, including the northern urban areas and towns in the southern mountainous areas, during the period from 1990 to 2020, the area of construction land more than doubled. The rising industry of tourism in the northern foot of the Qinling Mountains has promoted the construction of rural infrastructure and economic development in the area on one side; on the other side, it negatively impacted on the local ecosystem which resulting in the decline of habitat quality (Zhang S. et al., 2022; Han et al., 2023).

Despite the support of various government policies, the habitat quality of the northern foothills of the Qinling Mountains continued to decline from 1990 to 2020, mainly due to the continuous increase in construction land. However, there is a clear boundary between medium and high habitat quality in the northern foothills of the Qinling Mountains, distributed in the central region, and the habitat quality in this region is continuously improving. This indicates that the government has to some extent clarified the boundary between human activities and nature, and has constrained the scope of human activities through a series of measures such as returning farmland to forests, demolishing illegal buildings, and establishing nature reserves (Liu et al., 2018; Chen, 2019). In addition, as the growth rate of China's population slows down, the scale of urban expansion tends to stabilize (Hou et al., 2022), which will provide favorable conditions for the continuous improvement of habitat quality in the region.

TABLE 9 The results of interactive detection.

Interaction	Influence	Interaction	Influence
X1 ∩ X2 (0.391)	Enhance,bi-	X3 ∩ X4 (0.860)	Enhance,bi-
X1 ∩ X3 (0.812)	Enhance,bi-	X3 ∩ X5 (0.845)	Enhance,bi-
X1 ∩ X4 (0.501)	Enhance,bi-	X3 ∩ X6 (0.865)	Enhance,bi-
X1 ∩ X5 (0.570)	Enhance,bi-	X3 ∩ X7 (0.847)	Enhance,bi-
X1 ∩ X6 (0.492)	Enhance,bi-	X4 ∩ X5 (0.668)	Enhance,bi-
X1 ∩ X7 (0.462)	Enhance,bi-	X4 ∩ X6 (0.484)	Enhance,bi-
X2 ∩ X3 (0.822)	Enhance,bi-	X4 ∩ X7 (0.505)	Enhance,bi-
X2 ∩ X4 (0.508)	Enhance,bi-	X5 ∩ X6 (0.668)	Enhance,bi-
X2 ∩ X5 (0.579)	Enhance,bi-	X5 ∩ X7 (0.655)	Enhance,bi-
X2 ∩ X6(0.497)	Enhance,bi-	X6 ∩ X7 (0.466)	Enhance,bi-
X2 ∩ X7 (0.482)	Enhance,bi-		–

Enhance, bi-: means that the interaction between the two factors is a bi-factor enhancement.

Driving factors of habitat quality

During the study period, land use type was the main determinant of habitat quality, this is consistent with previous research results (Cui et al., 2022). followed by the NDVI index, which had a strong impact on habitat quality and was an important parameter reflecting vegetation growth status and coverage in the region. NDVI is closely related to habitat quality, which is different from Zhang X. et al. (2022a). Differences in the geographical environment of the study area led to different drivers of habitat quality. The interaction test results show that natural factors and social factors have a significant influence on the temporal and spatial changes of habitat quality in the study area. The interaction of all factors enhanced the impact on habitat quality, indicating that the interaction of two factors was much greater than that of single factors. The interaction between land use and other factors was significantly stronger than the interaction between other factors, indicating that land use was the main factor affecting habitat quality change. This indicates that the biodiversity maintenance function of the ecosystem is affected by many factors, but the land bearing the ecosystem is a decisive factor for the habitat quality of the ecosystem.

Limitations

In this study, the quantitative and computational results of HQ are visualized by the InVEST-HQ model. However, there are some limitations to our study. First of all, the regional scale results can only be used as a reference for the relationship between LULC changes and HQ changes in the northern foot of the Qinling Mountains. It is necessary to carry out large-scale and more comprehensive research on the study area to formulate appropriate ecological protection measures. Secondly, due to the limitation of data, this study only considers the impact of internal threat sources on the headquarters but does not evaluate the impact of threat sources outside the study area, so it may affect the evaluation results of HQ. Similarly, previous studies have shown that the internal mechanisms of habitat quality are complex and vary greatly in different regions, which may lead to unclear results. Further research is needed on the accuracy of regional headquarters assessments based on field survey data parameters. In addition, due to the limited data collected, although the resolution of the driver layer data is unified by resampling, there are still some uncertainties in the analysis of the geographic detector model, which needs to be further explored in future studies.

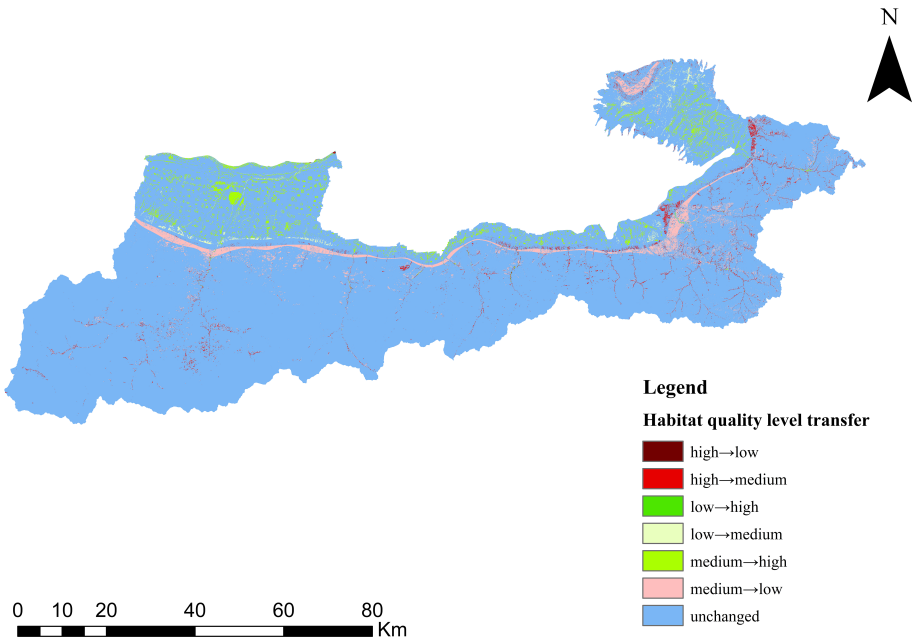

FIGURE 4
Changes in habitat quality transfer at different levels.

Conclusions

This research is completed using the InVEST-HQ model and Geodetector were used to study the spatiotemporal changes of the Xi'an section at the northern foothills of the Qinling Mountains and the factors driving the changes of the headquarters.The main conclusions are as follows:

During 1990–2020, the main land use types in the northern foothills of the Qinling Mountains are forest land, cultivated land, and grassland. The area of cultivated land, grassland, and water area decreased by 16.40%, 74.37%, and 35.39%, respectively, while the area of forest land, construction land, and water increased by 8.47% and 117.70%, respectively.

During 1990–2020, the average habitat quality index in the study area first increased and then decreased. The spatial distribution of habitat quality was high in the south, moderate in the north, and low in the northwest.

The single interactive factor detection results of the geodetic detector show that LULC is the main driving force for the change of HQ, followed by natural factors such as NDVI and altitude. Socioeconomic factors such as population density and GDP are secondary drivers of HQ.

Data availability statement

The original contributions presented in the study are included in the article/Supplementary Material. Further inquiries can be directed to the corresponding author.

Author contributions

LM: Conceptualization, Funding acquisition, Writing – review & editing. CW: Conceptualization, Writing – review & editing. LW: Formal analysis, Methodology, Visualization, Writing – original draft. SJ: Formal analysis, Visualization, Writing – original draft. XK: Software, Writing – original draft.

Funding

The author(s) declare financial support was received for the research, authorship, and/or publication of this article. This work was jointly supported by the Natural Science Basic Research Program of Shaanxi (Program No.2021JLM-56).

Conflict of interest

Authors LM, CW, LW, SJ, and XK were employed by Northwest Engineering Corporation Limited.

Publisher's note

Supplementary material

The Supplementary Material for this article can be found online at: https://www.frontiersin.org/articles/10.3389/fevo.2023.1284281/full#supplementary-material

References

Arunyawat, S., and Shrestha, R. P. (2016). Assessing land use change and its impact on ecosystem services in northern Thailand. *Sustainability* 8 (8), 768. doi: 10.3390/su8080768

Bagstad, K. J., Villa, F., and Johnson, G. W. (2011). *ARIES— artificial intelligence for ecosystem services : A guide to models and data, version 1.0 [R/OL]* (Burlington, VT: ARIES).

Cao, W., Li, R., Chi, X., Chen, N., Chen, J., Zhang, H., et al. (2017). Island urbanization and its ecological consequences: A case study in the Zhoushan Island, East China. *Ecol. Indic.* 76 (may), 1–14. doi: 10.1016/j.ecolind.2017.01.001

Chen, M., Bai, Z., Wang, Q., and Shi, Z. (2021). Habitat quality effect and driving mechanism of land use transitions: a case study of henan water source area of the middle route of the south-to-north water transfer project. *Land* 10. doi: 10.3390/land10080796

Chen, M., Su, X. L., Huang, H. M., and Gao, T. (2019). Assessment of river habitat quality in the Three Gorges Reservoir Region. *Acta Ecologica Sin.* 39 (1), 192–201.

Chen, Y. P. (2019). Significance and strategies on the ecological civilization construction at Qinling Mountains . *J. Earth Environ.* 10 (1), 1–11. doi: 10.7515/JEE182056

Chen, X., Qin, J., Yao, J., Yang, Z., and Li, X. (2023). The distribution and impact characteristics of small-scale carbon emissions in the Chengdu–Chongqing Region. *Atmosphere* 14, 216. doi: 10.3390/atmos14020216

Cui, G., Zhang, Y., Shi, F., Jia, W., Pan, B., Han, C., et al. (2022). Study of spatiotemporal changes and driving factors of habitat quality: a case study of the agro-pastoral ecotone in Northern Shaanxi, China. *Sustainability.* 14 (9), 5141. doi: 10.3390/su14095141

Fan, X., Gu, X., Yu, H., Long, A., Tiando, D. S., Ou, S., et al. (2021). The spatial and temporal evolution and drivers of habitat quality in the hung river valley. *Land.* 10, 1369. doi: 10.3390/land10121369

Han, R., Chen, C., Li, Y., Wen, Z., Li, Z., Li, W., et al. (2023). Response of vegetation coverage to climate changes in the qinling-daba mountains of China. *Forests* 14 (2), 425. doi: 10.3390/f14020425

He, N., Guo, W., Wang, H., Yu, L., Cheng, S., Huang, L., et al. (2023). Temporal and spatial variations in landscape habitat quality under multiple land-use/land-cover scenarios based on the PLUS-InVEST model in the Yangtze River Basin, China. *Land* 12, 1338. doi: 10.3390/land12071338

Hou, Y., Kuang, W., and Dou, Y. (2022). Analysis of urban expansion and fractal features in global 33 megacities from 2000-2020. *Acta Geographica Sinic.* 77 (11), 2687–2702.

Huang, M. Y., Yue, W. Z., Feng, S. R., and Zhang, J. H. (2020). Spatial-temporal evolution of habitat quality and analysis of landscape patterns in Dabie Mountain area of west Anhui Province based on InVEST model. *Acta Ecologica Sinic.* 40 (9), 2895–2906. doi: 10.5846/stxb201904260858

Jing, Y., Maogui, H. U., and Shaoying, Z. (2017). Influencing mechanism of spatial distribution difference in national γ Radiation dose rate based on geographical detector. *J. Geo-Information Sci.* 19 (5), 625–634. doi: 10.3724/SP.J.1047.2017.00625

Li, C. X., Gao, X., and Xi, Z. L. (2019). Characteristics, hazards, and control of illegal villa (houses): evidence from the Northern Piedmont of Qinling Mountains, Shaanxi Province, China. *Environ. Sci. pollut. Res.* 26, 21059–21064. doi: 10.1007/s11356-019-05515-1

Li, S., Zhang, H., Zhou, X., Yu, H., and Li, W. (2020b). Enhancing protected areas for biodiversity and ecosystem services in the Qinghai–Tibet Plateau. *Ecosystem Services* 43, 101090. doi: 10.1016/j.ecoser.2020.101090

Li, S., Liu, J., Lin, J., and Fan, S. L. (2020a). Spatial and temporal evolution of habitat quality in Fujian Province, China based on the land use change from 1980 to 2018. *Chin. J. Appl. Ecol.* 31 (12), 4080–4090. doi: 10.13287/j.1001-9332.202012.019

Li, Y., Vina, A., Yang, W., Chen, X. D., Zhang, J. D., Ouyang, Z. Y., Liang, Z., and Liu, J. G. (2013). Effects of conservation policies on forest cover change in giant panda habitat regions, China. *Land Use Policy.* 33, 42–53. doi: 10.1016/j.landusepol.2012.12.003

Li, Z., Hou, P., Jiang, W. G., Wang, X Y., and Hou, J. (2023). The driving effect of land use changes on ecosystem services:a case study at the Qinling Natural Reserve. *J. Beijing Normal Univ. (Natural Science)* 59 (02), 196–205. doi: 10.12202/j.0476-0301.2022034

Liu, S. T., Niu, X., Wang, B., Song, Q. F., and Tao, Y. Z. (2018). An ecological benefit assessment of the Grain for Green Project in Shaanxi Province. *ActaEcologicaSinica* 38 (16), 5759–5770. doi: 10.5846/stxb201707261342

Ma, L., Hong, Y., Chen, X., and Quan, X. (2022). Can green innovation and new urbanization be synergistic development empirical evidence from yangtze river delta city group in China. *Sustainability* 14 (10), 1–21. doi: 10.3390/su14105765

Ma, X., Bai, H., Deng, C., and Wu, T. (2019). Sensitivity of vegetation on alpine and subalpine timberline in qinling mountains to temperature change. *Forests* 10 (12), 1105. doi: 10.3390/f10121105

Moreina, M., Fonseca, C., Vengilio, M., Calado, H., and Gil, A. (2018). Spatial assossment of habitat conservation status in a Macaronesian island based on theInVEST model: a case study of Pico Island (Azores, Portugal). *Land Use Policy.* 78, 637–649. doi: 10.1016/j.landusepol.2018.07.015

Muñoz-Barcia, C. V., Lagos, L., Blanco-Arias, C. A., Díaz-Varela, R., and Fagúndez, J. (2019). Habitat quality assessment of Atlantic wet heathlands in Serra do Xistral, NW Spain. *Cuadernos Investigación Geográfica.* 45 (2), 533–549. doi: 10.18172/cig.3628

Mushet, D. M., Neau, J. L., and Euliss, N. H. (2014). Modeling effects of conservation grassland losses on amphibian habitat. *Biol. Conserv.* 174, 93–100. doi: 10.1016/j.biocon.2014.04.001

Newbold, T., Hudson, L. N., Hill, S. L. L., Contu, S., Lysenko, L., Senior, R. A., et al. (2015). Global effects of land use on local terrestrial biodiversity. *Nature* 520 (7545), 45–50. doi: 10.1038/nature14324

Ning, Y. Z., Zhang, F. P., Feng, Q., Wei, Y. F., Ding, J. B., and Zhang, Y. (2020). Temporal and spatial variation of water conservation function in Qinling Mountain and its influencing factors. *Chin. J. Ecol.* 39 (9), 3080–3091. doi: 10.13292/j.1000-4890.202009.031

Pan, Y., Yin, Y., Hou, W., and Han, H. (2022). Spatiotemporal variation of habitat quality in the source region of the Yellow River based on land use and vegetation cover changes. *Acta Ecologica Sin.* 32 (19), 1–11. doi: 10.5846/stxb202105131254

Qianqian, W., Mukadasi, A., Abudureheman, H., Kaixuan, Y., Lei, Y., Hua, T., et al. (2022). Temporal and spatial variation analysis of habitat quality on the PLUS-InVEST model for Ebinur Lake Basin, China. *Ecol. Indicators.* 145, 109632. doi: 10.1016/j.ecolind.2022.109632

Qu, Z., Zhao, Y., Luo, M., Han, L., Yang, S., and Zhang, L. (2022). The effect of the human footprint and climate change on landscape ecological risks: A case study of the loess plateau, China. *Land.* 11 (2), 1–19. doi: 10.3390/land11020217

Sallustio, L., De Toni, A., Strollo, A., Febbraro, M. D., Gissi, E., Casella, L., et al. (2017). Assessing habitat quality in relation to the spatial distribution of protected areas in Italy. *J. Environ. Management.* 201 (oct.1), 129. doi: 10.1016/j.jenvman.2017.06.031

Sharp, R., Douglass, J., Wolny, S., Arkema, K., Bernhardt, J., Bierbower, W., et al. (2020). *InVEST 3.8.7. User's Guide; Collaborative Publication by the Natural Capital Project, Stanford University, University of Minnesota, the Nature Conservancy, World Wildlife Fund.* (Stanford, CA, USA: Stanford University).

Sherrouse, B. C., Semmens, D. J., and Clement, J. M. (2014). An application of Social Values for Ecosystem Services (SolVES) to three national forests in Colorado and Wyoming. *Ecol. Indic.* 36, 68–79. doi: 10.1016/j.ecolind.2013.07.008

Shu-Yan, Y. (2002). Studies on the climate changes in the northern and the southern regions of the qinling mountains and correlated analysis between climate changes and el nino/la nina phenomenon during the recent 40 years. *J. Mountain Res.* 20 (4), 493–496. doi: 10.1002/mop.10502

Silvis, H. (2012). The economics of ecosystems and biodiversity in national and international policy making. *Eur. Rev. Agric. Economic* 39 (1), 186–188. doi: 10.1093/erae/jbr052

Sun, Y., Guan, Q., Wang, Q., Yang, L., Pan, H., Ma, Y., et al. (2021). Quantitative assessment of the impact of climatic factors on phenological changes in the Qilian Mountains, China. *For. Ecol. Management.* 499 (7), 119594. doi: 10.1016/j.foreco.2021.119594

Ting, L., Liu, K., Sheng, H. U., and Bao, Y. B. (2014). Soil erosion andecological benefits evaluation of Qinling Mountains based on the InVEST model. *Resour. Environ. Yangtze Basin* 23 (9), 1242–1250.

Wang, B., and Cheng, W. (2022). Effects of land use/cover on regional habitat quality under different geomorphic types based on InVEST model. *Remote Sens.* 14, 1279. doi: 10.3390/rs14051279

Wu, L., Sun, C., and Fan, F. (2021). Estimating the characteristic spatiotemporal variation in habitat quality using the inVEST model—A case study from Guangdong–Hong Kong–Macao greater bay area. *Remote Sens.* 13 (5), 1008. doi: 10.3390/rs13051008

Wynne, S. P., and Côté, I. M. (2007). Effects of habitat quality and fishing on Caribbean spotted spiny lobster populations. *Appl. Ecol.* 44, 488–494. doi: 10.1111/j.1365-2664.2007.01312.x

Yang, H., Huang, Q., Zhang, J., Songer, M., and Liu, J. (2021a). Range-wide assessment of the impact of China's nature reserves on giant panda habitat quality. *Sci. Total Environment.* 769, 145081. doi: 10.1016/j.scitotenv.2021.145081

Yang, Z., Wang, S., Guo, M., Tian, J., and Zhang, Y. (2021b). Spatiotemporal differentiation of territorial space development intensity and its habitat quality response in Northeast China. *Land.* 10, 573. doi: 10.3390/land10060573

Zhang, H. J., Gao, Y., Hua, Y. W., Zhang, Y., and Liu, K. (2019). Assessing and mapping recreationists' perceived social values for ecosystem services in the Qinling Mountains, China. *Ecosystem Services.* 39, 101006. doi: 10.1016/j.ecoser.2019.101006

Zhang, X., Zhang, B., Yao, Y., Wang, J., Yu, F., Liu, J., et al. (2022b). Dynamics and climatic drivers of evergreen vegetation in the Qinling-Daba Mountains of China. *Ecol. Indicators.* 136, 108625. doi: 10.1016/j.ecolind.2022.108625

Zhang, X., Lyu, C., Fan, X., Bi, R., Xia, L., Xu, C., et al. (2022a). Spatiotemporal variation and influence factors of habitat quality in loess hilly and gully area of yellow river basin: a case study of Liulin County, China. *Land.* 11 (1), 1–17. doi: 10.3390/land11010127

Zhang, X., Zhou, J., and Li, M. (2020). Analysis on spatial and temporal changes of regional habitat quality based on the spatial pattern reconstruction of land use. *Acta Geographica Sinica.* 75 (1), 160–178. doi: 10.11821/dlxb202001012

Zhang, Y. B., Wang, Y. Z., Phillips, N., Ma, K. P., Li, J. S., and Wang, W. (2017). Integrated maps of biodiversity in the Qinling Mountains of China for expanding protected areas. *Biol. Conserv.* 210, 64–71. doi: 10.1016/j.biocon.2016.04.022

Zhang, S. H., Zhou, Y. K., Yu, Y., Li, F., Zhang, R., and Li, W. (2022). Using the Geodetector method to characterize the spatiotemporal dynamics of vegetation and its interaction with environmental factors in the Qinba Mountains, China. *Remote Sens.* 14 (22), 5794. doi: 10.3390/rs14225794

Zhao, F., Lan, X., Li, W., Zhu, W., and Li, T. (2021). Influence of land use change on the surface albedo and climate change in the qinling-daba mountains. *Sustainability* 13 (18), 1–15. doi: 10.3390/su131810153

Zhou, Z. X., and Li, M. T. (2017). Spatial-temporal change in urban agricultural land use efficiency from the perspective of agricultural multi-functionality: a case study of the Xi'an metropolitan zone. *J. Geographical Sci.* 27, 1499–1520. doi: 10.1007/s11442-017-1449-6

frontiers | Frontiers in Ecology and Evolution

TYPE Original Research
PUBLISHED 18 December 2023
DOI 10.3389/fevo.2023.1319815

OPEN ACCESS

EDITED BY
Xue-Chao Wang,
Beijing Normal University, China

REVIEWED BY
Guoen Wei,
Nanchang University, China
Pengyan Zhang,
Henan University, China

*CORRESPONDENCE
Linglin Xie
xll@img.net

RECEIVED 11 October 2023
ACCEPTED 10 November 2023
PUBLISHED 18 December 2023

CITATION
Li P, Liao Y, Huang C, Yi L and Xie L (2023) Evolution and zoning of spatial ecosystem functional stability in the southern hilly region of China: a "structure–function" perspective.
Front. Ecol. Evol. 11:1319815.
doi: 10.3389/fevo.2023.1319815

Evolution and zoning of spatial ecosystem functional stability in the southern hilly region of China: a "structure–function" perspective

Peijin Li[1], Yixin Liao[2], Chen Huang[1], Lang Yi[1] and Linglin Xie[3]*

[1]School of Engineering Management, Hunan University of Finance and Economics, Changsha, China, [2]College of Natural Resources and Environment, South China Agricultural University, Guangzhou, Guangdong, China, [3]Key Laboratory of Natural Resources Monitoring and Supervision in Southern Hilly Region, Ministry of Natural Resources, Changsha, China

Introduction: A series of significant ecological construction projects in the southern hilly region have brought about substantial changes to the ecological status and comprehensive zoning of the region. Hunan Province, with its strategic significance, was chosen as a representative research subject in the southern hilly region.

Methods: We conducted a dynamic evaluation of the ecological status change and comprehensive zoning of Hunan Province from a structure–function perspective by applying the transfer matrix, Theil-Sen, Mann-Kendall, and ecosystem service trade-offs or synergies methods. The research goal was to integrate and harmonize structural complexity and functional diversification, providing valuable insights for optimizing both ecological background and territorial background.

Results: The main results are as follows: (1) The structural changes of ecosystems were mainly concentrated in settlement and Cropland ecosystems. While the area of bulti-up ecosystems has increased significantly, from 1.34% in 2000 to 2.72% in 2020. Cropland ecosystems marking a decrease of 1.39%, with a continued conversion of Cropland into construction land ecosystems. (2) Ecosystem function changes have introduced instability. Over time, NPP exhibited an oscillating trend of increase followed by a decrease. Spatially, there was a sharp decline in peripheral building land, and the regions of declining NPP displayed a lateral U-shaped distribution. (3) The overall trend in ecosystem service changes was positive. Quantitatively, GP and CS experienced an ascending-then-decreasing pattern, while HQ showed a weak decline and WY increased annually. At the county scale, there was noticeable spatial heterogeneity. Human socio-economic activities and environmental protection policies exert a significant impact on the ecological conditions within the study area. (4) Regarding the national territory space function partition, urban functional zones have primarily catered to residential functions and were mainly distributed in the Changsha-Zhuzhou-Xiangtan area.

Discussion: Ecological functional zones were mainly centered on ecological functions, and most were located in the mountainous areas of western and southern Hunan Province. The agricultural function areas were mainly to serve production functions and were mainly located in the Dongting Lake Plain, the nearshore plain of the mainstream and tributary systems of the rivers of Xiang, Zi, Yuan, and Li. In general, the changes in ecosystem structure and function in the study area reflect changes in ecological conditions. In the future, ecosystem diversity, stability, and sustainability should be improved from an integrated structure–function perspective.

KEYWORDS

southern hilly region, structure and function, ecosystem service clusters, national territory space function, ecosystem pattern transfer

1 Introduction

The analysis of changes in ecological status constitutes a pivotal model for the comprehensive assessment of ecosystems. These changes are primarily influenced by natural and human factors, resulting in significant changes in ecosystem structure, function, and services (Hou et al., 2015; He et al., 2021; Liu G.B. et al., 2023), such as the loss of Cropland (Zhu et al., 2022), fragmentation of landscape structure (Peng et al., 2017), and reduction of habitat quality (Ouyang and Zhu, 2020), among others. Ecosystem services, which emerge directly or indirectly from functioning (Hou et al., 2015), embody another facet of this functioning. Therefore, it is crucial to quantify the state of regional ecosystems from both structural and functional perspectives. This understanding is essential for evaluating regional high-quality development, optimizing regional territorial spatial planning, and making informed decisions.

As the primary determinant shaping the context and spatial variations of ecosystem function, ecosystem structure reveals the spatial distribution patterns of its internal subsystems and their spatial structural interrelationships (Xu et al., 2008; Ouyang et al., 2023). Ecosystem structure refers to the proportionality or composition of various ecosystems at a given scale. Ecosystem function can be represented by three key axes: maximum productivity, water utilization strategy, and carbon utilization strategy. When describing the condition of an ecosystem, the structure and function approach takes both aspects into account. The foremost key axis, contributing the most significantly, represents the ecosystem's maximum productivity and is mainly affected by vegetation structure (Migliavacca et al., 2021). Consequently, it is paramount to unveil changes in ecological status from both structural and functional perspectives in order to achieve integrated governance of ecosystem systems. This approach offers theoretical and practical reference values for the overall protection and synergistic governance of social-ecological systems (Dan et al., 2020; Wei et al., 2023a). To reinforce the cohesion and systemic coherence of ecosystems, fostering mutual feedback between their structure and function is needed. Many scholars have extensively investigated changes in ecological conditions from the perspectives of ecosystem structure and ecosystem function. Based on the ecosystem structure perspective, it is evident that frequent human activities can result in significant alterations in land use type, thereby impacting the landscape and ecosystem health of the region. Existing literature mainly employs methods such as the transfer matrix (Li et al., 2023; Zhang et al., 2023) and landscape pattern index (Liu et al., 2022b; Chen et al., 2023; Wei et al., 2023b). For example, the ecosystem transfer matrix was used to reveal temporal and spatial changes in the ecosystems of the Yellow River Basin over the past 35 years. The benefit transfer method and elasticity coefficient were utilized to evaluate their impact on ecosystem service values (Liu et al., 2021). Additionally, the landscape pattern index was used to construct an ecosystem health evaluation system for wetlands in the urban area of Xiongan, exploring its landscape pattern and ecological health status (Xu et al., 2020). As for the ecosystem function perspective, it can be categorized into methods evaluating value quantity and those evaluating physical quality (Zhao et al., 2023). For instance, the ecosystem service value equivalent factor was applied to estimate the ecosystem service value of known land use areas (Shi et al., 2022; Zhou et al., 2022). Using variables like NPP, water retention services, and habitat quality, the spatial pattern of ecosystem service functions in the Beijing-Tianjin-Hebei region was modeled. Next, the region's raster-scale ecosystem health variations were assessed (Ning et al., 2021). On the other hand, there are researchers who perceive ecosystem service clusters from a different perspective (Pan et al., 2021; Zhang et al., 2021; Liu et al., 2022b). Ecosystem service clusters encompass collections of ecosystem services occurring in close proximity in space (Li et al., 2016). They assist in coordinating the composite functional zoning of territorial space and support the overall optimization and improvement of local ecosystems. In particular, Zhang Chunyue et al. used K-Mean cluster analysis to identify clusters of ecosystem services and examined their synergistic relationships to improve the comprehensive ecosystem service capacity of the study area (Zhang et al., 2021). Likewise, Pan Ying et al. utilized the PAM module within the "cluster" package of the R language to conduct cluster

analysis of ecosystem services in the Daqing River Basin, identifying driving factors (Pan et al., 2021).

The structure and function of ecosystems are essential elements for partitioning the functions of national territory space, in line with the objective of achieving high-quality development. This comprehension stands as a pivotal aspect to understanding the evolution of ecological conditions and enabling comprehensive national territory space function partitioning. Some scholars have suggested that single dominant function zoning is inadequate in the current literature on qualitative analysis, and that the new era of territorial spatial function classification should be divided into multifunctional mixed zoning and combined with spatially secondary functions (Zou et al., 2022; Hu et al., 2023). In quantitative research, ecosystem macro-structure, NDVI, and NPP were used to examine changes in the ecological status of different principal functional zones within the Yangtze River Economic Zone (Wu et al., 2018).Remote sensing classification data was used to measure the ecological function, and its value was calibrated by integrating ecosystem service values. Consequently, the spatial function of land within Henan Province was evaluated, and the functional zoning was subsequently established based on the two-dimensional graph theory clustering algorithm (Zhou et al., 2020).

In general, numerous findings have emerged from studies focusing on ecosystem change through a single perspective of either structure or function. However, a comprehensive understanding of how ecosystem conditions evolve under the integrated structure–function perspective requires further investigation, particularly in terms of the synergistic effect of ecosystem structure and function on the functional zoning of land space. As a result, this study concentrates on addressing the following scientific issues: (1) how to characterize ecosystem changes from a structure–function perspective; (2) how to delineate different integrated functional regions from a service cluster perspective. The southern hilly mountainous belt stands as a significant ecological security barrier in southern China, containing the world's largest and most well-preserved meso-subtropical woodland ecosystems within the same latitudinal belt (Ma et al., 2021). Based on this, this paper employed methodologies, such as the transfer matrix and ecosystem service trade-offs or synergy, to reveal the spatio-temporal dynamic change patterns of ecosystem conditions and identify integrated functional areas in Hunan Province between 2000 and 2020. The ultimate goal is to furnish a scientific and theoretical foundation for ecological construction and planning within the context of the southern hilly mountainous belt.

2 Overview of the study area

The southern hilly region, which encompasses seven provinces: Zhejiang, Fujian, Jiangxi, Hunan, Guangdong, Guangxi, and Guizhou (Figure 1), is characterized by a wealth of heat and water and pleasant temperatures due to its subtropical monsoon climate. The southern hilly areas have made immeasurable contributions to the ecological security of China's southern region as an integral part of the country's "two screens and three belts" ecological pattern. They also play an indispensable role in exploring the spatial functional zoning of the country's land and fostering the high-quality development of the southern region.

Hunan Province is situated between latitude 24°38′–30°08′N and longitude 108°47′–114°15′E, sharing borders with Chongqing and Guizhou in the west, Jiangxi in the east, Guangxi and Guangdong in the south, and Hubei in the north (Figure 1), covering a total land area of 211,800 km^2. The majority of its landforms are mountains and hills, including the Mufu-Luoxiao mountain range in the east, the Nanling mountain range in the south, the Wuling and Xuefeng Mountains in the west, and the Dongting Lake Plain in the north (Zheng et al., 2023). The province's center consists of hills and valleys, a dense network of rivers, and well-established water systems across Hunan (Chen et al., 2019). In 2022, the GDP of Hunan Province was 4,867.037

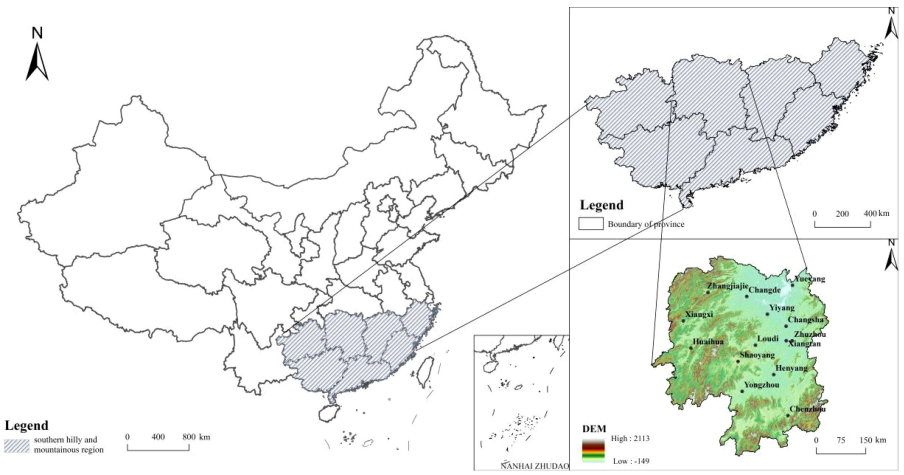

FIGURE 1
Schematic location diagram of Hunan Province.

billion yuan, with a resident population of 66.220 million people. The province contains 122 county-level divisions and 14 prefectural-level administrative districts. Being a key development axis in the central region, Hunan Province boasts diverse ecosystem types and performs ecosystem service activities such as water conservation, regional climate regulation, and biodiversity maintenance. It also serves as a significant ecological reserve and water conservation area in the southern hilly region, with its favorable ecological environment being essential for maintaining and sustaining regional ecosystem functions (Xiong et al., 2020). To provide an ecological foundation and a national territory foundation for the thorough implementation of the significant strategy of "three highs and four news" in Hunan Province, it is of utmost importance to study how to integrate changes in ecological conditions and spatial functional zoning of the national territory.

3 Data sources and processing and research methods

3.1 Data sources

The data utilized in this study primarily consists of the following: Social and natural economic development datasets were predominantly sourced from the Hunan Statistical Yearbook (2000–2020) and the China Meteorological Data Network.

(1) Ecosystem-type datasets were primarily ecosystem-type records for Hunan Province spanning from 2000, 2005, 2010, 2015, and 2020. The datasets were obtained from the Resource and Environmental Science and Data Center of the Chinese Academy of Sciences, accessible through the specific website (https://www.resdc.cn/). The spatial resolution was set at 0.03 km, with the transfer matrix generated post-processing using ArcGIS 10.2. This classification involves referencing the "Third National Land Survey Land Classification" alongside relevant findings pertaining to ecosystem-type divisions. The classification encompasses various types, including cropland, woodland, grassland, built-up, and waterbody, among others.

(2) Nighttime light data were acquired from the National Earth System Science Data Center (http://geodata.nnu.edu.cn/). The data processing procedure involves utilizing the Sigmoid function conversion, resampling SNPP-VIIRS data, and splicing DMSP-OLS from the Colorado School of Mines (http://eogdata.mines.edu/nighttime_light/) to obtain China-wide DMSP-OLS (1 km) spanning from 2000 to 2020.

(3) Net primary productivity (NPP) data from 2000 to 2020 were derived from the National Aeronautics and Space Administration MOD17A3HGFd dataset, which featured a spatial resolution of 0.5 km. The resolution was harmonized to 1 km for consistency

3.2 Research methods

3.2.1 Ecosystem pattern transfer matrix

The conversion link between ecosystem patterns in Hunan Province was examined at the start and the conclusion of the study period using the transfer matrix of the ecosystem pattern (Shi et al., 2000):

$$S_{ij} = \begin{vmatrix} S_{11} & S_{12} & \cdots & S_{1n} \\ S_{21} & S_{22} & \cdots & S_{2n} \\ \cdots & \cdots & \cdots & \cdots \\ S_{n1} & S_{n1} & \cdots & S_{nn} \end{vmatrix} \quad (1)$$

In the above equation, n is the number of ecosystem types; i, j refers to the ecosystems at the beginning and end of the study period; S_{ij} denotes the area where ecosystem type i was transferred to ecosystem type j during the study period.

3.2.2 Trend analysis of NPP changes

We examined the variations in vegetation NPP characteristics within Hunan Province using the Theil-Sen median trend analysis. Among these, the Theil-Sen median trend analysis employs the median function to generate the detection factor, signifying a reliable nonparametric calculation method unaffected by measurement errors and outlier data. This approach is commonly used for trend analysis of extensive time series data (Wan et al., 2023):

$$\beta = Median\left(\frac{NPP_i - NPP_j}{i - j}\right) \quad (2)$$

In the above equation, NPP_i and NPP_j denote the NPP values of the sample time series iand j, respectively; β denotes the median of the slopes for calculating $\frac{n(n-1)}{2}$ data combinations.

The Mann-Kendall significance test is a nonparametric statistical test that is unaffected by missing values and outliers and does not require that the measurement data follow a normal distribution or that the trend be linear (Wan et al., 2023):

$$S = \sum_{i=1}^{n-1} \sum_{j=i+1}^{n} \mathrm{sgn}(x_j - x_i) \quad (3)$$

$$\mathrm{sgn}(x_j - x_i) = \begin{cases} +1, x_j - x_i > 0 \\ 0, x_j - x_i = 0 \\ -1, x_j - x_i < 0 \end{cases} \quad (4)$$

$$Z = \begin{cases} \frac{S-1}{\sqrt{VAR(S)}}, S > 0 \\ 0, S = 0 \\ \frac{S+1}{\sqrt{VAR(S)}}, S < 0 \end{cases} \quad (5)$$

$$Var(S) = \frac{n(n-1)(2n+5) - \sum_{i=1}^{m} t_i(t_i-1)(2t_i+5)}{18} \quad (6)$$

The test statistics (*S*and *S*), the number of replicated data sets in the study time series (m), the number of repetitious data in the i_{th} set of replicated data (t_i), and the variance of *S* (*V*ar(*S*)) are all included in Equations (3–6). When the absolute value of *Z* is greater than 1.96 or 1.65, the significance test is considered to have been successfully conducted with a 95% or 90% confidence level. When the value is greater than 0, the table NPP displays an increasing trend; when the value is 0, a falling trend.

3.2.3 Ecosystem service clusters

The Self-Organizing Feature Mapping network (SOFM) is a neural network approach used in this study for unsupervised learning. It identifies ecosystem service clusters at the county scale and assigns each county unit to an ecosystem service cluster based on the spatial co-occurrence similarity of ecosystems (Xia et al., 2023). In order to guarantee consistency and comparability of defined ecosystem service clusters across a 20-year period, the SOFM implementation used normalized values for ecosystems of the same scale.

Food production exhibited inconsistency across different land-use types, and we evaluated the region's food supply capacity by converting food mass into corresponding energy (kJ/kg). (Li et al., 2016; Zhang et al., 2017). When combined with land cover data and biodiversity threat indicators, the InVEST model's Habitat Quality module serves as raster data. (Di Febbraro et al., 2018). To assess carbon storage in each cell, the InVEST model analyzes carbon densities and maps for each land-use type (Natural Capital Project, 2023). The InVEST model's water yield service module is based on Budyko's coupled hydrothermal equilibrium assumption. (Zhu et al., 2023). Water yield service typically represents the difference between precipitation and evapotranspiration, which measures the ecosystem's supply water capability.

The "Kohonen" package in R4.0 software was used to run SOFM, clustering and analyzing five distinct ecosystem services: food production, nighttime light index, habitat quality, carbon storage, and water yield service, across 122 counties (urban areas) throughout the entire study area in 2000, 2010, and 2020. These specific indexes are detailed in Table 1. Based on the features of each cluster's ecosystem services, they were designated as urban functional area, agricultural functional area, and ecological functional area (Zhang et al., 2019; Hu et al., 2022; Niu et al., 2022; Qiu et al., 2023). Radar diagrams were created to depict the ecosystem service cluster structures. SOFM has the advantage of being more stable and insensitive while dealing with a larger amount of data than general K-mean cluster analysis.

TABLE 1 Comprehensive zoning evaluation index system.

Function	Indicators	Explain	Calculation methods or Data sources
Production function	Grain production (GP)	Refers to the production of grain from agricultural land.	References (Li et al., 2016; Zhang et al., 2017)
Life function	Nighttime lights index (NLs)	Reflect the degree of economic growth to a certain extent.	References (Wu et al., 2022)
Ecological function	Ecologically functional habitat quality (HQ)	Reflect biodiversity in the region.	References (Di Febbraro et al., 2018; Natural Capital Project, 2023; Zhu et al., 2023)
	Carbon storage(CS)	Provide a variety of basic ecosystem services.	
	Water yield service(WY)	represents the surface water yield in the study area.	

HQ, habitat quality; WY, water yeild; GP, grain production; CS, carbon storage; NLs, nighttime lights.

3.2.4 Driving factor analysis

Several factors collaborate to influence changes in ecosystem conditions. These variables include those that are intrinsic to ecosystem changes, like temperature and precipitation; extrinsic variables, like human activity; and changes in ecosystem patterns, which are subject to the effect of national policy (Di Febbraro et al., 2018). In this study, the anthropogenic disturbance index was used to assess the impact of human activities on ecosystem conditions changes in Hunan Province. The least squares method was employed to analyze interannual trends in natural factors like temperature and precipitation.

Given that human activities affect different ecosystems to varying degrees, causing varying levels of disturbance, such as minimal disturbance to unutilized land and substantial disturbance to cropland, hierarchical assignments were assigned to each ecosystem. Anthropogenic disturbance indices were categorized into four levels (as shown in Table 2) based on the degree of disruption to different ecosystems. This categorization is referenced in the study by Zhao et al. (Zhao et al., 2023).

For a given region, ecosystem types with multiple disturbance grading indices generally exist simultaneously. Therefore, the composite human disturbance index for ecosystems in the region is calculated through a weighted summation method, resulting in a composite human disturbance index for ecosystems between 0 and 3:

$$D = \frac{\sum_{i=0}^{3} A_i \times P_i}{3\sum_{i=1}^{n} P_i} \tag{7}$$

In the above equation, *D* is the human disturbance index, A_i denotes the grading index of the ecosystem at level, and P_i denotes the percentage of area of the ecosystem at level i.

4 Results and analysis

4.1 Macro-structural change of the ecosystem

During the study period, significant changes occurred in various ecosystems (see Table 3). Notably, cropland ecosystems experienced

TABLE 2 Grading scale of human disturbance.

Type	Natural unused land	Natural regeneration	Anthropogenic regeneration	Anthropogenic non-regeneration
Ecosystem type	Unused land	Woodland, Grassland, Waterbody	Cropland	Built-up land
Disturbance grading index	0	1	2	3

a continuous 1.39% decline, equivalent to 2948.14 km^2, from 2000 to 2020. In contrast, bulti-up ecosystems spatially expanded by 2917.82 km^2, growing from 1.34% in 2000 to 2.72% in 2020. Woodland ecosystems and waterbody ecosystems increased slightly in their respective areas, with no substantial alterations observed. Grassland ecosystems continued to decrease, covering an area of 679.6 km^2. The area of unused land exhibited a fluctuating pattern, initially increasing and then decreasing, ultimately covering an area of 989.87 km^2 in 2020, accounting for only 0.47% of the total land area within the study area.

To illustrate the configuration of each ecosystem's land use type and the corresponding transitions occurring within Hunan Province from 2000 to 2020, this study employed a transfer matrix. The results of ecosystem transfers were then visually represented through a chordal diagram (Figures 2A–D). Within the four phases of ecosystem area transformation, the primary interchanges involved cropland and woodland, exhibiting bidirectional conversion attributes.

From 2000 to 2005, land-use conversion was significant, equivalent to 1.07% of the total area. This indicates the high intensity of human activities affecting land use during the study period, resulting in notable land-use alterations. Specifically, the principal conversions comprised cropland and woodland, totaling 1122.88 km^2 and 808.28 km^2, accounting for 49.36% and 35.53% of the transferred area, respectively. Notably, cropland mainly shifted to woodland, encompassing an area of 696.96 km^2, while woodland primarily converted to cropland, encompassing 542.08 km^2.

From 2005 to 2010, this phase predominantly followed the trajectory of ecosystem area conversion from the previous stage. The main types of conversion remained cropland(3,291.2 km^2) and woodland (1,747.24 km^2), accounting for 46.19% and 24.5% of converted areas, respectively. Cropland was primarily converted to woodland (1,931.16 km^2) and built-up land (745.36 km^2). This pattern aligns with the ongoing "Return Farmland to woodlands" initiative, which has already made a substantial impact. woodland, amounting to 556.6 km^2, was converted into built-up land as well, primarily driven by rapid urban development and the need for expanded built-up land areas, resulting in the encroachment on both cropland and woodland ecosystems.

From 2010 to 2015, the majority of conversions consisted of cropland (3,571.92 km^2) and grassland (484 km^2), accounting for 48.64% of the total transfer area. Grassland shifted mainly to woodland, while cropland was primarily converted to woodland (2691.04 km^2) and built-up land(454.96 km^2), showcasing the significant impact of the farmland-to-woodland conversion. A smaller amount of land was converted between 2015 and 2020, with the majority undergoing conversions to cropland (2,350.88 km^2) and woodland(2,550.22 km^2). During this stage, the transitions involved reciprocal conversions between cropland and woodland, with a substantial portion being converted into built-up land(1,258.25 km^2), reflecting the continued expansion of built-up land. Additionally, there was an increase in the proportion of waterbody ecosystem area, aligning with the effectiveness of returning cropland to water.

4.2 Spatiotemporal change of ecosystem function

4.2.1 Temporal variation characteristics of vegetation NPP

Figure 3 illustrates the trend in the annual average vegetation NPP within the study area from 2000 to 2020, demonstrating a noticeable upward trajectory ($p<0.01$). The trend exhibits a rate of 2.96 $gC/m^2/a$ and a mean value of 603.47 $gC/m^2/a$ for the given study period. This value is comparable to the estimated 2000–2019

TABLE 3 Land use types and proportions of land in Hunan Province from 2000 to 2020.

Ecosystem type	In 2000		In 2005		In 2010		In 2015		In 2020	
	Area(km^2)	%	Area(km^2)	%	Area(km^2)	%	Area(km^2)	%	Area(km^2)	%
Cropland ecosystem	62108.90	29.32	61746.57	29.15	60061.99	28.36	59695.20	28.18	59160.76	27.93
Woodland ecosystem	131399.80	62.04	131290.38	61.98	132335.08	62.48	132099.57	62.37	131772.25	62.21
Grassland ecosystem	7570.20	3.57	7553.48	3.57	6997.67	3.30	6946.73	3.28	6890.60	3.25
Waterbody ecosystem	7140.73	3.37	7314.05	3.45	7175.41	3.39	7202.87	3.40	7236.81	3.42
Built-up ecosystem	2847.19	1.34	3195.09	1.51	4241.64	2.00	4866.86	2.30	5765.01	2.72
Unused ecosystem	746.34	0.35	715.00	0.34	1003.11	0.47	1002.68	0.47	989.87	0.47

10.3389/fevo.2023.1319815

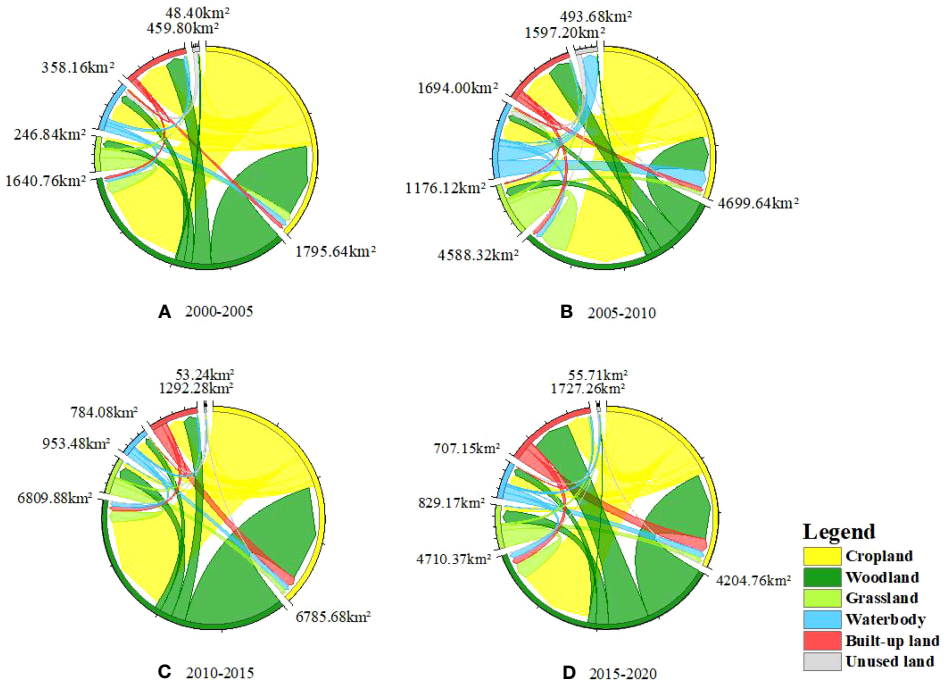

FIGURE 2
Ecosystem transfer in Hunan Province from 2000 to 2020. **(A)** 2000–2005, **(B)** 2005–2010, **(C)** 2010–2015, and **(D)** 2015–2020.

vegetation NPP of 566.92 gC/m^2/a, as assessed by Yan Yan et al. (2022) utilizing the CASA model. By including the mean NPP value for 2020, the present study's mean value increased to 625.37 gC/m^2/a. The highest value, 658.62 gC/m^2/a, was observed in 2015, while the lowest value, 549.97 gC/m^2/a, was recorded in 2000, reflecting a variation of 108.65 gC/m^2/a. From 2000 to 2015, there was an upward oscillation, whereas from 2015 to 2020, a downward oscillation was observed.

Figure 4 presents the distribution of the annual average vegetation NPP area share across different classes within the study

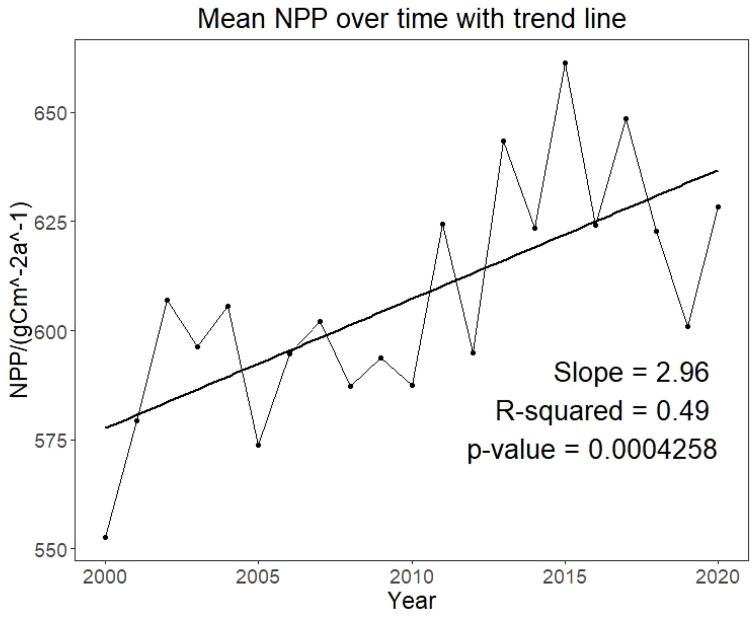

FIGURE 3
Inter-annual trend of NPP in Hunan Province, 2000–2020.

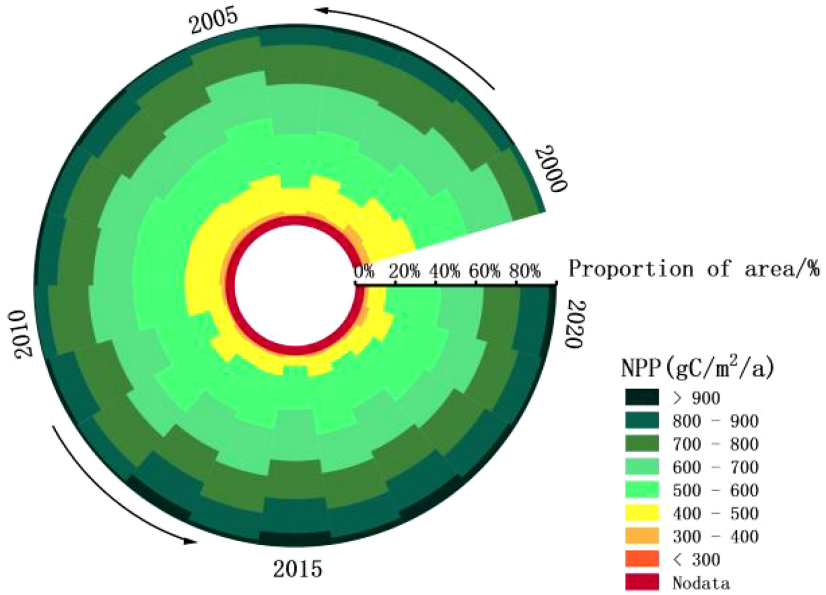

FIGURE 4
Circumferential stacking of NPP area share in Hunan Province, 2000–2020.

area from 2000 to 2020. This distribution can be divided into three subperiods based on their change characteristics: (1) The period 2000–2002 represents the growth phase, during which the area with NPP>500 experienced a 15.18% increase. (2) The period from 2003 to 2010 is characterized as the stabilization period, in which the area share of different grades remained within a narrow range. The maximum increase was 5.61%, and the maximum decrease was −5.18%, corresponding to the 400–500 range in 2003–2004 and 2004–2005, respectively. (3) The period from 2011 to 2020 can be viewed as the gearing period, with changes in the share of different grades showing fluctuation and some instability. Notably, the maximum increment of 305.26% and the maximum decrement of −59.42% occurred within the NPP intervals greater than 900 in 2012–2013 and 2013–2014, respectively.

4.2.2 Characteristics of vegetation NPP spatial distribution

The distribution of average vegetation NPP in Hunan Province from 2000 to 2020 (Figure 5) showed distinct characteristics: high along the southeast, even higher in the northwest, lower in the central areas, and further decreased in the northern parts. The southeastern part of the Xiangnan region experienced an average annual NPP exceeding 900 gC/m^2/a. In the northwestern part of the Great Xiangxi region, NPP ranged between 600–900 gC/m^2/a. The Dongting Lake region's north-central part and the CZT region's center had NPP proportions below 500 gC/m^2/a. The NPP values notably less than 300 gC/m^2/a, mainly distributed around built-up land. From 2000 to 2020, the average vegetation NPP in Hunan Province remained high in the southeast while being lower in the

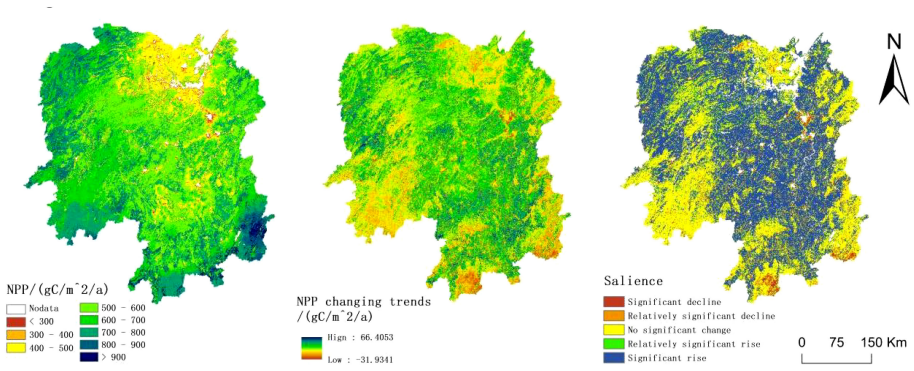

FIGURE 5
Spatial distribution and variation characteristics of NPP from 2000 to 2020.

central and northern regions. Throughout this period, the trend of vegetation NPP change in Hunan Province primarily centered around ±12 gC/m^2/a. Decreasing NPP trends mainly encompassed the northern part of the Dongting Lake area, the CZT area's center, the southwestern part of Daxiang, and the southeastern part of the Xiangnan area. This distribution exhibited a side U-shape pattern, covering a total area of 17.60%. In contrast, areas displaying an upward trend accounted for 77.76%, indicating an overall positive annual mean NPP in Hunan Province.

Combining the results of the Theil-Sen median trend analysis and Mann-Kendall significance test, and referring to the type classification of Liu G. et al. (2023), vegetation NPP changes in Hunan Province from 2000 to 2020 can be classified into five types: significant increase, relatively significant increase, no significant change, relatively significant decrease, and significant decrease (Liu et al., 2022a). Significantly declining areas accounted for 3.74% of the total area, mainly distributed in the southern Xiangnan region and around the CZT region's built-up land. The area proportion of regions with an upward trend was 58.54%, indicating a general increase in the average annual NPP over the study period. The area share of the average annual vegetation NPP change rate in Hunan Province from 2000 to 2020, greater than zero, accounted for 74.83%, while the proportion with a change rate below 25% was 4.24%. The downward trend in the NPP change rate corresponded with the main distribution around the Dongting Lake area and the CZT region, encircling built-up land. The southern part of the larger Xiangxi region displayed a less pronounced negative change characteristic.

4.2.3 Spatial and temporal changes in ecosystem services

Table 4 presents the quantities of four distinct types of ecosystem services and their temporal evolution. In Hunan Province, the average values of grain production, carbon storage, habitat quality, and water production services were 452.14 KJ/hm^2, 147.59 t/hm^2, 0.79, and 940.81mm in 2000, 2010, and 2020, respectively.

Over the past two decades, the maximum grain production increased by 70.94 t/hm^2, which can be largely attributed to advancements in grain production technology and ongoing improvements in agricultural infrastructure. During this period, both the maximum and minimum values of grain production have shown a steady rise. The province's average grain production exhibited a pattern of decrease followed by increase, a trend influenced by rapid urbanization occurring between 2000 and 2010, leading to a reduction in Cropland available for grain cultivation. However, with increasing emphasis on Cropland protection, implementation of stringent protection measures, and initiatives such as establishing high-standard basic farmland, the province's grain output rebounded and improved between 2010 and 2020.

Both carbon stock and habitat quality values underwent marginal changes during the study period. Specifically, habitat quality decreased by 0.007 over two decades, indicating some level of ecological disturbance in Hunan Province due to anthropogenic activities and the development and exploitation of land resources. In comparison, the mean value of the water production service has displayed an annual increase, rising by a total of 113.44 mm.

Figures 6A–L show the marked spatial heterogeneity of ecosystem services across different counties. Between 2000 and 2020, regions with elevated and even higher GP, CS, and HQ were primarily concentrated in the mountainous southwestern Hunan area, encompassing Suining, Xinning, and Chengbu counties. Similar patterns are observed in the western Hunan region, including Yongshun, Sangzhi, and Longshan counties, as well as the hilly southeastern Hunan regions, including Rucheng County, Guidong County, and Zixing City. These areas are characterized by abundant woodland, relatively plentiful water resources, and less human intervention. The coastal regions

TABLE 4 Changes in ecosystem services in Hunan Province, 2000–2020.

Type of service		2000	2010	2020
Grain production (KJ/hm^2)	Maximum	570.82	604.79	641.76
	Average value	433.91	417.59	504.91
	Minimum value	0.69	17.85	16.76
Carbon storage (t/hm^2)	The maximum	183.06	187.12	182.85
	Average value	147.66	147.81	147.31
	Minimum value	58.32	62.43	57.19
Habitat quality	Maximum	1	1	1
	Average value	0.793	0.791	0.786
	Minimum value	0	0	0
Water production service (mm)	Maximum	1732.17	1944.89	1662.37
	Average value	866.16	976.67	979.60
	Minimum value	0	0	0

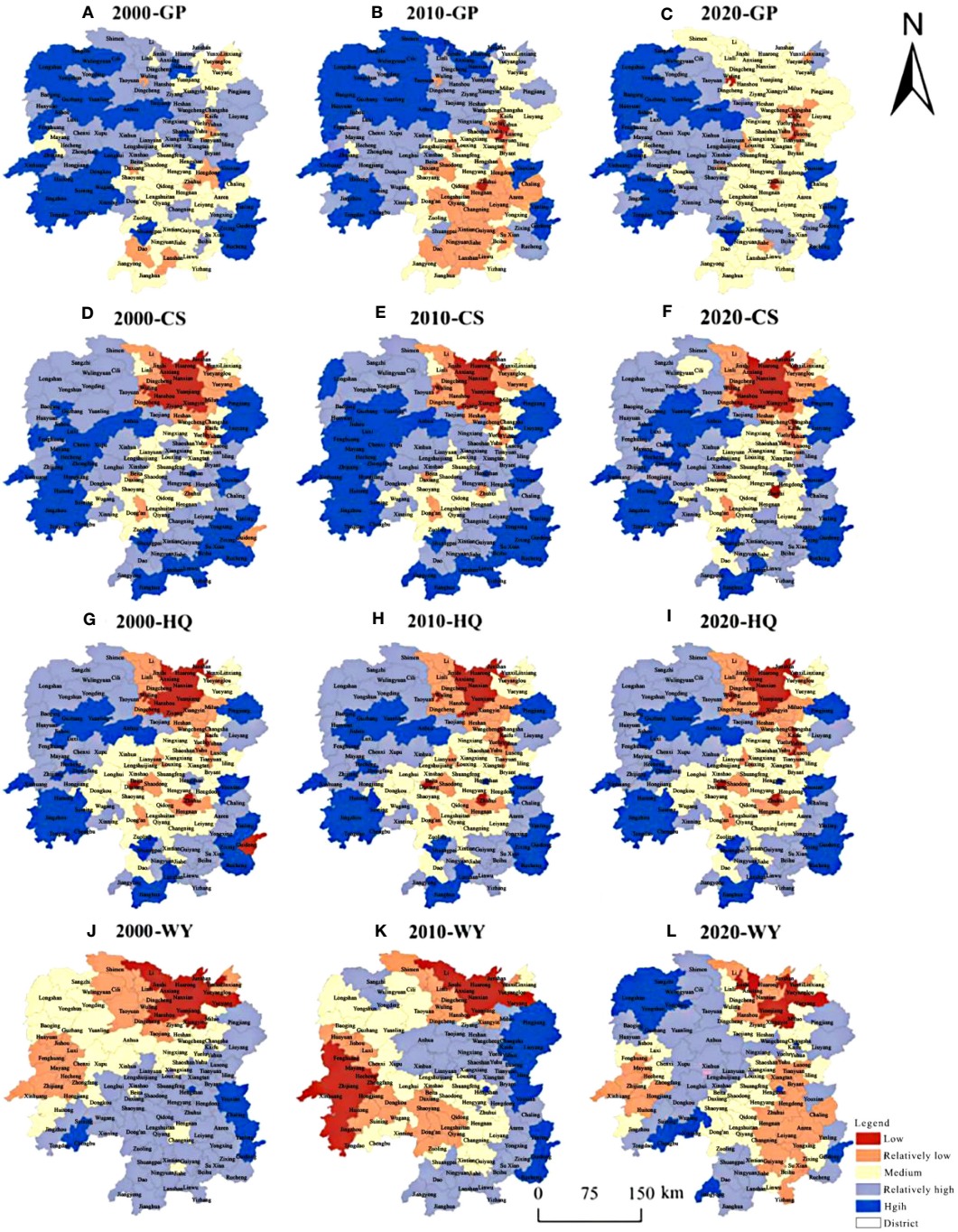

FIGURE 6
Spatial change of ecosystem services of Hunan Province in 2000-2020. **(A–C)** GP in 2000, 2010 and 2020, **(D–F)** CS in 2000, 2010 and 2020, **(G–I)** HQ in 2000, 2010 and 2020 and **(J–L)** WY in 2000, 2010 and 2020.

around Dongting Lake, including Yueyang County, Huarong County, and Yuanjiang City, predominantly exhibit lower values of WY, CS, and HQ. This disparity is attributed to factors such as flat topography, high population density, and significant agricultural activity in these areas, contributing to diminished levels of these three ecosystem services. These challenges are expanding due to ongoing ecosystem disturbance in these regions. Areas demonstrating average performance across the four ecosystem services are primarily located in the central Hunan region, which includes Lianyuan City, Shuangfeng County, and Xiangxiang City.

Hunan Province exhibits noticeable latitudinal and vertical heterogeneity in ecosystem services. In general, the capacity for ecosystem services in the hilly and mountainous regions in western and southern Hunan markedly surpassed that of the Dongting Lake Plain area in northern and central Hunan. Moreover, the ecosystem service capacity of the CZT urban agglomeration constituted the ecological weak point of the study area. In terms of the four

ecosystem services, GP exhibited a spatial distribution that is higher in the west and lower in the east. The number of counties with average GP values increased, and the spatial distribution of high and higher values gradually shrank to the west and became more compact. CS was mainly affected by the land-use type and the natural environment of the region, demonstrating a spatial pattern with the Dongting Lake area as the core low-value region, expanding irregularly towards the periphery. HQ remained relatively stable during the 20-year period, maintaining a capacity significantly higher than that of the Dongting Lake Plain area and Xiangzhong City Cluster, consistent with that of Cropland and built-up areas in various cities. Given that built-up land can negatively impact HQ significantly, counties with a larger proportion of built-up land tend to have relatively lower HQ values. HQ was concentrated in woodland with excellent ecological environments, while areas with intensive human activities exhibited lower HQ values. In terms of WY, a spatial pattern emerged with higher values in the south and lower values in the north. However, during the study period, WY did not show any noticeable regular geographical changes because it is mostly driven by natural precipitation.

5 Discussion and conclusion

5.1 Discussion

5.1.1 Impact factors of ecological condition change

Ecological condition change drivers include various factors that contribute to shifts in ecosystem utilization, encompassing natural factors, socio-economic dynamics, and policy systems. Natural drivers include climate, geomorphology, and plant succession, while socio-economic drivers include social, economic, and technological variables as well as those that have a direct impact on how regional ecosystems evolve over time (Ji et al., 2020; Hou et al., 2022; Yan et al., 2022; Zhang et al., 2022; Liu S. C., et al., 2023).

Hunan Province experiences a subtropical monsoon climate characterized by abundant sunlight, heat, and precipitation, with simultaneous rain and warmth. The region's topography is predominantly mountainous and hilly, flanked by mountains on three sides, resulting in elevated terrain in the south and lower elevation in the north. Climatic factors, such as temperature, precipitation, wind speed, and humidity, have a significant influence on the growth conditions of surface vegetation. Therefore, comprehending the impact of natural variables on changes in the land surface ecosystem pattern within the research area is essential. The ecological landscape of Hunan Province has transformed over the the past two decades, spanning from 2000 to 2020, driven by a synergy of natural and anthropogenic forces.

Climatic conditions in the study area are generally favorable, and factors like a suitable temperature and a low wind speed can directly affect the rate of change in both natural and human-influenced vegetation-based ecosystems (Niu and Liu, 2022). In addition, conditions that promote alterations in biodiversity and the extent of soil erosion can indirectly affect ecosystem changes in Hunan Province. In particular, average temperatures remained relatively stable within the study region from 2000 to 2020.

Socio-economic development stands as a pivotal driving factor that influences and changes the pattern of artificial ecosystems. Hunan Province has witnessed rapid socio-economic progress, with a substantial surge in GDP from 369.188 billion yuan in 2000 to 4,178.15 billion yuan in 2020, marking an increase of 1131.7%. Similarly, Hunan's population has increased considerably. Since 2000, alongside urbanization initiatives, a growing rural population has migrated to urban areas due to increasing settlement needs, particularly for residential land and transportation land. This trend has led to the continual conversion of surrounding Cropland and woodland ecosystem areas into urban infrastructure and residential zones, aligning with the findings of previous analyses (Xu et al., 2023).

Over the past two decades, Hunan Province has experienced significant landscape changes due to the successive implementation of various policies, including the Xiangjiang River Basin and Dongting Lake ecological protection and restoration project, the middle and upper reaches of the Yangtze River protective woodland project, the returning farmland to woodland project, and the pilot project for ecological protection and restoration of mountains, water, forests, fields, lakes, and grasses. Specifically, Cropland ecosystems, which accounted for 29.32% of the province's land area in 2000, shrank to 29.15% in 2005, 28.36% in 2010, 28.18% in 2015, and 27.93% in 2020, demonstrating a steady decline in Cropland area. About 5319.16 km^2 of Cropland was converted into woodland ecosystems, constituting 66.61% of the total transformed area. A smaller portion of Cropland was converted into watersheds. This transformation was primarily influenced by policies promoting the conversion of farmland back into woodland, leading to increased fragmentation of Cropland ecosystems. Over time, the Cropland ecosystems in the study area also displayed a trend toward simplification.

From 2000 to 2020, the comprehensive human disturbance level in Hunan Province experienced fluctuations, initially rising, then declining, and again rising (Table 5), exhibiting an overall upward trajectory and a net change of 0.0027. Specifically, the comprehensive human disturbance index from 2005 to 2010 increased by 0.0112 compared with that from 2000 to 2005. This increase was primarily attributed to the shift of cropland and woodland with lower disturbance levels into colonies with higher disturbance levels (Table 3). The rapid expansion of built-up land drove the augmentation of the composite human disturbance index.

TABLE 5 Human disturbance index.

	2000–2005	2005–2010	2010–2015	2015–2020
Composite Human Disturbance Index	0.4404	0.4516	0.4417	0.4431

Hunan Province initiated the farmland-to-forest project in 2002, which was followed by increased efforts by the national and provincial governments to conserve the environment. Policies encompassing returning farmland to woodland, closing mountains to forests, prohibiting cutting and logging, and reforestation initiatives have yielded significant outcomes. The composite human disturbance index decreased from 2010 to 2015 (Table 3), then again from 2015 to 2020 (Table 4), though at a slower rate than the preceding period, as higher-disturbance Cropland was converted to lower-disturbance wooded area. In 2020, there was a small increase of about 0.0014 compared with 2010–2015. The first period of the study was primarily focused on ecosystem transformation, while the subsequent period witnessed a reduction in the transformation of ecosystems, emphasizing the consolidation of earlier transformation outcomes. As a result, the average value of the comprehensive human disturbance index was higher in the first ten years than in the following decade.

5.1.2 Comprehensive national territory space function partition from the perspective of service clusters

National territory space function partition can guide the balance of supply and demand for social-ecological system services. The foundation of comprehensive zoning lies in delineating urban, ecological, and agricultural zones based on their dominant functions. The integration of main functional domains and social-ecological system components serves as a crucial avenue for achieving multifunctional territorial spatial functional comprehensive zoning (Hu et al., 2022; Qu et al., 2023).

The environmental service clusters in Hunan Province exhibited regional and temporal variations from 2000 to 2020 (Figures 7A–C). Urban functional zones, primarily concentrated in the CZT area and the core regions of rapidly urbanizing cities like Changde Wuling District and Hengyang Steam Xiang District, are primarily used for residential functions. The number of counties (districts) covered increased significantly from 31 to 49 between 2000 and 2020. The CZT urban agglomeration, witnessing continued population concentration, is a prominent region experiencing substantial transformations. In terms of the ecosystem service composition structure, NLs are more prominent, with other services slightly trailing at the mean level. Ecological function areas are mainly located in the mountainous terrains of western and southern Hunan province. These areas boast superior ecological environment quality, high vegetation cover, and better carbon sequestration services. However, due to topographic constraints, the proportion of both NLs and GPs in this region remains quite low.

In the overarching framework of ecosystem service composition, CS and HQ services are more prominent, and ecosystem regulating services significantly outweigh provisioning services. However, due to the rapid pace of urbanization, a discernible spatial shift in ecosystem services has occurred from regulating services to provisioning services. Additionally, the extent of ecological functional areas declined between 2000 and 2020. The agricultural functional area is dominated by the production function and is mainly located in Dongting Lake Plain, the near-shore plains of the four watercourses, and tributary water systems. These areas have rich natural resources and favorable geographic conditions, rendering them suitable for agricultural development. They represent the primary food source region in Hunan Province and are characterized by substantial human intervention, frequent agricultural activities, prominent GP, high WY, and good synergistic effects. However, the living and ecological functions within this zone are relatively weak. Overall, the agricultural functional area is in a state of growth.

5.1.3 Limitations

In summary, from a "structure–function" perspective, this paper analyzed the shifts in ecosystem macro-structure, functions, and services and integrated the driving factors of nature, social economy, and policy to explore their influence paths and degrees on structural and functional changes. Subsequently, guided by the service cluster concept, this paper explored the current "structure–function" scenario within territorial spatial comprehensive zoning, discussing potential optimization

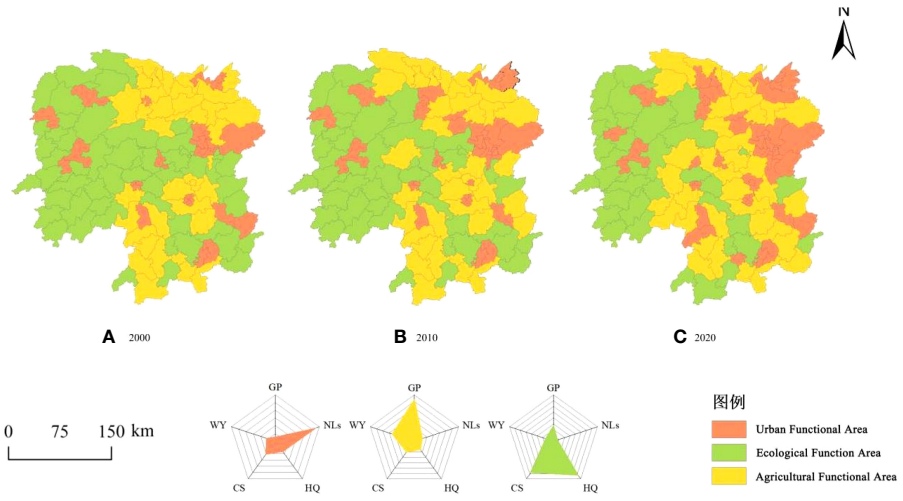

FIGURE 7
Spatial distribution and composition of ecosystem service clusters, 2000–2020. **(A)** 2000, **(B)** 2010 and **(C)** 2020.

strategies for future functional zoning. However, there are still several research limitations. First, given the universal applicability of single dominant function zoning and the study's focus on comprehensive zoning utilizing ecosystem service clusters, it becomes imperative to clarify the relationship and interconnection between dominant and secondary functions within the comprehensive zoning of the national territory space in subsequent studies. This clarification would provide insights into second-level guideline zoning. Second, this study first investigated the path toward second-level zoning, utilizing the spatial distribution of service clusters as the primary guideline and the compositional structure as the second-level guideline. In future studies, it is essential to meticulously refine the evaluation index system of comprehensive zoning to enhance the precision of functional zoning guidance. This refinement will facilitate a deeper exploration of primary functional areas based on "double evaluation" and land spatial planning. As a result, it will facilitate a more comprehensive connection between secondary zoning and planning, guiding the delineation of diverse primary comprehensive functional zones.

5.2 Conclusion

This study focuses on Hunan Province and utilizes land use data from five distinct periods (i.e., 2000, 2005, 2010, 2015, and 2020), we comprehensively analyzed the spatio-temporal characteristics of ecosystems and their directional shifts within the province. This analysis was accomplished using the transfer matrix, land use dynamics, human disturbance index, and ecosystem service clusters. Additionally, we explored the synergistic benefits of ecosystem services. The main results of the study are as follows:

(1) The ecosystem structure of Hunan Province has undergone substantial transformations from 2000 to 2020. Macro-structural changes were concentrated in the ecosystems of built-up land and Croplands. The area occupied by built-up land has increased significantly, while Cropland has experienced a marked decrease, steadily converting into built-up land. Therefore, to maintain the ecological stability of the province, a more cautious approach to growth should be adopted, with a focus on containing expansion within core areas and prioritizing the protection of regions that provide crucial ecological functions.

(2) Human socio-economic activities and environmental protection policies exert a significant impact on the ecosystem configuration within the study area. The urban periphery's Croplands are gradually yielding to the expanding city limits, caused mainly by the construction of residences, public infrastructure, and road networks, among others. Consequently, Croplands with lower disturbance levels are being transformed into areas with higher disturbance levels, leading to significant shifts in the ecosystem layout.

(3) The functional areas of towns and cities have steadily expanded, while the capacity of ecological functions within the ecological space has gradually contracted. During this period, the zones with significantly decreasing NPP change trends in Hunan Province experienced a U-shape distribution, with woodland ecosystems being prevalent. With the rapid development of society and economy, people are increasingly pursuing high-quality ecosystems that cater to recreational and cultural needs. However, ecosystems in closer proximity to areas of human production and habitation have experienced weakened capabilities in providing essential functions, primarily due to the continuous expansion of construction land.

(4) The overall trend of ecosystem service changes is favorable. Quantitatively, GP and CS experienced initial increases followed by declines, while HQ showed a gradual decline, and WY increased year by year. Spatially, these changes exhibited pronounced heterogeneity, marked by both latitudinal and vertical variations. Ecological functional zones were primarily designated for ecological functions, with a majority situated in the mountainous areas of western and southern Hunan. Agricultural functional zones were mainly designated for production functions, located mainly in the plains of Dongting Lake and the nearby plains of the four main streams of the Xiangzhi Yuanli water systems, along with their tributaries. The agricultural functional areas were primarily situated in the plains of Dongting Lake, as well as along the main streams and tributaries of the Xiangzhi Yuan and Li Rivers.

Data availability statement

The original contributions presented in the study are included in the article/supplementary material. Further inquiries can be directed to the corresponding author.

Author contributions

PL: Conceptualization, Formal analysis, Software, Supervision, Writing – original draft, Writing – review and editing. YL: Data curation, Formal analysis, Methodology, Writing – original draft. CH: Data curation, Formal analysis, Methodology, Software, Writing – original draft. LY: Data curation, Supervision, Writing – original draft. LX: Conceptualization, Resources, Validation, Writing – original draft.

Funding

The author(s) declare financial support was received for the research, authorship, and/or publication of this article. This paper was supported by the Research Foundation of the Department of Natural Resources of Hunan Province, China (2022-49), Hunan Province social Science Fund project (21YBA245) and the Open Topic of Key Laboratory of Natural Resources Monitoring and

Supervision in Southern Hilly Region, Ministry of Natural Resources, China, (NRMSSHR2022Z06).

Conflict of interest

The authors declare that the research was conducted in the absence of any commercial or financial relationships that could be construed as a potential conflict of interest.

Publisher's note

All claims expressed in this article are solely those of the authors and do not necessarily represent those of their affiliated organizations, or those of the publisher, the editors and the reviewers. Any product that may be evaluated in this article, or claim that may be made by its manufacturer, is not guaranteed or endorsed by the publisher.

References

Chen, L.-C., Guan, X., Li, H.-M., Wang, Q.-K., Zhang, W.-D., Yang, Q.-P., et al. (2019). Spatiotemporal patterns of carbon storage in forest ecosystems in Hunan Province, China. *For. Ecol. Management* 432, 656–666. doi: 10.1016/j.foreco.2018.09.059

Chen, J., Qi, Q., Wang, B., He, S., Li, Z., Wang, L., et al. (2023). Response of ecosystem services to landscape patterns under socio-economic-natural factor zoning: A case study of Hubei Province, China. *Ecol. Indicators* 153, 110417. doi: 10.1016/j.ecolind.2023.110417

Dan, Y. Z., Peng, J., Zhang, Z. M., Xu, Z. H., Mao, Q., and Dong, J. Q. (2020). Territorially ecological restoration zoning based on the framework of degradation pressure, supply state and restoration potential: a case study in the Pearl River Delta region. *J. Ecology* 23, 8451–8460. doi: 10.5846/stxb202004240982

Di Febbraro, M., Sallustio, L., Vizzarri, M., De Rosa, D., De Lisio, L., Loy, A., et al. (2018). Expert-based and correlative models to map habitat quality: Which gives better support to conservation planning? *Global Ecol. Conserv.* 16, e00513. doi: 10.1016/j.gecco.2018.e00513

He, Y. L., You, N. S., Cui, Y. P., Xiao, T., Hao, Y. Y., and Dong, J. W. (2021). Spatio-temporal changes in remote sensing-based ecological index in China since 2000. *J. Natural Resources.* 05, 1176–1185. doi: 10.31497/zrzyxb.20210507

Hou, J., Wang, J. W., Qin, T. L., Liu, S. S., Zhang, X., Yan, S., et al. (2022). Attribution identification of terrestrial ecosystem evolution in the Yellow River Basin. *Open Geosciences* 14, 615–628. doi: 10.1515/geo-2022-0385

Hou, P., Wang, Q., Shen, W., Zhai, J., Liu, H., and Yang, M. (2015). Progress of integrated ecosystem assessment: Concept, framework and challenges. *Geogr. Res.* 10, 1809–1823. doi: 10.11821/dlyj201510001

Hu, Q., Shen, W., and Zhang, Z. (2023). How does urbanisation affect the evolution of territorial space composite function? *Appl. Geography* 155, 102976. doi: 10.1016/j.apgeog.2023.102976

Hu, Q., Zhang, Z., and Niu, L. (2022). Identification and evolution of territorial space from the perspective of composite functions. *Habitat Int.* 128, 102662. doi: 10.1016/j.habitatint.2022.102662

Ji, Z. X., Xu, Y. Q., and Wei, H. J. (2020). Identifying dynamic changes in ecosystem services supply and demand for urban sustainability: insights from a rapidly urbanizing city in central China. *Sustainability* 12, 1-23. doi: 10.3390/su12083428

Li, B., Chen, D., Wu, S., Zhou, S., Wang, T., and Chen, H. (2016). Spatio-temporal assessment of urbanization impacts on ecosystem services: Case study of Nanjing City, China. *Ecol. Indicators* 71, 416–427. doi: 10.1016/j.ecolind.2016.07.017

Li, T., Zhang, Q., Wang, G., Singh, V. P., Zhao, J., Sun, S., et al. (2023). Ecological degradation in the Inner Mongolia reach of the Yellow River Basin, China: Spatiotemporal patterns and driving factors. *Ecol. Indicators* 154, 110498. doi: 10.1016/j.ecolind.2023.110498

Liu, Z., Huang, Q., Zhou, Y., and Sun, X. (2022b). Spatial identification of restored priority areas based on ecosystem service bundles and urbanization effects in a megalopolis area. *J. Environ. Management* 308, 114627. doi: 10.1016/j.jenvman.2022.114627

Liu, B., Pan, L. B., Qi, Y., Guan, X., and Li, J. S. (2021). Land use and land cover change in the yellow river basin from 1980 to 2015 and its impact on the ecosystem services. *Land* 10, 1-11. doi: 10.3390/land10101080

Liu, G. B., Shao, Q. Q., Fan, J. W., Ning, J., Rong, K., Huang, H. B., et al. (2023). Spatiotemporal evolution and driving forces of ecosystem service value and ecological risk in the Ulan Buh Desert. *Front. Environ. Sci.* 10. doi: 10.3389/fenvs.2022.1053797

Liu, S. C., Shao, Q. Q., Niu, L. N., Ning, J., Liu, G. B., and Zhang, X. Y. (2023). Changes of ecological and the characteristics of trade-offs and synergies of ecosystem services in the upper reaches of the Yangtze River. *J. Ecology* 03, 1028–1039. doi: 10.5846/stxb202110092798

Liu, S., Wang, Z., Wu, W., and Yu, L. (2022a). Effects of landscape pattern change on ecosystem services and its interactions in karst cities: A case study of Guiyang City in China. *Ecol. Indicators* 145, 109646. doi: 10.1016/j.ecolind.2022.109646

Ma, S., Wang, L.-J., Zhu, D., and Zhang, J. (2021). Spatiotemporal changes in ecosystem services in the conservation priorities of the southern hill and mountain belt, China. *Ecol. Indicators* 122, 107225. doi: 10.1016/j.ecolind.2020.107225

Migliavacca, M., Musavi, T., Mahecha, M. D., Nelson, J. A., Knauer, J., Baldocchi, D. D., et al. (2021). The three major axes of terrestrial ecosystem function. *Nature* 598, 468–472. doi: 10.1038/s41586-021-03939-9

Natural Capital Project (2023) *InVEST 3.13.0. Stanford university, University of Minnesota, Chinese Academy of Sciences, The Nature Conservancy, World Wildlife Fund, Stockholm Resilience Centre and the Royal Swedish Academy of Sciences*. Available at: https://naturalcapitalproject.stanford.edu/software/invest.

Ning, L. X., Liang, X. Y., and Cheng, C. X. (2021). Spatiotemporal variations of ecosystem health of Jing-Jin-Ji region based on the PSR model. *Ecol. Science* 06, 1–12. doi: 10.14108/j.cnki.1008-8873.2021.06.001

Niu, X. Y., and Liu, L. A. (2022). Change trend and restoration potential of vegetation net primary productivity in China over the past 20 years. *Remote Sens.* 14, 1-26. doi: 10.3390/rs14071634

Niu, G. Y., Wang, G. L., Lu, Q. C., and Xiong, C. H. (2022). Function evaluation and optimal strategies of three types of space in cross-provincial areas from the perspective of high-quality development: A case study of yangtze river delta, China. *Polish J. Environ. Stud.* 31, 2763–2777. doi: 10.15244/pjoes/144910

Ouyang, X., Wei, X., Wei, G., and Wang, K. (2023). The expansion efficiency of urban land in China's urban agglomerations and its impact on ecosystem services. *Habitat Int.* 141, 102944. doi: 10.1016/j.habitatint.2023.102944

Ouyang, X., and Zhu, X. (2020). Spatio-temporal characteristics of urban land expansion in Chinese urban agglomerations. *J. Geography* 03, 571–588. doi: 10.11821/dlxb202003010

Pan, Y., Zheng, H., Yi, Q. T., and Li, R. N. (2021). The change and driving factors of ecosystem service bundles: A case study of Daqing River Basin. *J. Ecology* 13, 5204–5213. doi: 10.5846/stxb202103100650

Peng, J., Liu, Y., Liu, Z., and Yang, Y. (2017). Mapping spatial non-stationarity of human-natural factors associated with agricultural landscape multifunctionality in Beijing-Tianjin-Hebei region, China. *Agriculture Ecosyst. Environment* 246, 221–233. doi: 10.1016/j.agee.2017.06.007

Qiu, Y., Zhou, A., Li, M., Guo, Y., Hao, C., and Ma, C. (2023). Territorial spatial usage regulation based on resources endowment and sustainable development: A case of Wuhan, China. *J. Cleaner Production* 385, 135771. doi: 10.1016/j.jclepro.2022.135771

Qu, Y., Dong, X., Su, D., Jiang, G., and Ma, W. (2023). How to balance protection and development? A comprehensive analysis framework for territorial space utilization scale, function and pattern. *J. Environ. Management* 339, 117809. doi: 10.1016/j.jenvman.2023.117809

Shi, P. J., Chen, J., and Pan, Y. Z. (2000). Landuse change mechanism in shenzhen city. *J. Geography* 02, 151–160. doi: 10.11821/xb200002003

Shi, J., Li, S., Song, Y., Zhou, N., Guo, K., and Bai, J. (2022). How socioeconomic factors affect ecosystem service value: Evidence from China. *Ecol. Indicators* 145, 109589. doi: 10.1016/j.ecolind.2022.109589

Wan, H., Xie, Y., Li, B., Cai, Y., and Yang, Z. (2023). An integrated method to identify and evaluate the impact of hydropower development on terrestrial ecosystem. *Environ. Impact Assess. Review.* 99, 107042. doi: 10.1016/j.eiar.2023.107042

Wei, G., Bi, M., Liu, X., Zhang, Z., and He, B. (2023a). Investigating the impact of multi-dimensional urbanization and FDI on carbon emissions in the belt and road initiative region: Direct and spillover effects. *J. Cleaner Production* 384, 135608. doi: 10.1016/j.jclepro.2022.135608

Wei, G., He, B., Sun, P., Liu, Y., Li, R., Ouyang, X., et al. (2023b). Evolutionary trends of urban expansion and its sustainable development: Evidence from 80 representative cities in the belt and road initiative region. *Cities* 138, 104353. doi: 10.1016/j.cities.2023.104353

Wu, Y. Z., Shi, K. F., Chen, Z. Q., Liu, S. R., and Chang, Z. J. (2022). Developing improved time-series DMSP-OLS-like data, (19922019) in China by integrating

DMSP-OLS and SNPP-VIIRS. *IEEE Trans. Geosci. Remote Sens.* 60, 1-14. doi: 10.1109/TGRS.2021.3135333

Wu, D., Zou, C. X., Lin, N. F., and Xu, M. J. (2018). Characteristic analysis of ecological status in the yangtze River economic belt based on the plan for major function-oriented zones. *Yangtze River Basin Resour. Environment* 08, 1676–1682. doi: 10.11870/cjlyzyyhj201808003

Xia, H., Yuan, S., and Prishchepov, A. V. (2023). Spatial-temporal heterogeneity of ecosystem service interactions and their social-ecological drivers: Implications for spatial planning and management. *Resources Conserv. Recycling.* 189, 106767. doi: 10.1016/j.resconrec.2022.106767

Xiong, Y., Sun, W. J., Wei, X., He, J. X., Zhao, D. D., Sun, B., et al. (2020). Cooperative development model of ecosystem services and rural communities in hilly-mountain of Southern China: a case study of eight villages in Lechang, Guandong Province. *J. Ecology* 18, 6505–6521. doi: 10.5846/stxb201911142420

Xu, X. L., Liu, J. Y., Shao, Q. Q., and Fan, J. W. (2008). The dynamic changes of ecosystem spatial pattern and structure in the Three-River Headwaters region in Qinghai Province during recent 30 years. *Geogr. Res.* 04, 829–838 + 974. doi: 10.11821/yj2008040011

Xu, Z., Peng, J., Liu, Y., Qiu, S., Zhang, H., and Dong, J. (2023). Exploring the combined impact of ecosystem services and urbanization on SDGs realization. *Appl. Geogr.* 153, 102907. doi: 10.1016/j.apgeog.2023.102907

Xu, Y., Yang, F., and Yan, C. Z. (2020). Ecological health assessment of urban wetland in Xiong'an based on landscape pattern. *J. Ecology* 20, 7132–7142. doi: 10.5846/stxb201912202744

Yan, X. L., Li, X. Y., Liu, C. H., Li, J. W., and Zhong, J. Q. (2022). Scales and historical evolution: methods to reveal the relationships between ecosystem service bundles and socio-ecological drivers-A case study of dalian city, China. *Int. J. Environ. Res. Public Health* 19, 1-20. doi: 10.3390/ijerph191811766

Zhang, C. Y., Bai, Y. P., Yang, X. D., Li, L. W., Liang, J. S., Wang, Q., et al. (2021). Identification of ecosystem service bundles in Ningxia Plain under multi-scenario simulation. *Geogr. Res.* 12, 3364–3382. doi: 10.11821/dlyj020220289

Zhang, D., Huang, Q., He, C., and Wu, J. (2017). Impacts of urban expansion on ecosystem services in the Beijing-Tianjin-Hebei urban agglomeration, China: A scenario analysis based on the Shared Socioeconomic Pathways. *Resources Conserv. Recycling.* 125, 115–130. doi: 10.1016/j.resconrec.2017.06.003

Zhang, J. F., Liu, C. Y., and Chang, F. (2019). A new approach for multifunctional zoning of territorial space: the panxi area of the upper yangtze river in China case study. *Sustainability* 11, 1-19. doi: 10.3390/su11082325

Zhang, T. J., Zhang, S. P., Cao, Q., Wang, H. Y., and Li, Y. L. (2022). The spatiotemporal dynamics of ecosystem services bundles and the social-economic-ecological drivers in the Yellow River Delta region. *Ecol. Indic.* 135, 1-14. doi: 10.1016/j.ecolind.2022.108573

Zhang, Y., Zheng, M., and Qin, B. (2023). Optimization of spatial layout based on ESV-FLUS model from the perspective of "Production-Living-Ecological": A case study of Wuhan City. *Ecol. Modelling.* 481, 110356. doi: 10.1016/j.ecolmodel.2023.110356

Zhao, Y., Wang, M., Lan, T., Xu, Z., Wu, J., Liu, Q., et al. (2023). Distinguishing the effects of land use policies on ecosystem services and their trade-offs based on multi-scenario simulations. *Appl. Geogr.* 151, 102864. doi: 10.1016/j.apgeog.2022.102864

Zheng, H., Xu, Z., Hu, T., Cheng, X., Xia, P., and Peng, J. (2023). A wavelet coherence approach to zoning supply-demand matching of carbon sequestration service. *Sci. Total Environ.* 901, 165641. doi: 10.1016/j.scitotenv.2023.165641

Zhou, H., Jin, P., and Xia, W. S. (2020). Functional zoning of territorial space in provincial level based on the production-living-ecological functions: A case of henan province. *China Land Science* 08, 10–17. doi: 10.11994/zgtdkx.20200731.164624

Zhou, Z., Sun, X., Zhang, X., and Wang, Y. (2022). Inter-regional ecological compensation in the Yellow River Basin based on the value of ecosystem services. *J. Environ. Management* 322, 116073. doi: 10.1016/j.jenvman.2022.116073

Zhu, C. M., Yang, L. X., Xu, Q. Y., Fu, J. W., Lin, Y., Sun, L., et al. (2022). A comparative analysis of farmland occupation by urban sprawl and rural settlement expansion in China. *Land* 11, 1-16. doi: 10.3390/land11101738

Zhu, C. X., Zhong, S. Z., Long, Y., and Yan, D. (2023). Spatiotemporal variation of ecosystem services and their drivers in the Yellow River Basin, China. *J. Ecol.* 1-15, 2502-2513. doi: 10.13292/j.1000-4890.202310. 005

Zou, L. L., Zhang, L. J., Liang, Y. F., and Wen, Q. (2022). Scientific cognition and research framework of territorial space function in the New Era. *J. Natural Resour.* 12, 3060–3072. doi: 10.31497/zrzyxb.20221203

frontiers | Frontiers in Environmental Science

TYPE Original Research
PUBLISHED 05 January 2024
DOI 10.3389/fenvs.2023.1334458

OPEN ACCESS

EDITED BY
Xiao Ouyang,
Hunan University of Finance and Economics, China

REVIEWED BY
Qimeng Ning,
Hunan City University, China
Yafen He,
Jiangxi University of Finance and Economics, China

*CORRESPONDENCE
Youping Xie,
xyp@img.net

RECEIVED 07 November 2023
ACCEPTED 12 December 2023
PUBLISHED 05 January 2024

CITATION
Huang X, Xie Y, Lei F, Cao L and Zeng H (2024), Analysis on spatio-temporal evolution and influencing factors of ecosystem service in the Changsha-Zhuzhou-Xiangtan urban agglomeration, China.
Front. Environ. Sci. 11:1334458.
doi: 10.3389/fenvs.2023.1334458

Analysis on spatio-temporal evolution and influencing factors of ecosystem service in the Changsha-Zhuzhou-Xiangtan urban agglomeration, China

Xuanhua Huang[1], Youping Xie[2]*, Fan Lei[2], Li Cao[2] and Haibo Zeng[2]

[1]School of Public Administratior, Hunan Normal University, Changsha, China, [2]Key Laboratory of Natural Resources Monitoring and Supervision in Southern Hilly Region, Ministry of Natural Resources, Changsha, China

Introduction: It is of great significance to strengthen the evaluation research and driving force analysis of ecosystem services value for the rational utilization and protection of the ecological environment of Changsha-Zhuzhou-Xiangtan (CZT) urban agglomeration and the promotion of the integration of urban agglomeration.

Methods: Based on the remote sensing image data, the spatial and temporal evolution characteristics and influencing factors of the ecosystem services value of CZT urban agglomeration were analyzed by the methods of ArcGIS10.2, Geoda, value equivalent and spatial statistics.

Results: The results showed that: 1) From 2000 to 2020, the total value of ecosystem service in the CZT urban agglomeration decreased gradually, with an overall decrease of 4,381.07 × 10^6 yuan. In the past 20 years, the ecosystem service Value (ESV) of cultivated land, forest land and grassland had declined, but the ESV of water area and unused land had fluctuated, and the single ESV had declined. 2) From 2000 to 2020, the spatial distribution of ESV in the CZT urban agglomeration showed an obvious pattern of "low in the middle and high in the surrounding areas", and the changes were quite different in different periods. 3) The spatial correlation between ESV and distance from county government, distance from railway, proportion of construction land, NDVI, population density, economic density, slope and precipitation were significant. The spatial distribution of the distance from the county government, the distance from the railway, NDVI and ESV were similar; the population density and economic density were consistent with the spatial distribution of ESV; and the spatial distribution of construction land proportion, slope, precipitation and ESV were different.

Discussion: The results of the study can provide some reference for the further development of ecological protection policies and related planning in urban agglomerations.

KEYWORDS

ecosystem service, spatio-temporal evolution, influencing factors, spatial statistics, Changsha-Zhuzhou-Xiangtan urban agglomeration

1 Introduction

Ecosystem services (ESs) refer to the environmental conditions and utilities provided by ecosystems to support human survival and development (Daily, 1997). Ecosystem service Value (ESV) is a monetary evaluation of ESs that can partially indicate the quality of the regional ecological environment (Zhao et al., 2014). Natural and social forces both have an impact on changes in ESV. Investigating the spatial and temporal changes in ESV and the spatial correlation between the drivers and ESV can aid in understanding the spatial and temporal variations of the drivers, and offer valuable insights for developing effective ecological management plans, enhancing ecological construction, and improving human wellbeing in the region.

Existing academic research on ESs has yielded significant findings, primarily focused on various aspects including the assessment of ESV, spatio-temporal characteristics, and influencing factors (Liu and Lv, 2009; Wei and Guo, 2015; Deng et al., 2019). For example, Rui et al. (2019), Liu et al. (2016), and Rao et al. (2013) conducted assessments on overall ecosystems, individual ecosystems, and specific ecosystem service, analyzing their functional values and corresponding driving factors. Studies were conducted at different spatial scales, such as natural areas (Sun et al., 2017; Nan et al., 2018), economic zones (Zhao et al., 2017), and administrative regions (Xue and Luo, 2015; Gao et al., 2016). Li. (2019) examined the spatial and temporal changes in the loss of ESV in karst mountainous areas, while Li (2014) explored the dynamics of ESV and its driving forces in the Guanzhong-Tianshui Economic Zone. Additionally, Li. (2019b), Mao and Chen (2010), and Lin (2019) evaluated the ESV in the Yangtze River Economic Zone, Jiangsu Province, and Guangzhou City, respectively. Traditional research methods primarily involve principal component analysis (Zhang et al., 2017), multiple regression (Qiao et al., 2015), and correlation analysis (Yang, 2018). However, with advancements in geographic information systems and remote sensing, newer statistical approaches like geoprospectors (Huang et al., 2019; Huang and Yang, 2019), spatial autocorrelation (Yang et al., 2012; Yao et al., 2015), the STIRPAT model (Sun et al., 2009; Ran et al., 2018), and geographically weighted regressions (Chen et al., 2014) have gained popularity. SU (2018) employed the InVEST and CASA models to evaluate the ecosystem service functions of sediment interception, water production, net primary productivity (NPP), carbon sequestration, oxygen release, and food production in the Upper Fen River Basin. Additionally, Tang et al. (2016) utilized the STIRPAT model and the GWR model to examine the drivers of ESV in Beijing. Previous studies have provided some guidance for quantitatively analyzing the driving factors of ESV. However, there are several deficiencies. Firstly, research areas were mainly selected at medium and large scales, such as national, provincial, prefectural, municipal, and watershed levels. Less attention was paid to changes at smaller scales, such as grids, which ignore the scale-dependence of geographic element distribution. Secondly, the selection of influencing factors mainly focused on natural and socio-economic aspects and the analysis of quantitative relationships, with less consideration of the influence of spatial location factors, thus resulting in a relatively weak analysis of relevant spatial characteristics. Furthermore, research methods were mainly traditional quantitative methods like correlation and principal components, which are difficult to reflect the spatially relevant characteristics of the influencing factors, although they can be better for the evaluation of the global effects of the influencing factors.

The "Three Trunks and One Track" project of the western loop of the CZT Railway, the accelerated construction of Changsha's southern new city and Zhuzhou's Yunlong Demonstration Zone, as well as the rapid transformation of Furong Avenue, Dongzhu Road, and Tanzhou Avenue in the CZT urban agglomeration, have all contributed to the integration of the three cities of the CZT. The population and economic activity between cities will increasingly rise as a result of this quickly developing integration process, having a substantial impact on the structure, operation, and function of ecosystem service. The urban ecological environment is likely to face increasing pressure, which might ultimately affect human wellbeing. We estimated the ESV in the CZT urban agglomeration area using remote sensing photos from 2005 to 2020, together with tools like GIS, SPSS, Geoda, and others, to better understand this phenomenon. We looked at the spatial and temporal evolution patterns of the ESs and their spatial interactions with the drivers using the methodologies of value equivalence, multiple regression, and bivariate spatial statistics. Our purpose was to offer better solutions for the urbanization of CZT and to improve the ESs. Moreover, we aimed to: quantify the ecosystem services change trends in CZT, and explore the effects of different driving forces on the ecosystem services, intending to provide guidance for ecological management and ecological construction in the CZT urban agglomeration area.

1.1 Overview of the study area

The CZT urban agglomeration, which is situated in Hunan Province's central and eastern region, is a significant component of the urban agglomeration in the middle reaches of the Yangtze River and serves as the province's focal point for economic and social growth as it gradually transforms into one of the driving forces behind the "Rise of Central China." CZT's three cities are located in the middle reaches of the Xiangjiang River. Along the Xiangjiang River was "Pin" shape distribution, two and two less than 40 km apart, in the middle of the ecological green heart of the natural isolation, but also has dense high-speed, urban railroad network connectivity, the urban agglomeration of the overall strength of the significant increase (Figure 1). The CZT urban agglomeration is located in the subtropical monsoon humid climate zone, with sufficient heat and abundant rainfall. Basin and hills are interlaced, urban areas and villages are intertwined, and the spatial combination is unique; a good combination of mountains, waters, and green heart form a unique ecological background, and the regional ecological environment is superior (Zhang et al., 2020). Referring to the studies of He and Zhou (2007) and Ouyang et al. (2019), the metropolitan area of the urban agglomeration was selected as the study area of this research, including the urban areas of Changsha, Zhuzhou, and Xiangtan (Zhuzhou County was changed to Bryan Kou District in 2018), as well as Changsha County and Xiangtan County. By the end of 2018, the CZT metropolitan area had a resident population of 9,041,600 people, with an average urbanization level of 80.46%, a gross regional product of

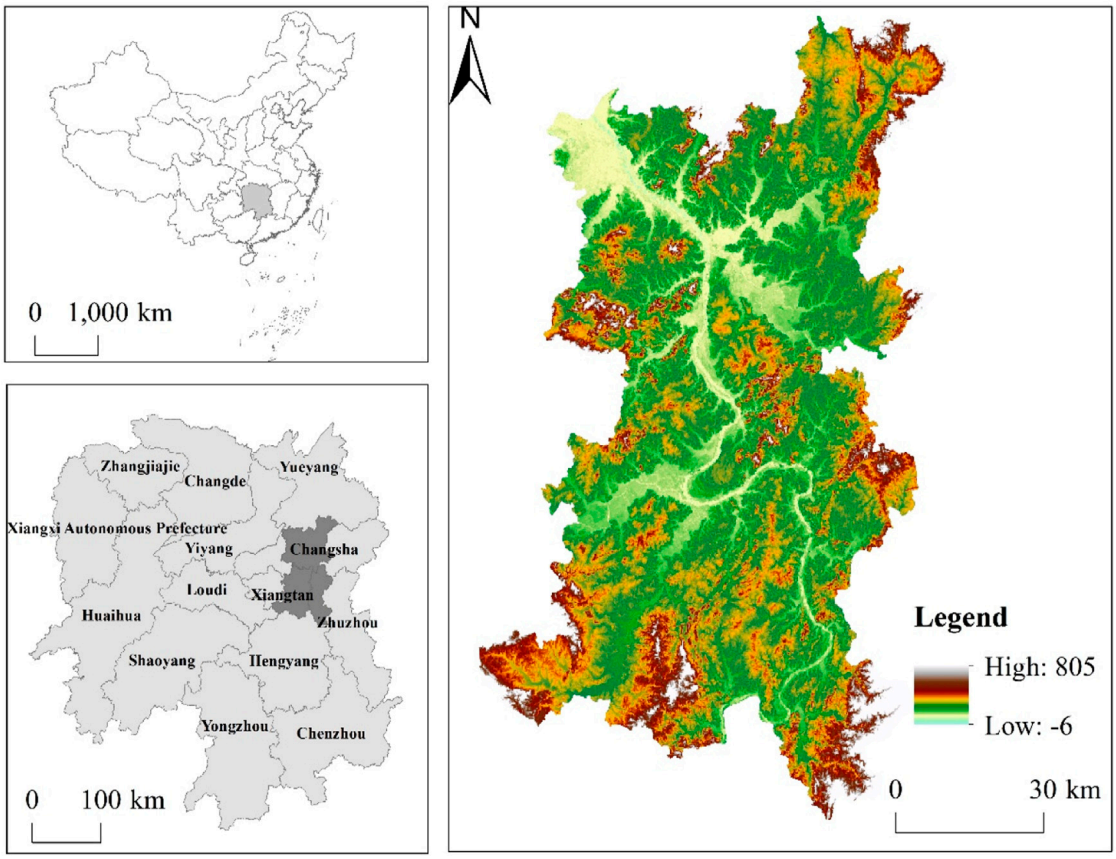

FIGURE 1
Location of the study area.

1,164,966 million yuan, accounting for about 73.43% of the CZT urban agglomeration, and a retail sales volume of all consumer goods of 534,823 million yuan.

2 Data sources and research methodology

2.1 Data sources and processing

2.1.1 Land use data

The Landsat TM/ETM remote sensing images of the CZT urban agglomeration from 2005, 2010, 2015, and 2020 were acquired from the Resource and Environment Science Data Center, Chinese Academy of Sciences (http://www.resdc.cn). The land use types were classified into six categories based on the national standard classification of land use and the study conducted by Liu et al. (2014): arable land, forest land, grassland, watershed, construction land, and unutilized land.

2.1.2 Selection of influencing factors

Changes in ecosystem services impact ecological health, affecting economic and social development and human wellbeing. Therefore, based on existing research results (Jiang, 2010; Ouyang et al., 2020), this study selected relevant influencing factors of ESV from three aspects: natural environment, socio-economy, and spatial location.

For the natural environment, five factors are chosen: Normalized Difference Vegetation Index (NDVI), air temperature, precipitation, elevation, and slope. NDVI reflects surface biomass and ESV (Chen et al., 2014). Temperature and precipitation influence ES functions like evapotranspiration and climate regulation. Higher elevations and slopes are associated with less human activity impact and more stable ESV. The NDVI, temperature, precipitation, and Digital Elevation Model (DEM) data were obtained from the Resource and Environment Science Data Center, Chinese Academy of Sciences (http://www.resdc.cn), while the slope was extracted from the DEM using the Slope Analysis module in ArcGIS.

In socio-economic aspects, three factors are selected: proportion of construction land, population density, and economic density (GDP density). Increasing population and economic densities exert pressure on ESs (Zuo and Ma, 2012). Proportion of construction land reflects spatial expansion of human activities (Xing, 2018). The proportion of construction land is obtained using the Attribution Select tool in ArcGIS, while population density and economic density are derived from the Resource and Environment Science Data Center, Chinese Academy of Sciences (http://www.resdc.cn).

Spatial location factors include distance to rivers, highways, county government, and railways. Rivers have two main effects

TABLE 1 Coefficient of ESV per unit area (yuan·hm^{-2}·a^{-1}).

Ecosystem service function	Land use type				
	Cultivated land	Wood land	Grass land	Water area	Unused land
Gas regulation	2,773.58	16,641.50	5,778.30	1964.62	231.13
Climate regulation	3,736.63	15,678.45	6,009.43	7,935.53	500.79
Water conservation	2,966.19	15,755.50	5,855.34	72,305.78	269.65
Soil formation and protection	5,662.73	15,485.84	8,628.93	1,579.40	654.87
Waste treatment	5,354.56	6,625.78	5,084.90	57,205.16	1,001.57
Biodiversity protection	3,929.24	17,373.42	7,203.61	13,213.04	1,540.88
Food production	3,852.20	1,271.23	1,656.45	2041.67	77.04
Raw materials	1,502.36	11,479.55	1,386.79	1,348.27	154.09
Recreational culture	654.87	8,012.57	3,351.41	17,103.77	924.53
Sum	30,432.38	108,323.85	44,955.17	174,697.25	5,354.56

on human activities: providing sufficient water for production and life, and offering convenient shipping conditions (Xie et al., 2003). The distance from highways, county government, and railways also reflects human influence on the ecological environment (Wartenberg, 1985). Vector data for rivers, highways, county government, and railways in the CZT metropolitan area were obtained from Urban Data Pie (https://www.udparty.com//). The distances were calculated using the Euclidean Distance tool in ArcGIS 10.2. The projected coordinates of all influencing factors were unified, and the values of each influencing factor in each grid were calculated using the Zonal Statistics as Table module in ArcGIS 10.2.

2.2 Study methods

2.2.1 Calculation of ecosystem service value (ESV)

The functional value method and the equivalent value method are the two main categories of assessment methods that have been developed thus far, but there is currently a lack of a comprehensive, unified, and scientific set of methods for accounting or assessing the ESV both domestically and internationally. In this work, we utilize the coefficients of ESV of CZT urban agglomeration of Ouyang Xiao et al. (Ouyang et al., 2019) for computation, referring to the equivalent ESV per unit area of Chinese terrestrial ecosystems as developed by Xie et al. (2003) (Eqs 1, 2). Since the ESV of construction land is zero, it is not listed in Table 1, and the ESV coefficients and calculation formulas for the CZT urban agglomeration are as follows:

$$ESV_f = \sum\left(A_k \times VC_{kf}\right) \quad (1)$$

$$ESV = \sum\left(A_k \times VC_k\right) \quad (2)$$

Where: ESV_f is the value of the f ecosystem service function, VC_{kf} is the value coefficient of the f ecosystem service function, ESV is the total ESV in the study area, A_k is the area of the k land use type, and VC_k is the ESV of the k land use type.

2.2.2 Driving forces of ESV

(1) Variance Inflation Factor (VIF)

The VIF is a method of the degree of multicollinearity between predictor variables. A VIF value > 10 is generally considered to provide evidence of multicollinearity (Luo et al., 2020), and no predictor variables had collinearity with the other variables.

(2) Spatial autocorrelation

Spatial autocorrelation offers significant advantages in analyzing the effects of spatial locational factors and relevant spatial features. By identifying patterns of similarity or dissimilarity and recognizing the spatial dependency between neighboring locations, it helps improve the accuracy of statistical models. By recognizing and incorporating the spatial relationships between neighboring locations, the model can better capture the underlying spatial structure of the data. The bivariate global autocorrelation and local autocorrelation are extended to show the correlation of the spatial distribution of various factors, with reference to the research of associated researchers (Eq. 3). The following is the formula (Gao et al., 2019):

$$I_{lm}^{p} = z_l^p \cdot \sum_{q=1}^{n} W_{pq} \cdot z_m^q \quad (3)$$

Where: $z_l^p = \frac{X_l^p - \overline{X_l}}{e_l}$; $z_m^q = \frac{X_m^q - \overline{X_m}}{e_m}$; X_l^p is the value of attribute l of the spatial cell p, X_m^q is the value of attribute m of the spatial cell q, $\overline{X_l}$ and $\overline{X_m}$ are the mean values of attribute l and m, respectively, and e and e are the variances of attribute l and m, respectively.

3 Results analysis

3.1 Spatio-temporal evolution of ESV

According to the change in total value, the CZT Urban Agglomeration's ESV decreased gradually between 2000 and 2020, falling from 64,955.87 × 10^6 yuan in 2000–60,574.80 × 10^6

TABLE 2 Change of ESV of individual land use types (10^6yuan).

Land use type / Year	Cultivated land	Wood land	Grass land	Water area	Unused land	ESV
2000	10,225.93	49,308.45	147.41	5,272.59	1.49	64,955.87
2005	10,068.54	48,797.51	145.15	5,270.53	1.64	64,283.37
2010	9,965.36	48,482.78	145.15	5,289.17	1.61	63,884.07
2015	9,271.85	47,014.54	139.68	5,113.37	2.98	61,542.43
2020	8,973.20	46,204.50	139.12	5,255.39	2.58	60,574.80

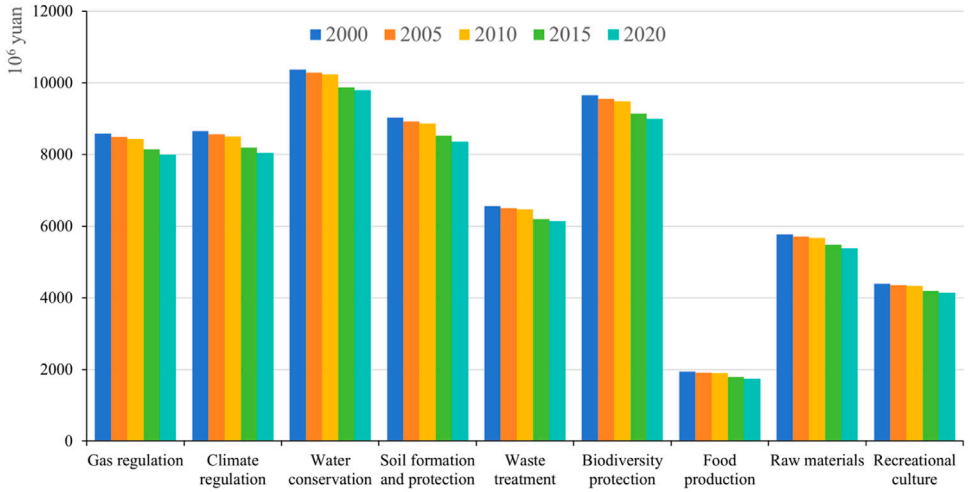

FIGURE 2
Change of individual ESV in 2000–2020.

yuan in 2020, a decrease of 4,381.07 × 10^6 yuan or 6.74% (Table 2). In the periods 2000–2005, 2005–2010, 2010–2015 and 2015–2020, it fell by 1.04%, 0.62%, 3.7% and 1.57%, respectively. From the perspective of each land use type, the ecological service value of cultivated land, wood land and grass land also showed a decreasing trend during the 20-year period, decreasing by 1,252.73 × 10^6 yuan, 3,103.95 × 10^6 yuan and 8.29 × 10^6 yuan from 2000 to 2020, with a decrease rate of 12.3%, 6.29%, and 5.62%, respectively. However, the ecological service value of water area and unused land is volatile, with the ecological service value of waters experiencing a fluctuating process of first decrease, then growth and then decrease, decreasing by a total of 17.2 × 10^6 yuan, with a decrease rate of 0.33%.

In terms of the value of individual ecosystem service, the value of all nine ecosystem service functions in the study area from 2005 to 2020 showed the same trend of change, i.e., a decreasing trend. As can be seen from Figure 2, ESs in the CZT urban agglomeration area are mainly dominated by the three functions of water conservation, biodiversity protection, and soil formation and protection, with three ESVs accounting for 16.05%, 14.86%, and 13.84% of the total value in 2020 in that order, followed by the functions of gas exchange and climate regulation, with the total share of gas exchange and climate regulation accounting for 26.55%; Food production is the weakest function, with only 2.91%. Meanwhile, waste treatment and raw materials accounted for 10.07% and 8.91%, respectively, which were much higher than that of food production. Due to the extensive distribution of the Xiangjiang River and its tributaries and lakes in the study area, the regional water conservation function is more prominent. Coupled with the increasingly strict ecological protection of the CZT ecological green center, the region provides a good ecological background for biodiversity conservation and soil formation and protection functions.

3.2 Spatial change of ESV

As can be seen in Figure 3, the spatial distribution of ESV in the CZT urban agglomeration from 2000 to 2020 shows an obvious pattern of "low in the middle and high in the surroundings", and the changes in different periods of time vary greatly, primarily in Changsha City and Xiangtan City but also concentrated in Tianyuan District. This decrease was largely driven by the rapid pace of CZT integration and "melting city" constructions, resulting in an accelerated expansion of construction land areas and significant declines in the ESV of the three urban areas. Overall, the ESV of the study area from 2005 to 2020 has decreased in a large area, spreading in a piecemeal fashion, with a significant decrease in

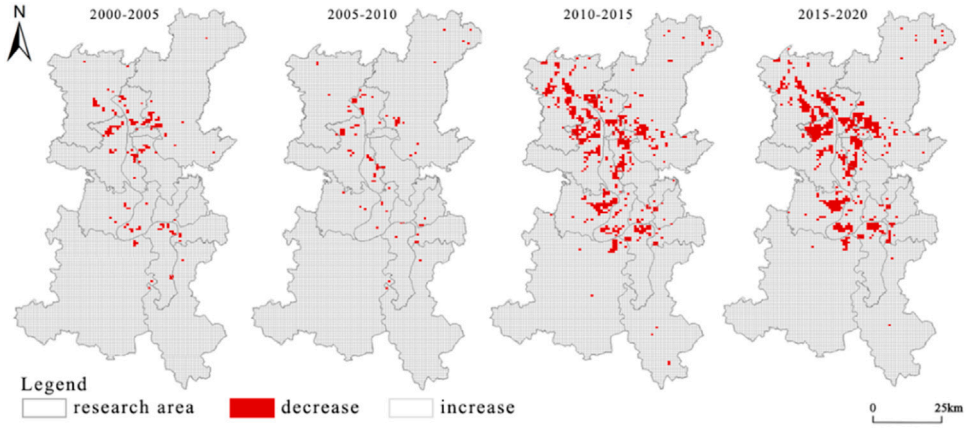

FIGURE 3
The spatial distribution of changes of ESV in 2000–2020 (10^6 yuan).

TABLE 3 Test of the influence factors.

Influencing factors	Proportion of construction land	NDVI	Temperature	Precipitation	Altitude	Slope
VIF	2.51	2.79	2.17	1.14	4.50	2.77
Influencing factors	Distance from river	Distance from highway	Distance from county government	Distance from railway	Population density	Economic density
VIF	4.81	1.37	4.00	3.66	10.13	9.34

the urban areas of CZT and an increase in the value of ecosystem service in the periphery of the urban areas. During the past 20 years, the urbanization level of CZT urban agglomeration and the integration construction of the three cities have increased the population density and the scale of economic activities in the region, which has intensified the squeeze and encroachment of urban land on arable land and ecological land and consequently led to a significant reduction of the ESV.

3.3 Analysis of influencing factors of ESV

Using SPSS23.0 to carry out the covariance test of the influence factors, it can be seen from Table 3 that among the 12 factors, only the inflated variance inflation factor (VIF) of population density is 10.13 > 10, and the VIF values of the rest of the factors are relatively small, which indicates that the level of covariance among the factors is low, and because population density is an important factor affecting the ESV, it is retained here. Through multiple stepwise regression of 12 factors, an adjusted R^2 of 0.60 was obtained, and the regression results passed the test of probability <0.05, and the factors affecting the ESV of CZT urban agglomeration were finally screened out to mainly include the factors of distance from district and county governments and distance from railways in terms of the locational conditions, the factors of NDVI, slope and precipitation in terms of the natural environment, as well as the proportion of construction land in terms of the socio-economic aspects, population density and economic density factors.

In order to investigate the relationship between the spatial distribution of the above eight major factors and the ESV in the study area, a bivariate spatial autocorrelation test was conducted using Geoda, and the results are shown in Table 4, the global Moran's I index of distance from Distance from county government, Distance from railway, Proportion of construction land, NDVI, Population density, Economic density, Slope and Precipitation with ESV were 0.23, 0.12, −0.45, 0.34, −0.33, −0.32, 0.26, and 0.05, respectively, while all these eight factors passed the 1% significance level test, indicating that their spatial correlation with ESV was significant. Among them, the proportion of construction land, population density and economic density are negatively correlated with the spatial distribution of ESV, and the spatial agglomeration of dissimilar values is significant. Besides, the remaining five factors have positive correlations with ESV in spatial distribution, and the similar values are spatially agglomeration significantly.

In Figures 4A, B, D, the spatial relationship between the three factors, distance from county governments, distance from railway, and NDVI, and ESV are similar, and the low-low concentration is dispersed throughout CZT's core urban areas. To be more precise, it is primarily concentrated in Yuelu District's northern portion, Kaifu District's southern portion, Furong District, Tianxin District's eastern and southern portions, Yuhua District's northern portion, the southwest portion of Changsha County, Yuhu District, Yetang District, Shifeng District, Hetang District, and portions of Tianyuan District. The southwest, Hetang, Yutang, Shifeng, Yuhu, and a portion of Tianyuan districts. High-high agglomeration areas are

TABLE 4 Spatial auto-correlation test of influencing factors.

Influencing factors	Distance to county government	Distance to railway	Proportion of construction land	NDVI	Population density	Economic density	Slope	Precipitation
Moran's I	0.23	0.12	−0.45	0.34	−0.33	−0.32	0.26	0.05
Z	22.77	11.94	−38.43	32.33	−31.54	−31.78	25.23	5.31

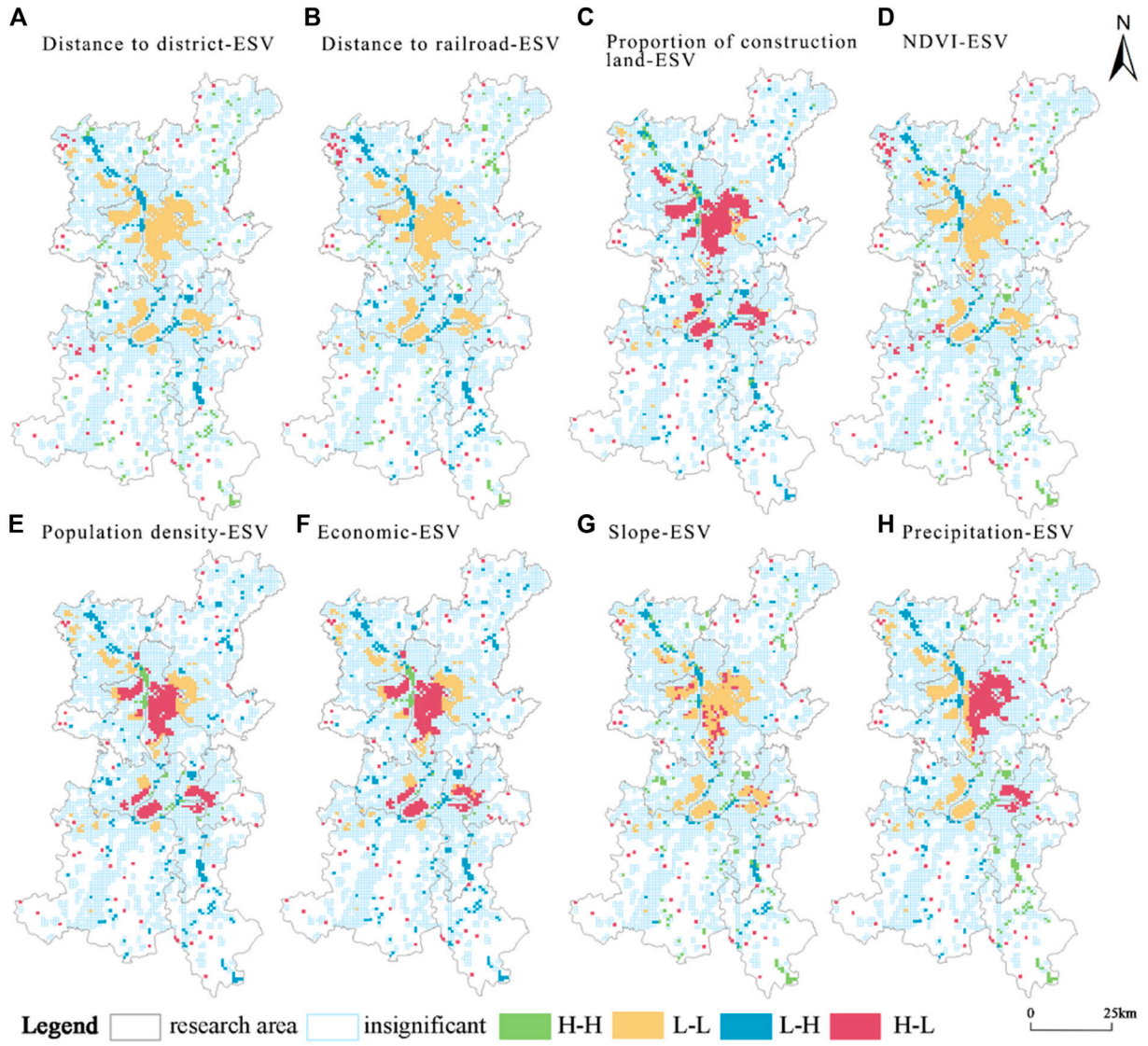

FIGURE 4
(A–H) Local spatial agglomeration graph of influencing factors and ESV.

concentrated in the northeastern part of the study area (Changsha County), the southern part (Xiangtan County, Zhuzhou County) and the ecological green heart, and other areas with lush vegetation cover, whose ecological environments are well protected due to their good vegetation cover, resulting in high ESV. The low-high value areas are mainly distributed along the Xiangjiang River and lakes, which are generally highly developed and utilised, resulting in a lower ESV; the high-low value areas are scattered in the peripheral areas of the urban area, which is mainly related to the planning of transport routes. The high and low ESV areas in Figure 4C are primarily found in Changsha City, Xiangtan City, Xiangtan County, and Shifeng, Hetang, and Tianyuan Districts in Zhuzhou City. These areas are concentrated in urban areas due to population density and economic activity, rising levels of urbanization, and rising land demand, which causes land to expand quickly for construction, significantly lowering the ESV of the area. Value of the area's

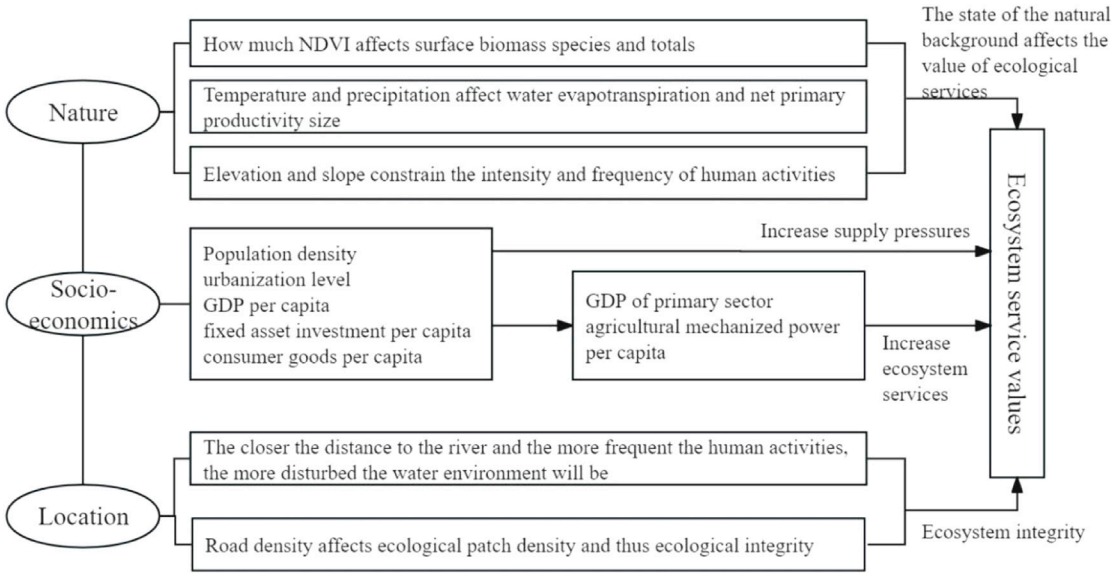

FIGURE 5
The relationship between each influencing factor and ESV.

services. The low-low agglomeration area is located in the southwestern part of Changsha County, the northwestern part of Wangcheng District, and the periphery of Yuhu District and Xiangtan County, which is far away from the urban area, sparsely populated, economically inactive, and mostly farmable land with a low ESV in general. The high - high agglomeration is mainly along the Xiangjiang River, with a high proportion of construction land, but the ESV is also relatively high due to the proximity of the Xiangjiang River and lakes and wetlands.

In Figures 4E, F, the spatial distribution of population and economic densities and ESV is consistent, i.e., the high-low ESV areas are mainly distributed in the inner five districts of Changsha, Yuhu and Yutang districts of Xiangtan, and Shifeng, Tianyuan and Hetang districts of Zhuzhou. In comparison to the neighboring counties and districts, these districts have a higher population density, more economic activity, and a higher demand for ESs from human civilization. As a result, the ecological environment is under more stress and has a lower value. However, Changsha County, Wangcheng District, Xiangtan County, and other towns and cities with lower population and economic densities are primarily found on the periphery of the low-low agglomeration. The low-low agglomeration is primarily concentrated in the urban regions of Changsha, Xiangtan and its surrounding counties and towns, as well as Shifeng, Tianyuan, and Hetang districts of Zhuzhou. The spatial distribution of slope and ESV in Figure 4G displays variability. Meanwhile, the high - low anomalies are also intertwined and distributed in these areas. In the spatial distribution of precipitation and ESV in Figure 4H, the low-low agglomeration area is mainly distributed in the central and western parts of CZT urban agglomeration, while the high-low anomaly area is mainly distributed in the central-eastern part of the study area, including Furong, Tianxin, Yuhua, and southwestern Changsha counties, and Shifeng, Hetang, and Tianyuan districts. The high - high agglomeration is mainly concentrated in the northeastern part of Changsha County and the southeastern part of Zhuzhou County, due to the rich vegetation, sloping topography, and more abundant precipitation, thus making the value of ecosystem service higher than that of the urban areas.

4 Conclusions and discussion

4.1 Conclusion

Taking CZT urban agglomeration as the study area, based on the remote sensing image data and multifactor raster data from 2000 to 2020, using the value equivalent method, multivariate regression and bivariate spatial statistical methods, we analyzed the temporal and spatial change characteristics and driving factors of ESV in the study area, and obtained the following main conclusions: The total ESV in CZT urban agglomeration shows a changing trend of decrease. The ESV of different land use type were declining trends. The ESs in the CZT urban agglomeration area are mainly dominated by the three functions of water conservation, biodiversity conservation and soil formation and protection, followed by gas exchange and climate regulation functions, and the weakest food production function. The spatial distribution of ESV in the CZT urban agglomeration shows an obvious pattern of “low in the middle and high in the surroundings”. The spatial correlation between distance from the county government, distance from the railway, Proportion of construction land, NDVI, population density, economic density, slope, precipitation, and ESV are significant.

4.2 Discussion

This study utilizes grid analysis to quantify the spatial and temporal changes in the value of ESs in the CZT urban

agglomeration from 2005 to 2020, and finds that it shows a decreasing trend in time, with an obvious decreasing trend; the spatial distribution shows an obvious "low in the middle, high in the periphery" pattern, which is consistent with Ouyang et al. This is basically consistent with the conclusion of (Ouyang et al., 2019) that "ESs in the CZT urban agglomeration in 2015 showed a spatial pattern of "center-periphery" distribution, and showed a spatial distribution trend of outward increase". It is basically consistent. Unlike most of the previous studies at the scale of administrative division, economic division and natural division, the grid can avoid the influence of artificial division boundaries to a certain extent, and can more accurately reflect and portray the micro-scale spatial changes of ESV and its influencing factors.

The sharp decline in the ESV is primarily caused by the rapid urbanization of urban agglomerations since 2005, the rapid migration of rural residents to cities and towns, the conversion of significant amounts of Cultivated land into construction land and industrial land, mining, and transportation purposes, and the growing intensity of economic activities. Industrialization has exacerbated environmental pollution and ecological damage, thus changing the structure, function and development process of ecosystems, and bringing about a decline in ecological environment quality. The decline in ecological environment quality is manifested in the reduction of ESV, which affects the sustainable survival and development of human beings. In urban areas with a high level of economic development, the population density and economic activity levels are high, and human demand for ESs is high. This combination creates an ecological crisis caused by a lack of regional ESs, which limits the scale of economic development and has an adverse impact on the improvement of people's quality of life. While in the periphery of urban agglomerations with a lower level of economic development, the area of ecological land is large, and with the low intensity of economic activities, the ESV is high *per capita*, but the ESV is low. The ESV is high, but the economic development of the peripheral areas is slow and the development gap with the core urban areas is large. It can be seen that the spatial imbalance of ESs will constrain the coordinated integration and sustainable development between the core and peripheral areas to a greater extent. The result the consistent with Jiang. (2010) "the result of key area was contrary to the whole study area".

In addition to the natural and socio-economic factors like climate, topography, population, and economic and social factors, the spatial location of each grid was also taken into account when choosing the influencing factors (Figure 5). Four influencing factors, such as distance to rivers, distance to different transportation roads, and distance to county government were chosen, based on the studies of Jiang. (2010) and Xing. (2018). In general, the direction of changes in the value of ecosystem service is determined by the amount to which human activities have an impact on different spatial regions' ecosystems. The closer the distance from rivers, highways, county government and railway, and the more intensive the human activities, the more the ESs are affected by human society, and the value of ecosystem service tends to decrease. The spatial distribution correlation between ESV and the influencing factors in CZT urban agglomeration is presented visually using SPSS 23.0 to screen the pertinent influencing factors, and Geoda and ArcGIS 10.2 software. This is of great importance for the urban agglomeration to harmonize the ecological environment, adjust the ecological management, and advance the experiment of reforming the "two-type" society in the future. This will help to coordinate ecological management in the urban agglomeration in the future and will support the reform experiment of a "two types" society. However, since it is difficult to identify the local anomalies of the influencing factors, more accurate spatial heterogeneity detection model should be applied in future studies. Moreover, with the improvement of transportation conditions and information networks, the linkage between urban agglomerations will also affect the value of ecosystem service, and the spatial interactions between cities should be quantified in the future. Meanwhile, the assessment and analysis of multi-scale grids will be strengthened in the future in order to more accurately recognize the scale effect.

In view of the declining trend of the total ESV and the value of individual services in the CZT urban agglomeration, under the background of accelerated urbanization and integrated urban development, there are the following suggestions for the planning and ecological construction of the urban agglomeration in the future: First, appropriately promote the urbanization of CZT cities, reasonably regulate the scale and speed of construction land expansion, advocate saving and intensive use of construction land, and improve the efficiency of land use; reasonably evacuate the population in areas with high population and economic density and poor ecosystem service function. Second, adhere to the red line of basic farmland protection, encourage farming where farming is appropriate, strengthen the efficient and modernized production of basic farmland, increase the food production per unit area of farmland, and enhance the capacity and security of regional food supply. Third, strengthen the protection of ecological land in urban agglomerations, plan and utilize the natural ecological environment in the peripheral areas of urban agglomerations and green heart areas, and rationally deploy ecosystem service to create an ecological environment in urban agglomerations that is pleasant to live in, pleasant to work in, and pleasant to visit.

Data availability statement

The original contributions presented in the study are included in the article/Supplementary Material, further inquiries can be directed to the corresponding authors.

Author contributions

XH: Conceptualization, Formal Analysis, Methodology, Software, Supervision, Writing–original draft, Writing–review and editing. YX: Formal Analysis, Methodology, Writing–original draft. FL: Data curation, Methodology, Software, Writing–original draft. LC: Data curation, Investigation, Resources, Visualization, Writing–original draft. HZ: Data curation, Formal Analysis, Software, Writing–original draft.

Funding

The author(s) declare financial support was received for the research, authorship, and/or publication of this article. The Open Topic of Key Laboratory of Natural Resources Monitoring and

Supervision in Southern Hilly Region, Ministry of Natural Resources (NRMSSHR 2022Z06).

Conflict of interest

The authors declare that the research was conducted in the absence of any commercial or financial relationships that could be construed as a potential conflict of interest.

Publisher's note

References

Chen, F., Liu, Y., and Liu, Q. (2014). Spatial downscaling of TRMM 3B43 precipitation considering spatial heterogeneity. *Int. J. Remote Sens.* 35 (9-10), 3074–3093. doi:10.1080/01431161.2014.902550

Daily, G. C. (Editors) (1997). *Nature's Service: Societal Dependence on Natural Ecosystems*. Washington: Island Press.

Deng, C., Zhong, X., Xie, B., Wan, Y., and Song, X. (2019). Spatial and temporal changes of land ecosystem service value in Dongting Lake area in 1995-2015. *Geogr. Res.* 12, 4. doi:10.11821/dlyj020170999

Gao, H., Han, H., Luo, X., Yu, H., and Han, M. (2016). Spatial correlation of socioeconomic factors and ecosystem service values in guizhou province. *Res. Soil Water Conservation* 23, 5. doi:10.13869/j.cnki.rswc.2016.02.048

Gao, J., Yu, Z., Wang, L., and Vejre, H. (2019). Suitability of regional development based on ecosystem service benefits and losses: a case study of the Yangtze River Delta urban agglomeration, China. *Ecol. Indic.* 107, 105579. doi:10.1016/j.ecolind.2019.105579

He, Y., and Zhou, G.-h. (2007). Delimitation of the changsha-zhuzhou-xiangtan city-and-town concentrated area. *Trop. Geogr.* 27, 6.

Huang, L., Yang, P., Wang, L. J., and Zhang, X. L. (2019). Spatio-temporal evolution characteristics and influencing factors of LandEcological security in the Yangtze River Economic belt. *Resour. Environ. Yangtze Basin* 71, 11–21. doi:10.11870/cjlyzyyhj201908003

Huang, M., Fang, B., Yue, W., and Feng, S. (2019). Spatial differentiation of ecosystem service values and its geographical detection in Chaohu Basin during 1995-2017. *Geogr. Res.* 38, 14. doi:10.11821/dlyj020181075

Jiang, T. (2010). *Change of farmland ecosystem services values and its driving forces in northwestern arid area: a case study on minqin county*. Lanzhou: Lanzhou University.

Li, D. (2019a). *Time and space evolution and driving forces ofFarmland ecosystem service value loss in karst areas: a case study ofLibo county*. Guizhou: Guizhou Normal University.

Li, H. (2014). *Study on changes in the value of ecological services in guanzhong-tianshui economic zone and its driving factors*. Shaanxi: Shaanxi Normal University.

Li, X. (2019b). *A study on the measurement and influence factors of Ecosystem service value in the Yangtze River Economic belt.* Jiangxi: Jiangxi University of Finance and Economics.

Lin, H. (2019). *Spatio-temporal evolution of ecosystem Service Value and its driving mechanism in Guangzhou*. Guangzhou: Guangzhou University.

Liu, J., Kuang, W., Zhang, Z., Xu, X., Qin, Y., Ning, J., et al. (2014). Spatiotemporal characteristics, patterns and causes of land use changes in China since the late 1980s. *Acta Geogr. Sin.* 69, 12. doi:10.11821/dlxb201401001

Liu, M., Zeng, S., Sun, F., and Liu, Y. (2016). Analysis on the evolution law and driving force of water ecosystem services in beijing-tianjin-hebei region. *Environ. Impact Assess.* 38, 5. doi:10.14068/j.ceia.2016.06.010

Liu, X., and Lv, X. (2009). Driving forces analysis of wetland ecosystem services change. *J. Arid Land Resour. Environ.* 5, 1.

Luo, Y., Lü, Y., Liu, L., Liang, H., Li, T., and Ren, Y. (2020). Spatiotemporal scale and integrative methods matter for quantifying the driving forces of land cover change. *Sci. Total Environ.* 739, 139622. doi:10.1016/j.scitotenv.2020.139622

Mao, C., and Chen, Y. (2010). The driving force and prediction of the evolution of land use and ecosystem services value——a case study of Jiangsu province. *Res. Soil Water Conservation* 17, 7.

Nan, B., Yang, Z., Bi, X., Fu, Q., and Li, B. (2018). Spatial-temporal correlation analysis of ecosystem services value and human activities——a case study of Huayang lakes area in the middle reaches of Yangtze Rive. *China Environ. Sci.* 38, 11. doi:10.19674/j.cnki.issn1000-6923.2018.0382

Ouyang, X., He, Q., and Zhu, X. (2020). Simulation of lmpacts of urban agglomeration land use change on Ecosystem services value under multi-scenarios: case study in changsha-zhuzhou-xiangtan urban agglomeration. *Econ. Geogr.* 10, 1. doi:10.15957/j.cnki.jjdl.2020.01.011

Ouyang, X., Zhu, X., and He, Q. (2019). Spatial interaction between urbanisation and ecosystem services: a casestudy in Changsha-Zhuzhou-Xiangtan urban agglomeration, China. *J. Ecol.* 39, 7502–7513. doi:10.5846/stxb201809081922

Qiao, X., Gu, Y., Tang, H., and Yang, Y. (2015). Service values change of farmland ecosystem and its influence factors analysis in Weigan River Basin. *Agric. Res. Arid Areas* 000, 237–245. doi:10.16302/j.cnki.1000-7601.2015.02.039

Ran, F., Luo, Z., Cao, L., Zhao, J., and Zhao, Y. (2018). Analysis on the change of ecological service value and its driving factors in nanchang. *Res. Soil Water Conservation* 25, 7. doi:10.13869/j.cnki.rswc.2018.03.025

Rao, E., Xiao, Y., Ouyang, Z., and Zheng, H. (2013). Spatial characteristics of soil conservation service and its impact factors in Hainan Island. *Acta Ecol. Sin.* 33, 10. doi:10.5846/stxb201203240400

Rui, H., Sun, S., Guo, L., and Chen, Y. (2019). Evolution of ecosystem service value and analysis of driving forces in the east region of sichuan province, China. *J. Ecol. Rural Environ.* 35, 8. doi:10.19741/j.issn.1673-4831.2018.0596

Su, C. W. (2018). Yalu. Evolution of ecosystem services and its driving factors in the upper reaches of the Fenhe River watershed, China. *Acta Ecol. Sin.* 38 (22), 7886–7898. doi:10.5846/stxb201711061986

Sun, H., Yang, G., Wan, R., and Wu, Y. (2009). According analysis of the change of ecosystem service value and the differentiation of the driving factors in kunshan. *Resour. Environ. Yangtze Basin* 18, 6.

Sun, X., Guo, H., Lian, L., Liu, F., and Li, B. (2017). The spatial pattern of water yield and its driving factors in nansi lake basin. *J. Nat. Resour.* 32, 11. doi:10.11849/zrzyxb.20160460

Tang, X., Hao, X., Liu, Y., Pan, Y., and Li, H. (2016). Driving factors and spatial heterogeneity analysis of ecosystem services value. *Trans. Chin. Soc. Agric. Mach.* 47, 7.

Wartenberg, D. (1985). Multivariate spatial correlation: a method for exploratory geographical analysis. *Geogr. Anal.* 17, 263–283. doi:10.1111/j.1538-4632.1985.tb00849.x

Wei, H., and Guo, D. (2015). Dynamic change and its driving forces of alpine meadow ecosystem in Maqu, Gansu, China. *J. Desert Res.* 8, 33.

Xie, G., Lu, C., Leng, Y., Zheng, D., and Li, S. (2003). Ecological assets valuation of the Tibetan Plateau. *J. Nat. Resour.* (02), 189–196. doi:10.11849/zrzyxb.2003.02.010

Xing, L. (2018). *Study on the spatio-temporal impacts of urbanization on the ecosystem services value and ecological sustainability assessment*. Huazhong: Huazhong University of Science and Technology.

Xue, M., and Luo, Y. (2015). Dynamic variations in ecosystem service value and sustainability of urban system: a case study for Tianjin city, China. *Cities* 46, 85–93. doi:10.1016/j.cities.2015.05.007

Yang, C. (2018). *Study on spatial-temporal differentiation of land ecosystem service value and driving factors in central plains urban agglomeration*. Hebei: Hebei University of Economics and Business.

Yang, L., Yang, G., Yao, S., and Yuan, S. (2012). A study on the spatial heterogeneity of grain yield per hectare and driving factors based on ESDA-GWR. *Econ. Geogr.* 32, 7.

Yao, X., Zeng, J., and Li, W. (2015). Spatial correlation characteristics of urbanization and land ecosystem service value in Wuhan Urban Agglomeration. *Trans. Chin. Soc. Agric. Eng.* 31, 8.

Zhang, H., Wang, S., and Liu, Y. (2017). Research on spatial differentiation of land ecological quality and main controlling factors identification based on city scale:——a case study of Jiaozuo City. *Agric. Res. Arid Areas* 35, 9.

Zhang, P., Zhu, Y., Shi, Y., and Hu, Y. (2020). *Chang-zhu-tan urban agglomeration regional plan (2008-2020) (2014 revision)*.

Zhao, Z., Wang, K., and Xie, X. (2014). Assessment on ecosystem services value of foothills county——taking taoyuan county of hunan province as an example. *Hubei Agric. Sci.* 53, 6. doi:10.14088/j.cnki.issn0439-8114.2014.06.068

Zhao, Z., Yu, D., Han, C., and Wang, K. (2017). Ecosystem services value prediction and driving forces in the Poyang Lake Ecoeconomic Zone. *Acta Ecol. Sin.* 37, 11. doi:10.5846/stxb201612042489

Zuo, M., and Ma, Y. (2012). Analysis of the evolution of yiwu ecological service value and its driving factors. *J. Zhejiang Agric. Sci.* 5, 2.

frontiers | Frontiers in Ecology and Evolution

TYPE Original Research
PUBLISHED 10 January 2024
DOI 10.3389/fevo.2023.1308310

OPEN ACCESS

EDITED BY
Xue-Chao Wang,
Beijing Normal University, China

REVIEWED BY
Qimeng Ning,
Hunan City University, China
Guoen Wei,
Nanchang University, China

*CORRESPONDENCE
Benqing Zhang
zhang1667799@foxmail.com

RECEIVED 06 October 2023
ACCEPTED 11 December 2023
PUBLISHED 10 January 2024

CITATION
Yin X, Lu Z and Zhang B (2024) Study on the factors influencing ecological environment and zoning control: a study case of the Dongting Lake area. *Front. Ecol. Evol.* 11:1308310. doi: 10.3389/fevo.2023.1308310

Study on the factors influencing ecological environment and zoning control: a study case of the Dongting Lake area

Xiangpeng Yin[1,2], Zhaoyan Lu[3] and Benqing Zhang[2]*

[1]School of Marxism, Hunan University of Science and Technology, Xiangtan, China, [2]School of Marxism, Hunan University of Finance and Economics, Changsha, China, [3]Economic College, Hunan Agricultural University, Changsha, China

Introduction: Protecting the ecosystem of the Dongting Lake area is of utmost importance for maintaining ecological balance and achieving human well-being.

Methods: This study identifies the key factors influencing the remote sensing based ecological index (RESI) in the Dongting Lake area based on the spatial and temporal evolution characteristics of the RESI and environmental changes and anthropogenic disturbance factors. The priority zoning for ecological restoration was delineated in combination with the anthropogenic composite index (ACI). By exploring the influence of anthropogenic disturbances on RESI, the zoning locations were determined using spatial statistics and linear regression methods.

Results: The overall RESI of the Dongting Lake area showed a decline from 2001 to 2020, with the mean value decreasing from 0.52 to 0.48. High-quality zones were mainly located in mountainous and forested areas, while low-quality zones were mainly distributed in more developed cities in the east urban area. Anthropogenic factors were the main reasons for the decline in the ecological environment, while natural factors showed a positive correlation with RESI. Based on the RESI and ACI, four ecological control zones (H-H, H-L, L-H, and L-L) were delineated, which accounted for a total of 45.66% of the Dongting Lake area. Among them, 3.91% required immediate control and management, while 17.80% required artificial maintenance. This study explores the influencing factors and mechanisms of the ecological environment quality in the Dongting Lake area, and explores the effective spatial paths for the implementation of ecological restoration zoning control and differentiated restoration strategies in the Dongting Lake area.

Discussion: This study provides a scientific basis for mitigating ecological and environmental problems in the Dongting Lake area, and provides a reference for ecological restoration and regulation and the realization of sustainable development goals in China and global regions with complex environmental problems.

KEYWORDS

Dongting Lake area, ecological environment, zoning control, influencing factors, ecological restoration

1 Introduction

Environmental changes, such as precipitation and temperature, along with human disturbances, can lead to a range of ecological effects that impact ecological health (Su et al., 2010; He et al., 2019). In recent decades, the Dongting Lake area has faced numerous threats to its ecological quality due to intensive and continuous human activities, including lake encirclement, dam construction, urban expansion, agricultural surface pollution, and irrational exploitation. Of particular concern is the over-exploitation of resource elements (Yu et al., 2018; Zhang et al., 2018b). These activities have resulted in the decline of wetland area, deterioration of water quality, destruction of ecosystem structure and habitats, and loss of biodiversity, ultimately leading to a significant decline in ecological quality and weakening of ecological service function (Wang et al., 2022). Consequently, there is an urgent need to effectively evaluate the RESI within the Dongting Lake area and implement comprehensive spatial protection measures for this national territory.

Numerous studies have been conducted to monitor and evaluate the status or changes in the ecological environment. Among these studies, remote sensing indices have been employed for evaluation purposes. These indices include the Normalized Vegetation Index (Kobayashi and Dye, 2005), enhanced vegetation index (Matsushita et al., 2007), Normalized Difference Water Index (Taloor et al., 2021), and the Normalized Difference moisture Index (Jin and Sader, 2005). Scholars have increasingly combined these remote sensing indices with socio-economic factors to construct pressure-state-response models for evaluating ecological health (Zhang et al., 2012; Qin et al., 2023). However, the subjectivity involved in applying hierarchical analysis to determine the weight of each factor reduces the credibility of the evaluation results (Cheng et al., 2022). Alternatively, some scholars have proposed a comprehensive ecological index, known as the Remote Sensing Based Ecological Index (RESI), which integrates four major ecological indicators: moisture, dryness, heat, and greenness. The principal component analysis of covariance is used to determine the weights of each factor on ecological quality. This approach emphasizes the objectivity and reasonability of the evaluation results by highlighting the influence of each indicator's impact on ecological quality based on data characteristics rather than subjective factors (Xu et al., 2018). Thus, the use of the RESI to evaluate changes in ecological quality in the Dongting Lake area is both feasible and reliable.

Researchers have identified various factors that influence RESI, including climate, land use change, population, and economy (Ouyang et al., 2019; Hasan et al., 2020; Yang et al., 2022). The composition and health of different land use types serve as direct indicators of ecological quality (Hasan et al., 2020). Temperature and precipitation are significant climatic influences (Zou et al., 2020), while population density and socio-economic development contribute as prominent anthropogenic disturbances (Liu et al., 2023). It is reasonable to expect that higher population density will have a greater negative impact on ecological health (Wei et al., 2023). Therefore, it is imperative to study the factors influencing RESI in the Dongting Lake area and identify key factors responsible for the changes in RESI. However, current research on RESI has certain limitations. Firstly, it primarily focuses on urban areas, neglecting the lake area. Secondly, it fails to consider long-term changes in RESI and the varying intensity of influencing factors across different time periods.

Climate change and large-scale land development have led to changes in the structure and function of the lake and wetland ecosystems in the region, and it is necessary to curb ecological degradation by promoting ecological restoration. Efficient zoning control strategies and rapid improvement of ecological quality remain challenging. In this study, based on a 2 km × 2 km grid scale covering the Dongting Lake area, the ecological environment quality index (EEQI) was calculated from 2001 to 2020 by integrating four indicators, namely, humidity, dryness, heat and greenness, and the influencing factors of EEQ were analyzed by using GWR (geographically-weighted regression), and the relationship between ACI (Anthropogenic Composite Index) and RSEI was quantified to determine the priority areas for ecological restoration by combining the Anthropogenic Finally, the relationship between ACI and RSEI was quantified by combining the ACI to determine the ecological restoration priority areas. The study aims to address the following scientific questions: (1) What are the temporal and spatial characteristics of continuous changes in the RESI in the Dongting Lake area during the study period. (2) What are the potential factors that affect changes in the RESI in the Dongting Lake area. The ultimate goal is to provide guidance for formulating ecological restoration plans in the Dongting Lake area.

2 Materials and methods

2.1 Study area

The Dongting Lake area, centered on the waters of Dongting Lake, exhibits diverse landscapes transitioning into wetlands, plains, hills, and mountains (Tan et al., 2020). It serves as a significant ecological zone for regulating water levels in the middle and lower reaches of the Yangtze River. Additionally, it represents a fragile zone where land and water ecosystems intertwine at the confluence of four rivers: Xiang, Zizhi, Yuan, and Li. The region has a subtropical monsoon climate characterized by abundant precipitation, simultaneous rain and heat, and rich water, air, soil, and biological resources. It hosts diverse ecosystems, including wetlands, grasslands, forests, farmlands, and urban areas (Tan et al., 2020; Xiong et al., 2022). At present, the ecological environment of Dongting Lake is mainly facing problems such as unstable water quality, degradation of wetlands, declining water levels, loss of biodiversity, floods and land use conflicts. These problems affect the ecological balance of the lake, the sustainable use of water resources and the livelihoods of local residents.

To enhance the ecological quality of the Dongting Lake Basin, the Hunan Provincial People's Government implemented the Three-Year Action Plan for the Ecological Environment of Dongting Lake (2018–2020). This plan encompassed measures such as addressing agricultural surface pollution, reforestation and wetland conservation, the removal of invasive poplars in the

core area of the Dongting Lake Nature Reserve, and wetland restoration. The implementation of these measures has resulted in notable improvements in the habitat quality of the Dongting Lake Basin. However, serious threats to habitat quality persist. Hence, studying the habitat quality in the Dongting Lake area is both typical and representative. The study area includes selected counties (cities and districts) in Yueyang, Yiyang, and Changde, three prefecture-level cities located in the Dongting Lake area (Figure 1). It covers an area of approximately 25,800 km^2, accounting for about 12.18% of Hunan Province. The resident population was approximately 10,705,800 by the end of 2020, constituting 16.11% of the province's total, with a gross domestic product (GDP) of around 710,440 million yuan, representing approximately 17% of the province's total.

2.2 Study methods

(1) Remote Sensing Based Ecological Index (RESI)

The Remote Sensing Based Ecological Index (RSEI) evaluates the quality of the ecological environment using four indicators: moisture, dryness, heat, and greenness. These indicators are closely related to the human living environment. They can be obtained by analyzing remote sensing images, and the specific data acquisition methods can be found in the data source section. Compared with the Ecological Environment Status Index, RSEI provides a more accurate assessment of the strengths and weaknesses of regional ecological environments (Lakes and Kim, 2012; Xu, 2013; Zheng et al., 2022). In this study, we utilized the ENVI 5.3 platform to calculate the indicators of moisture, dryness, heat, and greenness based on different bands of remote sensing images. Moisture was represented by WET values, dryness was determined by integrating surface building and surface bare soil indices, heat was derived through the inversion of a single window algorithm, and greenness was expressed using the Normalized Vegetation Index (NVI).

(2) Selection of Factors Influencing RSEI

When it comes to the selection of variables that affect RSEI, moisture, dryness, heat, and greenness are the main factors. These factors directly reflect the status of RESI. Moreover, the quality of the ecological environment is affected by both natural and human factors (Ouyang et al., 2021). Natural factors encompass climatic and geographical aspects, with temperature and precipitation being key climatic influences, while slope is an important geographical factor (Peng et al., 2017). Human factors incorporate disturbances such as proximity to the county government, population size, and socio-economic development (Retallack, 2021; Li et al., 2022). Since RSEI is constructed based on the metrics of moisture, dryness, heat, and greenness, these factors were not taken into account during the analysis of potential influencing factors. This study quantitatively analyzed the relationship between the entire RSEI mean and factors

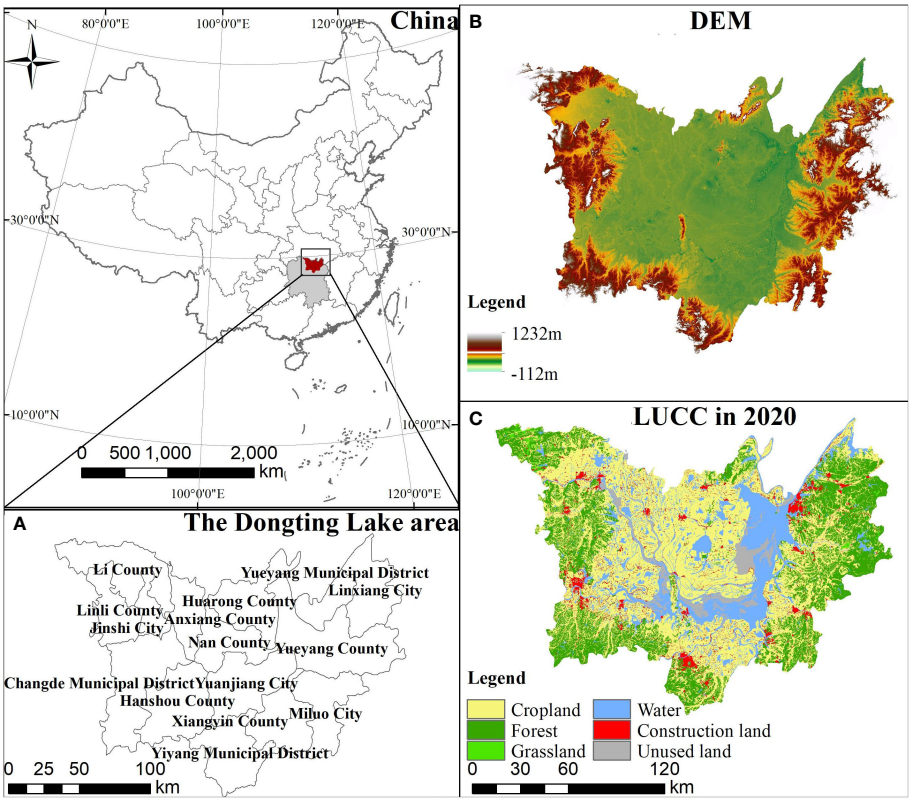

FIGURE 1
Study area. **(A)** Dongting Lake area; **(B)** DEM; **(C)** LUCC.

such as slope, temperature, rainfall, population density, GDP, and proximity to the county government using geographically weighted regression to dissect the correlation between natural factors and natural factors on RSEI.

(3) Selection of spatial priority areas for ecological restoration

This study utilized the Anthropogenic Composite Index (ACI) to measure the intensity of human activities within each 2 km × 2 km grid in the Dongting Lake area of Hunan Province, quantify the relationship between ACI and RSEI" for concision (Equation 1), and identify priority zones for ecological restoration using a spatial statistical method that considers the removal of water bodies. The calculation formula is as follows:

$$ACI = (G_{std} + P_{std} + N_{std})/3 \quad (1)$$

Where, G_{std} is the standardized value of GDP, P_{std} is the standardized value of population density, N_{std} is the standardized value of nighttime lighting index, all expressed in terms of a 2 km × 2 km grid.

Based on the bivariate local Moran's I (bi-LISA) method (Equation 2), the spatial correlation between the RSEI and the ACI was investigated to quantify the significance of ΔRSEI and ΔACI in image elements and their neighbouring shares at the 2 km grid scale. The calculation is as follows:

$$I_{B,i} = z_{x,i} \sum_{j=1,j\neq i}^{N} W_{i,j}\, z_{y,j} \quad (2)$$

Where, x is the average change in the ΔACI of a pixel and y represents the average change in ΔRSEI of pixels nearby called j. The first-order queen-neighbor matrix serves as the foundation for the spatial weight matrix, $W_{i,j}$. Using significant values of p 0.001, 0.005, 0.01, and 0.05 as the discriminating criterion, the results revealed that the restoration priority locations had four significant value types: high-high (H-H), high-low (H-L), low-high (L-H), and low-low (L-L).

2.3 Data sources

The data used in this study were mainly derived from the Resource and Environment Science Data Centre of the Chinese Academy of Sciences (www.resdc.cn); China statistical yearbook (www.stats.gov.cn); OpenStreetMap (www.openstreetmap.org); Landscan (https://landscan.ornl.gov); and National Aeronautics and Space Administration (www.earthdata.nasa.gov). This study considers paddy fields, drylands, construction land, and bare land as potential threat sources due to their frequent human activities or harsher natural environments. In this study, NDVI, NDBSI, LST and WET data were calculated based on Landsat surface reflectance data, and then RSEI was further measured. The Landsat surface reflectance data were obtained from the USGS (United States Geological Survey) (https://lpdaac.usgs.gov) with a resolution of 500m. The parameter settings, including habitat suitability, weights of stressors, maximum stress distance, and sensitivity of habitat types to stressors, were adopted from relevant literature.

3 Results

3.1 Temporal and spatial characteristics of RESI

Based on the results of the spatial and temporal evolution of the ecological quality of Dongting Lake at a raster scale of 2 km × 2 km from 2001 to 2020 (Figure 2) and the categorical statistics of the ecological quality area (Table 1), there was an overall slight downward trend in the mean value of ecological quality. Over time, the mean value of RESI in the Dongting Lake area decreased from 0.52 in 2000 to 0.48 in 2020. The minimum value of RESI fluctuated with a decrease from 0.28 in 2000 to 0.22 in 2020, while the maximum value showed a fluctuating trend of ups and downs.

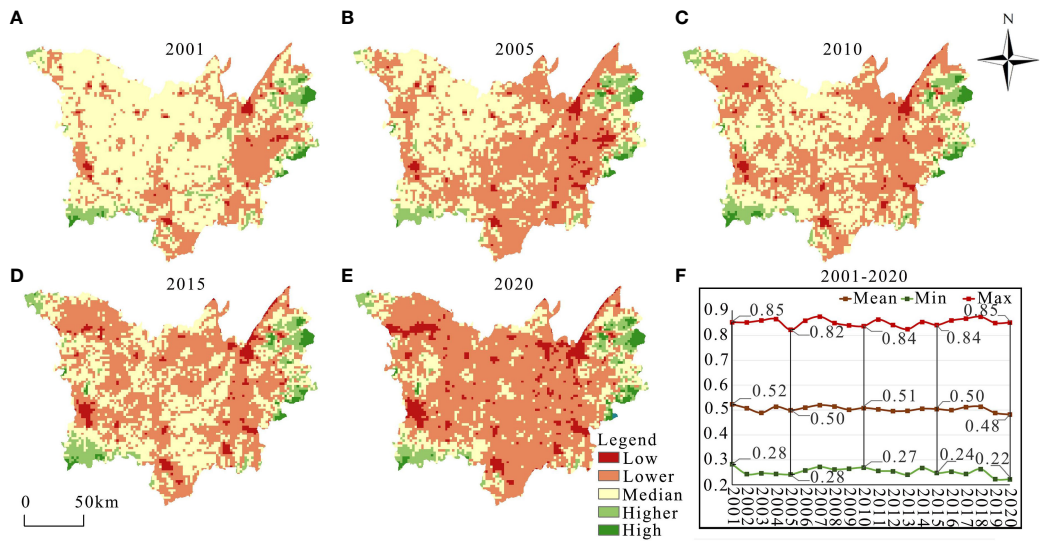

FIGURE 2
Spatial and temporal evolution of RESI in Dongting Lake region, 2001–2020. **(A–E)** 2001, 2005, 2010, 2015 and 2020 of RESI, **(F)** mean, min and max of RESI from 2001 to 2020.

10.3389/fevo.2023.1308310

TABLE 1 Classification statistics of RESI in Dongting Lake area, 2001–2020/km^2.

Year	Low	Lower	Medium	Higher	High
	0.2–0.4	0.4–0.5	0.5–0.6	0.6–0.7	0.7–0.9
2001	5620	115400	25560	21920	5336
2005	12812	202980	154508	18980	4556
2010	9716	186264	166516	23692	7648
2015	15764	194940	150048	25972	7112
2020	30572	258712	73292	23080	8180

From a spatial perspective, the RESI in the Dongting Lake region exhibits a concentration of high values and a dispersion of low values. High-value and higher-value areas are primarily found in Dingcheng District, Linxiang City, and other mountainous areas with abundant vegetation cover. On the other hand, low-value areas cluster in the eastern part of the Dongting Lake Basin, particularly in regions characterized by extensive urban construction and development, such as Heshan District, Yueyanglou District, and Yunxi District. Between 2000 and 2020, the process of urban expansion has led to a more extensive spatial distribution of low-value and lower-value areas of ecological quality in the Dongting Lake area. The area occupied by low-value areas increased by 4.43 times, while lower-value areas increased by 1.24 times. These areas have experienced rapid economic development, intense exploitation of land resources, and high population concentration, resulting in significant disturbances to the ecosystem.

During the period from 2001 to 2020, there were variations in the transfer of RESI levels in Hunan Province, demonstrating an overall gradient downward trend from high values to medium values and then to low values (Figure 3).

Specifically, the transfer of different RSEI levels occurred in an area of 15,222.85 km^2 within the Dongting Lake area. The largest proportion of transfers was from the middle value to the lower value, accounting for 74.62% of the area (11,359.01 km^2), followed by transfers from the lower value to the lower value, accounting for 8.04% of the area (1,223.52 km^2). Transfers from the high value to the

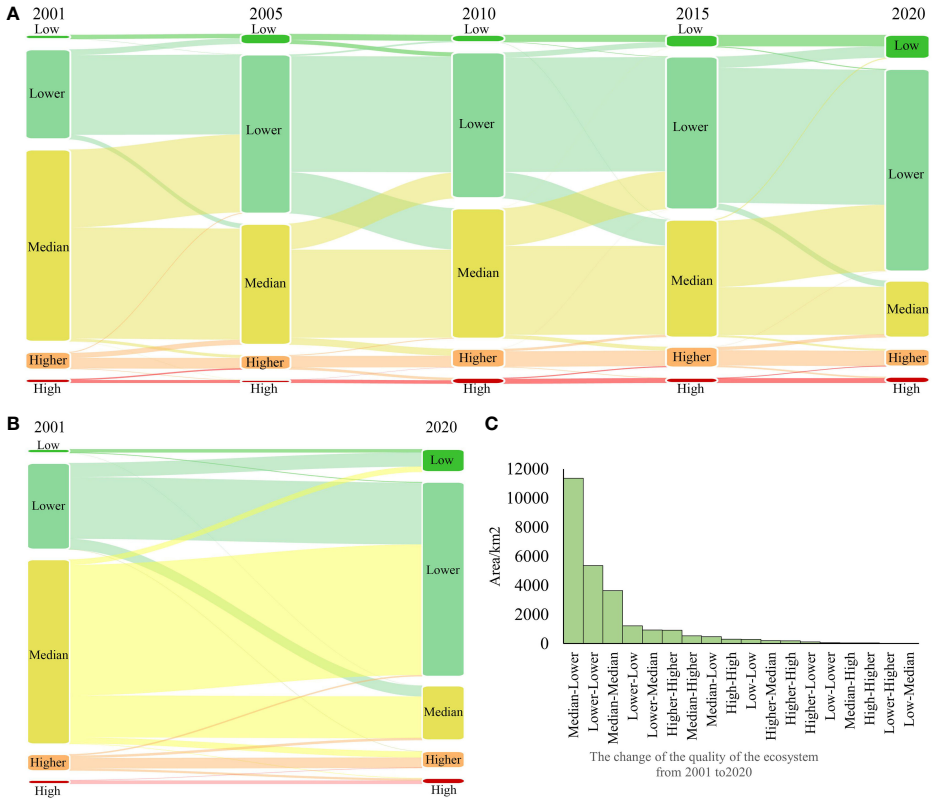

FIGURE 3
Transfer of RESI level in Dongting Lake region, 2001–2020. **(A)** Transfer of RESI in 2001–2005, 2005–2010, 2010–2015 and 2015–2020; **(B)** transfer of RESI from 2001 to 2020; **(C)** change of RESI from 2001 to 2020.

higher value accounted for 1.38%, and transfers from the higher value to the lower value accounted for 1.4%. Higher values were transferred to higher values in 1.38% of the area, covering an area of 43.42 km^2.

3.2 Analysis of influencing factors

In this study, the Geographically Weighted Regression (GWR) model was developed to assess the ecological environment's quality in the Dongting Lake area. The dependent variable was ecological environmental quality, while the independent variables included population (POP), GDP, road network density (RND), nighttime light index (NLI), elevation (DEM), slope (SP), temperature (TEM), precipitation (PRE), sunshine duration (SD), and NDVI. The GWR model's goodness of fit was evaluated using R^2, corrected R^2, residual sum of squares (RSS), and AICC. A fixed bandwidth of 3113.034 was selected for the regression. Table 2 provides the corresponding parameters used in this study. The results indicated that the GWR model yielded a corrected R^2 of 0.58, 0.68, and 0.72 for the years 2001, 2010, and 2020, respectively, which demonstrated a good fit.

The spatial distribution of each factor's influence on the quality of the ecological environment was visualized and analyzed using the GWR model, indicated by the regression coefficients (Figure 4). Areas with the highest significance of influence were primarily located in regions with high ecological environment's quality values and concentrated human activities. These regions included Dingcheng District, Linxiang City, Wuling District, and Yueyanglou District. Moreover, the center of gravity of the significantly influential areas gradually shifted from the western to the eastern part of the country during the period of 2001–2020.

Regarding human factors, POP, GDP, RND, and NLI were found to be negatively correlated with the RSEI of the Dongting Lake area. The mean regression coefficients for POP in 2001, 2010, and 2020 were −0.14, −1.62, and −2.13. For GDP, the mean regression coefficients were −5.16, −8.35, and −9.19 during the same years. The RND had mean regression coefficients of −1.24, −0.65, and −0.45, while NLI had mean regression coefficients of −5.41, −9.45, and −15.70.

The negative influence of POP, GDP, and NLI on the RSEI showed a gradual increase over time. This can be attributed to accelerated industrialization and urbanization, which have led to higher levels of disturbance and pollution in densely populated areas, resulting in a decline in the ecological quality of the Dongting Lake area. However, the negative impact of RND on RESI decreased gradually as there were fewer excavation projects in the past two decades, leading to a relatively stable spatial pattern.

TABLE 2 Statistical test of GWR results in 2001,2010 and 2020.

Year	Bandwidth parameter	Residual sum of squares	Effective number	AICC	R^2	Correction R^2
2001	3113.034	7.576	41.132	−21352.916	0.584	0.580
2010	3113.034	7.643	42.139	−19654.469	0.681	0.678
2020	3113.034	9.463	40.755	−20092.645	0.722	0.720

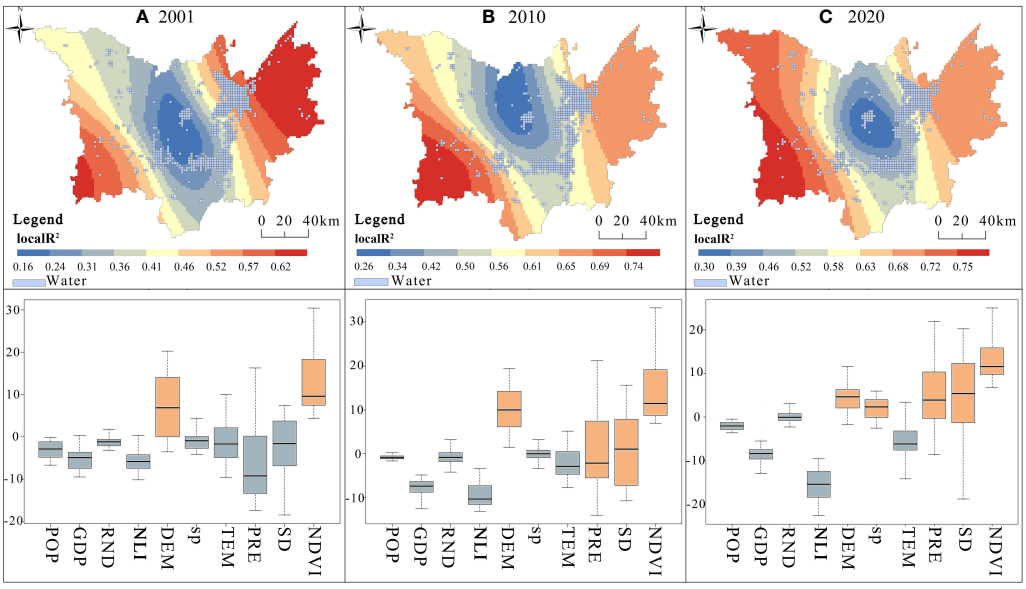

FIGURE 4
Spatial distribution of GWR residual sum of squares and visualization of regression coefficients. **(A)** 2001; **(B)** 2010; **(C)** 2020.

As for natural factors, DEM, SP, TEM, PRE, SD, and NDVI were positively correlated with the quality of the ecological environment during 2001–2020. The mean regression coefficients for elevation in 2001, 2010, and 2020 were 7.27, 10.10, and 4.36, respectively. The mean regression coefficients for SP were −0.95, −0.15, and 1.91. TEM had mean regression coefficients of −1.51, −2.16, and −5.39, while PRE had mean regression coefficients of −6.8 and 0.8. SD had mean regression coefficients of −2.39, 1.10, and 5.09, and NDVI had mean regression coefficients of 13.10, 14.97, and 14.44.

The positive influence of natural factors on RSEI increased from two factors (DEM and NDVI) in 2001 to five factors (DEM, SP, PRE, SD, and NDVI) in 2020. Specifically, SP, PRE, and SD exhibited an increasing positive trend, while the impact of NDVI consistently showed a high positive correlation with the quality of the ecological environment. Furthermore, under the backdrop of global warming, the annual mean temperature in the Dongting Lake area gradually exerted a negative effect on the ecological quality.

3.3 Delineation of ecological priority zones

In order to identify potential areas for ecological restoration, RSEI and ACI were used to perform spatial statistical tests. After the spatial calculations, ΔRSEI and ΔACI for the period 2001–2020 were utilized for significance tests to classify the grids in the Dongting Lake region of Hunan Province into four categories. The four ecological restoration priority areas include critical ecological restoration areas, important ecological restoration site areas, artificial ecological restoration site areas and natural base ecological restoration areas. The ecological restoration priority areas are considered as potential targets for artificial reconstruction or natural restoration. Critical ecological restoration areas represent pixels with large changes in ACI and large changes in neighboring RSEI, which have the potential to provide more high-quality ecosystem services. Critical ecological restoration site areas indicate pixels with large changes in ACI and small changes in neighboring RSEI, which have higher ecological sensitivity. Artificial ecological restoration site areas indicate pixels with small changes in ACI and large changes in the surrounding RSEI, which have a high urbanization intensity, and changes in the intensity of urbanization at a low level have a greater impact on the RSEI. Natural-based ecological restoration areas represent image elements with low ACI change and surrounding RSEI change, which are characterized by low ACI and low RSEI within the ecological red line, and ecosystems can be restored through nature-based solutions. We classified 3106 grids measuring 2 km × 2 km as priority control areas for ecological conservation in the Dongting Lake region, accounting for 45.66% of all grids. Among these, 3.91% exhibited significant ecological significance as the high-high type, 7.95% as the high-low type, 17.80% as the low-high type, and 16.00% as the low-low type (Figure 5).

The high-high type areas were primarily located in the municipal districts of Yueyang City, Changde City, Yiyang City, and surrounding areas such as Linli County. The high-low-type areas indicated regions with long-term urbanization and high levels of human disturbance, mainly concentrated in the central built-up areas of cities and counties. The low-high type areas were primarily

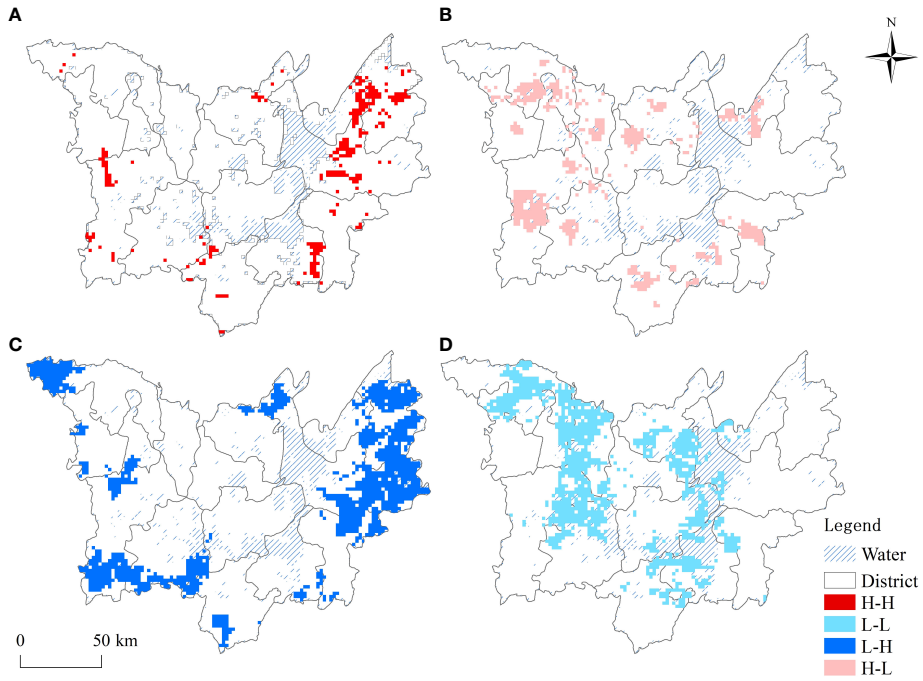

FIGURE 5
Priority areas for ecological restoration in the Dongting Lake region of Hunan Province. **(A)** H-H; **(B)** H-L; **(C)** L-H; **(D)** L-L.

distributed in regions with relatively favorable ecological conditions, such as the suburbs of Linxiang City, Yueyang County, and Li County. These areas are characterized by abundant vegetation and minimal human interference, and their ecological quality is mainly influenced by natural conditions such as climate and topography. The low-low type areas were mainly found in Anxiang County, Huarong County, and Hanshou County, exhibiting more stable ecological environments.

4 Discussion

4.1 Mechanism of ecological quality impact

The RESI in this area is a complex process influenced by a variety of factors, according to the findings of the spatio-temporal characteristics of the RESI and the analysis of influencing factors through GWR in the Dongting Lake region of Hunan Province (Figure 6). Specifically, urbanization and the level of economic development are considered to be among the most important factors affecting the ecological environment (Li et al., 2023). The advancement of urban expansion and industrialization has intensified pollutant emissions and land resource exploitation, thus exerting pressure on the ecosystem. Areas with high road network density contribute to land fragmentation and ecosystem destruction, negatively impacting the ecosystem.

Natural factors such as DEM, SP, PRE, SD, and NDVI positively influence the quality of the ecosystem. The positive effect of NDVI suggests that vegetation cover has a beneficial impact on ecosystem improvement, with higher NDVI values indicating healthier vegetation. Areas at higher elevations typically exhibit better ecological conditions, while regions with sufficient PRE and SD are favorable for vegetation growth and maintaining ecological balance.

However, the gradual increase in average annual temperature has a negative impact on ecological conditions. Global warming may lead to water scarcity, ecosystem disturbances, and species extinction, thus affecting the quality of the ecological environment. By comprehensively understanding and summarizing the mechanisms influencing the quality of the ecological environment, we can promote the orderly functioning of both natural and artificial ecosystems, ultimately improving the regional ecological environment. We can play a good role as a spatial carrier of the ecological environment in urban activities, which is essential in supporting human survival and promoting economic and social development in the Dongting Lake region.

4.2 Suggestions for zoning control

High-high type zoning refers to image elements with significant changes in anthropogenic disturbance intensity and surrounding RESI. High-low type zoning denotes image elements with significant changes in anthropogenic disturbance intensity but minimal changes in the quality of the surrounding ecological environment. Low-high type zoning indicates pixels with low changes in anthropogenic disturbance intensity but high changes in the quality of the surrounding ecosystem. Low-low type zoning

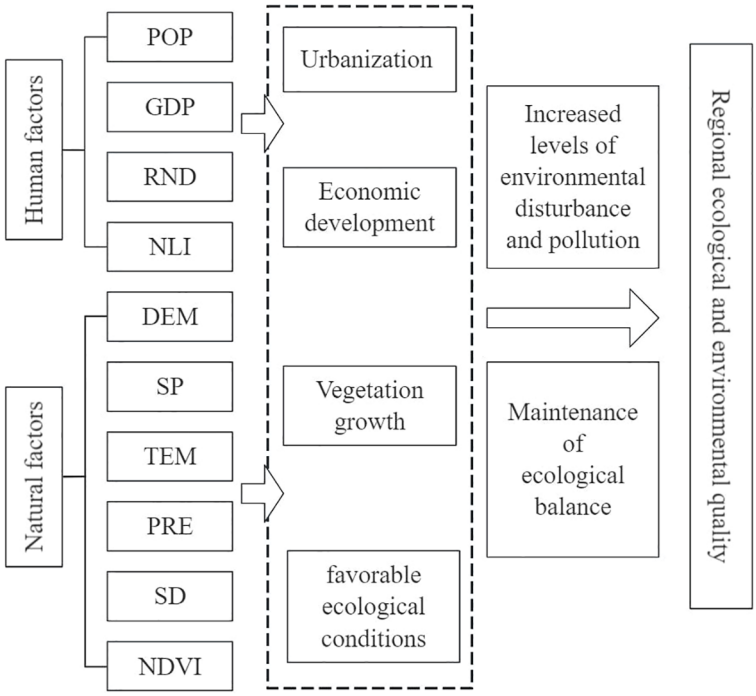

FIGURE 6
Mechanism of ecological quality impact in the Dongting Lake region of Hunan Province.

represents image elements with low changes in anthropogenic disturbance intensity and low changes in the quality of the surrounding ecological environment. These categories, respectively, represent critical control areas (KERS), important control areas (IERS), artificially maintained areas (AERS), and naturally maintained areas (NERS). This study put forward suggestions for zoning control, which was in line with the findings of Lv et al. (2023) and Zhang et al. (2023).

Therefore, to address the decline in RESI in the Dongting Lake region during the period 2001–2020, it is crucial to exercise strict control over construction land expansion while considering the restoration of other land use types, such as land remediation and lake restoration (Zhang et al., 2018a; Niu et al., 2022). Changes in both the extent and quality of different land use types can better explain variations in the RESI of the Dongting Lake basin. It is strongly recommended to implement effective management plans, particularly those focused on ecological restoration, for crucial land use types within areas exhibiting low RSEI values.

4.3 Limitation and future research directions

This study presents a case study on the spatial and temporal variations in RSEI within the Dongting Lake area. Moreover, it quantifies the influence of ten key drivers on RSEI changes at a 2 km × 2 km grid scale, taking into account the contributions of human activities and natural factors. These findings offer valuable insights for future urbanization and ecological preservation efforts in the Dongting Lake region. However, it is essential to acknowledge the limitations of this study.

Firstly, it should be noted that the findings of this study are specific to the Dongting Lake region and may not be generalizable. While the Dongting Lake area possesses valuable wetland ecosystems and represents a typical level of ecological damage, conducting experiments on a larger scale and in additional regions would yield a more comprehensive understanding. This approach would enable researchers to assess if similar conclusions can be drawn for other urban areas.

Secondly, this study underscores that anthropogenic factors exert the most significant influence on regional RSEI, aligning with previous research findings. Notably, human activities such as urban expansion largely contribute to the ecological disparities among the three key urban agglomerations in the Yangtze River Economic Belt. However, balancing societal development and environmental preservation remains a challenging task. Therefore, it is essential to identify other influential factors that impact RSEI, thus facilitating its improvement through effective urban planning. For instance, factors such as the distribution of green infrastructure, the establishment of ecological redlines, and energy consumption play pivotal roles in addressing the regional disparity between RSEI and human social development.

In conclusion, despite certain limitations, this study offers valuable insights into the dynamics and determinants of RSEI in the Dongting Lake region. Conducting future research on a broader scale, encompassing multiple cities, and considering additional factors like the distribution of green infrastructure will enhance our comprehensive understanding of the underlying reasons behind the RSEI imbalance and provide pathways towards its resolution. Moreover, such research will contribute to well-informed urban planning and ecological enhancement efforts.

5 Conclusion

This study is to evaluate the spatial and temporal evolution of RESI in the Dongting Lake area and to analyze its relationship with various anthropogenic and natural factors. The overall RESI of the Dongting Lake area exhibited a declining trend from 2001 to 2020, with the mean value dropping from 0.52 in 2001 to 0.48 in 2020. The high-quality areas were primarily located in mountainous and forested regions, whereas the low-quality areas were concentrated in zones characterized by extensive urban construction and development, particularly in the eastern watershed area. The GWR results show that urban expansion and economic development have significant negative impacts on the ecological environment, which are related to economic development, land resource development and population agglomeration, and also reflect the importance of balance and sustainability between human factors and natural factors. The geographically weighted regression (GWR) analysis revealed a positive relationship between urban expansion and the expansion of low-quality areas. This can be attributed to economic development, land resource exploitation, and population concentration. POP, GDP, RND, and NLI displayed negative correlations with ecological quality, and these detrimental effects intensified over time. Natural factors, including DEM, SP, PRE, SD and NDVI, exhibited a positive influence on ecological quality, with NDVI consistently showing a positive effect. The mean annual temperature had an incrementally adverse impact on RESI, possibly attributable to global warming. These divisions provide governments and decision makers with information on how to undertake sustainable ecological management and policy development. Policies and plans can be developed accordingly for each type of area to balance the need for resource utilization and ecological protection. It provides a strong basis for targeted control and management, ensuring effective resource utilization and ecological protection.

Data availability statement

The raw data supporting the conclusions of this article will be made available by the authors, without undue reservation.

Author contributions

XY: Conceptualization, Data curation, Formal analysis, Writing – original draft, Writing – review & editing. ZL: Visualization, Writing – review & editing. BZ: Formal analysis, Supervision, Validation, Writing – review & editing, Writing – original draft.

Funding

The author(s) declare financial support was received for the research, authorship, and/or publication of this article. Humanities and Social Science Fund of Ministry of Education (23YJA710051).

Conflict of interest

The authors declare that the research was conducted in the absence of any commercial or financial relationships that could be construed as a potential conflict of interest.

Publisher's note

References

Cheng, H., Zhu, L., and Meng, J. (2022). Fuzzy evaluation of the ecological security of land resources in mainland China based on the Pressure-State-Response framework. *Sci. Total Environ.* 804, 150053. doi: 10.1016/j.scitotenv.2021.150053

Hasan, S. S., Zhen, L., Miah, M. G., Ahamed, T., and Samie, A. (2020). Impact of land use change on ecosystem services: A review. *Environ. Dev.* 34, 100527. doi: 10.1016/j.envdev.2020.100527

He, J., Pan, Z., Liu, D., and Guo, X. (2019). Exploring the regional differences of ecosystem health and its driving factors in China. *Sci. Total Environ.* 673, 553–564. doi: 10.1016/j.scitotenv.2019.03.465

Jin, S., and Sader, S. A. (2005). Comparison of time series tasseled cap wetness and the normalized difference moisture index in detecting forest disturbances. *Remote Sens. Environ.* 94, 364–372. doi: 10.1016/j.rse.2004.10.012

Kobayashi, H., and Dye, D. G. (2005). Atmospheric conditions for monitoring the long-term vegetation dynamics in the Amazon using normalized difference vegetation index. *Remote Sens. Environ.* 97, 519–525. doi: 10.1016/j.rse.2005.06.007

Lakes, T., and Kim, H.-O. (2012). The urban environmental indicator "Biotope Area Ratio"—An enhanced approach to assess and manage the urban ecosystem services using high resolution remote-sensing. *Ecol. Indic.* 13, 93–103. doi: 10.1016/j.ecolind.2011.05.016

Li, F., Yin, X., and Shao, M. (2022). Natural and anthropogenic factors on China's ecosystem services: Comparison and spillover effect perspective. *J. Environ. Manage.* 324, 116064. doi: 10.1016/j.jenvman.2022.116064

Li, W., Kang, J., and Wang, Y. (2023). Spatiotemporal changes and driving forces of ecological security in the Chengdu-Chongqing urban agglomeration, China: Quantification using health-services-risk framework. *J. Clean. Prod.* 389, 136135. doi: 10.1016/j.jclepro.2023.136135

Liu, C., Liu, Y., Giannetti, B. F., Almeida, C. M. V. B., Sevegnani, F., and Li, R. (2023). Spatiotemporal differentiation and mechanism of anthropogenic factors affecting ecosystem service value in the Urban Agglomeration around Poyang Lake, China. *Ecol. Indic.* 154, 110733. doi: 10.1016/j.ecolind.2023.110733

Lv, T., Zeng, C., Lin, C., Liu, W., Cheng, Y., and Li, Y. (2023). Towards an integrated approach for land spatial ecological restoration zoning based on ecosystem health assessment. *Ecol. Indic.* 147, 110016. doi: 10.1016/j.ecolind.2023.110016

Matsushita, B., Yang, W., Chen, J., Onda, Y., and Qiu, G. (2007). Sensitivity of the enhanced vegetation index (EVI) and normalized difference vegetation index (NDVI) to topographic effects: a case study in high-density cypress forest. *Sensors* 7, 2636–2651. doi: 10.3390/s7112636

Niu, L., Shao, Q., Ning, J., and Huang, H. (2022). Ecological changes and the tradeoff and synergy of ecosystem services in western China. *J. Geographical Sci.* 32, 1059–1075. doi: 10.1007/s11442-022-1985-6

Ouyang, X., Shao, Q., Zhu, X., He, Q., Xiang, C., and Wei, G. (2019). Environmental regulation, economic growth and air pollution: Panel threshold analysis for OECD countries. *Sci. Total Environ.* 657, 234–241. doi: 10.1016/j.scitotenv.2018.12.056

Ouyang, X., Tang, L., Wei, X., and Li, Y. (2021). Spatial interaction between urbanization and ecosystem services in Chinese urban agglomerations. *Land Use Policy* 109, 105587. doi: 10.1016/j.landusepol.2021.105587

Peng, J., Liu, Y., Li, T., and Wu, J. (2017). Regional ecosystem health response to rural land use change: A case study in Lijiang City, China. *Ecol. Indic.* 72, 399–410. doi: 10.1016/j.ecolind.2016.08.024

Qin, X., Hu, X., and Xia, W. (2023). Investigating the dynamic decoupling relationship between regional social economy and lake water environment: The application of DPSIR-Extended Tapio decoupling model. *J. Environ. Manage.* 345, 118926. doi: 10.1016/j.jenvman.2023.118926

Retallack, M. (2021). The intersection of economic demand for ecosystem services and public policy: A watershed case study exploring implications for social-ecological resilience. *Ecosyst. Serv.* 50, 101322. doi: 10.1016/j.ecoser.2021.101322

Su, M., Fath, B. D., and Yang, Z. (2010). Urban ecosystem health assessment: A review. *Sci. Total Environ.* 408, 2425–2434. doi: 10.1016/j.scitotenv.2010.03.009

Taloor, A. K., Drinder Singh, M., and Chandra Kothyari, G. (2021). Retrieval of land surface temperature, normalized difference moisture index, normalized difference water index of the Ravi basin using Landsat data. *Appl. Comput. Geosci.* 9, 100051. doi: 10.1016/j.acags.2020.100051

Tan, J., Yu, D., Li, Q., Tan, X., and Zhou, W. (2020). Spatial relationship between land-use/land-cover change and land surface temperature in the Dongting Lake area, China. *Sci. Rep.* 10, 9245. doi: 10.1038/s41598-020-66168-6

Wang, H., Huang, L., Guo, W., Zhu, Y., Yang, H., Jiao, X., et al. (2022). Evaluation of ecohydrological regime and its driving forces in the Dongting Lake, China. *J. Hydrology: Regional Stud.* 41, 101067. doi: 10.1016/j.ejrh.2022.101067

Wei, G., He, B.-J., Sun, P., Liu, Y., Li, R., Ouyang, X., et al. (2023). Evolutionary trends of urban expansion and its sustainable development: Evidence from 80 representative cities in the belt and road initiative region. *Cities* 138, 104353. doi: 10.1016/j.cities.2023.104353

Xiong, J., Wang, X., Zhao, D., and Zhao, Y. (2022). Spatiotemporal pattern and driving forces of ecological carrying capacity during urbanization process in the Dongting Lake area, China. *Ecol. Indic.* 144, 109486. doi: 10.1016/j.ecolind.2022.109486

Xu, H. (2013). A remote sensing urban ecological index and its application. *Acta Ecol. Sin.* 33, 7853–7862. doi: 10.5846/stxb201208301223

Xu, H., Wang, M., Shi, T., Guan, H., Fang, C., and Lin, Z. (2018). Prediction of ecological effects of potential population and impervious surface increases using a remote sensing based ecological index (RSEI). *Ecol. Indic.* 93, 730–740. doi: 10.1016/j.ecolind.2018.05.055

Yang, S., Liu, J., Wang, C., Zhang, T., Dong, X., and Liu, Y. (2022). Vegetation dynamics influenced by climate change and human activities in the Hanjiang River Basin, central China. *Ecol. Indic.* 145, 109586. doi: 10.1016/j.ecolind.2022.109586

Yu, Y., Mei, X., Dai, Z., Gao, J., Li, J., Wang, J., et al. (2018). Hydromorphological processes of dongting lake in China between 1951 and 2014. *J. Hydrology* 562, 254–266. doi: 10.1016/j.jhydrol.2018.05.015

Zhang, D., Jia, Q., Xu, X., Yao, S., Chen, H., and Hou, X. (2018a). Contribution of ecological policies to vegetation restoration: A case study from Wuqi County in Shaanxi Province, China. *Land Use Policy* 73, 400–411. doi: 10.1016/j.landusepol.2018.02.020

Zhang, X., Ma, C., Zhan, S., and Chen, W. (2012). Evaluation and simulation for ecological risk based on emergy analysis and Pressure-State-Response Model in a coastal city, China. *Proc. Environ. Sci.* 13, 221–231. doi: 10.1016/j.proenv.2012.01.021

Zhang, Y., Hu, X., Wei, B., Zhang, X., Tang, L., Chen, C., et al. (2023). Spatiotemporal exploration of ecosystem service value, landscape ecological risk, and their interactive relationship in Hunan Province, Central-South China, over the past 30 years. *Ecol. Indic.* 156, 111066. doi: 10.1016/j.ecolind.2023.111066

Zhang, Y., Tian, Y., Shen, M., and Zeng, G. (2018b). Heavy metals in soils and sediments from Dongting Lake in China: occurrence, sources, and spatial distribution by multivariate statistical analysis. *Environ. Sci. Pollut. Res.* 25, 13687–13696. doi: 10.1007/s11356-018-1590-5

Zheng, Z., Wu, Z., Chen, Y., Guo, C., and Marinello, F. (2022). Instability of remote sensing based ecological index (RSEI) and its improvement for time series analysis. *Sci. Total Environ.* 814, 152595. doi: 10.1016/j.scitotenv.2021.152595

Zou, F., Li, H., and Hu, Q. (2020). Responses of vegetation greening and land surface temperature variations to global warming on the Qinghai-Tibetan Plateau 2001–2016. *Ecol. Indic.* 119, 106867. doi: 10.1016/j.ecolind.2020.106867

frontiers | Frontiers in Ecology and Evolution

TYPE Original Research
PUBLISHED 17 January 2024
DOI 10.3389/fevo.2023.1342766

OPEN ACCESS

EDITED BY
Xiao Ouyang,
Hunan University of Finance and Economics, China

REVIEWED BY
Siyun Chen,
Hunan University of Finance and Economics, China
Xue-Chao Wang,
Beijing Normal University, China

*CORRESPONDENCE
Fusheng Zeng
zengfusheng@163.com

RECEIVED 22 November 2023
ACCEPTED 14 December 2023
PUBLISHED 17 January 2024

CITATION
Tan F, Lu Z and Zeng F (2024) Study on the trade-off/synergy spatiotemporal benefits of ecosystem services and its influencing factors in hilly areas of southern China.
Front. Ecol. Evol. 11:1342766.
doi: 10.3389/fevo.2023.1342766

Study on the trade-off/synergy spatiotemporal benefits of ecosystem services and its influencing factors in hilly areas of southern China

Fenglian Tan[1,2], Zhaoyan Lu[1,2] and Fusheng Zeng[1,2]*

[1]Economic College, Hunan Agricultural University, Changsa, China, [2]Malanshan New Media College, Changsha University, Changsa, China

Introduction: This study aims to investigate the factors influencing ecosystem service trade-offs/synergies (TOSs) in major agricultural production areas in the southern hilly region and to propose optimization strategies to promote ecosystem sustainability in agricultural areas.

Methods: The study used a geographical detector to analyze the determinants influencing the ecosystem service trade-offs as well as correlation analysis, geographically weighted regression (GWR), and a geographical detector to analyze the spatial and temporal evolution of ecosystem service and TOS relationships from 2000 to 2020 in Hunan Province.

Results: The results showed that the comprehensive value of ecosystem services in Hunan Province showed an increasing trend from 2000 to 2020. With spatial heterogeneity, the areas with high values were mainly distributed in the hilly areas in the west, south, and east of Hunan Province, and the areas with low values were mainly distributed in the Dongting Lake Plain and the Xiangzhong Hilly Basin. There was a trade-off relationship between food production (FP) and all other ecosystem services, of which FP has the strongest trade-off effect with habitat quality (HQ). The synergy effect between HQ, water yield (WY), carbon storage (CS), and soil conservation (SC) shows an increasing trend. Gross domestic product (GDP) and SLOPE are the dominant factors for the strength of trade-offs between food supply and other ecosystem services, and Digital Elevation Model (DEM) and Normalized Difference Vegetation Index (NDVI) are the dominant factors for the strength of synergy effects among ecosystem services. The strength of TOS effects of ecosystem services is determined by interactions or co-influences between the two services rather than by a single component.

Discussion: The results of this study can provide a reference basis for the enhancement of ecosystem services and the sustainable planning of agricultural landscapes in the southern hilly areas.

KEYWORDS

ecosystem services, trade-offs effect, geographical detector, influencing factors, hilly areas of southern China

1 Introduction

Ecosystem services (ESs) are provisioning (e.g., raw materials and food), regulating (e.g., climate and gases), supporting (e.g., biodiversity and soil conservation), and cultural (e.g., outdoor recreation and aesthetic landscapes) services that are directly or indirectly provided by ecosystem structures, processes, and functions, and that link ecosystems to human wellbeing (Costanza et al., 1998; Ouyang et al., 2021a). However, the increasing demand for food as well as agricultural land over the past decades has had important impacts on biodiversity, water resources, carbon cycle, etc., leading to TOS mutual gains among ecosystem services (Li et al., 2020; Zhang et al., 2023). Coordinating the multi-objective conflicts of ecosystem management and mitigating the trade-off relationships and intensity among ecosystem services are now unavoidable choices for achieving the diversification of ecosystem services and high-quality regional agriculture development. Therefore, it is of great significance to explore the spatial and temporal changes of ecosystem services and the characteristics of the TOS relationship, and to propose spatially differentiated ecosystem service optimization countermeasures to enhance the synergies and mitigate the trade-offs, in order to maximize the comprehensive benefits of ecosystem services.

There are synergy relationships (simultaneous increase or decrease of two services) and trade-off relationships (increase of one service leads to decrease of another) among ecosystem services (Bennett et al., 2010). Currently, the existing studies form a variety of revealing ES and TOS relationships. Among them, ES TOS relationship methods include spatiotemporal correlation analysis (Xu et al., 2017) for quantifying ES TOS relationships in time and spatial, while using a geographically weighted regression and binary spatial autocorrelation analyses to reflect spatial TOS relationships (Zhang et al., 2020). The analysis of ecosystem service trade-offs and synergy relationships is a prerequisite for improving the level of ecosystem service provision. Currently, many scholars have focused on the quantification of ecosystem service TOS relationships at a single spatial scale, lacking multi-scale analyses. In addition to the analysis of ES TOS relationships, it is important and challenging to use ES-related results to enlighten territorial spatial planning. Most of the existing studies focus on administrative or physical geographic scales such as county or watershed (Gong et al., 2022; Liu et al., 2019), and there are fewer studies using grids as zoning units, which is not conducive to small-area scale studies and refined management. In addition, the analysis of ecosystem service TOSs and influencing factors for the subregion is relatively lacking, which cannot effectively provide recommendations for subregional management. Thus, research on how to better integrate spatiotemporal changes in ecosystem services and TOSs at many scales to explicitly assist spatial planning remains unrepresentative despite the advancements in spatiotemporal and cross-scale assessments of ecosystems. There is an urgent need to explicitly link ES information to policy development, regional planning, and implementation. Numerous and intricate elements affect TOSs (Feng et al., 2021). TOSs are influenced by a multitude of natural and anthropogenic factors, including DEM, slope, temperature, precipitation, population growth, urban expansion, economic development, and planning policies (Ouyang et al., 2023).

The southern hilly region accounts for 13% of China's national land area and is the southern hilly and mountainous belt in the "two screens and three belts" of the national main ecological function zoning, which is an important part of the national ecological security pattern (Shao et al., 2023). In the process of urbanization in China, significant natural resource plunder and extensive ecological destruction have occurred in the pursuit of development. This has resulted in a significant conflict between ecological conservation and utilization in the southern hilly and mountainous regions. The consequences include severe water pollution, degraded forest quality, encroachment of urbanization on ecological spaces, loss of ecological functionality in certain areas, as well as issues such as soil and water erosion, rocky desertification, and more. Hunan Province, serving as a crucial developmental axis in the central region, also grapples with similar challenges, with soil pollution being a particularly pressing issue. Most studies on ecosystem services and TOS relationships in the southern hilly areas are currently conducted from a single static ecosystem service dimension, and lack quantitative geo-spatial information in long time series, making it difficult to apply in China's territorial spatial planning. In view of this, this paper reveals the spatial and temporal evolution of TOSs between five ecosystem services—food production, water yield, carbon storage, soil conservation, and habitat quality—over the period 2000–2020 and selects the factors influencing them with the use of a geographical detector. This study's main contributions are as follows: First, we quantified the major ESs to identify areas for ecological concerns. Next, we used GWR and Spearman's correlation to quantify TOSs between ES. Finally, we investigated into the grid scale contributions of the TOS components. Based on this, the ecosystem management measures are put forward, in order to promote the southern hilly area ecosystem service differentiation control and the modern development of harmonious coexistence between man and nature.

2 Overview of the study area, study methods, and data sources

2.1 Overview of the study area

The southern hilly region is the area south of the Qinling Mountains, east of the Yunnan-Guizhou Plateau, and north of the Leizhou Peninsula in China, covering seven provinces, namely, Zhejiang, Fujian, Jiangxi, Hunan, Guangdong, Guangxi, and Guizhou, with a total land area of approximately 1,276,000 km^2 (Shao et al., 2023), constituting one of the important components of China's "two screens and three belts" ecological pattern (see Figure 1). The region is interspersed with mountains, hills, and plains, with a variety of ecosystems and the largest and most well-

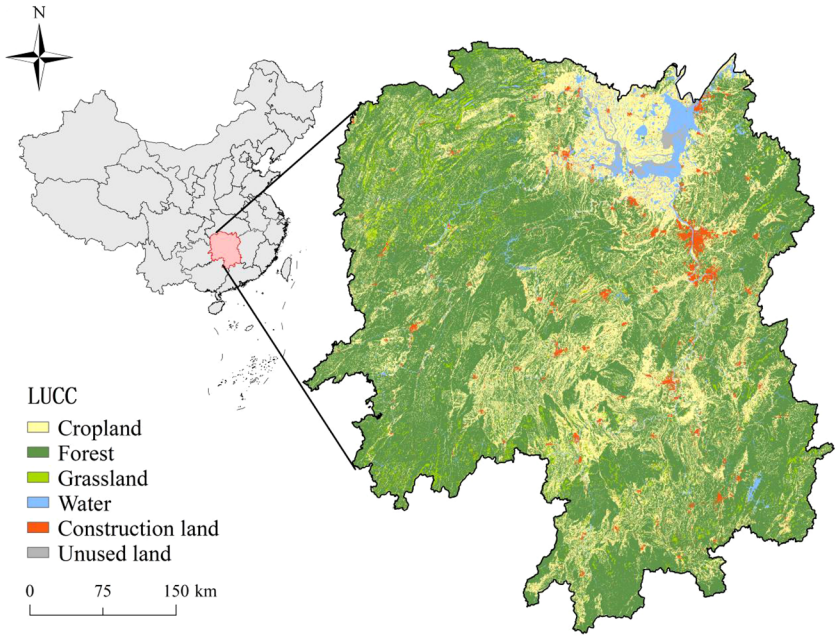

FIGURE 1
Location diagram of Hunan Province.

preserved middle-subtropical forest ecosystem in the same latitude band. Hunan Province is located in the central part of the southern mountainous and hilly region, with geographical coordinates of 24° 38'–30°08'N, 108°47'–114°15'E. Hunan Province has a humid subtropical monsoon climate, with an average annual temperature of 16–19°C. The average annual precipitation is 1,200–1,800 mm, and the change of seasons is obvious, which is suitable for human habitation and the growth of crops and green plants.

2.2 Study methods

2.2.1 Ecosystem service calculation

The InVEST model and the ArcGIS software were utilized in this study to quantitatively evaluate five ecosystem services: food production, water yield, carbon storage, soil conservation, and habitat quality. The precise formulas are provided (see Ouyang et al., 2023). The results of the above five ecosystem service types were used to normalize the extremes and then averaged to measure the ESV.

2.2.2 Ecosystem service trade-offs/synergies

2.2.2.1 Temporal trade-off/synergy analyses

Pearson's non-parametric correlation analysis was used in this study to determine trade-offs or synergy relationships between different ecosystem service groups. A positive correlation implies a synergy relationship, while a negative correlation is a trade-off relationship (Gou et al., 2021). Pearson correlation analyses of five ecosystem service bundles at three time scales, 2000, 2010, and 2020, and at grid scale were performed using the "corrplot" package in R4.3.1 software. Between 2000 and 2020, Hunan Province's urbanization experienced rapid development, resulting in notable ecological changes. At the same time, 2000, 2010, and 2020 were selected considering the periodicity of ecological change.

2.2.2.2 Spatial trade-off/synergy analysis

In addition to the general synergies and trade-offs obtained through correlation analyses, in order to gain a more in-depth understanding of the patterns in the spatial distribution of these types of ecosystem services, this study used GWR to define the spatial interaction correlations of TOSs. The GWR model modifies the traditional regression framework to detect spatial non-stationarity in the relationships between samples (Xue et al., 2023). The strength and direction of the relationship between the dependent variable and its predictors may change in response to changes in the environmental components in the GWR, which fits with one of the mechanisms that generate ecosystem service trade-offs (common drivers affecting multiple ecosystem services simultaneously). In addition, common drivers contribute to the spatial heterogeneity and spatial non-stationarity of ecosystem service TOSs. Since we only use ecosystem service variables as independent and dependent variables, there is no problem of multicollinearity. The GWR model (Equation 1) is formulated as follows:

$$y_i = \beta_0(\mu_i, v_i) + \sum_{k=1}^{p} \beta_k(\mu_i, v_i) X_{jk} + \varepsilon_i \quad (1)$$

where (μ_i, v_i) is the spatial location of the point, p is the number of independent variables, y_i is the dependent variable, X_{jk} is the independent variable, ϵ_i represents the random error, $\beta_0(\mu_i, v_i)$

represents the intercept at i point, and $\beta_k(\mu_i, v_i)$ represents the regression coefficient. Positive regression coefficients indicate spatial synergies and negative regression coefficients indicate spatial trade-offs.

2.2.2.3 Geographical detector

A geographical detector (GD) is used to detect the strength of the effect of a single factor and the interaction of two factors on the dependent variable, and to avoid the problem of multivariate covariance (Wang et al., 2016). The GD model (Equation 2) is formulated as follows:

$$q = 1 - \frac{1}{Kw^2}\sum_{h=1}^{L} K_h w_h^2 \quad (2)$$

where q is the influence of factors, K and K_h are the number of the grids, L is the number of index samples, w^2 and w_h^2 is the discrete variance of the resilience of the study area and grid h.

We used each influencing factor as an independent variable and the strength of ecosystem service trade-offs as the dependent variable in this study. To analyze the degree of influence of each driving factor and factor combinations on the spatial heterogeneity of the degree of ecosystem service trade-offs, we selected the "factor detection" and "interaction detection" in geographical detector. Specific influencing factors are shown in Table 1; Figure 2.

TABLE 1 The influencing factors selected for this study.

Factor name	Factor description
Mean annual precipitation	Based on the interpolation of daily precipitation data of surrounding stations
Elevation	Based on DEM data
Slope	Based on ArcGIS surface analysis
NDVI	Vegetation cover
GDP density	Reflects the GDP distribution of a 1-km^2 grid
Population density	Reflects the population distribution of a 1-km^2 grid

2.3 Data sources

Land use data: The land use data from 2000 to 2020 were from the Resource and Environmental Science Data Center of the Chinese Academy of Sciences (www.resdc.cn), with a spatial resolution of 30 m. Vegetation type data: MODIS13Q1 NDVI was derived from the NASA Earth Data Center (www.earthdata.nasa.gov) with a spatial resolution of 250 m. Digital Elevation Model (DEM) data: from the geospatial data cloud, spatial resolution of 30 m; GDP density and POP density are derived from the Resource and Environmental Science Data Center of the Chinese Academy of Sciences (www.resdc.cn), with a spatial resolution of 1 km. Grain production: from 2000–2020, "Hunan Statistical Yearbook" and "Hunan Rural Statistical Yearbook". Finally, the resolution resampling of each factor raster data is unified to 1 km, and the projection coordinate system is unified by WGS_1984_Albers.

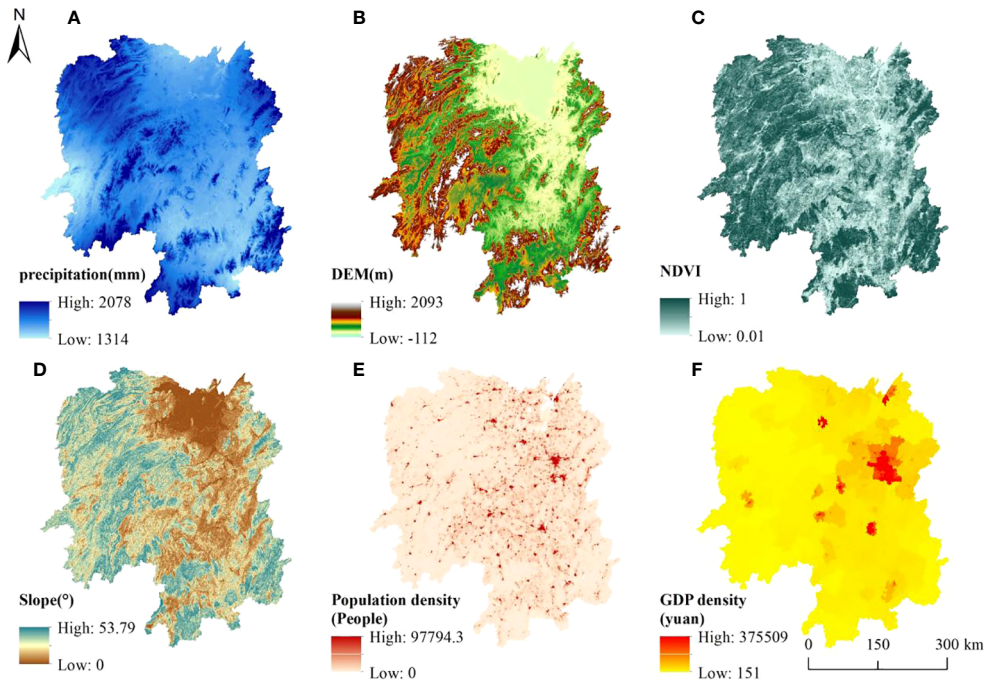

FIGURE 2
The spatial of influencing factors. **(A)** Precipitation, **(B)** DEM; **(C)** DEM; **(D)** Slope; **(E)** Population density and **(F)** GDP density.

3 Analysis of the results

3.1 Spatiotemporal changes of ecosystem services

The trend of integrated services in Hunan Province from 2000 to 2020 exhibited an overall upward trajectory. Specifically, the average values of integrated ecosystem services at the provincial grid scale in 2000, 2010, and 2020 were 0.533, 0.528, and 0.613, respectively. From a spatial perspective, areas with high integrated ecosystem service values at the provincial grid scale were predominantly located in the western, southern, and eastern hilly regions of Hunan Province. These areas boasted low population density and high vegetation coverage rates, as depicted in Figure 3. On the other hand, the areas with low values are mainly distributed in the Dongting Lake Plain and Xiangzhong Hilly Basin, in which the built-up areas of cities with intensive human activities have the lowest integrated ecosystem services, due to the flat terrain, high proportion of surrounding farmland, high population density, and the high degree of interference with the natural ecosystems, which leads to the low integrated ecosystem services in these areas.

3.2 Ecosystem service trade-offs and synergies

From the temporal dimension (Figure 4A), in 2000, HQ and SC, HQ and CS, and SC and CS in Hunan Province were highly positively correlated, with correlation coefficients of 0.67, 0.93, and 0.63, respectively. These three ecosystem service pairs passed the significance test of 0.001, indicating that there was a strong synergy effect between them. Similarly, there was a strong positive correlation between HQ and WY, WY and SC, and WY and CS, with correlation coefficients of 0.11, 0.24, and 0.19, respectively, which also passed the significance test of 0.001. FP and HQ, FP and WY, FP and SC, and FP and CS showed strong negative correlations, with correlation coefficients of −0.53, −0.04, −0.47, and −0.46, respectively. Among them, FP vs. HQ, FP vs. CS, and FP vs. SC passed the significance test of 0.001, indicating a strong trade-off effect between them.

In 2010, HQ and SC, HQ and CS, SC and CS, HQ and WY, WY and SC, and WY and CS still maintained strong spatial synergy effects, with correlation coefficients of 0.59, 0.93, 0.55, 0.09, 0.19, and 0.14, respectively. The spatial trade-off effects of FP and HQ, FP and WY, and FP and SC diminished, with correlation coefficients of −0.51, −0.01, and −0.39.

In 2020, a strong synergy relationship was still maintained among the six ecosystem service pairs consisting of HQ, WY, CS, and SC in Hunan Province. The highest correlation coefficient of 0.93 was found between HQ and CS, and strong synergy effects were also found between HQ and WY, HQ and SC, WY and SC, WY and CS, and SC and CS, with correlation coefficients of 0.13, 0.65, 0.93, 0.32, 0.18, and 0.61, respectively. The correlation coefficients between HQ-WY, WY-CS, WY-SC, CS-SC, and HQ-SC showed a significant increasing trend at the grid scale of 2000–2020. However, FP-HQ and FP-SC showed a decreasing trend.

From the spatial dimension (Figure 4B), the proportion of spatial synergies between HQ, WY, CS, and SC at the grid scale in Hunan Province was significantly higher than the proportion of spatial trade-offs, indicating that the spatial relationships among these four types of ecosystem services were dominated by synergy relationships. The areas with strong spatial synergies were mainly distributed in the hilly areas of southern Hunan Province (e.g., HQ-CS, WY-HQ, and CS-SC) and western Hunan Province (e.g., SC-WY, WY-HQ, and CS-SC). In contrast, the areas of spatial trade-offs between FP and other ecosystem services were mainly concentrated in the western (FP-WY and FP-CS), southern (FP-HQ, FP-WY, FP-CS, and FP-SC), and northern (FP-HQ, FP-CS, and FP-SC) regions of Hunan Province.

3.3 Influencing factors of trade-offs/synergies

At the grid scale, GDP has the highest degree of influence on the trade-off effects of FP-CS, FP-HQ, FP-SC, and FP-WY, as well as the highest degree of influence on the synergy effects of HQ-WY. SLOPE has the second highest degree of influence on the trade-off effects of FP-CS, FP-HQ, and FP-SC, and PRE has the lowest degree of influence (see Figure 5).

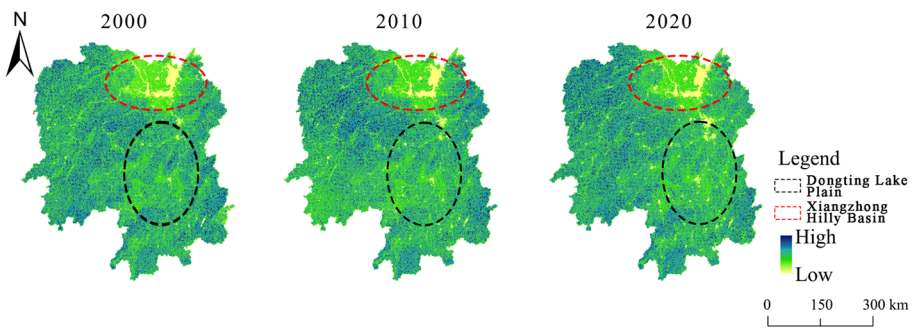

FIGURE 3
Integrated services of grid ecosystems in Hunan Province, 2000–2020.

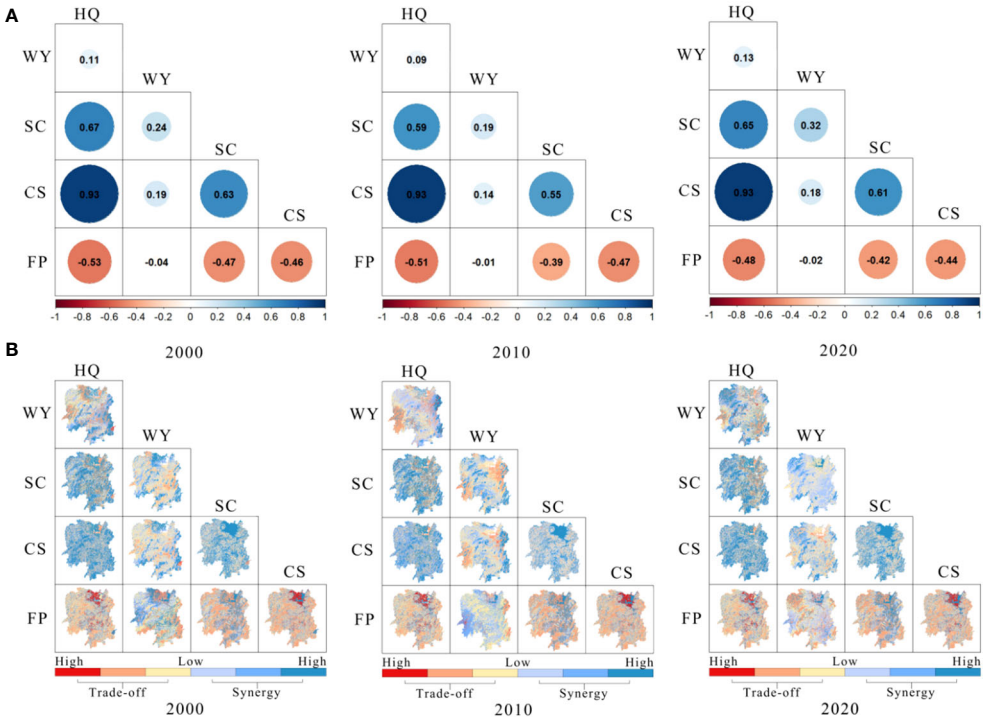

FIGURE 4
Changes in trade-offs and synergies of ecosystem services at grid scale in Hunan province. **(A)** Temporal dimension and **(B)** spatial dimension.

In the results of the synergy effects of FP-WY, GDP has the highest degree of influence with a *q*-value of 0.10, which is slightly higher than DEM and PRE, followed by NDVI and SLOPE, and POP is the lowest with a *q*-value of 0.05. In the results of the synergy effects of SC-CS, the degree of influence of DEM is much higher than that of other factors, with a *q*-value of 0.31, followed by SLOPE with a *q*-value of 0.26. This indicates that in the synergy relationship between SC-CS, the altitudinal position and topographic conditions have a greater influence. NDVI and GDP both had *q*-values of 0.12, while POP was lower than 0.08, and PRE was the lowest at 0.03.

In the results of the synergy influence of HQ-CS, DEM has the highest degree of influence with a *q*-value of 0.21, followed by SLOPE with a *q*-value of 0.15, while GDP, POP, and NDVI have *q*-values of 0.10, 0.08, and 0.10, respectively, and PRE is the lowest at 0.03. In the results of the synergy effect of the influence of HQ-SC, DEM, SLOPE, NDVI, GDP, POP, and PRE had *q*-values of 0.19, 0.18, 0.17, 0.15, 0.10, and 0.02, respectively. In the synergy effect impact results of HQ-WY, GDP, DEM, NDVI, SLOPE, PRE, and POP had *q*-values of 0.09, 0.07, 0.07, 0.05, 0.04, and 0.03, respectively.

In the synergy effect impact results of WY-CS, the *q*-values of DEM, SLOPE, GDP, POP, NDVI, and PRE are 0.28, 0.27, 0.20, 0.16, 0.12, and 0.03, respectively. In the synergy effect impact results of WY-SC, the *q*-values of DEM, POP, GDP, SLOPE, PRE, and NDVI are 0.20, 0.17, 0.17, 0.16, 0.14, and 0.09, respectively.

At the 1-km grid scale of interaction detection results in Table 2, the interaction results among the factors were more balanced compared to the city and county levels. With a score of 0.54, 0.53, 0.52, 0.54, 0.55, 0.56, and 0.55, respectively, NDVI has the largest influence among them in the trade-off interaction detection of FP-SC, FP-HQ, FP-SC, FP-WY, HQ-SC, HQ-CS, and HQ-WY, while the GDP had the highest amount of influence in the synergistic detection of SC-CS, WY-CS, and WY-SC, with detections of 0.53, 0.80, and 0.64, respectively.

4 Discussion

During the study period, the value of integrated ecosystem services showed an increasing trend over time and heterogeneity in space, which has important implications for decision-making related to sustainable development, environmental protection, and regional planning. There was an overall trade-off relationship between FP and any other ecosystem services, with the strongest trade-off effect between FP and HQ, which was spatially distributed mainly in the hilly and mountainous regions of the western part of the Xiangxi region, which have favorable environmental conditions. The synergy effect between HQ, WY, CS, and SC generally showed an increasing trend during the study period (Shen et al., 2023). The GD can then explore how the selected drivers affect TOSs at the gird scale, and also investigate if there are any nonlinear effects between the drivers on TOSs (Ouyang et al., 2023). TOSs were influenced by a combination of natural conditions, socio-economic, and other factors. Among them, GDP and slope factors had the greatest influence on food production, along with other influencing factors. Economic development led to a corresponding decrease in the area of arable land, which, in turn, caused a decline in food production services. However, the impact of human management

10.3389/fevo.2023.1342766

FIGURE 5
Correlation coefficient of different factors and ES.

TABLE 2 Interactive influence coefficients of different factors and ES.

Ecosystem service	Interaction dominant factor 1	Interaction dominant factor 2	Interaction dominant factor 3	Interaction dominant factor 4	Interaction dominant factor 5
FP-CS	POP∩SLOPE:0.252	PRE∩POP:0.377	GDP∩PRE:0.522	NDVI∩GDP:0541	DEM∩GDP:0.411
FP-HQ	POP∩SLOPE:0.233	PRE∩POP:0.362	GDP∩PRE:0.512	NDVI∩GDP:0.535	DEM∩NDVI:0.377
FP-SC	POP∩SLOPE:0.180	PRE∩POP:0.328	GDP∩PRE:0.478	NDVI∩GDP:0.522	DEM∩NDVI:0.362
FP-WY	POP∩SLOPE:0.210	PRE∩POP:0.440	GDP∩POP:0.520	NDVI∩GDP:0.543	DEM∩GDP:0.7377

(Continued)

TABLE 2 Continued

Ecosystem service	Interaction dominant factor 1	Interaction dominant factor 2	Interaction dominant factor 3	Interaction dominant factor 4	Interaction dominant factor 5
HQ-CS	POP∩SLOPE:0.314	PRE∩POP:0.330	GDP∩PRE:0.540	NDVI∩GDP:0.560	DEM∩NDVI:0.481
HQ-SC	POP∩SLOPE:0.258	PRE∩POP:0.343	GDP∩PRE:0.508	NDVI∩GDP:0.544	DEM∩NDVI:0.445
HQ-WY	POP∩SLOPE:0.176	PRE∩POP:0.280	GDP∩PRE:0.516	NDVI∩GDP:0.557	DEM∩GDP:0.368
SC-CS	POP∩SLOPE:0.316	PRE∩POP:0.334	GDP∩PRE:0.534	NDVI∩GDP:0.534	DEM∩NDVI:0.498
WY-CS	POP∩SLOPE:0.547	PRE∩POP:0.586	GDP∩POP:0.808	NDVI∩POP:0.714	DEM∩GDP:0.655
WY-SC	POP∩SLOPE:0.371	PRE∩POP:0.552	GDP∩POP:0.641	NDVI∩POP:0.494	DEM∩GDP:0.557

activities on agriculture can have a positive effect on food production. The more economically developed the region, the higher the cost and management inputs in the agricultural production process, leading to a higher intensity of agricultural management measures such as agricultural fertilizers, farmland irrigation, and agricultural machinery. These measures can effectively increase crop yields and enhance food production services.

This study analyzed the relationship between ecosystem services, which can help to form spatially oriented strategies to improve ecosystem service relationships and promote the sustainable development of social–ecological systems. However, there are limitations to the study, as only five representative ecosystem services were analyzed. The study's mapping results may be less uncertain if these ecological indicators are improved, data quality is raised, and the spatially explicit models used to calculate ecosystem supply and demand are updated. These actions may also have further policy and planning impacts. Considering how the socio-ecological drivers of ecosystem service TOSs evolve over time and scale is a next step to be taken in this study.

Despite some shortcomings, this study provides an attempt to gain a deeper understanding of the various influences of socio-ecological determinants on TOSs between ecological settings. Firstly, spatially explicit details of the TOSs among ESs are mapped as opposed to traditional correlation analyses that only provide statistical results. In addition, a technique for quantifying the degree of TOSs among ESs is suggested. In conclusion, many connections between ESs and potential drivers have been revealed and their spatial differentiation has been explored. The analysis then explores the spatial implications of different drivers and offers more theoretical and practical recommendations for local policymakers. Furthermore, the study's methodology and data are applied to other places, making it a useful case study and resource for ecological management in the hilly southern regions. (Li et al., 2019; Li et al., 2022). Additionally, a technique is proposed to quantify the extent of TOSs among ESs. In summary, this study identifies numerous connections between ESs and potential drivers, and examines their spatial variability. The analysis then explores the spatial implications of different drivers and offers more theoretical and practical recommendations for local policymakers. Furthermore, the study's methodology and data are applied to other places, making it a useful case study and resource for ecological management in the hilly southern regions (Xia et al.,2023).

5 Conclusion

This study quantitatively assessed the temporal and spatial change characteristics of five ecosystem services in Hunan Province from 2000 to 2020, including water production, soil conservation, carbon storage, habitat quality, and food production. We measured the TOS relationships among these ecosystem services using correlation analysis and GWR. Additionally, we identified the primary influencing factors and factor combinations for the degree of trade-offs in ecosystem services by applying a geographical detector. The comprehensive value of ecosystem services in Hunan Province showed an increasing trend from 2000 to 2020, with high values mainly distributed in the hilly areas in the west, south, and east of Hunan Province, while low values were mainly distributed in the Dongting Lake Plain and the Xiangzhong Hilly Basin.

There was a trade-off relationship between FP and all other ecosystem services, with the strongest trade-off effect found between FP and HQ. The synergy effect among HQ, WY, CS, and SC showed an increasing trend. GDP and slope were the dominant factors for the strength of trade-offs between food supply and other ecosystem services, while DEM and NDVI were the dominant factors for the strength of synergies among ecosystem services. Therefore, the strength of trade-offs and synergies between ecosystem services was not affected by a single factor. The interactions or the driving of common influencing factors between the two services determined the relationship.

Data availability statement

The raw data supporting the conclusions of this article will be made available by the authors, without undue reservation.

Author contributions

FT: Conceptualization, Data curation, Formal analysis, Methodology, Software, Supervision, Writing – original draft. ZL: Data curation, Methodology, Software, Writing – original draft. FZ: Funding acquisition, Supervision, Validation, Writing – original draft.

Funding

The author(s) declare financial support was received for the research, authorship, and/or publication of this article. The Major Bidding Project of Hunan Social Science Fund, "Research and Interpretation of the Spirit of the 6th Plenary Session of the 19th National Congress of the Communist Party of China and the Spirit of the 12th Party Congress of Hunan Province" (22ZDA020), and the Youth Project of Hunan Social Science Fund, "Model Selection and Efficiency Optimization of Effective Connection between Poverty Alleviation and Rural Revitalization in Ethnic Areas of Hunan.

Conflict of interest

The authors declare that the research was conducted in the absence of any commercial or financial relationships that could be construed as a potential conflict of interest.

Publisher's note

References

Bennett, E. M., Peterson, G. D., and Gordon, L. J. (2010). Understanding relationships among multiple ecosystem services. *Ecol. Lett.* 12 (12), 1394–1404. doi: 10.1111/j.1461-0248.2009.01387.x

Costanza, R., Arge, R., and De G, R. (1998). The value of the world's ecosystem services and natural capital. *Ecol. Economics* 25 (1), 3–15. doi: 10.1016/S0921-8009(98)00020-2

Feng, R., Wang, F., Wang, K., and Xu, S. (2021). Quantifying influences of anthropogenic-natural factors on ecological land evolution in mega-urban agglomeration: A case study of Guangdong-Hong Kong-Macao greater Bay area. *J. Cleaner Production* 283, 125304. doi: 10.1016/j.jclepro.2020.125304

Gong, J., Jin, T., Liu, D., Zhu, Y., and Yan, L. (2022). Are ecosystem service bundles useful for mountainous landscape function zoning and management? A case study of Bailongjiang watershed in western China. *Ecol. Indic.* 134, 108495. doi: 10.1016/j.ecolind.2021.108495

Gou, M., Li, L., Ouyang, S., Wang, N., La, L., Liu, C., et al. (2021). Identifying and analyzing ecosystem service bundles and their socioecological drivers in the Three Gorges Reservoir Area. *J. Cleaner Production* 307, 127208. doi: 10.1016/j.jclepro.2021.127208

Li, T., Lü, Y. H., Fu, B. J., Hu, W. Y., and Comber, A. J. (2019). Bundling ecosystem services for detecting their interactions driven by large-scale vegetation restoration: enhanced services while depressed synergies. *Ecol. Indic.* 99, 332–342. doi: 10.1016/j.ecolind.2018.12.041

Li, W., Xiong, W., Yang, W. B., Wang, T., Lian, H. L., Liu, Y. L., et al. (2022). Poplar trees do not always act as a water pump: evidence from modeling deep drainage in a low-coverage-mode shelterbelt in China. *J. Of Hydrology* 605, 127383. doi: 10.1016/j.jhydrol.2021.127383

Li, Z., Deng, X., Jin, G., Mohmmed, A., and Arowolo, A. O. (2020). Tradeoffs between agricultural production and ecosystem services: A case study in Zhangye, Northwest China. *Sci. Total Environ.* 707, 136032. doi: 10.1016/j.scitotenv.2019.136032

Liu, Y., Li, T., Zhao, W., Wang, S., and Fu, B. (2019). Landscape functional zoning at a county level based on ecosystem services bundle: Methods comparison and management indication. *J. Environ. Manage.* 249, 109315. doi: 10.1016/j.jenvman.2019.109315

Ouyang, X., Tang, L.-S., Wei, X., and Li, Y.-H. (2021a). Spatial interaction between urbanization and ecosystem services in Chinese urban agglomerations. *Land Use Policy* 109, 105587. doi: 10.1016/j.landusepol.2021.105587

Ouyang, X., Wei, X., Wei, G., and Wang, K. (2023). The expansion efficiency of urban land in China's urban agglomerations and its impact on ecosystem services. expansion efficiency of urban land in China's urban agglomerations and its impact on ecosystem services. *Habitat Int.* 141, 102944. doi: 10.1016/j.habitatint.2023.102944

Shao, Y., Xiao, Y., Kou, X., and Sang, W. (2023). Sustainable land use scenarios generated by optimizing ecosystem distribution based on temporal and spatial patterns of ecosystem services in the southern China hilly region. *Ecol. Inf.* 78, 102275. doi: 10.1016/j.ecoinf.2023.102275

Shen, J., Li, S., Wang, H., Wu, S., Liang, Z., Zhang, Y., et al. (2023). Understanding the spatial relationships and drivers of ecosystem service supply-demand mismatches towards spatially-targeted management of social-ecological system. *J. Cleaner Production* 406, 136882. doi: 10.1016/j.jclepro.2023.136882

Wang, J., Zhang, T., and Fu, B. (2016). A measure of spatial stratified heterogeneity. *Ecol. Indic.* 67, 250–256. doi: 10.1016/j.ecolind.2016.02.052

Xia, H., Yuan, S., and Prishchepov, A. V. (2023). Spatial-temporal heterogeneity of ecosystem service interactions and their social-ecological drivers: Implications for spatial planning and management. *Resources Conserv. Recycling* 189, 106767. doi: 10.1016/j.resconrec.2022.106767

Xu, S., Liu, Y., Wang, X., and Zhang, G. (2017). Scale effect on spatial patterns of ecosystem services and associations among them in semi-arid area: A case study in Ningxia Hui Autonomous Region, China. *Sci. Total Environ.* 598, 297–306. doi: 10.1016/j.scitotenv.2017.04.009

Xue, C., Chen, X., Xue, L., Zhang, H., Chen, J., and Li, D. (2023). modelling the spatially heterogeneous relationships between TOSs among ecosystem services and potential drivers considering geographic scale in Bairin Left Banner, China. *Sci. Total Environ.* 855, 158834. doi: 10.1016/j.scitotenv.2022.158834

Zhang, Z., Liu, Y., Wang, Y., Liu, Y., Zhang, Y., and Zhang, Y. (2020). What factors affect the synergies and tradeoff between ecosystem services, and how, from a geospatial perspective? *J. Cleaner Production* 257, 120454. doi: 10.1016/j.jclepro.2020.120454

Zhang, Z., Tong, Z., Zhang, L., and Liu, Y. (2023). What are the dominant factors and optimal driving threshold for the synergies and tradeoff between ecosystem services, from a nonlinear coupling perspective? *J. Cleaner Production* 422, 138609. doi: 10.1016/j.jclepro.2023.138609

Frontiers in
Ecology and Evolution

Ecological and evolutionary research into our natural and anthropogenic world

This multidisciplinary journal covers the spectrum of ecological and evolutionary inquiry. It provides insights into our natural and anthropogenic world, and how it can best be managed.

Discover the latest Research Topics

See more →

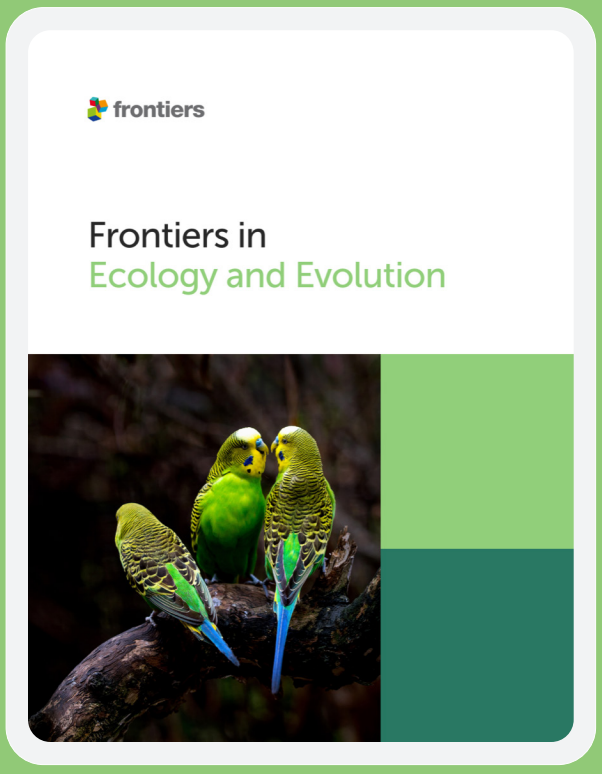

Frontiers

Avenue du Tribunal-Fédéral 34
1005 Lausanne, Switzerland
frontiersin.org

Contact us

+41 (0)21 510 17 00
frontiersin.org/about/contact